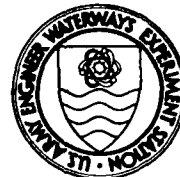


MISCELLANEOUS PAPER SL-81-14



# EVALUATION OF CONDITION OF LAKE SUPERIOR REGULATORY STRUCTURE SAULT STE. MARIE, MICHIGAN

by

Henry T. Thornton, Jr., Carl E. Pace, Richard L. Stowe  
Barbara A. Pavlov, Roy L. Campbell, A. Michel Alexander

Structures Laboratory  
U. S. Army Engineer Waterways Experiment Station  
P. O. Box 631, Vicksburg, Miss. 39180

June 1981  
Final Report

Approved For Public Release; Distribution Unlimited

DTIC  
S JUL 20 1981  
A



Prepared for U. S. Army Engineer District, Detroit  
Detroit, Michigan 48231

81 7 20 007

AD A101604

DTIC FILE COPY

Destroy this report when no longer needed. Do not return  
it to the originator.

The findings in this report are not to be construed as an official  
Department of the Army position unless so designated  
by other authorized documents.

The contents of this report are not to be used for  
advertising, publication, or promotional purposes.  
Citation of trade names does not constitute an  
official endorsement or approval of the use of  
such commercial products.

Unclassified

SECURITY CLASSIFICATION OF THIS PAGE (When Data Entered)

REPORT DOCUMENTATION PAGE		READ INSTRUCTIONS BEFORE COMPLETING FORM
1. REPORT NUMBER Miscellaneous Paper SL-81-14	2. GOVT ACCESSION NO. AD-A101 604	3. RECIPIENT'S CATALOG NUMBER
4. TITLE (and Subtitle) EVALUATION OF CONDITION OF LAKE SUPERIOR REGULATORY STRUCTURE, SAULT STE. MARIE, MICHIGAN		5. TYPE OF REPORT & PERIOD COVERED Final report.
7. AUTHOR(s) Henry T./Thornton, Jr. Barbara A./Pavlov Carl E./Pace Roy L./Campbell Richard L./Stowe A. Michel Alexander		8. CONTRACT OR GRANT NUMBER(s) D13/MP/SL-81
9. PERFORMING ORGANIZATION NAME AND ADDRESS U. S. Army Engineer Waterways Experiment Station Structures Laboratory P. O. Box 631, Vicksburg, Miss. 39180		10. PROGRAM ELEMENT, PROJECT, TASK AREA & WORK UNIT NUMBERS
11. CONTROLLING OFFICE NAME AND ADDRESS U. S. Army Engineer District, Detroit P. O. Box 1027 Detroit, Mich. 48231		12. REPORT DATE June 1981
14. MONITORING AGENCY NAME & ADDRESS (if different from Controlling Office)		13. NUMBER OF PAGES 376
		15. SECURITY CLASS. (of this report) Unclassified
		15a. DECLASSIFICATION/DOWNGRADING SCHEDULE
16. DISTRIBUTION STATEMENT (of this Report)  Approved for public release; distribution unlimited.		
17. DISTRIBUTION STATEMENT (of the abstract entered in Block 20, if different from Report)		
18. SUPPLEMENTARY NOTES  Available from National Technical Information Service, 5285 Port Royal Road, Springfield, Va. 22151.		
19. KEY WORDS (Continue on reverse side if necessary and identify by block number)  Concrete tests                      Laboratory tests Foundation conditions              Lake Superior Hydraulic structures		
20. ABSTRACT (Continue on reverse side if necessary and identify by block number)  X In May 1978 the U. S. Army Engineer District, Detroit (NCE) requested the U. S. Army Engineer Waterways Experiment Station (WES) to participate in the organization and execution of a program to accomplish detailed testing to deter- mine the condition of the Lake Superior Regulatory Structure and its foundation.  WES helped to plan and direct a testing program that included nondestructive and microseismic tests, concrete core drilling, laboratory analysis of core samples, tests and analysis of the steel structure and machinery. (Continued)		

DD FORM 1 JAN 73 1473 EDITION OF 1 NOV 65 IS OBSOLETE

Unclassified  
SECURITY CLASSIFICATION OF THIS PAGE (When Data Entered)

4/1/85

**SECURITY CLASSIFICATION OF THIS PAGE(When Data Entered)**

structural analysis of the substructure and superstructure, and preparation of written reports and recommendations.

Laboratory tests of the concrete cores indicate some minor amounts of surface frost-damaged concrete in three of the piers, and some alkali-silica reaction damage in one of those three. The interior concrete of the aprons and piers is in good condition and should continue to give excellent service.

The concrete piers were found to be adequate in their resistance to overturning and base pressure, but inadequate to sliding. Remedial stability measures are recommended.

Recommendations for future action are made where warranted in each area of evaluation in this investigation.

[illegible]

SECURITY CLASSIFICATION OF THIS PAGE(When Data Entered)



## PREFACE

The work reported here was performed for the U. S. Army Engineer District, Detroit (NCE), by members of the staff of the U. S. Army Engineer Waterways Experiment Station (WES). The preliminary engineering studies and field testing program were accomplished in FY 79 and were authorized by DA Form 2544 No. NCE-IA-79-005 dated 24 October 1978, Change No. 1 dated 7 November 1978, and DA Form 2544 No. NCE-IA-79-043 dated 30 January 1979. The compilation and evaluation of all test data, the completion of the structural stability and stress analysis, and the preparation of the final report were accomplished in FY 80 and were authorized by DA Form 2544 No. NCE-IA-80-022-EN dated 19 October 1979.

The detailed testing program was accomplished under the direction of Mr. Bryant Mather, Chief of the Structures Laboratory (SL); Mr. William Flathau, Assistant Chief, SL; Mr. John M. Scanlon, Chief, Engineering Mechanics Division (EMD); and Mrs. Katharine Mather, formerly Chief, Engineering Sciences Division (ESD); all of WES. Soils tests and borehole camera work were performed by members of the staff of the Geotechnical Laboratory (GL), WES; Mr. Gene P. Hale (GL) supervised the direct shear testing, and Mr. Richard W. Hunt performed the borehole camera work. The core-drilling program was accomplished by Mobile District drill crews under the supervision of Mr. Clyde Gambrell. Mr. Joe Kubinski of the NCE was on site during the drilling program and served as logistics coordinator. Messrs. Robert K. Jones and Jim Smith of the NCE served as overall project managers. Mr. Jim Bray, Sault Area Engineer, and his staff provided assistance during the course of the investigation.

Members of the WES staff who performed the work are Ms. B. A. Pavlov, Dr. C. E. Pace, Messrs. R. L. Campbell, E. F. O'Neil, R. L. Stowe, H. T. Thornton, Jr., A. M. Alexander, D. Glass, D. E. Wilson, and G. S. Wong, all of SL, and Messrs. J. C. Oldham, R. C. Hosemann, and T. E. Stukes of GL. Mr. Thornton served as Project Leader for the WES effort. Dr. Pace was responsible for coordinating and completing the work pertaining to stress, stability, and microseismic analysis.

Mr. Stowe was responsible for coordinating and completing the work pertaining to geology, foundation exploration, and concrete and rock testing. Ms. Pavlov, Tr. Pace, and Messrs. Stowe, Campbell, and Alexander coauthored this report with Mr. Thornton.

The Commanders and Directors of WES during the conduct of the investigation and preparation and publication of the report were COL John L. Cannon, CE, and COL Nelson P. Conover, CE. Mr. F. R. Brown was Technical Director.

## CONTENTS

	<u>Page</u>
PREFACE . . . . .	1
CONVERSION FACTORS, INCH-POUND TO METRIC (SI) UNITS OF MEASUREMENT . . . . .	5
PART I: INTRODUCTION . . . . .	6
Location of Area . . . . .	6
Background . . . . .	9
Objective . . . . .	12
Scope . . . . .	12
PART II: PRELIMINARY ENGINEERING STUDY AND TESTING . . . . .	13
Visual Inspections . . . . .	13
Review of Records and Drawings . . . . .	13
Survey and Soundings . . . . .	13
Underwater Video Inspection . . . . .	13
Ultrasonic Velocity Tests of Concrete . . . . .	14
In-Office Stability Calculations . . . . .	16
PART III: FIELD TESTING AND EXPLORATION . . . . .	21
Gates and Operating Machinery . . . . .	21
Microseismic In-Place Stability and Deterioration Evaluations . . . . .	27
Results of Preparatory Studies . . . . .	30
Foundation Exploration . . . . .	35
Scouring . . . . .	40
Geology . . . . .	47
PART IV: LABORATORY TESTS AND ANALYSIS . . . . .	53
Test Specimens and Test Procedures . . . . .	53
Core Test Results and Discussion . . . . .	56
Structural Stability Analysis . . . . .	73
Stability of Concrete-Foundation Interface . . . . .	76
Stability in Foundation Below Concrete-Foundation Interface . . . . .	77
Stress Analysis of Gate Operating Machinery . . . . .	81
Stress Analysis of Sluice Gates . . . . .	83
Automatic Operation of Sluice Gates . . . . .	84
PART V: SUMMARY AND RECOMMENDATIONS . . . . .	87
Summary . . . . .	87
Recommendations . . . . .	91
REFERENCES . . . . .	93
TABLE 1	
APPENDIX A: MATERIAL SUPPLEMENTARY TO PRELIMINARY ENGINEERING STUDY AND TESTING . . . . .	A1

APPENDIX B:	NDT AND LOAD TEST RESULTS, GATES AND OPERATING MACHINERY . . . . .	B1
APPENDIX C:	FOUNDATION EXPLORATION, REFERENCE MATERIAL AND BOREHOLE PHOTOGRAPHY . . . . .	C1
APPENDIX D:	BORING LOCATION PLAN AND GEOLOGIC CROSS SECTIONS . .	D1
APPENDIX E:	LABORATORY TEST RESULTS OF CONCRETE AND ROCK CORES . . . . .	E1
APPENDIX F:	STRUCTURAL STABILITY ANALYSIS, FIGURES AND COMPUTATIONS . . . . .	F1
APPENDIX G:	STRESS ANALYSIS OF GATES AND OPERATING MACHINERY, FIGURES AND COMPUTATIONS . . . . .	G1

CONVERSION FACTORS, INCH-POUND TO METRIC (SI)  
UNITS OF MEASUREMENT

Inch-pound units of measurement used in this report can be converted to metric (SI) units as follows:

<u>Multiply</u>	<u>By</u>	<u>To Obtain</u>
cubic feet	0.02831685	cubic metres
degrees (angular)	0.1745329	radians
feet	0.3048	metres
feet per minute	0.00508	metres per second
feet per second	0.3048	metres per second
foot-kips (force)	1355.818	joules
inches	0.0254	metres
inches per pound	0.571015	centimetres per newton
inch-pounds (force)	0.1129848	newton metres
kips (force)	4448.222	newtons
kips (force) per square foot	47.88026	kilopascals
miles (U. S. statute)	1.609344	kilometres
pounds (force)	4.448222	newtons
pounds (force) per foot	14.59390	newtons per metre
pounds (force) per square foot	47.88026	pascals
pounds (force) per square inch	6.894757	kilopascals
pounds (mass)	0.4535924	kilograms
pounds (mass) per cubic foot	16.01846	kilograms per cubic metre
square feet	0.09290304	square metres
tons (force) per square foot	0.09576052	megapascals
tons (2,000 lb, mass)	907.1847	kilograms

EVALUATION OF CONDITION OF LAKE SUPERIOR  
REGULATORY STRUCTURE, SAULT STE. MARIE,  
MICHIGAN

PART I: INTRODUCTION

Location of Area

1. The Lake Superior Regulatory Structure is located at the head of the St. Mary's Rapids between the twin cities of Sault Ste. Marie, Michigan, and Ontario. The St. Mary's River forms the only outlet from Lake Superior and links Lake Superior at its most easterly point with Lakes Michigan and Huron. Figure 1a shows vicinity and locality maps and a general plan view of the area. At this point the St. Mary's River flow is distributed among the following man-made structures, named from the Canadian to the United States side: the power canal of the Great Lakes Power Corporation, the Canadian Ship Canal, the Regulatory Structure, the power canal of the U. S. Government power plant, the two U. S. ship canals which serve four navigation locks, and the Edison Sault Electric Company's power canal. The Regulatory Structure consists of 16 gates, numbered 1 through 16 commencing on the Canadian side. Gates 1 through 8 are owned, operated, and maintained by the Great Lakes Power Corporation Limited, based in Sault Ste. Marie, Ontario. Gates 9 through 16 are owned, operated, and maintained by the U. S. Army Corps of Engineers. For the sake of water, that organization has entered into a contract with the local U. S. utility, the Edison Sault Electric Company, the terms of which permit the Corps of Engineers to use monies to repair the structure using the services of the Edison Company. An aerial photograph of the Regulatory Structure, with all gates in the full-open position, is shown on Figure 1b.





Figure 1b. Regulatory Structure, Sault Ste. Marie, aerial photographs



## Background

2. The Lake Superior Regulatory Structure was constructed by private firms between 1913 and 1919. There are 16 gates, 8 in Canada and 8 in the United States, used to control the water level in Lake Superior. The Canadian portion of the structure (gates No. 1 through 8) is owned, maintained, and operated by the Great Lakes Power Corporation (privately held). The U. S. portion (gates 9 through 16) is owned by the U. S. Government, but is maintained and operated by Edison Sault Electric Company at the direction of and under the administration of the U. S. Army Corps of Engineers. In 1976 the Lake Superior Board of Control requested a testing program as a basis for future decisions on the structure, i.e., need for repairs, rehabilitation, modernization, replacement, etc. The U. S. portion of the structure is in the jurisdiction of the U. S. Army Engineer District, Detroit (NCE) who was given the responsibility for coordination of the U. S. testing program. In a letter dated 12 May 1978 to the Commander and Director of the U. S. Army Engineer Waterways Experiment Station (WES), subject: Detailed Testing of the Lake Superior Regulatory Structure, the Chief, NCE, requested WES to participate in the organization and execution of a program to accomplish the testing of the U. S. part of the structure jointly owned and operated by Canada and the U. S. An enclosure to the letter of 12 May 1978 was a copy of a letter dated 3 December 1976 from the Lake Superior Board of Control transmitting a proposed program for the "detailed testing" to the International Joint Commission for Regulation of the Great Lakes Water Levels. A part of the preface to the proposed program is quoted here to present the rationale supporting the need for such a program:

The time has come when the U. S. and Canada must take under consideration the future usefulness of the Compensating Works at Sault Ste. Marie to meet the expanding needs of the International Joint Commission for Regulation of the Great Lakes Water Levels and as the interest of each country may appear.

The existing works were constructed between 1901 and 1921 on the approval by the governments of the U. S.

and Canada of a proposal by the Michigan Northern Power Company and the Algoma Steel Corporation to construct the compensating works for power purposes.

They have provided fifty-five years of excellent service but their condition is now considered to be sufficiently questionable as to justify an extensive examination on both sides of the border to test their suitability for continued service with or without reconstruction for a reasonable number of additional years.

Recent discoveries of local failures suggesting deterioration of underlying strata is obvious evidence of advancing age and perhaps inadequate repairs which creates further uncertainties with respect to the capability of the structures to sustain the use which would be required of it by several of the proposed Great Lakes Regulation plans. Furthermore, these plans call for a more responsive operation than would be possible with the present hand operated gates.

A further situation in Canada which must be resolved before final plans can be drawn up is a proposal by the Great Lakes Power Company to construct a new hydro plant in the region of the rapids and phase out the old obsolete plant.

Obviously these opinions must be investigated. Typical but not all inclusive questions are:

Is the current compensating structure structurally sound?

If no, should it be repaired?

Should it be modernized?

Should a multi-purpose structure with hydro power be constructed, etc.?

The first step to all these questions is a detailed engineering investigation of the present structure and its foundation. The investigation must be of sufficient detail that firm engineering data will be available to allow all potential future uses to be analyzed.

3. After the request by NCE for WES participation in the testing program a meeting was held in Sault Ste. Marie, Michigan. Attendees included representatives from the U. S. Army Engineer District, Mobile, (SAM), who had been asked to handle the core drilling, WES, NCE, and the Sault Area Office. The capabilities of the organizations represented

were discussed, as well as how such a testing program might be accomplished, and problems that might be encountered. WES was asked to study the proposed program and make recommendations based on testing capabilities and previous experience with similar testing programs. Figure A1 in Appendix A\* outlines the detailed testing program prepared jointly by WES and NCE. This outline presents the items of work and the proposed test standards and specifications to be used or referred to in accomplishing each item. The outline covers all items of the original program proposed by the Lake Superior Board of Control except the item addressing the "Coordination of (Committee) Assignments" which provides for the formation of an International Ad Hoc Committee to coordinate testing and analysis standards recognized by the scientific and professional community. The Ad Hoc Committee will also review both U. S. and Canadian test reports to assure that the study was conducted in accordance with these standards and that the findings and tentative recommendations are technically sound. The Ad Hoc Committee will act in a purely advisory capacity to the Lake Superior Board. Appointments to the International Ad Hoc Committee were:

United States Section

Mr. P. McCallister, Detroit District - Chairman  
Mr. W. C. Otto, Detroit District  
Mr. R. E. Philleo, Office, Chief of Engineers  
Mr. Jose Ordonez, North Central Division  
Mr. J. Bray, Sault Area Engineer  
Mr. H. T. Thornton, Jr., WES

Canadian Section

Mr. K. A. Rowsell, Canada Department of Public Works - Chairman  
Mr. R. Seawright, Canada Department of Public Works - Project Manager  
Mr. P. Siiman, Canada Department of Public Works - Structural Engineer  
Mr. D. Cuthbert, Canada Department of Public Works - Hydraulic Engineer  
Mr. E. Ashton, Canada Department of Public Works - Area Representative  
Mr. J. Bouchard, St. Lawrence Seaway Authority, International Lake Superior Board of Control - On-Site Representative

---

\* Figures, tables, and plates placed in appendixes will be referred to in the text with alpha-numeric characters designating those appendixes.

The Committee met 7 September 1978 in Sault Ste. Marie, Ontario, 19 October 1978 at WES, Vicksburg, Mississippi, and 16 August 1979 at Sault Ste. Marie, Michigan, U. S. A. The Committee approved the detailed testing program as presented in Appendix A. These of the Committee actions satisfy the requirements of the first group of work items, Coordination of (Committee) Assignments, until the Canadian section presents a program of proposed work. The Committee will review both U. S. and Canadian test reports and complete the testing program with one joint recommendation to the Lake Superior Board.

#### Objective

4. The objective of WES in this effort was to assist the NCE in the planning, implementation, and execution of a detailed testing program to determine the overall condition of the Regulatory Structure and its foundation.

#### Scope

5. The testing program included:

- a. Preliminary engineering study and testing.
  - (1) Visual inspections and collection and review of all available records and data.
  - (2) Survey, soundings, and underwater inspection.
  - (3) Ultrasonic velocity measurements in concrete.
  - (4) In-office stability analysis of substructure and superstructure.
- b. Field testing and exploration.
  - (1) Core-drilling program.
  - (2) Nondestructive testing (NDT) and load tests of gates and operating machinery.
  - (3) Microseismic analysis of piers.
  - (4) Foundation exploration and geology.
- c. Laboratory tests and analysis.
  - (1) Tests and analysis of concrete and rock cores.
  - (2) Structural stability analysis.
  - (3) Stress analysis of gates and operating machinery.

## PART II: PRELIMINARY ENGINEERING STUDY AND TESTING

### Visual Inspections

6. In May 1978 representatives from NCE, SAM, and WES made an inspection of the Regulatory Structure, and with the help of Sault Area Office representatives gathered information on the logistics problems that might be encountered in the overall planning and execution of the detailed testing program. The collection of data by visual means continued during the remainder of the testing program for use as direct input or as supplementary data in the overall assessment of the Structure.

### Review of Records and Drawings

7. All available records and drawings of the Structure were collected and reviewed. The items available for review included construction drawings, maintenance records, prior underwater inspections, modification plans for winter operation, boring logs, and foundation reports. Specific references to these records and drawings are made in appropriate parts of this report.

### Survey and Soundings

8. In January 1979 WES received a print of drawing No. DC-103-25, Compensating Works Condition Survey, showing elevations of the upstream and downstream aprons and adjacent river bottom. Pier elevations from results of prior surveys were obtained by telephone from members of the Sault lock staff. Information on water levels recorded upstream from the structure were also furnished. These data provided input for the office analysis of stability and later were used in developing the geologic cross section and assessing the condition of the foundation.

### Underwater Video Inspection

9. The underwater video inspection was originally scheduled to be performed in the fall of 1978. Difficulties with underwater video equipment and inclement weather conditions caused a change in scheduling.

This work was accomplished during the summer of 1979. WES received videotapes which recorded the complete upstream and downstream underwater inspection of the aprons and gates of bays 9 through 16. The information obtained from viewing these tapes provided valuable input to the evaluation of the structural stability of the dam and made possible a more complete assessment of the condition of the foundation.

#### Ultrasonic Velocity Tests of Concrete

10. In November 1978 ultrasonic velocity measurements were made through the concrete piers in the U. S. part of the Regulatory Structure. This NDT method is used to establish the uniformity or continuity of concrete structures and to provide indications of the general quality of the concrete in the structure. The equipment used for these tests was similar to that described in the Corps of Engineers test method CRD-C 51-72 (ASTM 597-71) (U. S. Army Engineer Waterways Experiment Station 1949). Ultrasonic pulse waves are transmitted through the concrete and the time of travel from the transmitter to the receiver, through a measured section of concrete, is electronically measured. Knowing the time of travel and the path length, the velocities through the material can be computed by using the following formula:

$$\text{Pulse velocity, ft/sec} = \frac{\text{Path length, ft}}{\text{Effective time, sec}}$$

This velocity provides an index of the condition or quality of concrete through which the readings are taken. Although mixture design and properties of materials used in various concrete mixtures affect velocities, the generally accepted correlation of velocity versus condition for mature concrete is given in the following tabulation (Leslie and Chessman 1949) of suggested concrete pulse velocity ratings:

<u>Pulse Velocity, ft/sec</u>	<u>General Conditions</u>
Above 15,000	excellent
12,000 to 15,000	good
10,000 to 12,000	questionable
7,000 to 10,000	poor
Below 7,000	very poor

11. To facilitate the velocity testing, members of the Sault Area Office designed and fabricated a rig with portable ladders and platforms to provide access to the sides of the concrete piers (see Figure 2). The aluminum ladders fit over the piers like a saddle. They are very light and easy to move from pier to pier.

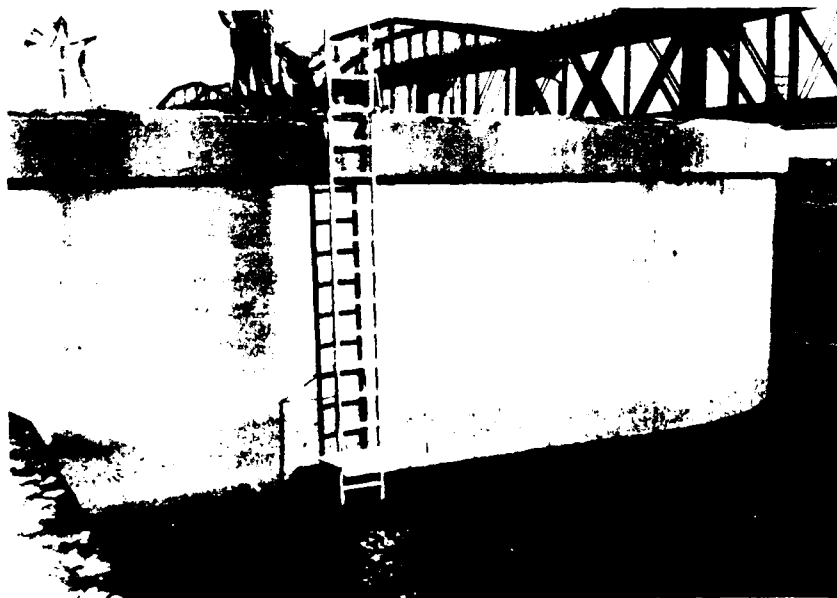


Figure 2. Portable aluminum ladders with platforms provided access to sides of piers

12. A total of 68 velocity measurements were made through the concrete in piers 9 through 16. Data stations were located on the vertical faces of each pier to provide for the accurate placement of

the transmitting and receiving transducers. Figure 3 shows the layout of data stations for piers 10, 11, 12, 14, 15, and 16. These piers are 8 ft wide\* and 34.6 ft long downstream from the gates. Figure 4 shows the layout of data stations on piers 9 and 13. These two piers are 9 ft wide and 40.6 ft long downstream from the gates.

13. Velocity data for piers 10, 11, 12, 14, 15, and 16 are given in Table A1. The high mean velocities indicate excellent quality concrete in these piers. The extraordinary roughness near the waterline on pier 12 probably caused the lower velocities obtained at stations 1b, 3b, and 4b. Velocities obtained from measurements on the larger piers, No. 9 and 13, are presented in Table A2. Again, the mean velocities indicate excellent quality concrete. The velocities obtained from pier 13 indicate a quality of concrete somewhat lower than that of the other piers. The fact that this pier has been patched in an area near the waterline indicates that the concrete in pier 13 is less resistant to the mechanism causing the waterline deterioration of the piers (see Figure 5). There is a vertical crack near data station 3a that may be the result of a change in the foundation near the downstream end of the pier.

14. These initial velocity measurements did not produce anomalies of alarming characteristics. The data indicate that the concrete is of generally good to excellent quality and that there are no areas which need to be regarded as deficient with respect to structural integrity. The ultrasonic velocity investigation of the concrete provided the desired input for stability analysis and overall assessment of condition of the structure.

#### In-Office Stability Calculations

15. At an early stage in the investigation of a concrete structure, the engineer is limited to what he can observe at the surface of

---

\* A table of factors for converting inch-pound units of measurements to metric (SI) units is presented on page 5.





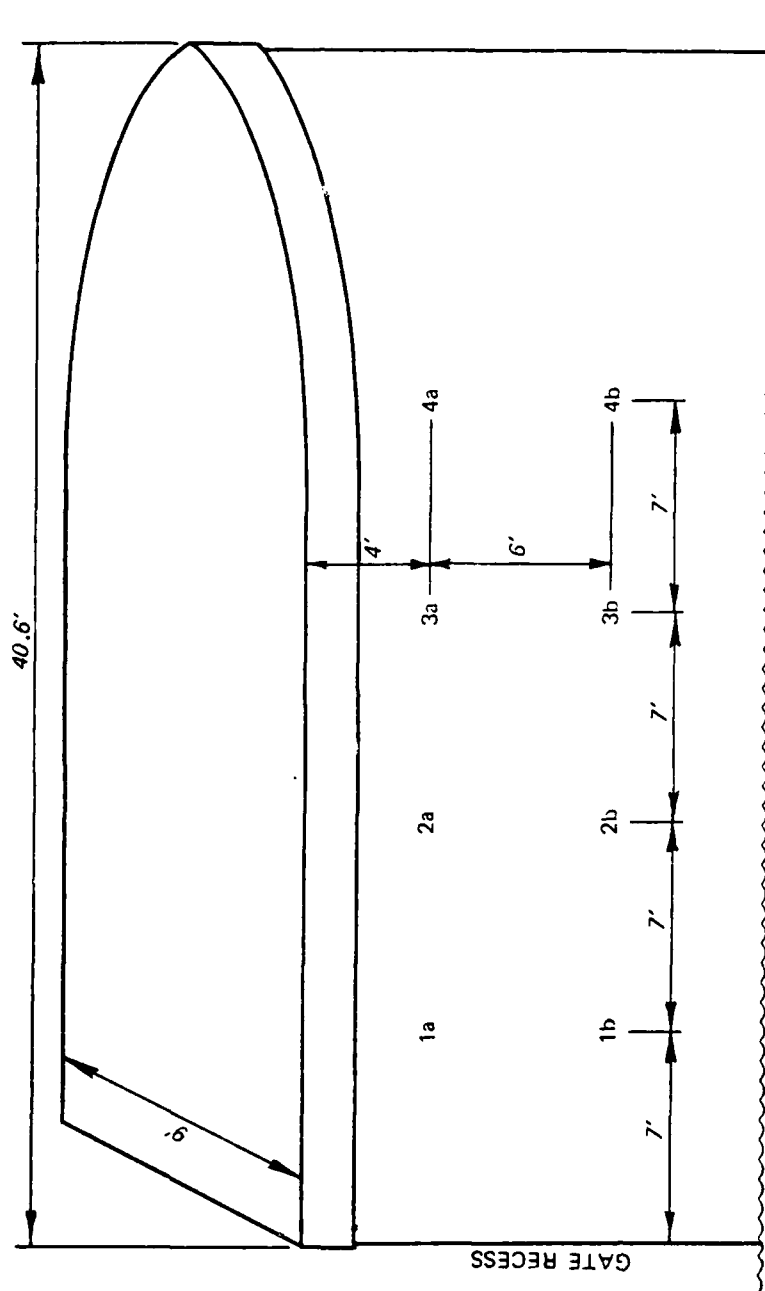


Figure 4. Ultrasonic velocity tests, Lake Superior Regulatory Structure.  
Typical layout of data stations, piers No. 9 and 13

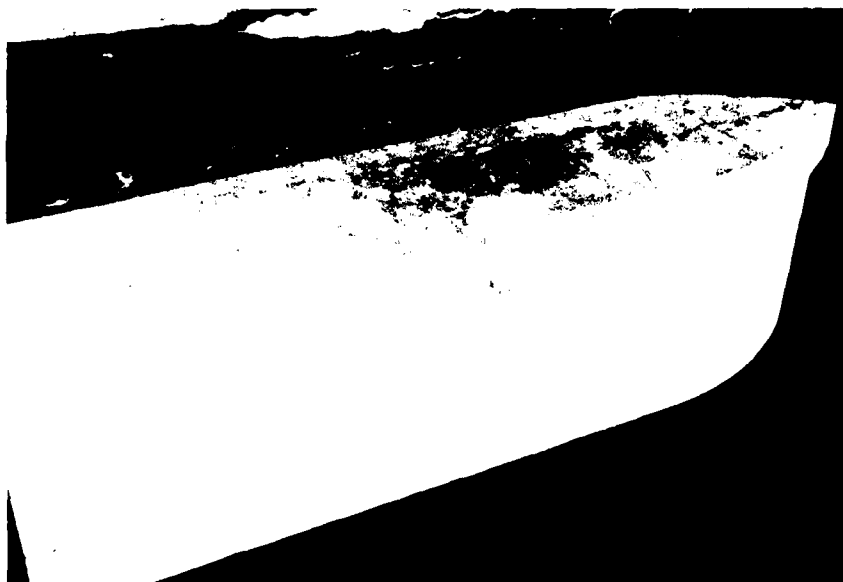


Figure 5. Pier No. 13, note patched area near waterline and slabbing near gate

the structure, and thus is limited in evaluating the whole structure. The interior condition of the concrete, such as deterioration and cracking, and the base condition of the structure are concerns which need to be investigated as an interrelated whole, but this is possible only after detailed field and office investigations. The preliminary analysis involved:

- a. Performing a preliminary conventional stability analysis to determine, in general, the adequacy of the piers to resist overturning, sliding, and base pressures.
- b. Preparation for a microseismic study to determine the in-place structural stability of the piers and to obtain an evaluation of the total structural system in relation to structural integrity.

The preliminary stability analysis used the following assumed properties:

Concrete weight =  $150 \text{ lb/ft}^3$

Angle of internal friction between pier and foundation = 30 deg

Cohesion between pier and foundation = 0

Strut resistance = 0

The strut resistance was initially assumed as zero because:

- a. Scour downstream of the dam was suspected but unknown.
- b. The condition and strength properties of the apron to act as a strut against the piers were unknown.

16. The results of the preliminary stability analysis indicated that the piers were adequate in their resistance to overturning and base pressures and were probably inadequate in their resistance to sliding.

### PART III: FIELD TESTING AND EXPLORATION

#### Gates and Operating Machinery

##### Magnetic particle and ultrasonic inspection

17. In June 1979 Peabody Testing Service was requested to perform an on-site determination of the best methods for evaluation of the condition of the steel and cast iron gate lift machinery and to advise WES representatives on other tests to be performed, such as rivet sounding and gate skin measurements. Individuals certified at Level III in NDT according to the American Society for Nondestructive Testing, recommended practice SNT-TC-1A (areas of magnetic particle, liquid penetrant, ultrasonics, and radiography testing), made the inspection and furnished a letter report recommending the use of dry magnetic particle and ultrasonic tests.

18. During the period of 8 August 1979 to 12 September 1979, dry magnetic particle inspections were performed on the accessible portions of the gears and lifting chains of the eight pairs of lifting mechanisms of gates No. 9 through 16; ultrasonic inspections were performed on the shafts of the eight pairs of lifting mechanisms (see Figures 6 and 7); and ultrasonic plate gaging and length measurements were performed on the gate skins and rivets.

19. Magnetic particle test results. The following discontinuities were found:

Gate No. 9 East - a 5-in. crack in a weight secured to a lifting chain link.

Gate No. 9 West - a 2-in. crack in the bolt hole in a lifting chain link.

Gate No. 15 West - a 3-in. crack in a weight secured to a lifting chain link.

All the discontinuities were circled, numbered, and marked with a white paint marker. The discontinuities that were found are not considered to be of a nature that could cause failure in the lifting mechanisms. No other discontinuities were indicated in the lifting mechanisms inspected using the magnetic particle technique.



Figure 6. Shafts and lifting chain of operating mechanism



Figure 7. Gear mechanism in operation

20. Ultrasonic inspection (gate skins and shafts) results. The ultrasonic inspection of the shafts of the eight pairs of lifting mechanisms produced no indications of processing or fatigue defects. The results of the ultrasonic plate gaging performed on the gate skins are given in Plates B1 through B8. Most of the measurements were made in the lower portion of the gates where maximum hydraulic pressure is exerted. Each of the 20 sections of steel plate in the lower portion of each of the eight gates was scanned to determine the thickness of the plates. Scans were made in areas near the four corners and in the center of each section. Some sections of the steel plate in the upper portions of gates No. 12, 13, and 14 were scanned to check the uniformity of thickness between upper and lower sections. The number of scans taken per gate is as follows:

Gates No. 9, 10, 11, 15, and 16 - 100

Gates No. 12 and 13 - 120

Gate No. 14 - 130

The construction drawings specify that the gate skin plates contain sections of medium steel of 0.375-in. thickness. Evaluation of data given in Plates B1 through B8 shows that only 24 of the 870 areas scanned produced apparent thicknesses less than 0.375 in. The mean thickness measurements for the eight gate skin plates ranged between 0.39 in. and 0.41 in. The grand mean for the eight gates is 0.40 in. The apparent presence of 0.025 in. of steel thickness is not considered to be unusual since it is not uncommon for steel plate to be over-toleranced in order to assure compliance with specifications. It is difficult to ascertain what were standard practices on tolerance setting in the early 1900's when this steel was manufactured. The data obtained from the ultrasonic inspections do not indicate that there has been any appreciable loss in gate skin thickness.

21. Ultrasonic inspection (rivets) results. The rivets used to fabricate the sluice gates were of medium steel, 7/8-in. diam, and had round heads (see Figure 8). The round heads made it extremely difficult to check the rivets for continuity using ultrasonic inspection. After consulting with experts in the conduct of these types of tests,

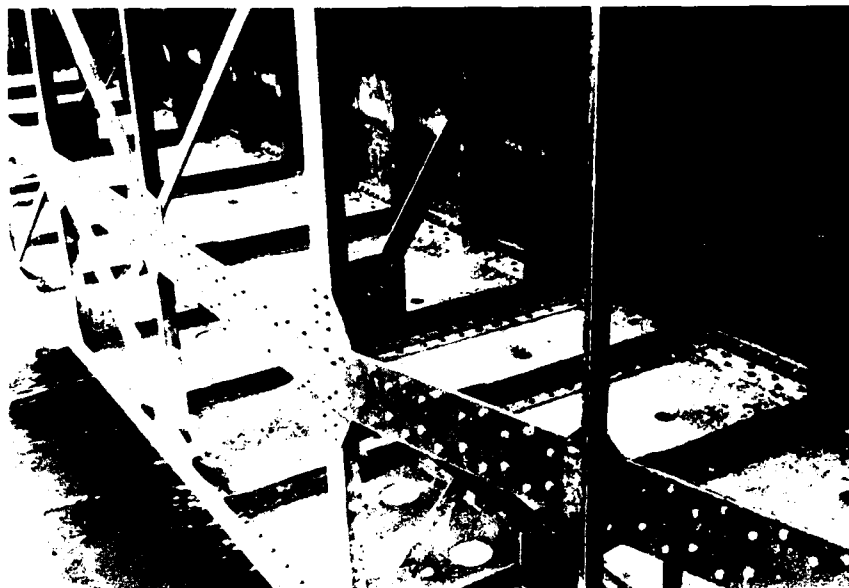


Figure 8. View of downstream side of sluice gate

it was determined that there were no alternatives to ultrasonics that would simplify or substitute for this type of measurement. It was apparent from the outset that satisfactory contact between the ultrasonic transducer and the rivet could not be made without grinding the head of the rivet. This had to be done by hand and was very tedious since the surface had to be flat and normal to the rivet axis. The degree of difficulty, the time and access restrictions imposed by a stringent schedule of gate manipulation, and the fact that field personnel were needed to complete other work resulted in a limited effort in rivet inspection. Plates B9 and B10 show the locations and results of measurements made on gates No. 11 and 12. A total of 60 rivets were sounded. Only six measurements indicated possible flaws. These flaws, if they were present, were very near the end of the rivet in each case. The fact that these six indications of defective rivets could have been caused by a lack of normalcy between the plane of contact and the rivet axis allows one to speculate that maybe none of the rivets tested were defective. The results of these tests do not show cause for concern about the rivets with respect to the integrity of the gates.



#### Load tests of gate machinery

22. After a study of the drawings showing the gate lifting machinery, the sprocket chain, and the hookup to the sluice gates, it was determined that the best way to make measurements of the gate hoisting loads would be to insert load cells into the hoisting system. This method was chosen over that of strain gaging the eye bars to eliminate the need for laboratory calibration of load versus strain for this particular steel. Since the purpose of these tests was to determine the combined total of gate and friction loads of several gates, it was necessary only to calibrate in the laboratory load versus output in millivolts of the load cells to be used and then record the output continuously during the operation of the gates.

23. The sheets showing strains and loads were examined along with photographs. Nominal loads to be expected during the operation of the gates were computed to be 30,750 lb per side. Replacement eye bars were designed to accommodate two 50,000-lb capacity load cells (one on each side of the gate) and to be substituted for the eye bars connecting the lifting chains to the gate (see Figures 9 and 10). The replacement eye bars were fabricated in the Sault Ste. Marie Area Office machine shop. The load cells were transported to the site along with the measurement instrumentation (see Figure 11), and the measurements were made during the period of 15-18 August 1979.

24. Loads were monitored continuously on gates No. 9, 10, 15, and 16 during normal raising operations. The results of these measurements are tabulated in Tables B1 through B4 and plotted in Plates B11 through B14. The gates were raised a distance of 10 to 13 ft at a nominal rate of 1.2 ft/min. Single side loads ranged between 30,250 and 36,400 lb. Gates No. 9 and 10 showed noticeable differences in loads between sides. Gate No. 9 at one point showed a difference of 2450 lb, and gate No. 10 showed a 5550-lb difference at one point. It was observed that the counterweights on some gates may not have been symmetrically spaced. These differences could also be caused by friction loading.



Figure 9. Fifty thousand pound capacity load cell



Figure 10. Load cell and replacement eye bars

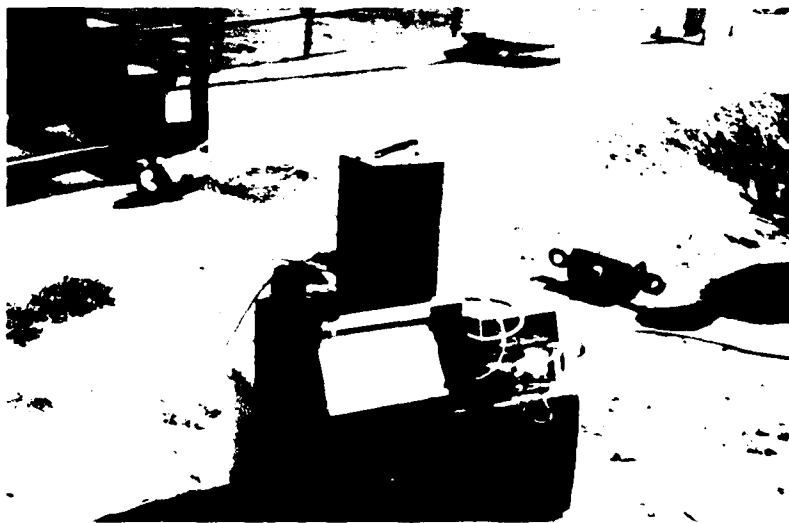


Figure 11. Load measurement instrumentation

## Microseismic In-Place Stability and Deterioration Evaluations

### Introduction

25. For many years, dynamic E calculations have been made and used to indicate the state of deterioration of freeze-and-thaw beams in standard laboratory tests. The deterioration need not be caused by freezing and thawing conditions. The dynamic E as obtained from a response after dynamically exciting a structure is a measure of the elastic qualities of the total structure and is a good indicator of its structural integrity.

26. In the past, the stability of a structure has been determined by conventional calculations. These calculations are based on certain assumptions, such as laboratory test results, to represent the behavior of foundation and structure materials, a flat base structure, assumptions concerning the properties of backfill materials, etc. In the past, it has been demonstrated that these methods, even though they are approximate, can produce a safe structural system. It is very probable that the structural designs are overconservative and if the actual stability of the in-place structure could be known, especially when older structures are being evaluated, large amounts of money could be saved by eliminating expensive remedial measures for inadequate stability, as reflected by conventional computations. The best way to determine the in-place stability of a structure is to push on it with increasing horizontal static forces and determine the static horizontal force and deflection relationship. This does not directly give the stability of the in-place structure because some criteria must be available to evaluate what this horizontal force-deflection relationship means in relation to sliding safety. The way to make this evaluation is not by developing new criteria which must be proven with time; but to relate the horizontal force-deflection relationship as determined in the field to conventional stability analysis in such a way as to determine the safety factor against sliding in relation to conventional sliding safety factor calculations. This relationship can be obtained by using the same laboratory test data as are used in performing the conventional

stability analysis computations in conjunction with in-place measurements. Laboratory tests are used to determine the angle of internal friction and cohesion of the weakest plane or combination of planes below a structure. Shear tests, which give this data, also give the load-deflection characteristics of these shear planes.

27. The safety factor as determined by the laboratory test data can be ratioed by  $\frac{\text{laboratory deflection/load}}{\text{field deflection/load}}$  to obtain the in-place

factor of safety against sliding. This is saying, quite simply, if the structure is harder to displace in the field than laboratory test data indicate, it is safer in its resistance to sliding. The monoliths at the Regulatory Structure are very stable against overturning and base pressures; therefore, the in-place sliding resistance is all that is needed to evaluate the in-place stability of the Structure.

28. The only problem with the above analysis is that a reaction-block type system would be needed to push on the in-place structure, and sensitive deflection gages would be needed to measure the small deflections. This problem can be eliminated by using dynamic excitation and the equivalent static force-deflection relationship for the structure from load cell and accelerometer measurements. The deflection is obtained by Fast Fourier measurement and analysis instruments (FFT) (see Figure 12), which will give the deflection at zero frequency and the corresponding static load associated with the dynamic excitation. The FFT is used mainly for impedance measurements but will also give instant velocity and displacement feedback from the accelerometer measurement.

29. The FFT is excellent for obtaining data from structure response (after excitation by a dynamic energy input) which can be used to evaluate in-place structure stability and structure integrity.

#### Preparatory studies

30. Since the dynamic technique had never been used to determine in-place stability and structure integrity, it was necessary to perform some preliminary tests to get ideas, techniques, and equipment to best perform the field tests. Various size model structures were obtained and shakers of various sizes were used to put sinusoidal or swept-sine

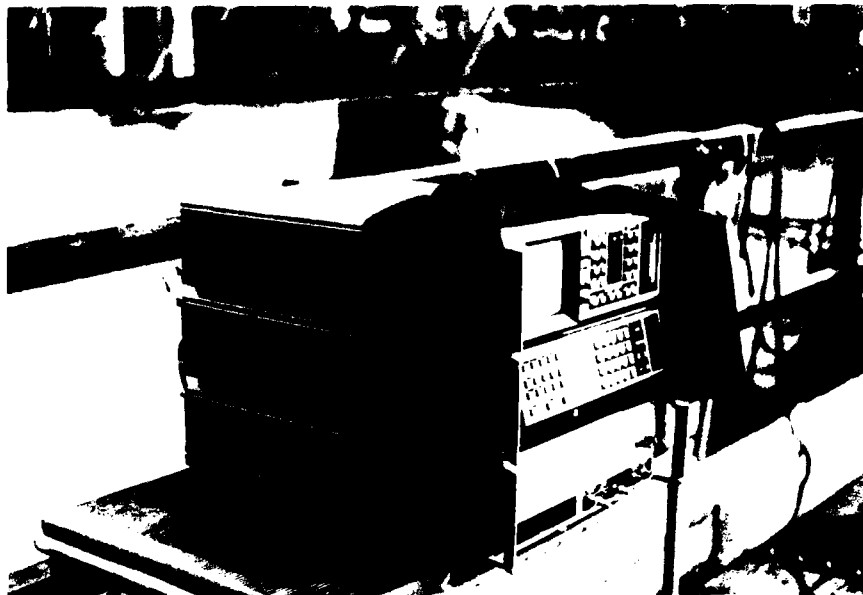


Figure 12. Real-time Fourier analyzer (FFT)

input into the structure. The output was measured with an accelerometer and the data reduced by an elaborate instrumentation system which has been used in the analysis of vibration data by the SL at the WES. This system was too expensive and was abandoned in favor of an impulse loading with the data being reduced by an FFT. This system was best, due to portability of equipment, less cost, speed of measurements, speed of data analysis, and increased capability. The investigation not only included studying the feasibility of the resonant technique for determining the integrity of a field structure but also determined the feasibility of using the impulse technique to excite the structure rather than the more commonly used sinusoidal or swept-sine technique. The impact resonance method was used on the same structures as the sinusoidal method, and the same resonant frequencies were obtained. The impulse method was verified, and it could be used economically on the piers at the Regulatory Structure. The FFT made it possible to calculate functions such as spectrums, transfer relationships, coherence, and many other on-site

structural response characteristics. In addition to on-site analysis, the data were stored on magnetic tape and analyzed in the laboratory.

31. The impact tests were made on rectangular blocks, two of which are shown in Figures 13 and 14. Some model structure sizes, weights, resonant frequencies, and dynamic E's are presented below:

<u>Structure</u>	<u>Structure Size</u>	<u>Mass, lb</u>	<u>Resonant Frequency, Hz</u>	<u>Dynamic E, psi</u>
1	18 by 18 by 26 in.	765	2280	$5.84 \text{ by } 10^6$
2	3 by 6 by 6 ft	16,800	564	$3.54 \text{ by } 10^6$
3	3 by 6 by 10 ft	28,140	322	$5.73 \text{ by } 10^6$

#### Results of Preparatory Studies

32. Structure 2 (16,800 lb) had a lower dynamic E as calculated by the fundamental frequency equations of Pickett (1945). This specimen had a number of large cracks which were visible before the structure surface was grouted and painted. This demonstrates that diminished structural integrity will be reflected by the dynamic modulus calculations. The determining of the resonant frequency allows one to know at what frequencies the structure will be more effected by loadings. During the laboratory tests it was found that it took a static load of 10,000 lb to fail the 28,140-lb structure in sliding. At its natural frequency, it failed at approximately 250 lb. This indicates a reduction by a factor of 40 in sliding resistance, which very drastically illustrates the undesirability of exciting the structure near its resonant frequency. This consideration has been of concern and interest in many situations of the past. For example, companies of soldiers must break step when crossing bridges due to the risk of creating large motions at resonant frequencies. The Tacoma Narrows Bridge in Washington State was destroyed by the wind exciting the structure at a resonant frequency. Tests on other laboratory structures were performed and similar results as those stated above were obtained.

Figure 14. Block  
Dimensions 3 by 6  
by 10 ft

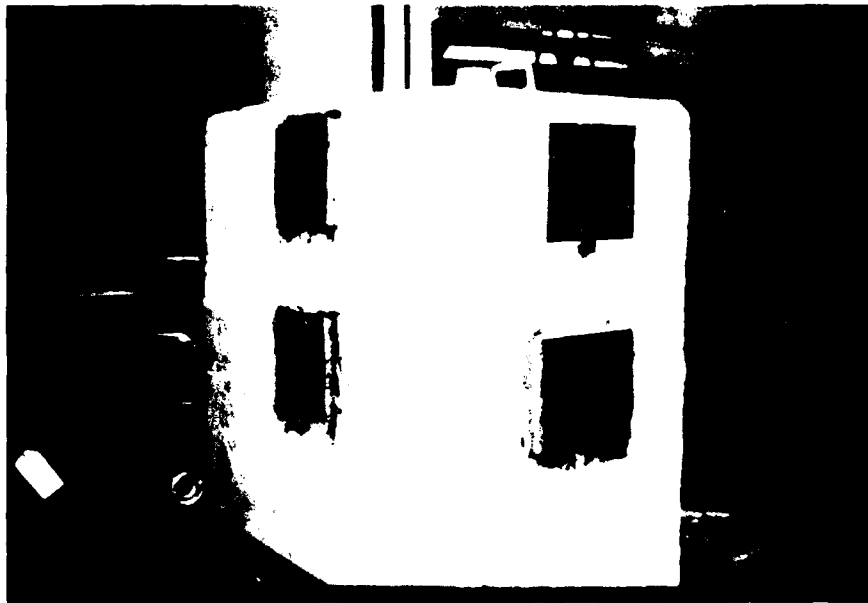


Figure 13. Block  
Dimensions 3 by 6  
by 6 ft

### Field tests

33. Resonant frequency measurements were performed on all eight piers American controlled at the Regulatory Structure using the impact technique. Each of the piers was measured in the flexural mode. As the resonant frequency is directly related to the dynamic modulus of a specimen the test permits a dynamic evaluation of the mechanical integrity of the structure. A FFT was used to process the force and acceleration signals in real time.

34. A 550-lb weight was swung in a small arc using a tripod system (Figure 15). This weight struck a 200-lb reaction block that was

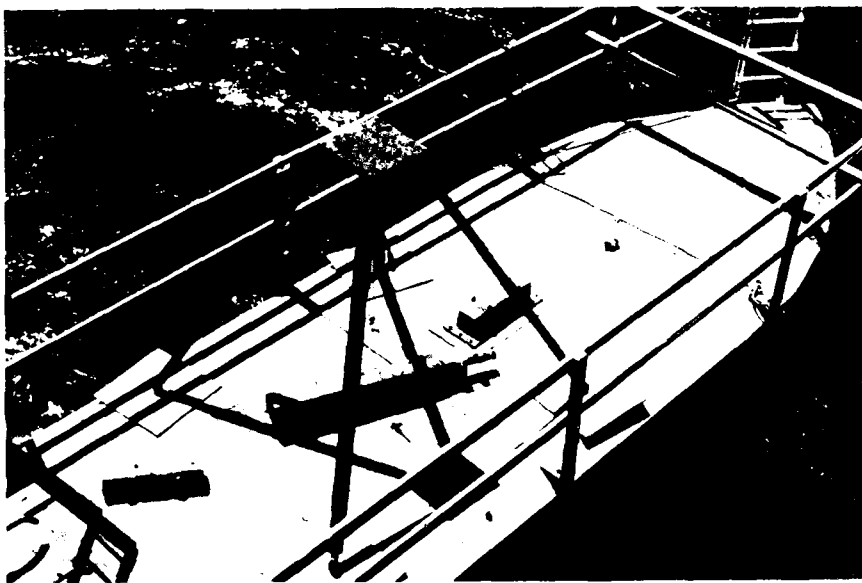


Figure 15. System to generate load pulse: A-frame, 550-lb impactor, reaction block, steel plate, concrete pier

bolted to a large 3/4-in.-thick steel plate anchored by bolts and epoxied to the concrete surface. A force pulse was generated that was typically 5000-lb peak, existing for about 15 msec. The pulse contained excitation energy from 0 to about 100 Hz. Previous mathematical calculations had



shown that the fundamental resonant frequency vibrating in flexure should be in that range. The mathematical equations used were derived for rectangular shaped specimens that are unrestrained. Tests made on a physical model in the laboratory showed that the resonant frequency was higher for the specimen when the ends were sawed to resemble the shape of the piers. Also, when the model was epoxied to a very rigid base to restrain movement, simulating the case in the field, the fundamental flexural frequency showed further increase. The frequency for the physical model increased 36 percent from a rectangular, unrestrained specimen to a sawed, restrained specimen. Calculations indicated expectations of about 50 Hz from one of the smaller piers at Soo if it was rectangular and unrestrained. Increasing that by 36 percent yields an expected value of near 68 Hz. The actual measurements were about 76 Hz for those particular piers. Although accurate calculations of the dynamic modulus from the resonant frequencies are impossible to obtain because of the shape and restraint affect, still it is possible to gain significant information from the resonant frequencies. The fact that all six of the smaller piers had resonant frequencies within less than 2 Hz of each other indicates that all six piers are in like condition with respect to mechanical integrity, and the fact that the frequencies tend toward the higher side of the range of frequencies produced by the mathematical calculations indicates that the piers are of good quality rather than poor. If we assume that all six piers are seeing the same restraint at the base, then because they all have the same geometry, the frequency deviation of almost 2 Hz is due to modulus alone. Mathematical calculations were made to determine the variation of modulus required to produce a difference in resonant frequency of 2 Hz. The computed variation was about half a million psi. Since these assumptions represent the worst case, it is likely that the deviation of the modulus between piers is not that high, since the bridgework supported by the piers as well as the slight differences in foundation could account for some variation. The test data are given in the following tabulation:

	<u>Pier No.</u>	<u>Frequency, Hz</u>	<u>Deviation, Hz</u>
Larger	9	62.500	
Piers	13	63.000	
	10	76.562	0.122
	11	78.125	1.685
Smaller	12	75.000	-1.44
Piers	14	76.172	-0.268
	15	77.000	0.56
	16	75.781	-0.659
<hr/>			
Average		76.44	--

Although pier 11 seems to be of better quality, the small variation of 1.7 Hz may not be significant if allowed for some measurement error. Since piers 9 and 13 are reading within 1/2 cycle of each other, indications are that both are of the same quality and, again, because of reading on the high side of the frequency range calculated from the mathematical model, the dynamic modulus appears to be high. No discontinuities are indicated in any of the piers, nor are any significant differences in the restraint offered by the foundation of any of the piers indicated.

#### Results

35. By exciting a structure with an impact force and analyzing the output, the integrity and the in-place stability of the structure can be predicted. The resonant technique is a measurement which gives characteristics of the total structure and foundation system.

36. From the above measurements, it was determined that the piers are all structurally sound.

37. The data for stability evaluations were limited because of gate opening schedules at the structure while the testing was in progress, which afforded too little time to make and evaluate a sufficient number of deflection measurements at the base of the piers.

38. The deflection obtained at the base of piers where measurements were made was in the range of  $2.0$  to  $4.0 \times 10^{-7}$  in./lb. The laboratory data give values of approximately  $2.0 \times 10^{-8}$  in./lb for the shaley sandstone and  $6.0 \times 10^{-9}$  for the very hard sandstone and concrete

interface. Since the shaley sandstone seam governed, there is an indication from field data that the piers are less stable than conventional calculations indicate. The indication is that the conventional safety

factor is reduced roughly  $\frac{2 \text{ to } 4 \times 10^{-7}}{2 \times 10^{-8}} = 10 \text{ or } 20 \text{ times}$ . This seems

unreasonable and since time was limited such that detailed on-site evaluations could not be made, it is suggested that the conventional stability results in Part be used and the piers be posttensioned to the foundation to assure their safety.

#### Foundation Exploration

39. A review of previous boring location maps, boring logs, a foundation report for the New Poe Lock, and other foundation data in the vicinity of the Regulatory Structure has been made; see Appendix C for a partial list of materials used. The review revealed that there was no major geologic structure in the area that might affect the dam's stability, that bedding was nearly horizontal with weak soft seams of varying thicknesses, and that competent foundation rock could be expected to be present beneath the dam. No information was found concerning settlement or misalignment of the dam structure, which if found, could indicate foundation problems.

#### Previous exploration

40. The first three locks built at Sault Ste. Marie, State, Weitzel, and Old Poe Locks, were built without foundation explorations.

41. In 1907 foundation explorations for Davis and Sabin Locks were made. Ten borings were drilled with a highest top elevation of 585.5 ft and a deepest bottom elevation of 504.0 ft.

42. In 1942 foundation explorations for MacArthur Lock (new first lock) were made. Eleven borings were drilled with a deepest elevation of 521.2 ft. In 1958 and 1959, 29 borings were made in exploration for design of the New Poe Lock (new second lock).

43. In 1962 additional foundation explorations were made at New Poe Lock during a re-evaluation of lock design and foundation

requirements. Fifty-two borings were made with a highest top elevation of 590.19 ft and a deepest bottom elevation of 509.39 ft.

44. From 1964 to 1967, 301 borings were made during the construction of New Poe Lock. Highest top elevation drilled was 594.2 ft and deepest bottom elevation was 497.1 ft.

45. In 1974 foundation explorations were made for New Sabin Lock. Five borings were drilled with a highest top elevation of 589.7 ft and a deepest bottom elevation of 452.0 ft.

46. In 1975 additional foundation explorations were conducted for New Sabin Lock. Two borings were drilled with a highest top elevation of 603.59 ft and a deepest bottom elevation of 487.19 ft.

47. In 1960, 44 borings were made in foundation excavations for the Sault Ste. Marie International Bridge by the Michigan State Highway Department. The bridge is about 400 ft downstream of the Regulatory Structure. The highest elevation for top of bedrock encountered in the borings is 605.5 ft and the deepest bottom of the borings is 563.5 ft. Bedrock at the bridge site is believed to be similar to that found in the most recent borings at the Regulatory Structure.

#### Drilling at Regulatory Structure

48. A total of 30 borings was drilled at the Regulatory Structure (see Plate D1). One was drilled through the spoil dike at the south end of the Regulatory Structure. Four were drilled approximately 80 ft upstream of the centerline of the Regulatory Structure. Eight were drilled approximately 6 ft upstream of the centerline of the Regulatory Structure. Thirteen were drilled through the downstream end of the piers and apron, and four were drilled approximately 62 ft downstream. Seven cores had 6-in. diam, and 23 cores had 4-in. diam. These borings were made from 14 June to 7 July 1979. Drilling was done by personnel of SAM. The field drilling logs for all borings are presented in Exhibit A, which is on file at the Soo Locks and the Detroit District Office. Figure 16 shows typical drill rig set-ups. Figure 16a shows the drill rig on a cantilevered work platform attached to Scow 15. This set-up was used to drill the upstream borings adjacent to the structure. Figure 16b



a. Setup for drilling upstream boring adjacent to the structure



b. Setup for drilling the piers

Figure 16. Typical rig setups

illustrates how the drill rig was set up to drill the piers; note guardrail around top of pier.

49. Depths of holes ranged from 10 ft to 53.5 ft when concrete is included or from 7.1 ft to 30.7 ft when only rock is measured. Total footage was 730.5 ft. This includes 464.25 ft of rock, 26.5 ft of fill, 1.5 ft of overburden, and 238.25 ft of concrete.

50. Core recovery was good, usually above 97 percent. The boring CW-35 through the spoil dike had only 40 percent recovery due to grinding and washing away of the fill material. The lowest core recovery for the remaining 29 holes was 90.9 percent in CW-19.

51. Drilling was accomplished using two skid rigs: a Longyear 38 and a 43 SA Failing Holemaster. Core barrels used were 4- by 5-1/2-in. double tube and 6- by 7-3/4-in. double tube core barrels. A pressure pump was used to supply bypass water for drilling (with a 1-1/2-in. discharge hose).

52. Transportation to and from the jobsite, marine floating plant, and crane support were supplied by the Area Engineer Office at the Sault Locks. Drill rigs were set up on piers with a Manitowoc 140-ton crane mounted on the 40-ton Derrick boat HARVEY. Upstream holes were drilled from an 18- by 75-ft barge (Scow 15) with a 40-ft launch as tender ALCONA. Downstream holes were drilled from a 30- by 60-ft barge MMN-1-BAY CITY with a 16-ft skiff as tender. As core was removed from the core barrel, it was logged, marked, photographed, and preserved using one of two methods. The photographs of the cores are presented in Exhibit B on file at the Detroit District Office. In the first method, the core was wrapped in sheet plastic, then sealed inside heavy plastic tubing which was taped shut and fused at the ends. The second method involved wrapping the core in plastic food wrap, then in cheesecloth and coating the core and cheesecloth with a thick layer of wax. The preserved core was then placed in appropriately sized boxes lined with sawdust. The core boxes were stored at the jobsite until shipment to WES.

#### Borehole photography

53. Stagg and Zienkiewicz (1968) point out the necessity of

determining the strike, dip, continuity, joint spacing, and coating thickness when planning an excavation in rock or computing the resistance of a rock structure to loading. The shape and location of a potential failure surface will be strongly influenced by the orientation of the rock mass discontinuities and the shearing resistance along them. The rigidity of the rock mass is particularly sensitive to joint continuity and spacing.

54. To assist in determining the features listed above, a WES borehole camera was run in the nine borings through the U. S. piers. Continuous, 360-deg, oriented, color photographs were taken in borings to depths ranging from 1.5 to 51.5 ft. A detailed description of the borehole camera can be found in Trantina and Cluff (1963).

55. Strikes and dips of prominent discontinuities were measured from the borehole camera logs. Indications from surficial geology and core logs showed that many of the discontinuities shown on the camera film were, in fact, bedding features since they possessed westerly directed dips of less than 10 deg. Joint frequency diagrams by borings are given in Plates C1-C5. Symbols are used to represent joint dips greater and less than 10 deg, filled or partially open joints and open joints. Joint frequencies are shown for each 5-ft depth of boring beginning at the concrete bedrock interface. Joint strike rosettes showing all non-bedding joints (>10-deg dip) are presented in Plates C6 and C7.

56. A total of 51 prominent joints were observed on the photographs. Of these, 18 had dips  $\geq 70$  deg. The remaining 33 joints had dips between 10 and 35 deg. Plates C6 and C7 show two prominent joint sets that are perpendicular; one oriented north-south and the other oriented east-west. By aligning the joint strike rosette with the axis of the Regulatory Structure, the north-south joint set is oriented 15 deg northwest of the structure's axis. The other joint set is then oriented 15 deg north of a line running in an upstream-downstream direction.

57. Viewing joints from above water and on the underwater videotapes, the joints are generally continuous in plan view. When viewing the jointing in section, they appear to be of limited extent (rarely

exceeding 3 ft in height). The joints observed in the core logs and the underwater videotapes cut through one or two beds and terminate on a bedding plane. As described under Scouring, the jointing is classified as "moderately fractured" (fracture spacing 1 to 3 ft) to unfractured (fracture spacing >6 ft). The majority of joints have 1 to 3 ft spacing.

58. Sandstone along the joints is often leached white in contrast to the red sandstone. Some incipient joints, where no opening is visible along the joint, were easily detected by the white leached outline made by the joint. Of the 51 prominent joints, 75 percent were classified as tight, 22 percent were open joints (1/32 to 1/8 in.), and 2 were clay filled (1/16 to 1/4 in. thickness).

59. It is not known if leaching along joints occurred in the geologic past or is a continuing process. The relatively small number of open joints beneath the structure as observed in the photographs suggest that if it is a continuing process, then it is a slow process. Open joints are present adjacent to the structure in the bedrock. In order to ascertain if seepage is occurring along joints in the bedrock beneath the dam, a detailed study would have to be performed. A traceable material could be injected into a sealed borehole upstream and then monitored just downstream of the dam. The rather heavy silting observed in the videotapes towards the right abutment (gates 15 and 16) suggests that water was not flowing beneath the structure in this area.

#### Scouring

60. Soundings at the Regulatory Structure were taken most recently in 1978-79 by personnel at the Sault Locks. The results of the soundings are presented in plan view on drawing DC-103-25, dated January 1979, and titled "Compensating Works Condition Survey - 1978"; the drawing is on file at the Area Engineer Office, Sault Locks. Selected elevations along certain sections, concrete thicknesses from boring logs, and underwater videotape pictures were used to study undercutting and bedrock scouring in front of and behind the dam. See Figures 17 and 18 for profiles containing soundings and concrete thickness data.



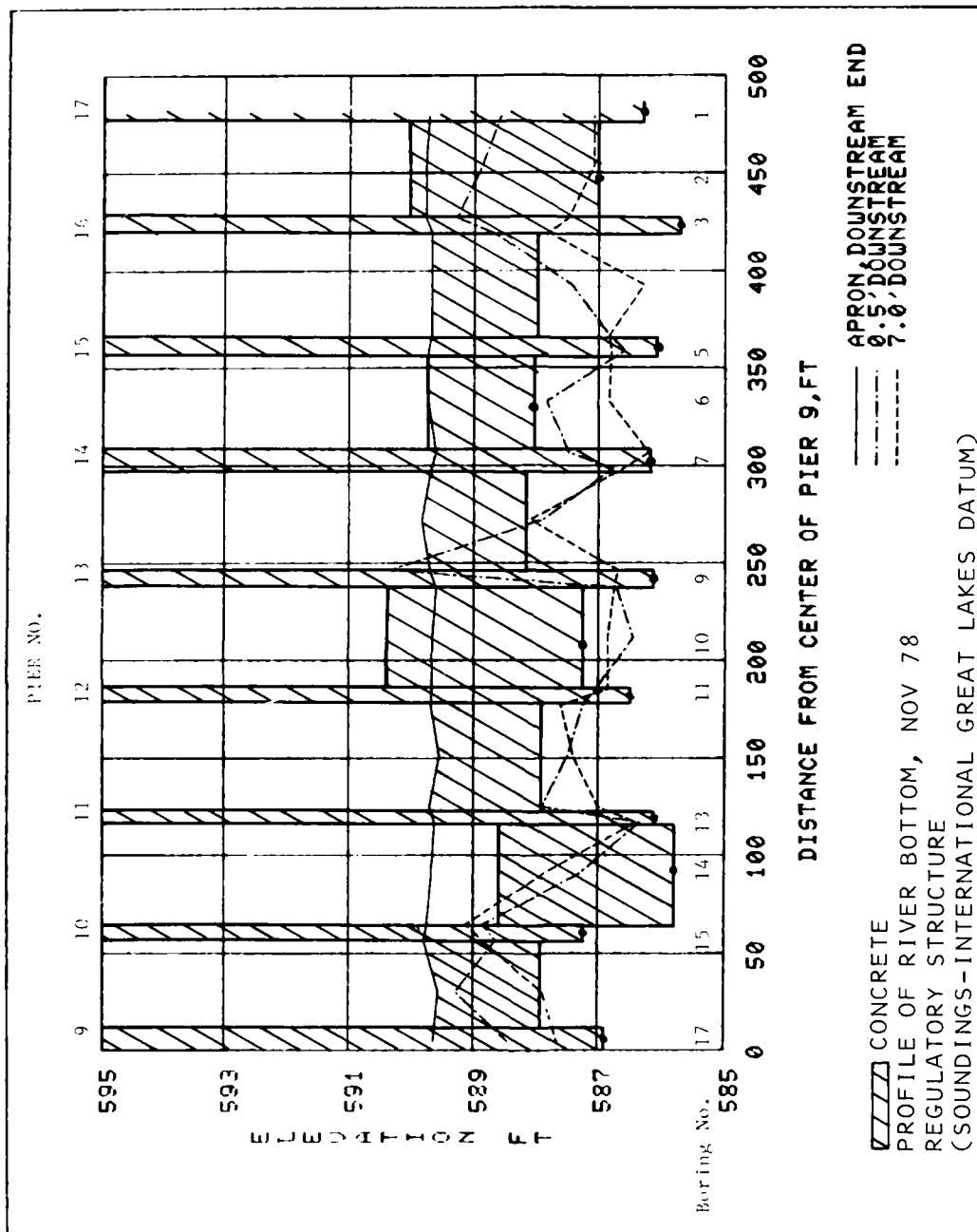


Figure 17. Downstream profile of soundings and concrete thickness data

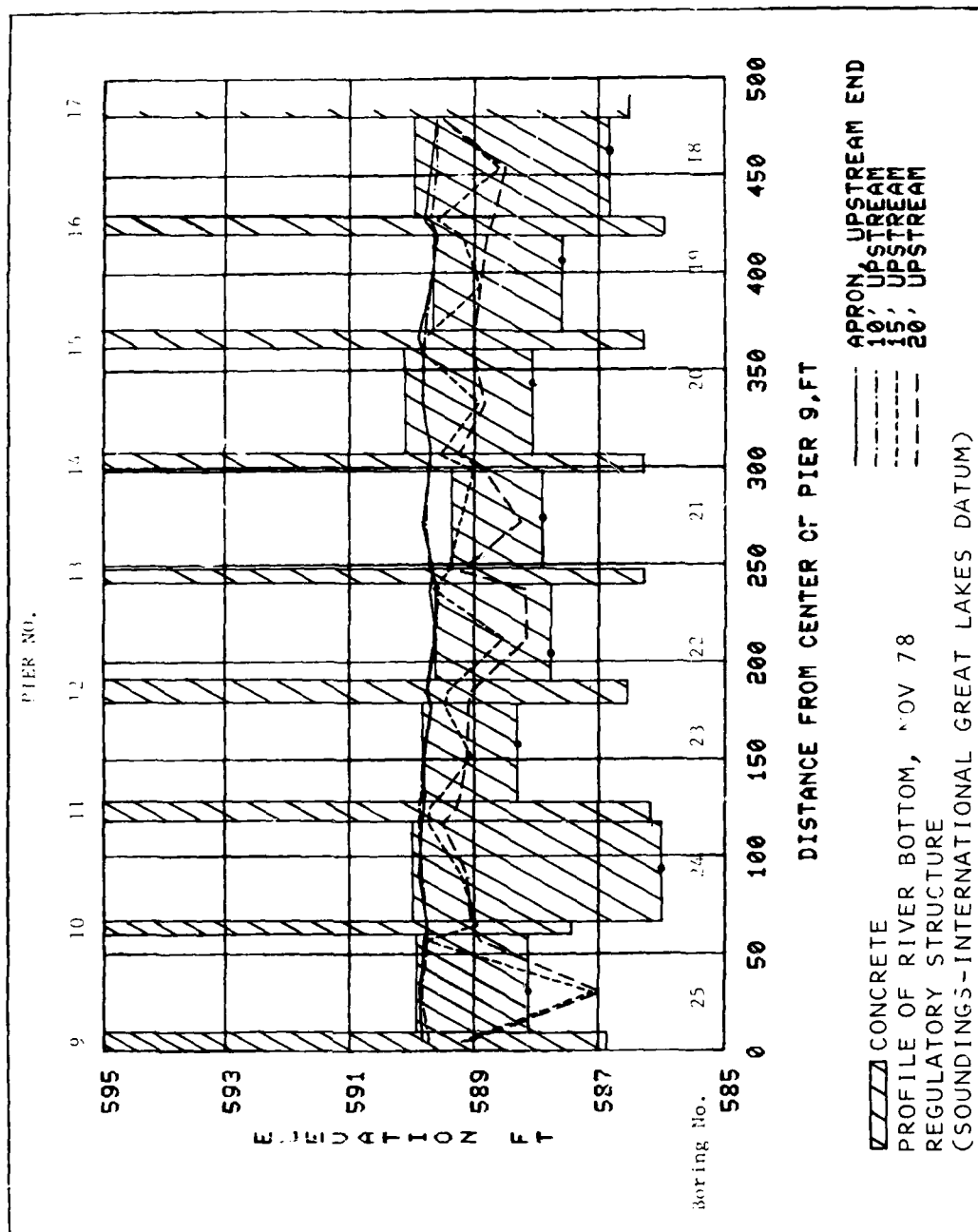


Figure 18. Upstream profile of soundings and concrete thickness data

61. Figure 17 contains three profiles; the solid line indicates top of apron and the dashed lines represent profiles taken at 0.5 and 7.0 ft downstream of the apron end. Figure 18 contains four profiles; the solid line at top of apron and the three dashed lines represent profiles taken 10, 15, and 20 ft upstream of the apron end.

62. Figure 17 indicates that at six locations on the 0.5-ft profile the scouring action of the water has removed rock to a depth below the base of the apron. Apron thickness on the downstream side of the dam varies from an assumed 18 in. (shown on working drawings) to 3.2 ft as revealed in boring CW-10. The 18-in. apron thickness was used for those gate bays where borings were not made. Top and bottom elevations of borings are shown with a dot. Figure 18 indicates only one area where the bedrock appears to have been removed to a depth below the base of the apron at pier 9. Upstream apron thickness was measured on concrete core recovered in each gate bay apron about 6.5 ft upstream from the gates; apron thickness varied from 1.4 to 3.9 ft. In general, the apron thickness was similar at the upstream and downstream ends of individual gate bays. The different apron thickness is probably due to removal of less desirable rock during construction.

63. The following general discussion describes the condition of the underwater concrete and bedrock adjacent to the downstream and upstream apron. The reason a general discussion is presented is that accurate measurements of concrete and bedrock removal were not taken during the underwater survey. A videotape camera was used during the survey.

64. The video from the underwater filming of the Regulatory Structure was of excellent quality. The filming was done in such a logical and orderly manner that the viewer had no trouble with orientation between the location being viewed and the construction drawings. However, the carpenter scale used in the film was too small to be read. The black tape that secured the scale to the support rod could have been uniformly spaced on 1-ft centers to make it readable. However, this was not the case and often on close-up viewing the tape covered the foot marker, making it impossible to read the scale accurately.

65. In general, the concrete in the piers and aprons, upstream and downstream of the gates, appears to be in good condition. Pier 9 has very severe scaling\* of the concrete along a horizontal construction joint for a distance of about 6 ft. The scaling occurs on the downstream south edge of the pier. The concrete surfaces of the piers and aprons show evidences of light to medium scaling.\* A crack in the upstream apron of gate 13 was noted. It traverses the apron from the gate to the upstream edge of the apron, as shown on working drawings. The crack width appeared to be about 0.24 in. A few much smaller cracks were noted in several other apron sections; these cracks are not structurally significant. Repair of the very severe scaled area on pier 9 and the apron crack in gate bay 13 should be made at the next opportunity.

66. Bed thickness of the foundation rock varies from thin beds (beds less than 4 in. thick) to thick beds (beds from 1 to 3 ft thick) (Office, Chief of Engineers 1975). The majority of observed beds were classified as thick. Shale and clay seams could be seen quite easily; however, they did not occur frequently in the 5 ft or so of rock exposed just below the top of the aprons. At several locations the softer seams were partially removed. Bedding surfaces were smooth and flat.

67. The degree of fracturing (jointing) varied from moderately fractured (fracture spacing 1 to 3 ft) to unfractured (fracture spacing >6 ft) (Office, Chief of Engineers 1975). The majority of observed fractures were classified as moderate. Fractures were vertical, linear, and had smooth surfaces. There were at least two joint sets intersecting at about 90 deg. The bedding thickness and frequency of jointing resulted in tabular (flat or bladed) shape rock blocks with dimensions from 1 to 3 ft. In viewing the videotapes, it was evident that the water action

---

\* Light scaling: Loss of surface mortar without exposure of coarse aggregate. Medium scaling: Loss of surface mortar up to 0.20 to 0.39 in. in depth and exposure of coarse aggregate. Very severe scaling: Loss of coarse aggregate particles as well as surface mortar and mortar surrounding aggregate, generally greater than 0.79 in. in depth (American Concrete Institute 1980).

could easily remove the tabular blocks and flip them about.

68. The working drawing showed that the apron and piers were to be founded in bedrock; the underwater pictures indicate that this was done. The apron face was formed as evidenced by its smooth appearance and vertical position. However, most all of the downstream apron face (about 18 in.) is now exposed. Bedrock just beyond the apron has been removed by scouring for a depth of from 2 to 3 ft below top of apron. Local areas appear to be deeper than 3 ft, maybe as deep as 5 ft. The extent of removal downstream is unknown because pictures were taken looking upstream from about 5 ft off the apron. The scouring (removal of tabular blocks) terminates on horizontal bedding surfaces that form a series of ledges (stair-step appearance). There appears to be a common ledge where most of the scouring has terminated at about 3 ft below top of apron. In a few of the sluiceways, portions of the apron face are covered by rock; however, the rock only extends a few feet downstream and then stairsteps downwards. It is conservative to assume that there is no strut resistance downstream of the apron for a depth of 5 ft below top of apron.

69. Two of the eight sluiceway aprons are undercut up to about 6 ft. In some cases, the rock just downstream of the apron and the apron were undercut. It was difficult to ascertain the true extent of undercutting. The conscious of the people viewing the underwater pictures was that the undercutting areas were severe and needed to be filled. One small area (maybe 3 by 3 ft) was sunken in about 1 ft; the area probably had been undercut and then collapsed.

70. The working drawings show the upstream apron terminating 6 ft upstream from its starting point near the gates. The underwater pictures show that at this terminating point, the apron face appears to have been formed; this is seen near pier 9. The pictures reveal that the concrete apron continues upstream for about 14 more ft, ending with a semiround feather-edging. The feather-edge has generally held up well.

71. The upstream vertical apron face is exposed at only one location. The apron face, adjacent to and where it abuts into the north side of pier 9, is exposed. From the point where the apron abuts into

pier 9 and upstream along the pier to the upstream edge of the pier, the base of the pier is exposed. Portions of this section of the pier are undercut to what appears to be several inches. Scouring action has removed the bedrock down to the base of the pier and below the base of the apron. If the apron near pier 9 extended the additional 14 ft, as it was in the other gate bays, then a 14-ft wide strip of concrete apron and bedrock has been removed in order to expose the apron face. Maintenance records show that in 1972 repair of the foundations of piers 6, 7, and 8 was carried out by anchoring steel forms to the foundation, filling the forms with aggregate, and grouting the aggregate in-place. This work was done by the Canadians (Lake Superior Board of Control 1979). The available records do not indicate whether the repairs were done upstream or downstream. The present bedrock conditions near the upstream portion of pier 9 are probably similar to those that existed near piers 6, 7, and 8 in 1972.

72. The apron is undercut at four other locations to at least 6 ft, i.e., the aprons of gates 10, 11, 12, and 13. Little bedrock has been removed upstream of the apron of gates 14, 15, and 16. From gate 14 to gate 9, the bedrock has been scoured to a depth of from several inches to about 3 ft; only a few areas go to depths of 3 ft. The scouring action upstream has formed a series of ledges in the bedrock just like scouring did downstream of the dam. Jointing in the upstream bedrock is similar to that described for the downstream bedrock. There did not appear to be any apron sections where undercutting at the downstream apron was connected to undercutting at the upstream apron or vis-a-vis.

73. In 55 years of scouring, 5 ft of rock has been removed from at least one area, which translates into a removal rate of 1 ft in 11 years. The rate of undercutting of the apron is slightly greater, 1 ft in every 9.2 years. It is recommended that a protective apron be placed upstream and downstream of the existing apron in order to eliminate undercutting of the dam and removal of rock adjacent to the dam. A protective apron of concrete or grouted in-place aggregate should be considered.

## Geology

### Geomorphology

74. The description of geomorphology of the work area is as follows: "The Regulatory Structure is located on the St. Mary's Rapids. The rapids are 1/4 mile wide, 3/4 mile long. From Lake Superior to Sugar Island, St. Mary's River Valley is bounded on the north by the escarpment of a dissected peneplane, the Gros Cap Batholith, with elevations 400 to 600 ft above the valley floor. The south boundary is defined by morainal highlands and terraces of glacial lake sediments. Valley width ranges between 3 miles near St. Mary's Rapids to 9 miles at Waiska Bay near the river head. St. Mary's River occupies most of the valley and has a maximum width of 5 miles at Point Iroquois Shoals - Waiska Bay. The river has a general appearance of several interconnected bays (U. S. Army Engineer District, Detroit 1974)."

### Overburden

75. The overburden in the dike on the southern end of the Regulatory Structure is probably fill from excavations made at the Soo Locks and the Regulatory Structure. Boring CW-35 was drilled through this overburden consisting of boulder, cobble, gravel, and sand sized pieces of the Jacobsville sandstone. The fines were washed away in drilling so that any clay or shale present in the overburden was not detected. Compaction is poor since no water return occurred during drilling until bedrock was reached.

### Effects of glaciation on bedrock

76. As a result of construction and the washing action of the St. Mary's River, all of the glacial overburden had been removed at the Regulatory Structure. No glacial overburden was detected in the borings put down during this investigation. Glacial drift can be found adjacent to the town of St. Sault Marie, Michigan.

77. Due to glacial activity, the loading and unloading of the bedrock probably caused jointing to form in the bedrock. This activity likely modified the stresses in the rock to be something other than due to superincumbent loading.

### Stratigraphy

78. Bedrock at the Regulatory Structure belongs to the Jacobsville Formation of Cambrian Age. The Jacobsville extends from the Keeweenaw Peninsula eastward to Sault Ste. Marie and Sugar Island and from the south shore of Lake Superior south approximately 30 miles. It extends several miles northward beneath Lake Superior from the south shore. Northernmost boundary has not yet been established. The thickness of the Jacobsville is variable because it was deposited on an irregular pre-Cambrian rock surface.

79. The rock at the Regulatory Structure is an arkosic sandstone (containing up to 20 percent feldspar). The sandstone is fine- to medium-grained and cemented together by fine particles of quartz mixed with sericite, illite, and iron oxide. Shale and clay seams are found in the sandstone. The sandstone, clay, and shale are all predominantly red in color with variations ranging from white to purplish-red. Mottling occurs in many areas. Rock at the Regulatory Structure is located geologically slightly upsection from that examined at New Poe Lock (U. S. Army Engineer District, Detroit 1974).

80. Hamblin (1958) divides the Jacobsville into four facies based on grain size and bedding pattern. The rock found at Sault Locks and at the Regulatory Structure probably belong to the red siltstone facies and the lenticular sandstone facies. For classification purposes this report will not use the facies descriptions but instead will adopt a classification system based on engineering geology characteristics as first used by the U. S. Army Engineer District, Detroit (1974) at New Poe Lock. The rock is divided into shaly, hard, and very hard sandstone units.

81. The very hard sandstone unit is fine- to medium-grained; well-cemented; sometimes cross bedded; mottled or banded; colored purple, pink, or occasionally deep red; with varicolored reduction spots. Units range in the borings from <1 ft to 5 ft in thickness. Thin shale and clay seams are found in this unit and occur most predictably at the upper and lower contacts of all three rock units. The shale and clay are often thinly bedded.



82. The hard sandstone unit is fine- to medium-grained, plane bedded, well-compacted, and colored red with gray reduction spots. Thickness ranges from 3 ft to 13 ft in the three units found in the borings. The contacts of this unit grade almost imperceptibly horizontally and vertically into very hard sandstone or shaly sandstone (U. S. Army Engineer District, Detroit 1974). Thin beds of very hard and shaly sandstone are interbedding in the hard sandstone unit, making classification quite difficult. Thin shale and clay seams are present in the hard sandstone unit.

83. The shaly sandstone unit is fine-grained, colored light to dark red with gray reduction spots, and contains shaly bedding. The unit is then bedded with inner beds of hard sandstone. Thickness of the unit ranges from 2.75 ft to 4.5 ft in the two units exposed in the borings. Thin shale and clay seams occur in the shaly sandstone unit.

84. Ripple marks were observed on some of the shaly bedding. The shaly sandstone was observed at the project site as a fill material and as protection along the south dam abutment. Hand samples show the shaly seams are badly weathered, and the rock appears to have undergone rapid deterioration after exposure to freezing and thawing. Underwater videotape pictures taken at the Regulatory Structure reveal areas where the concrete apron is undercut due to scouring. It is probably the shaly sandstone that has been scoured.

85. The shaly sandstone would be the least desirable of the three rock units as a foundation material.

86. Classification of the sandstone into the three separate units was done primarily on the basis of hardness. Interbeds less than 1 ft in thickness were not distinguished in the cross sections, although strength tests were performed on several samples taken from these interbeds.

87. The samples of clay from borings CW-1, 6, 11, and 31 were analyzed by X-ray diffraction. Composition of the clay is: illite, chlorite, mixed-layer clay, K-spar, and quartz. The mixed-layer clay is composed in part of smectite, a swelling clay of the montmorillonite group. The amount of swelling in the clay should be tested in following

reports. No swelling clays were found in the clay examined at New Poe Lock (U. S. Army Engineer District, Detroit 1974).

#### Geologic cross sections

88. Seven cross sections were drawn from the 30 borings. Cross-section A-A' (Plate D1) was constructed from the borings drilled 6 ft upstream of the gate centerline. Section B-B' (Plate D2) was constructed from borings drilled 80 ft upstream from the gate centerline. Section C-C' (Plate D3) was constructed from borings drilled 62 ft downstream of the piers. Section D-D' (Plates D4) was constructed from borings drilled through concrete piers and apron near the downstream end of the piers. Sections E-E' (Plate D5), F-F' (Plate D6), and G-G' (Plate D7) were constructed perpendicular to the Regulatory Structure using borings found in the other cross sections. Plate D8 contains characterization and engineering design properties cross-referenced to the geologic cross sections.

89. The designation for clay is CL; shale is SH. SH/CL designates a shaly clay, clayey shale, or finely interlayered clay and shale seams. The clay and shale at times grade imperceptibly into one another. Shale stringers are noted in the cross sections. These are discontinuous lenses of shale which occur parallel to bedding in the sandstone.

#### Structure

90. Dip of the beds beneath the Regulatory Structure is approximately 3 ft per 100 ft to the west. Minor variations exist due to the presence of cross bedding and fluvial troughs.

91. Bedding is continuous over the length of the Regulatory Structure. Individual shale and clay seams are believed continuous over the installation, although only a small number are actually shown connected on the cross sections. The U. S. Army Engineer District, Detroit (1974) was able to examine exposed rock face in the excavation of New Poe Lock in 1964-1967 for distances of about 2000 ft. They showed all clay and shale seams as small as 0.01 ft to be continuous over the excavation. Not all clay and shale seams may have been detected, especially those <0.01 ft which may exist only as a thin film on the bedding plane, making logging difficult.

92. High-angle fractures are considered to occur along cross bedding or current bedding (well-defined channel structure), especially in boring CW-19. Information from the core about jointing was included under Borehole Photography.

93. Shale breccia and conglomerates were found in three cores. Shear fractures of limited extent were present in five cores. All shear fractures were either horizontal or low angle. One was clay filled; two were shale filled. Three of the shear fractures occurred in the same unit--the topmost hard sandstone unit. The other two shear fractures occurred in the same position--at the contact between the second shaly sandstone unit and the second hard sandstone unit.

94. A 0.3- to 0.6-ft core loss occurred in the same sandstone unit in three more or less adjacent borings: CW-21, 22, 19 (see Plate D1, Sheets 2 and 3). Boring CW-31 exhibited the largest variety and concentration of weak zones of all cores taken. CW-31 was drilled 62 ft downstream from the downstream end of pier 14. It contained four sets of joints in various sandstone units, all clay-coated. It contained seven zones of highly fractured rock totaling 2.3 ft in length. It contained a proportionately larger number of clay and shale seams than the other cores.

95. Fractured rock was found in a number of cores in thin bands less than 0.2 ft. An exception is found in boring CW-17 which contains 1.35 ft of highly fractured rock at the base of the concrete in pier 9.

96. Possible weak zones in the foundation rock are the soft clay and shale seams within a few feet of the bottom of the apron and gate piers. These seams are continuous under the piers. Scouring has removed bedrock from behind the dam several feet deeper than the base elevation of the piers. The weak seams are thus exposed, which suggests major foundation problems in terms of sliding. With similar bedrock conditions existing upstream, the piers are considered to be resting on a pedestal that is underlaid with clay and shale. The apron and possibly the piers are undercut in a number of places up to a depth of 6 ft; the undercutting adds to the problem.

97. Solution activity along joints has occurred and has probably

contributed to the bedrock scouring. The solution activity has discolored the rock adjacent to the joints; a white band on either side of the joint results. Where clay is present in the joints, the solution activity would remove the clay leaving a gap. Where these gaps exist, scouring can occur more readily. It is not known whether or not solution channels have thus been created and exist beneath the dam. There was no evidence of water passing through any of the joints during the underwater inspection with the video-type camera. At the present time solution activity is considered not to be a problem. If protection against scouring is carried out by placing material upstream and downstream of the dam, joints adjacent to the aprons could be pressure grouted as an added protection against further solution activity.

## PART IV: LABORATORY TEST AND ANALYSIS

### Test Specimens and Test Procedures

#### Cores received

98. Concrete and rock core from 30 borings were received at WES. Shipment of the core was by commercial motor freight. The cores were received in good condition. Pertinent information concerning the cores are presented in Table E1.

#### Selection of test specimens

99. A detailed visual examination of cores was made in the laboratory to supplement the field boring logs and to assist in the selection of representative test specimens. Concrete specimens were selected for testing based upon physical condition of the concrete and depth in order to obtain representative properties throughout the structure.

100. Concrete specimens were selected from five borings in the upstream apron, eight borings in the piers, and four borings in the downstream apron. Two specimens from borings in the aprons were tested where core length permitted. Test specimens from the deep borings in the piers were selected from the top, middle, and bottom of the core. Test specimen depths shown in the tables of test results represent the midsection of the test specimen; i.e., el 608.75 ft is the midpoint of a piece of core with top el being 609.08 ft and the bottom el being 608.42 ft. Four-inch-diameter by nominally eight-inch-long concrete and rock cores were used for testing, the exception being the specimens for direct shear testing. The direct shear specimens were 4 in. diam by nominal 4 in. long.

101. An attempt was made to select test specimens to be representative of the rock units (very hard, hard, and shaly sandstone) in close proximity to the base of the structure. Soft clay and shale seams were obtained for testing as seams within the host rock and as individual (intact) test specimens where they were large enough to be tested separately from the host rock. Specimens with natural joints were selected for testing after viewing the surface condition of the jointed surfaces.

The test assignment locations can be obtained from appropriate tables of test results. Locations of the core tested in direct shear are also presented in the geologic cross sections (Plates D1-D16) as series numbers adjacent to boring profiles.

102. Test specimens were selected for testing concurrent with the detailed logging of core; the logging began the day core arrived at the laboratory. The test specimens were rewrapped and stored in a moist curing room until time for testing; the moist room is maintained at  $73.4 \pm 3^\circ\text{F}$  ( $23 \pm 1.7^\circ\text{C}$ ).

Laboratory testing program

103. Concrete cores. The laboratory testing program of the concrete cores consisted of the following tests on representative selected cores.

- a. Density,  $\gamma$ .
- b. Compression Wave Velocity,  $V_p$ .
- c. Compressive Strength.
- d. Tensile Splitting Strength,  $T_s$ .
- e. Elastic Moduli,  $E$ .
- f. Poisson's Ratio,  $\nu$ .

104. Rock cores. The laboratory testing of the bedrock cores consisted of the following tests on representative selected cores. The tests are grouped under either characterization tests or engineering design tests. Photographs of cores after they were tested were taken.

- a. Characterization tests.
  - (1) Wet and Dry Unit Weight,  $\gamma_m$  and  $\gamma_d$ .
  - (2) Water Content,  $w$ .
  - (3) Compressive Strength,  $q_u$ .
  - (4) Direct Tensile Strength,  $T_D$ .
- b. Engineering design tests.
  - (1) Elastic Moduli,  $E$ .
  - (2) Poisson's Ratio,  $\nu$ .
  - (3) Triaxial Strength.
  - (4) Direct Shear Strength.
    - (a) Concrete to rock, bond strength (maximum).

- (b) Concrete on rock, precut (residual).
- (c) Intact (maximum and residual).
- (d) Precut (residual).
- (e) Clay and shale seams (maximum and residual).
- (f) Natural joint (maximum and residual).
- (g) Cross bed (maximum).

105. Testing of the granular dike material was to be done; however, no samples from the one boring in the dike were taken. The dike material consisted of boulder, cobble, gravel and sand-size pieces of sandstone.

#### Test procedures

106. The characterization properties tests and the engineering design properties tests were conducted in accordance with the appropriate test method tabulated below:

<u>Property</u>	<u>Test Method</u>
<u>Characterization</u>	
Wet Unit Weight (As Received), $\gamma_m$	RTM 109-77*
Dry Unit Weight, $\gamma_d$	RTM 109-77
Water Content, $w$	RTM 106-77
Compressional Wave Velocity, $V_p$	RTM 110-77 (ASTM D 2845)
Compressive Strength, $q_u$	RTM 111-77 (ASTM D 2938)
Direct Tensile, $T_D$	RTM 112-77
Tensile Splitting Strength, $T_s$	CRD-C 77-72 (WES 1949)
<u>Engineering Design</u>	
Elastic Modulus, $E$	RTM 201-77 (ASTM D 2148)
Direct Shear Strength	RTM 203-77
Poisson's Ratio, $\nu$	RTM 201-77
Triaxial Strength	RTM 202-77

---

\* Proposed Rock Test Method, Corps of Engineers, in review prior to publication.

107. For the compression and triaxial compression tests, the specimens were cut with a diamond-blade saw and the cut surfaces were ground flat to 0.001 in.; specimens were checked for parallel ends and the perpendicularity of ends to the axis of the specimen. Electrical resistance

strain-gages were used for strain measurements. Two each were used in the axial and horizontal directions. The modulus of elasticity and Poisson's ratio were computed from the strain measurements. Axial specimen load was applied with a 440,000-lbf capacity universal testing machine. Confining pressure during the triaxial tests was applied using an electro-hydraulic pump.

108. The concrete-to-rock specimens (for bond strength) were fabricated using a general mass concrete mixture having an approximate compressive strength of 2000 psi at 28-days age. The concrete was wet sieved over a 1-in. sieve, and the portion passing was cast on top of rock cores contained in the bottom section of a 4-in.-diam mold. Rock surfaces onto which the concrete was cast were smooth and horizontal. Rock cores used for these tests were taken from within 2 ft of the base elevation of the dam.

#### Core Test Results and Discussion

##### General comments for concrete

109. The following general comments pertain to the condition of the concrete over the U. S. half of the Regulatory Structure. These comments are the result of examination of the cores recovered from the works (Table E1). Individual structural elements, aprons, and piers within the works will be discussed separately. The results of the concrete characterization and engineering design tests are presented in Table E2. Stress-strain relations for concrete cores are presented in Plates E1-E8. These data will be referred to as appropriate.

110. New concrete was recovered only in boring CW-9, which was drilled in pier 13; two areas of new concrete were seen. The newer concrete (0.5 ft thick) contained red sandstone river-run aggregate, which differs from the older concrete that contains igneous aggregates. Below the 0.5-ft thick newer concrete was a new appearing concrete that extended to 2.4 ft; it contained the igneous aggregates found in the old concrete. The post construction concrete (0 to 2.4 ft) is the result of resurfacing efforts. An inspection of the exterior of the pier



reveals that the top section of the pier has been resurfaced as well as a section from about 5 ft above the low pool to low pool. It appears that two repairs to the top of the pier have been made.

111. The older concrete was nonair-entrained. It varies in color from tan to gray with a predominantly tan matrix. It is hard, dense, has occasional tiny voids, and contains igneous and metamorphic, angular, coarse and fine aggregates. The coarse aggregate size ranges from 1/2 to 2 in. Basalt, granite, quartzite, syenite, rhyolite, diorite, and andesite are the common rocks found in the concrete. The concrete was well consolidated as evidenced by its dense nature and absence of honeycombing and other voids. It is structurally sound and should serve its intended purpose.

112. Minor frost damage, as evidenced by subparallel cracks, was detected in only three of the nine borings drilled into the piers. The damage is caused by freezing and thawing. The deteriorated concrete was found in the top portions of two of the three borings extending to a minimum depth of 0.8 ft. The third boring contained frost damage in a 5-ft zone beginning about 10 ft from the top of the pier. The concrete recovered in the apron borings, those started below water, were not damaged by freezing and thawing.

113. A total of 21 borings were drilled through concrete and into bedrock. In 57 percent of these borings the contact between concrete and rock was well bonded. The contact was loose in the remaining 43 percent of the borings. It is suspected that the majority of the loose contacts were caused as the core was removed from the core barrel.

#### Upstream apron

114. Concrete deterioration. One contact, boring 18 (upstream apron), was described as weathered, open, and with loose sand grains. A second contact, boring 20, was described as tight but had weathered vesicles in the concrete adjacent to the bedrock. Figure 18 does not indicate the apron as being undercut near these two borings. Water passing along vertical or near vertical joints in the bedrock could have caused the weathered condition; if so, this is the first observed occurrence of such weathering. Cracking in the upstream apron is

considered minor. The surface of apron shows evidences of light to medium scaling, which would be expected for concrete subjected to the abrasive action of running water for 50 some years. A large amount of concrete is suspected of having been removed from the apron adjacent to pier 9; see Scouring for explanation.

115. Average physical properties. The average physical properties of the concrete core from the upstream apron are listed below:

<u>Test</u>	<u>Avg Value</u>
Wet unit weight, pcf	158.8
Comp wave velocity, fps	15,290
Compressive strength, psi	7,250
Tensile strength, psi	490
Modulus of elasticity, $\times 10^6$ psi	5.89
Poisson's ratio	0.19

The physical properties are characteristic of good quality concrete. The standard deviations,  $s$ , for the unit weights ( $\pm 2.5$ ), velocity ( $\pm 719$ ), modulus ( $\pm 0.99$ ), and the Poisson's ratio ( $\pm 0.02$ ) are considered small and therefore indicate uniformity. The compressive strengths for the four cores recovered from the upstream apron had a standard deviation of  $\pm 2300$  psi. The highest strength was 11,220 psi, while the lowest was 5440 psi. The lowest strength indicates sound strong concrete.

#### Piers

116. Concrete deterioration. Only three of the nine borings in the piers showed evidences of freezing and thawing action. Characteristic subparallel cracking of the concrete to the face surface was observed. The core from borings CW-1 (pier 17) and CW-3 (pier 16) has frost damage to depths of 0.1 and 0.2 ft, respectively. Core from boring CW-7 (pier 13) has damaged concrete in a small zone near the top of the pier, 0.5 to 0.8 ft, and in a zone from 10.5 to 15.8 ft. The damaged top zone is the result of freezing and thawing action. The damaged zone from 0.5 to 0.8 ft probably occurred prior to the second repair; all of the bad concrete was not removed, and a portion was covered up with the newer concrete. The 5.3-ft zone beginning and terminating at elevations 599.3 and 594.0 ft is described as weathered, containing horizontal and vertical hairline fractures and white reaction products.

117. The core appears sound despite the hairline fractures. A petrographic examination revealed that the white reaction product is the result of alkali-silica reaction. The reaction products appear to be local, as they were not detected in any of the other concrete cores. A weathered zone like this one was not seen in the other borings. It is likely that the concrete in pier 13 has been damaged slightly due to the effects of freezing and thawing. Water has found its way into the pier along cracks, like the vertical crack toward the downstream end of the pier, and upon freezing and thawing, has caused the hairline fractures and alkali-silica reaction. The ultrasonic velocities taken in pier 13 are about 9 percent lower than the velocities obtained from the remaining eight piers on the U. S. side of the Regulatory Structure. This fact further indicates the internal damage of the concrete due to freezing and thawing.

118. If the internal concrete continues to get free water, the zone of deterioration will grow. If the water is not allowed to enter the concrete, then the damage due to freezing and thawing and alkali-silica reaction will be significantly reduced. At the present time the pier is considered structurally sound, considering the available field and laboratory test results.

119. At a depth of 19 ft (el 590.7 ft) an open horizontal crack exists that is partially coated with red silt clay. The surfaces were described as being water worn on the field drilling log (see Exhibit A). A closer look in the laboratory at the crack revealed that a clay ball had been entrapped in the concrete during construction, and the boring happened to pass through it.

120. Average physical properties. The average physical properties of the concrete core from the piers are listed below. The properties from the concrete cores from pier 13 were averaged with the properties from the cores of the other piers.

<u>Test</u>	<u>Near Surface Concrete</u>	<u>Middle of Core Concrete</u>	<u>Bottom of Core Concrete</u>	<u>Percentage Difference</u>
Wet unit weight, pcf	158.3 (±2.6)*	159.0 (±3.1)	161.0 (±1.6)	-1.7
Comp wave velocity, fps	15,650 (±895)	15,693 (±738)	15,597 (±661)	0.6
Compressive strength, psi	7,140 (±1313)	7,490 (±920)	7,640 (±2043)	-6.5
Tensile strength, psi	490 (±79)	--	--	
Modulus of elasticity, × 10 <sup>6</sup> psi	6.21 (±0.95)	5.97 (±1.05)	6.52 (±1.76)	-8.4
Poisson's Ratio	0.21 (±0.04)	0.19 (±0.03)	0.21 (±0.03)	-10.0

---

\* Standard deviation given in parentheses.

The percentage difference was calculated using the bottom of core concrete value as the base number; the highest or lowest value of the near surface (closest to top of pier) and middle of core value was used to get the greatest percentage difference. The percentage difference indicates that there is no real significant difference between the near surface, middle, and bottom concretes. Concrete core test samples from the piers were taken about 10 ft apart.

121. The physical properties of the concrete from the piers are characteristic of good quality concrete; it is similar in quality to the concrete in the upstream apron. The standard deviations for the pier cores are considered small and indicative of uniform concrete. The lowest compressive strength from the pier cores is 5180 psi, which indicates sound concrete.

#### Downstream apron

122. Concrete deterioration. There was no evidence of damage in the concrete core recovered from the four borings put through the downstream apron.

123. Average physical properties. The average physical properties of the concrete recovered as cores from the downstream apron are listed below.

<u>Test</u>	<u>Avg Value</u>
Wet unit weight, pcf	158.3
Comp wave velocity, fps	15,230
Compressive strength, psi	8,620
Modulus of elasticity, $\times 10^6$ psi	6.35
Poisson's ratio	0.20

124. The physical properties of the core from the downstream apron are quite similar to the properties of the core from the piers and the upstream apron. Again, the physical properties of the downstream apron concrete are indicative of good quality concrete. The concrete is uniform, as indicated by the small standard deviation for the unit weight ( $\pm 3.1$ ), velocity ( $\pm 983$ ), modulus ( $\pm 1.90$ ), and Poisson's ratio ( $\pm 0.05$ ). The standard deviation of the compressive strength is  $\pm 2750$ . The relatively large deviation indicates a wide scatter in the strength data. The lowest strength is 6,530 psi, while the highest strength is 12,650 psi.

125. In summary, the concrete core recovered from the Regulatory Structure shows that the concrete in the aprons and piers is structurally sound, hard, dense, and durable. It contains a minor quantity of frost damage that is localized in a few areas. The concrete should continue to give excellent service even in the severe winter environment in which it has survived for over 50 plus years. The fact that the concrete is nonair-entrained and has survived in severe weather is further testimony to its excellent quality.

#### Characterization properties of foundation rock

126. The results of the characterization properties tests are presented in Tables E3, E4, and E5 for the very hard sandstone, the hard sandstone, and the shaly sandstone, respectively. Stress-strain curves for the three rocks are presented in Plates E9-E18. Photographs of cores after they were tested for compressive, tensile, and triaxial strength are presented in Plates E19-E22, E23-E24, and E25-E26, respectively.

127. The following tabulation is a summary of the average characterization properties for the three rocks:

<u>Property</u>	<u>Very Hard Sandstone</u>	<u>Hard Sandstone</u>	<u>Shaly Sandstone</u>
Wet unit weight, pcf	156.3	156.8	157.0
s*	1.9	2.5	1.7
n	38	33	24
Dry unit weight, pcf	152.9	151.6	151.9
s	2.1	2.8	3.8
n	37	28	24
Water content, pcf	2.5	3.4	3.4
s	0.7	0.8	0.9
n	37	28	24
Compressive strength, psi	14,730	8,830	7,580
s	3,170	770	1,030
n	8	7	10
Tensile strength, psi	50	65	32
s	21	--	27
n	2	1	3

\* Standard deviation (s), number of tests (n).

128. The average wet unit weights of the three rocks are very nearly the same. The relatively low standard deviation indicates consistency within the three types of rocks and denotes a small amount of dispersion in the wet unit weights. The dry unit weights were calculated using the wet unit weights and water contents. The water contents are consistent within each of the three rock units, as indicated by the standard deviation.

129. A large difference in compressive strength exists between the very hard sandstone and the hard and shaly sandstones. The very hard sandstone is 1.67 times and 1.94 times stronger than the hard and shaly sandstone, respectively. The hard sandstone is about 1.2 times as strong as the shaly. All the compressive strength data for the sandstone indicate that the foundation rock is not critical in terms of bearing capacity. The standard deviations of the hard and shaly sandstone indicate a small degree of disparity within the samples tested. The stress-strain curves (see Plates E9-E11) for the very hard sandstone are typical for a strong sandstone; i.e., the curve is initially plastic (in this case

slightly concave upwards) and followed by a definite linear portion. The hard and shaly sandstones have the same plastic-elastic behavior; however, as seen in Plates E12-E18, the curves have a pronounced concave upward portion. The three rocks do not yield significantly and were observed to have a brittle-type failure. Moduli and Poisson's ratios were calculated from the stress-strain curves; the modulus is a tangent value calculated at one-half the compressive strength.

130. A limited number of direct tensile strengths were obtained. The standard deviation shows a fair amount of scatter for the few specimens tested. The shaly sandstone had the lowest strengths, as was expected due to the inherent weak planes of shale. The difference in tensile strength for the very hard and hard sandstone is small. These strengths are lower than what were expected, considering the high compressive strengths. The general rule is that the tensile strengths of rocks are between 10 and 20 percent of the compressive strength. For all three rocks, the tensile strength is less than 1 percent of the compressive strength. The moisture content and the bedding planes of the sandstone contributed to the low tensile strengths.

131. The unit weights, water contents, and strengths of some of the rock cores reported in this report are similar to the test results reported in U. S. Army Engineer Division, Ohio River (1975, 1976). The rock identified in U. S. Army Engineer Division, Ohio River (1975) is just above the section of rock tested during this investigation. It all belongs to the Jacobsville Formation and was expected to have similar characterization properties.

Engineering design  
properties of foundation rock

132. The individual moduli and Poisson's ratio computed from the stress-strain curves obtained from the very hard, hard, and shaly sandstone are presented in Tables E3, E4, and E5. Presented in the following tabulation are the average values of moduli and Poisson's ratio for the three rocks.

<u>Property</u>	<u>Very Hard Sandstone</u>	<u>Hard Sandstone</u>	<u>Shaly Sandstone</u>
Modulus of elasticity, $\times 10^6$ psi	5.31	2.33	1.70
s*	1.31	0.51	0.3
n	8	7	11
Poisson's ratio	0.20	0.32	0.37
s	0.03	0.05	0.08
n	8	7	11

\* Standard deviation (s), number of tests (n).

The difference in modulus and Poisson's ratio between the three sandstones is reasonable. The shaly sandstone was expected to undergo greater deformation under load than the other two rocks. The shaly sandstone was weaker and contained shale laminae that would be expected to consolidate somewhat under load.

#### Maximum and residual shear stress criteria

133. The following discussion of shear stress criteria is taken from Zeigler (1972) and is followed in this report.

134. Designers are commonly interested in the maximum available shear strength. The maximum shear stress points are identified as  $\tau_{\max}$  in Figure 19. The maximum shear stress usually corresponds to the peak of the shear stress versus displacement plot (curve a of Figure 19); however, some confusion may arise where strain-hardening is encountered. When strain-hardening occurs, an initial peak usually occurs at a relatively small displacement, followed by an increase in shear stress to a value greater than the initial peak. When this happens, the first peak is termed the maximum shear stress corresponding to initial failure and the latter is the ultimate shear stress.

135. If the residual shear strength is to be determined, then displacement is continued until the shear stress approaches the horizontal asymptotic value of residual shear stress  $\tau_R$  (curve a of Figure 19). When the zone tested exhibits only a residual shear strength, curve b of Figure 19 may be obtained. In such cases, the maximum shear stress attained is the residual shear strength. By testing a number of



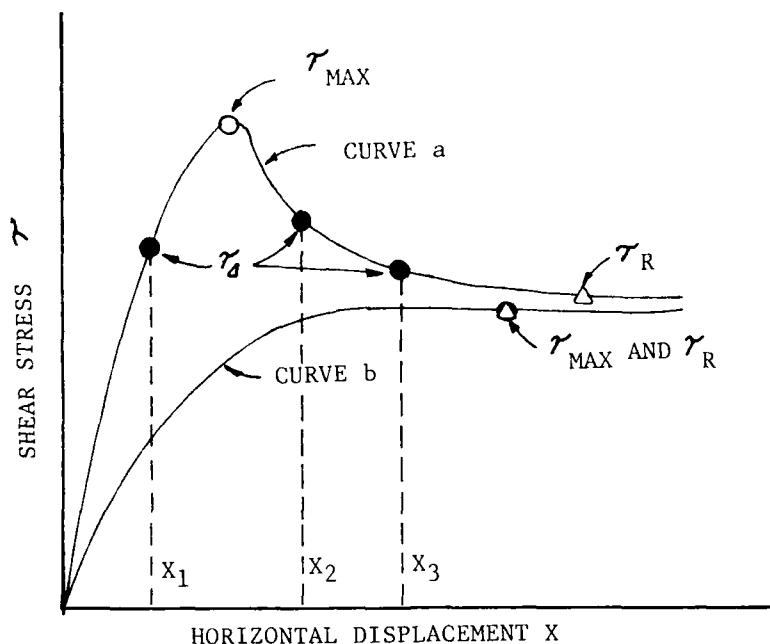


Figure 19. Maximum and residual shear stress, and displacement failure criteria (after Ziegler 1972)

specimens, each at a different normal load, the maximum and residual strength failure envelopes are developed by plotting maximum and residual shear stresses versus corresponding normal stresses.

#### Maximum and residual shear strengths

136. Two types of direct shear tests were conducted to ascertain maximum strength of intact specimens and sliding friction characteristics of discontinuous specimens. Maximum strengths were measured for intact sandstones, sandstones containing concrete to rock interfaces, soft clays and shales; residual strengths were obtained where available. Sliding friction properties were measured for specimens along either precut surfaces, clay and shale seams, or naturally occurring joints. The direct shear test results are presented on laboratory report sheets, Plates E27-E32, E33-E38, and E39-E43, for the very hard, hard, and shaly sandstones, respectively. The shear stress versus shear deformation and normal deformation versus shear deformation curves from the direct shear tests

are presented in Plates E44-E60, E61-E71, and E72-E84 for the very hard, hard, and shaly sandstone, respectively. Maximum and residual strength failure envelopes for the individual test series (intact, precut, etc.) are illustrated in Plates E85-E90, E91-E95, and E96-E100 for the very hard, hard, and shaly sandstone.

137. Typical photographs of specimens after having been tested in direct shear are presented in Plates E101-E103. It will be noted in these photographs that most of the sheared surfaces were along bedding planes that are relatively smooth. The bedding planes observed in the rock core were quite smooth. The photograph of the natural jointed core is likewise smooth, as were most all the other natural joints observed in the core.

138. The direct shear tests were performed in two shear devices. A single plane shear device, designated MRD, was used for the 4-in.-diameter cores; most tests were run in this device. A few clay seams, large enough to be removed from the host rock, were tested in the 1- by 3- by 3-in. soils direct shear device. Normal loads were selected to cover anticipated normal loads at the structure.

139. The majority of direct shear tests were conducted using three different specimens and three different normal loads, one normal load per specimen. Four tests were run differently to check on the residual strength of intact specimens, clay seams, and shale seams. Four to five specimens were used per test with each specimen having a different normal load applied. A specimen was consolidated with a normal load, sheared, and a peak load determined. The shear and normal loads were removed, the specimen repositioned, the same normal load reapplied and sheared again. This sequence was continued with the same specimen until a residual strength was obtained. Another specimen was likewise tested at a greater normal load, and so forth. The peak and residual shear stress values from the four or five specimens were used to construct maximum and residual strength failure envelopes; thus, maximum and residual  $\phi$  angles were determined. The residual  $\phi$  from the intact very hard sandstone,  $\phi_r = 29.9^\circ$ , compared quite well with a similar value from the precut very hard sandstone,  $\phi_r = 32.9^\circ$ . The lowest

residual value obtained during the testing program was obtained using this technique.

140. The plots for each direct shear test, intact, precut, etc., for the three rock types (see Plates E85-E100) show very little scatter of the shear stress values. Failure envelopes were fitted through the data points using a linear regression fit. For a few plots, the envelopes were shifted to have a zero cohesion.

141. A summary plot of all the failure envelopes for the very hard, hard, and shaly sandstone is presented in Figures 20, 21, and 22. The bedrock feature having the lowest residual strength is the shale seam (1 in. thick) found in the shaly sandstone; the residual shear strength is  $\phi_r = 21^\circ$  and  $c = 0$ . The same shale seam has a maximum shear strength  $\phi = 31.4^\circ$  and  $c = 1.4$  tsf; see Figure 22. It will be noted in Figure 22 that the thicker shale seam (seams were removed from the host rock and tested as intact specimens) has higher shearing resistance than the thinner shale seams. An explanation may be that the thicker seam more fully developed its resistance to shearing by uniformly distributing the shear load throughout a homogenous material (all shale). In contrast, the thinner shale seam within the host rock developed an uneven stress distribution due to the two discontinuities adjacent to the seam. Uneven stress concentrations resulted, and the full shear strength of the shale was not reached.

142. A small number of core samples had slickensides along horizontal bedding, which is evidence of previous movement along the bedding planes. The residual shear strengths for the thin (1 in. thick) shale seams would be a conservative value to consider for sliding stability analysis.

143. The shear stress-shear deformation curves were generally characteristic of the two curves presented in Figure 19. It will be noted that on the majority of the shear stress-shear deformation plots, the curves look as if the specimens underwent strain hardening. Between 0.1- and 0.2-in. deformation, the curves turn sharply upwards. Some strain hardening probably has occurred for some of the specimens. However, it is believed that the rather sharp increase in shear stress is

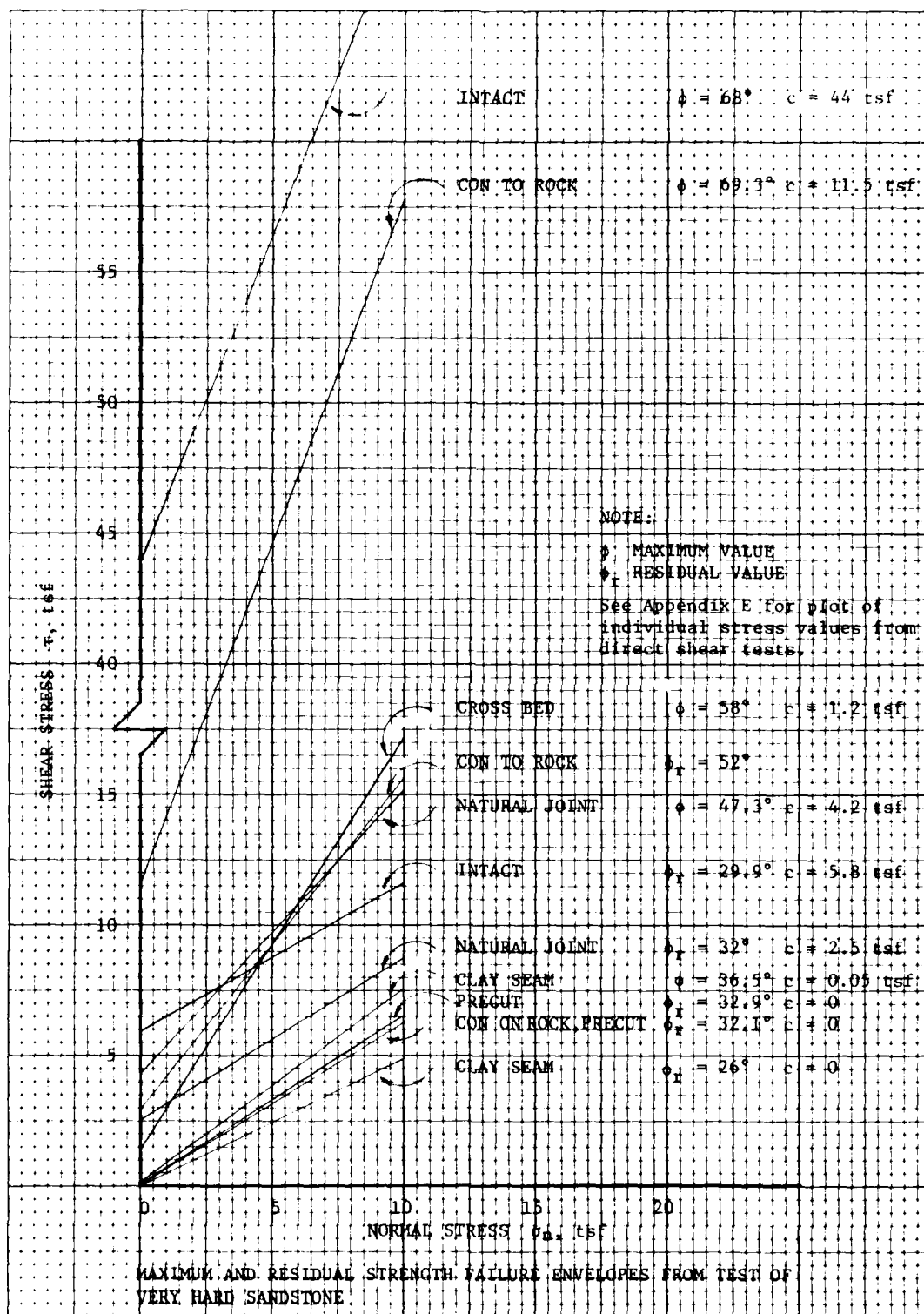


Figure 20. Summary of plot of very hard sandstone failure envelopes

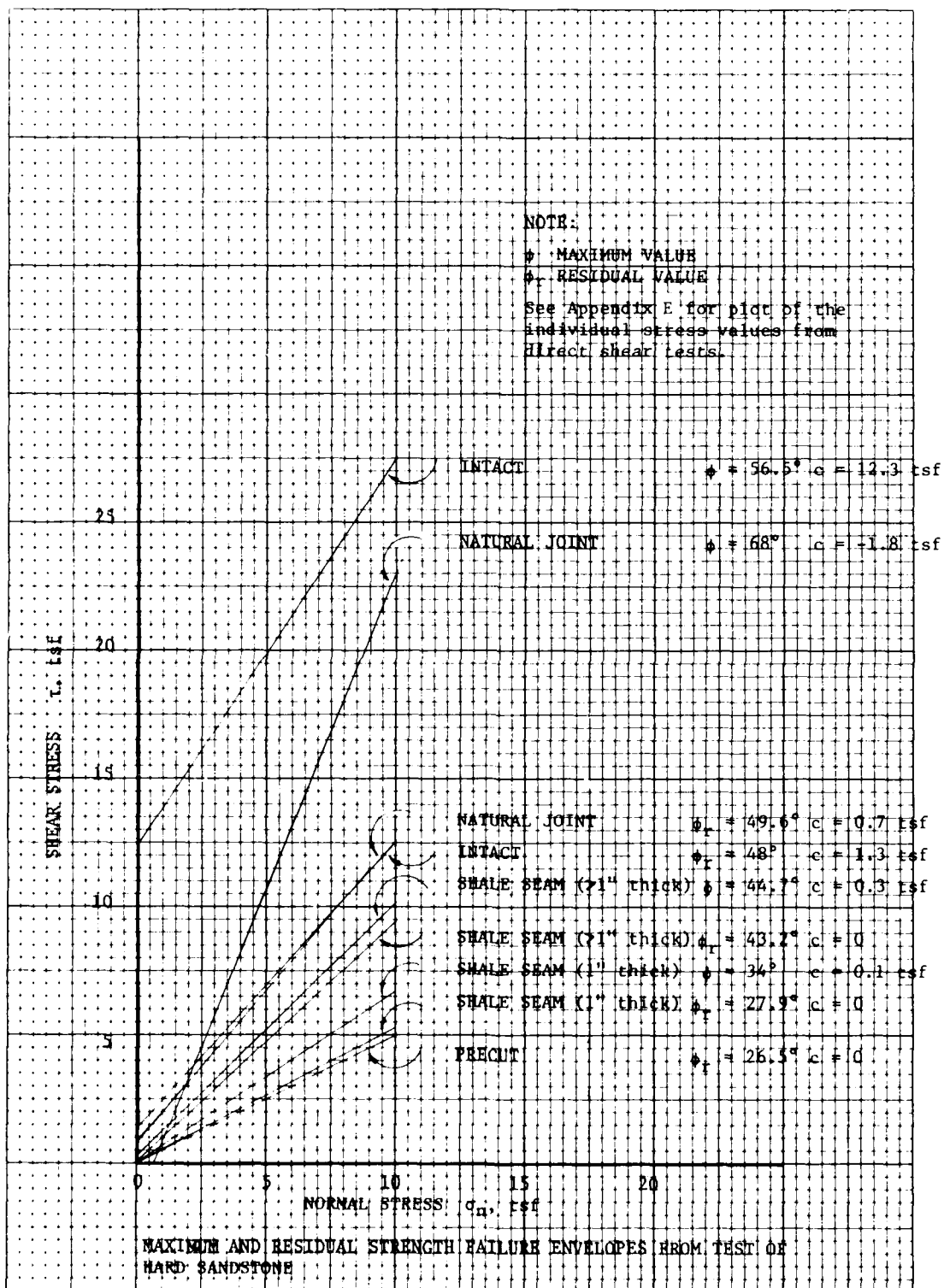


Figure 21. Summary of plot of hard sandstone failure envelopes

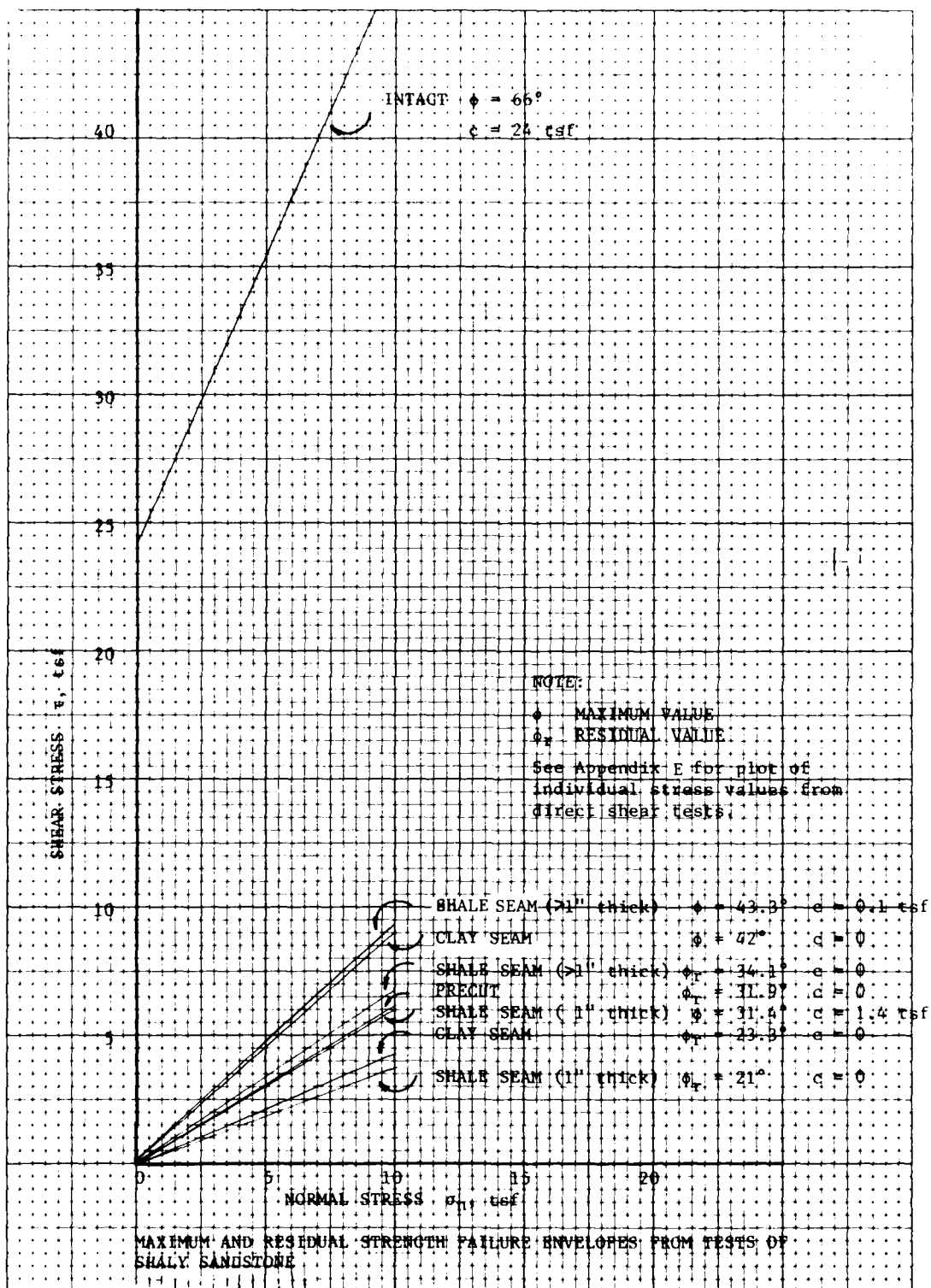


Figure 22. Summary plot of shaly sandstone failure envelopes

due to a combination of things. Some of the tests were set up with too small a gap between the shear blocks, causing the blocks to bind together during a test. And with some of the tests, the bonding agent holding the specimens in the shear blocks was set too high and came into contact during testing. The test data are not in question for those curves that do not rise sharply at about 0.2 in. of deformation and between zero and about 0.2 in. of deformation.

144. U. S. Army Engineer District, Detroit (1974) presents a range of coefficient of friction for the shaly seams in the bedrock at the New Poe Lock. The same rock formation with similar rock types is present at the New Poe Lock and the Regulatory Structure. The coefficient of friction from U. S. Army Engineer District, Detroit (1974) ranged from 0.40 to 1.75; in this report, the range for similar shaly seams is 0.38, lowest residual value, to 2.25, highest maximum value. The friction values compare well.

#### Triaxial shear strengths

145. The stress-strain relations for the cores tested under triaxial loading conditions are presented in Plates E101-E104. Mohr stress circles are presented in Plates E105-E107 for the very hard, hard, and shaly sandstone. The maximum and minimum stress values obtained during the testing are presented in Table E6, along with other pertinent information.

146. A failure envelope for the very hard sandstone was not drawn. An envelope could not be easily fitted to the stress circles. The angle of shearing resistance ( $\phi = 54^\circ$ ) correlates well with the angle of shearing resistance obtained on the intact hard sandstone specimens tested in direct shear ( $\phi$  is  $56.5^\circ$ ). The same comparison for the shaly sandstone is not as good,  $\phi = 55^\circ$  for triaxial and  $\phi = 66^\circ$  for direct shear. Cohesion for the hard and shaly sandstone is 1200 and 1440 psi, respectively.

#### Recommended design values

147. Design should consider rock types and the various bedrock structural features described herein. Guidance is presented in following tabulation as to proper choice of design parameters.

	<u>Very Hard Sandstone</u>	<u>Hard Sandstone</u>	<u>Shaly Sandstone</u>
Wet unit weight, pcf	156.3	156.8	157.0
Dry unit weight, pcf	152.9	151.6	151.9
Compressive strength, psi	14,730	8,830	7,580
Tensile strength, psi	50	65	32
Shear strength:			
Concrete to rock	$\phi = 69.3^\circ$ $c = 11.5$ tsf		
Concrete on rock, precut	$\phi = 32.10$ $c = 0$		
Intact	$\phi = 68^\circ$ $c = 44$ tsf $\phi_r = 29.9^\circ$	$\phi = 56.5^\circ$ $c = 12.3$ tsf $\phi_r = 48^\circ$	$\phi = 66^\circ$ $c = 24$ tsf
Precut	$c = 5.8$ tsf $\phi_r = 32.9^\circ$ $c = 0$	$c = 1.3$ tsf $\phi_r = 26.5^\circ$ $c = 0$	$\phi_r = 31.9^\circ$ $c = 0$
Clay seam (CL)	$\phi = 36.5^\circ$ $c = 0.05$ tsf $\phi_r = 26^\circ$ $c = 0$		$\phi = 42^\circ$ $c = 0$ $\phi_r = 23.3^\circ$ $c = 0$
Shale seam			
1 in. thick		$\phi = 34^\circ$ $c = 0.1$ tsf $\phi_r = 27.9^\circ$ $c = 0$	$\phi = 31.4^\circ$ $c = 1.4$ tsf $\phi_r = 21^\circ$ $c = 0$
>1 in. thick		$\phi = 44.7^\circ$ $c = 0.3$ tsf $\phi_r = 43.2^\circ$ $c = 0$	$\phi = 43.3^\circ$ $c = 0.1$ tsf $\phi_r = 34.1^\circ$ $c = 0$
Natural joint	$\phi = 47.3^\circ$ $c = 4.2$ tsf $\phi_r = 32^\circ$ $c = 2.5$ tsf	$\phi = 68^\circ$ $c = 0$ $\phi_r = 49.6^\circ$ $c = 0$	
Cross bed	$\phi = 58^\circ$ $c = 1$ tsf $\phi_r = 51^\circ$ $c = 0$		
Modulus of elasticity, $\times 10^6$ psi	5.31	2.33	1.70
Poisson's ratio	0.20	0.32	0.37



## Structural Stability Analysis

### Introduction

148. Even though monoliths of the Lake Superior Regulatory Structure at Sault Ste. Marie, Michigan, have been in service since 1919, it is important that they be examined in view of present-day criteria and in relation to deterioration experienced to assure continued structural adequacy. If the design or the deterioration makes the structures fail to satisfy current criteria, thereby producing unsafe or doubtful conditions of safety, the structure must be modified to conform to good engineering practice.

149. One of the main considerations for structural adequacy of the dam is the stability of the various monoliths when subjected to possible loading conditions. The stability study involves analyzing the various monoliths, taking into account reasonable loadings, structure condition, and foundation conditions to determine if they have adequate resistance against overturning, sliding, and base pressures. Practicably the analysis could be generalized to consider the smaller piers (piers 10, 11, 12, 14, 15, and 16) and the larger piers (piers 9 and 13) as groups and only one pier from each group analyzed. The analysis and evaluation of one pier from each group are adequate for an evaluation of all monoliths. Figures and computations for the structural stability analysis are presented in Appendix F.

150. In general, the stability study was done in accordance with the applicable portions of the following Engineer Manuals and Engineer Technical Letters.

- a. EM 1110-2-2200, Gravity Dam Design, 1958.
- b. EM 1110-2-2607, Navigation Dam Masonry, 1958.
- c. ETL 1110-2-184, Gravity Dam Design Stability, 1974.
- d. ETL 1110-2-22, Design of Navigation Lock Gravity Walls, 1967.
- e. EM 1110-2-2602, Planning and Design of Navigation Lock Walls and Appurtenances, 1960.
- f. EM 1110-2-2502, Retaining Walls, 1961.

151. The adequacy of the structure to resist overturning can be judged by the location of the resultant with respect to the base of the section where stability is being considered, within the monolith, or at the base-foundation interface. In general, the gravity monoliths where stability against overturning is being considered are required to have the resultant of applied loads fall within the kern of the base of the section being analyzed when subjected to active earth pressures or for monoliths not subjected to earth pressures. For operating conditions with earthquake, the resultant only has to fall within the base, but the allowable foundation stresses should not be exceeded.

152. The percent effective base (percent of the base which is in compression) is a good way to present where the resultant falls in a rectangular base section. It is a good guide for representing overturning resistance for any shape base. For example, for a rectangular base:

<u>Percent Effective Base</u>	<u>Resultant Location Within Base</u>
100	Within middle 1/3 or in kern area
75	At 1/4 points of base
50	At 1/6 points of base

153. Sliding resistance of a monolith is calculated by choosing a trial failure plane or combination of planes and calculating the resistance along this path. The critical section for sliding must be determined. It may be within the monolith, at the base-foundation interface, or at a plane or combination of planes below the base.

154. The resistance may be composed of several types. The sliding resistance due to friction and cohesion for a horizontal surface between the monolith and its foundation is calculated by the formula given in ETL 1110-2-184. The safety factor is obtained by dividing the horizontal resistance by the horizontal driving force. These formulas are inadequate for evaluating structural sliding on inclined planes. For inclined planes, the safety factor is obtained by dividing the resistance along the plane by the driving force along the plane with any passive resistance taken into consideration. The sliding resistance due to all or any part of the failure plane extending through either the concrete monolith or the foundation is calculated from the shearing or diagonal

tensile strength of the material acting over the length in which the stress occurs. If other restraints, such as strut action, exist, they must also be considered in the evaluation. The factors of safety used for sliding evaluations are as follows:

- a. Residual and precut shear strength parameters:
  - (1) 1.0 for normal operation case loading with earthquakes;
  - (2) 1.5 for other case loadings.
- b. Maximum shear strength parameters:
  - (1) 1-1/3 for normal operation case loading with earthquakes;
  - (2) 2 for other case loadings.

The factors of safety for maximum shear strength parameters have been reduced from accepted criteria because it is felt that the above values are adequate and will be acceptable for the stability evaluations of the Lake Superior Regulatory Structure.

155. The base pressures are the sum of the contact and uplift pressures on the concrete-foundation interface.

156. The dam monoliths were investigated for the following case loadings:

- a. Normal operation.
- b. Normal operation plus earthquake.
- c. Normal operation plus ice.
- d. High water condition.

### Results

157. There are two sizes of piers with similar geometry and an abutment monolith at the Regulatory Structure. The smaller piers (piers 10, 11, 12, 14, 15, and 16, Figure F5) and the larger piers (piers 9 and 13, Figure F20) have the same shape geometry and are embedded in an apron section. Consideration was given to analyzing the piers individually, but there is not enough available data to define the concrete-foundation interface plane for individual pier evaluation. The core locations provide only local determinations of in-place pier and apron depths and, in fact, may reflect local variations in foundation geometry. Also, by

viewing underwater videotapes, it was possible only to determine a general depth of 5 ft below the top of the apron to competent downstream strut resistance. With these considerations the best approach is to perform some overall, conservative evaluations. In this case, the stability analysis of one small and one large pier is sufficient.

158. The stability analysis will first be performed for the small and large piers considering overturning, sliding, and base pressures at the concrete-foundation interface (Figures F6 through F8, F10 through F13, F21, and F28). The second consideration will be the safety factor against sliding for the small and large piers considering the failure just below the pier-foundation interface (Figure F9). The third consideration will be the failure from center line to center line between piers (Figures F19 and F29). This consideration will be for sliding in the foundation material and can be viewed as a failure of one or a number of pier sections of the dam.

#### Stability of Concrete-Foundation Interface

159. The stability summaries and computations are presented in Figures F6 through F8 and Figure 21, respectively, for the small and large piers when the failure plane is at the concrete-foundation interface.

160. The small piers are considered adequate in their resistance to overturning even though for normal operation with ice the percent effective base is 93.6 percent (Figure F6). Posttensioning, which is recommended later for sliding deficiencies, will make the 93.6 percent effective base within the allowable. The safety factors against sliding at the concrete-foundation interface are adequate (Figure F7). The base pressures are within the allowable (Figure F8).

$$\begin{array}{l} \text{Allowable base pressure} = \frac{(7250 \text{ psi})}{4(1000 \text{ \#/K})} \frac{144 \text{ in.}^2}{\text{ft}^2} = 261 \text{ KSF} \\ \text{(Safety Factor} = 4, \\ \text{concrete governs)} \end{array}$$

161. The larger piers are adequate in their resistance to overturning. These results are not presented because the larger piers are

of the same height as the smaller piers but with greater base area; therefore, the presentation of results showing the adequacy in overturning is unnecessary. The safety factors for sliding at the base-foundation interface for the larger piers are adequate (Figure F21). The base pressures for the larger piers are within the allowable and the results are not presented. The base pressures are very low as can be seen from the results for the smaller piers.

#### Stability in Foundation Below Concrete-Foundation Interface

##### Introduction

162. Establishing the safety of the small and large piers against sliding below the concrete-foundation interface is the remaining concern for the stability of the dam at the Lake Superior Regulatory Structure. The first concern for the evaluation of sliding in the foundation is to determine whether or not the resisting forces increase faster than the driving forces as the depth of the sliding plane increases. This will allow a determination of whether the safety factor increases or decreases as the depth to the sliding plane increases. Because of analysis, which will be presented subsequently, the sliding plane will be considered horizontal. Figure F1 presents the variation of the safety factor against sliding versus the elevation of the sliding plane. The most critical seam (smaller  $\phi$  and  $c$ ) was used; therefore, the resisting forces increase faster in relation to the driving forces as the depth of the sliding plane increases.

163. The above-referenced computations and analysis establishes that a particular sliding plane will be more critical the closer it is located to the concrete-foundation interface. Figure F4 shows that the seams which were actually found by boring logs are at or very close to the concrete-foundation interface. The condition and erosion of the foundation influenced engineering judgments concerning taking conservative approaches in the analysis for sliding stability.

164. The foundation upstream and downstream of the Lake Superior Regulatory Structure has been removed by water action to a depth of 2 to

3 ft below the top of the apron. Local areas of scour appear to have removed rock from 3 to 5 ft below the top of the apron. The foundation is jointed and the clay and shale seams are predominately continuous. The following argument is in support of the concept that the shale and clay seams can possibly occur throughout the foundation profile. Figure F4 shows that the clay and shale seams that were actually found in the core are at or very close to the concrete foundation interface. The sandstone was classified into three separate units, although, interbeds less than 1 ft in thickness were not distinguished in the cross sections. Since clay and shale seams occur in each of the three rock units (very hard, hard, and shaly sandstone), it is possible that a seam such as 35a could be only a small distance away from the base of the structure. Previous cuts through the sandstone units at The New Poe Lock show that the clay and shale seams as thin as 0.01 ft occur and are continuous over the excavation. Not all clay and shale seams may have been detected; especially those less than 0.01 ft which may exist only as a thin film on the bedding plane making logging difficult. Considering the (1) interbeds of sandstone less than 1 ft in thickness were not distinguished in the cross sections, (2) clay and shale seams occur in each sandstone unit, (3) the clay and shale seams are predominately continuous, (4) due to drilling action and logging some seams may have not been detected, and (5) all seams were found at or near the concrete-foundation interface, it was assumed that the clay and shale seams can occur throughout the foundation profile. The assumptions were that:

- a. The most critical seam and failure geometry may occur just below the concrete-foundation interface. This makes evaluations using less critical shear strength parameters and geometries of no importance because they will not govern the sliding evaluations.
- b. Since the core holes are at isolated points with considerable distance between them ( $\frac{1}{4}$  to  $\frac{1}{2}$  between piers >60 ft), they do not define with certainty the three-dimensional base of the structure or foundation; therefore, the pier base-foundation interface was taken as that originally planned for the structures (el 585.75) even though the cores indicate an average pier depth of 1.2 ft below the planned pier depth. Some cores

indicate that certain pier bases (15 and 17) were constructed at or close to the planned elevation.

- c. Even though the general dip of the bedding is 3 ft per 100 ft from downstream to upstream, the local dip under the Regulatory Structure as can be determined from available data (the geological cross sections) will not support downstream to upstream dip under the structure. In fact, in certain cases the dip appears to be from upstream to downstream. A presentation of the various clay and shale seams are presented in Figures F3 and F4, respectively, for the upstream and downstream section of core holes transverse to the dam (Plate D1).

Viewing the general location of the seams from upstream to downstream, it is seen that a sliding plane dip under the structure from downstream to upstream is not supported. The general locations of the seams close to a given elevation and in or on the boundary of a particular sandstone unit is considered without a detailed look at the matching of point locations of the material to particular bedding planes from borehole to borehole. Without extensive work with the original core logs, and possibly more drilling, this approach is considered to be within the accuracy of the data, and a more detailed development of sliding planes from the geological cross sections is conjecture. Much difficulty was encountered in the attempt to develop a more detailed connection of seams, and consequently, was eliminated from consideration. An example considering the general dip of the bedding planes can be seen in Figure F2. Seam 14 is at approximate el 586 in the upstream section of boreholes and at el 585 in the downstream section of boreholes (Figure F3). This indicates a possible upstream to downstream dip of the bedding plane.

#### Stability of piers just below concrete-foundation interface

165. The stability summary and computations for the piers just below the concrete-foundation interface are presented in Figures F9 and F22, respectively for the small and large piers. Some of the safety factors for sliding are below available but do not control because the factors of safety for the pier and apron section are lower and govern.

Stability of pier and  
apron section just below  
concrete-foundation interface

166. The stability summary and computations for the pier and apron sections are presented in Figures F19 and F29, respectively, for the small and large piers. The critical seam for sliding is Seam 14 for maximum strength parameters (Figure 19) and Seam 35a for residual shear strength parameters (Figure F19). The sliding factors of safety for Seam 14 is 1.75 (small piers) and 1.94 (larger piers) and that for Seam 35a is 0.73 (small piers) and 0.83 (larger piers). Seam 35a governs and requires a total posttensioning force of 765 kips and 656 kips, respectively, for the small and large piers. Four posttensioning holes are suggested as shown in Figure F30 with a capacity of 191 and 164 kips per tendon, respectively, for the small and large piers. The stability at a plane of el 584.75 is also considered to give comparative values for safety factors at a deeper location of the critical sliding plane. Considering past experience it is felt that the required posttensioning forces will not overstress the concrete or foundation (Pace and Campbell 1978).

167. A 25-ft foundation embedment depth should be used for the rock anchors. A 25-ft embedment depth and a 20-ft anchor length is conservative for foundation or bond failure, but from a practical standpoint the foundation is layered with the presence of hydrostatic pressures; therefore, this embedment depth is considered adequate but not excessively conservative.

168. It is recommended that a cement or epoxy grout be used to anchor the tendons. The lower 20 ft of the tendon should be grouted and after sufficient grout strength, they should be posttensioned. The reason for only grouting the lower 20 ft of the tendon is to avoid producing tensile or shear stress concentrations in the foundation immediately below the concrete-foundation interface. The foundation material is characterized by predominant bedding planes. Scour from water action downstream of the dam shows that it can be completely removed and scour can produce undercutting in the softer layers of foundation



material. This suggests that it is best to avoid producing tensile or shear stress concentrations in the foundation immediately below the concrete-foundation interface and produce a desirable compressive stress field in the first 5 ft of foundation material immediately below the concrete-foundation interface to tighten the bedding planes in this region. The space around the tendons inside the concrete monolith and the unbonded 5 ft of tendon in the foundation should be filled with a noncorrosive grout to protect the tendons. This should be done only after there is negligible loss of posttensioning with time.

#### Stress Analysis of Gate Operating Machinery

169. Stresses obtained in the analysis of gears are not precise because of many factors, such as stress concentrations, residual stresses, load cycles, tooth hardness, polish of the root of the fillet, misalignments, tooth error, etc. For example, the stresses at the root of the gear tooth may have a concentration factor which varies from 1 to 2. In most cases, it is very hard to be sure that the load is properly shared by two or more teeth simultaneously, and the actual shape of the stress diagram across the root of the gear tooth is difficult to establish.

170. In the analysis of the gears at the Regulatory Structure, the stresses in the gears are estimated using conservative loading; and if the stresses are sufficiently low, they can be considered adequate. If they are not low, a more detailed analysis must be performed to give consideration to their adequacy.

171. In the gear analysis which follows, the load is considered to be carried by a single tooth and to be applied at the tooth tip. The gears at the Regulatory Structure were made at a time when the best gears were not manufactured very accurately, and the above assumptions are considered best for the present analysis.

172. A schematic diagram of the gears is presented in Figure G1 (sheet 1) for terminology purposes in the analysis and discussion of the gear stresses. A picture of the gears is presented in Figure 23.



Figure 23. Gate operating machinery, Lake Superior  
Regulatory Structure

Pertinent gear details are also presented in Figure G1 (sheet 2).

173. Gate load tests were performed (Part III) by placing a load cell in the gate lifting linkage just above and on each side of the gate. This was done for four typical gates to get an idea of how much force is required to raise the gates under normal operating conditions. The tests showed that a maximum force between 30,250 and 36,400 lb was required in the linkage at the end of the gates while they were being raised. The force transmitted to the gear teeth is reduced by the weight of the counterweight. This makes the balancing of the gates with the counterweight system very important. Considering the difference in the force required in raising the gates and the counterweight force, the torque and force on the gears can be determined. The forces on the gear teeth are computed and presented in Figure G1 (sheet 3). The stresses in the gears are then calculated. The calculations are also presented in Figure G1 (sheet 4). The maximum tensile and compressive stress in the teeth of the gears is about 6300 psi, which is low. Since the computed stress in the gear teeth is low, even though a conservative maximum stress of 20,000 psi was assumed for cast iron, the gears are considered to be adequate under normal loading conditions.

174. The shear stress in the shafts is presented in Figure G1 (sheet 5). The shafts are adequate, considering a computed stress of approximately 3000 psi being present under normal operating conditions.

175. The stress in the chain is presented in Figure G1 (sheet 6) and is not excessive.

176. The chain, shafts, and gears are adequate under normal operating conditions. As long as modifications, such as automatic gate operation, do not increase the stresses, the operating gate machinery is not overstressed.

### Stress Analysis of Sluice Gates

177. The stress analysis of the sluice gates is presented in Figure G2. The stress in the ribs and plates of the gates is excessive for the case loading of normal operation plus ice (Figure G2, sheets 10, 13,

15) in relation to an allowable stress of 18,000 psi. The calculated stresses in the rib and plate of girder "C" is 61,800 psi and 43,500 psi, respectively. The rivets are also overstressed for the case of normal operation plus ice. The method of calculating the stresses is conservative in some respects. For example, the girders are considered to be simply supported at their ends. The ice loading on the gates is highly indeterminate, and the analysis could be overconservative in that it uses 2 ft of ice thickness at 5000 lb/ft<sup>2</sup>.

178. The stresses in the ribs and plates for the normal operation case are below 20,000 psi and are considered acceptable.

179. Since the gates have not shown any signs of distress over a long period of service, it is recommended that they not be modified but observed each winter and if any signs of distress become apparent, corrective action can be undertaken at that time. It is believed that the ice loadings are not as severe as assumed, and the gates will continue to operate satisfactorily in the future.

#### Automatic Operation of Sluice Gates

180. An estimate was made in 1975 for modification of the Regulatory Structure sluice gates for automatic and winter operation. The estimate was made by the Sault Area Office based on H. G. Acres and Company's report of March 1972 entitled, "Lake Superior Regulatory Structure Feasibility Study for Improvements to Lake Superior Control Works." The estimate provides for housing all eight United States owned gates, the furnishing of electric power to the eight gates, electric drive to each gate, and heating arrangements for three gates for winter operation.

181. For electrifying the Regulatory Structure, motor driven gear reducers would be installed at each end of the gate. Vertical gate movement would be approximately 1 ft/min. Electric controllers with push buttons would be mounted to the west of and between the gates on the working deck so that a gate could be operated from either end. Push buttons would also be located at the downstream side of the gate at a location permitting observation of gate movement from downstream pier

level. Controller enclosures would be NEMA 3\*. Four electric controllers would be furnished with gate and gain heater magnetic contactors and associated circuit breakers.

182. A cofferdam fabricated beforehand of steel or wood would be sunk to cover the bulkhead gate slot areas and also for work of installing the gain heaters. Two such cofferdams would be fabricated so that work on both slots could be accomplished simultaneously. Cofferdam size would be such as to permit two men to work in the dry. For work on the gate gains, the Stoney roller gates would have to be raised completely out of their slots while necessary modification work is being accomplished. A monorail trolley supported by steel bents at each pier at locations above the bulkhead slot for the three regulatory gate openings would be provided. This trolley would permit raising the bulkhead for positioning into the pier slots, as well as to traverse north or south for transferring the bulkhead to the adjacent sluice.

183. An estimated capital cost and average annual costs for winter operation for electrifying eight gates and heating three gates on the United States side are presented in Table 1 as computed in 1975. Useful service life was considered to be 40 years and interest rate compounded annually at 7 percent.

184. The total capital cost as figured in 1975 was \$745,000 with an annual operating cost of \$58,938. Inflation since 1975 has caused construction costs to rise dramatically and would cause the above figures to increase significantly. In present-day economics a proposal of this magnitude would probably be cost-prohibitive. The necessity for consideration of such an extensive modification at this time is questionable, since the gate positions are adjusted only several times a year, and usually only a few gates are moved at any one time.

185. It is recommended that an automatic system be implemented by installing proper gear reducers on the gear system and that the gates be operated from each end using battery packs which can be carried to and from the site.

---

\* National Electric Manufacturers Association designation for outdoor electrical enclosures.

186. A representative of a manufacturer and installer of electro-mechanical operating devices for doors, gates, and turnstiles visited the Regulatory Structure and studied the automatic operation problem. It is concluded that the automatic operation of the gates by proper gear reducers and battery packs is feasible.

## PART V: SUMMARY AND RECOMMENDATIONS

### Summary

#### NDT of piers, gates and operating machinery

187. Subsequent to the preliminary engineering study, which included visual inspections, review of records and drawings, the accomplishment of a survey and soundings, and an underwater video inspection, NDT methods were employed to collect qualitative and quantitative data for assessment of the adequacy and condition of various structural materials contained in the Regulatory Structure. NDT methods and applications included (1) magnetic particle inspection of the accessible portions of the gears and lifting chains of the eight pairs of gate lifting mechanisms, (2) ultrasonic inspection of the concrete piers, the shafts of the eight pairs of lifting mechanisms, and the gate skins and rivets, and (3) microseismic in-place deterioration and stability evaluations of the structure. The magnetic particle tests revealed three discontinuities in the lifting mechanisms that are considered to be of a nature that could cause failure. The ultrasonic inspections did not produce anomalies that should cause concern. The concrete is indicated to be of generally good to excellent quality with no areas which are regarded as deficient with respect to structural integrity. Gate skin thicknesses averaged 0.40 in., which is 0.025 in. thicker than the design specifications. Also, ultrasonic test results indicate no cause for concern about the rivets with respect to the integrity of the gates. The results of the microseismic tests of the structure indicate the piers are all in similar condition with respect to mechanical integrity, are of good quality, and are structurally sound. Time was not available for a sufficient number of microseismic measurements to afford a good in-place evaluation of structural stability; therefore, the results of the conventional stability analysis are used in the assessment of the adequacy of the structure with respect to stability and in determining necessary remedial measures.

Load tests--  
operating machinery

188. Load cells were inserted into the gate hoisting systems of four gates in order to determine the combined total of gate and friction loads present during operation of the gates. The load cells were instrumented so that loading data could be continuously recorded for each side of the gates during the lifting operation. Nominal loads to be expected during hoisting were computed to be 30,750 lb per side. Single side loads ranged between 30,250 lb and 36,400 lb. Gates No. 9 and 10 showed noticeable differences in loads between sides (maximum 5550 lb). These differences could be caused by counterweight imbalance or friction, or both.

Concrete quality

189. A small quantity of new concrete applied as patches or overlays is in good condition. Old exterior concrete in the aprons and piers shows evidence of light to medium scaling. Severe scaling ( $>0.79$  in.) was noted in several small areas. Minor amounts of frost-damaged concrete are present in three of the nine U. S. piers. Maximum detected depth of damage is 0.3 ft. The damaged concrete was caused by cycles of freezing and thawing. Scaled and frost-damaged areas could be repaired during regular maintenance periods.

190. A 5.3-ft zone of damaged concrete exists in pier 13. The cause of the damage is partially freezing and thawing and partially alkali-silica reaction. Fine parallel cracking and white reaction product were found in the damaged zone. Ultrasonic velocities obtained in the field from measurements made on the pier were about 9 percent lower than similar velocities obtained from the other eight piers. The pier is considered structurally sound.

191. The interior concrete of the aprons and piers is in good condition. It is structurally sound, hard, dense, and durable. The concrete should continue to give excellent service even in the severe winter environment in which it has survived for over 50 years. The concrete is of excellent quality.



#### Foundation condition

192. Bedrock stratigraphy. The overburden in the dike at the southern end of the Regulatory Structure is probably spoil from the excavations of the Regulatory Structure and the Soo Locks. It consists of boulders, cobbles, gravel, and sand from the Jacobsville sandstone. It was intended to take drive samples of the overburden for testing purposes. However, a drive barrel could not be advanced and a core barrel was used to finish the one boring in the overburden. No test samples were recovered.

193. Bedrock at the Regulatory Structure site is the Jacobsville Formation of Cambrian age. The rock penetrated by drilling during this investigation is an arkosic sandstone. It is fine to medium grained and cemented primarily with quartz. The sandstone is red in color, dense, hard, and quite sound. Thin clay and shale seams are found throughout the sandstone. The bedrock is divided into very hard, hard, and shaly sandstone units for ease of classification. The three units contain mottled or banded areas and vari-colored reduction spots. Classification of the three units was done primarily on the bases of hardness.

194. Geologic cross sections. Seven cross sections were drawn to provide an overview of the bedrock material. They show the variations in bed thickness, bed sequence, the continuity and attitude of beds and the thin weak seams, and the location of the weak clay and shale seams in relation to the base of the structure.

195. Structure. The bedrock in the vicinity of the Regulatory Structure dips 3 ft per 100 ft to the west. Bed thickness is 1 to 13 ft and the beds are continuous beneath the Structure. Thin weak clay and shale seams (0.01 to 0.4 ft thick) are found throughout the bedrock and commonly occur between the three sandstone units. The clay and shale seams are considered to be the weakest zones within the bedrock.

196. Two prominent joint sets exist. They are orthogonal, with one set oriented 15 deg northwest of the Structure's axis, and the other 15 deg north of a line running in an upstream-downstream direction. The jointing is classified as moderately fractured (1- to 3-ft spacing) to unfractured (>6-ft spacing) with the prominent spacing in the moderate

range. The joints are continuous in plan view but of limited extent in section. Joints rarely exceed 3 ft in height and generally terminate on bedding planes. Joint dips can be placed into two groups, 0 to 35 deg and  $\geq 70$  deg.

197. It is not known if solution activity has occurred along the joints in the geologic past or is a continuing process. Information obtained from the borehole photography records and core logs suggest that if solutioning is occurring along joints, that it is a slow process. A more detailed study is required to ascertain if seepage along joints is occurring beneath the structure.

198. Deterioration of the underlying strata has occurred. Scouring upstream and downstream of the structure has caused undercutting of the apron to depths of 6 ft. Scour depths upstream have reached 3 ft below top of the apron, while downstream the scouring has removed rock to depths 5 ft below the top of the apron. Apron thickness is 18 in. Due to the scouring action, the piers are left standing on rock pedestals. Continuous weak clay and shale seams exist in the bedrock and are within 1 ft of the base of the structure in several places. The weak seams are thus exposed, which suggests major foundation problems in terms of sliding. It is conservative to assume that there is no strut resistance downstream of the apron for a depth of 5 ft below top of apron. The undercut and scoured areas pose uncertainties with respect to the safety of the structure. However, if these two areas are repaired, it is anticipated that the foundation would be sound in terms of stability of the structure. Adequately repaired, the foundation should serve its original intended purpose.

#### Structural stability

199. The piers are adequate in their resistance to overturning and base pressures. The resistance of the piers to sliding is inadequate. By conventional design the safety factor against sliding is below 1.0 for the case loading of normal operation plus ice. The sliding factor of safety is well below allowables for the other case loadings; therefore, remedial stability measures should be performed.

### Stress analysis

200. The stresses in the gears of the gate lifting mechanisms were calculated using conservative loading estimates. The calculated expected stresses were low; therefore, the gears are considered to be adequate for normal loading performance. The shafts and chains are also considered to be adequate since the computed stresses expected during their operation were below allowable.

201. The stress in the ribs, rivets, and plates was found to be excessive for the case loading of normal operation plus ice, but acceptable for normal operation. Since the gates have not shown any signs of distress over a long period of service, and since the actual ice loading on the gates is highly indeterminate (2-ft thickness at 5000 lb/ft<sup>2</sup> was used), it is possible that the stress analysis for this case loading is overconservative.

### Automatic gate operation

202. In 1975 the Soo Area Office prepared a work-cost estimate for the modification of the sluice gates for automatic and winter operation based on a report by H. G. Acres and Company prepared in March 1972. In present-day economics, a proposal of this magnitude would probably be cost-prohibitive. The necessity for consideration of such an extensive modification at this time is questionable, since the gate positions are adjusted only several times a year, and usually only a few gates are moved at any one time.

### Recommendations

203. It is recommended that an extensive repair and rehabilitation program for the Regulatory Structure be planned and executed in the very near future.

204. The areas of severely scaled, deteriorated, and frost-damaged concrete should be repaired during regular maintenance periods, or in conjunction with a major repair and rehabilitation program.

205. Pier No. 13 should be checked periodically for signs of further concrete deterioration. Visual inspections and other appropriate methods such as ultrasonic velocity tests should be employed.

206. It is recommended that a protective apron be placed upstream and downstream of the existing apron in order to eliminate further undercutting of the dam and removal of concrete or grouted in-place aggregate.

207. If protective aprons are installed at the structure, it is recommended that a study be initiated to monitor any seepage along joints. Such a study could be done where and if cofferdams are used for installing additional apron sections.

208. The remedial stability measures presented in Part IV should be implemented to ensure adequate sliding resistance of the piers. These measures will produce a compressive stress field in the 5 ft of foundation material immediately below the concrete-foundation interface, and will enhance the structural characteristics of the foundation. It is considered sufficient, cost-effective, and conducive to a better job to perform dewatering, foundation preparation, and concreting (scoured areas and placement of protective aprons) as a part of a total rehabilitation program if accomplished in the near future.

209. Modifications of the gates and operating machinery, such as for automatic operation, should not be accomplished without first considering the possibility of producing increased stresses in the gears, shafts, and chains, with the result of overstressing these elements.

210. The sluice gates should be observed closely during the winter for signs of overstressing due to ice loading.

211. If automatic operation of the gate machinery becomes desirable, it is recommended that a proper system of gear reducers be installed for operation by portable battery packs from each end of the gate.

212. It is further recommended that the technology developed in the field by CE districts, and through research efforts by WES, pertinent to repair and rehabilitation of old or damaged concrete structures, be considered in the planning of any extensive repair program.

## REFERENCES

- American Concrete Institute. 1980. "Guide for Making a Condition Survey of Concrete in Service," Manual of Concrete Practice, No. 65-67, Part 1, Detroit, Mich.
- Hamblin, W. Kenneth. 1958. "The Cambrian Sandstone of Northern Michigan," Michigan State Geological Survey, Publication 51.
- Lake Superior Board of Control. 1979. "Tabulated Record of Maintenance to Compensating Works," U. S. Army Engineer District, CE, Detroit, Detroit, Mich.
- Leslie, J. R., and Cheesman, W. J. 1949 (Sep). "An Ultrasonic Method of Studying Deterioration and Cracking in Concrete Structures, Proceedings, ACI Journal, Vol 46, No. 1, pp 17-36.
- Office, Chief of Engineers, Department of the Army. 1975 (Mar). "Geologic Mapping Procedures Open Excavations," Engineer Technical Letter No. 1110-2-203.
- Pace, Carl E., and Campbell, Roy L. 1978 (Dec). "Stability and Stress Analysis of Brandon Road Dam, Illinois Waterway," Miscellaneous Paper C-78-18, U. S. Army Engineer Waterways Experiment Station, CE, Vicksburg, Miss.
- Pickett, Gerald. 1945 (Sep). "Equations for Computing Elastic Constants from Flexural and Torsional Resonant Frequencies of Vibration of Prisms and Cylinders," Bulletin 7, Research Laboratory of the Portland Cement Association, Chicago, Ill.
- Stagg, K. G., and Zienkiewicz, O. C. 1978. Rock Mechanics in Engineering Practice, Wiley, London, p 49.
- Trantina, John A., and Cluff, Lloyd. 1963. "NX Bore-Hole Camera," Symposium on Soils Exploration, Special Technical Publication No. 351, American Society for Testing and Materials, Philadelphia, Pa.
- U. S. Army Engineer District, Detroit, CE. 1974 (Dec). "Foundation Report, New Poe Lock, Sault Ste. Marie, Michigan," Office of the Area Engineer, Detroit, Mich.
- U. S. Army Engineer Division, Ohio River, CE. 1975 (Mar). "New Sabin Lock Project, Results of Laboratory Rock Core Tests," Cincinnati, Ohio.
- \_\_\_\_\_. 1976 (Apr). "Sault Ste. Marie, Results of Laboratory Rock Core Tests," Cincinnati, Ohio.
- U. S. Army Engineer Waterways Experiment Station, CE. 1949. Handbook for Concrete and Cement (with quarterly supplements), Vicksburg, Miss.

Zeigler, T. W. 1972 (Nov). "In Situ Tests for the Determination of Rock Mass Shear Strength," Technical Report No. S-72-12, U. S. Army Engineer Waterways Experiment Station, CE, Vicksburg, Miss.

Table 1  
1975 Estimated Capital Cost and Average Annual Costs  
for Winter Operation of Sluice Gates at Compensating Works

	<u>Initial Capital Costs</u>	<u>Annual Costs</u>
<u>Capital Costs</u>		
Installation of gain and gate heaters (3 gates), including structural modifications to pier structures and providing one bulkhead and monorail with trolley	\$407,400	\$28,518
Power supply from Northwest Pier feeder to controller at Regulatory Structure	104,000	7,800
Telephone line from Northwest Pier to Regulatory Structure (use locks telephone exchange switchboard)	1,000	75
Modifications to motorize 8 gates including controllers and connections	113,000	8,475
Metal-clad enclosures over 8 gates $(115,000 \times 0.8 \times 130\%) =$ $119,600 \times .07 = 8372$ $119,600 \times .005 = \underline{598}$ <span style="padding-left: 100px;">8970</span>	<u>119,600</u>	<u>8,970</u>
Total capital costs	\$745,000	
	Subtotal	\$53,838
<u>Annual Maintenance</u>		
Routine maintenance of heating equipment, motorized drives, controllers, lighting. Estimate two defective heaters per year requiring scuba diving personnel and dropping bulkhead in pier slots		\$ 2,500
Snow removal at site		300
Routine maintenance of power cable, terminal equipment, messenger cable, and poles.		500
Routine maintenance of telephone line		100

(Continued)

Table 1 (Concluded)

	<u>Initial Capital Costs</u>	<u>Annual Costs</u>
Repainting of cladding and frame, over service life.		<u>500</u>
	Subtotal	\$ 3,900
<u>Annual Operations</u>		
Annual operations for gate heating and lighting (assuming power is supplied by the U. S. Government Hydroelectric Plant at current cost of 4.6 mills under contract DA-20-064-ENG-632, Supplemental Agreement Modification No. 6 under the description as 'appurtenant work' to the St. Marys Falls Canal. Three months - 150 KW at 75% load factor)		\$ 500
Annual cost for gate operation including winter and summer (in past required six men on job - can be reduced to four) usual charges for operation approximately \$900		600
Annual cost of telephone operation (calls to outside through locks exchange)		<u>100</u>
	Subtotal	\$ 1,200
	Total Annual Costs -	\$58,938



APPENDIX A  
MATERIAL SUPPLEMENTARY TO  
PRELIMINARY ENGINEERING STUDY AND TESTING

Table A1  
Ultrasonic Velocity Data

Pier No. 10		Pier No. 11		Pier No. 12	
Station	Velocity fps	Station	Velocity fps	Station	Velocity fps
1a	17,620	1a	16,950	1a	17,780
b	17,465	b	16,160	b	16,325
2a	17,780	2a	16,770	2a	17,740
b	17,545	b	16,425	b	26,950
3a	17,355	3a	16,840	3a	17,580
b	17,545	b	16,065	b	16,325
4a	17,390	4a	17,770	4a	17,505
b	16,840	b	16,840	b	16,325
mean = 17,445 fps		mean = 16,465 fps		mean = 17,065 fps	
std dev = 280 fps		std dev = 420 fps		std dev = 665 fps	

Pier No. 14		Pier No. 15		Pier No. 16	
Station	Velocity fps	Station	Velocity fps	Station	Velocity fps
1a	17,020	1a	16,950	1a	16,950
b	15,840	b	17,095	b	17,205
2a	16,565	2a	16,770	2a	16,840
b	17,165	b	16,915	b	16,840
3a	16,565	3a	16,840	3a	16,565
b	16,130	b	16,950	b	16,325
4a	16,130	4a	16,840	4a	16,950
b	16,805	b	16,495	b	16,565
mean = 16,530 fps		mean = 16,855 fps		mean = 16,780 fps	
std dev = 465 fps		std dev = 175 fps		std dev = 280 fps	

Table A2  
Ultrasonic Velocity Data

<u>Pier No. 9</u>		<u>Pier No. 13</u>	
<u>Station</u>	<u>Velocity fps</u>	<u>Station</u>	<u>Velocity fps</u>
1a	17,145	1a	15,490
b	16,950	b*	16,070
		c	15,650
2a	17,145	2a	15,385
b	17,440	b	16,100
		c	15,790
3a	16,730	3a	15,100
b	16,915	b	15,735
		c	15,845
4a	16,665	4a	15,760
b	16,915	b	15,845
		c	15,790
mean = 16,700 fps		mean = 15,715 fps	
std dev = 250 fps		std dev = 280 fps	

\* On pier No. 13 the "c" stations were placed  
2 ft below the "b" stations on a patched area.

DETAILED TESTING PROGRAM  
UNITED STATES PORTION  
LAKE SUPERIOR REGULATORY STRUCTURE

Work Item	Standard
1. Conduct Survey, Soundings, & Underwater Inspection	
2. Conduct Ultrasonic Velocity Tests of Concrete	CRD-C 51-72 (ASTM C 597-71), "Pulse Velocity Through Concrete."
3. Detailed Visual Inspection	
4. Office Analysis of Substructure & Superstructure Stability	EM 1110-2-2200, "Gravity Dam Design." EM 1110-2-2607, "Navigation Dam Masonry." ER 1110-2-1806, "Earthquake Design and Analysis for COE Dams." EM 1110-1-2101, "Working Stresses for Structural Design."
5. Interim Report Preparation	
6. Finalize Borehole Locations	
7. Mobilize Equipment at Soo Locks	
8. Transport Equipment to Jobsite	
9. Conduct Drilling of Core Holes	
10. Ultrasonic Plate Gaging, Rivet Sounding	ASTM A-388-77, "Ultrasonic Pulse-Echo Straight-Beam Testing by the Contact Method." Guide Specification CE 270.02, "Ultrasonic Inspection of Plates." ASTM A 388-75, "Ultrasonic Examination of Heavy Steel Forgings." ASNT Recommended Practice: SNT-TC-1A

Figure A1. Detailed testing program prepared jointly by WES and DD (Sheet 1 of 3)

Work Item	Standard
11. Machinery Testing (Evaluate load capabilities, etc.)	
12. Machinery Testing (Magnetic Particle & Liquid Penetrant, if necessary)	ASTM E 109-63, "Dry Magnetic Particle." ASTM E 138-63, "Wet Magnetic Particle." ASTM A 275-74, "Magnetic Particle Inspection of Steel Forgings." ASTM E 165-75, "Liquid Penetrant Inspection Method."
13. Continuation of Ultrasonic Velocity Tests (borehole)	
14. Televiewer/borehole camera (maximum 10 holes)	WES Geophysical Manual in Draft
15. Rebound Hammer*	CRD-C 22-76 (ASTM C 805-75T), "Rebound Number of Hardened Concrete."
16. Laboratory Testing - Concrete/Masonry	
a. Compressive Strength	CRD-C 14-73 (ASTM C 39-72)
b. Tensile Splitting Strength	CRD-C 77-72 (ASTM C 496-71)
c. Freeze-Thaw Durability*	CRD-C 20-77 (ASTM C 666-77)
d. Wetting-Cooling, Dry-Heating*	ORDL Wet-Dry Test
e. Dynamic Modulus "E" of Concrete	CRD-C 18-59
f. Static Modulus "E" of Concrete	CRD-C 19-75 (ASTM C 469-65)
g. Density of Concrete	CRD-C 23-76 (ASTM C 642-75)
17. Laboratory Testing - Rock Specimens	
a. Weathering (Wet-Dry)*	
b. Compressive Strength	ASTM D 2938-71a
(1) Alone	ASTM D 3148-72
(2) With Modulus of Elasticity "E"	ASTM D 3148-72
(3) With Poisson's Ratio	

\* WES does not recommend this test for this testing program.

Figure A1. (Sheet 2 of 3)

Work Item	Standard
c. Tensile Strength (1) Ring Method*	ASTM D 2936-71
(2) Direct	
d. Shear Strength	
(1) Direct, w/o Deformation Readings	RTH 203-77
(2) With Sliding Friction	RTH 203-77
(3) Direct, w/Deformation Readings	RTH 203-77
(4) Direct, w/Deformation Readings & Sliding Friction	RTH 203-77
e. Sliding Friction (Rock on Rock)	
f. Shear (Bored) Strength	
(1) Grout on Rock	RTH 203-77
(2) Grout on Rock w/Sliding	RTH 203-77
g. Moisture Content	RTH 106-77
h. Unit Weight	RTH 109-77
i. Specific, Ga, Gm	RTH 107-77
j. Rock Core Triaxial (Q)	ASTM D 2664-67
k. Photographs of Sample	RTH 102-77
18. Laboratory Testing - Granular Dike Materials	
a. Determination of Angle of Internal Friction of all Materials in Land Connection Dike	EM 1110-2-1906
b. Determine Permeability of Materials in Land Connection Dike	EM 1110-2-1906
c. Unit Weight of Land Connection Dike Materials	EM 1110-2-1906
d. Moisture Content of Land Connection Dike Materials	EM 1110-2-1906
19. Complete Structural Stability Analysis & Prepare Final Report - FY 1980	

\* WES does not recommend this test for this testing program.

Figure A1. (Sheet 3 of 3)

APPENDIX B  
NDT AND LOAD TEST RESULTS,  
GATES AND OPERATING MACHINERY

Table B1  
Load Tests of Gate Machinery, Gate No. 9

<u>Travel of Gate, ft</u>	<u>Time, min</u>	<u>North Side Load, lb</u>	<u>South Side Load, lb</u>
0	0	0	0
1	1.05	32,750	34,400
2	1.90	33,300	34,400
3	2.70	33,100	34,000
4	3.35	34,150	35,000
5	4.15	33,750	35,250
6	4.90	33,800	36,250
7	5.60	34,050	35,850
8	6.35	34,200	35,900
9	7.05	34,250	36,400
10	7.70	33,500	35,800

Table B2  
Load Tests of Gate Machinery, Gate No. 10

<u>Travel of Gate, ft</u>	<u>Time, min</u>	<u>North Side Load, lb</u>	<u>South Side Load, lb</u>
0	0	0	0
1	1.10	30,750	34,750
2	1.90	31,250	35,600
3	2.75	30,500	34,700
4	3.60	31,300	35,400
5	4.45	31,250	35,800
6	5.25	31,250	36,000
7	6.00	31,350	36,150
8	6.80	30,250	35,800
9	7.70	30,900	35,950
10	8.45	30,200	35,700



Table B3

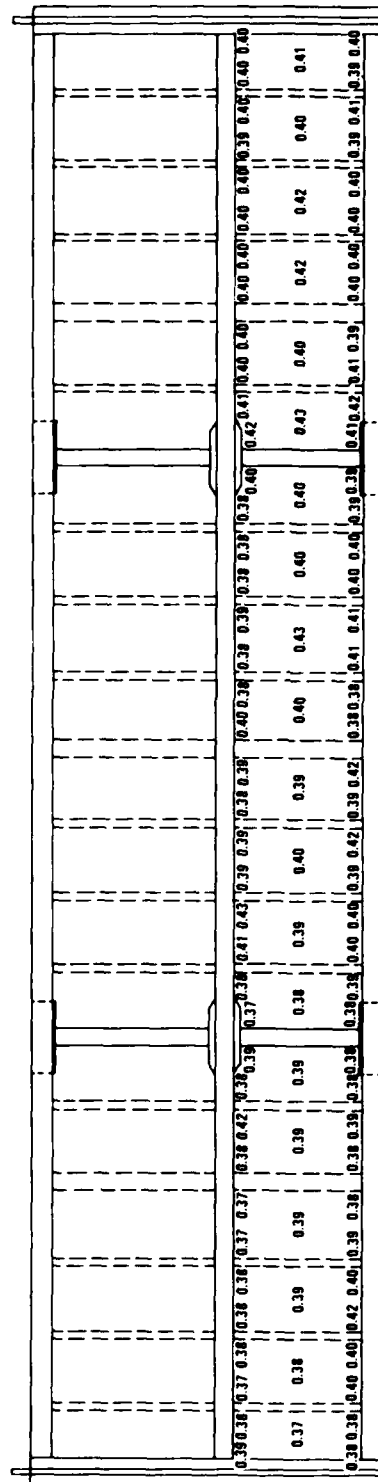
Load Tests of Gate Machinery, Gate No. 15

<u>Travel of Gate, ft</u>	<u>Time, min</u>	<u>North Side Load, lb</u>	<u>South Side Load, lb</u>
0	0	0	0
1	1.20	30,400	32,100
2	1.70	29,800	30,600
3	2.40	30,500	31,100
4	3.30	30,900	31,400
5	4.15	31,300	31,600
6	5.05	31,950	32,050
7	5.90	32,200	33,200
8	6.85	31,500	32,300
9	7.85	32,400	31,850
10	8.65	31,350	31,350
11	9.60	31,300	31,300
12	10.40	31,250	31,250
13	11.20	31,250	31,250

Table B4

Load Tests of Gate Machinery, Gate No. 16

<u>Travel of Gate, ft</u>	<u>Time, min</u>	<u>North Side Load, lb</u>	<u>South Side Load, lb</u>
0	0	0	0
1	0.65	31,500	32,300
2	1.45	31,400	32,350
3	2.35	32,250	32,600
4	3.10	31,400	32,500
5	4.00	31,500	32,950
6	4.90	31,500	32,600
7	5.80	31,750	32,850
8	6.60	31,500	32,050
9	7.45	31,700	31,700
10	8.35	31,750	31,300
11	9.25	31,600	31,100
12	10.00	31,600	31,200



NOTE: THICKNESS OF GATE SKIN IN INCHES

DETAILED TESTING  
LAKE SUPERIOR REGULATORY STRUCTURE  
UPSTREAM SIDE, GATE 9

NOTE: THICKNESS OF GATE SKIN IN INCHES.

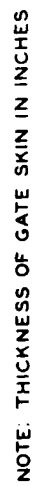


PLATE B3







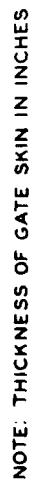
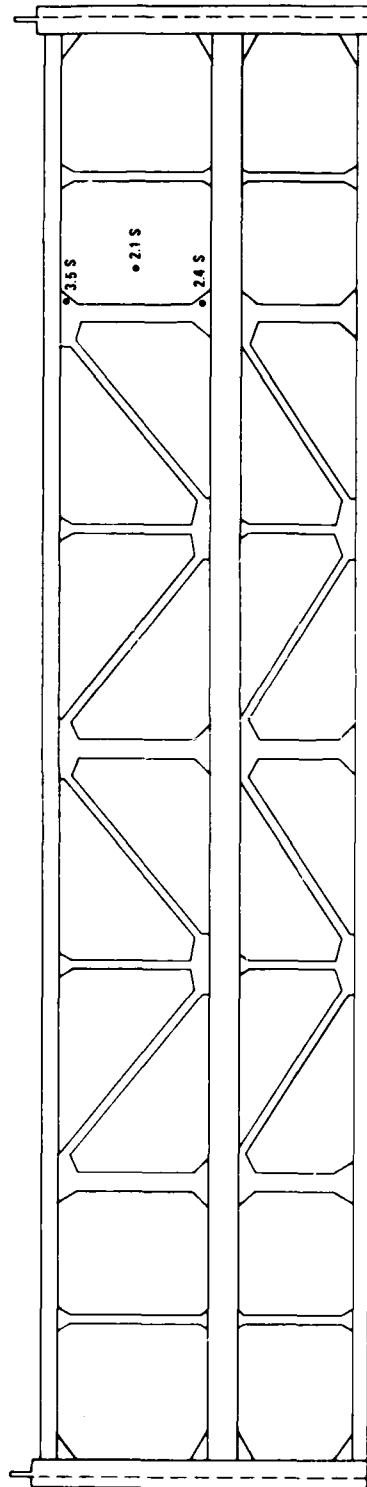


PLATE B7



**DETAILED TESTING  
LAKE SUPERIOR REGULATORY STRUCTURE  
UPSTREAM SIDE, GATE 16**



NOTE: MEASUREMENT OF RIVET LENGTH IN INCHES  
 S = ULTRASONICS INDICATED SAME AS ACTUAL  
 MEASURED LENGTH  
 B = INDICATES CRACKED RIVETS

DETAILED TESTING  
 LAKE SUPERIOR REGULATORY STRUCTURE  
 DOWNSTREAM SIDE, GATE 11

DETAILED TESTING  
LAKE SUPERIOR REGULATORY STRUCTURE  
DOWNSTREAM SIDE, GATE 12

NOTE: MEASUREMENT OF RIVET LENGTH IN INCHES.  
S = ULTRASONICS INDICATED SAME AS ACTUAL MEASURED LENGTH.  
B = INDICATES CRACKED RIVETS.

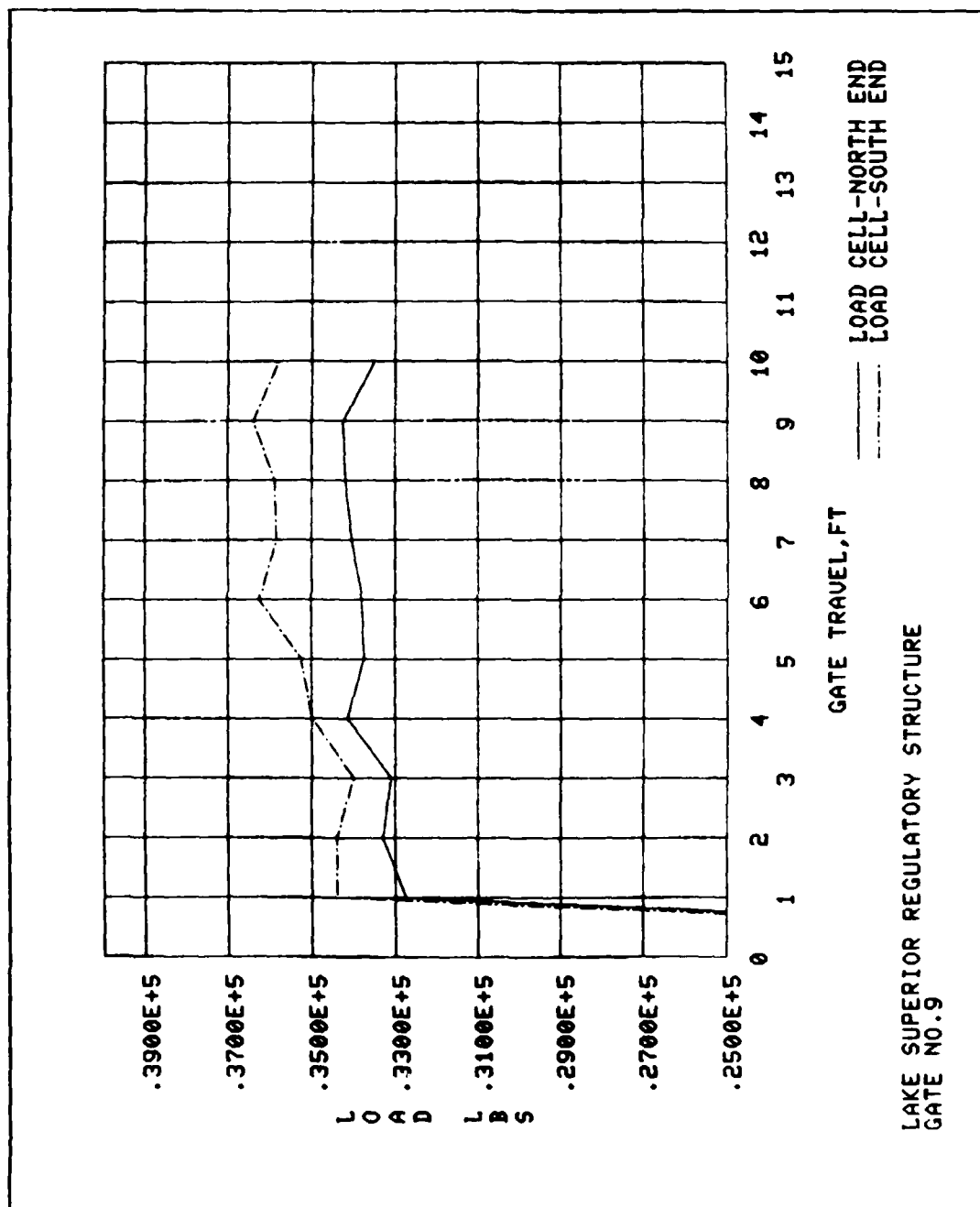
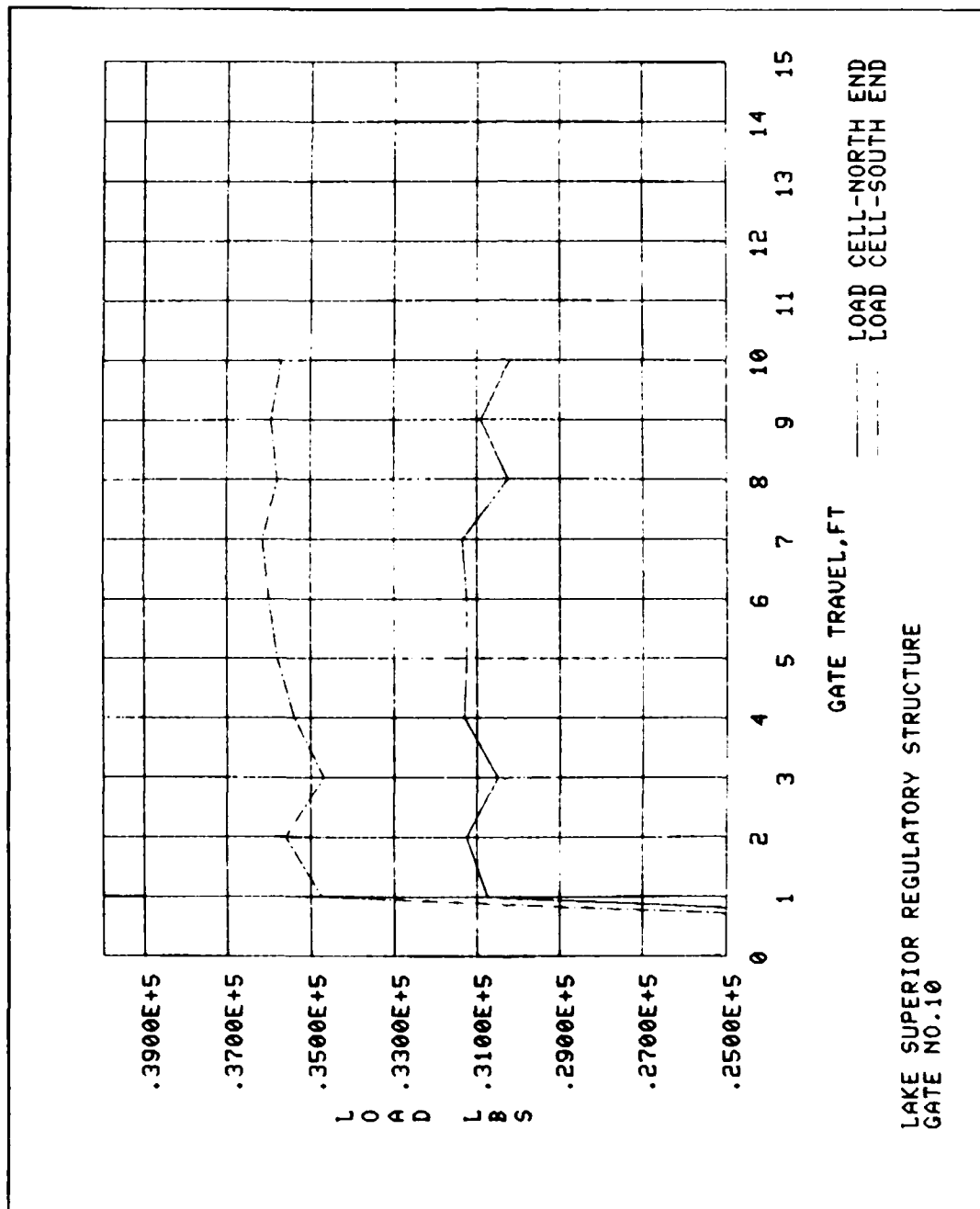


PLATE B11

PLATE B12



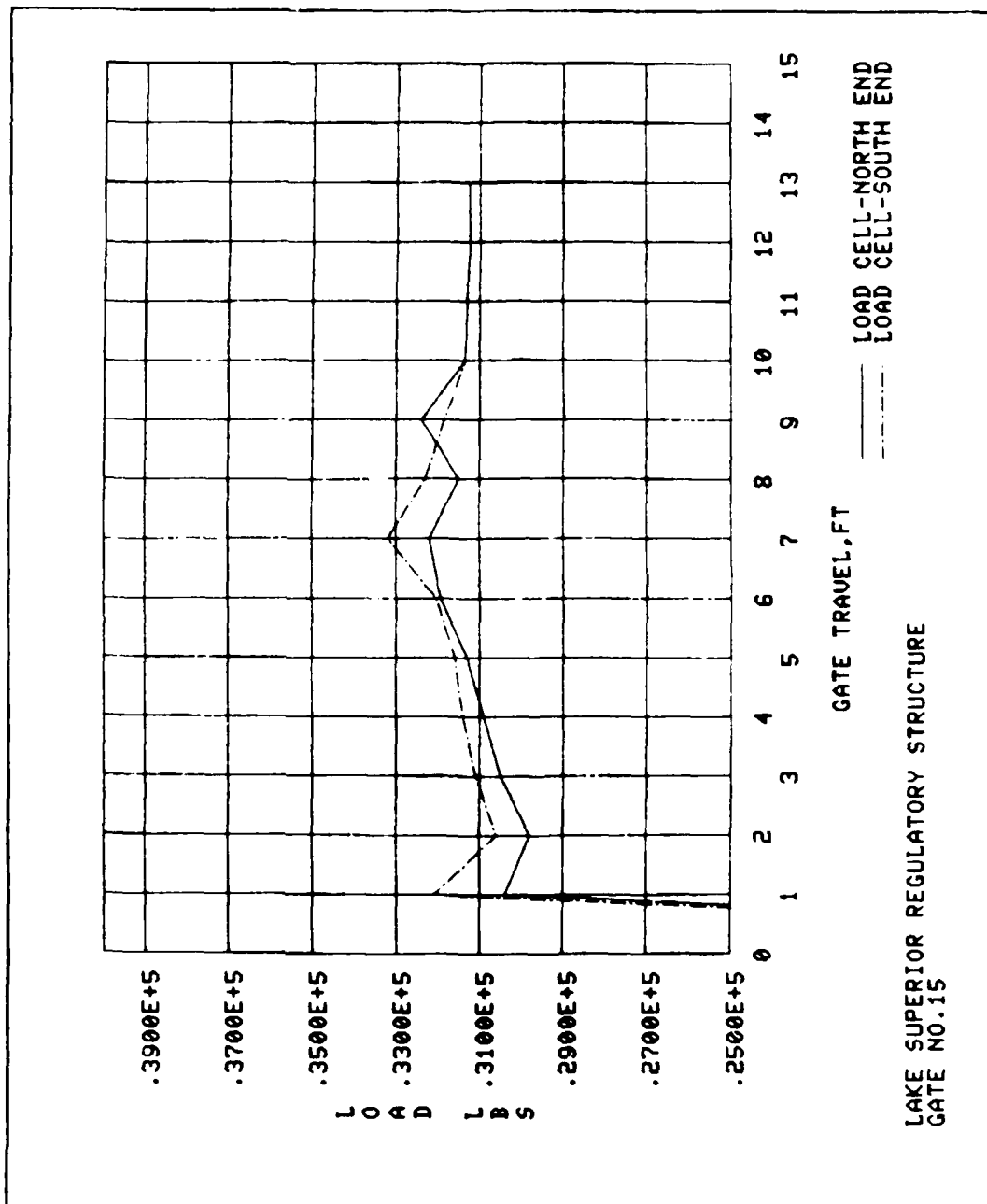
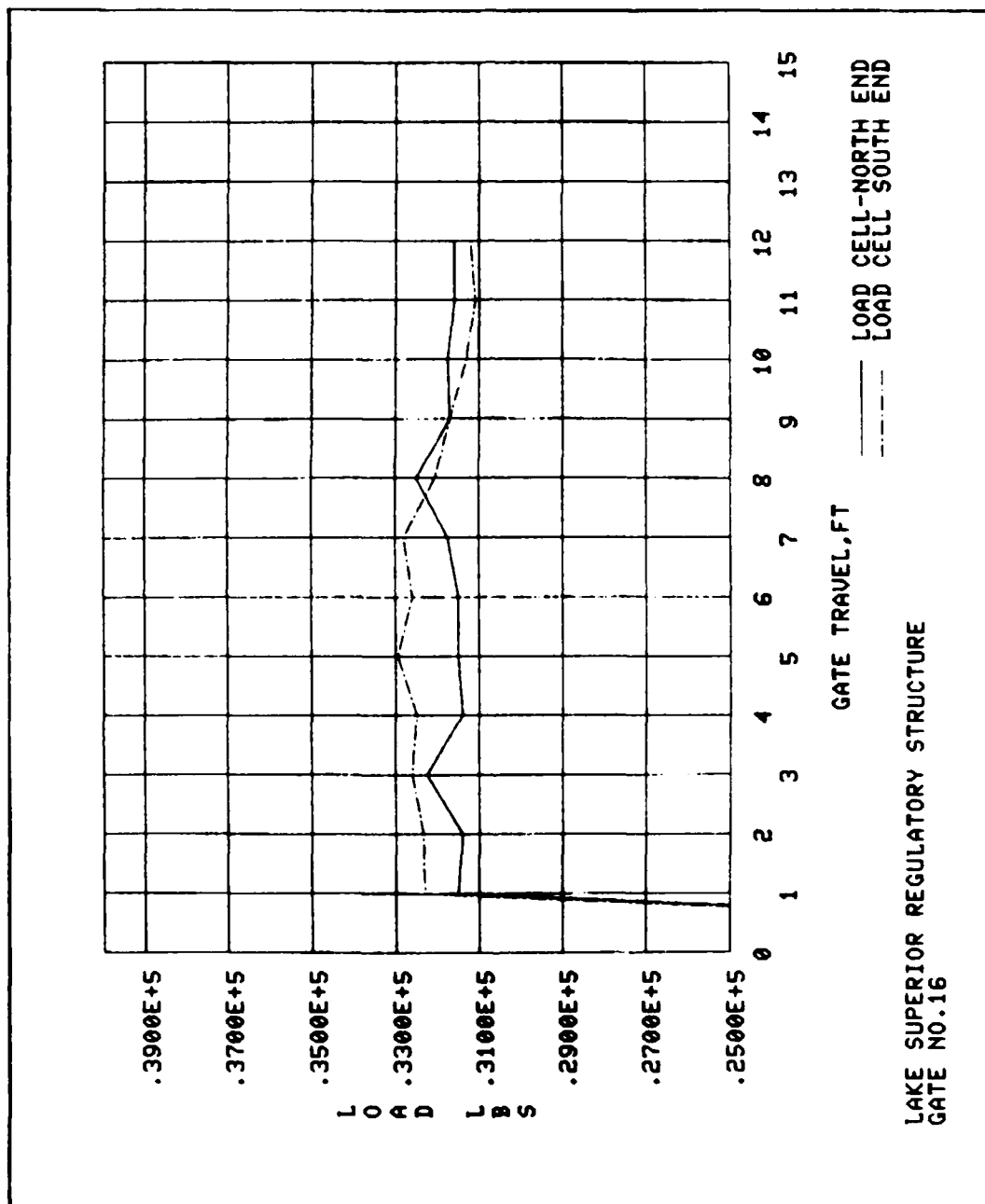


PLATE B13

PLATE B14



APPENDIX C  
FOUNDATION EXPLORATION,  
REFERENCE MATERIAL AND BOREHOLE PHOTOGRAPHY  
REGULATORY STRUCTURE  
SAULT STE. MARIE, MICHIGAN



1. Joint frequency diagrams give the number of observed joints per 5-ft depth interval a boring. The legend on Plates C1-C7 shows different size rectangular boxes; some are clear while others are partially or fully blackened.

2. The boxes in the interval between the base of the concrete and the 25-ft depth represent a depth interval of less than 5 ft. This was done for the convenience of reading the depth scale on the left of the diagrams.

3. The different height boxes represent different joint dips. The taller boxes represent dips between the vertical and 10 deg either side of the vertical. The shorter boxes represent dips between the horizontal and 10 deg either side of the horizontal.

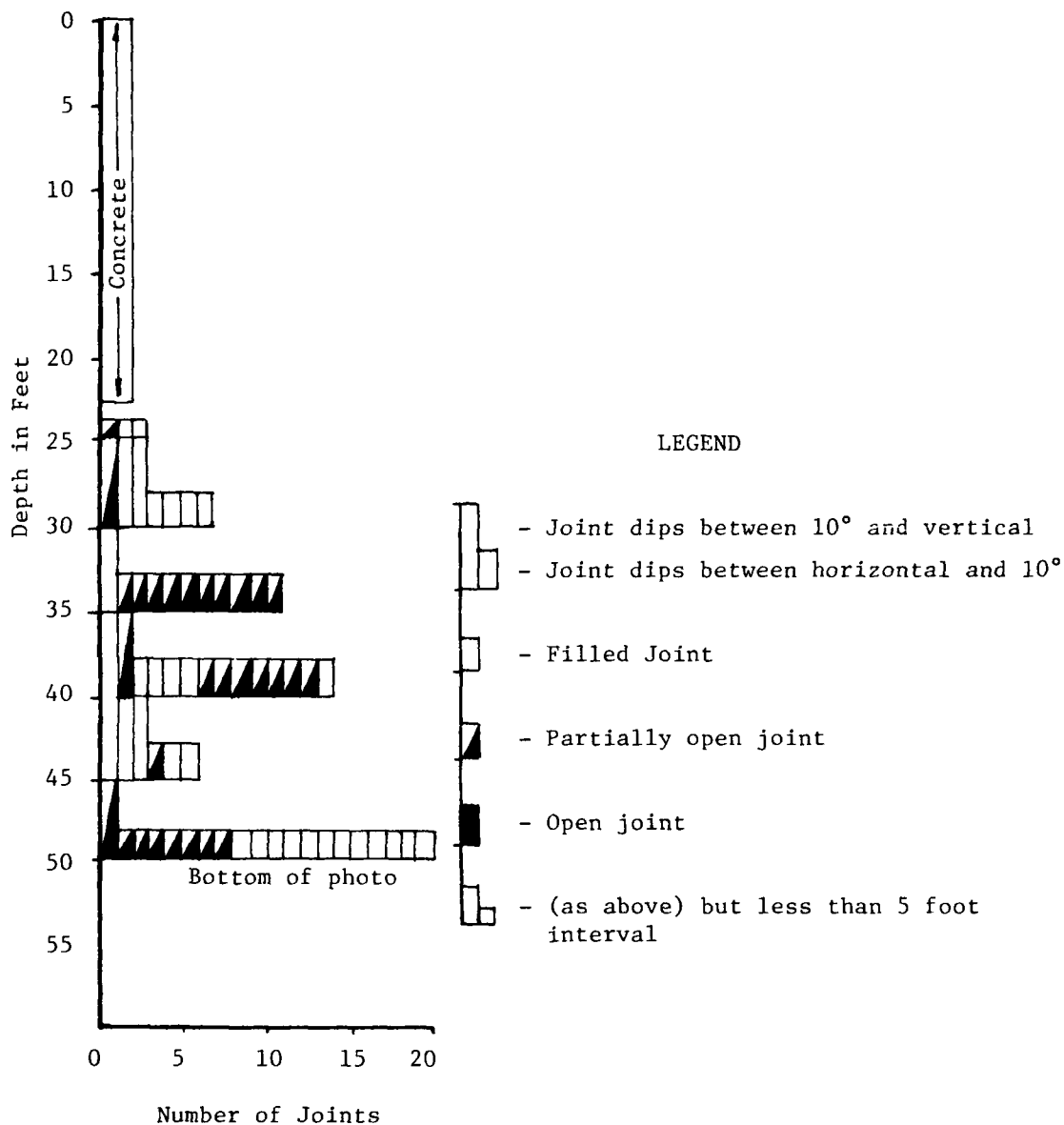
4. The filled joints are depicted with clear (or open) boxes, the partially opened joints are depicted with one-half blackened boxes, and the open joints are shown by fully blackened boxes.

5. The following reference material was supplied by the Detroit District to be reviewed for the foundation investigation and testing program, Regulatory Structure, Sault Ste. Marie, Michigan.

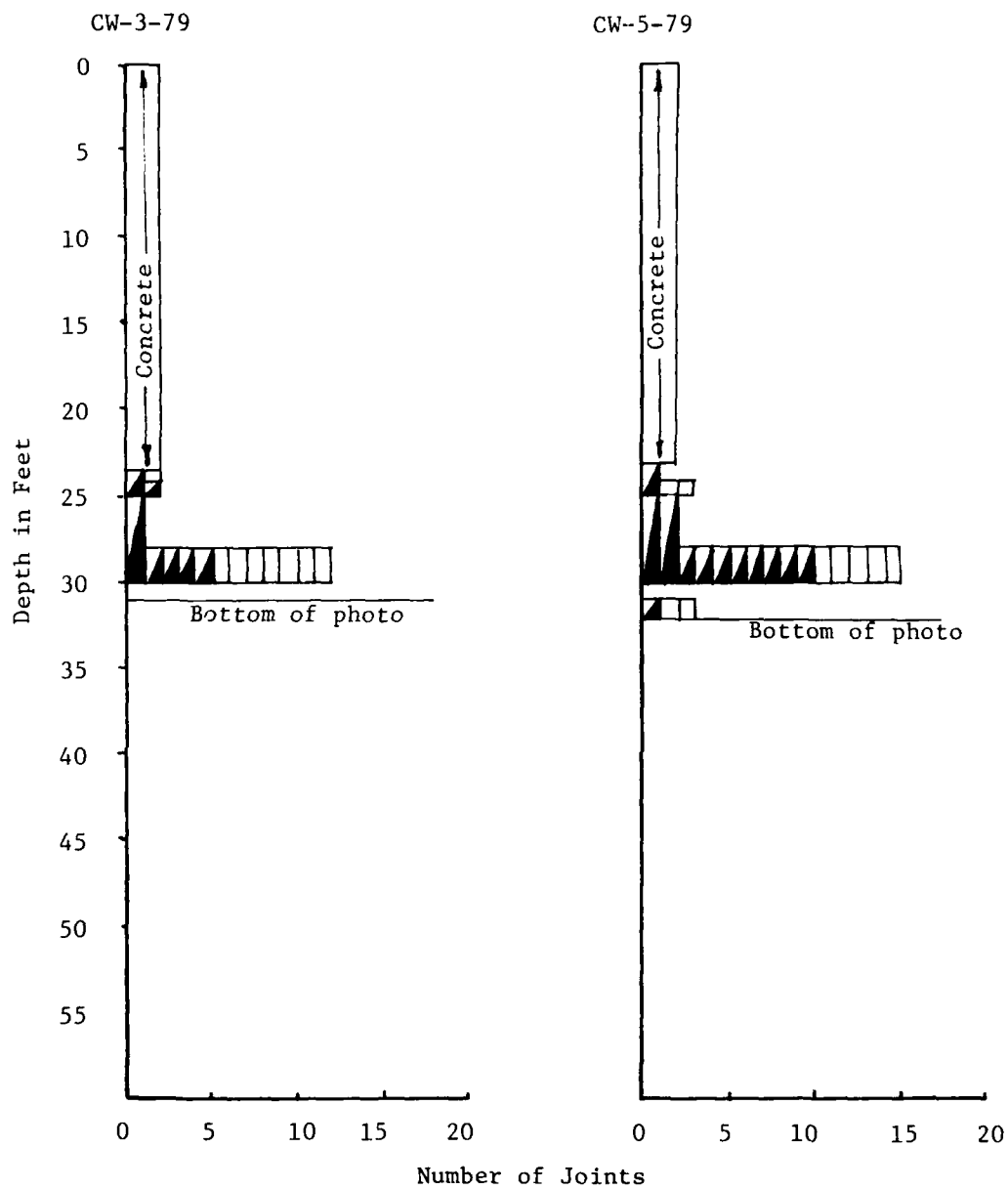
- a. Location Map for "P" Holes (1958-1959).
- b. 1958-1959 Boring Field Logs - Holes 1P, 2P, 3P, 4P, 4P-1, 5P, 6P, 7P, 8P, 9P, 9PW, 10P, 10PW, 11P, 12P, 13P, 13P-1, 14P, 15P, 16P, 17P, 18P, 19P, 19P-1, 20P, 21P, 22P, 23P.
- c. Location Map for 1907, 1945, 1974, and 1975 Borings.
- d. 1974 Boring Logs - S1-74, S2-74, S3-74, S4-74, S5-74.
- e. 1945 Boring Logs - Test Pit No. 1, Test Pit No. 2, Test Pit No. 3, Test Pit No. 4, Test Pit No. 5, Hole No. 6, Hole No. 7A, Hole No. 8, Hole No. 9, Hole No. 10, Hole No. 11, Hole No. 12A, Hole No. 13, Hole No. 20, Hole No. 21.
- f. 1907 Boring Logs - Hole Nos. 7, 8, 9, and 10.
- g. 1975 Boring Logs - S2-75, S3-75.
- h. Drawn Boring Logs - S1-74, S2-74, S3-74, S4-74, S5-74.
- i. Piezometer Logs - S2-74, S3-74, S4-74, S3-75.
- j. Profile of Piezometer Installations - S2-74, S3-74, S4-74.
- k. Field Logs of 1974 Borings - S1-74, S2-74, S3-74, S4-74, S5-74.

- l. Article on Cofferdam for New Locks at St. Mary's Falls Canal by Mr. W. J. Graves.
- m. Boring Hole Folders - P Calyx-9, PNX-1, PNX-3, PNX-4, PNX-6, PNX-10, PNX-11, PL-1, PL-1A, PL-2, PL-3, & Calyx-3, PL-4, PL-5A, PL-6, PL-7, PL-8A & 8B, PL-9, PL-12, PL-13, PL-14, PL-16, PL-17, PL-18, PL-19, PL-20, PL-21, PL-22, PL-23, PL-24, PL-25.
- n. Profile of New Second Lock - 1962.
- o. New Second Lock - Rock Symbols and Descriptions for Core Logs.
- p. 1962 Office Log Borings - PM-1, PL-1A, PL-2, PM-2, PM-3, PM-4, PM-5, PM-6, PM-7, PM-8, PM-9, PM-10, PM-11, PM-12, PM-13, PM-14, Calyx-1, Calyx-2, PL-3, PL-4 & 4A, PL-5A, PL-6, PL-8B, PL-9, PL-12, PL-13, PL-14, PL-16, PL-17, PL-18, PL-19, PL-20, PL-21, PL-22, PL-23, PL-24, PL-25.
- q. DF dated 30 August 1962, subject: Testing Rock Core Samples of Sandstone - New Second Lock, Sault Ste. Marie, Michigan.
- r. Boring Logs - Sault Ste. Marie International Bridge - 1960.
- s. Divers Report - "Inspection of Compensating Dam, Upstream Side," for Great Lakes Power Co., by the Canada Gunitite Co., Ltd., August 16, 1976.

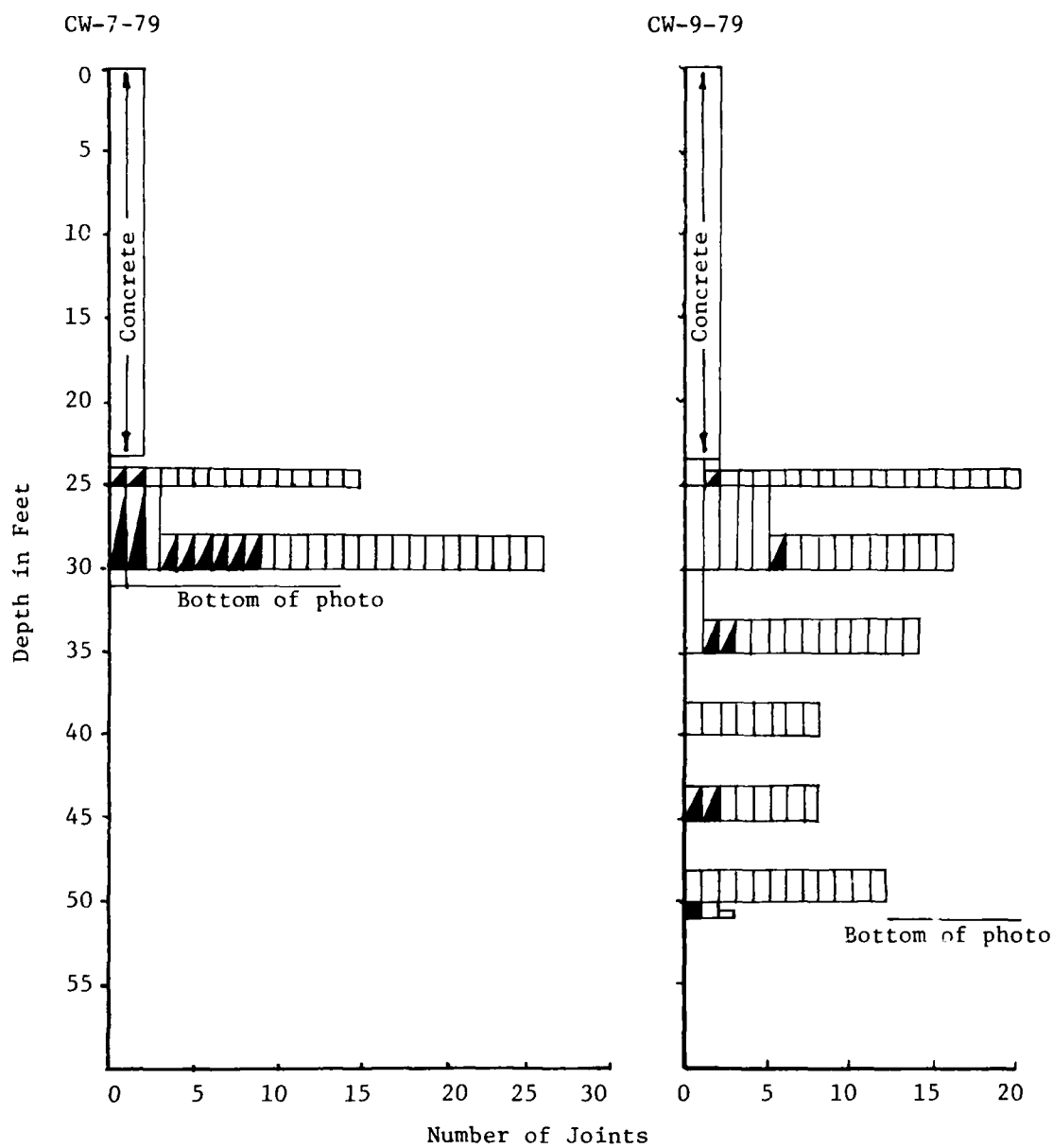
CW-1-79



Joint Frequency Diagrams, 5 Foot Intervals

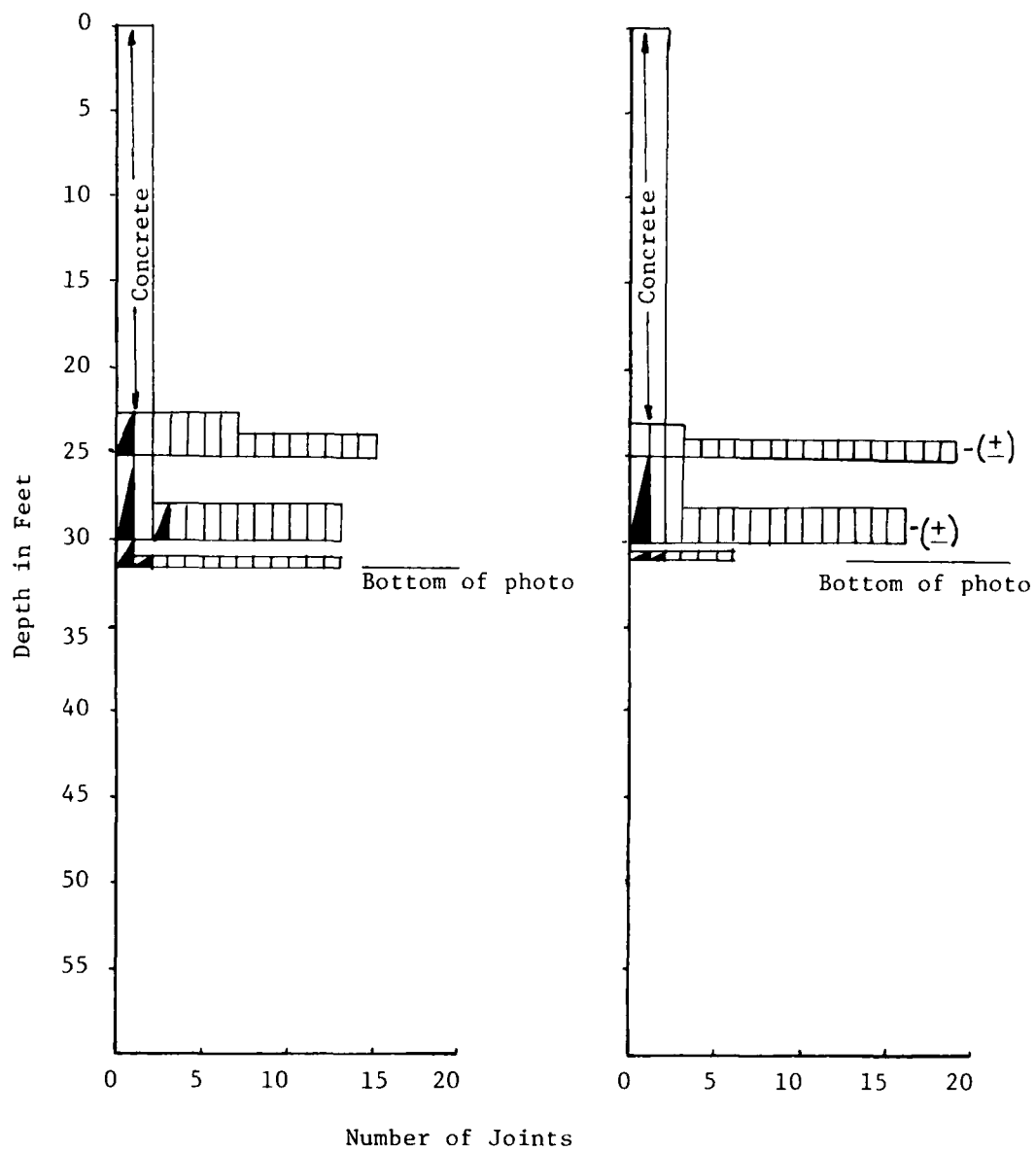


Joint Frequency Diagrams, 5 Foot Intervals

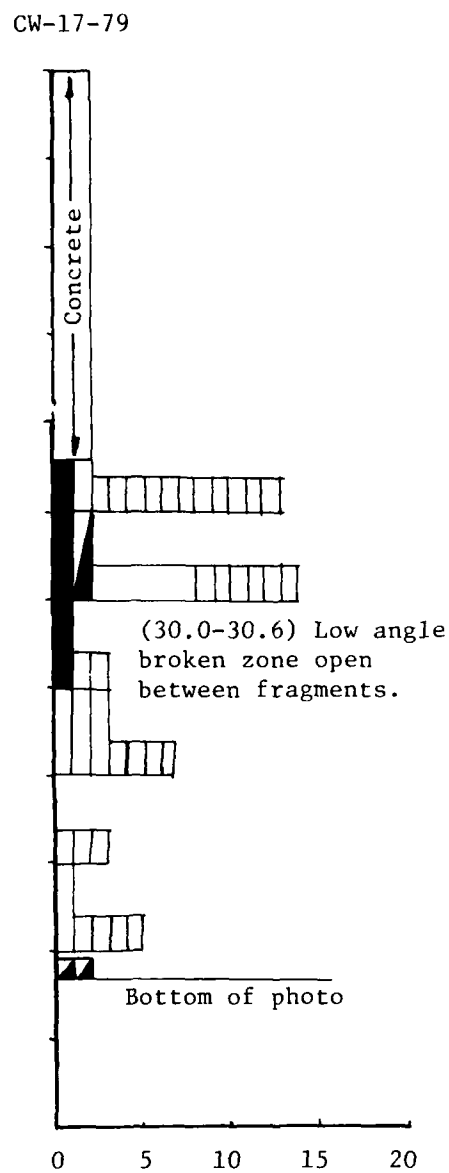
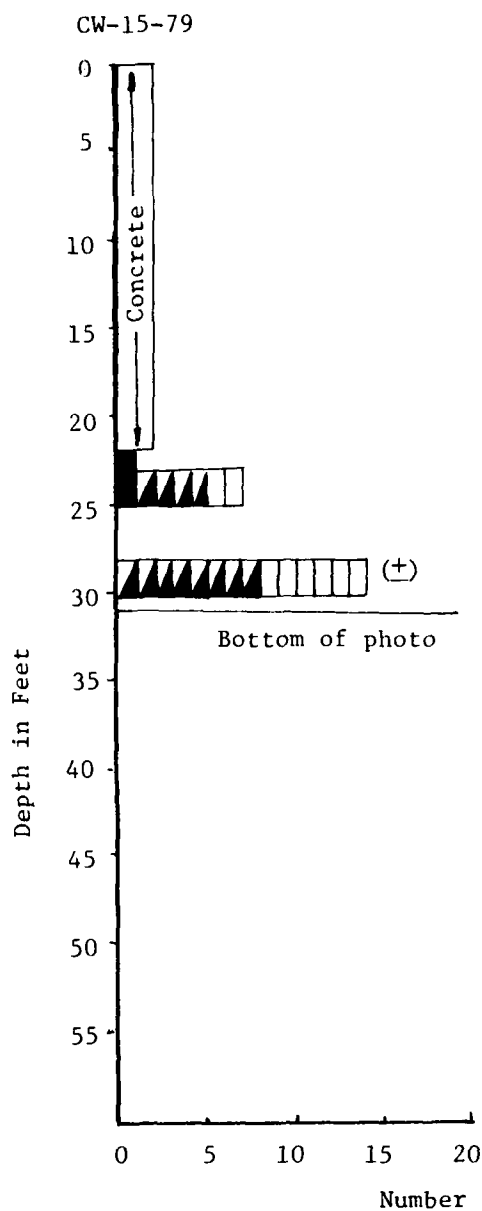


Joint Frequency Diagrams, 5 Foot Intervals

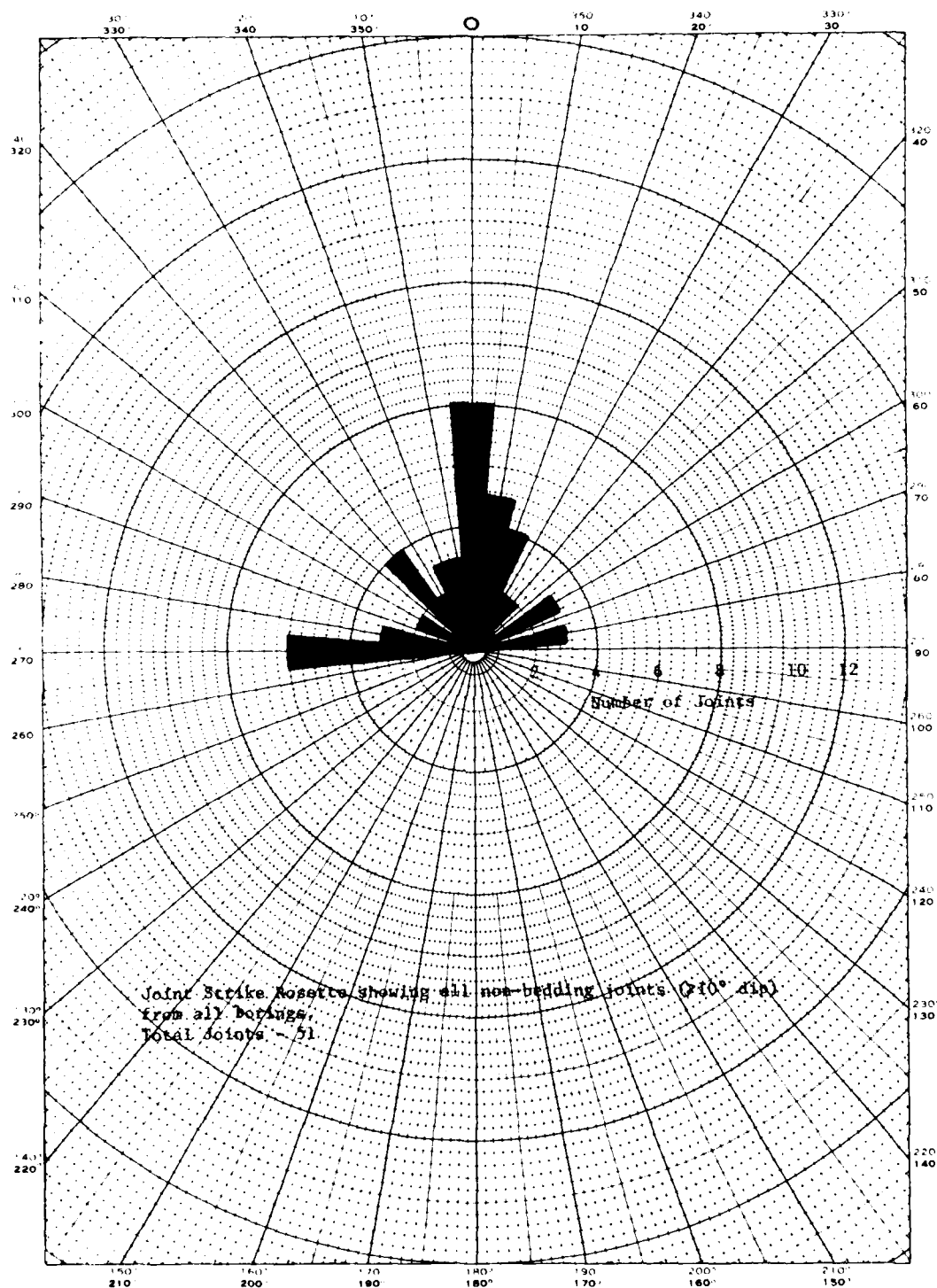
CW-13-79



### Joint Frequency Diagrams, 5 Foot Intervals



Joint Frequency Diagrams, 5 Foot Intervals





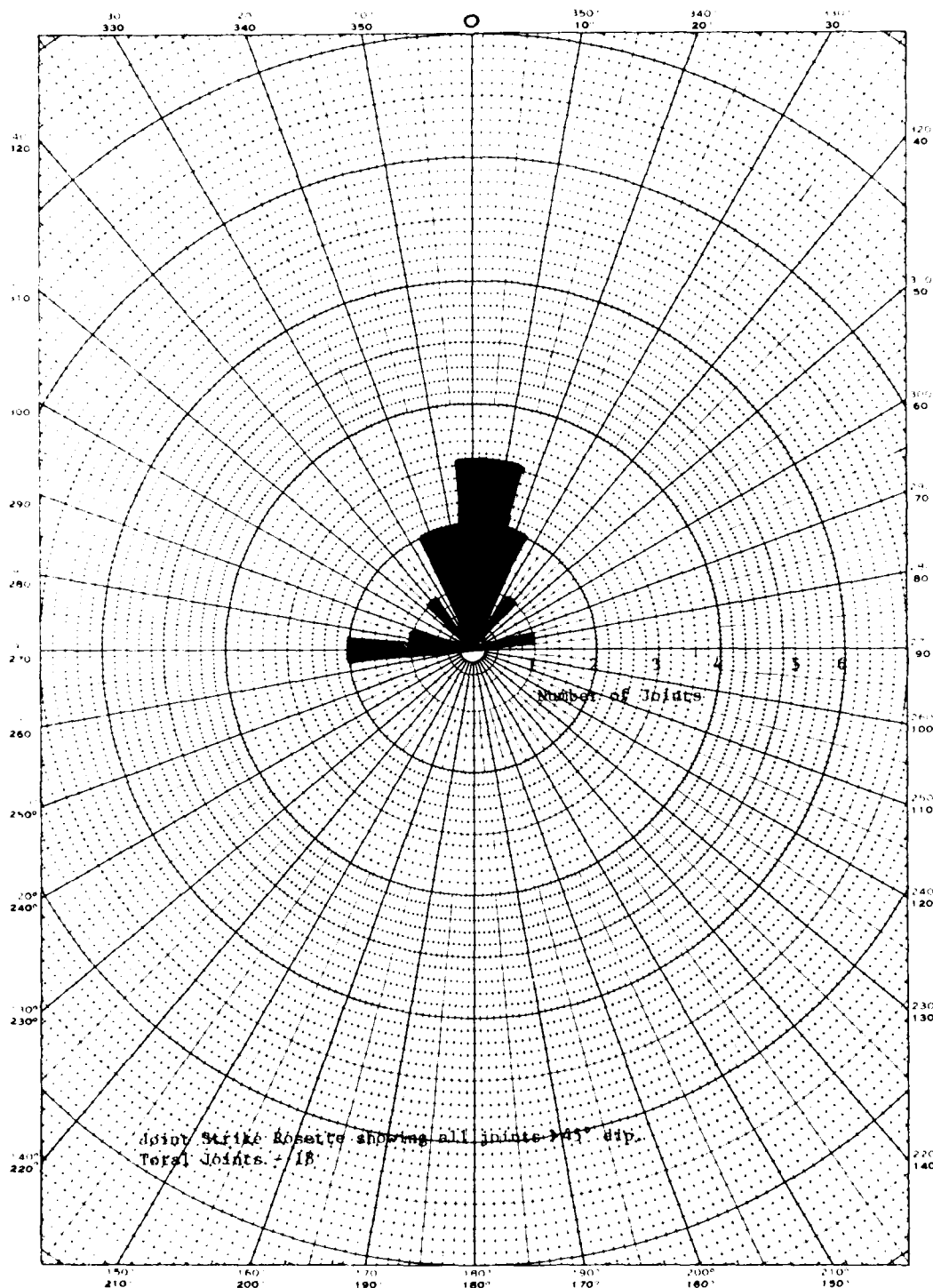
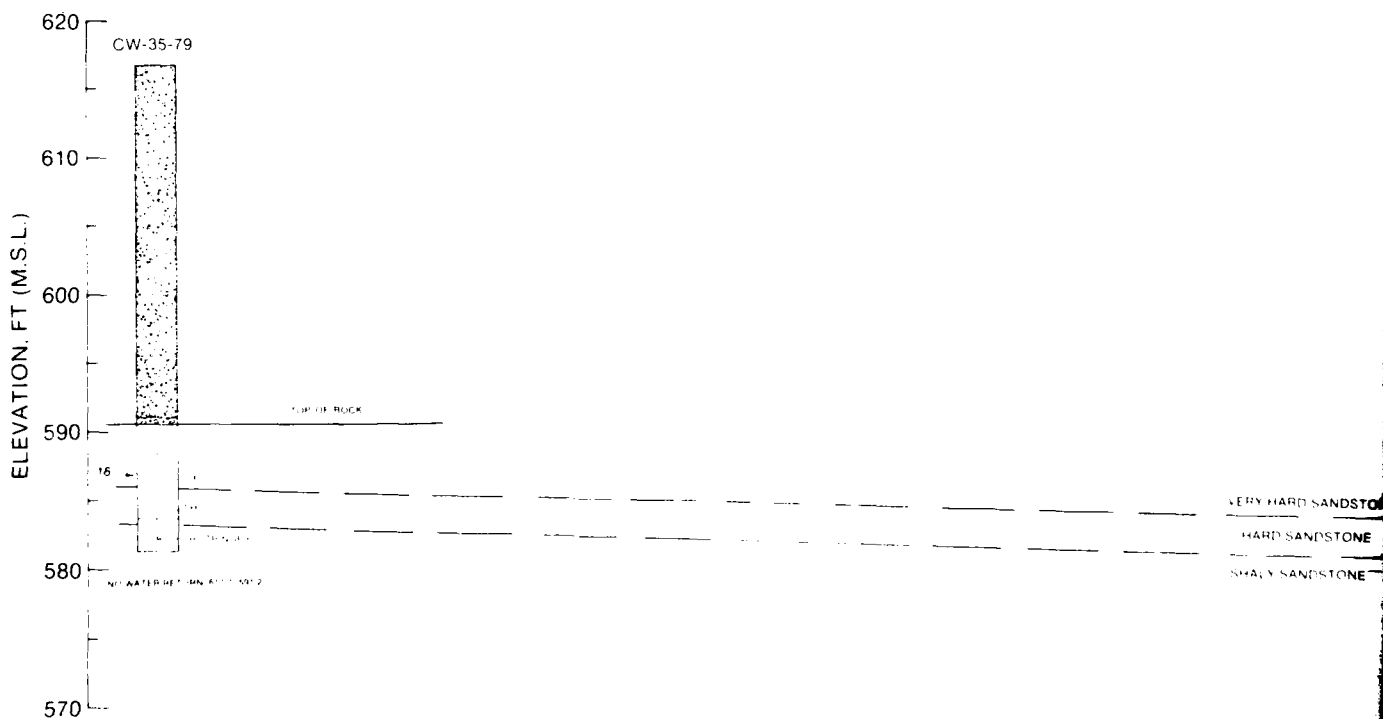
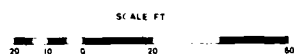


PLATE C7

APPENDIX D  
GEOLOGY, BORING LOCATION AND  
CROSS SECTIONS  
REGULATORY STRUCTURE

<u>Plate No.</u>	<u>Description of Plates</u>
D1	Boring Location Plan & Geologic Cross Section, Section A-A' in Foundation Exploration, Geologic Cross Section, Section A-A'
D2	Geologic Cross Section, Section B-B'
D3	Geologic Cross Section, Section C-C'
D4	Geologic Cross Section, Section D-D'
D5	Geologic Cross Section, Section E-E'
D6	Geologic Cross Section, Section F-F'
D7	Geologic Cross Section, Section G-G'
D8	Characterization and Engineering Design Properties

# BORING LOCATION PLAN

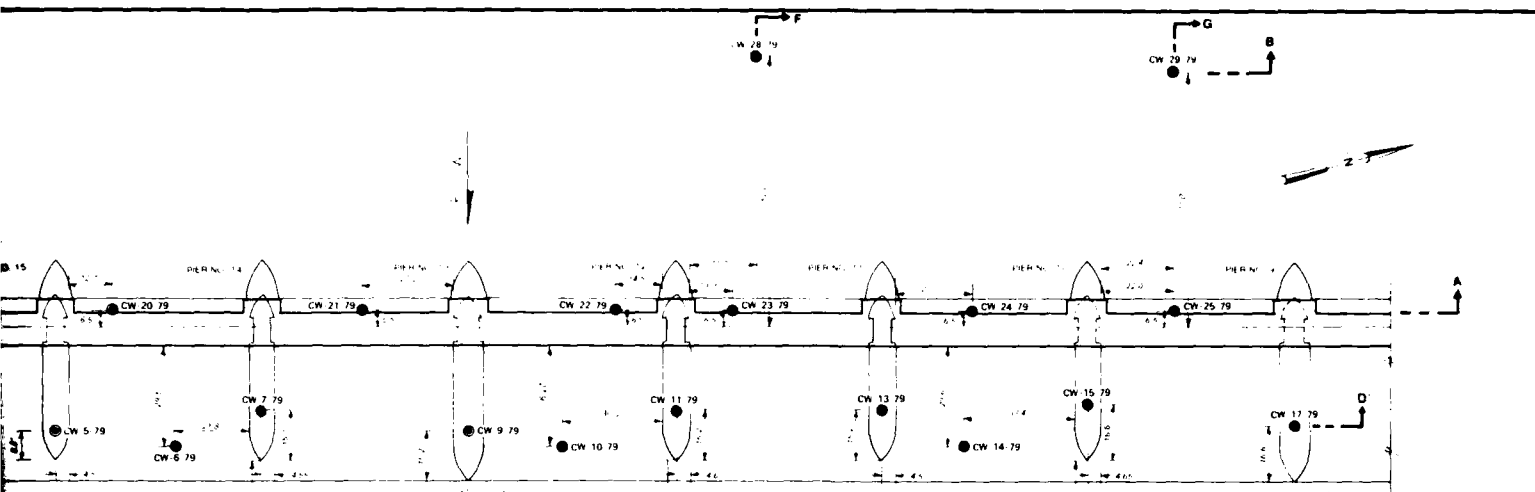


SEE PLATE D1 (SHEET 2 OF 4) FOR LEGEND

SEE PLATE D8 FOR CHARACTERIZATION AND ENGINEERING DESIGN PROPERTIES OF THE FOUNDATION ROCK

NUMBERS ADJACENT TO BORINGS IDENTIFY LOCATION OF TEST SPECIMENS AND TEST RESULTS GIVEN ON PLATE D8

BORING NUMBER	ELEVATION FT		CORE SIZE IN	CORE RECOVERY %
	TOP OF BORING	BOTTOM OF CORE		
CW-35-79	616.75	581.35	4	40
CW-18-79	589.8	575.8	6	100

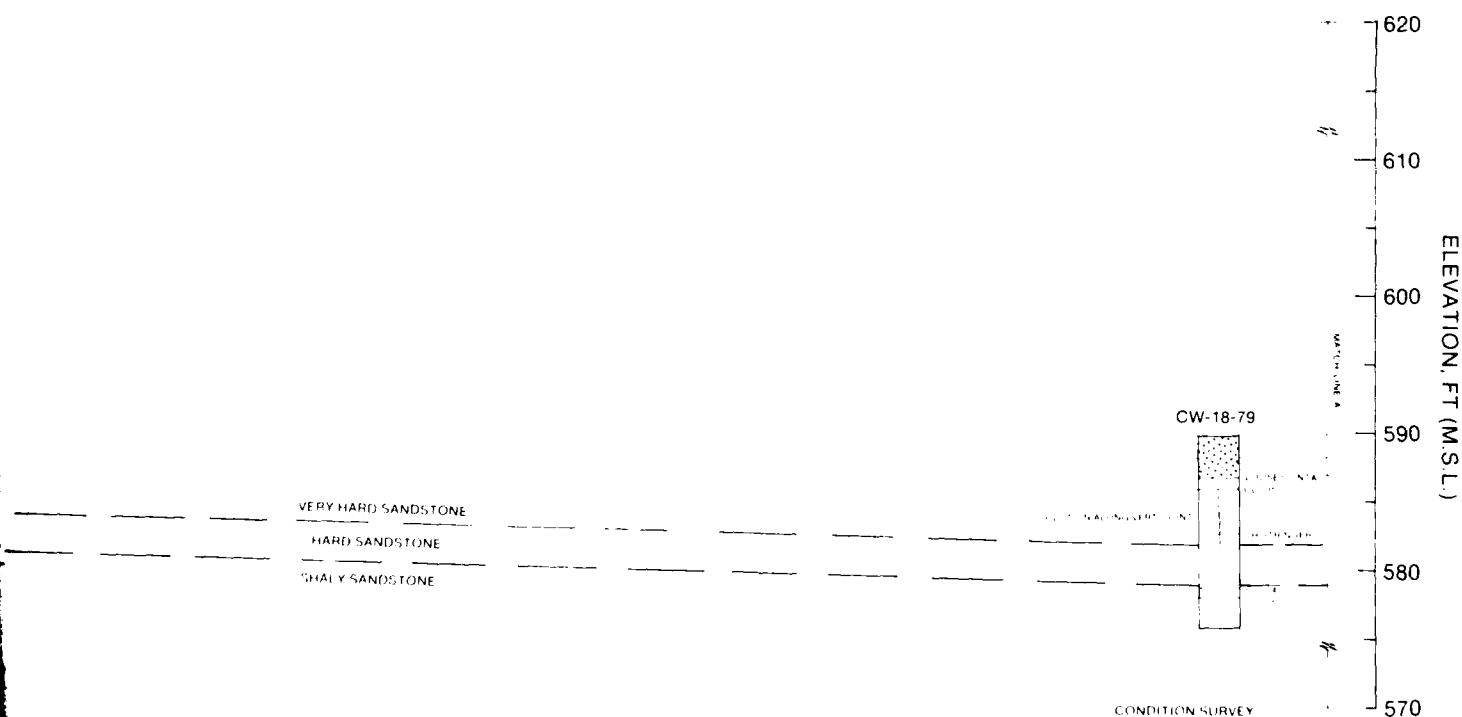


● CW-31-79

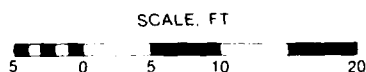
● CW-32-79

● CW-33-79

SYMBOLS  
 PROPOSED  
 C  
 DESCRIPTION  
 6 CORE HOLE  
 4 CORE HOLE  
 COMPLETED  
 ●



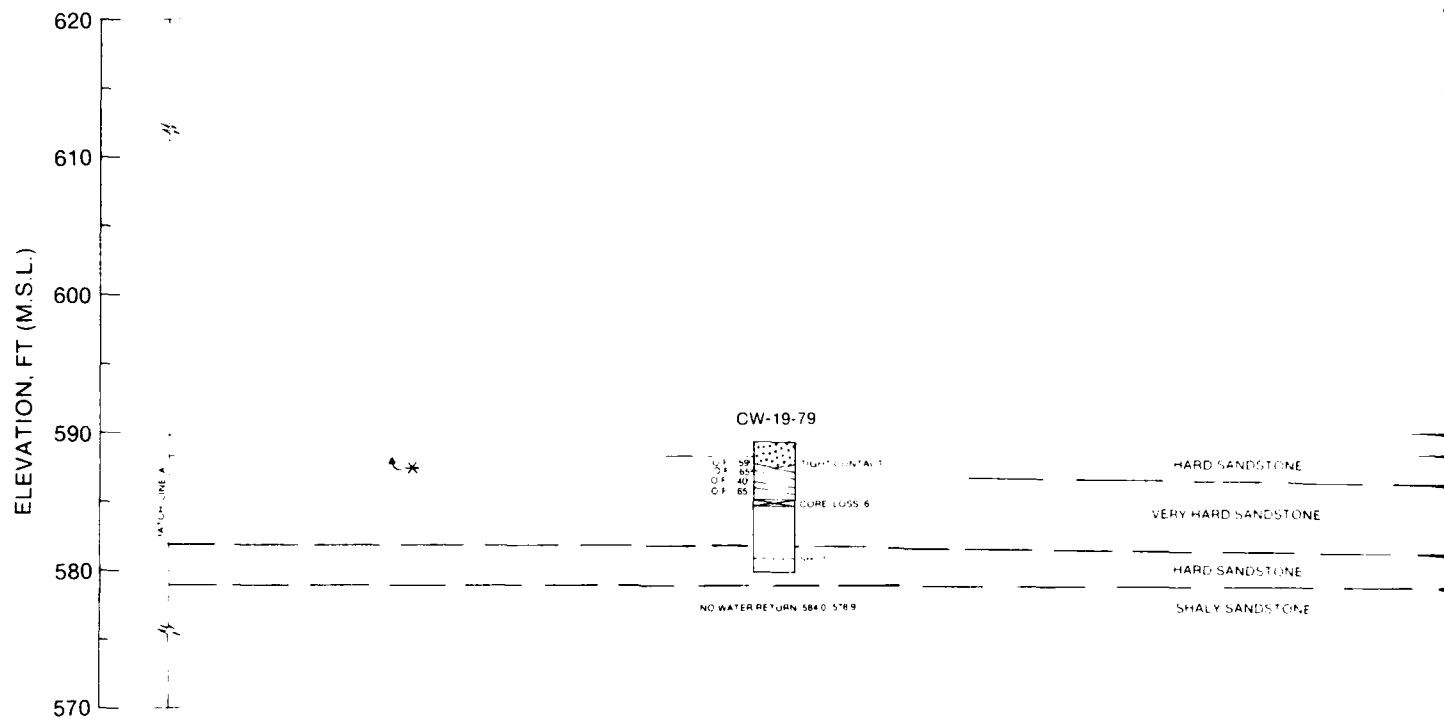
FT	CORE SIZE IN	CORE RECOVERY %
BTM		
135	4	40
138	6	100



CONDITION SURVEY  
 DECEMBER 1979  
 COMPENSATING WORKS  
 SAULT STE MARIE, MICHIGAN  
**BORING LOCATION PLAN &  
 GEOLOGIC CROSS SECTION**  
 SECTION A-A'

SHEET 1 OF 4

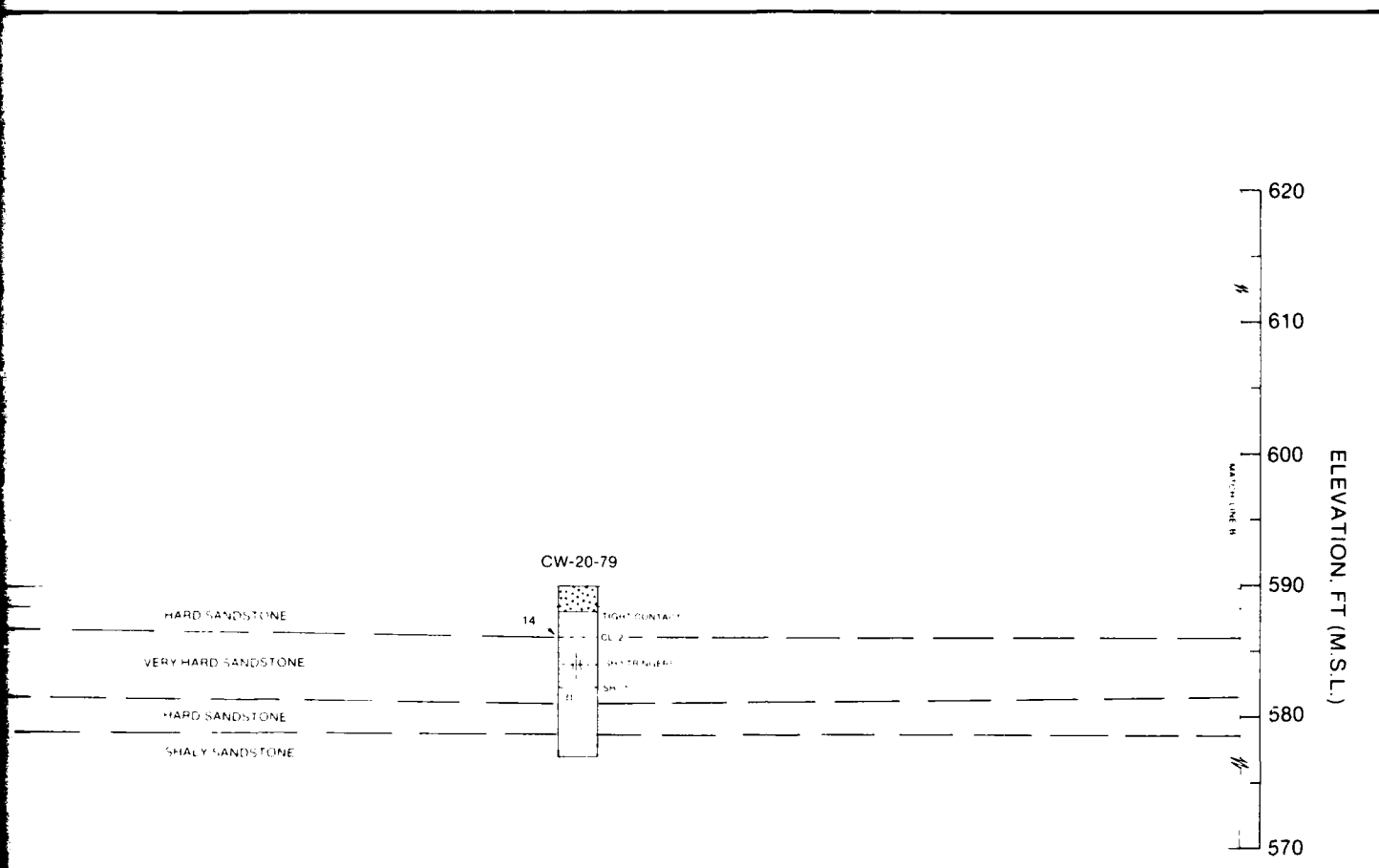
PLATE D1



BORING NUMBER	ELEVATION FT		CORE SIZE IN	CORE RECOVERY %
	TOP OF BORING	BOTTOM OF CORE		
CW-19-79	588.5	578.9	4	90.9
CW-20-79	589.9	576.9	6	99.7

#### LEGEND

- ROCK UNIT CONTACT
- CONCRETE
- SHALE, CLAY, OR CLAY-SHALE SEAM
- CORE LOSS ZONE
- FRACTURE, JOINT, OR PARTING
- OF OPEN FRACTURE, JOINT, OR PARTING
- CF CLOSED FRACTURE, JOINT, OR PARTING
- CL CLAY SEAM
- SH SHALE SEAM
- CL-SH CLAY-SHALE SEAM
- \* BASE OF CONCRETE AS SHOWN ON WORKING DRAWINGS



# LEGEND

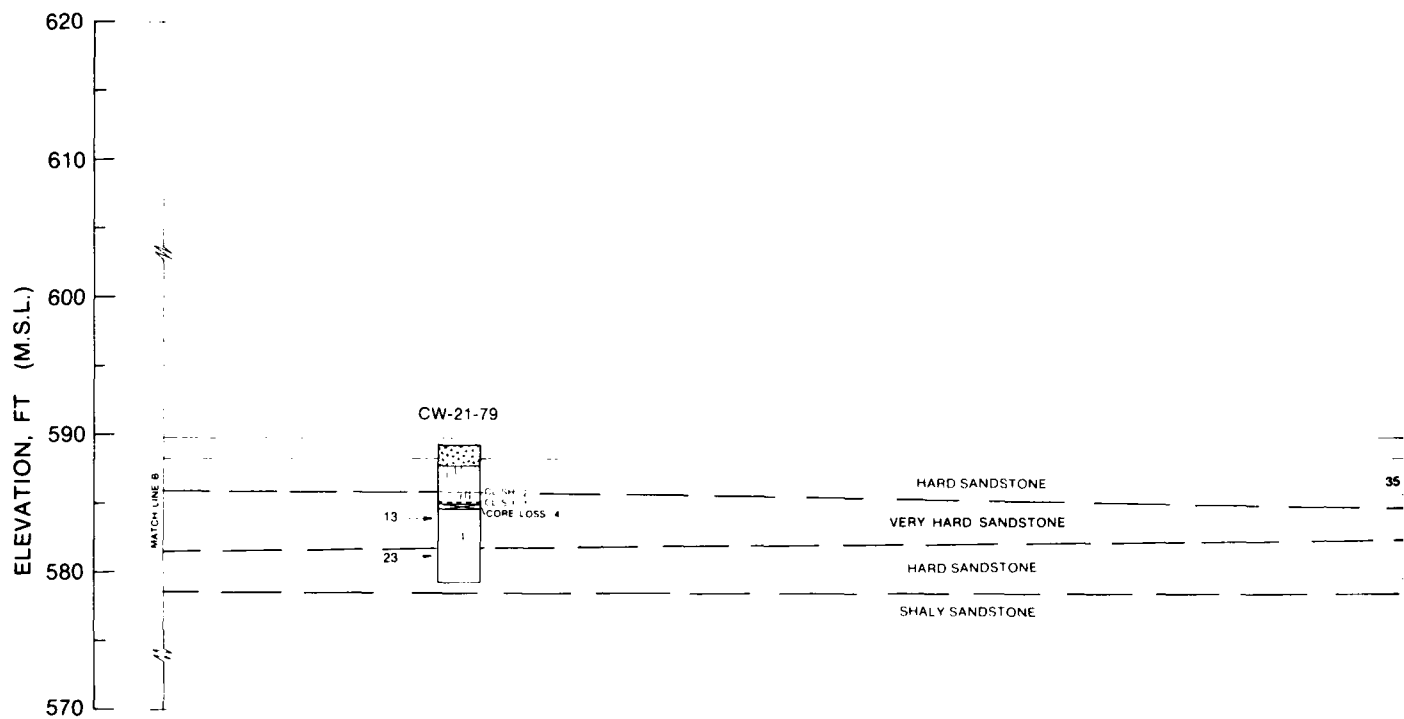
- ROCK UNIT CONTACT
- CONCRETE
- SHALE, CLAY, OR CLAY-SHALE SEAM
- CORE LOSS ZONE
- FRACTURE, JOINT, OR PARTING
- OF OPEN FRACTURE, JOINT, OR PARTING
- OF CLOSED FRACTURE, JOINT, OR PARTING
- CLAY SEAM
- SHALE SEAM
- CLAY-SHALE SEAM
- OF CONCRETE AS SHOWN ON WORKING DRAWING

CONDITION SURVEY  
 DECEMBER 1979  
 COMPENSATING WORKS  
 SAULT STE. MARIE, MICHIGAN  
**GEOLOGIC CROSS SECTION**

SECTION A—A'

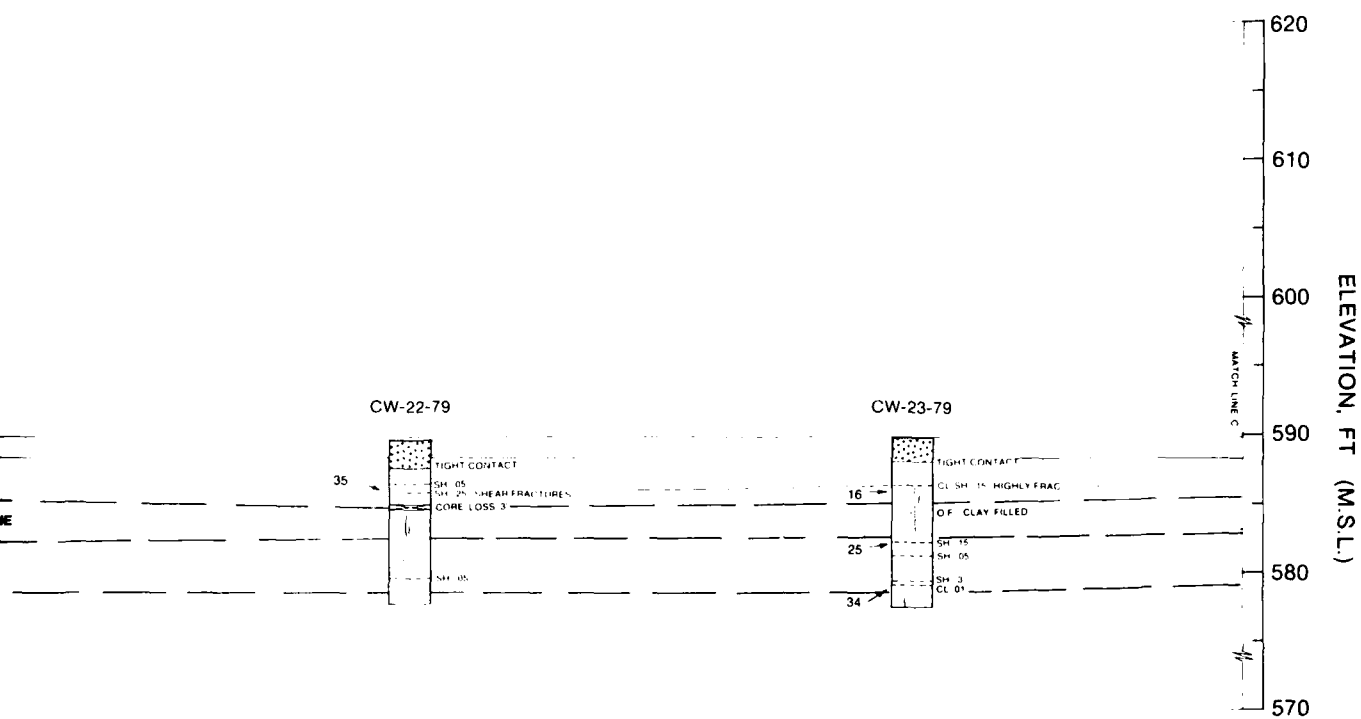
SHEET 2 OF 4

PLATE D1



BORING NUMBER	ELEVATION, FT		CORE SIZE, IN	CORE RECOVERY, %
	TOP OF BORING	BOTTOM OF CORE		
CW-21-79	589.2	579.35	4	94
CW-22-79	589.5	577.6	4	95.8
CW-23-79	589.7	577.4	4	100





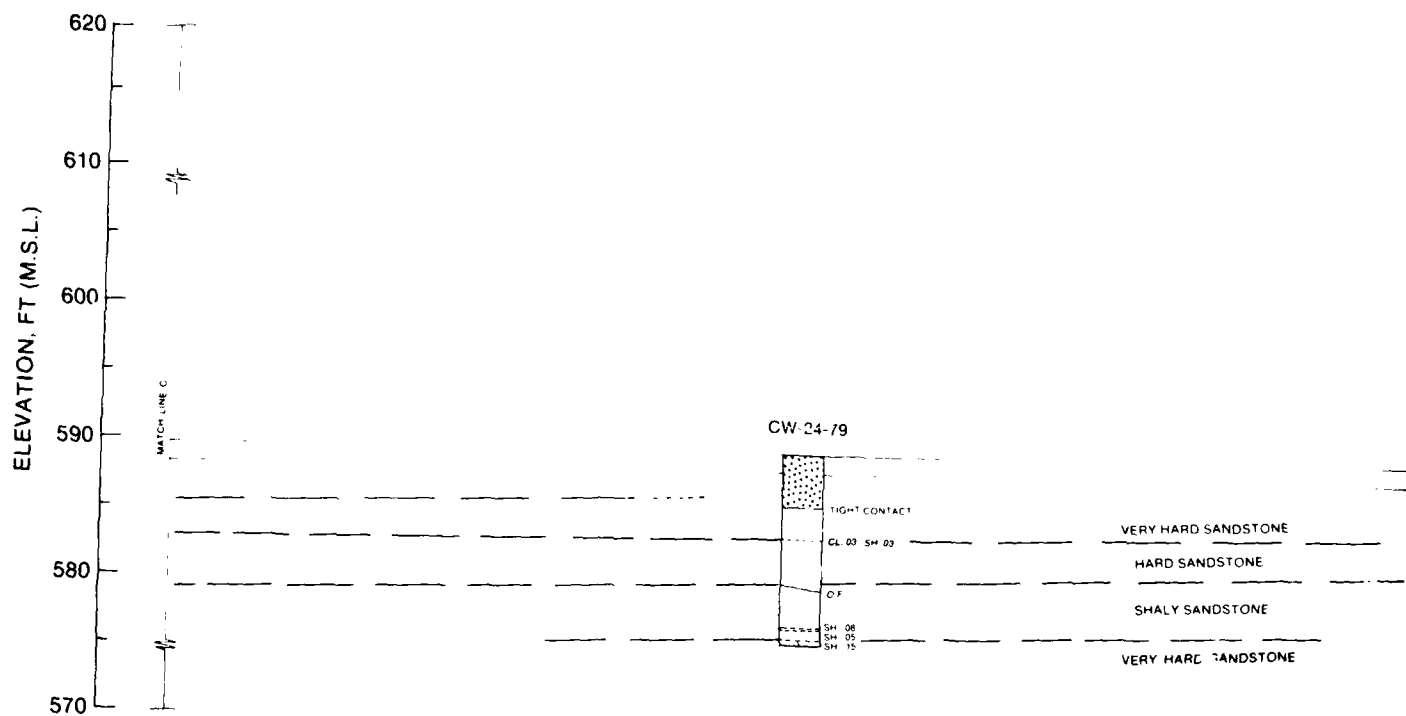
CONDITION SURVEY  
DECEMBER 1979  
COMPENSATING WORKS  
SAULT STE MARIE, MICHIGAN  
**GEOLOGIC CROSS SECTION**

SECTION A-A'

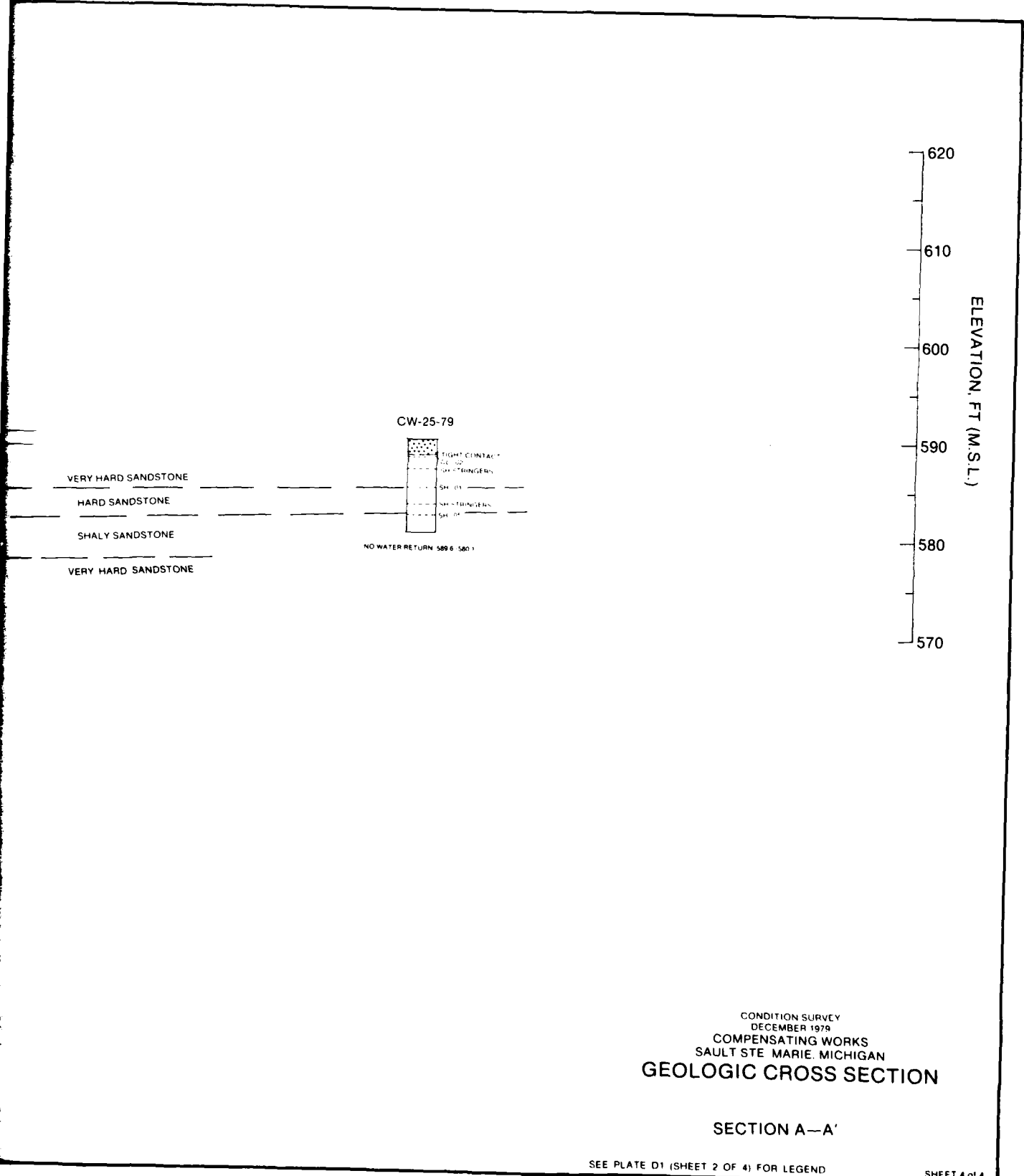
SEE PLATE D1 (SHEET 2 OF 4) FOR LEGEND

SHEET 3 of 4

PLATE D1



BORING NUMBER	ELEVATION, FT		CORE SIZE, IN	CORE RECOVERY, %
	TOP OF BORING	BOTTOM OF CORE		
CW-24-79	589.7	575.7	4	100
CW-25-79	589.6	580.1	4	95



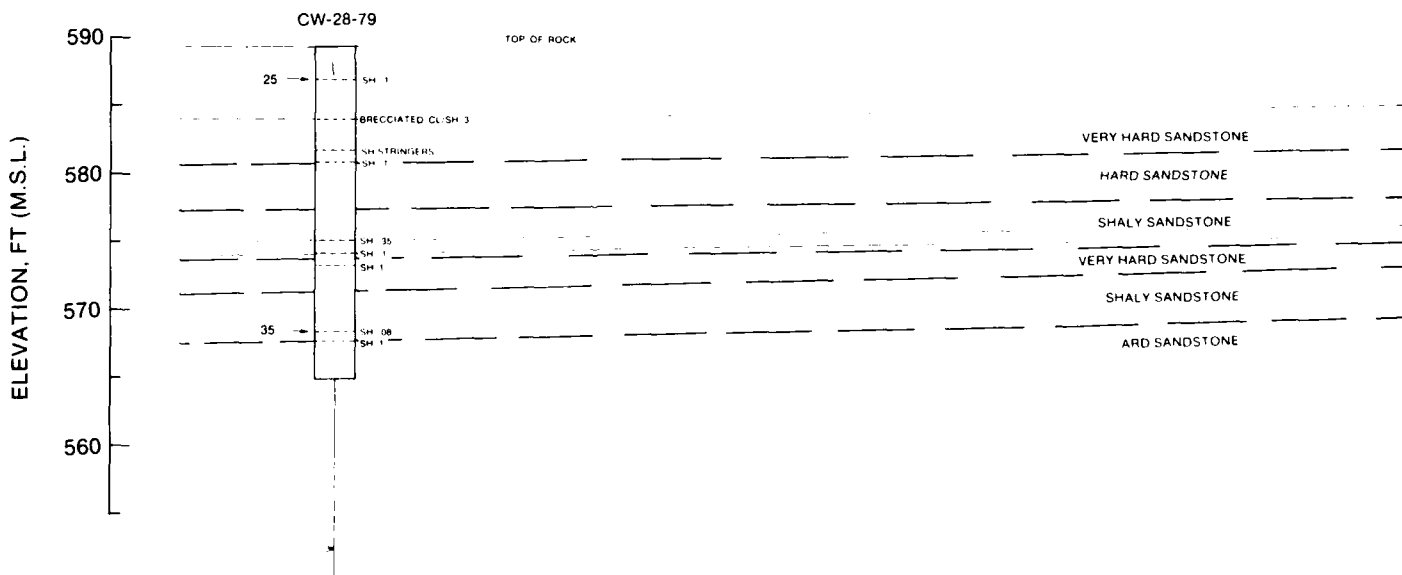
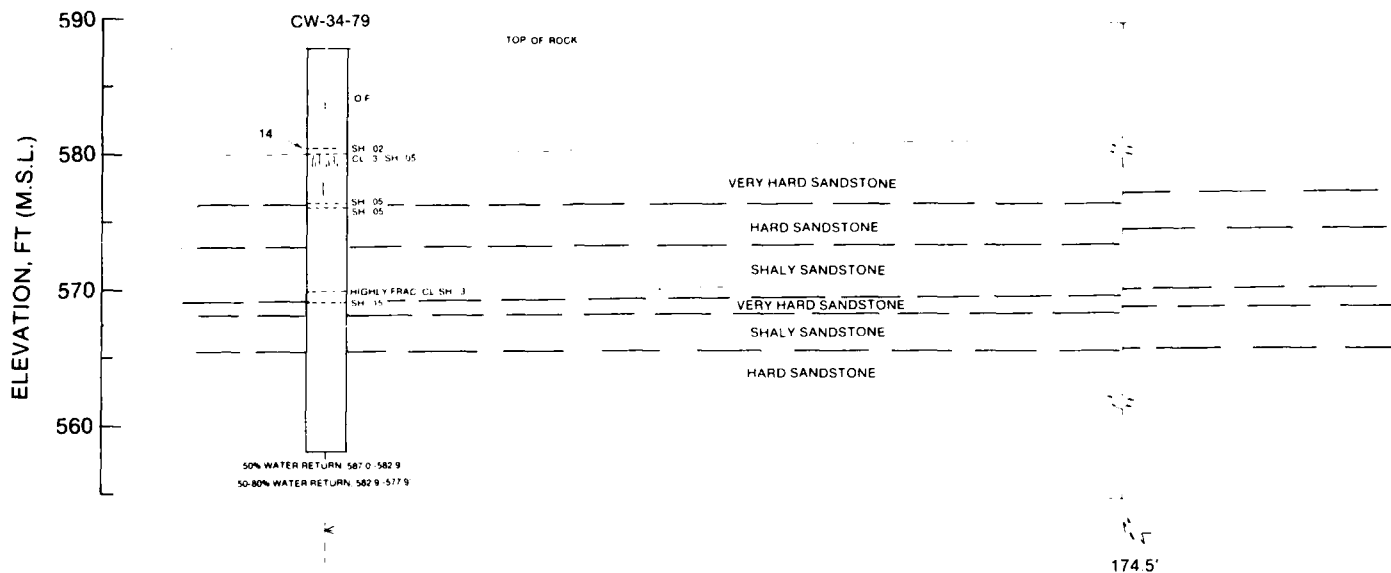
CONDITION SURVEY  
DECEMBER 1979  
COMPENSATING WORKS  
SAULT STE MARIE, MICHIGAN  
**GEOLOGIC CROSS SECTION**

SECTION A—A'

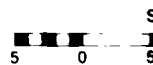
SEE PLATE D1 (SHEET 2 OF 4) FOR LEGEND

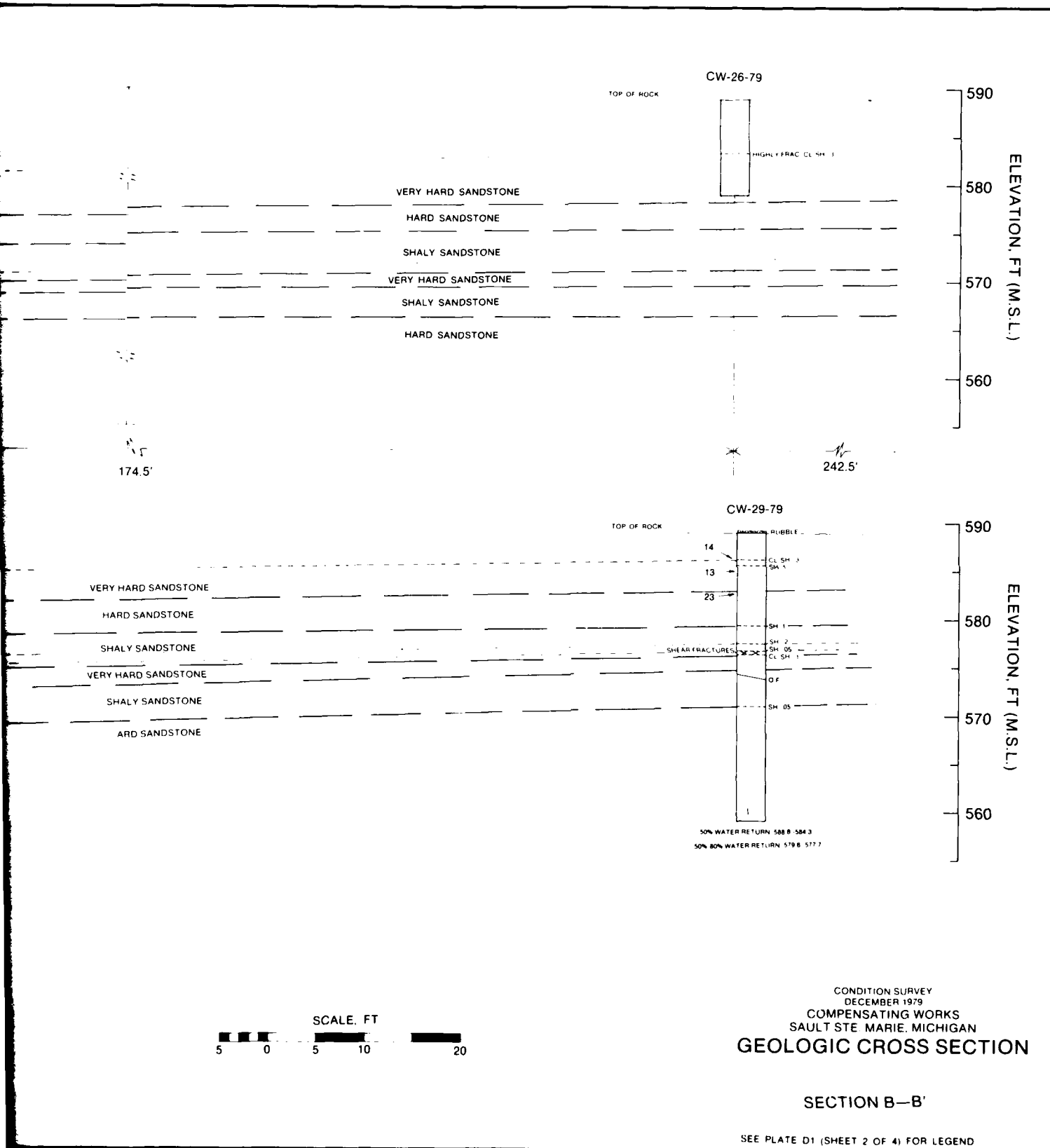
SHEET 4 of 4

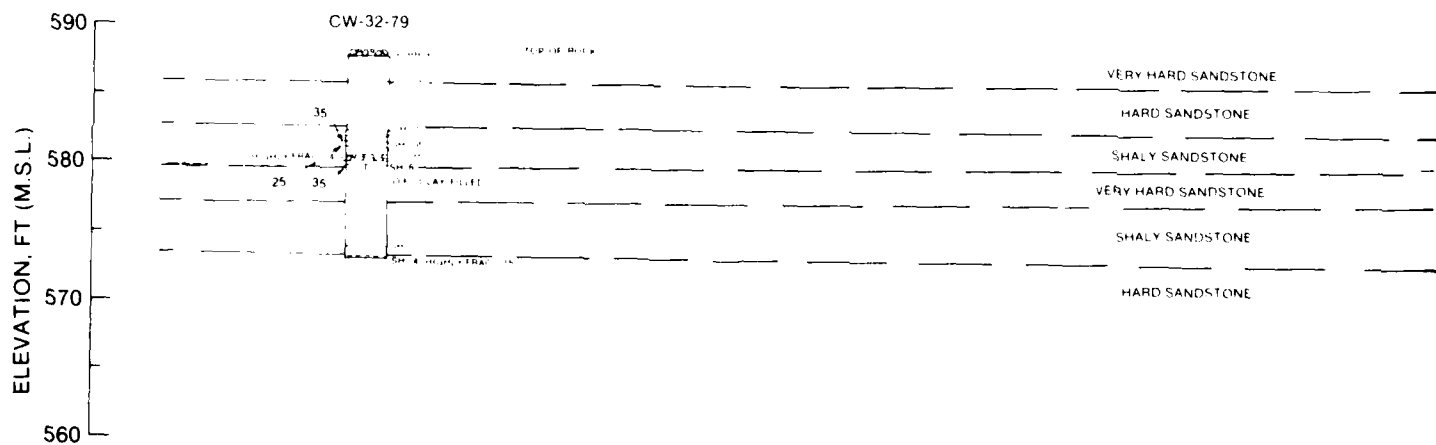
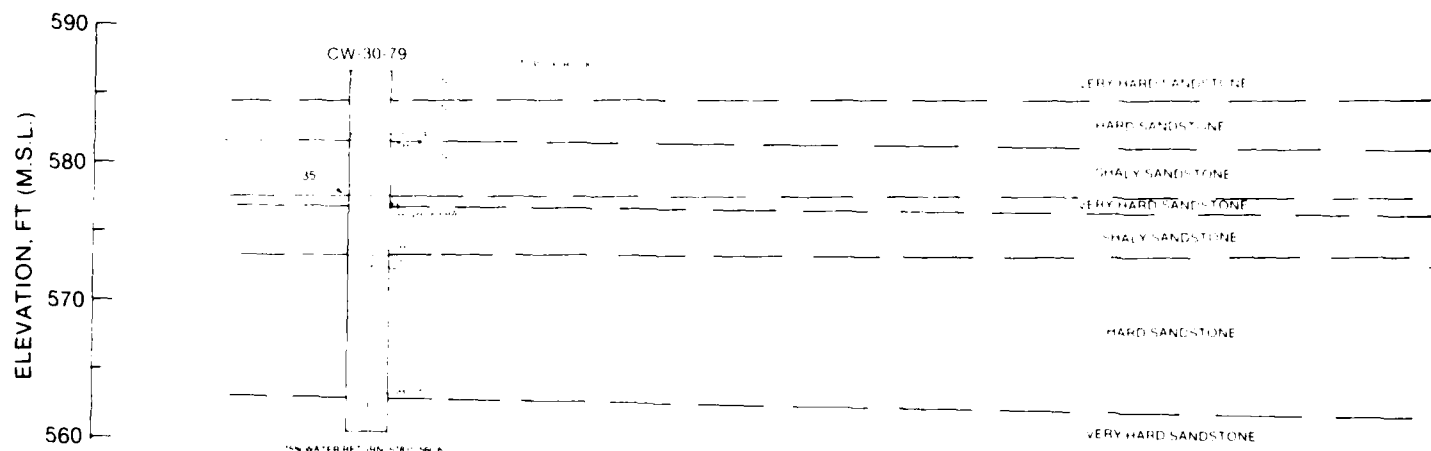
PLATE D1



BORING NUMBER	ELEVATION, FT		CORE SIZE, IN	CORE RECOVERY, %
	TOP OF BORING	BOTTOM OF CORE		
CW-34-79	587.9	558.2	4	99.0
CW-26-79	588.9	579.0	6	98
CW-28-79	589.4	565.0	4	98.4
CW-29-79	589.3	559.1	4	98.7



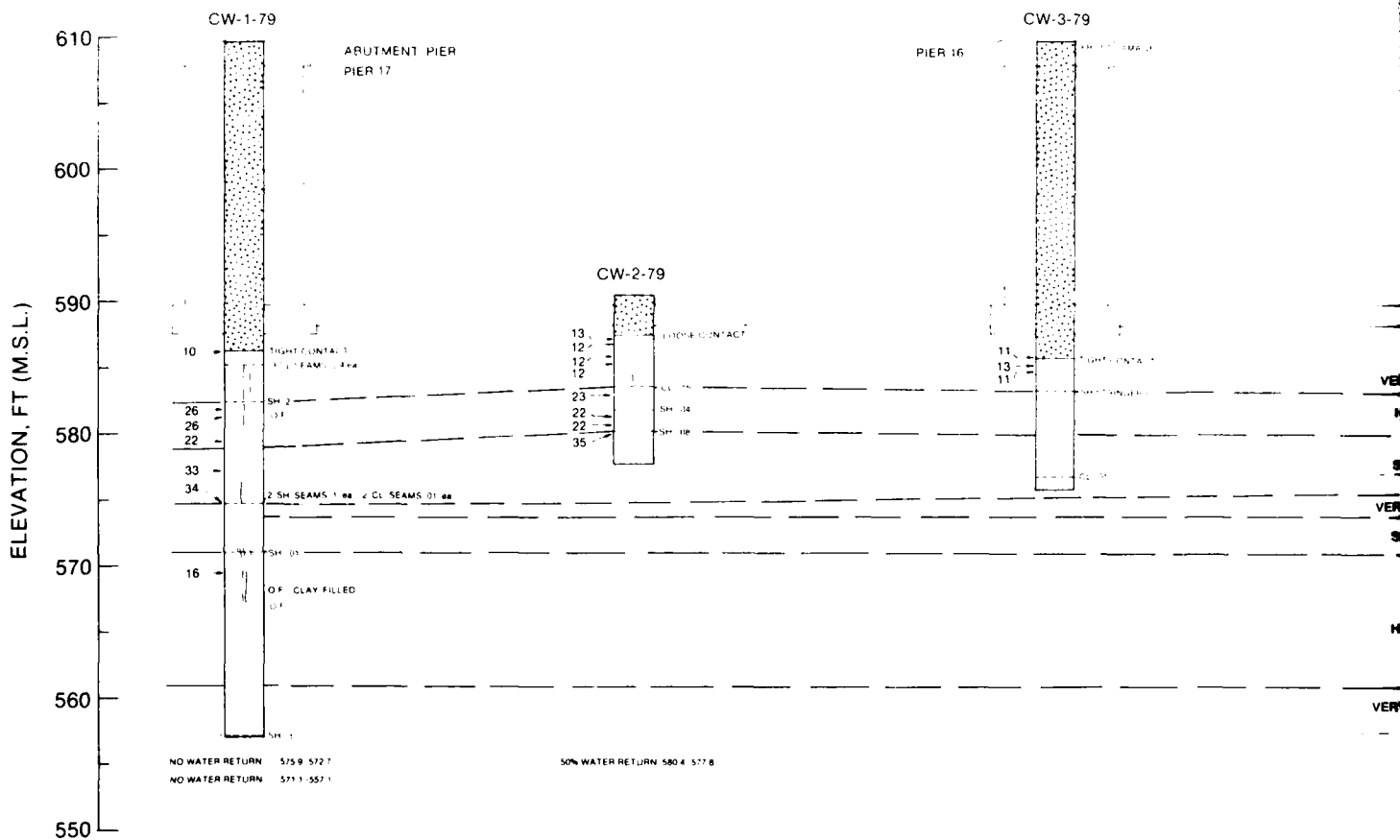




BORING NUMBER	ELEVATION, FT		CORE SIZE IN	CORE RECOVERY %
	TOP OF BORING	BOTTOM OF CORE		
CW-30-79	586.7	560.6	4	100
CW-31-79	589.6	560.8	4	97.4
CW-32-79	588.6	573.4	4	100
CW-33-79	588.7	564.9	4	96.2

5 0



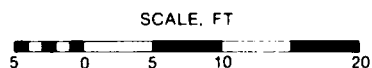
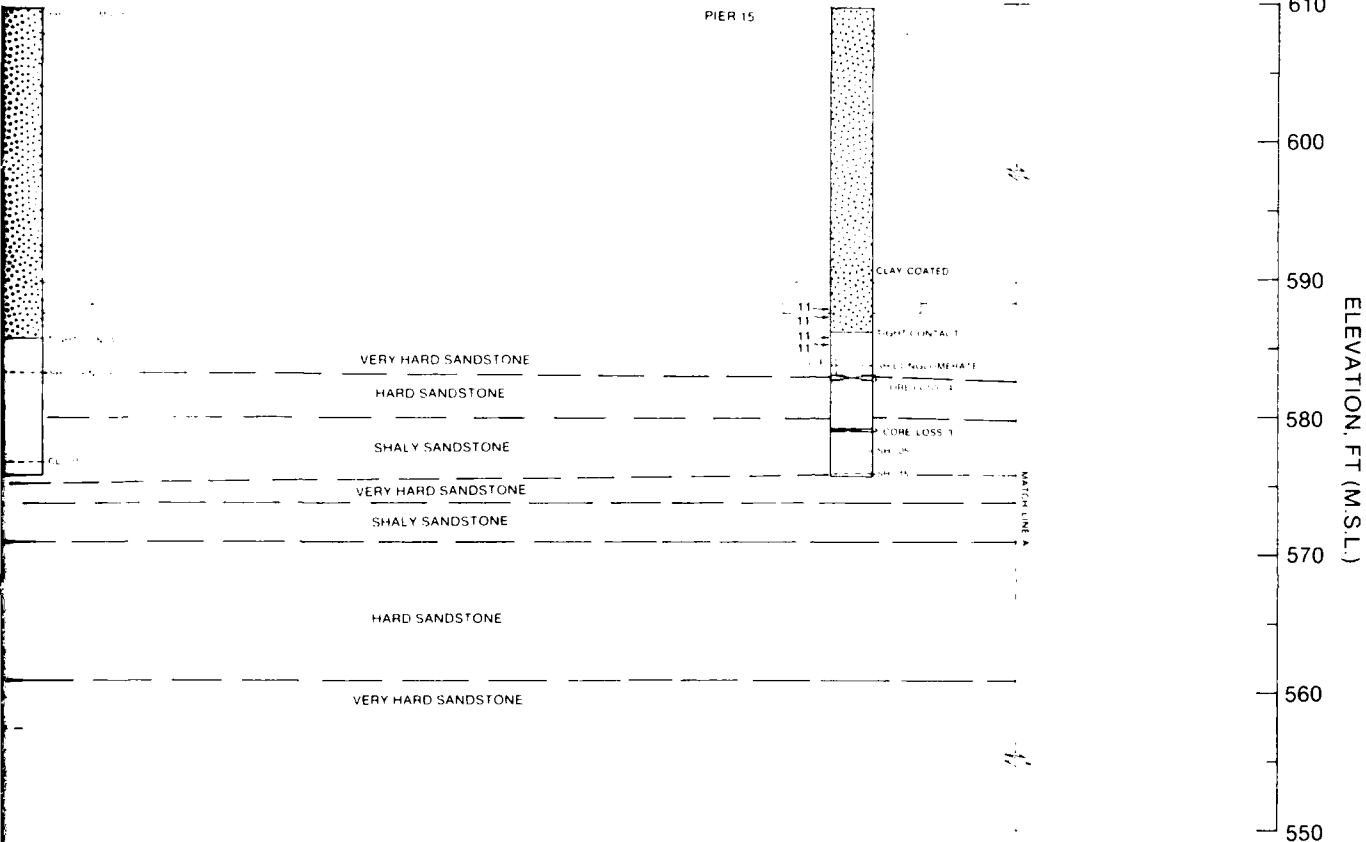




W-3-79

CW-5-79

PIER 15



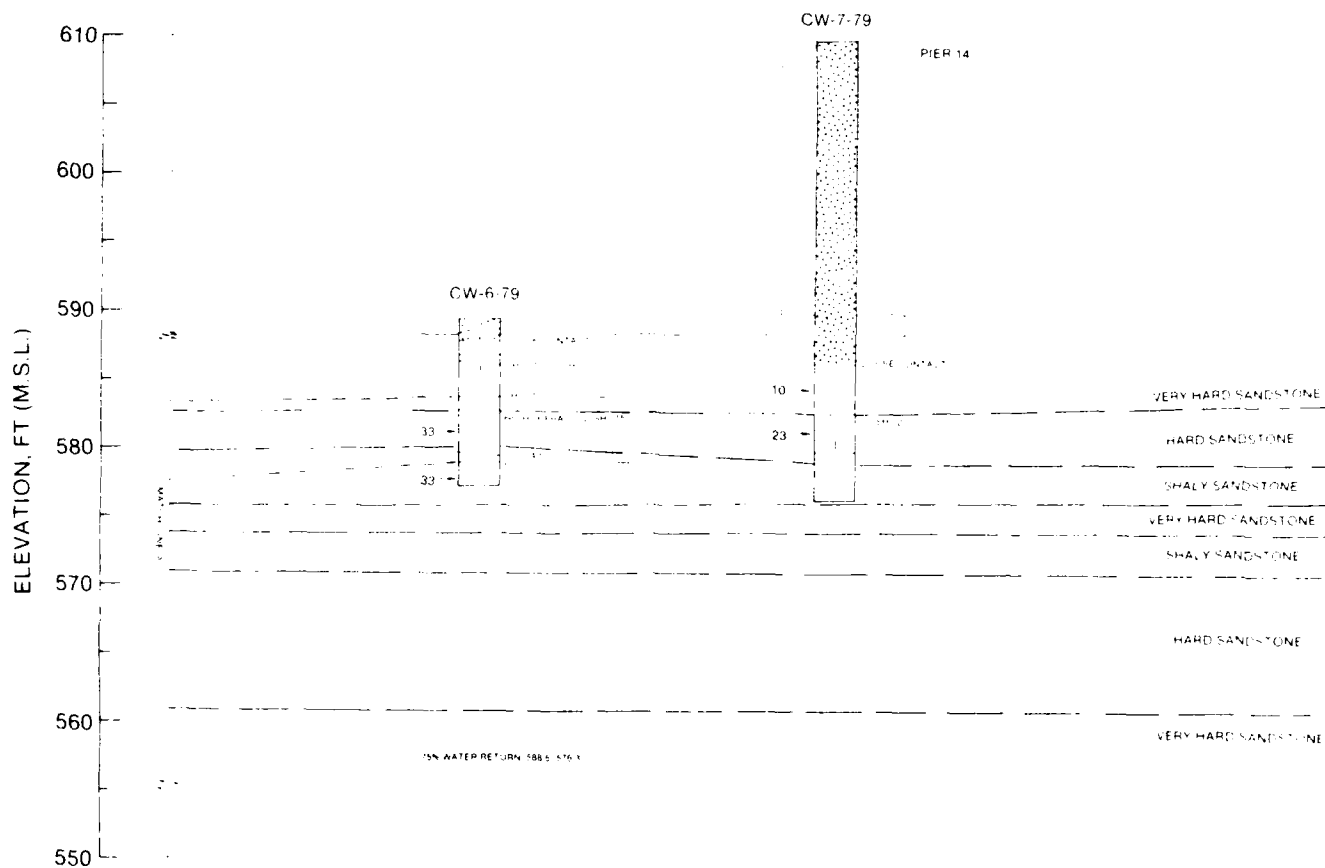
CONDITION SURVEY  
DECEMBER 1979  
COMPENSATING WORKS  
SAULT STE MARIE, MICHIGAN  
**GEOLOGIC CROSS SECTION**

SECTION D-D'

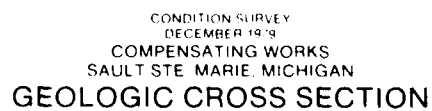
SEE PLATE D1 (SHEET 2 OF 4) FOR LEGEND

SHEET 1 OF 4

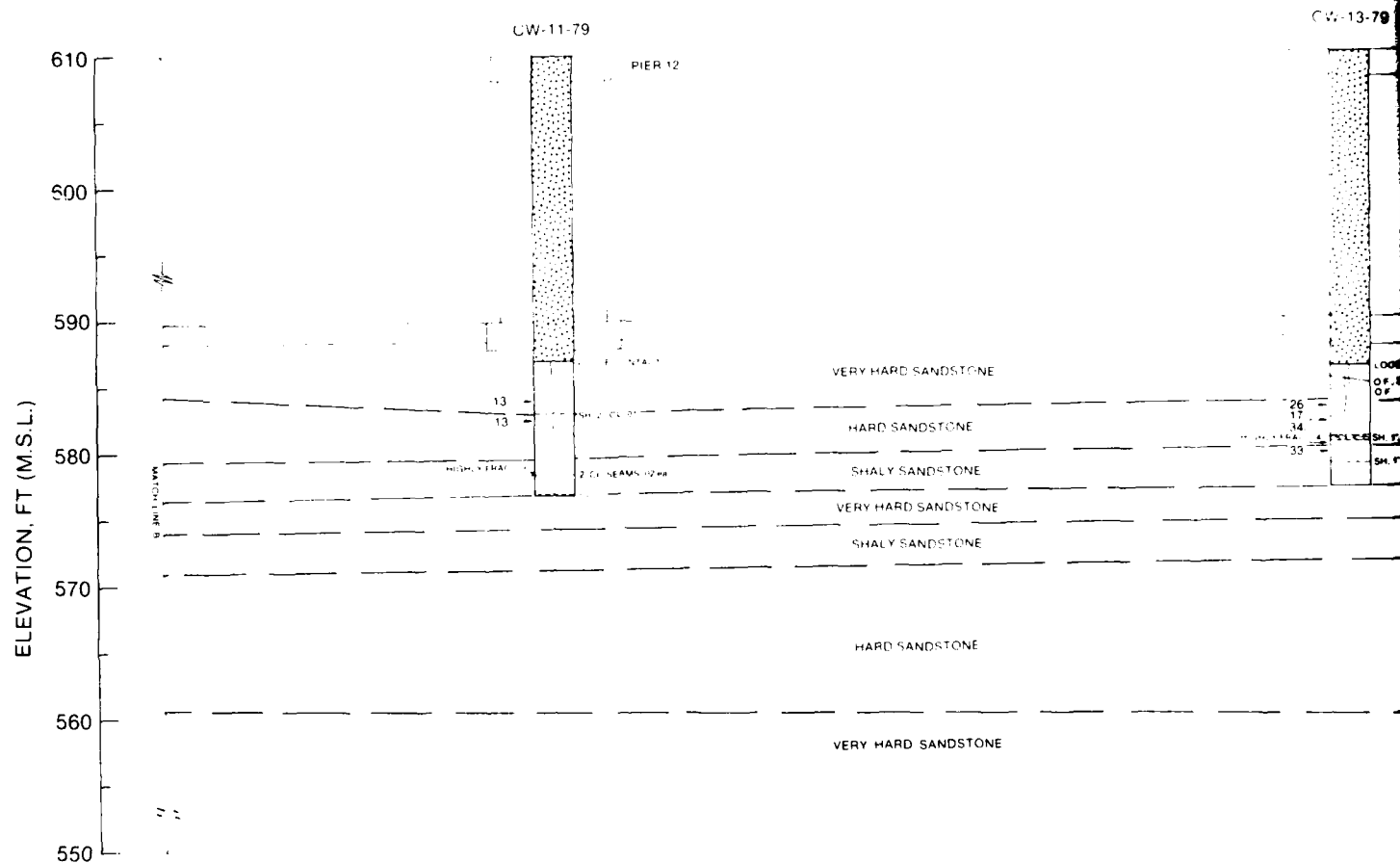
PLATE D4



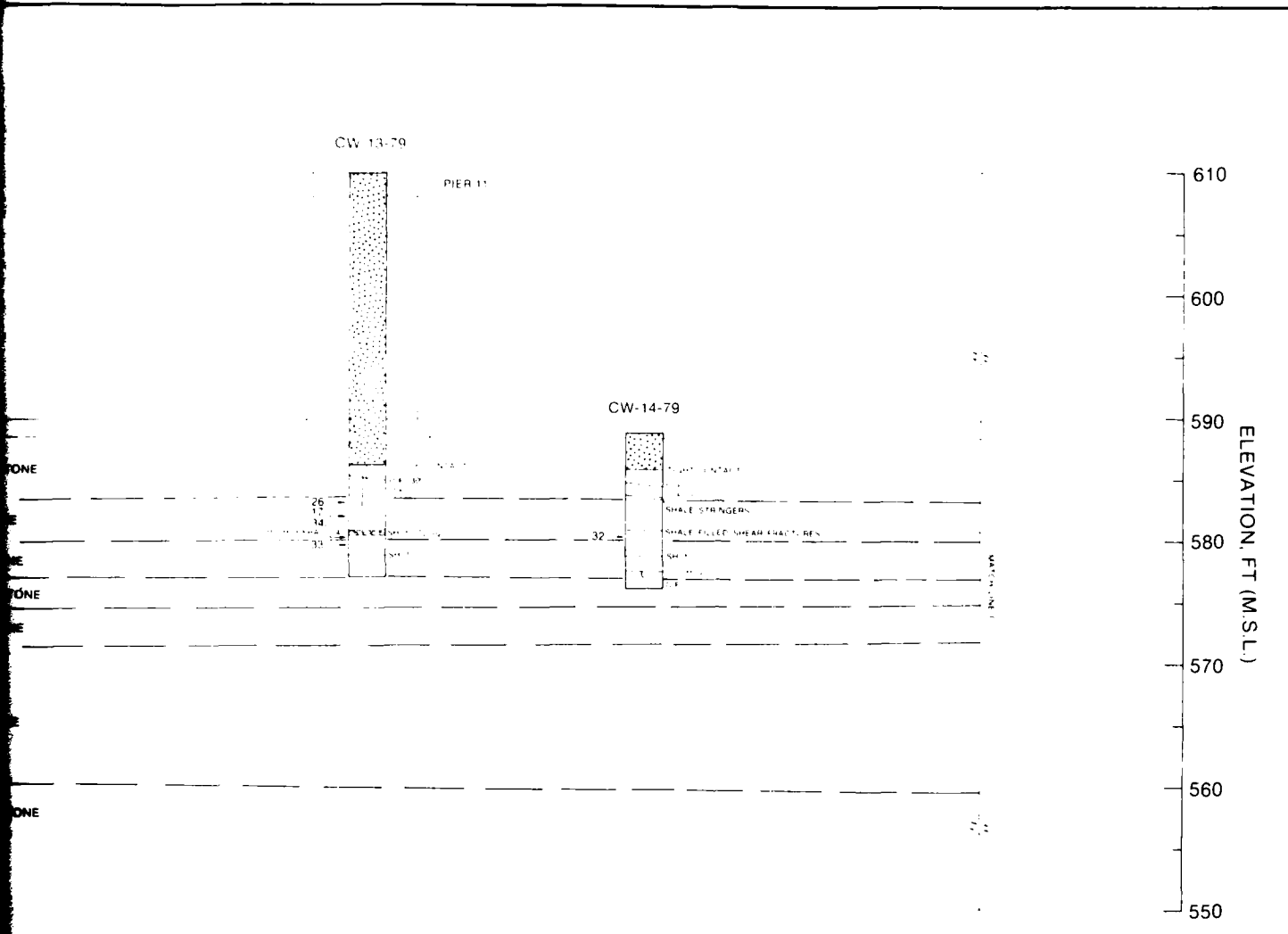
BORING NUMBER	ELEVATION FT		CORE SIZE IN	CORE RECOVERY %
	TOP OF BORING	BOTTOM OF CORE		
CW 6-79	589.75	577.5	4	100
CW 7-79	609.75	576.35	4	100
CW 9-79	609.83	556.73	6	100
CW 12-79	590.5	577.40	4	97



SHEET 2 of 4



BORING NUMBER	ELEVATION FT		CORE SIZE IN	CORE RECOVERY %
	TOP OF BORING	BOTTOM OF CORE		
CW-11-79	609.73	576.73	4	100
CW-13-79	609.74	576.99	4	100
CW-14-79	588.65	576.15	4	100



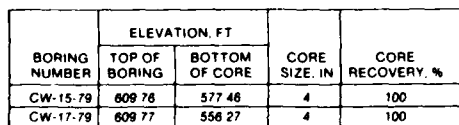
CONDITION SURVEY  
DECEMBER 1979  
COMPENSATING WORKS  
SAULT STE MARIE, MICHIGAN  
**GEOLOGIC CROSS SECTION**

SECTION D—D'

SEE PLATE D1 (SHEET 2 OF 4) FOR LEGEND

SHEET 3 OF 4

PLATE D4



BORING NUMBER	ELEVATION, FT		CORE SIZE, IN	CORE RECOVERY, %
	TOP OF BORING	BOTTOM OF CORE		
CW-15-79	609 76	577 48	4	100
CW-17-79	609 77	556 27	4	100

CW-17-79

PIER 9

HIGHLY FRAC. 135

LOOSE CONTACT  
OF CLAY FILLED  
CL SH

22

33

HIGHLY FRAC. CL SH 35

CL W CL SEAMS 01 03 CL FILLED SHEAR FRACTURES  
HIGHLY FRAC. NOT SEPARATED 65

25

SH 1

SH 1

SH 1

2 SH SEAMS 05 00

610

600

590

580

570

560

550

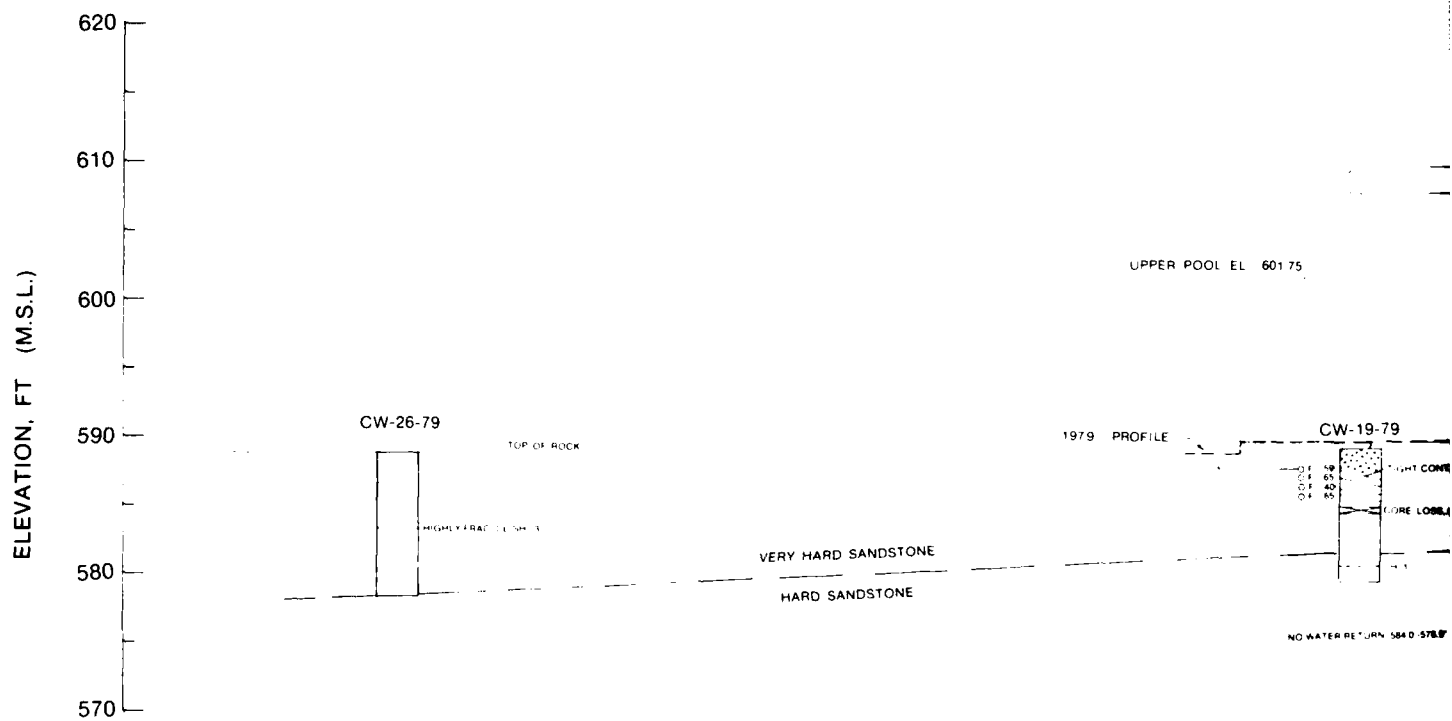
ELEVATION, FT (M.S.L.)

CONDITION SURVEY  
DECEMBER 1979  
COMPENSATING WORKS  
SAULT STE. MARIE, MICHIGAN  
**GEOLOGIC CROSS SECTION**  
SECTION D—D'

SEE PLATE D1 (SHEET 2 OF 4) FOR LEGEND

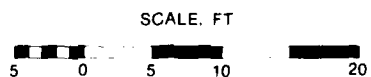
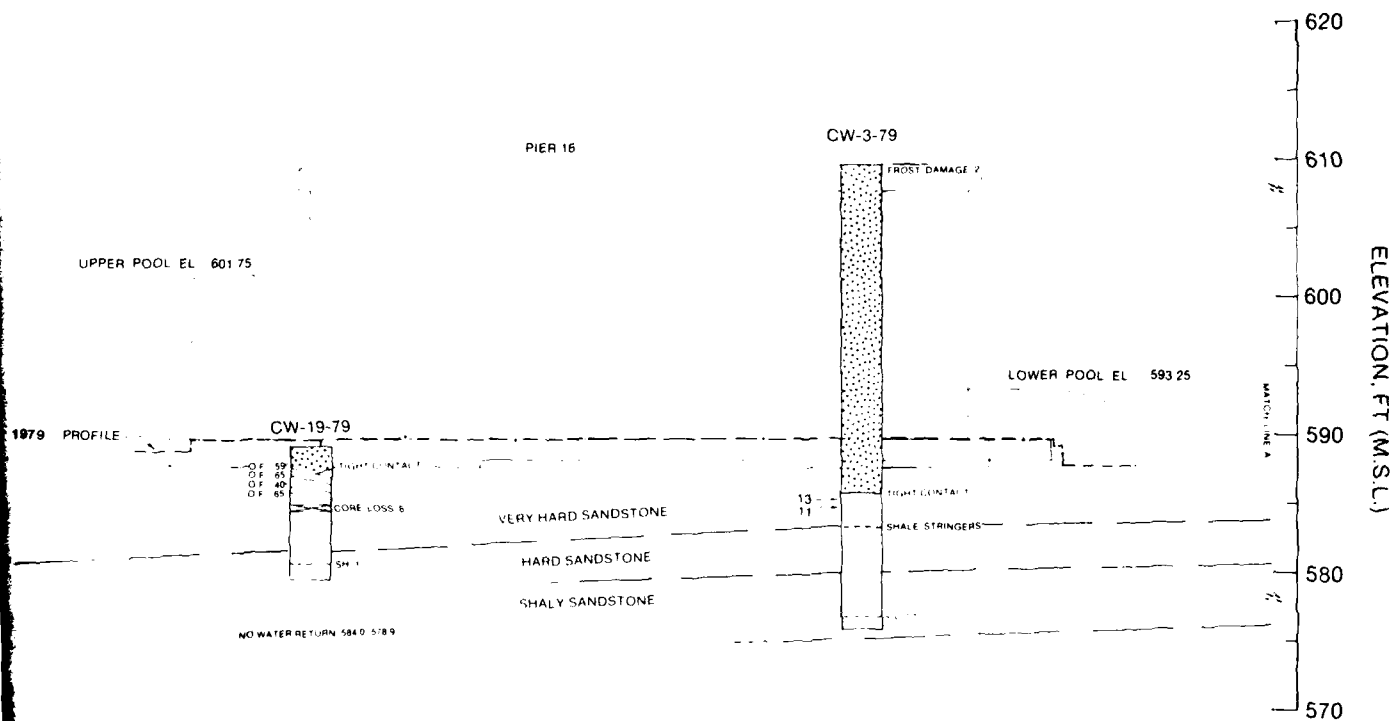
SHEET 4 of 4

PLATE D4



BORING NUMBER	ELEVATION FT		CORE SIZE IN	CORE RECOVERY %
	TOP OF BORING	BOTTOM OF CORE		
CW-26-79	588.9	579.0	6	98
CW-19-79	589.5	579.9	4	90.9
CW-3-79	609.73	575.98	6	99





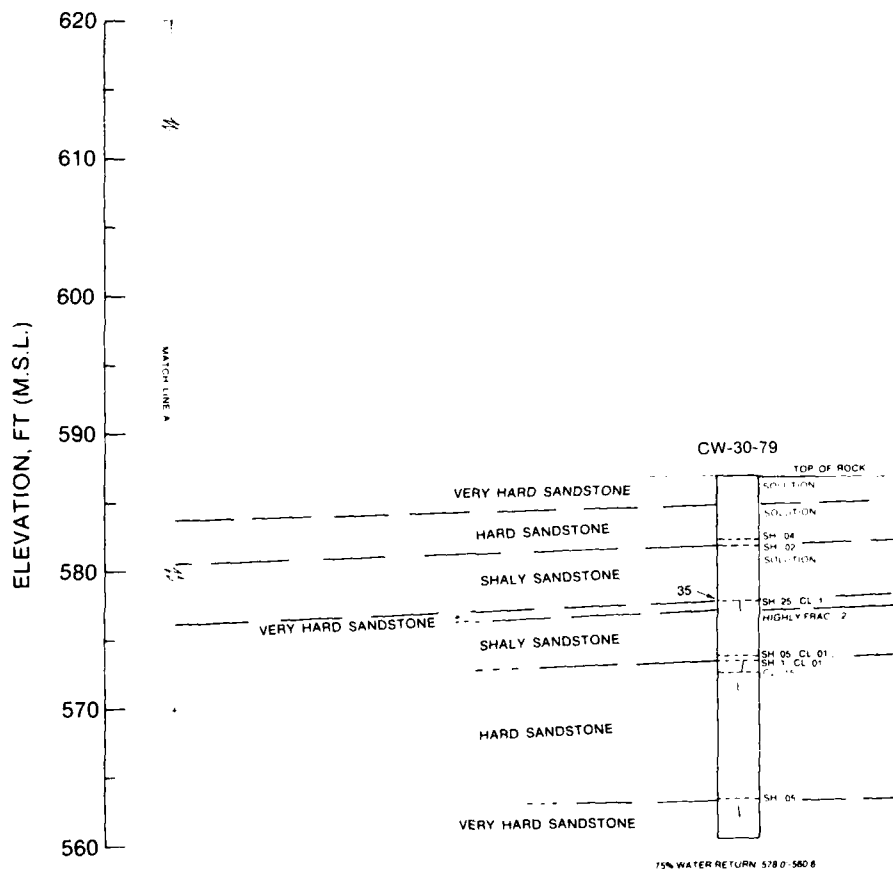
CONDITION SURVEY  
DECEMBER 1979  
COMPENSATING WORKS  
SAULT STE MARIE, MICHIGAN  
**GEOLOGIC CROSS SECTION**

SECTION E-E'

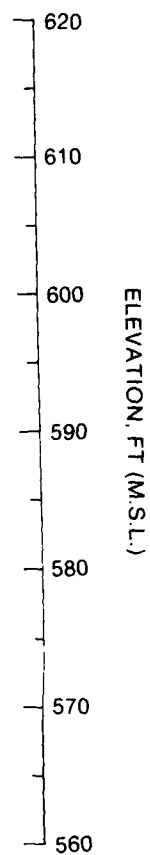
SEE PLATE D1 (SHEET 2 OF 4) FOR LEGEND

SHEET 1 of 2

PLATE D5



BORING NUMBER	ELEVATION, FT		CORE SIZE IN	CORE RECOVERY %
	TOP OF BORING	BOTTOM OF CORE		
CW-30-79	586.7	560.6	4	100

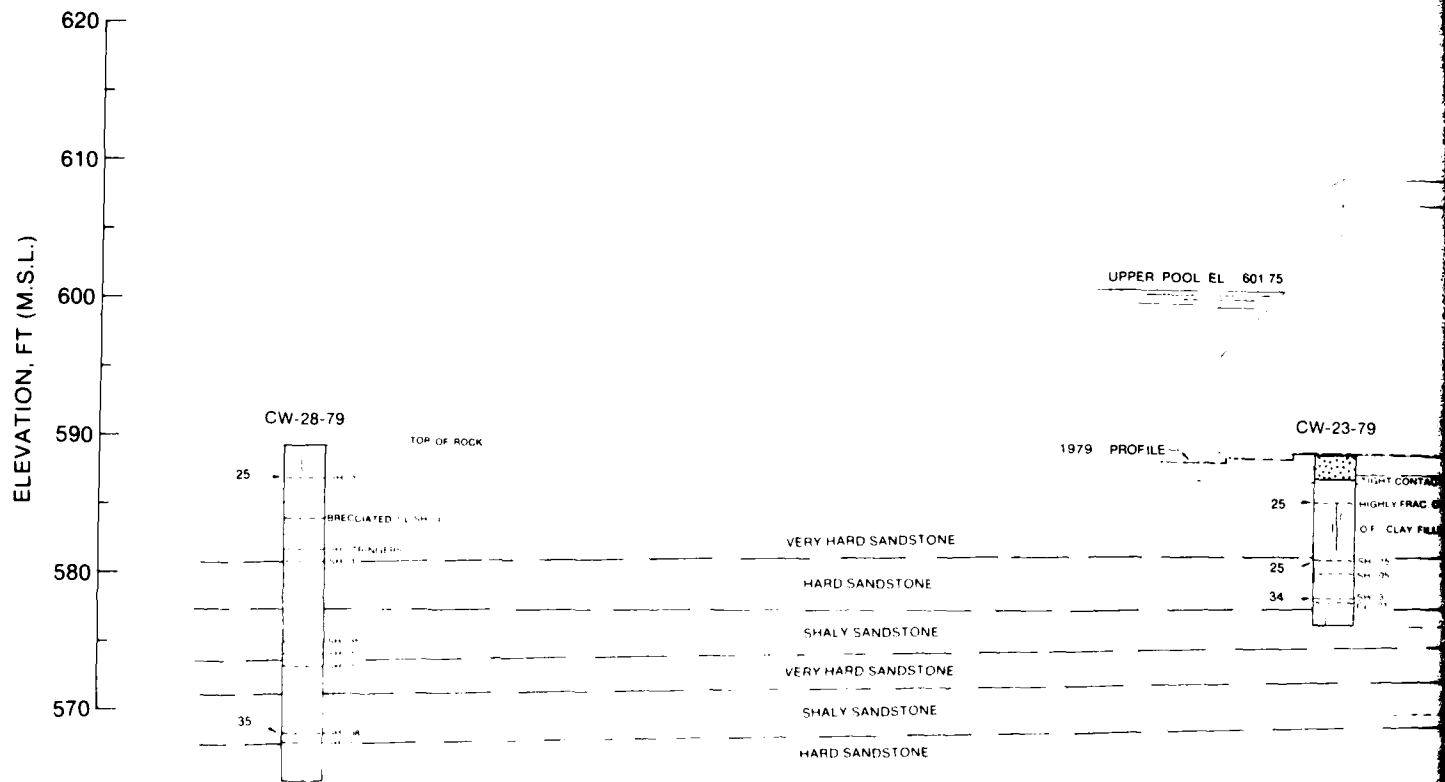


CONDITION SURVEY  
DECEMBER 1979  
COMPENSATING WORKS  
SAULT STE MARIE, MICHIGAN  
**GEOLOGIC CROSS SECTION**  
SECTION E—E'

SEE PLATE D1 (SHEET 2 OF 4) FOR LEGEND

SHEET 2 of 2

PLATE D5



BORING NUMBER	ELEVATION FT		CORE SIZE IN	CORE RECOVERY %
	TOP OF BORING	BOTTOM OF CORE		
CW-28-79	589.4	565.0	4	98.4
CW-23-79	589.7	577.4	4	100
CW-11-79	609.73	576.73	4	100



1

ELEVATION, FT (M.S.L.)

620

610

600

590

580

570

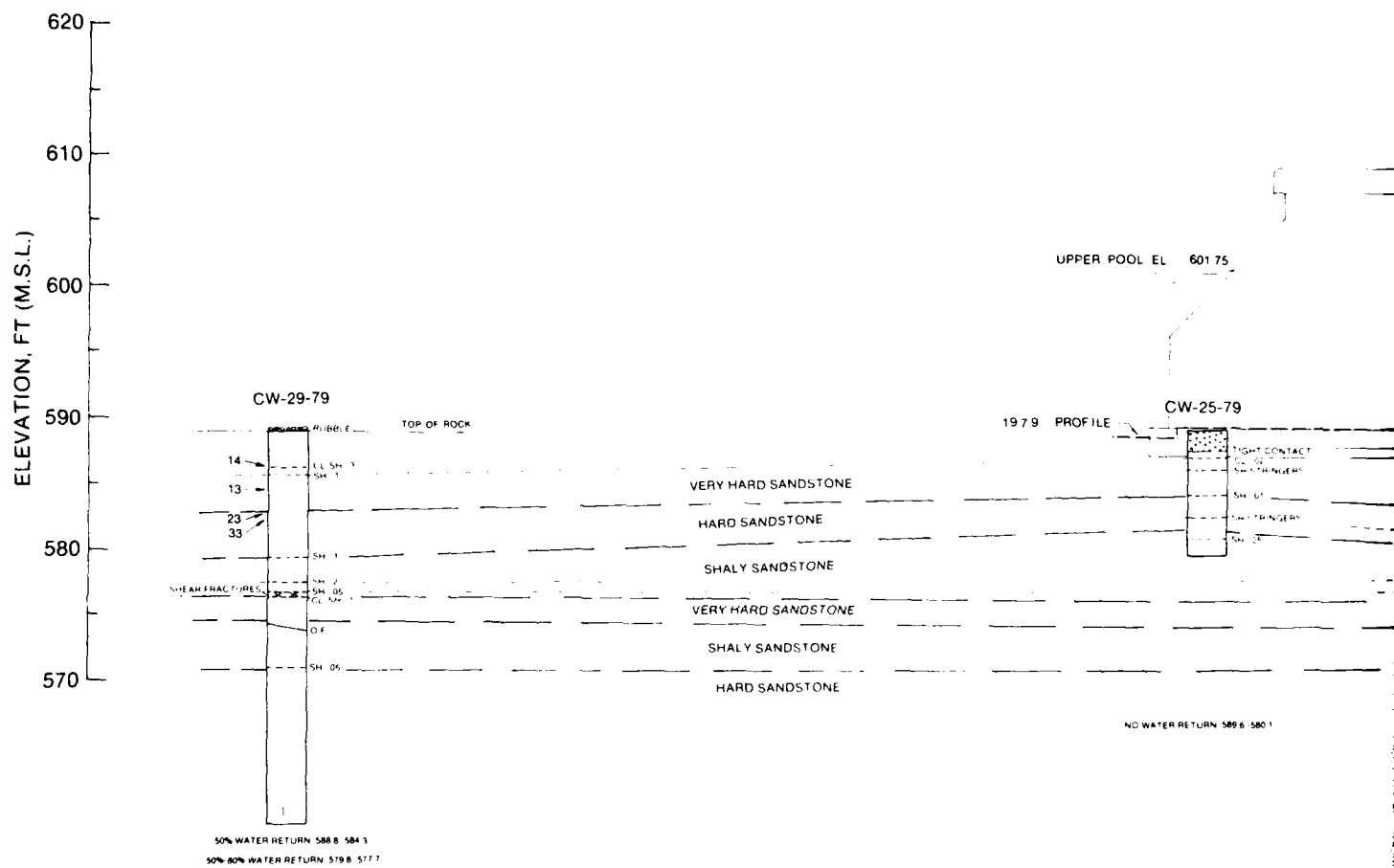
CONDITION SURVEY  
DECEMBER 1979  
COMPENSATING WORKS  
SAULT STE. MARIE, MICHIGAN  
GEOLOGIC CROSS SECTION

SECTION F—F'

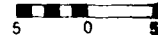
SEE PLATE D1 (SHEET 2 OF 4) FOR LEGEND

SHEET 2 of 2

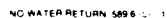
PLATE D6

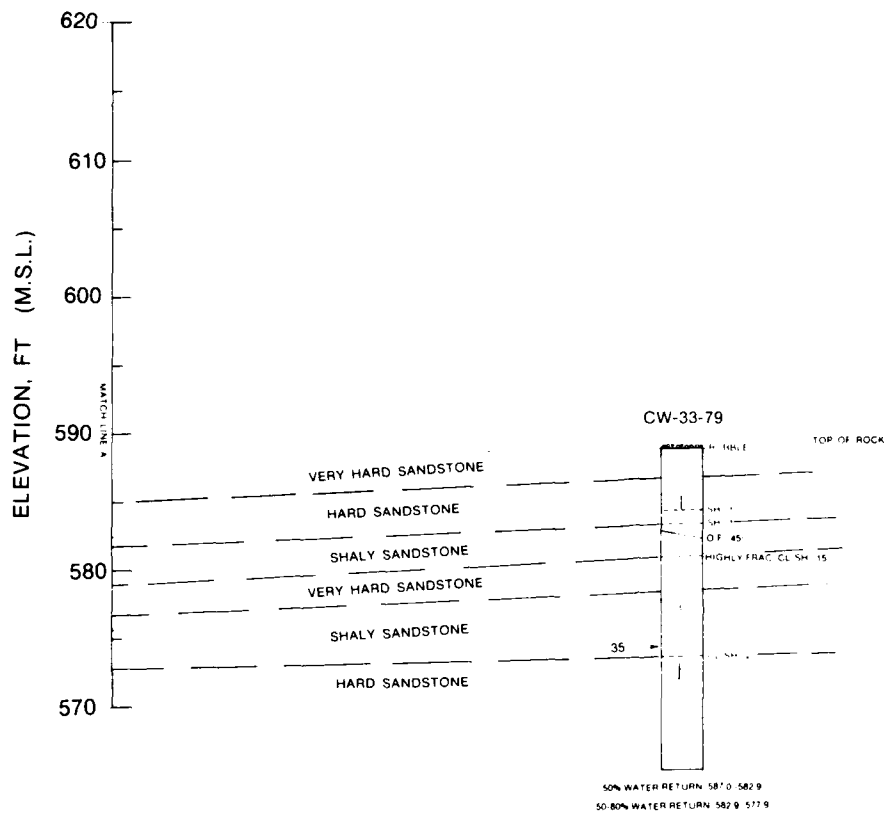


BORING NUMBER	ELEVATION, FT		CORE SIZE, IN	CORE RECOVERY %
	TOP OF BORING	BOTTOM OF CORE		
CW-29-79	589.3	559.1	4	98.7
CW-25-79	589.6	580.1	4	95
CW-15-79	609.76	577.46	4	100









BORING NUMBER	ELEVATION FT		CORE SIZE IN	CORE RECOVERY %
	TOP OF BORING	BOTTOM OF CORE		
CW-33-79	588.7	564.9	4	96.2

620  
610  
600  
590  
580  
570

ELEVATION, FT (M.S.L.)

CONDITION SURVEY  
DECEMBER 1979  
COMPENSATING WORKS  
SAULT STE MARIE, MICHIGAN  
**GEOLOGIC CROSS SECTION**

SECTION G—G'

SEE PLATE D1 (SHEET 2 OF 4) FOR LEGEND

SHEET 2 of 2

PLATE D7

# AVERAGES

## 10 VERY HARD SS

$\gamma_m = 156.3 \text{ lb/ft}^3$   
 $\gamma_d = 152.9 \text{ lb/ft}^3$   
 $w = 2.2\%$   
 $q_u = 14,730 \text{ psi}$   
 $f = 5.31 \times 10^6 \text{ psi}$   
 $\mu = 0.20$   
 $I_{10} = 50 \text{ psi}$

## 20 HARD SS

$\gamma_m = 156.8 \text{ lb/ft}^3$   
 $\gamma_d = 151.6 \text{ lb/ft}^3$   
 $w = 3.4\%$   
 $q_u = 8,830 \text{ psi}$   
 $f = 2.33 \times 10^6 \text{ psi}$   
 $\mu = 0.32$   
 $I_{10} = 65 \text{ psi}$

## DIRECT SHEAR

10 Con to rk  $\phi = 69.3^\circ$   
 $c = 11.5 \text{ tsf}$   
 11 Con on rk, precut  $\phi = 32.1^\circ$   
 $c = 0$   
 12 Intact  $\phi = 68^\circ$   $\phi_f = 29.9^\circ$   
 $c = 44 \text{ tsf}$   $c = 5.8 \text{ tsf}$   
 13 Precut  $\phi_f = 32.9^\circ$   
 $c = 0 \text{ tsf}$   
 14 Clay seam (CL)  $\phi = 36.5^\circ$   
 $c = 0.05 \text{ tsf}$   
 $\phi_f = 26^\circ$   
 $c = 0$   
 15 Shale seam  
 16 Natural joint  $\phi = 47.3^\circ$   
 $c = 4.2 \text{ tsf}$   
 $\phi_f = 32^\circ$   
 $c = 2.5 \text{ tsf}$   
 17 Cross bed\*  $\phi = 58^\circ$   
 $c = 1 \text{ tsf}$   
 $\phi_f = 51^\circ$   
 $c = 0$

## DIRECT SHEAR

20 Con to rk  
 21 Con on rk, precut  
 22 Intact  $\phi = 56.5^\circ$   $\phi_f = 4$   
 $c = 12.3 \text{ tsf}$   $c = 1$   
 23 Precut  $\phi_f = 26.5^\circ$   
 $c = 0$   
 24a Clay seam  
 24b Clay seam\*  
 25 Shale seam  
 a 1" thick  $\phi = 34^\circ$   
 $c = 0.1 \text{ tsf}$   
 $\phi_f = 27.9^\circ$   
 $c = 0$   
 b > 1" thick  $\phi = 44.7^\circ$   
 $c = 0.3 \text{ tsf}$   
 $\phi_f = 43.2^\circ$   
 $c = 0$   
 26 Natural joint  $\phi = 68^\circ$   
 $c = 1.8 \text{ tsf}$   
 $\phi_f = 49.6^\circ$   
 $c = 0$   
 27 Cross bed

\* Soils 3 x 3 x 1 direct shear

## NOTE

The rock properties are arranged in columns by rock type. Series numbers for each rock type appear next to the direct shear test results. Like series numbers appear on the geologic cross sections adjacent to the borings and at the elevations from which test specimens were taken. In some cases a series number, ie., 35, which denotes a shale seam in shaly sandstone, will appear in either the very hard or hard sandstone rock unit. The reason for this occurring is that rock units less than 1 ft thick have not been differentiated.

20 HARD SS

$\gamma_m = 156.8 \text{ lb/ft}^3$   
 $\gamma_d = 151.6 \text{ lb/ft}^3$   
 $w = 3.4\%$   
 $q_u = 8,830 \text{ psi}$   
 $E = 2.33 \times 10^6 \text{ psi}$   
 $\nu = 0.32$   
 $I_{(1)} = 65 \text{ psi}$

30 SHALY SS

$\gamma_m = 157.0 \text{ lb/ft}^3$   
 $\gamma_d = 151.9 \text{ lb/ft}^3$   
 $w = 3.4\%$   
 $q_u = 7,580 \text{ psi}$   
 $E = 1.70 \times 10^6 \text{ psi}$   
 $\nu = 0.37$   
 $I_{(1)} = 32 \text{ psi}$

DIRECT SHEAR

20 Con to rk

21 Con on rk, precut

22 Intact  $\phi = 56.5^\circ$   $\phi_f = 48^\circ$   
 $c = 12.3 \text{ tsf}$   $c = 1.3 \text{ tsf}$   
 23 Precut  $\phi_f = 26.5^\circ$   
 $c = 0$

24a Clay seam

24b Clay seam\*

25 Shale seam  
 a 1" thick  $\phi = 34^\circ$   
 $c = 0.1 \text{ tsf}$   
 $\phi_f = 27.9^\circ$   
 $c = 0$   
 b > 1" thick  $\phi = 44.7^\circ$   
 $c = 0.3 \text{ tsf}$   
 $\phi_f = 43.2^\circ$   
 $c = 0$   
 26 Natural joint  $\phi = 68^\circ$   
 $c = -1.8 \text{ tsf}$   
 $\phi_f = 49.6^\circ$   
 $c = 0$

27 Cross bed

DIRECT SHEAR

30 Con to rk

31 Con on rk, precut

32 Intact  $\phi = 66^\circ$   
 $c = 24 \text{ tsf}$   
 33 Precut  $\phi_f = 31.9^\circ$   
 $c = 0$

34 Clay seam

$\phi = 42^\circ$   
 $c = 0$   
 $\phi_f = 23.3^\circ$   
 $c = 0$

35 Shale seam  
 a 1" thick  $\phi = 31.4^\circ$   
 $c = 1.4 \text{ tsf}$   
 $\phi_f = 21.0^\circ$   
 $c = 0$

b > 1" thick  $\phi = 43.3^\circ$   
 $c = 0.1 \text{ tsf}$   
 $\phi_f = 34.1^\circ$   
 $c = 0$

36 Natural joint

37 Cross bed

\* Soils 3" x 3" x 1" direct shear

CONDITION SURVEY  
 DECEMBER 1979  
 COMPENSATING WORKS  
 SAULT STE. MARIE, MICHIGAN  
 CHARACTERIZATION AND  
 ENGINEERING DESIGN  
 PROPERTIES

APPENDIX E  
LABORATORY TEST RESULTS OF  
CONCRETE AND ROCK CORES

## TABLES

<u>Table No.</u>	<u>Description of Tables</u>
E1	Cores Received at WES, Regulatory Structure, Sault Ste. Marie
E2	Concrete Core Test Results, Regulatory Structure, Sault Ste. Marie
E3	Characterization and Engineering Design Properties of Foundation Rock, Very Hard Sandstone
E4	Characterization and Engineering Design Properties of Foundation Rock, Hard Sandstone
E5	Characterization and Engineering Design Properties of Foundation Rock, Shaly Sandstone
E6	Triaxial Test Results

## PLATES

<u>Plate No.</u>	<u>Description of Plates</u>
E1-E8	Compressive stress-strain curves, concrete cores
E9-E18	Compressive stress-strain curves, rock cores
E19-E22	Photographs, compressive strength
E23-E24	Photographs, tensile strength
E25-E26	Photographs, triaxial strength
E27-D32	Direct shear laboratory report sheets, very hard sandstone
E33-E38	Direct shear laboratory report sheets, hard sandstone
E39-E43	Direct shear laboratory report sheets, shaly sandstone
E44-E60	Shear stress-shear deformation curves, very hard sandstone
E61-E71	Shear stress-shear deformation curves, hard sandstone
E72-E84	Shear stress-shear deformation curves, shaly sandstone
E85-E90	Maximum and residual strength failure envelopes, very hard sandstone
E91-E95	Maximum and residual strength failure envelopes, hard sandstone

<u>Plate No.</u>	<u>Description of Plates</u>
E96-E100	Maximum and residual strength failure envelopes, shaly sandstone
E101-E103	Typical photographs of specimens tested in direct shear
E104-E107	Triaxial stress versus strain curves, three rock types
E108-E110	Mohr stress circles



Table E1

Cores Received at WES, Regulatory Structure, Sault Ste. Marie

WES Reference	Drill Hole No.	Date Rec'd	Core Diam in.	Box No.	Depth ft	Elevation, ft		Remarks
						Depth Intervals	Top of Hole	
DET-1 DC-21	CW-1-79	7-31-79	4	1 of 13	0.0 - 4.5	609.75-605.25	609.75	Concrete
				2 of 13	4.5 - 9.2	605.25-600.55		Concrete
				3 of 13	9.2 - 13.5	600.55-596.25		Concrete
				4 of 13	13.5 - 18.1	596.25-591.65		Concrete
				5 of 13	18.1 - 22.8	591.65-586.95		Concrete
				6 of 13	22.8 - 27.2	586.95-582.55		Concrete and sandstone
				7 of 13	27.2 - 31.5	582.55-578.25		Sandstone
				8 of 13	31.5 - 35.1	578.25-574.65		Sandstone
				9 of 13	35.1 - 38.6	574.65-571.15		Sandstone
				10 of 13	38.6 - 42.6	571.15-567.15		Sandstone
				11 of 13	42.6 - 46.1	567.15-563.65		Sandstone
				12 of 13	46.1 - 50.3	563.65-559.45		Sandstone
				13 of 13	50.3 - 52.6	559.45-557.15		Sandstone
DET-1 DC-22	CW-2-79	7-31-79	4	1 of 3	0.0 - 4.8	590.5 - 585.7	590.5	Concrete and sandstone
				2 of 3	4.8 - 11.5	585.7 - 579.0		Sandstone
				3 of 3	11.5 - 13.5	579.0 - 577.0		Sandstone
DET-1 DC-23	CW-3-79	7-31-79	6	1 of 9	0.0 - 2.2	609.73-607.53	609.73	Concrete
				2 of 9	2.2 - 6.2	607.53-603.53		Concrete
				3 of 9	6.2 - 10.3	603.53-599.43		Concrete
				4 of 9	10.3 - 14.6	599.43-595.13		Concrete
				5 of 9	14.6 - 18.4	595.13-591.33		Concrete
				6 of 9	18.4 - 22.85	591.33-586.88		Concrete
				7 of 9	22.85-26.6	586.88-583.13		Concrete and sandstone
				8 of 9	26.6 - 30.0	583.13-579.73		Sandstone
				9 of 9	30.0 - 33.75	579.73-575.98		Sandstone
				1 of 8	0.0 - 4.5	609.71-605.21	609.71	Concrete
				2 of 8	4.5 - 9.0	605.21-600.71		Concrete
				3 of 8	9.0 - 13.3	600.71-596.41		Concrete
				4 of 8	13.3 - 17.2	596.41-592.51		Concrete
DET-1 DC-24	CW-5-79	7-31-79	6	5 of 8	17.2 - 20.0	592.51-589.71		Concrete and sandstone
				6 of 8	20.0 - 25.2	589.71-584.51		Sandstone
				7 of 8	25.2 - 29.9	584.51-579.81		Sandstone
				8 of 8	29.9 - 34.1	579.81-575.61		Sandstone
				1 of 3	0.0 - 4.2	588.5 - 584.3	588.5	Concrete and sandstone
				2 of 3	4.2 - 8.3	584.3 - 580.2		Sandstone
				3 of 3	8.3 - 12.2	580.2 - 576.3		Sandstone
				1 of 8	0.0 - 4.5	609.75-605.25	609.75	Concrete
				2 of 8	4.5 - 8.9	605.25-600.85		Concrete
				3 of 8	8.9 - 13.4	600.85-596.35		Concrete

(Continued)

(Page 1 of 4)

Table E1 (Continued)

WES Reference	Drill Hole No.	Date Rec'd	Core Diam in.	Box No.	Depth ft	Elevation, ft		Remarks
						Depth Intervals	Top of Hole	
DET-1 DC-27	CW-9-79	7-31-79	6	4 of 8	13.4 - 18.2	596.35-591.55		Concrete
				5 of 8	18.2 - 22.4	591.55-587.35		Concrete
				6 of 8	22.4 - 26.0	587.35-583.75		Concrete and sandstone
				7 of 8	26.0 - 30.1	583.75-579.65		Sandstone
				8 of 8	30.1 - 33.4	579.65-576.35		Sandstone
				1 of 13	0.0 - 3.7	609.83-606.13	609.83	Concrete
				2 of 13	3.7 - 7.5	606.13-602.33		Concrete
				3 of 13	7.5 - 12.5	602.33-597.33		Concrete
				4 of 13	12.5 - 16.85	597.33-592.98		Concrete
				5 of 13	16.85-20.85	592.98-588.98		Concrete
				6 of 13	20.85-25.1	588.98-584.73		Concrete and sandstone
				7 of 13	25.1 - 29.2	584.73-580.63		Sandstone
				8 of 13	29.2 - 33.3	580.63-576.53		Sandstone
DET-1 DC-28	CW-10-79	7-31-79	4	9 of 13	33.3 - 36.85	576.53-572.98		Sandstone
				10 of 13	36.85-41.0	572.98-568.83		Sandstone
				11 of 13	41.0 - 44.9	568.83-564.93		Sandstone
				12 of 13	44.9 - 48.7	564.93-561.13		Sandstone
				13 of 13	48.7 - 53.1	561.13-556.73		Sandstone
				1 of 3	0.0 - 4.6	590.5 - 585.9	590.5	Concrete and sandstone
				2 of 3	4.6 - 9.3	585.9 - 581.2		Sandstone
				3 of 3	9.3 - 13.5	581.2 - 577.0		Sandstone
				1 of 6	0.0 - 6.2	609.73-603.53	609.73	Concrete
				2 of 6	6.2 - 12.3	603.53-597.43		Concrete
				3 of 6	12.3 - 19.1	597.43-590.63		Concrete
				4 of 6	19.1 - 25.2	590.63-584.53		Concrete and sandstone
				5 of 6	25.2 - 29.2	584.53-580.53		Sandstone
DET-1 DC-30	CW-11-79	7-31-79	4	6 of 6	29.2 - 33.0	580.53-576.73		Sandstone
				1 of 6	0.0 - 5.3	609.74-604.44	609.74	Concrete
				2 of 6	5.3 - 11.6	604.44-598.14		Concrete
				3 of 6	11.6 - 17.5	598.14-592.24		Concrete
				4 of 6	17.5 - 24.0	592.24-585.74		Concrete
				5 of 6	24.0 - 29.7	585.74-580.04		Concrete and sandstone
				6 of 6	29.7 - 32.75	580.04-576.99		Sandstone
				1 of 3	0.0 - 4.9	588.65-583.75	588.65	Concrete and sandstone
				2 of 3	4.9 - 8.6	583.75-580.05		Sandstone
				3 of 3	8.6 - 12.5	580.05-576.15		Sandstone
				1 of 8	0.0 - 4.5	609.76-605.26	609.76	Concrete
				2 of 8	4.5 - 8.4	605.26-601.36		Concrete
				3 of 8	8.4 - 12.7	601.36-597.06		Concrete
DET-1 DC-32	CW-15-79	7-31-79	4	4 of 8	12.7 - 16.6	597.06-593.16		Concrete

(Continued)

(Page 2 of 4)

Table E1 (Continued)

WES Reference	Drill Hole No.	Date Rec'd	Core Diam in.	Box No.	Depth ft	Elevation, ft		Remarks
						Depth Intervals	Top of Hole	
DET-1 DC-33	CW-17-79	7-31-79	4	5 of 8	16.6 - 20.8	593.16 - 588.96	609.77	Concrete
				6 of 8	20.8 - 25.05	588.96 - 584.71		Concrete and sandstone
				7 of 8	25.05 - 29.3	584.71 - 580.46		Sandstone
				8 of 8	29.3 - 32.3	580.46 - 577.46		Sandstone
				1 of 9	0.0 - 6.6	609.77 - 603.17		Concrete
				2 of 9	6.6 - 13.4	603.17 - 596.37		Concrete
				3 of 9	13.4 - 20.8	596.37 - 588.97		Concrete
				4 of 9	20.8 - 27.2	588.97 - 582.57		Concrete and sandstone
				5 of 9	27.2 - 33.0	582.57 - 576.77		Sandstone
				6A of 9	33.0 - 37.1	576.77 - 572.67		Sandstone
				6B of 9	37.1 - 41.05	572.67 - 568.72		Sandstone
				7 of 9	41.05 - 45.0	568.72 - 564.77		Sandstone
				8 of 9	45.0 - 49.65	564.77 - 560.12		Sandstone
				9 of 9	49.65 - 53.5	560.12 - 556.27		Sandstone
DET-1 DC-34	CW-18-79	7-31-79	6	1 of 4	0.0 - 4.1	589.8 - 585.7	589.8	Concrete and sandstone
				2 of 4	4.1 - 8.2	585.7 - 581.6		Sandstone
				3 of 4	8.2 - 11.0	581.6 - 578.8		Sandstone
				4 of 4	11.0 - 14.0	578.8 - 575.8		Sandstone
DET-1 DC-35	CW-19-79	7-31-79	4	1 of 2	0.0 - 7.0	588.5 - 581.5	588.5	Concrete and sandstone
				2 of 2	7.0 - 9.9	581.5 - 578.6		Sandstone
DET-1 DC-36	CW-20-79	7-31-79	6	1 of 3	0.0 - 4.1	589.9 - 585.8	589.9	Concrete and sandstone
				2 of 3	4.1 - 8.4	585.8 - 581.5		Sandstone
DET-1 DC-37	CW-21-79	7-31-79	4	3 of 3	8.4 - 13.0	581.5 - 576.9	589.2	Sandstone
				1 of 2	0.0 - 7.0	589.2 - 582.2		Concrete and sandstone
DET-1 DC-38	CW-22-79	7-31-79	4	2 of 2	7.0 - 10.0	582.2 - 579.2	589.5	Sandstone
				1 of 2	0.0 - 7.0	589.5 - 582.5		Concrete and sandstone
DET-1 DC-39	CW-23-79	7-31-79	4	2 of 2	0.0 - 6.8	582.5 - 577.5	589.7	Sandstone
				1 of 2	7.0 - 12.0	589.7 - 582.9		Concrete and sandstone
DET-1 DC-40	CW-24-79	7-31-79	4	2 of 2	6.8 - 12.3	582.9 - 577.4	589.7	Sandstone
				1 of 2	0.0 - 6.7	589.7 - 583.0		Concrete and sandstone
DET-1 DC-41	CW-25-79	7-31-79	4	2 of 2	6.7 - 14.0	583.0 - 575.7	589.6	Sandstone
				1 of 2	0.0 - 2.7	589.6 - 586.9		Concrete and sandstone
DET-1 DC-42	CW-26-79	7-31-79	6	2 of 2	2.7 - 10.0	586.9 - 579.6	588.9	Sandstone
				1 of 3	0.0 - 4.0	588.9 - 584.9		Sandstone
DET-1 DC-43	CW-28-79	7-31-79	4	2 of 3	4.0 - 8.1	584.9 - 580.8	589.4	Sandstone
				3 of 3	8.1 - 10.2	580.8 - 578.7		Sandstone
				1 of 4	0.0 - 6.1	589.4 - 583.3		Sandstone
				2 of 4	6.1 - 12.2	583.3 - 577.2		Sandstone
				3 of 4	12.2 - 19.1	577.2 - 570.3		Sandstone
				4 of 4	19.1 - 25.0	570.3 - 564.4		Sandstone

(Cont Inued)

(Page 3 of 4)

Table E1 (Continued)

WES Reference	Drill Hole No.	Date Rec'd	Core Diam in.	Box No.	Depth ft.	Elevation, ft		Remarks
						Depth Intervals	Top of Hole	
DET-1 DC-44	CW-29-79	7-31-79	4	1 of 5	0.0 - 7.3	589.3 - 582.0	589.3	Sandstone
				2 of 5	7.3 - 13.1	582.0 - 576.2		Sandstone
				3 of 5	13.1 - 19.6	576.2 - 569.7		Sandstone
				4 of 5	19.6 - 26.5	569.7 - 562.8		Sandstone
				5 of 5	26.5 - 30.2	562.8 - 559.1		Sandstone
DET-1 DC-45	CW-30-79	7-31-79	4	1 of 6	0.0 - 4.7	586.7 - 582.0	586.7	Sandstone
				2 of 6	4.7 - 8.6	582.0 - 578.1		Sandstone
				3 of 6	8.6 - 13.2	578.1 - 573.5		Sandstone
				4 of 6	13.2 - 17.0	573.5 - 569.7		Sandstone
				5 of 6	17.0 - 21.3	569.7 - 565.4		Sandstone
DET-1 DC-46	CW-31-79	7-31-79	4	6 of 6	21.3 - 26.1	565.4 - 560.6		Sandstone
				1 of 7	0.0 - 4.6	589.6 - 585.0	589.6	Sandstone
				2 of 7	4.6 - 8.7	585.0 - 580.9		Sandstone
				3 of 7	8.7 - 12.7	580.9 - 576.9		Sandstone
				4 of 7	12.7 - 17.3	576.9 - 572.3		Sandstone
DET-1 DC-47	CW-32-79	7-31-79	4	5 of 7	17.3 - 21.7	572.3 - 567.9		Sandstone
				6 of 7	21.7 - 26.2	567.9 - 563.4		Sandstone
				7 of 7	26.2 - 29.0	563.4 - 560.6		Sandstone
				1 of 4	0.0 - 5.0	588.6 - 583.6	588.6	Sandstone
				2 of 4	5.0 - 9.1	583.6 - 579.5		Sandstone
DET-1 DC-48	CW-33-79	7-31-79	4	3 of 4	9.1 - 13.0	579.5 - 575.6		Sandstone
				4 of 4	13.0 - 15.2	575.6 - 573.4		Sandstone
				1 of 4	0.0 - 7.3	588.7 - 581.4	588.7	Sandstone
				2 of 4	7.3 - 13.5	581.4 - 575.2		Sandstone
				3 of 4	13.5 - 22.0	575.2 - 566.7		Sandstone
DET-1 DC-49	CW-34-79	7-31-79	4	4 of 4	22.0 - 24.0	566.7 - 564.7		Sandstone
				1 of 5	0.0 - 6.6	587.9 - 581.3	587.9	Sandstone
				2 of 5	6.6 - 13.5	581.3 - 574.4		Sandstone
				3 of 5	13.5 - 20.0	574.4 - 567.9		Sandstone
				4 of 5	20.0 - 26.5	567.9 - 561.4		Sandstone
DET-1 DC-50	CW-35-79	7-31-79	4	5 of 5	26.5 - 30.0	561.4 - 557.9		Sandstone
				1 of 2	26.5 - 30.5	591.25 - 587.25	617.75	Sandstone
				2 of 2	30.5 - 35.4	587.25 - 582.35		Sandstone

Table F.2

Drill Hole No.	Elev. ft.	Depth of Core ft.	Characterization Tests					Engineering Design Tests		
			Wet Unit Wt. Y <sub>m</sub> , lb/ft <sup>3</sup>	Dry Unit Wt. Y <sub>d</sub> , lb/ft <sup>3</sup>	Water Content W, %	Comp. Wave Velocity V <sub>pw</sub> , fps	Tensile Splitting Strength T <sub>st</sub> , psi	Elastic Modulus E x 10 <sup>6</sup>	Poisson's Ratio	
										Comp. Strength UC, psi
CW-1-79	608.75	1.0	157.9	152.6	3.5	16,260	8,530	7.25	0.26	
CW-1-79	598.75	11.0	157.9	151.7	4.1	15,151	8,240	6.25	0.16	
CW-1-79	587.45	22.3	160.4	154.8	3.6	15,340	8,850	5.33	0.21	
CW-2-79	589.90	0.6	161.7	156.7	3.2	16,562	12,650	7.69	0.23	
CW-3-79	608.13	1.6	160.4	156.0	2.8	14,322	4,930			
CW-3-79	606.93	2.8	159.2			15,555		560		
CW-5-79	609.21	0.5	161.1	155.4	3.7	14,553	5,900	5.80	0.17	
CW-5-79	608.21	1.5	161.1			15,939		405		
CW-5-79	597.21	12.5	161.1	155.4	3.7	16,325	9,010			
CW-5-79	587.01	22.7	162.9	157.5	3.4	16,256	7,820			
CW-6-79	589.70	0.7	156.7	149.2	5.0	14,402	7,390			
CW-7-79	609.25	0.5	154.2	146.9	5.0	15,151	5,180			
CW-7-79	597.75	12.0	156.1	149.0	4.8	14,814	6,430	4.63	0.16	
CW-7-79	586.65	23.1	159.8	153.8	3.9	15,873	6,900			
CW-9-79	606.73	3.1	156.7	150.2	4.3	14,925	6,640	5.10	0.18	
CW-9-79	604.63	5.2	159.8			15,272		505		
CW-9-79	594.83	15.0	156.7	149.4	4.9	14,962	6,910	5.43	0.21	
CW-9-79	586.73	23.1	158.6	151.3	4.8	14,767	5,560	5.44	0.20	
CW-10-79	590.00	0.5	154.8	147.0	5.3	14,583	7,910	5.00	0.16	
CW-13-79	608.54	1.2	158.6	153.1	3.6	15,674	7,810			
CW-13-79	597.04	12.7	156.1	148.0	5.5	15,674	6,740	6.06	0.18	
CW-13-79	586.64	23.1	162.9	158.0	3.1	16,458	8,530			
CW-14-79	587.85	0.8	159.8	152.8	4.6	15,384	6,530			
CW-15-79	608.46	1.3	161.7	157.0	3.0	17,214	8,570			
CW-15-79	598.76	11.0	163.6	159.5	2.6	16,260	7,260	9.09	0.22	
CW-15-79	588.26	21.5	161.7	156.7	3.2	14,814	11,630	6.67	0.22	
CW-17-79	608.57	1.2	157.9	153.0	3.2	15,773	8,000	7.46	0.24	
CW-17-79	596.97	12.8	161.7	156.5	3.3	16,666	7,860	6.25	0.22	
CW-17-79	587.47	22.3	160.4	154.7	3.7	15,674	7,160	6.80	0.19	
CW-18-79	588.20	1.6	161.1	155.2	3.8	16,196	11,220			
CW-18-79	587.30	2.5	159.2			15,456		490		
CW-20-79	589.30	0.6	159.8	155.3	2.9	15,448	7,180	6.25	0.20	
CW-22-79	589.00	0.5	154.2	146.6	5.2	14,007	5,440	4.49	0.18	
CW-24-79	589.20	0.5	157.9			15,151	6,220			
CW-25-79	588.70	0.9	160.4	154.5	3.8	15,503	6,190	6.02	0.16	
CW-18-79		2.5	159.2							

Table E3  
Very Hard Sandstone Test Results, Regulatory Structure, Sault Ste. Marie

Drill Hole No.	Elev. ft	Depth of Core ft	Characterization Tests					Engineering Design Tests		
			Wet Unit Wt <sub>3</sub> γ <sub>m</sub> , lb/ft <sup>3</sup>	Dry Unit Wt <sub>3</sub> γ <sub>d</sub> , lb/ft <sup>3</sup>	Water Content W, %	Comp. Strength UC, psi	Direct Tensile Strength T <sub>d</sub> , psi	Elastic Modulus E x 10 <sup>6</sup>	Poisson's Ratio	
CW-1-79	559.8	49.95	157.3	153.2	2.7	14,300		4.38	0.25	
CW-2-79	584.1	6.40	157.3	153.3	2.6	14,220		5.83	0.22	
CW-28-79	583.0	6.40	153.6	150.6	2.0	16,580		5.00	0.21	
CW-28-79	572.9	16.50	156.1	151.4	3.1	9,690		3.85	0.16	
CW-31-79	587.2	2.40	152.3	149.9	1.6	15,890		7.27	0.19	
CW-31-79	562.3	27.30	156.1	153.6	1.6	20,680		7.14	0.19	
CW-33-79	579.2	9.80	154.2	150.4	2.5	13,430		4.67	0.19	
CW-9-79	574.0	35.83	157.3	151.8	3.6		35			
CW-9-79	570.2	39.63	158.6	154.7	2.5		65			
CW-26-79	581.8	7.10	156.7							
CW-14-79	581.4	7.25	151.7	147.0	3.2	13,050		4.33	0.20	
		Avg	155.6	151.6	2.5	14,730	50	5.31	0.20	
		s	2.2	2.2	0.7	3,170	21	1.31	0.03	
		n	11	10	10	8	2	8	8	
Grand Avg	*		156.3	152.9	2.2					
	s		1.9	2.1	0.7					
	n		38	37	37					

\* Grand Avg includes all available data from characterization and direct shear tests.  
s = standard deviation  
n = number of tests

Table E4  
Hard Sandstone Test Results, Regulatory Structure, Sault Ste. Marie

Drill Hole No.	Elev. ft	Depth of Core ft	Characterization Tests					Engineering Design Tests		
			Wet Unit Wt <sub>3</sub> Y <sub>m</sub> , lb/ft <sup>3</sup>	Dry Unit Wt <sub>3</sub> Y <sub>d</sub> , lb/ft <sup>3</sup>	Water Content W, %	Comp. Strength UC, psi	Direct Tensile Strength T <sub>d</sub> , psi	Elastic Modulus E x 10 <sup>6</sup>	Poisson's Ratio	
CW-1-79	563.2	46.55	158.6	153.5	3.3	8280		1.71	0.39	
CW-2-79	582.6	7.90	154.2	150.4	2.5	8680		2.05	0.34	
CW-19-79	581.4	8.10	157.3	153.6	2.4	7530		2.47	0.29	
CW-29-79	575.9	13.40	154.8	149.1	3.8	9490		2.35	0.33	
CW-32-79	574.9	13.70	154.2	149.1	3.4	8900		2.05	0.32	
CW-33-79	570.8	18.20	152.3	147.1	3.5	9830		3.33	0.22	
CW-34-79	559.7	28.20	154.8	149.3	3.7	9070	65	2.37	0.35	
CW-18-79	580.2	9.60	157.3							
CW-18-79	579.2	10.60	157.9	152.9	2.9					
Avg			155.7	150.6	3.2	8830	65	2.33	0.32	
s			2.1	2.4	0.5	770	--	0.51	0.05	
n			9	8	8	7	1	7	7	
Grand Avg *			156.8	151.6	3.4					
s			2.5	2.8	0.8					
n			33	28	28					

\* Grand Avg includes all available data from characterization and direct shear tests.  
s = standard deviation  
n = number of tests

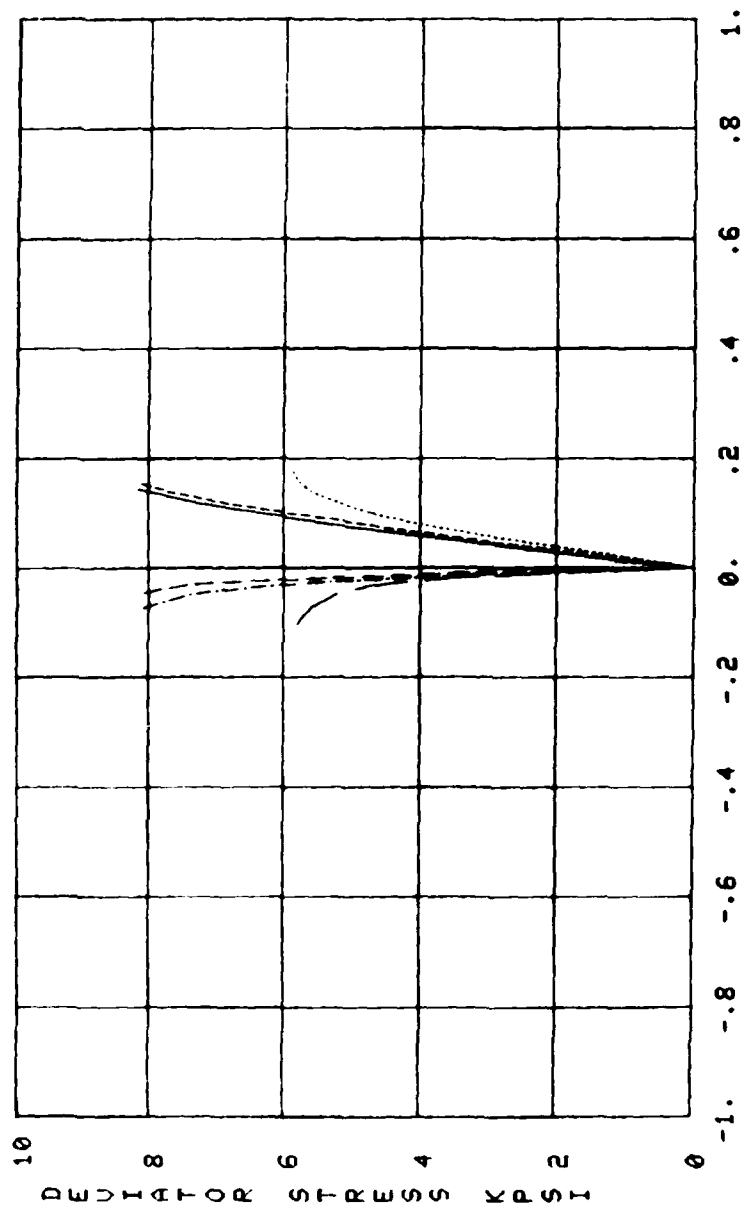
Table E5  
Shaly Sandstone Test Results, Regulatory Structure, Sault Ste. Marie

Drill Hole No.	Elev. ft	Depth of Core ft	Characterization Tests					Engineering Design Tests		
			Wet Unit Wt. $\gamma_m$ , lb/ft <sup>3</sup>	Dry Unit Wt. $\gamma_d$ , lb/ft <sup>3</sup>	Water Content W, %	Comp. Strength UC, psi	Direct Tensile Strength T <sub>d</sub> , psi	Elastic Modulus E x 10 <sup>6</sup>	Poisson's Ratio	
CW-1-79	565.4	44.35	158.6	153.4	3.4	7670		1.52	0.46	
CW-9-79	572.4	37.43	157.9	152.9	3.3	7010		1.75	0.38	
CW-10-79	578.4	12.10	157.3	151.5	3.8	5690		1.14	0.47	
CW-14-79	578.2	10.45	157.3	152.6	3.1	8890		2.00	0.24	
CW-30-79	567.3	19.40	156.1	151.4	3.1	8200		1.71	0.37	
CW-33-79	574.6	14.40	153.6	148.5	3.4	9050		2.25	0.29	
CW-33-79	574.0	15.00	156.1	151.3	3.2	7030		1.76	0.32	
CW-34-79	572.2	15.70	156.7	152.3	2.9	7510		1.31	0.48	
CW-34-79	568.6	19.30	156.1	151.0	3.4	8080		1.67	0.41	
CW-17-79	580.4	29.37	154.8	149.6	3.5		60			
CW-25-79	582.7	6.90	157.9	152.6	3.5		5			
CW-31-79	583.8	5.80	154.2	149.3	3.3		30			
CW-17-79	583.7	26.05	158.6	152.8	3.8	6640		1.65	0.38	
CW-17-79	584.6	25.17	154.2	149.4	3.2	8080		1.90	0.27	
Avg			156.4	151.3	3.4	7580	32	1.70	0.37	
s			1.7	1.6	0.3	1030	27	0.3	0.08	
n			14	14	14	10	3	11	11	
Grand Avg			157.0	151.9	3.4					
s			1.7	3.8	0.9					
n			24	24	24					



Table F6  
Triaxial Test Results, Sault Ste. Marie

Drill Hole No.	Elev. ft	Depth of Core, ft	Characterization Tests			Engineering Design Tests					
			Effective Unit Wt, lb/ft <sup>3</sup>	Dry Unit Wt, lb/ft <sup>3</sup>	Water Content, %	Minor Prin Stress, psi	Major Prin Stress, psi	Prin Stress Difference, psi	Modulus of Elasticity, E x 10 <sup>6</sup> , psi	Poisson's Ratio	
Very Hard Sandstone											
CW-17-79	578.3	31.47	153.6	148.4	3.5	100	14,200	14,100	3.55	0.16	
CW-17-79	577.5	32.27	157.9	152.3	3.7	300	17,550	17,250	6.77	0.18	
CW-17-79	576.2	33.57	154.8	151.0	2.5	900	17,330	16,430	2.78	0.34	
Hard Sandstone											
CW-23-79	580.6	9.10	154.8	150.6	2.8	200	11,810	11,610	2.32	0.29	
CW-24-79	582.5	7.20	154.2	150.9	2.2	600	18,090	17,490	3.41	0.23	
CW-24-79	581.8	7.90	157.7	152.9	2.5	1800	25,530	23,730	3.93	0.23	
CW-28-79	584.5	4.90	153.0	147.8	3.5	1800	26,860	25,060	4.03	0.27	
Shaly Sandstone											
CW-28-79	575.8	13.60	156.1	151.1	3.3	200	9,650	9,450	2.35	0.19	
CW-28-79	575.1	14.30	155.5	151.0	3.0	600	12,800	12,200	2.35	0.29	
CW-28-79	570.4	19.00	155.5	151.0	3.0	1800	26,010	24,210	4.80	0.26	



STRAIN AXIAL, DIAMETRIC (-), PCT

COMPRESSIVE STRESS-STRAIN, CONCRETE CORE  
 CU-1: 1.0 FT, 11.0 FT, 22.3 FT  
 PIER, SAULT STE MARIE

AXIAL	1.0 FT
DIAMETRIC	1.0 FT
AXIAL	11.0 FT
DIAMETRIC	11.0 FT
AXIAL	22.3 FT
DIAMETRIC	22.3 FT

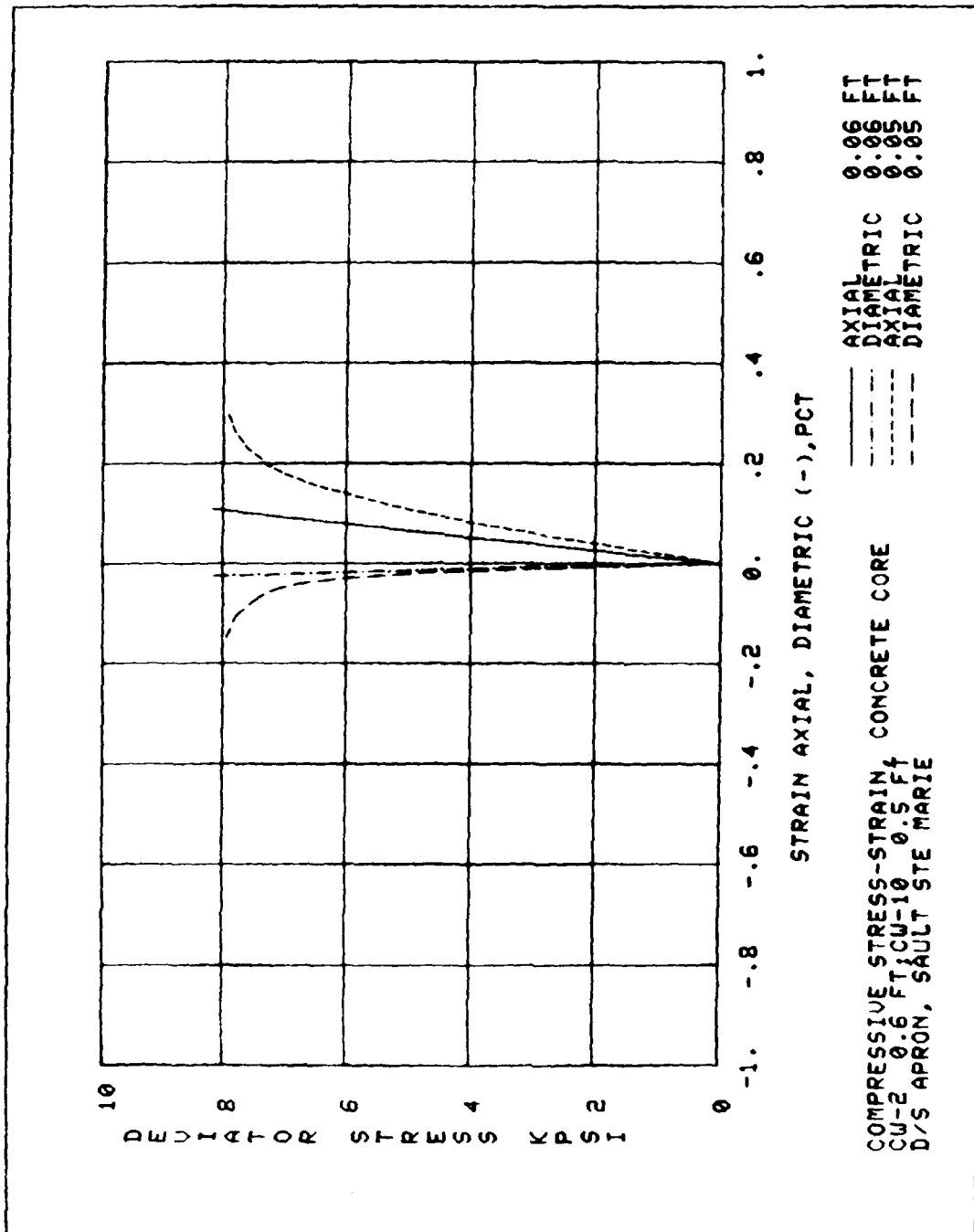


PLATE E2

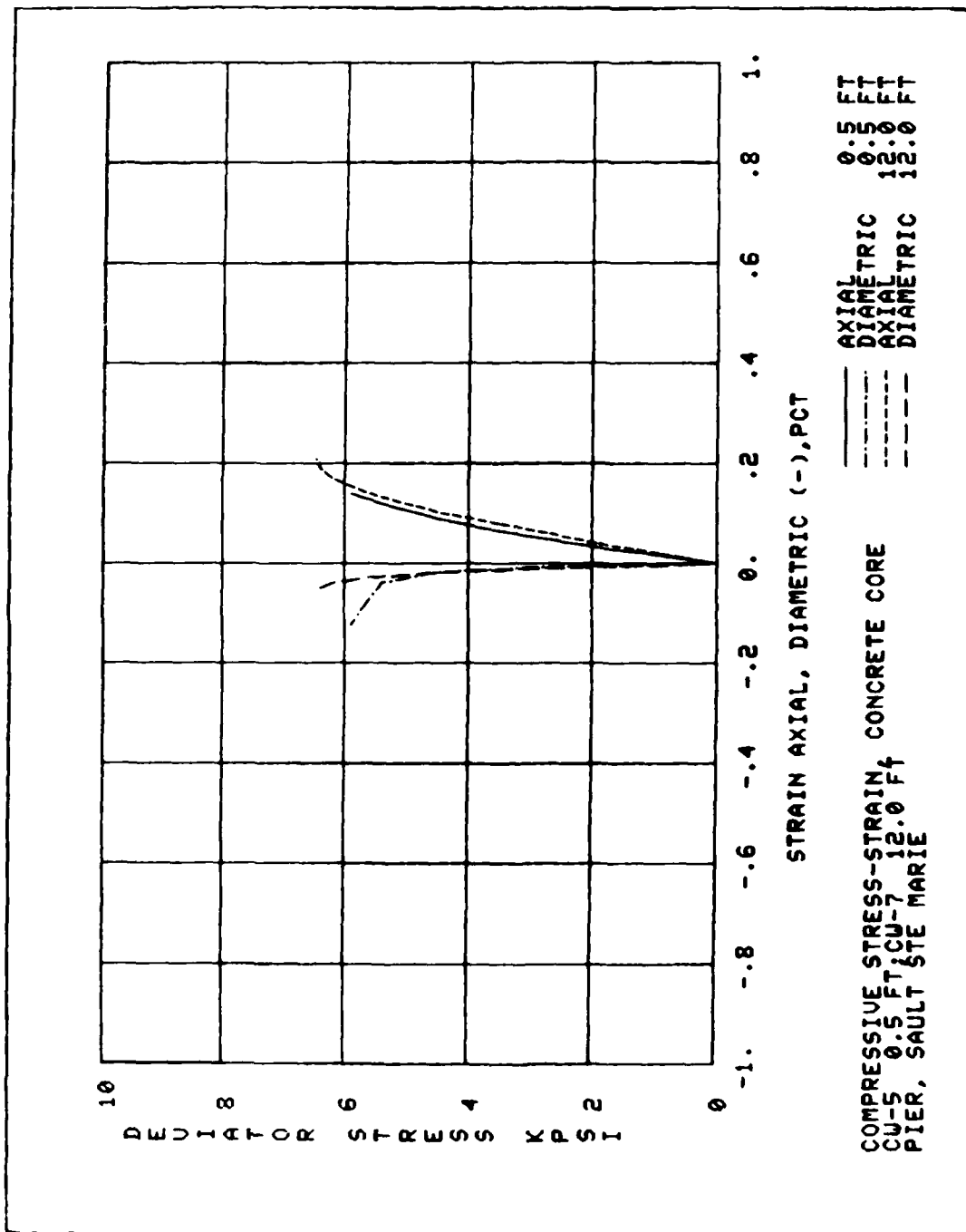
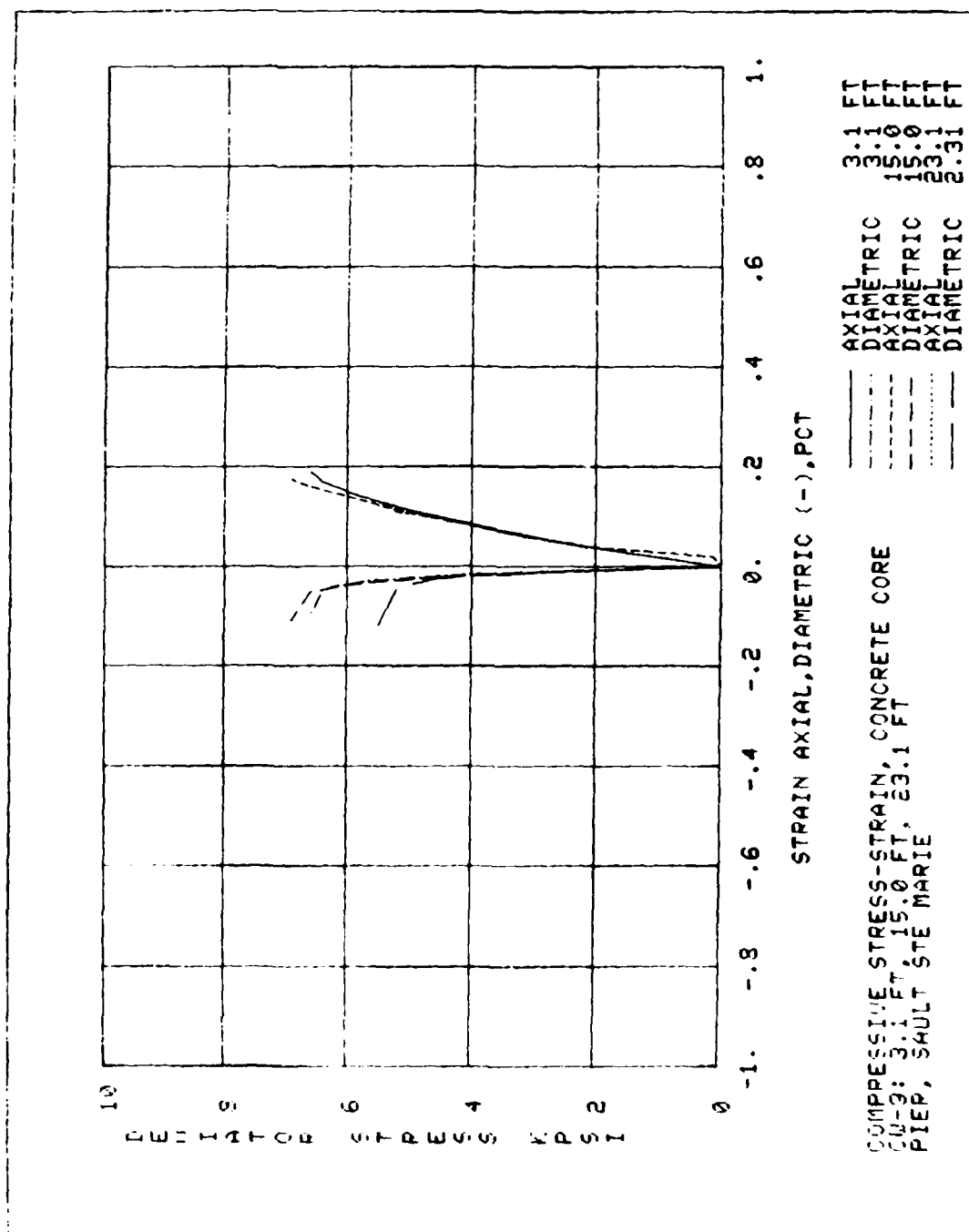


PLATE E4



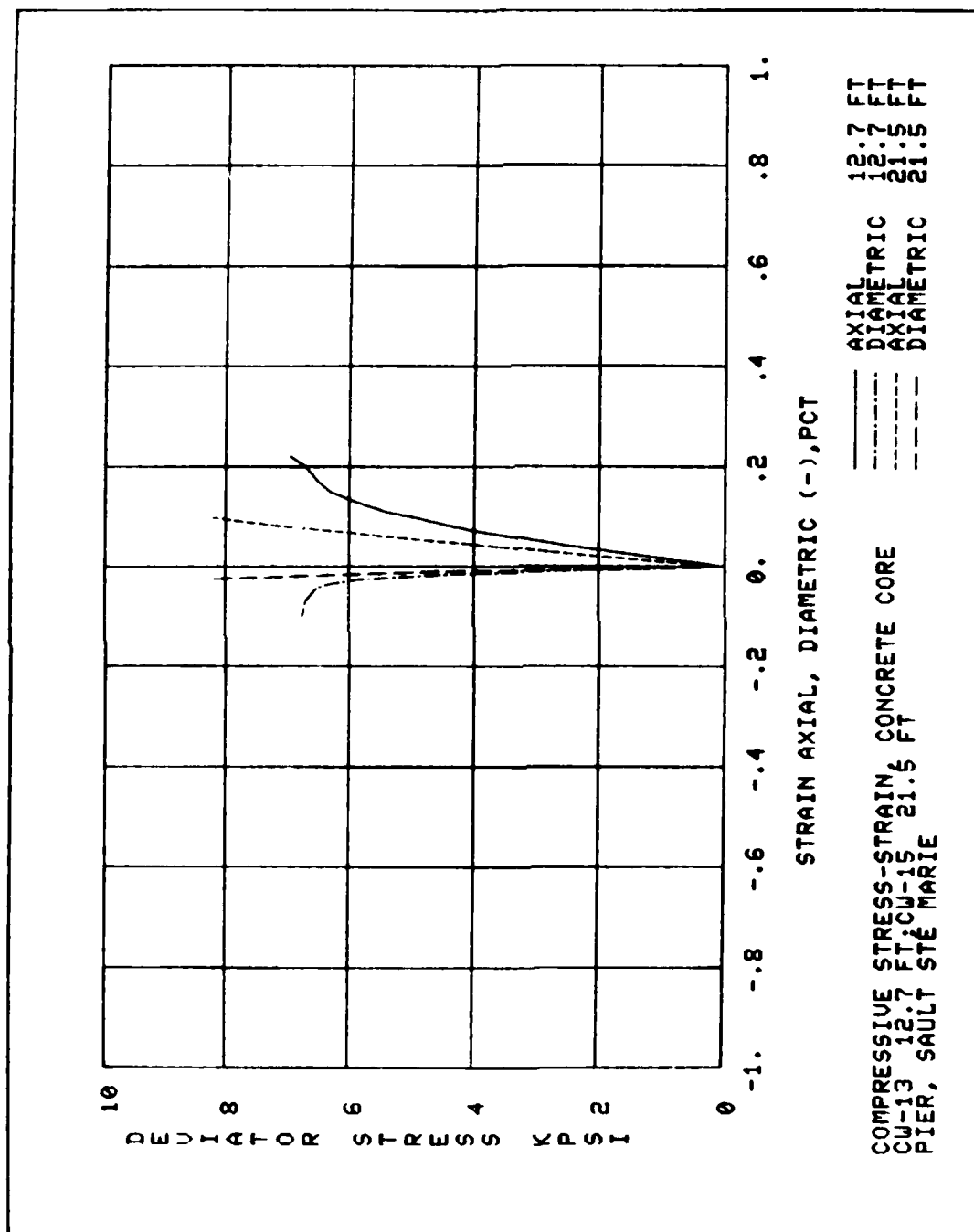


PLATE E5

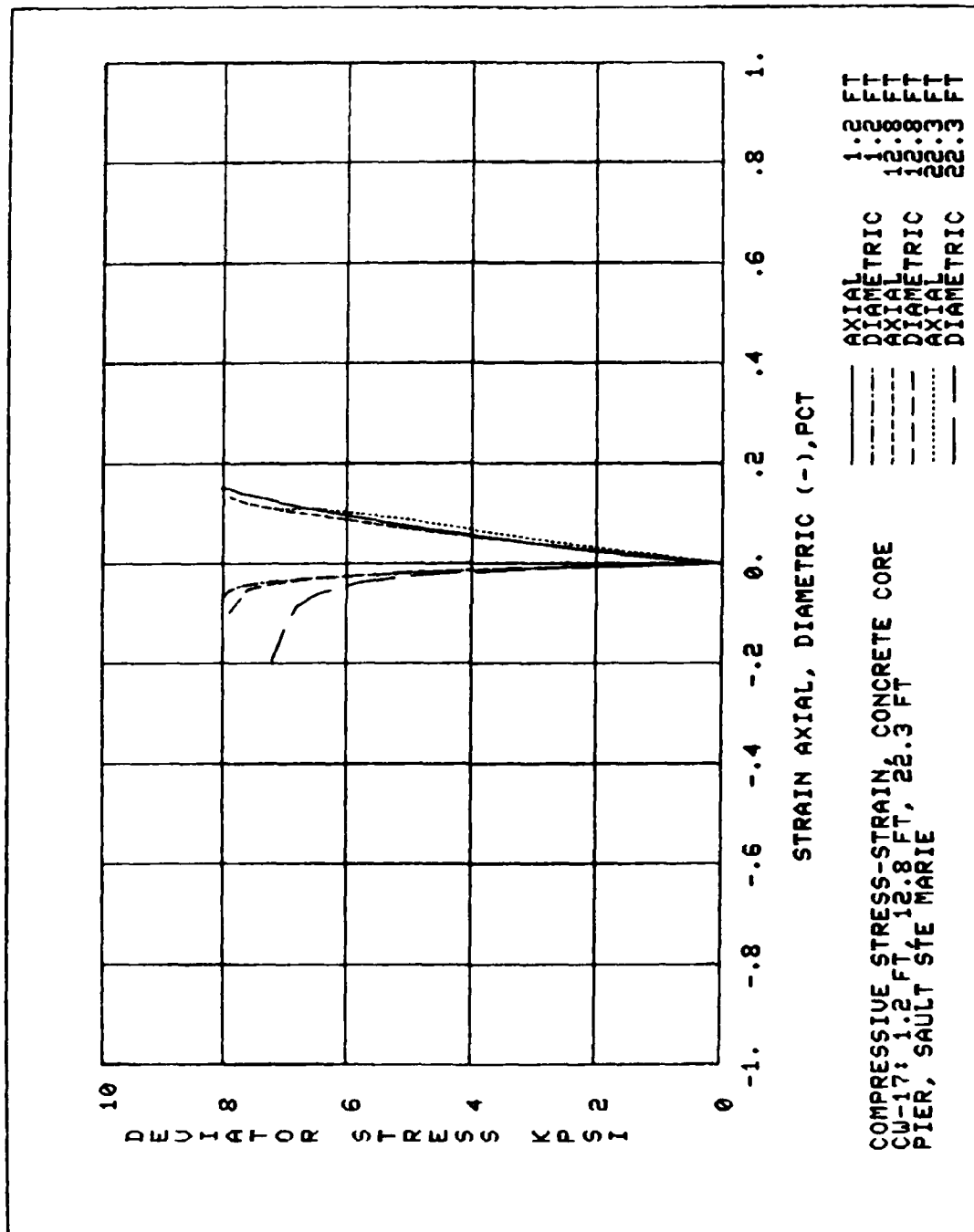


PLATE E6

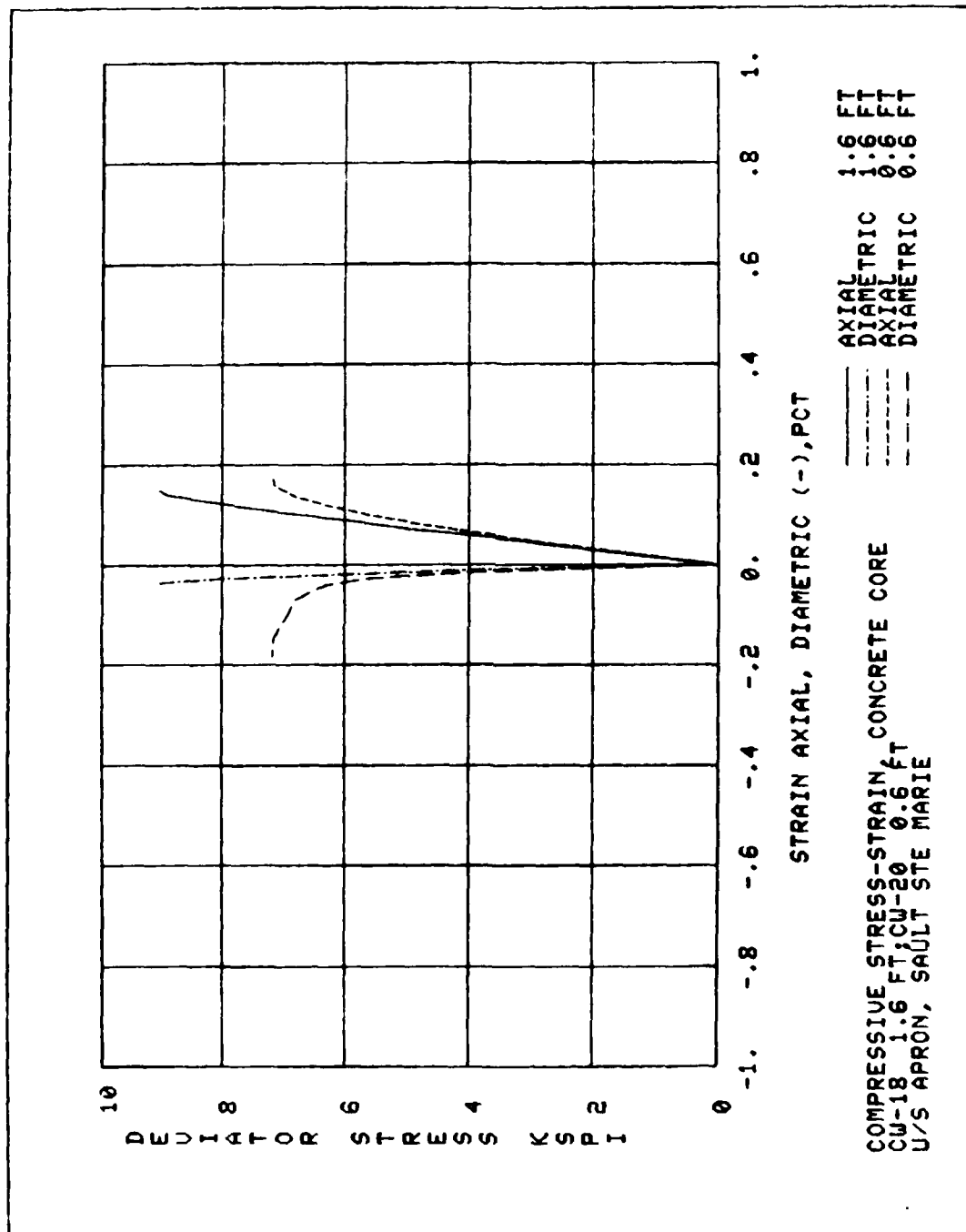


PLATE E7



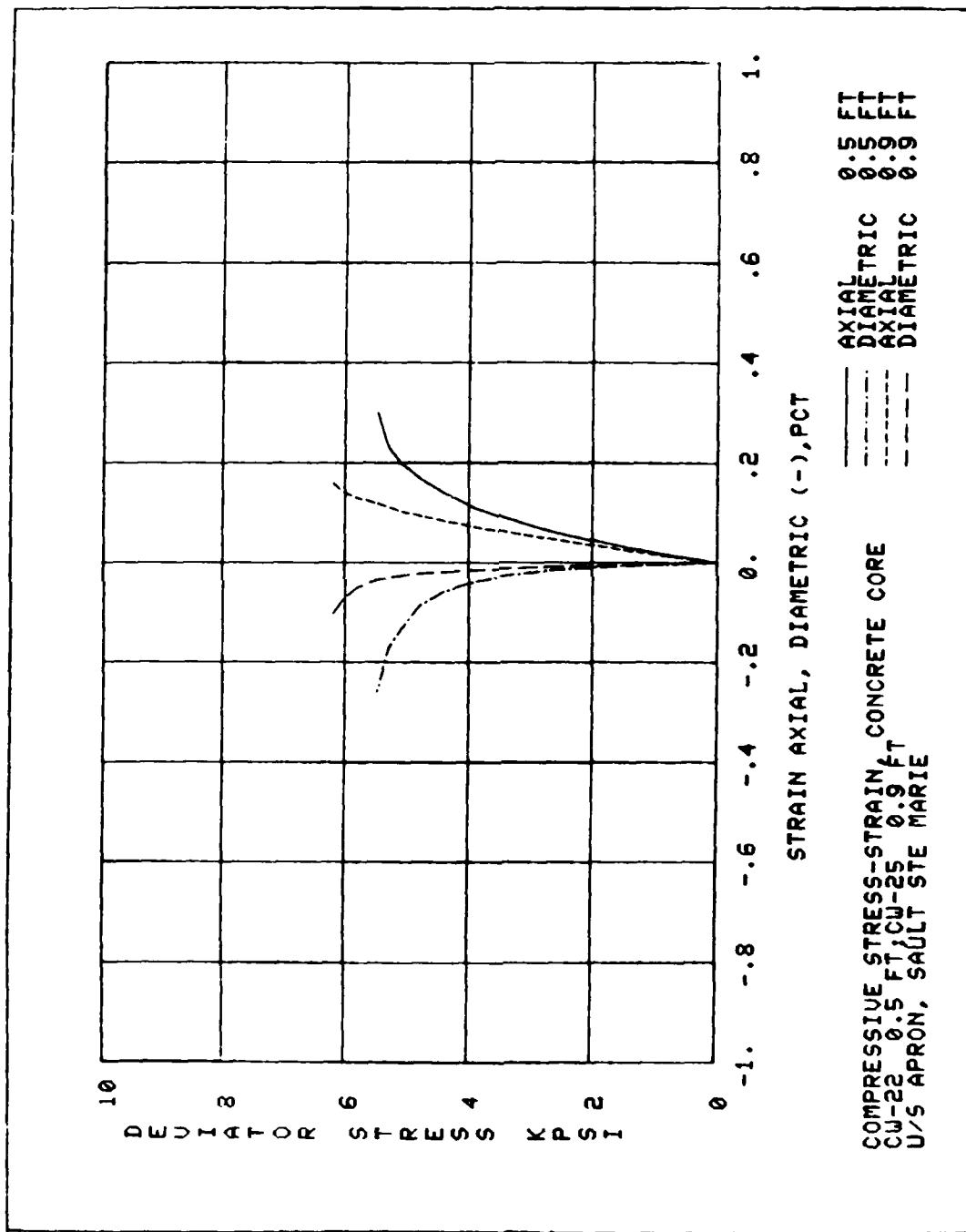
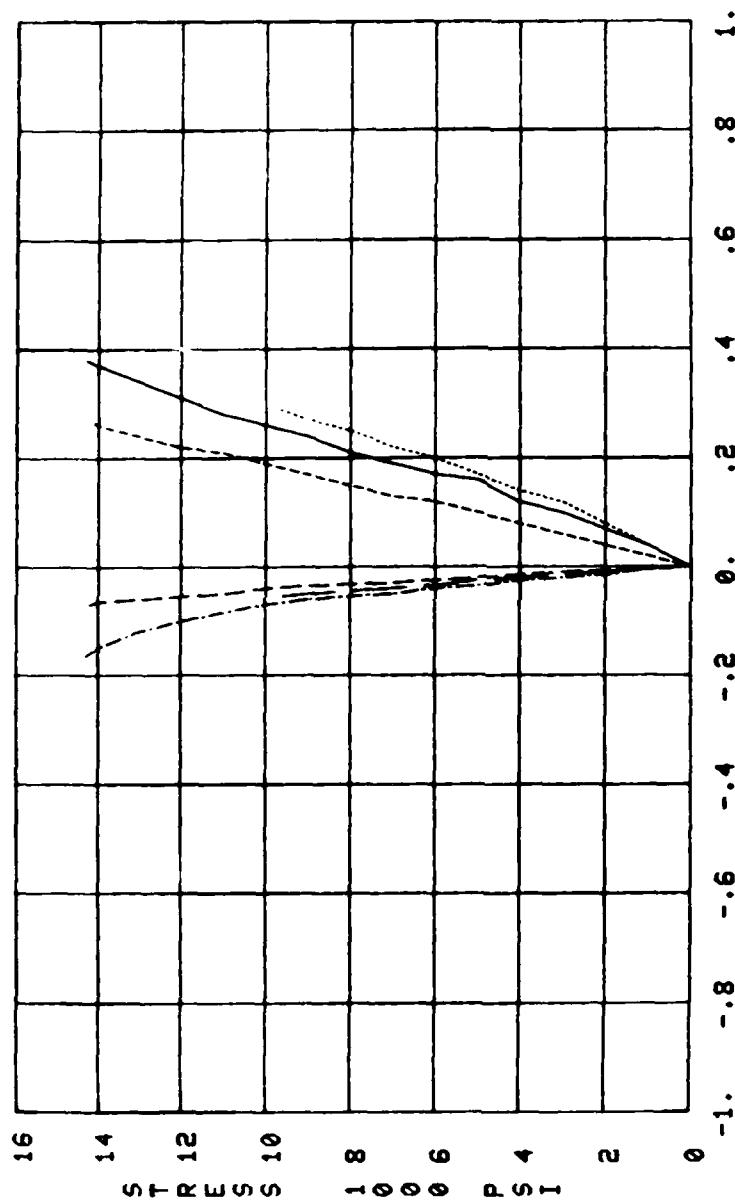


PLATE E8



STRAIN + AXIAL, DIAMETRIC (-), PCT

AXIAL DIAMETRIC 49.95 FT  
 AXIAL DIAMETRIC 49.95 FT  
 AXIAL DIAMETRIC 6.40 FT  
 AXIAL DIAMETRIC 16.50 FT

COMPRESSION STRENGTH - VERY HARD SANDSTONE  
 SAULT ST MARIE  
 CW-1 49.95 FT; CW-2 6.40 FT; CW-28 16.50 FT

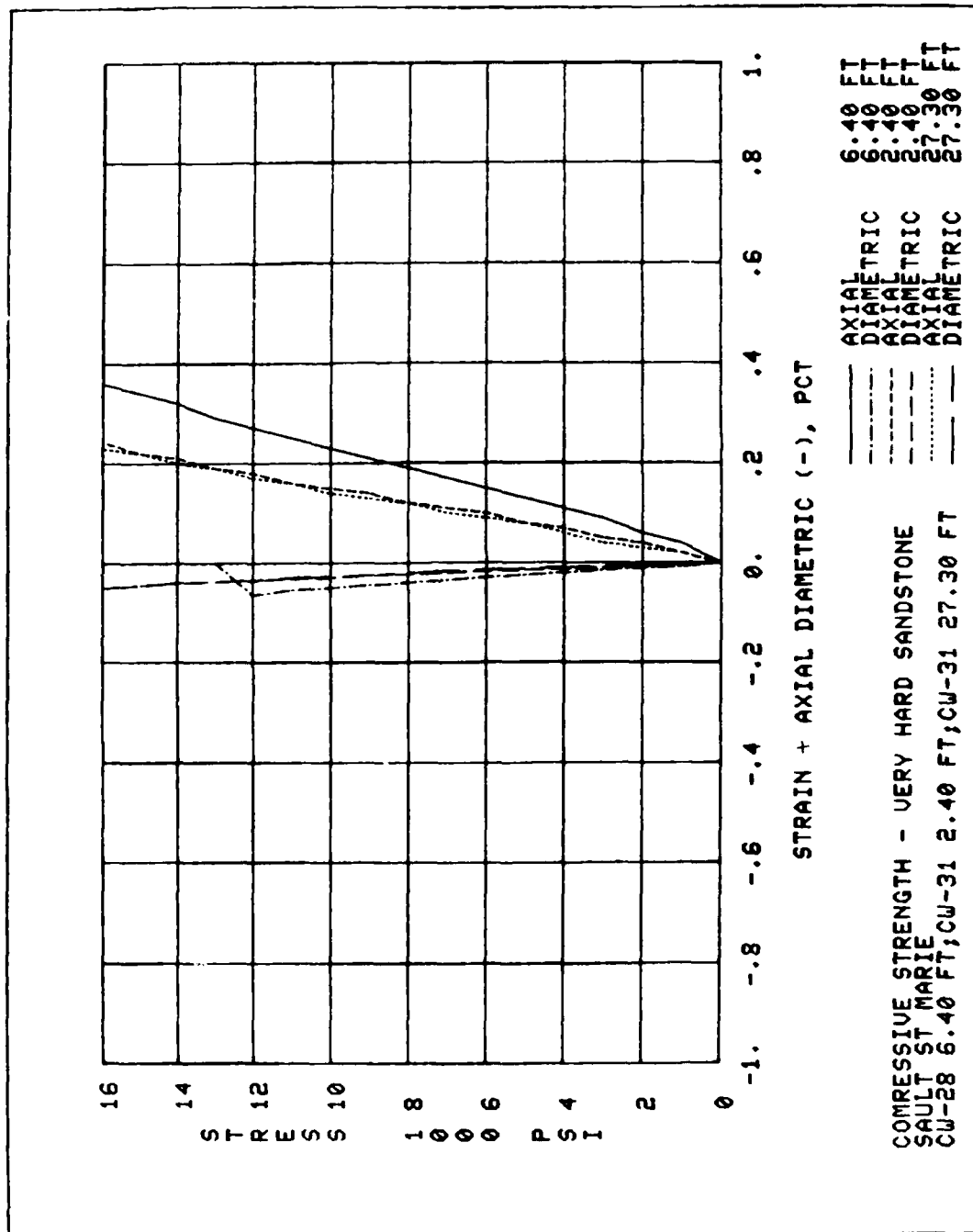
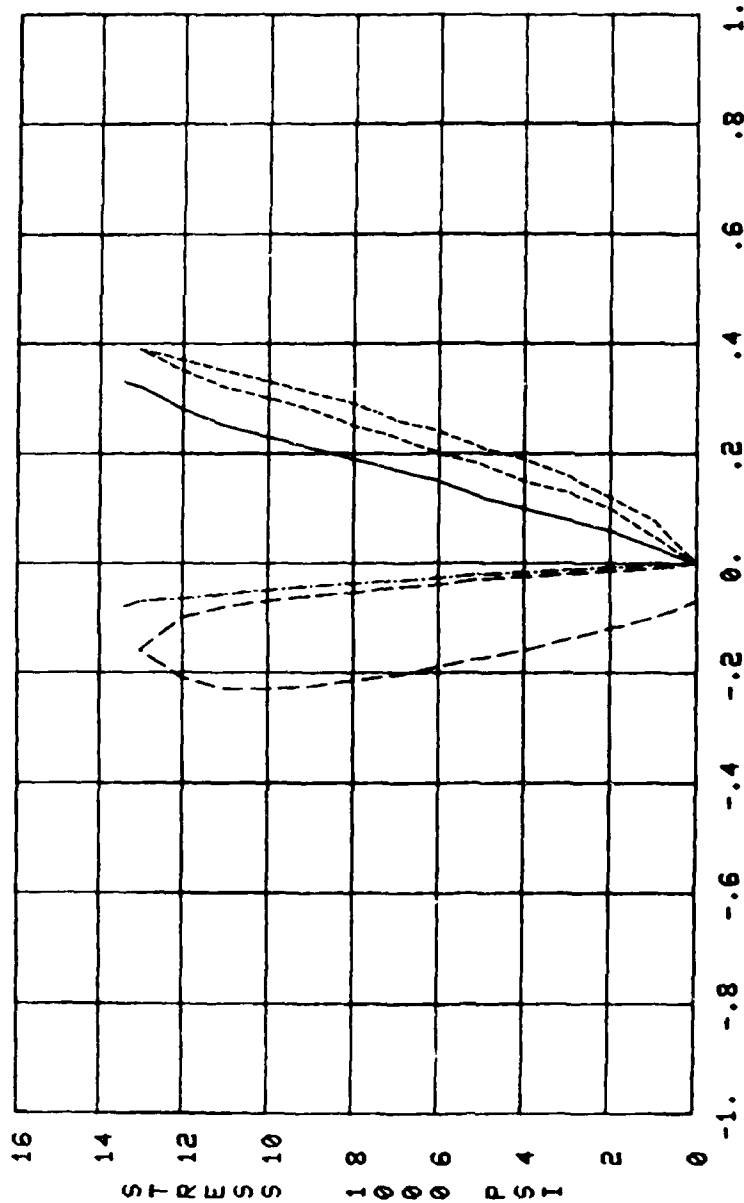
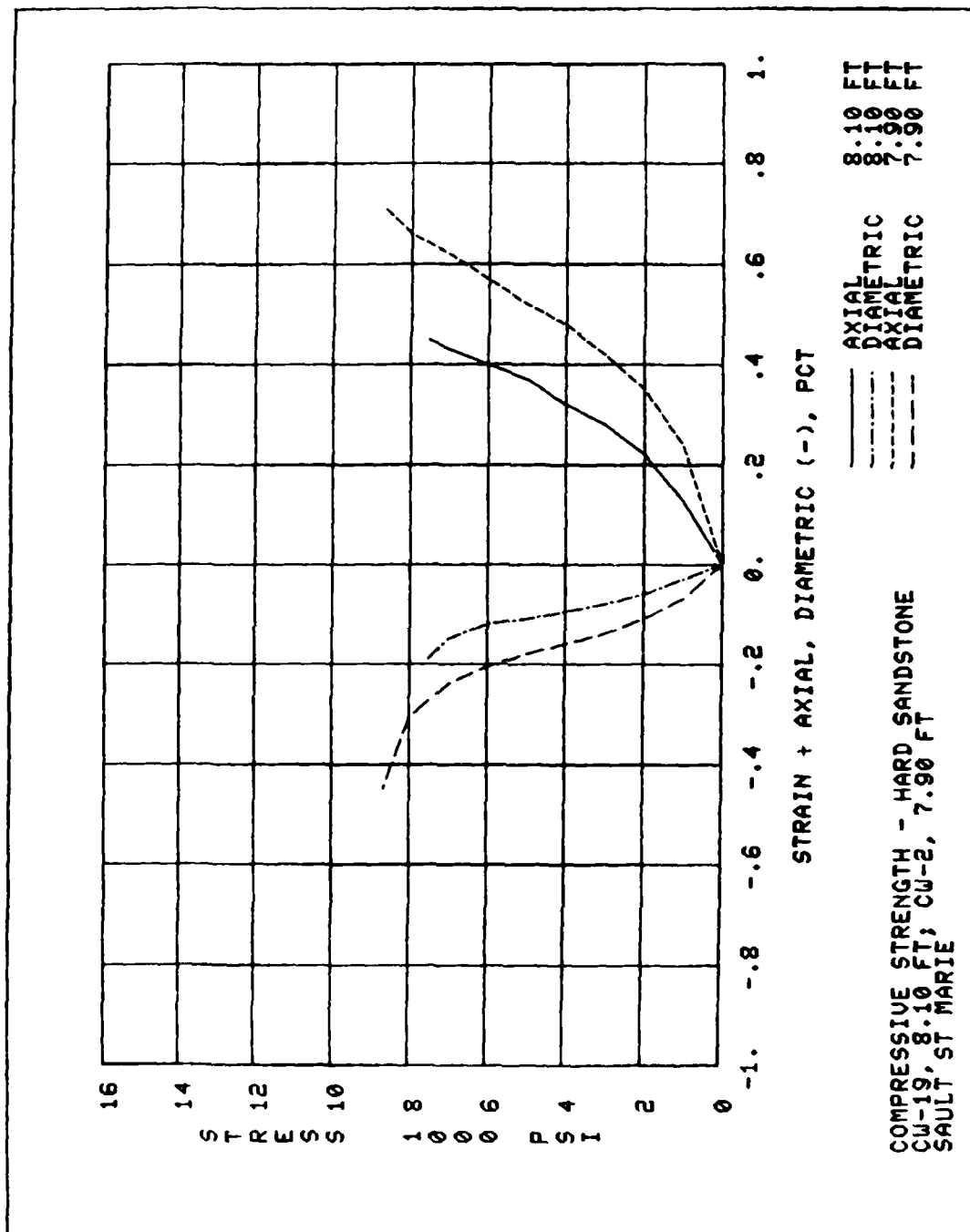


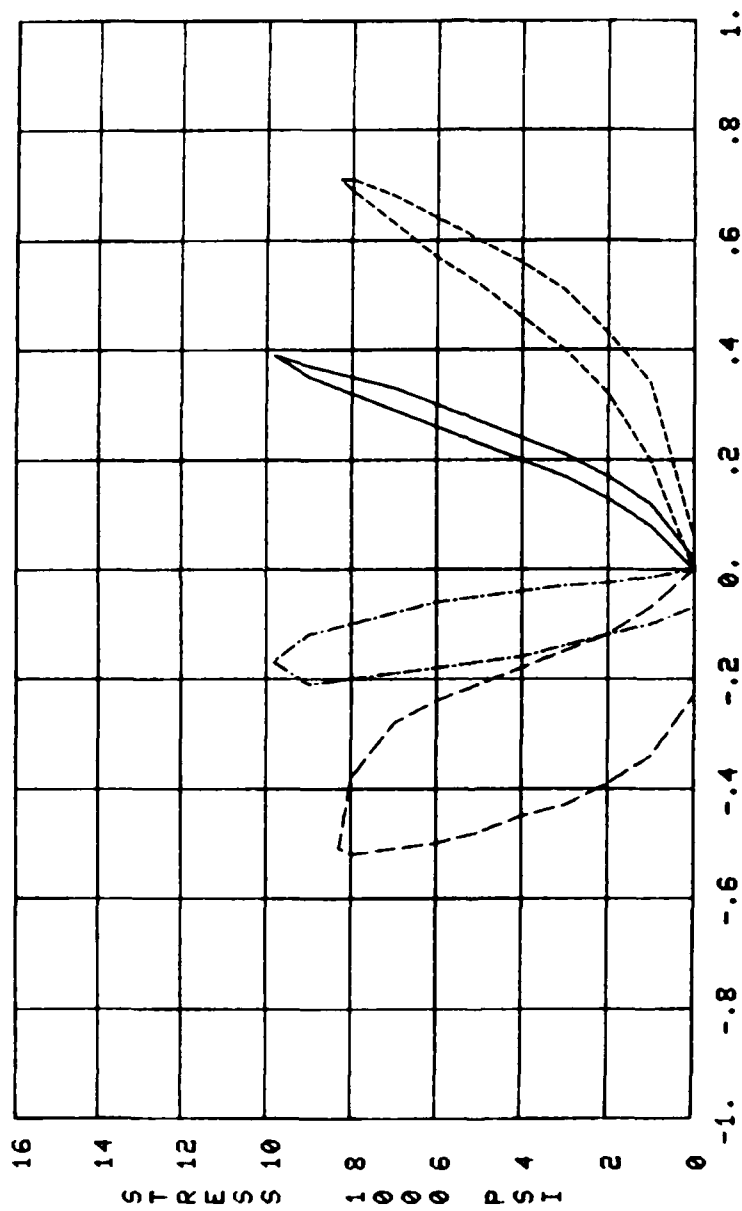
PLATE E10



COMPRESSION STRENGTH - VERY HARD SANDSTONE  
CU-33, 9.80 FT; CU-14, 7.25 FT  
SAULT ST MARIE

PLATE E12





STRAIN + AXIAL, DIAMETRIC (-), PCT

AXIAL 18.20 FT  
 AXIAL 18.20 FT  
 AXIAL 46.55 FT  
 DIAMETRIC 46.55 FT

COMPRESSION STRENGTH - HARD SANDSTONE  
 CW-33, 18.20 FT; CW-1, 46.55 FT  
 SAULT ST MARIE

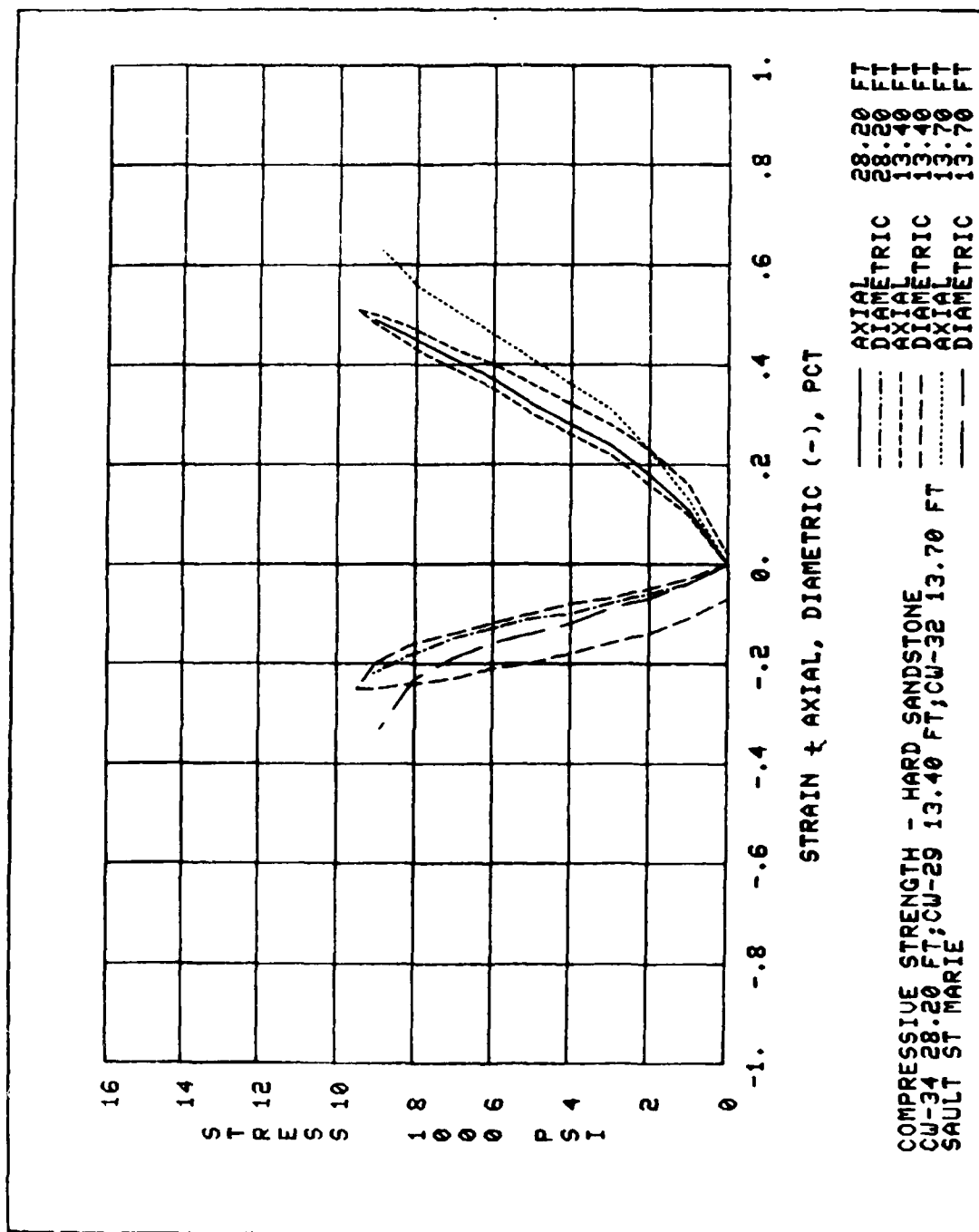


PLATE E14

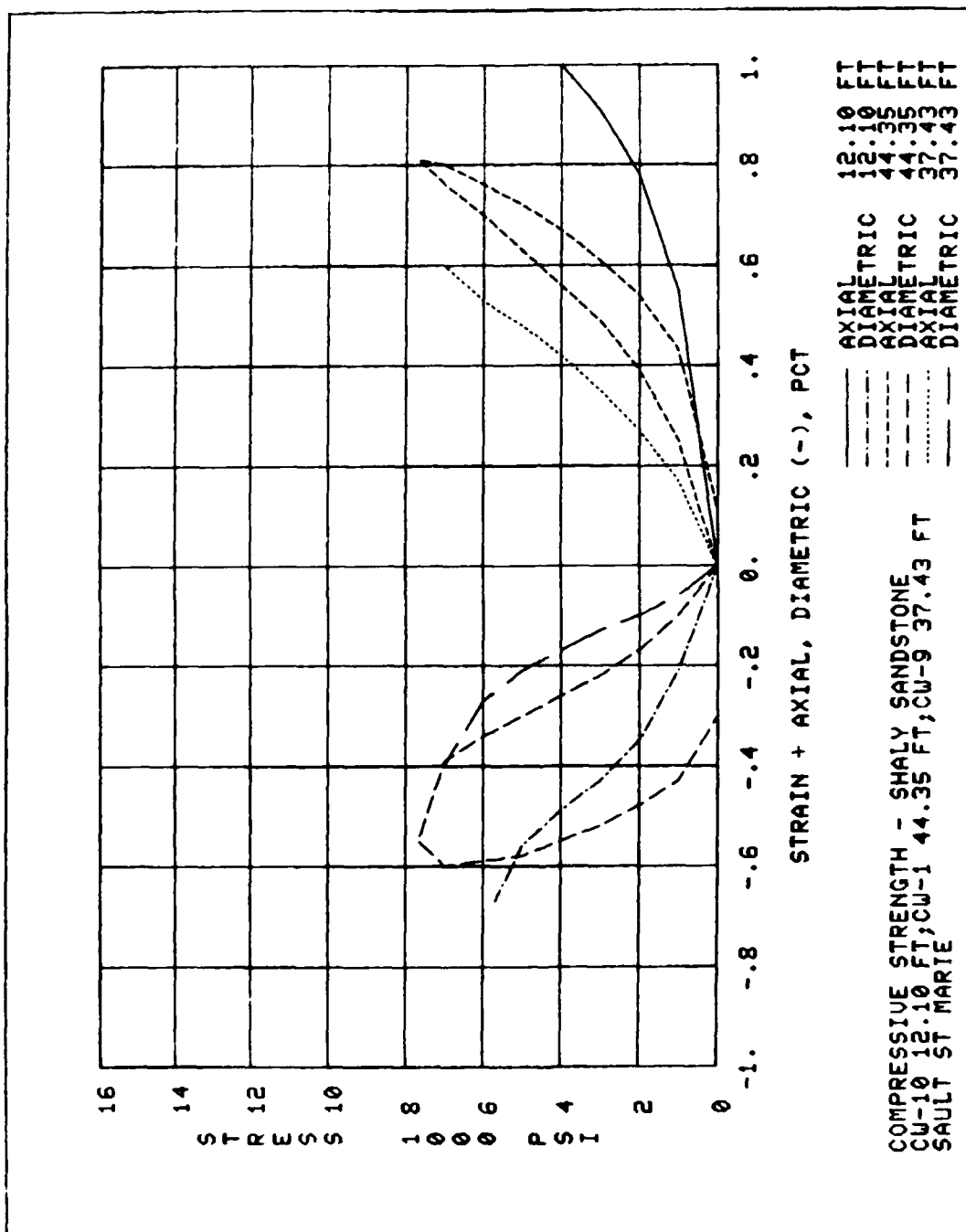


PLATE E15



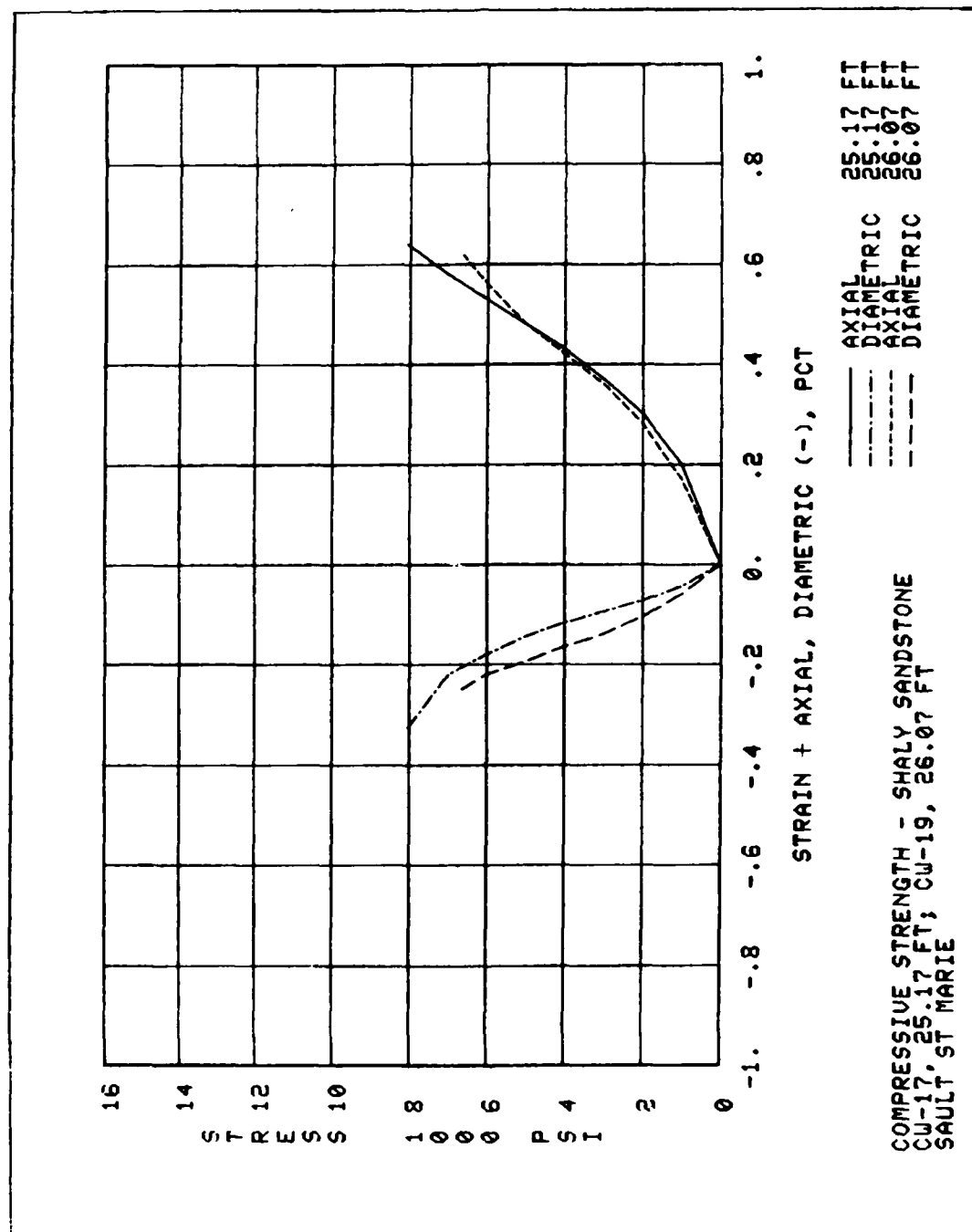
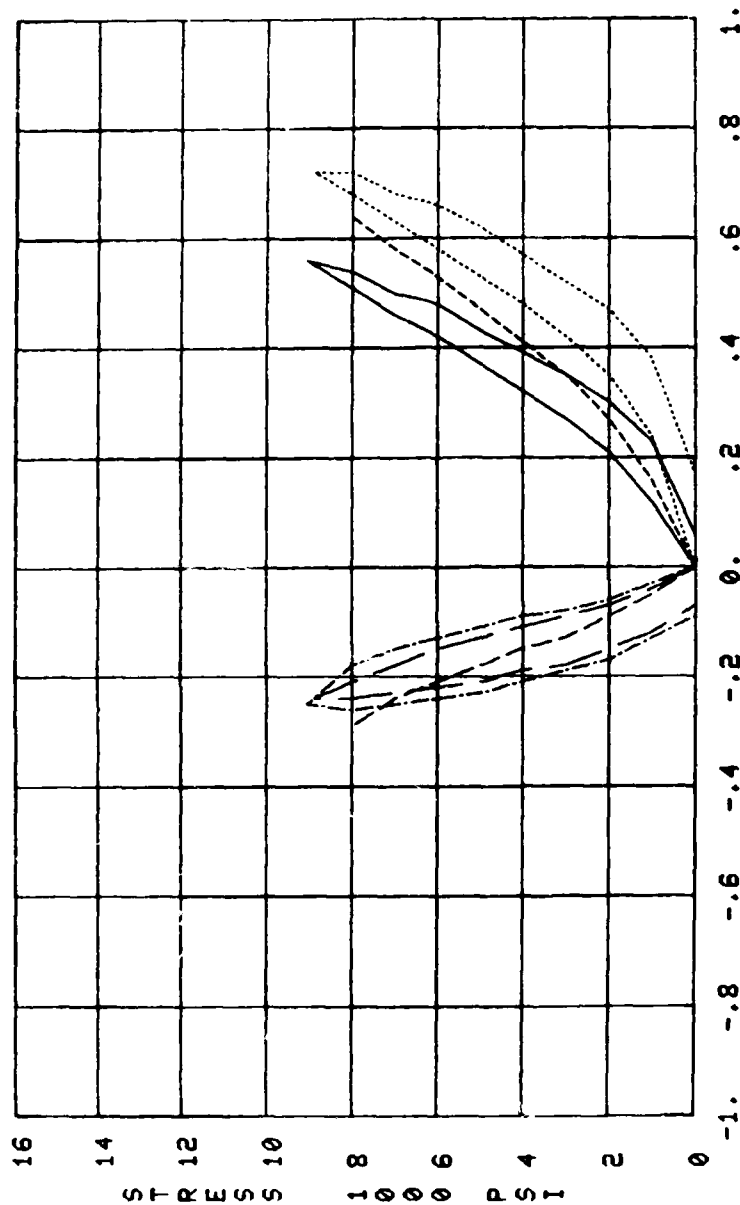


PLATE EI6



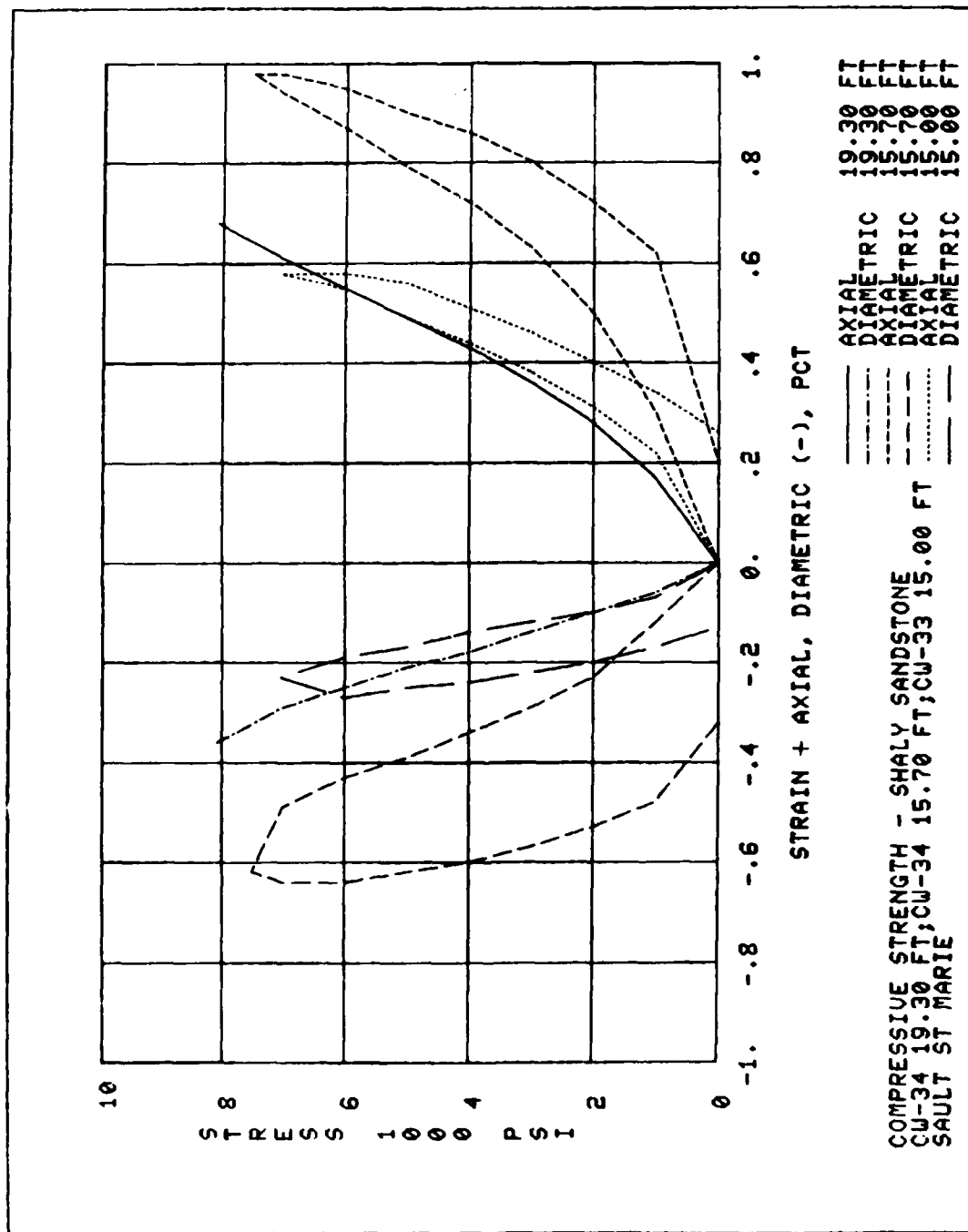
STRAIN + AXIAL, DIAMETRIC (-), PCT

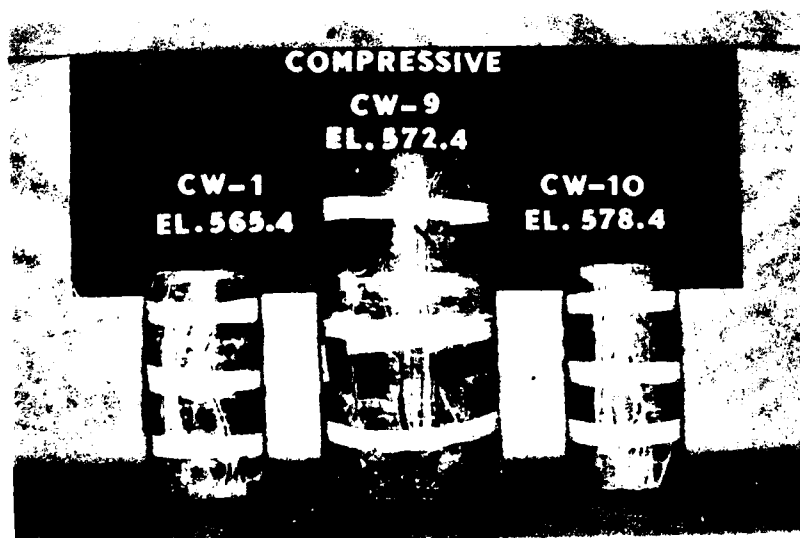
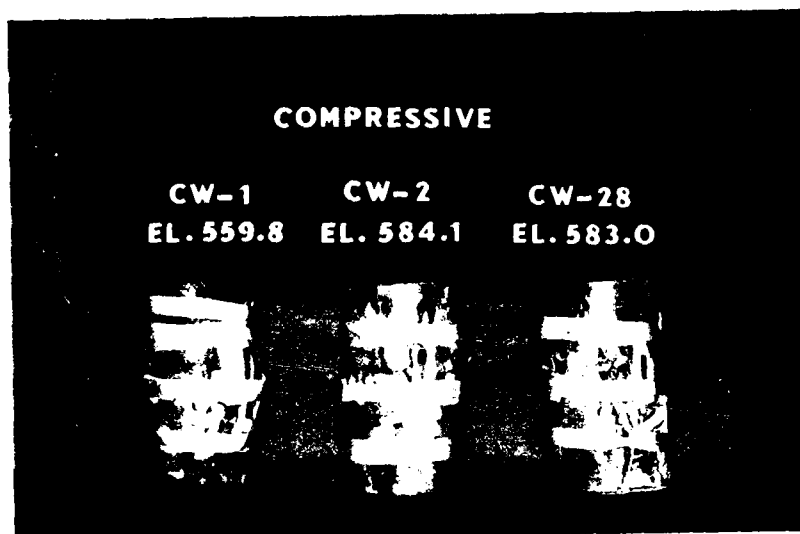
AXIAL  
DIAMETRIC  
AXIAL  
DIAMETRIC  
AXIAL  
DIAMETRIC

14.40 FT  
14.40 FT  
19.40 FT  
19.40 FT  
10.45 FT  
10.45 FT

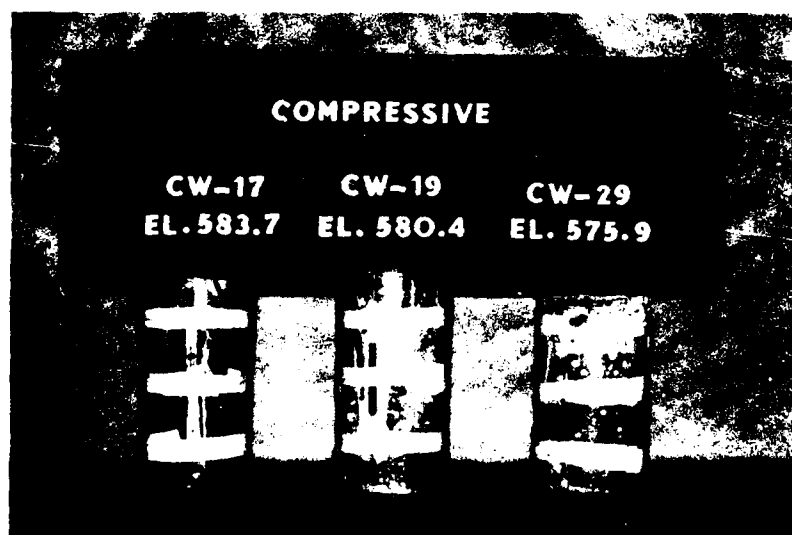
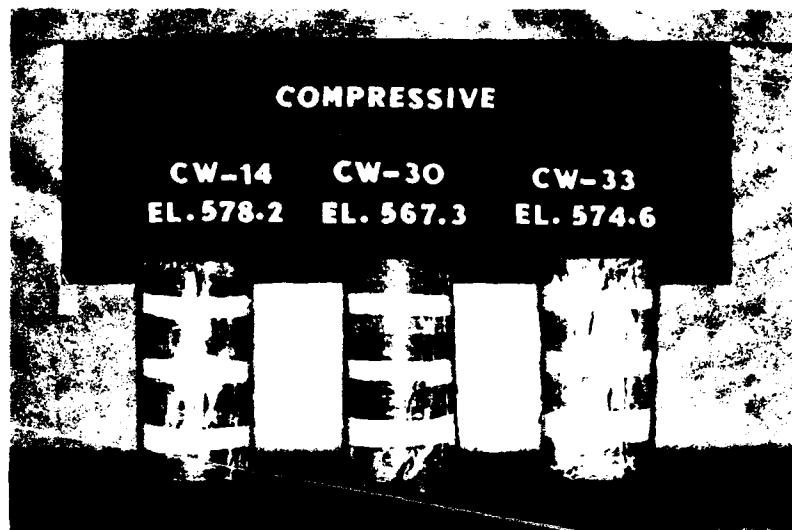
COMPRESSION STRENGTH - SHALY SANDSTONE  
CU-33 14.40 FT; CU-30 19.40 FT; CU-14 10.45 FT  
SAULT ST MARIE

PLATE E18

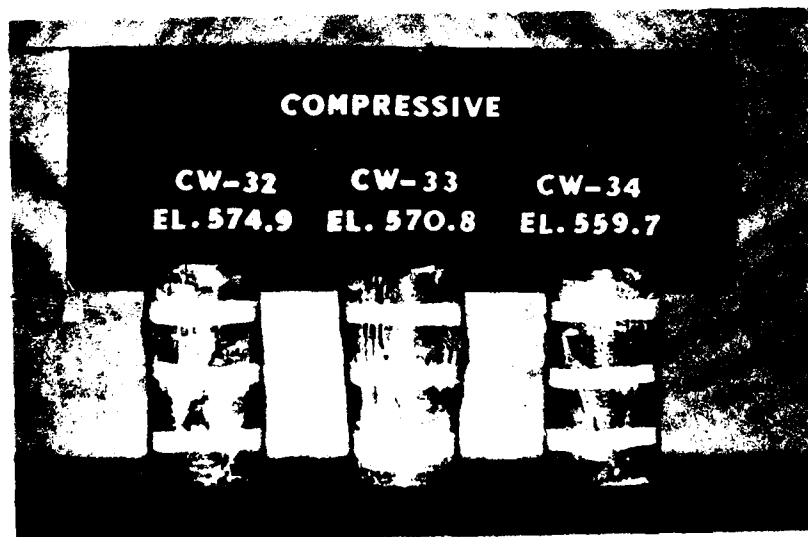
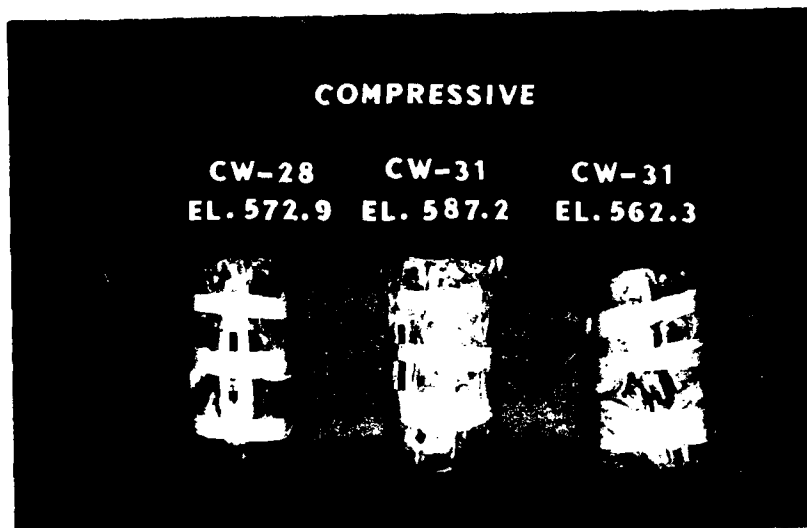




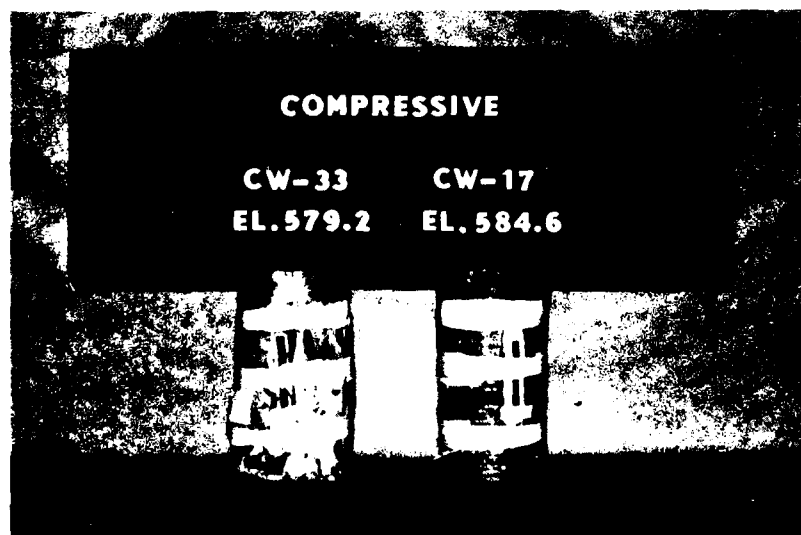
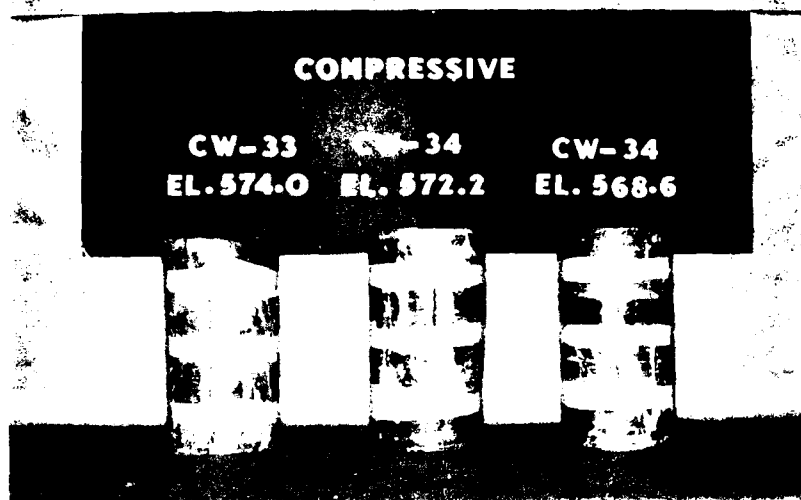
Photographs of core after compressive tests



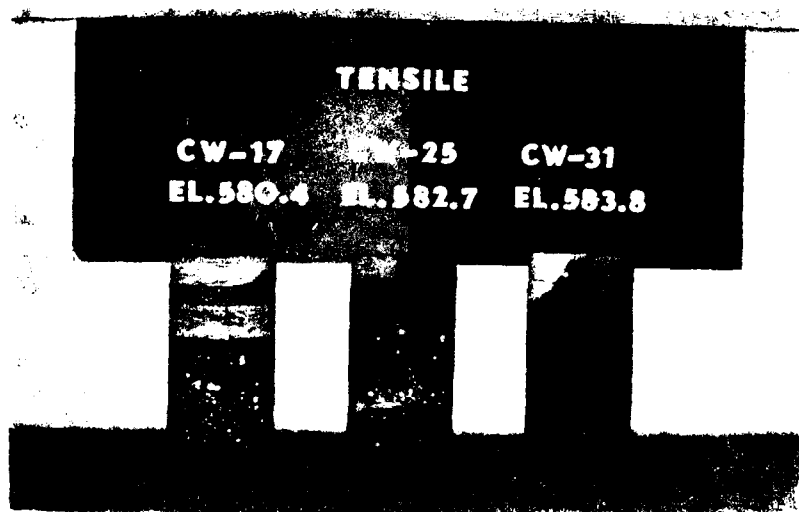
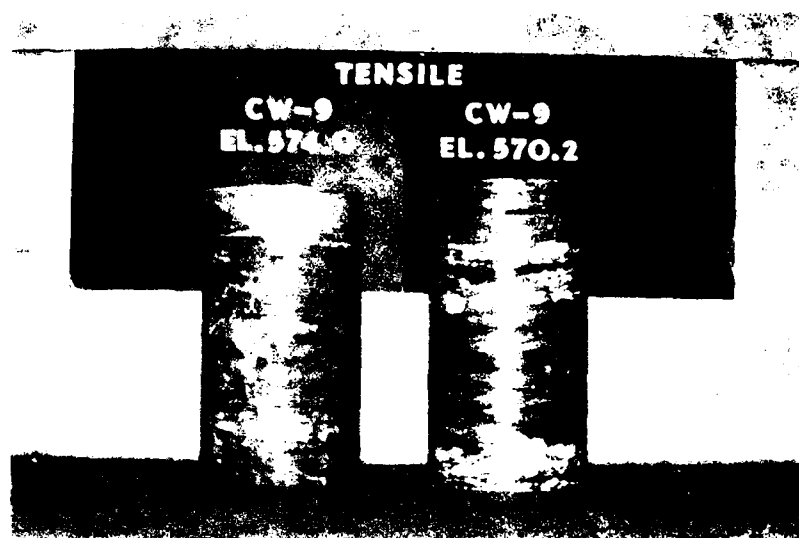
Photographs of core after compressive tests



Photographs of core after compressive tests

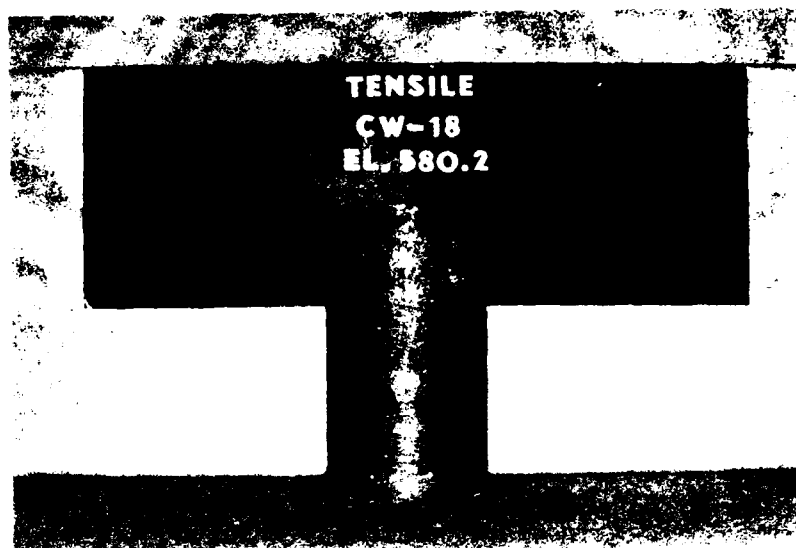


Photographs of core after compressive tests

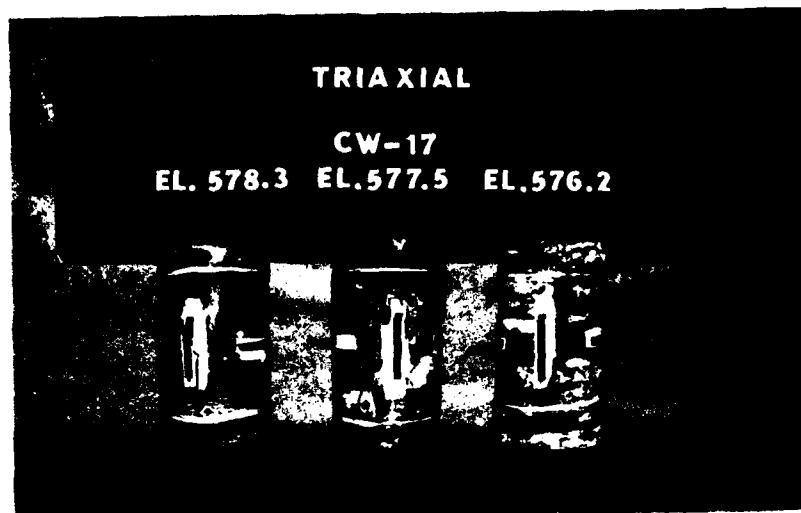


Photographs of core after direct tensile tests

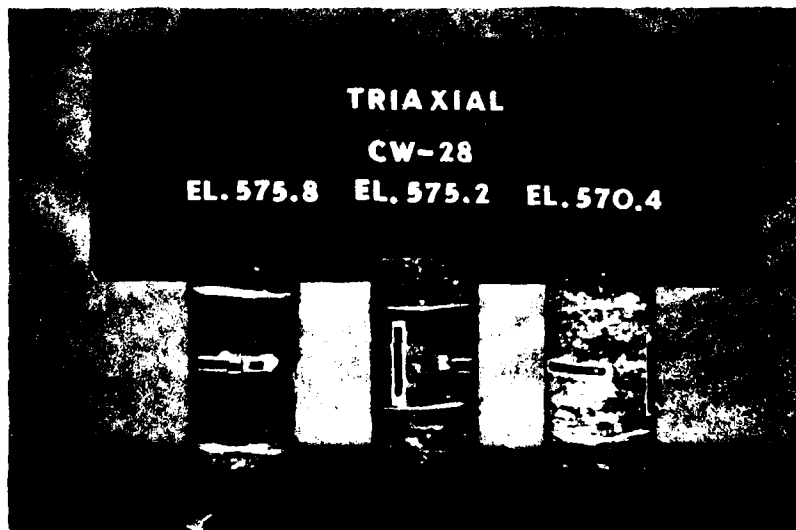
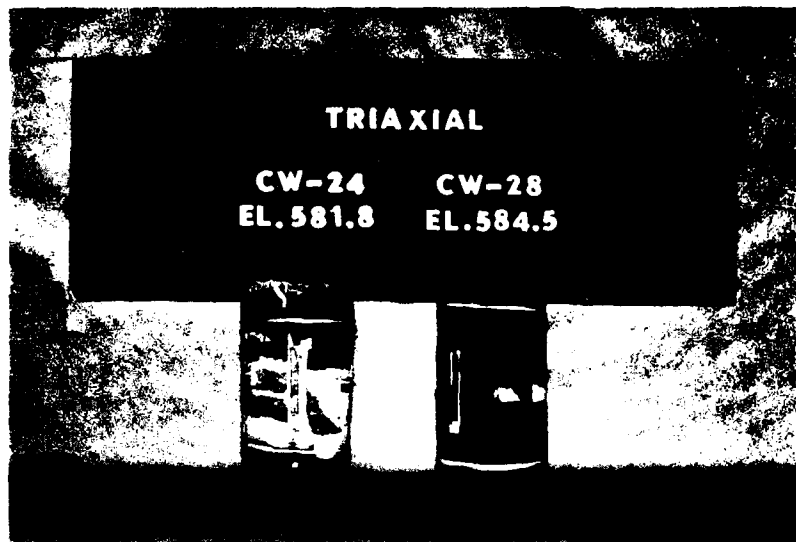




Photographs of core after direct tensile tests



Photographs of core after triaxial tests



Photographs of core after triaxial tests

PLATE E27  
SHEET NO.

SHEAR STRESS $\tau$ , TSP		SHEAR STRESS $\sigma$ , TSP		SHEAR STRENGTH PARAMETERS		SHEAR STRENGTH PARAMETERS	
MAXIMUM		MAXIMUM		MAXIMUM		MAXIMUM	
ULTIMATE		ULTIMATE		ULTIMATE		ULTIMATE	
SHEAR DEFORMATION, IN. $\times 10^{-3}$		SHEAR DEFORMATION, IN. $\times 10^{-3}$		SHEAR DEFORMATION, IN. $\times 10^{-3}$		SHEAR DEFORMATION, IN. $\times 10^{-3}$	
TAN $\phi =$		TAN $\phi =$		TAN $\phi =$		TAN $\phi =$	
C =		C =		C =		C =	
TEST NO. (Boring No. & Depth, ft)		CW-6		CW-2		CW-21	
WET DENSITY, PCF		156.3		154.6		157.1	
WATER CONTENT		0.9 %		1.3 %		2.3 %	
NORMAL STRESS, TSP		1.5		2.5		4.0	
MAXIMUM SHEAR STRESS, TSP		46.76		48.72		51.37	
TIME TO FAILURE, MINUTES		40		161		52	
ULTIMATE SHEAR STRESS, TSP		7.15		9.62		10.22	
INITIAL DIAMETER, IN.		3.96		3.96		3.96	
INITIAL HEIGHT, IN.		3.96		3.96		3.96	
DESCRIPTION OF MATERIAL: Very hard sandstone; Intact							
REMARKS							
PROJECT: Sault St Marie - Compensating Works							
AREA							
BORING NO. see Test No. SAMPLE NO.							
DEPTH see Test No. DATE 24 Oct 1979							
DIRECT SHEAR TEST REPORT (ROCK)							

WES FORM 1490 EDITION OF JUN 65 IS OBSOLETE  
 PLATE E28a SHEET NO

SHEAR STRESS $\tau$ , TSP		SHEAR STRESS $\sigma$ , TSP		SHEAR STRENGTH PARAMETERS		SHEAR STRENGTH PARAMETERS	
MAXIMUM		MAXIMUM		MAXIMUM		MAXIMUM	
ULTIMATE		ULTIMATE		ULTIMATE		ULTIMATE	
SHEAR DEFORMATION, IN. $\times 10^{-3}$		SHEAR DEFORMATION, IN. $\times 10^{-3}$		SHEAR DEFORMATION, IN. $\times 10^{-3}$		SHEAR DEFORMATION, IN. $\times 10^{-3}$	
TAN $\phi =$		TAN $\phi =$		TAN $\phi =$		TAN $\phi =$	
C =		C =		C =		C =	
TEST NO. (Boring No. & Depth, ft)		CW-29		CW-34		CW-20	
WET DENSITY, PCF		130.5		133.2		139.4	
WATER CONTENT		13.6 %		13.4 %		17.0 %	
NORMAL STRESS, TSP		1.0		2.0		3.0	
MAXIMUM SHEAR STRESS, TSP		0.78		1.44		3.12	
TIME TO FAILURE, MINUTES		11		1.47		2.08	
ULTIMATE SHEAR STRESS, TSP		0.60		1.12		1.47	
INITIAL DIAMETER, IN.		D <sub>0</sub>		D <sub>0</sub>		D <sub>0</sub>	
INITIAL HEIGHT, IN.		H <sub>0</sub>		H <sub>0</sub>		H <sub>0</sub>	
DESCRIPTION OF MATERIAL: Silty clay seam taken from very hard sandstone; Clay is classified as a lean clay (CL).							
REMARKS							
PROJECT: Sault Ste Marie Compensating Works							
AREA							
BORING NO. see Test No. SAMPLE NO.							
DEPTH see Test No. DATE Sept 1979							
DIRECT SHEAR TEST REPORT (ROCK)							

WES FORM 1490 EDITION OF JUN 65 IS OBSOLETE  
 PLATE E28b SHEET NO



SHEAR STRESS $\tau$ , TSF		SHEAR STRENGTH $s$ , TSF	
NORMAL DEFORMATION, IN. $\times 10^{-3}$		NORMAL STRESS $\sigma$ , TSF	
		SHEAR STRENGTH PARAMETERS	
		<u>MAXIMUM</u> <u>ULTIMATE</u>	
		$\phi =$ _____	
		TAN $\phi =$ _____	
		$c =$ _____ TSF	
	SHEAR DEFORMATION, IN. $\times 10^{-3}$		

TEST NO. (Boring No. & Depth, ft)	CW-3	CW-5	CW-5			
	24.70	23.85	24.25			
WET DENSITY, PCF	$\gamma_d$ 156.5	158.1	158.5			
WATER CONTENT	$w$ 3.0 %	2.1 %	1.8 %			
NORMAL STRESS, TSF	$\sigma$ 2.0	4.0	8.0			
MAXIMUM SHEAR STRESS, TSF	$\tau_f$					
TIME TO FAILURE, MINUTES	$t_f$ 72	63	103			
ULTIMATE SHEAR STRESS, TSF	$\tau_r$ 1.27	2.61	5.05			
INITIAL DIAMETER, IN.	$D_o$ 5.96	5.93	5.96			
INITIAL HEIGHT, IN.	$H_o$					

DESCRIPTION OF MATERIAL      Very hard sandstone, concrete on rock, precut

REMARKS	PROJECT      Sault St Marie Compensating Works AREA BORING NO. See test no.      SAMPLE NO. DEPTH      See test no.      DATE 24 Aug 1979 EL
DIRECT SHEAR TEST REPORT (ROCK)	





SHEAR STRESS  $\tau$ , TSF

SHEAR STRENGTH  $s$ , TSF

NORMAL DEFORMATION, IN.  $\times 10^{-3}$

NORMAL STRESS  $\sigma$ , TSF

SHEAR STRENGTH PARAMETERS

MAXIMUM      ULTIMATE

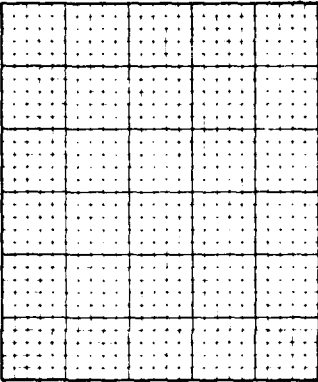
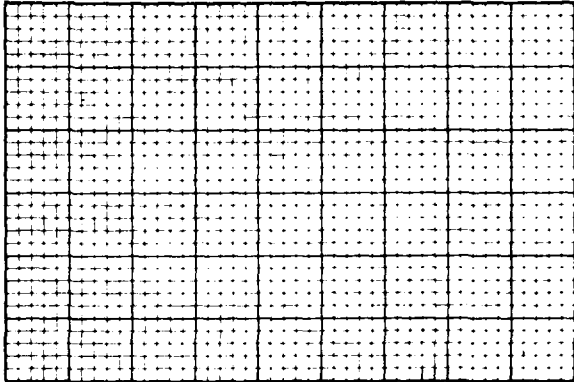
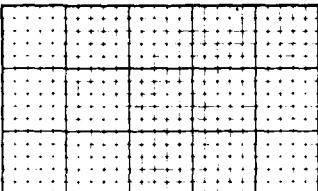
$\phi =$  \_\_\_\_\_

TAN  $\phi =$  \_\_\_\_\_

$c =$  \_\_\_\_\_ TSF

TEST NO. (Boring No. & Depth, ft)		CW-1	CW-23	CW-18	CW-35	CW-18	
WET DENSITY, PCF	$\gamma_d$	155.3	158.6	157.7	157.4	157.2	
WATER CONTENT	$w$	3.3 %	1.8 %	1.8 %	1.9 %	1.9 %	%
NORMAL STRESS, TSF	$\sigma$	2.0	4.0	4.0	8.0	8.0	
MAXIMUM SHEAR STRESS, TSF	$\tau_f$	9.70	6.60	5.56	11.40	16.06	
TIME TO FAILURE, MINUTES	$t_f$	13	11	10	7	7	
ULTIMATE SHEAR STRESS, TSF	$\tau_u$	3.88	6.22	3.81	7.65	14.04	
INITIAL rectangle, in.	$D_0$	3.7x3.9	3.9x3.9	3.6x4.8	3.9x3.6	4.6x3.9	
INITIAL HEIGHT, IN.	$H_0$						
DESCRIPTION OF MATERIAL <u>Very hard sandstone, natural joint</u>							
REMARKS _____		PROJECT <u>Sault St Marie</u>					
		Compensating Works					
		AREA _____					
		BORING NO. <u>see Test No.</u>			SAMPLE NO. _____		
		DEPTH EL. <u>see Test No.</u>			DATE <u>21 Feb 1980</u>		
DIRECT SHEAR TEST REPORT (ROCK)							



SHEAR STRESS $\tau$ , TSF  NORMAL DEFORMATION, IN. $\times 10^{-3}$		SHEAR STRENGTH $s$ , TSF		NORMAL STRESS $\sigma$ , TSF  SHEAR STRENGTH PARAMETERS MAXIMUM      ULTIMATE  $\phi =$ _____ TAN $\phi =$ _____ $c =$ _____ TSF
SHEAR DEFORMATION, IN. $\times 10^{-3}$				

TEST NO. (Boring No. & Depth, ft)	CW-10 9.55	CW-17 26.80	CW-10 9.85				
WET DENSITY, PCF	$\gamma_d$ 160.0	158.0	159.9				
WATER CONTENT	$w$ 1.7 %	3.8 %	2.5 %	%	%	%	%
NORMAL STRESS, TSF	$\sigma$ 6.0	8.0	8.0				
MAXIMUM SHEAR STRESS, TSF	$\tau_f$ 23.85	18.93	26.44				
TIME TO FAILURE, MINUTES	$t_f$ 0.35	0.48	0.17				
ULTIMATE SHEAR STRESS, TSF	$\tau_r$ 9.72	9.20	10.22				
INITIAL DIAMETER, IN.	$D_o$ 3.945	3.954	3.905				
INITIAL HEIGHT, IN.	$H_o$						
DESCRIPTION OF MATERIAL      Hard sandstone, intact							
REMARKS				PROJECT      Sault Ste Marie			
				Compensating Works			
				AREA			
				BORING NO. see Test No.		SAMPLE NO.	
				DEPTH EL      see Test No.		DATE 12 Jan 1980	
DIRECT SHEAR TEST REPORT (ROCK)							

SHEAR STRESS $\tau$ , TSF  NORMAL DEFORMATION, IN. $\times 10^{-3}$  SHEAR DEFORMATION, IN. $\times 10^{-3}$				NORMAL STRESS $\sigma$ , TSF  SHEAR STRENGTH PARAMETERS MAXIMUM      ULTIMATE $\phi =$ _____ $\tan \phi =$ _____ $c =$ _____ TSF
--	--	--	--	--

TEST NO. (Boring No. & Depth, ft)	CW-22 3.8	CW-15 31.1	CW-11 26.8	CW-30 8.8		
WET DENSITY, PCF	$\gamma_d$ 155.1	152.8	153.0	157.5		
WATER CONTENT	$w$ 7.7 %	3.8 %	6.1 %	6.5 %	%	%
NORMAL STRESS, TSF	$\sigma$ 1.5	2.5	4.0	8.0		
MAXIMUM SHEAR STRESS, TSF	$\tau_f$ 1.0	2.42	6.2	7.61		
TIME TO FAILURE, MINUTES	$t_f$ 0.45	0.17	0.18	0.25		
ULTIMATE SHEAR STRESS, TSF	$\tau_u$ 0.7	2.0	5.5	6.94		
INITIAL DIAMETER, IN.	$D_o$ 3.96	3.92	3.79	3.96		
INITIAL HEIGHT, IN.	$H_o$					
DESCRIPTION OF MATERIAL    Hard sandstone - red shale seams intact (>1" thick)						

REMARKS    Specimens thick enough to be taken from host rock	PROJECT    Sault St Marie Compensating Works AREA BORING NO. See test no.    SAMPLE NO. DEPTH                            See test no.    DATE 14 Jan 1980 EL DIRECT SHEAR TEST REPORT (ROCK)
---	--

SHEAR STRESS $\tau$ , TSF  NORMAL DEFORMATION, IN. $\times 10^{-3}$  SHEAR DEFORMATION, IN. $\times 10^{-3}$	SHEAR STRENGTH $s$ , TSF  NORMAL STRESS $\sigma$ , TSF  SHEAR STRENGTH PARAMETERS MAXIMUM      ULTIMATE $\phi =$ _____ $\tan \phi =$ _____ $c =$ _____ TSF																																																																														
<table border="1" style="width: 100%; border-collapse: collapse;"> <tr> <td style="width: 15%;">TEST NO (Boring N. &amp; Depth, ft)</td> <td style="width: 10%;">CW-15</td> <td style="width: 10%;">CW-15</td> <td style="width: 10%;">CW-23</td> <td style="width: 10%;">CW-15</td> <td style="width: 10%;"></td> <td style="width: 10%;"></td> </tr> <tr> <td></td> <td>26.5</td> <td>27.3</td> <td>1.8</td> <td>26.9</td> <td></td> <td></td> </tr> <tr> <td>WET DENSITY, PCF</td> <td><math>\gamma_d</math></td> <td>158.6</td> <td>154.8</td> <td>151.3</td> <td>158.7</td> <td></td> </tr> <tr> <td>WATER CONTENT</td> <td>w</td> <td>2.6 %</td> <td>2.3 %</td> <td>2.4 %</td> <td>2.6 %</td> <td>%</td> </tr> <tr> <td colspan="7"> </td> </tr> <tr> <td>NORMAL STRESS, TSF</td> <td><math>\sigma</math></td> <td>2.0</td> <td>4.0</td> <td>6.0</td> <td>8.0</td> <td></td> </tr> <tr> <td>MAXIMUM SHEAR STRESS, TSF</td> <td><math>\tau_f</math></td> <td>1.0</td> <td>1.52</td> <td>2.14</td> <td>3.47</td> <td></td> </tr> <tr> <td>TIME TO FAILURE, MINUTES</td> <td><math>t_f</math></td> <td>8</td> <td>7</td> <td></td> <td></td> <td></td> </tr> <tr> <td>ULTIMATE SHEAR STRESS, TSF</td> <td><math>\tau_u</math></td> <td></td> <td></td> <td></td> <td></td> <td></td> </tr> <tr> <td>INITIAL DIAMETER, IN.</td> <td><math>D_o</math></td> <td>3.96</td> <td>3.98</td> <td>3.97</td> <td>3.98</td> <td></td> </tr> <tr> <td>INITIAL HEIGHT, IN.</td> <td><math>H_o</math></td> <td></td> <td></td> <td></td> <td></td> <td></td> </tr> </table>			TEST NO (Boring N. & Depth, ft)	CW-15	CW-15	CW-23	CW-15				26.5	27.3	1.8	26.9			WET DENSITY, PCF	$\gamma_d$	158.6	154.8	151.3	158.7		WATER CONTENT	w	2.6 %	2.3 %	2.4 %	2.6 %	%								NORMAL STRESS, TSF	$\sigma$	2.0	4.0	6.0	8.0		MAXIMUM SHEAR STRESS, TSF	$\tau_f$	1.0	1.52	2.14	3.47		TIME TO FAILURE, MINUTES	$t_f$	8	7				ULTIMATE SHEAR STRESS, TSF	$\tau_u$						INITIAL DIAMETER, IN.	$D_o$	3.96	3.98	3.97	3.98		INITIAL HEIGHT, IN.	$H_o$					
TEST NO (Boring N. & Depth, ft)	CW-15	CW-15	CW-23	CW-15																																																																											
	26.5	27.3	1.8	26.9																																																																											
WET DENSITY, PCF	$\gamma_d$	158.6	154.8	151.3	158.7																																																																										
WATER CONTENT	w	2.6 %	2.3 %	2.4 %	2.6 %	%																																																																									
NORMAL STRESS, TSF	$\sigma$	2.0	4.0	6.0	8.0																																																																										
MAXIMUM SHEAR STRESS, TSF	$\tau_f$	1.0	1.52	2.14	3.47																																																																										
TIME TO FAILURE, MINUTES	$t_f$	8	7																																																																												
ULTIMATE SHEAR STRESS, TSF	$\tau_u$																																																																														
INITIAL DIAMETER, IN.	$D_o$	3.96	3.98	3.97	3.98																																																																										
INITIAL HEIGHT, IN.	$H_o$																																																																														
DESCRIPTION OF MATERIAL <u>Hard sandstone, precut</u>																																																																															
REMARKS _____ _____ _____ _____ _____	PROJECT <u>Sault St Marie</u> <u>Compensating Works</u> AREA _____ BORING NO. See test no.      SAMPLE NO. _____ DEPTH EL See test no.      DATE <u>13 May 1980</u> DIRECT SHEAR TEST REPORT (ROCK)																																																																														

SHEAR STRESS  $\tau$ , TSF

SHEAR STRENGTH  $s$ , TSF

NORMAL STRESS  $\sigma$ , TSF

SHEAR STRENGTH PARAMETERS

MAXIMUM    ULTIMATE

$\phi$  = \_\_\_\_\_

TAN  $\phi$  = \_\_\_\_\_

$c$  = \_\_\_\_\_ TSF

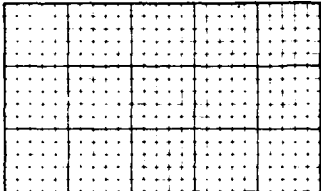
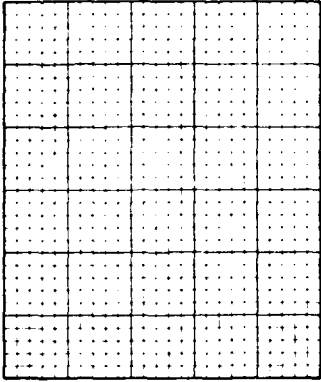
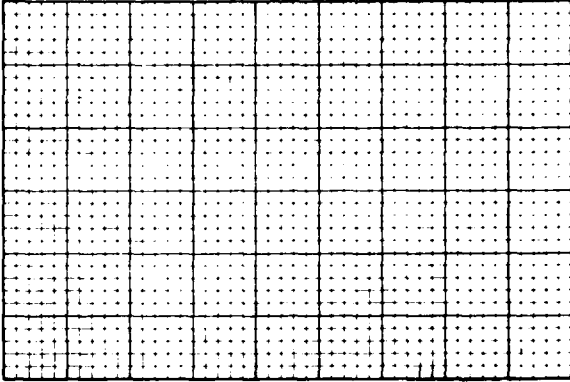
NORMAL DEFORMATION, IN.  $\times 10^{-3}$

SHEAR DEFORMATION, IN.  $\times 10^{-3}$

TEST NO.(Boring No. & Depth,ft)		CW-17 46.4	CW-28 2.35	CW-32 6.60	CW-23 7.00		
WET DENSITY, PCF	$\gamma_d$	160.6	155.0	159.0	155.0		
WATER CONTENT	w	3.2 %	3.1 %	5.7 %	4.1 %	%	%
NORMAL STRESS, TSF	$\sigma$	1.5	2.5	4.0	6.0		
MAXIMUM SHEAR STRESS, TSF	$\tau_f$	1.14	1.68	2.90	4.13		
TIME TO FAILURE, MINUTES	$t_f$	4	15	17	11		
ULTIMATE SHEAR STRESS, TSF	$\tau_r$	0.67	0.93	1.45	3.05		
INITIAL DIAMETER, IN.	$D_o$	3.97	3.98	3.94	3.97		
INITIAL HEIGHT, IN.	$H_o$						
DESCRIPTION OF MATERIAL    Hard Sandstone with shale seams (<1/16" to 1" thick)							

REMARKS \_\_\_\_\_  
 \_\_\_\_\_  
 \_\_\_\_\_  
 \_\_\_\_\_  
 \_\_\_\_\_

PROJECT	Sault St Marie		
	Compensating Works		
AREA			
BORING NO.	See test no.	SAMPLE NO.	
DEPTH EL	See test no.	DATE	29 Jan 1980
DIRECT SHEAR TEST REPORT (ROCK)			

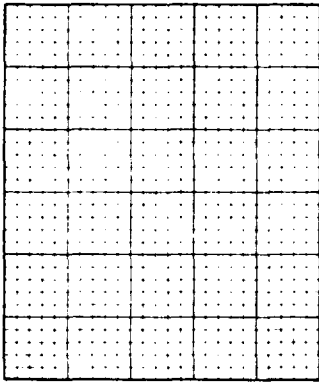
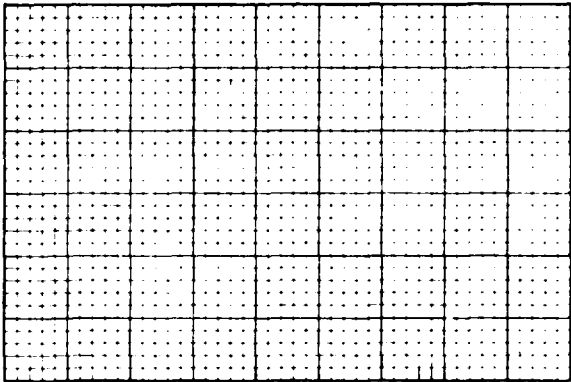
NORMAL DEFORMATION, IN. $\times 10^{-3}$	SHEAR STRESS $\tau$ , TSF	SHEAR STRENGTH $s$ , TSF	NORMAL STRESS $\sigma$ , TSF
			SHEAR STRENGTH PARAMETERS MAXIMUM      ULTIMATE $\phi =$ _____ $\tan \phi =$ _____ $c =$ _____ TSF
SHEAR DEFORMATION, IN. $\times 10^{-3}$			

TEST NO.(Boring No. & Depth,ft)	CW-1 27.6	CW-1 27.9	CW-13 26.6			
WET DENSITY, PCF	$\gamma_d$ 157.4	155.3	160.0			
WATER CONTENT	$w$ 3.1 %	3.1 %	2.4 %	%	%	%
NORMAL STRESS, TSF	$\sigma$ 2.0	4.0	8.0			
MAXIMUM SHEAR STRESS, TSF	$\tau_f$ 2.04	10.03	17.73			
TIME TO FAILURE, MINUTES	$t_f$ 19	14	13			
ULTIMATE SHEAR STRESS, TSF	$\tau_r$ 1.98	7.05	9.58			
INITIAL rectangle, in.	$D_o$ 3.6x3.9	3.7x4.0	3.7x3.9			
INITIAL HEIGHT, IN.	$H_o$					

DESCRIPTION OF MATERIAL Hard sandstone, natural joint

REMARKS _____ _____ _____ _____ _____	PROJECT <u>Sault St Marie</u> <u>Compensating Works</u> AREA _____ BORING NO. <u>See test no.</u> SAMPLE NO. _____ DEPTH <u>See test no.</u> DATE <u>3 March 1980</u> EL _____
---	---

DIRECT SHEAR TEST REPORT (ROCK)

SHEAR STRESS $\tau$ , TSF          NORMAL DEFORMATION IN. $\times 10^{-3}$	SHEAR STRENGTH $s$ , TSF	NORMAL STRESS $\sigma$ , TSF					
		SHEAR STRENGTH PARAMETERS MAXIMUM      ULTIMATE $\phi =$ _____ $\tan \phi =$ _____ $c =$ _____ TSF					
SHEAR DEFORMATION, IN. $\times 10^{-3}$							
TEST NO. (Boring No. & Depth, ft)	CW-10 7.4	CW-10 7.75	CW-32 4.0				
WET DENSITY, PCF	$\gamma_d$ 155.9	$\gamma_d$ 155.6	$\gamma_d$ 156.0				
WATER CONTENT	$w$ 3.2 %	$w$ 3.6 %	$w$ 3.0 %	%	%	%	%
NORMAL STRESS, TSF	$\sigma$ 2.0	$\sigma$ 4.0	$\sigma$ 8.0				
MAXIMUM SHEAR STRESS, TSF	$\tau_f$ 2.6.6	$\tau_f$ 37.1	$\tau_f$ 41.5				
TIME TO FAILURE, MINUTES	$t_f$ 33	$t_f$ 37	$t_f$ 35				
ULTIMATE SHEAR STRESS, TSF	$\tau_r$						
INITIAL DIAMETER, IN.	$D_o$ 3.97	$D_o$ 3.93	$D_o$ 3.95				
INITIAL HEIGHT, IN.	$H_o$						
DESCRIPTION OF MATERIAL      Shaly sandstone, intact							
REMARKS				PROJECT      Sault Ste Marie			
				Compensating Works			
				AREA			
				BORING NO.      see Test No.		SAMPLE NO.	
				DEPTH EL      see Test No.		DATE      13 May 1980	
DIRECT SHEAR TEST REPORT (ROCK)							

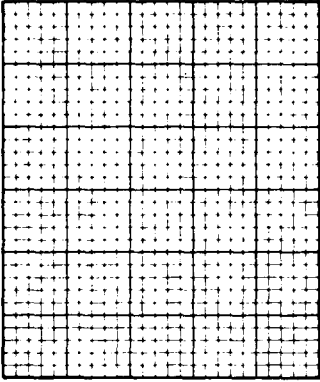


SHEAR STRESS $\tau$ , TSF  NORMAL DEFORMATION, IN. $\times 10^{-3}$	SHEAR STRENGTH $s$ , TSF	NORMAL STRESS $\sigma$ , TSF  SHEAR STRENGTH PARAMETERS MAXIMUM      ULTIMATE  $\phi =$ _____ $\tan \phi =$ _____ $c =$ _____ TSF

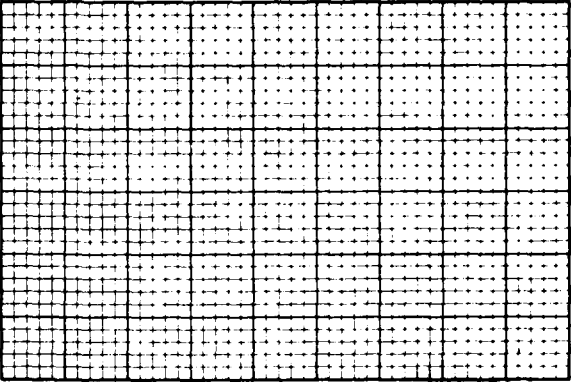
TEST NO.(Boring No. & Depth,ft)	CW-32	CW-33	CW-31			
	7.95	14.6	24.35			
WET DENSITY, PCF	$\gamma_d$ 153.0	142.5	157.7			
WATER CONTENT	$w$ 3.7 %	4.6 %	6.0 %			
NORMAL STRESS, TSF	$\sigma$ 2.0	4.0	8.0			
MAXIMUM SHEAR STRESS, TSF	$\tau_f$ 1.41	4.66	7.83			
TIME TO FAILURE, MINUTES	$t_f$ 11	18	7			
ULTIMATE SHEAR STRESS, TSF	$\tau_r$ 1.03	3.39	5.29			
INITIAL DIAMETER, IN.	$D_o$ 3.96	4.11	3.93			
INITIAL HEIGHT, IN.	$H_o$					
DESCRIPTION OF MATERIAL      Shaly sandstone - red shale with thin clay seams						
intact (>1" thick)						
REMARKS      Specimens thick enough	PROJECT      Sault Ste Marie					
to be taken from host rock						
	AREA					
	BORING NO. see Test No.			SAMPLE NO.		
	DEPTH EL      see Test No.			DATE      9 Jan 1980		
DIRECT SHEAR TEST REPORT (ROCK)						



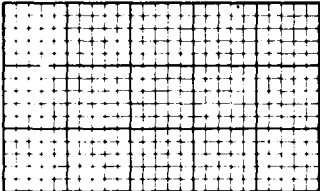
SHEAR STRESS  $\tau$ , TSF



SHEAR STRENGTH  $s$ , TSF



NORMAL DEFORMATION, IN.  $\times 10^{-3}$



SHEAR DEFORMATION, IN.  $\times 10^{-3}$

NORMAL STRESS  $\sigma$ , TSF

SHEAR STRENGTH PARAMETERS

MAXIMUM      ULTIMATE

$\phi =$  \_\_\_\_\_

$\tan \phi =$  \_\_\_\_\_

$c =$  \_\_\_\_\_ TSF

TEST NO.(Boring No. & Depth,ft)		CW-13 29.50	CW-23 10.25	CW-10 10.60	CW-15 28.90	CW-1 34.80	
WET DENSITY, PCF	$\gamma_d$	142.5	144.2	143.9	147.4	142.5	
WATER CONTENT	w	5.1 %	4.2 %	4.4 %	4.6 %	6.1 %	%
NORMAL STRESS, TSF	$\sigma$	1.5	2.5	4.0	6.0	8.0	
MAXIMUM SHEAR STRESS, TSF	$\tau_f$	0.58	5.18	3.70	11.72	11.42	
TIME TO FAILURE, MINUTES	$t_f$	15	15	16	34	77	
ULTIMATE SHEAR STRESS, TSF	$\tau_r$	0.49	2.60	1.54	4.81	5.42	
INITIAL DIAMETER, IN.	$D_o$	3.98	3.91	3.97	3.96	4.04	
INITIAL HEIGHT, IN.	$H_o$						

DESCRIPTION OF MATERIAL Shaly sandstone, thin clay seams (<1/8" thick)

REMARKS \_\_\_\_\_

\_\_\_\_\_

\_\_\_\_\_

\_\_\_\_\_

\_\_\_\_\_

PROJECT Sault Ste Marie

Compensating Works

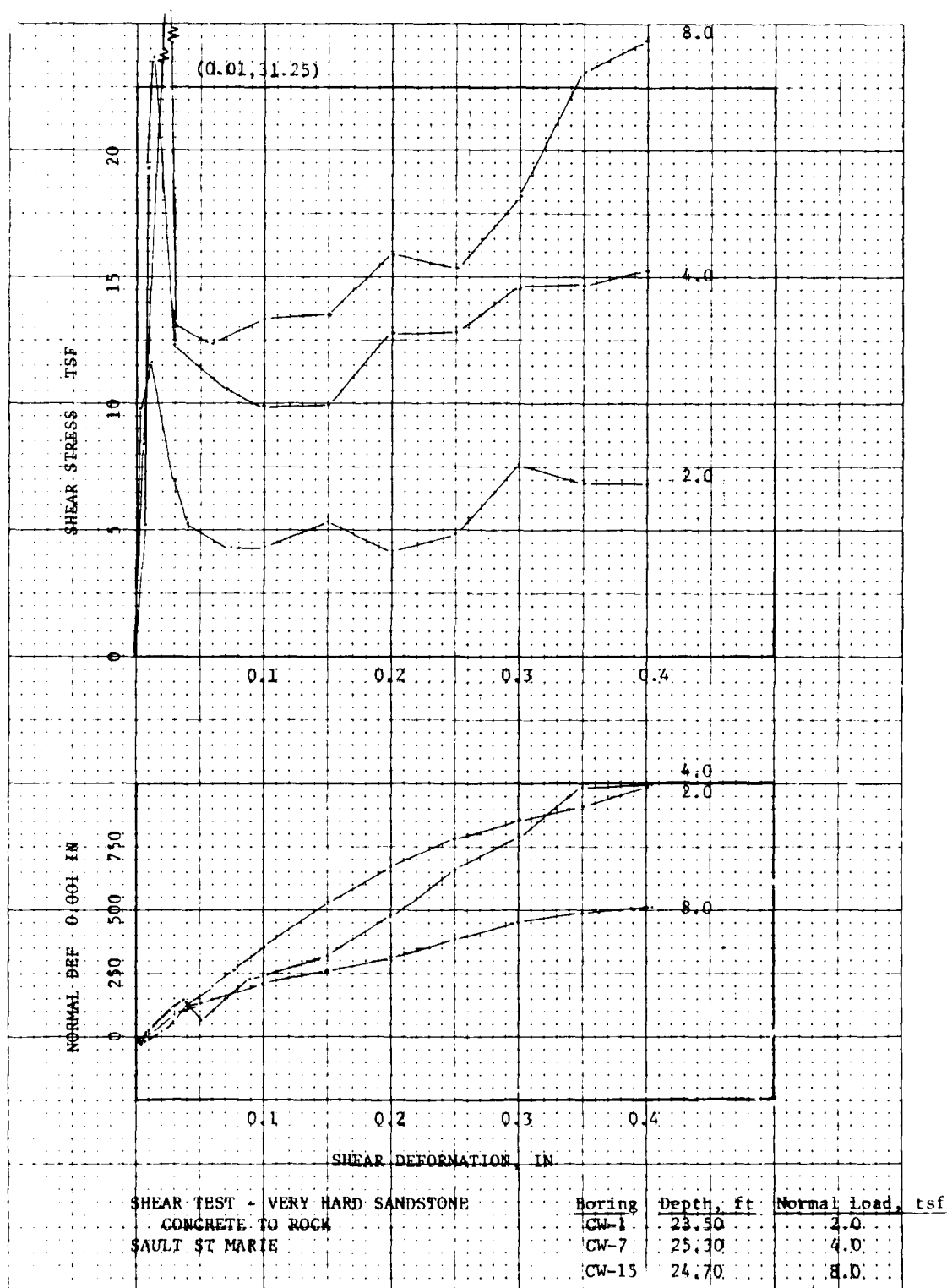
AREA \_\_\_\_\_

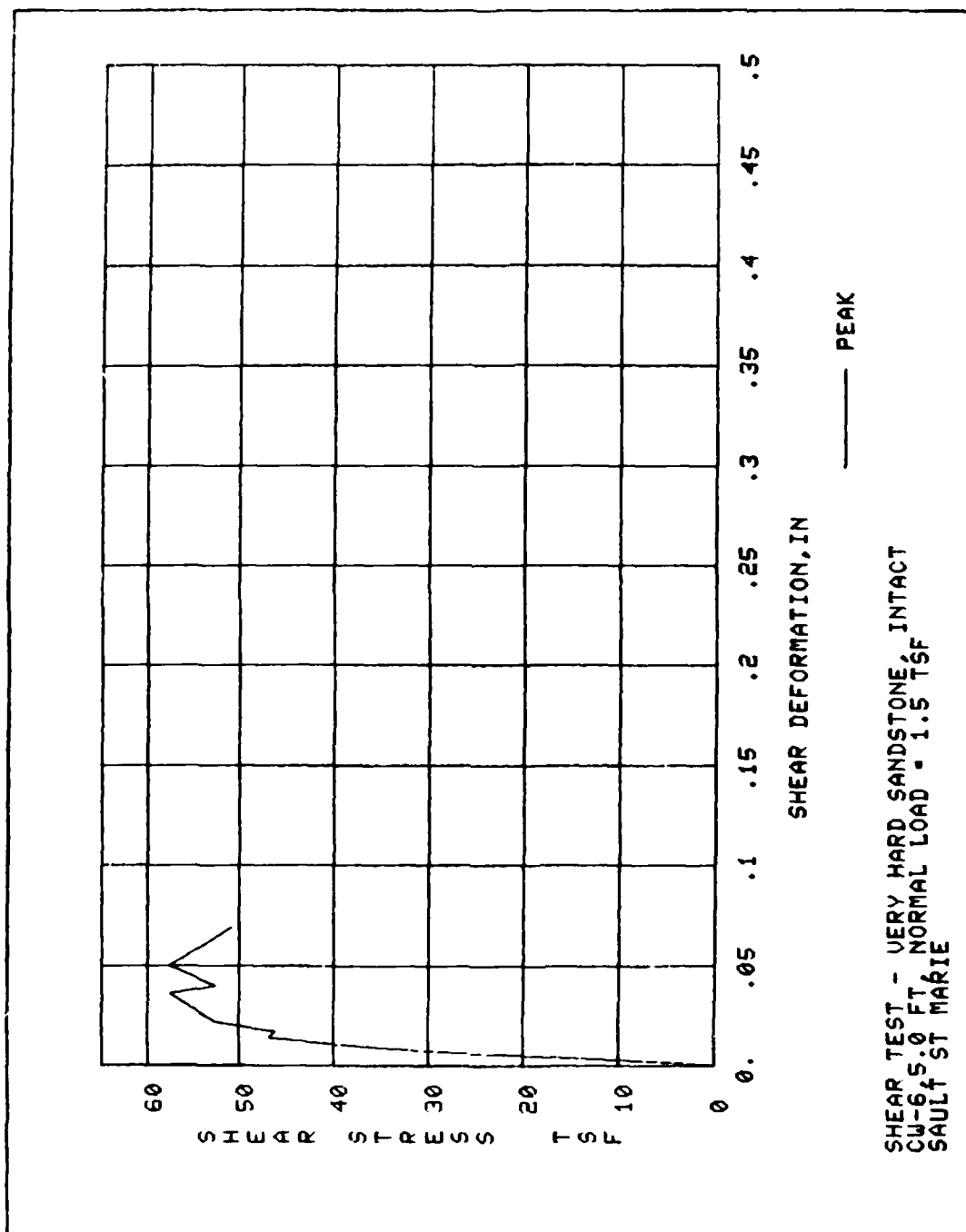
BORING NO. see Test No.      SAMPLE NO. \_\_\_\_\_

DEPTH see Test No.      DATE 30 Oct 1979

DIRECT SHEAR TEST REPORT (ROCK)

SHEET NO.





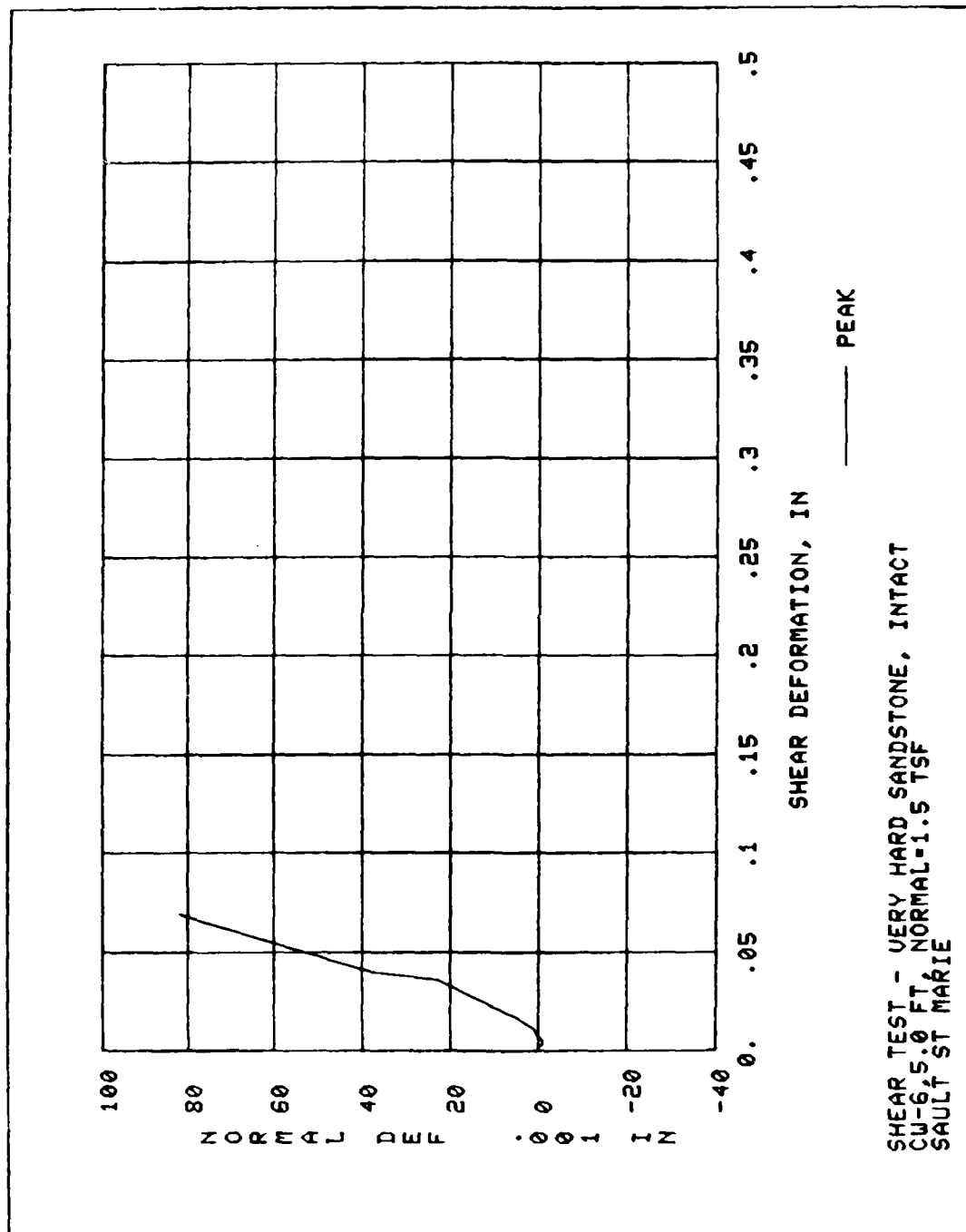
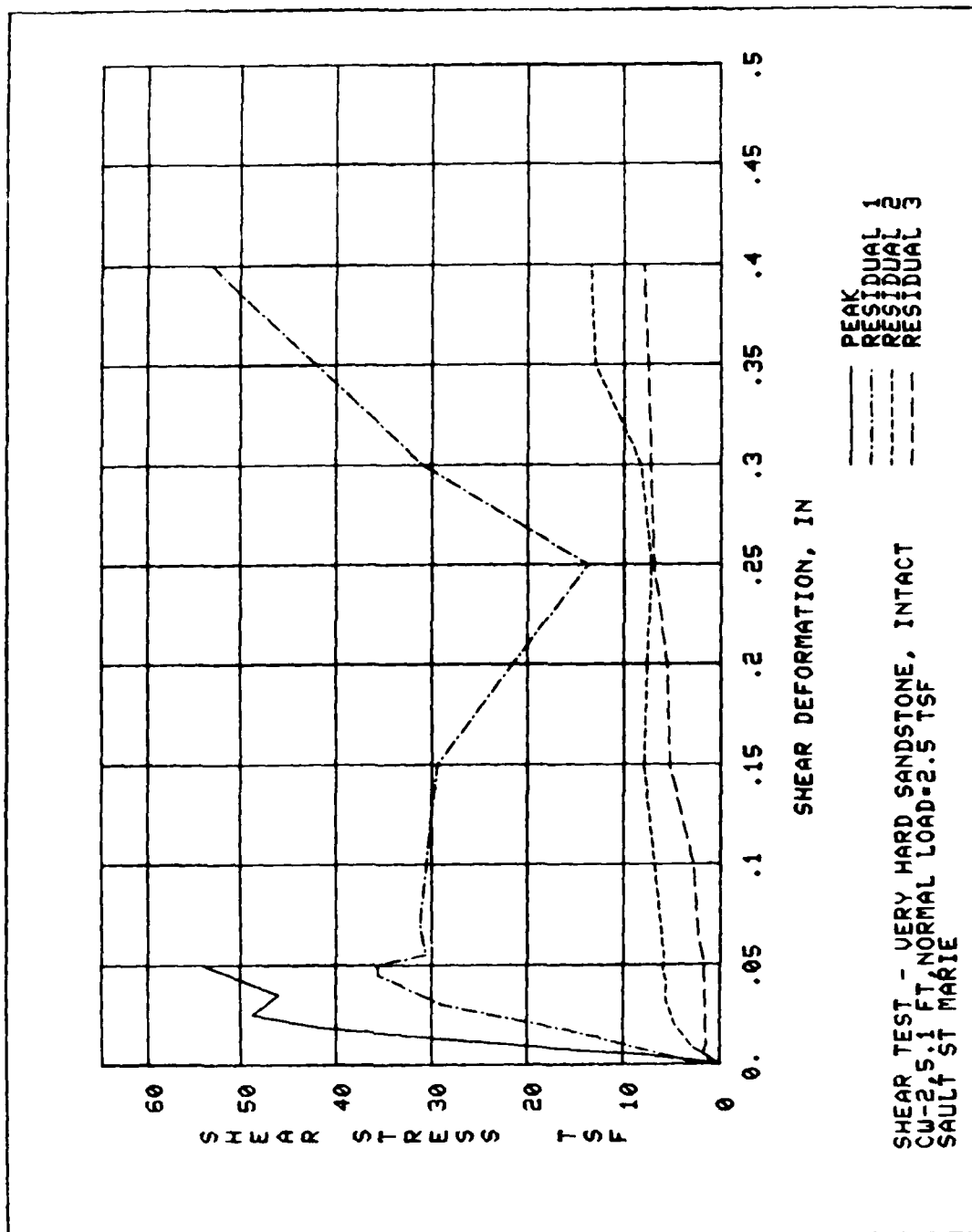


PLATE E46





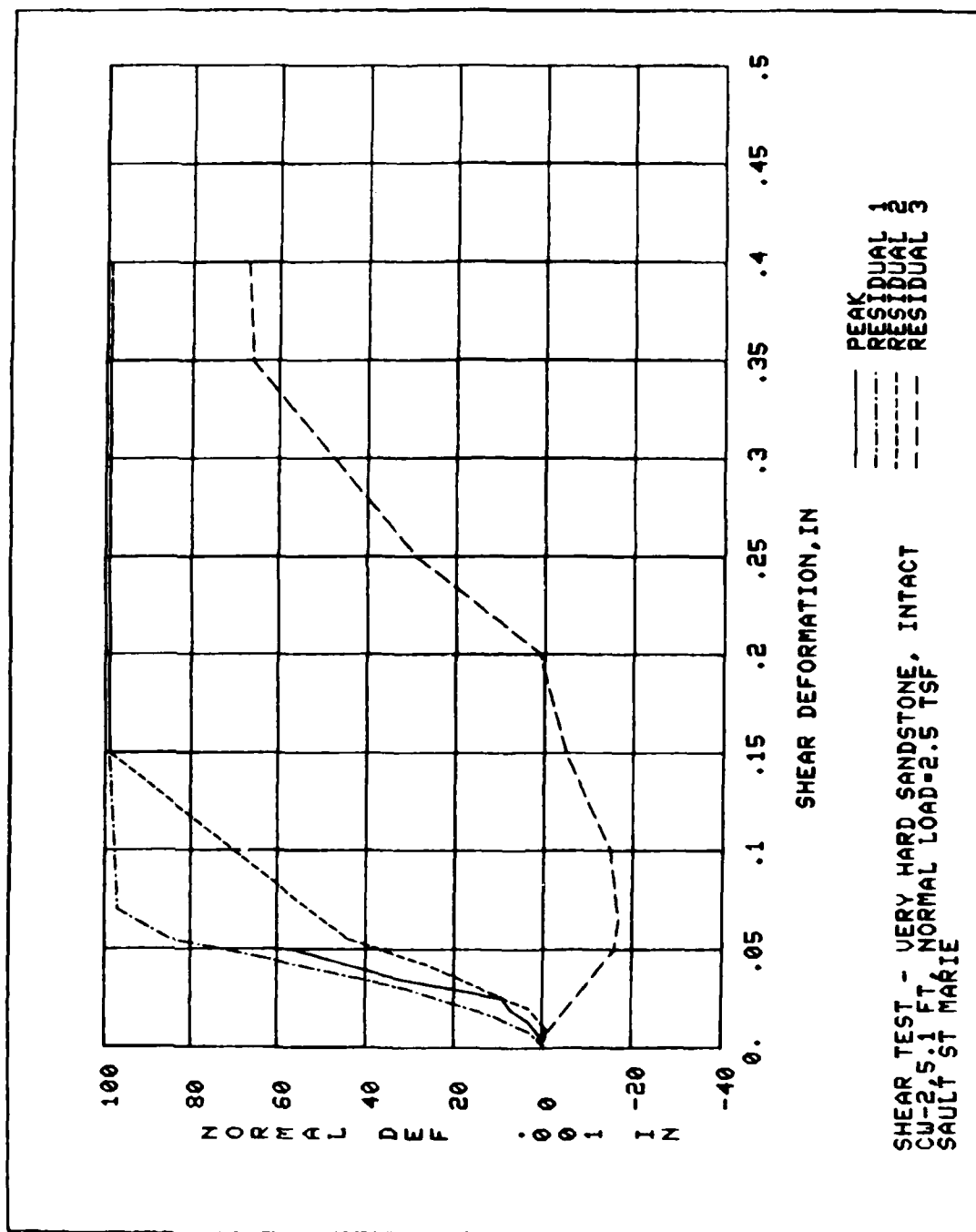
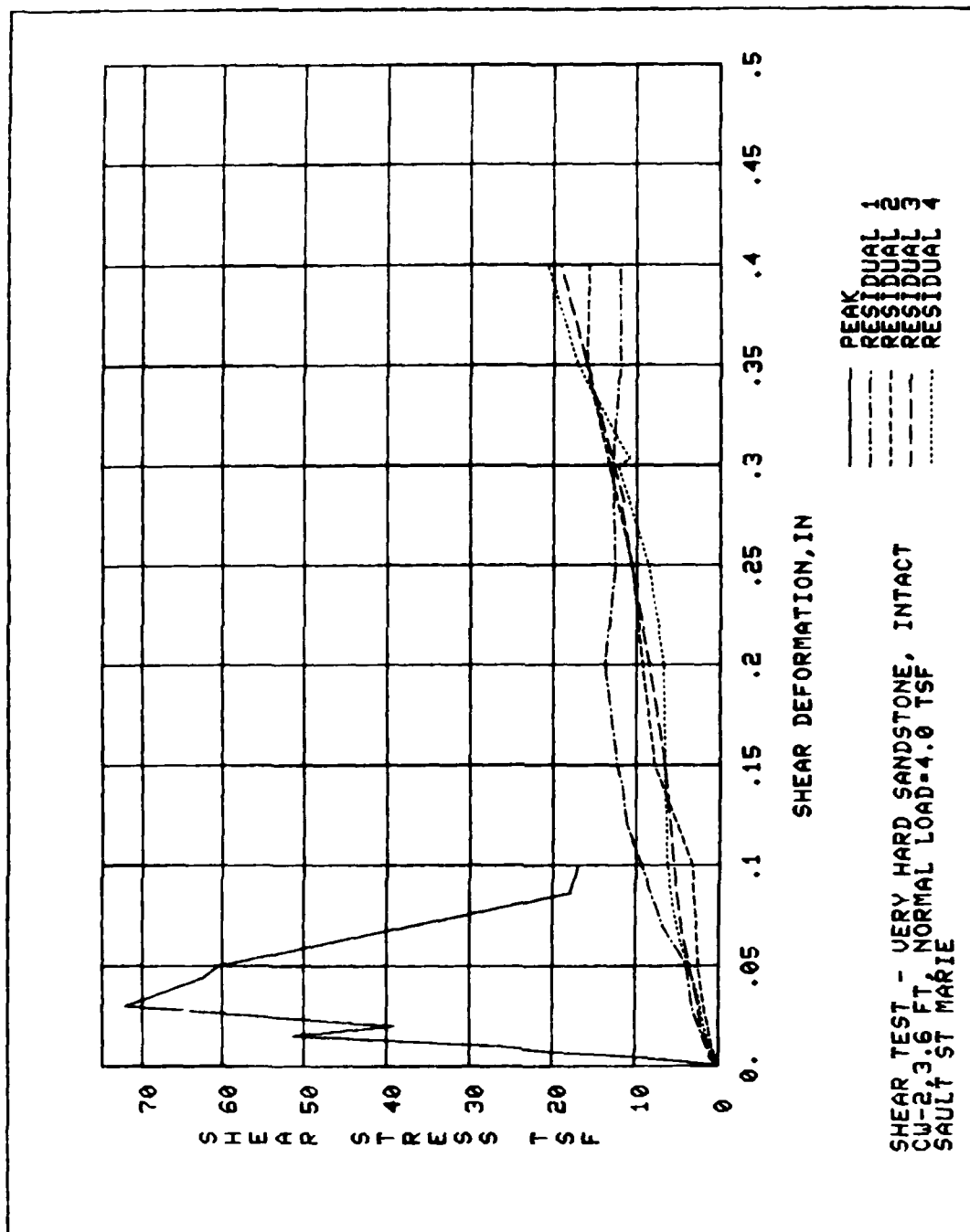


PLATE E48



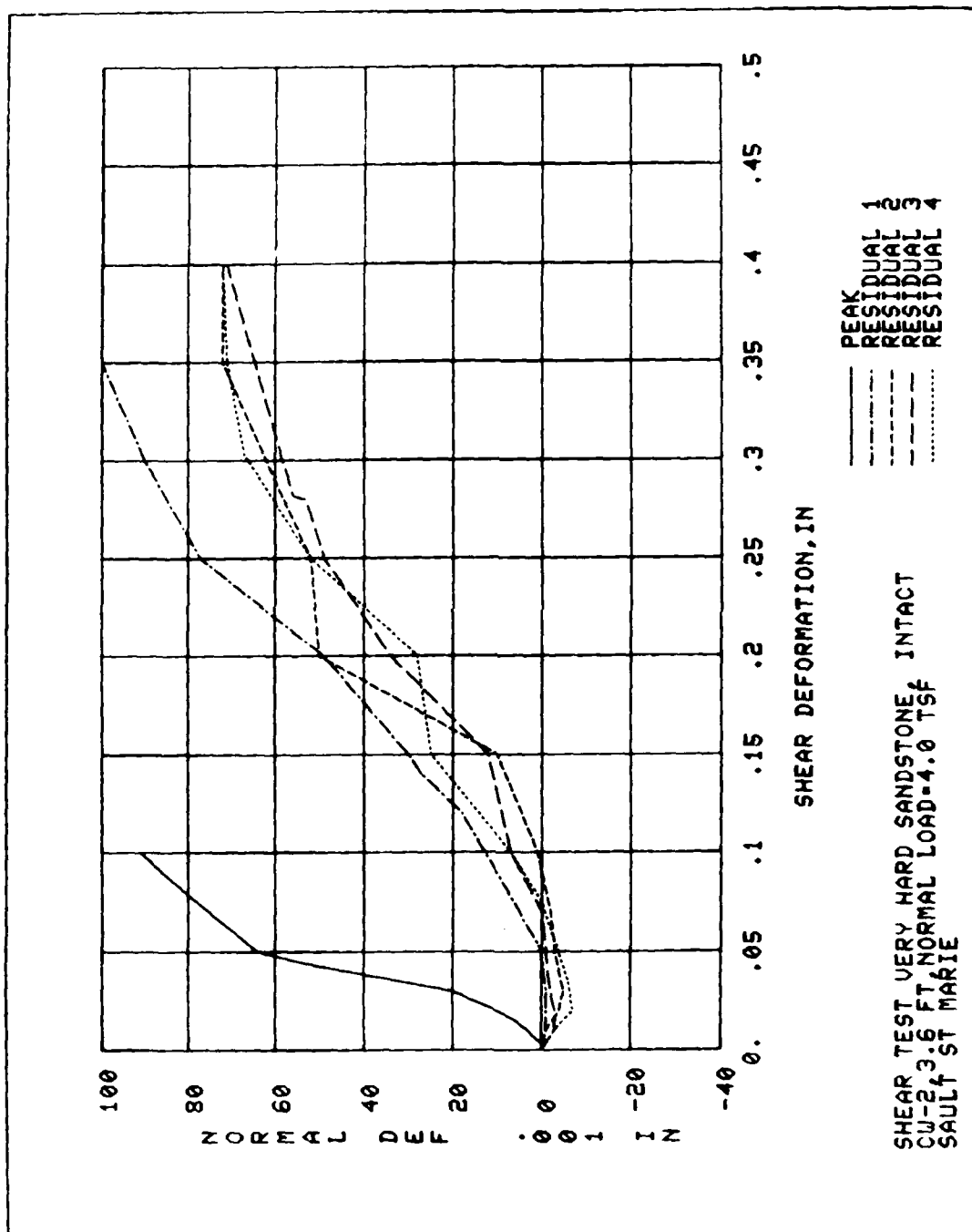


PLATE E50

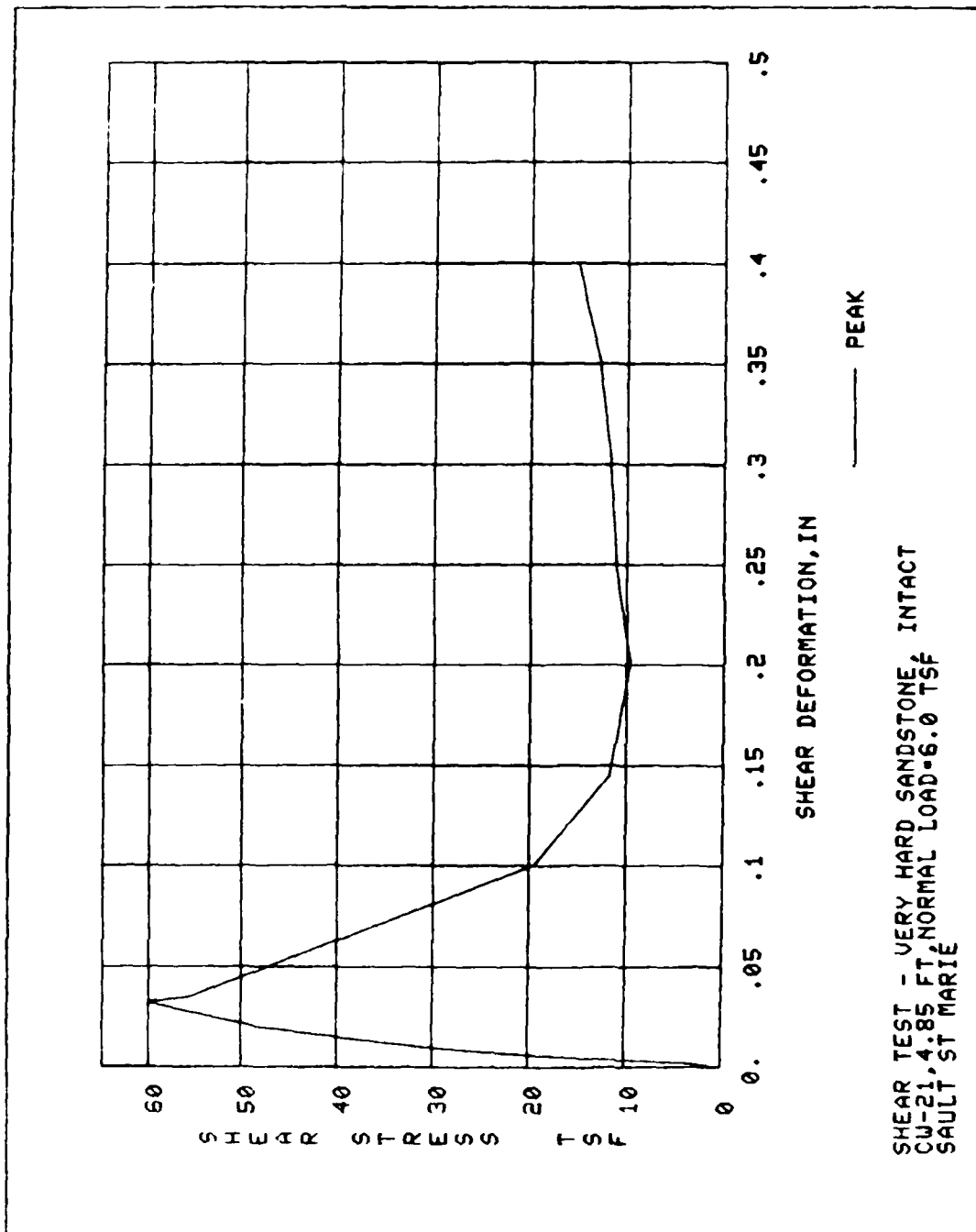


PLATE E51

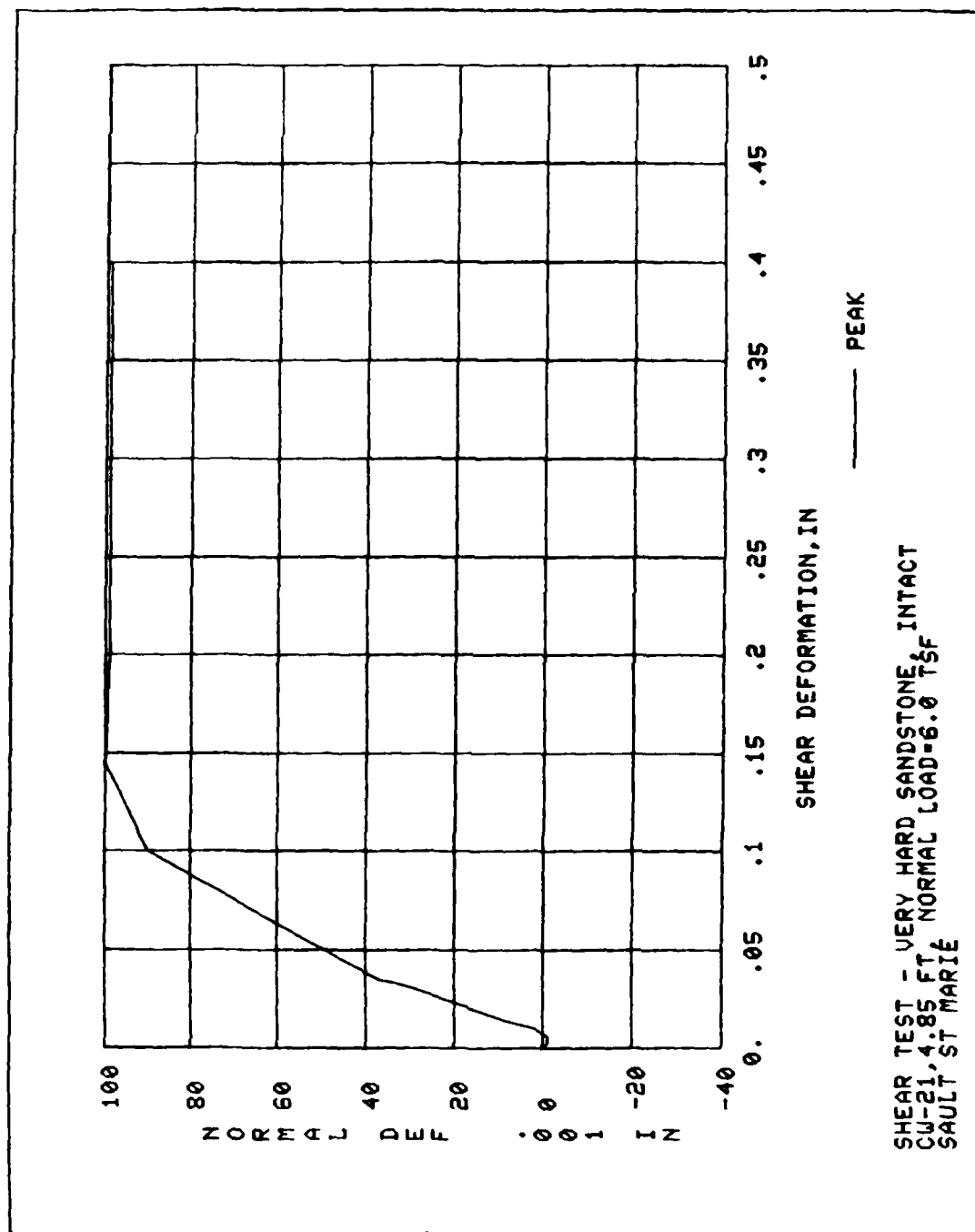
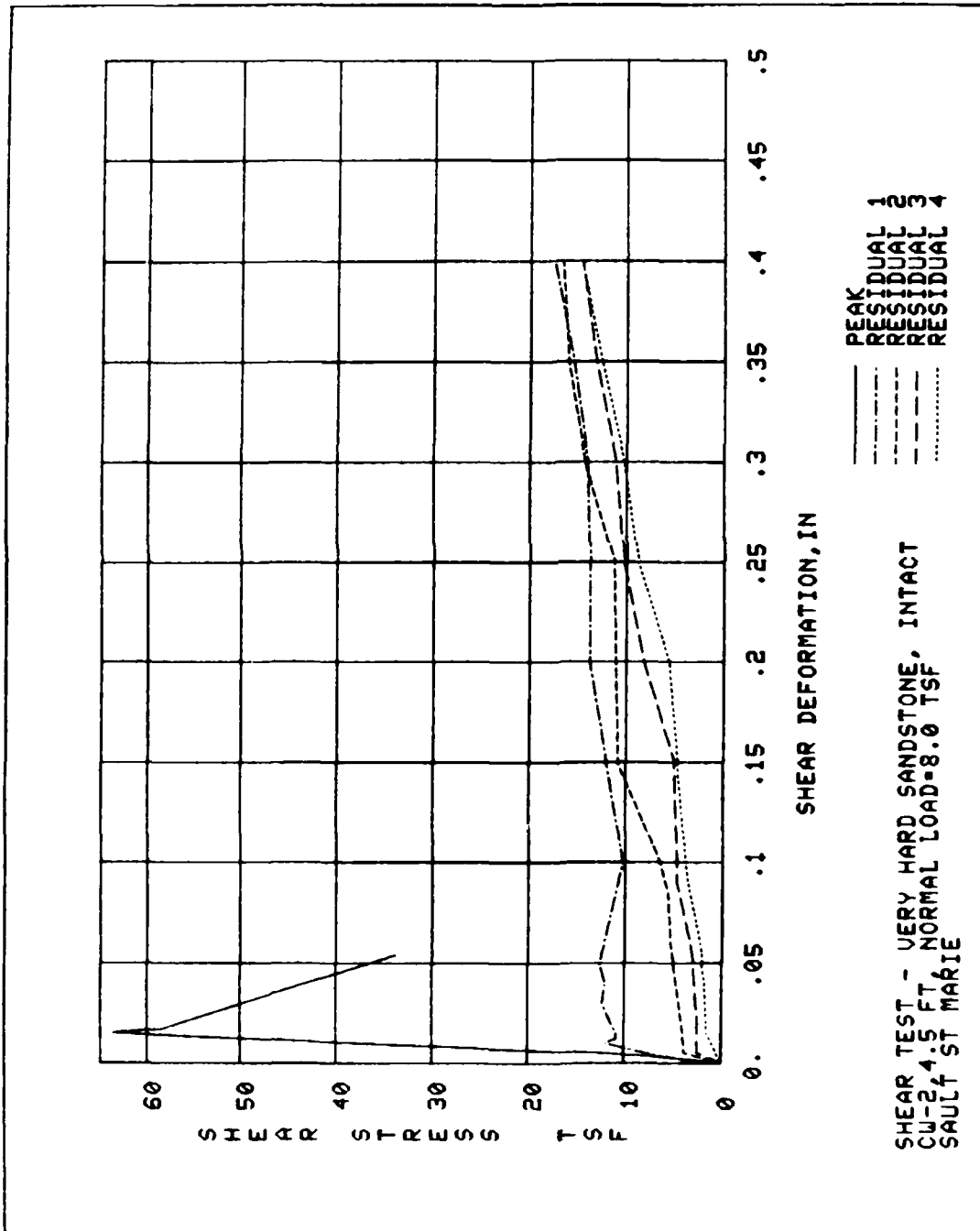


PLATE E52



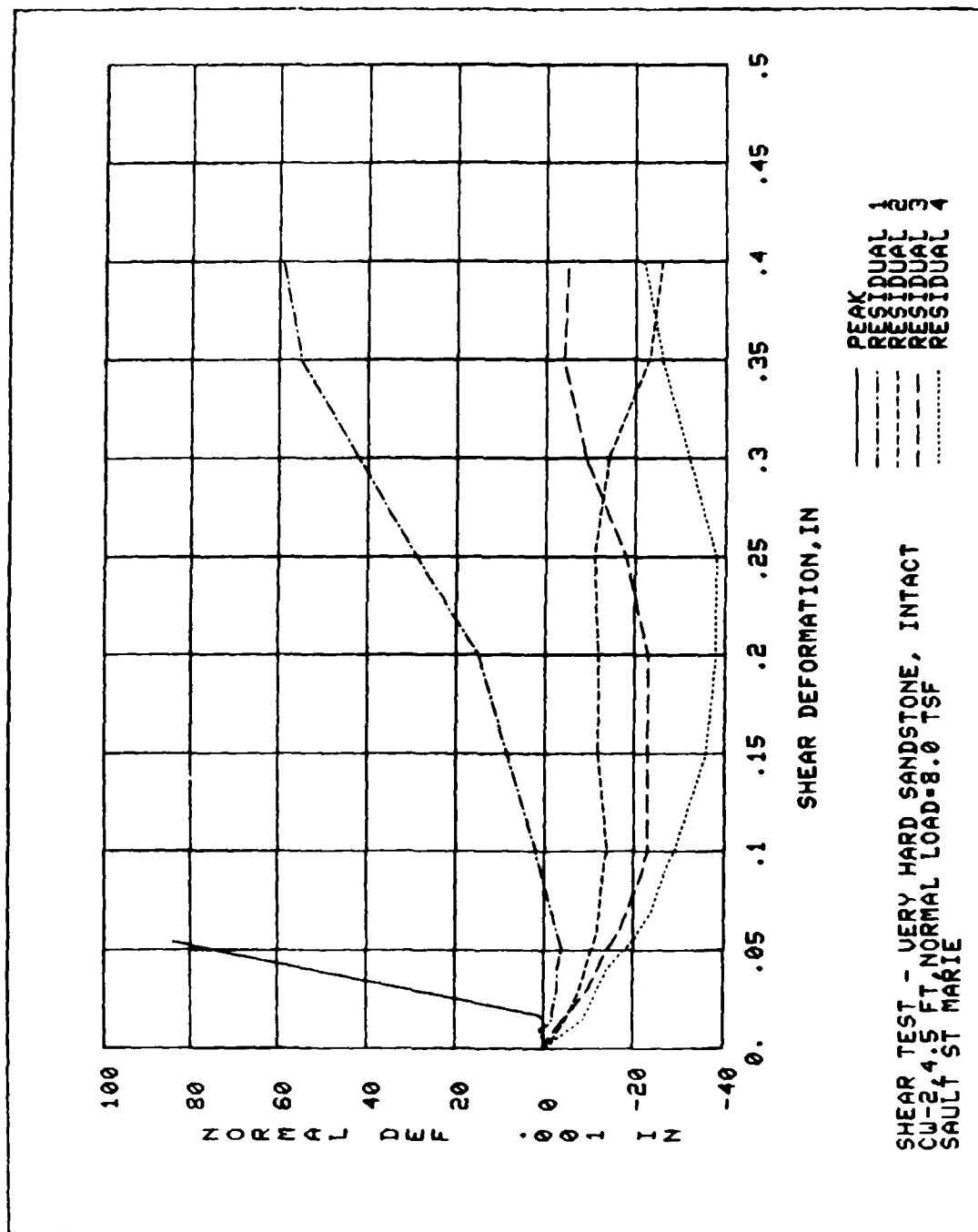
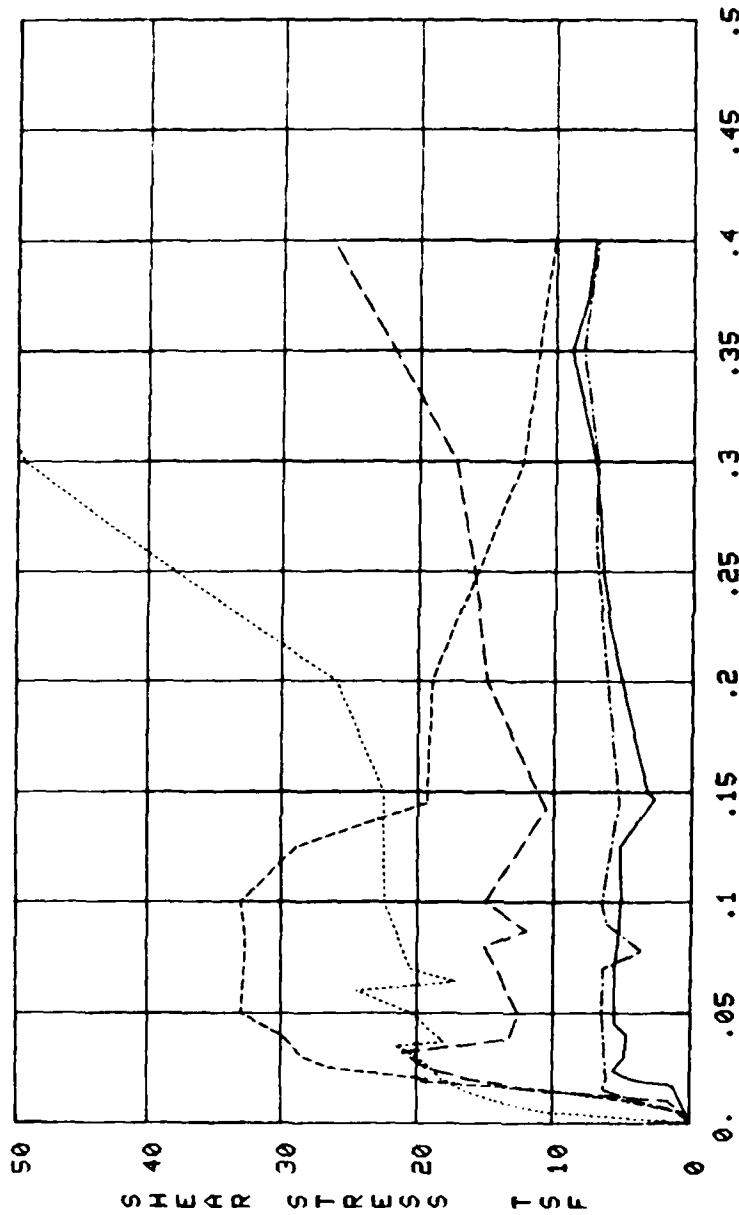


PLATE E54

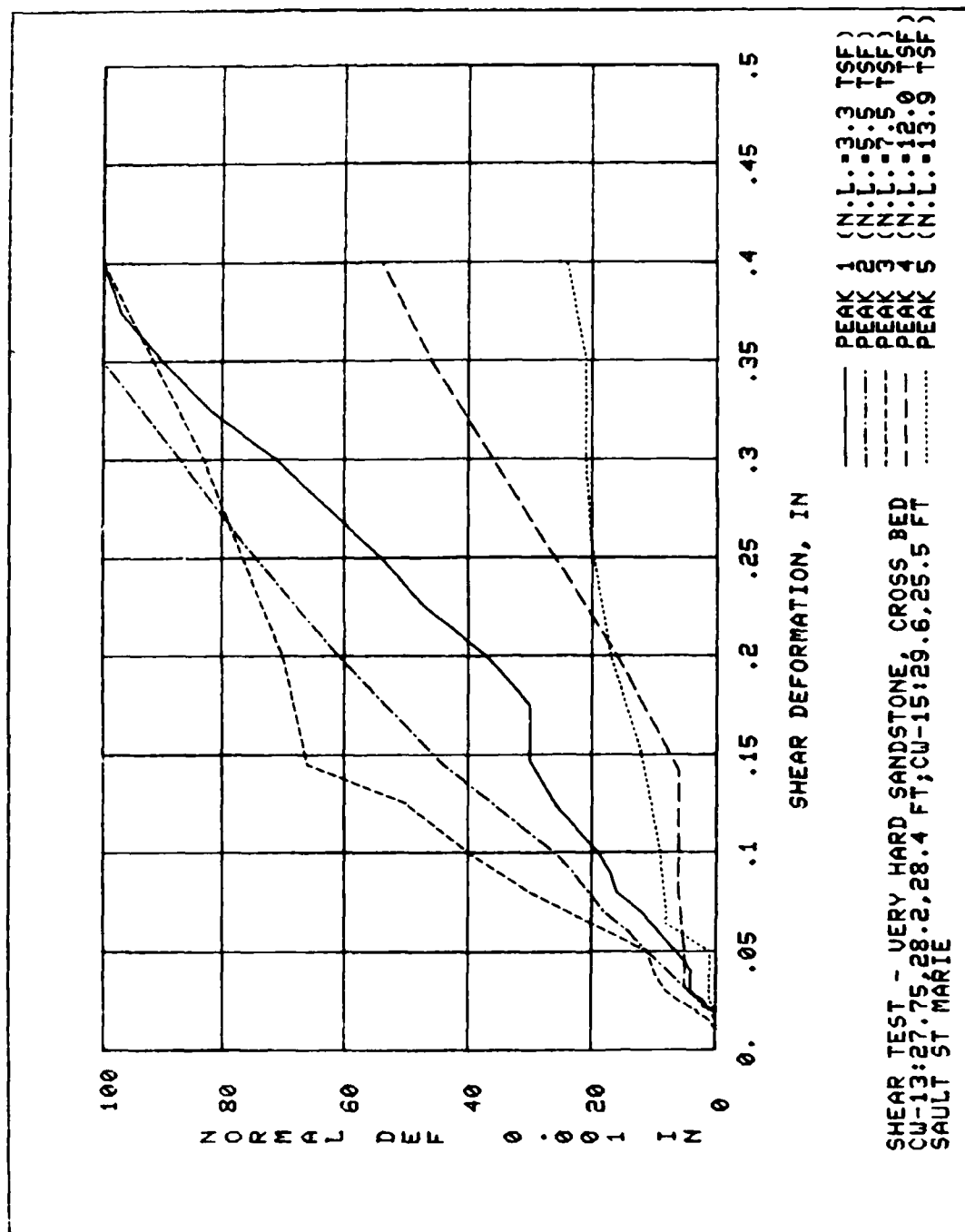


SHEAR DEFORMATION, IN

PEAK 1 (N.L.: 3.3 T.S.F.)  
 PEAK 2 (N.L.: 5.5 T.S.F.)  
 PEAK 3 (N.L.: 7.5 T.S.F.)  
 PEAK 4 (N.L.: 12.9 T.S.F.)  
 PEAK 5 (N.L.: 13.9 T.S.F.)

SHEAR TEST - VERY HARD SANDSTONE, CROSS BED  
 CU-13:27.75, 28.2, 28.4 FT; CU-15:26.6, 25.5 FT  
 SAULT ST MARIE





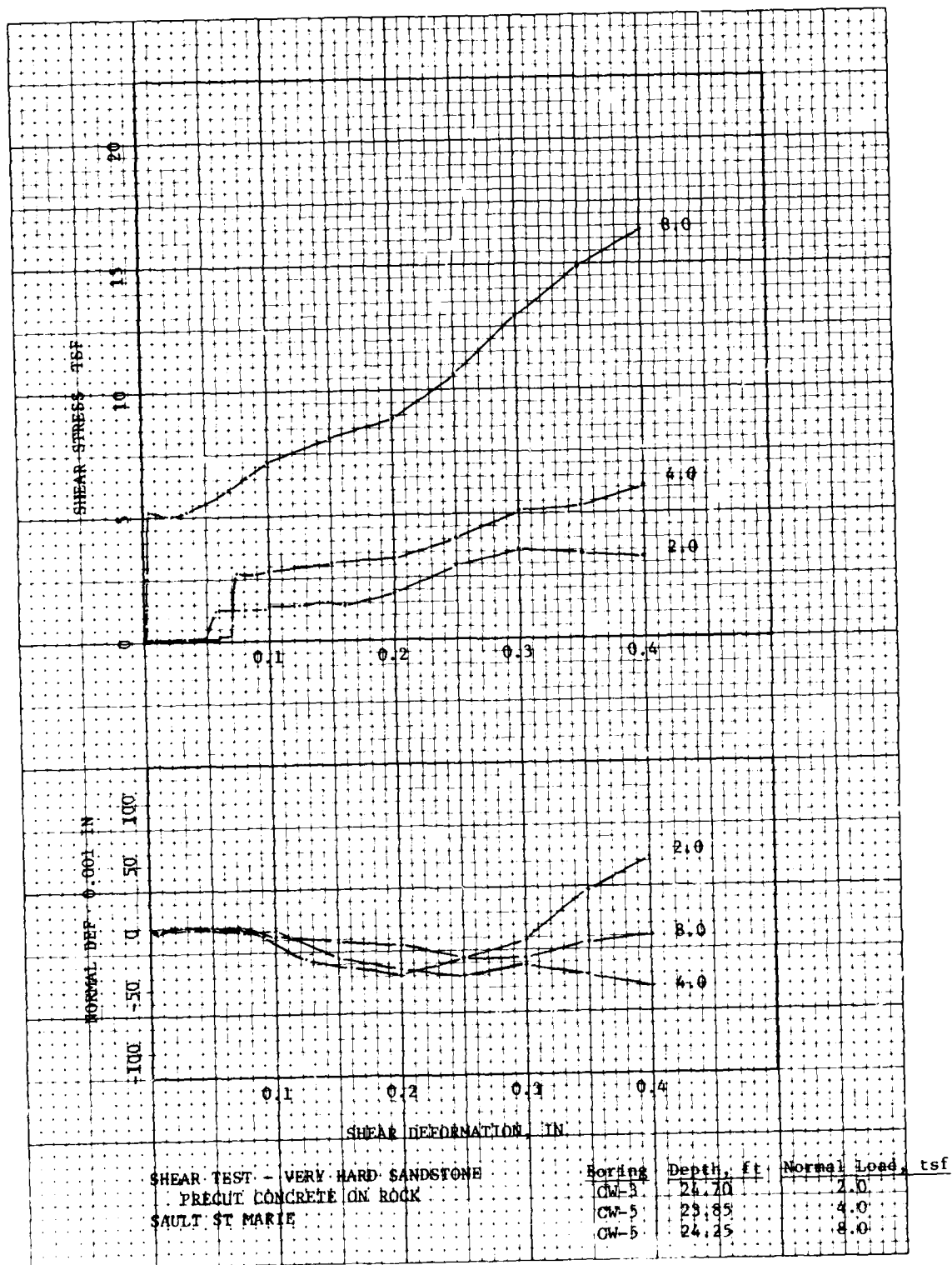


PLATE E57

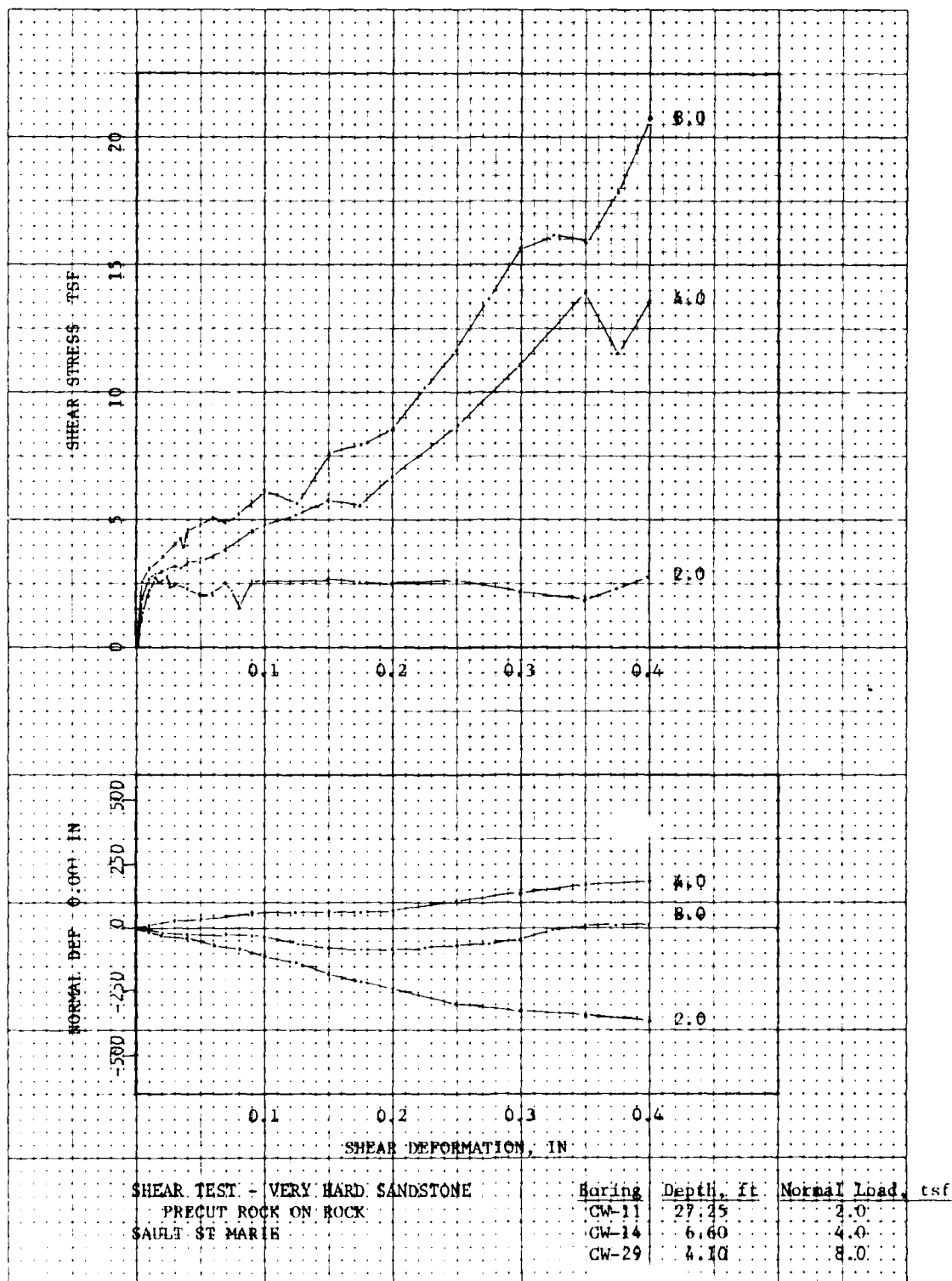
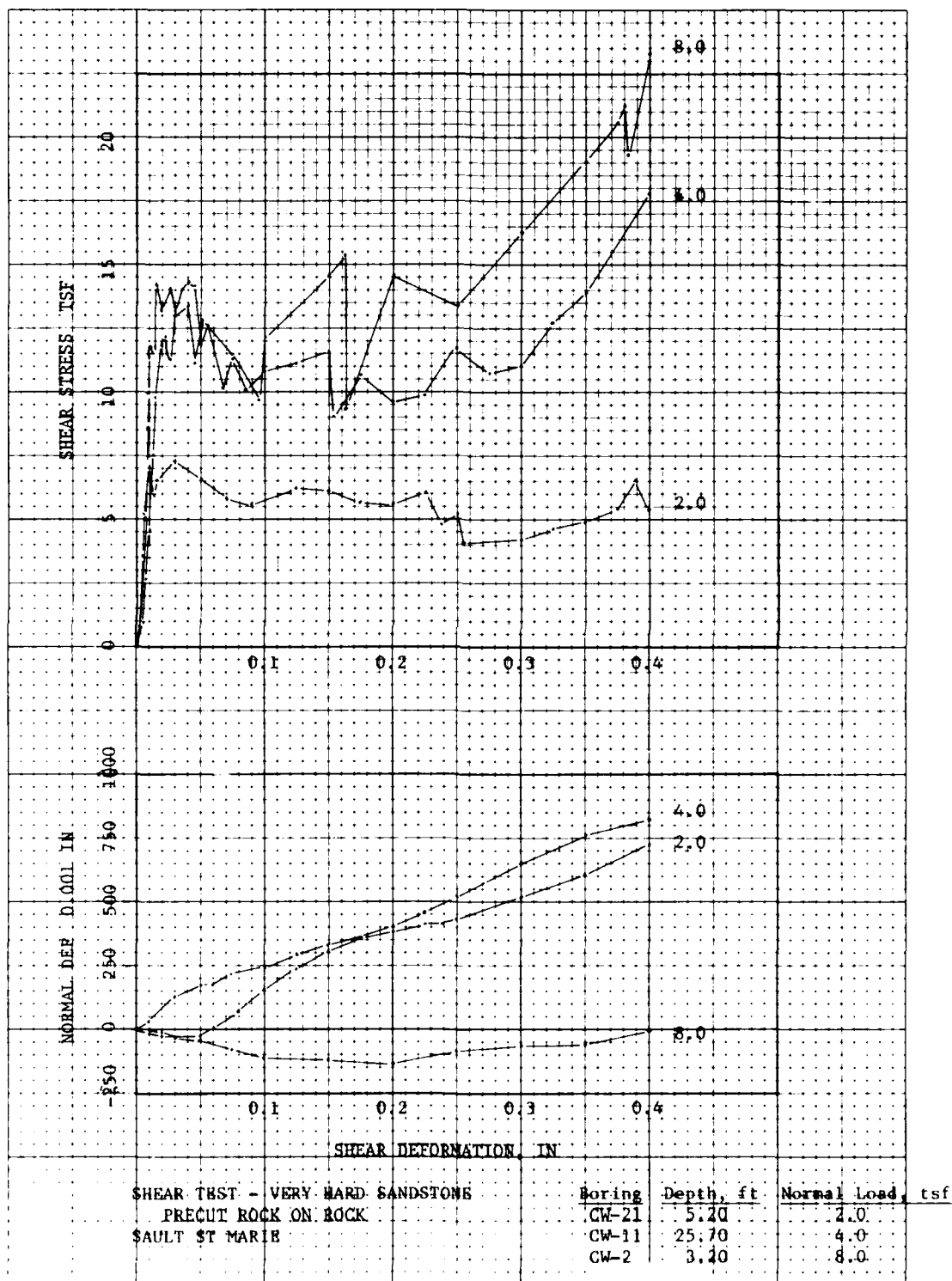


PLATE E58



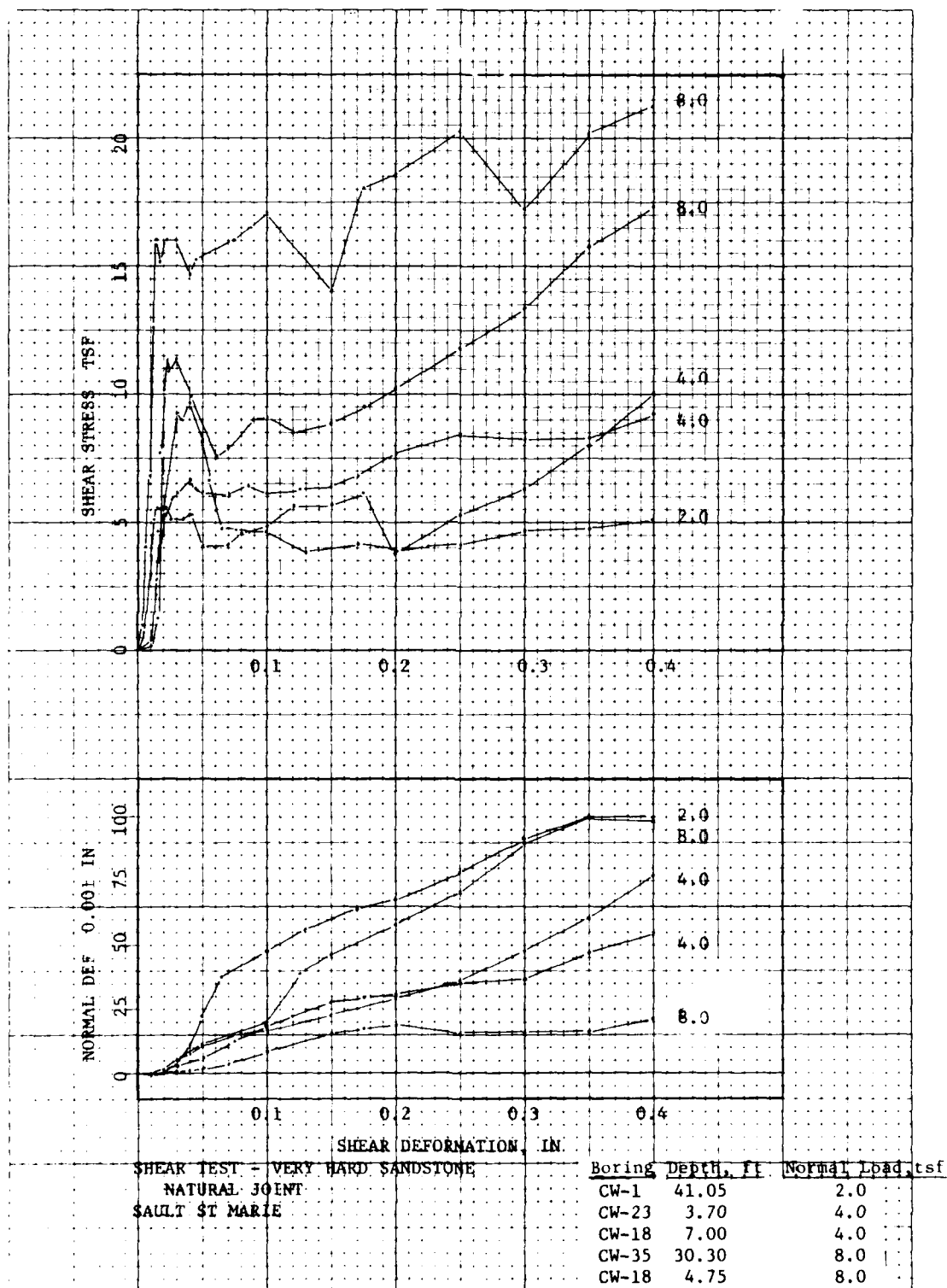


PLATE E60

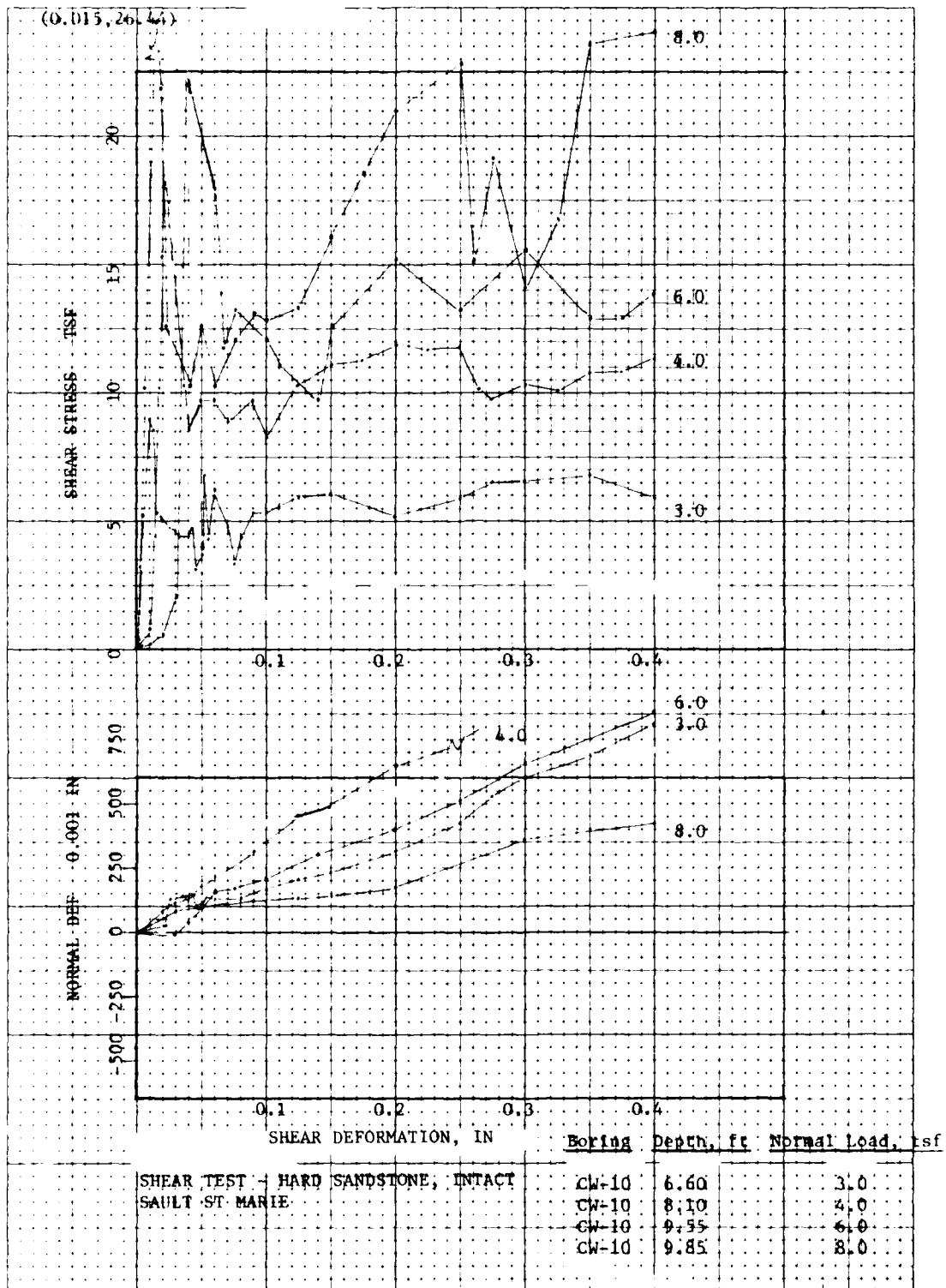


PLATE E61

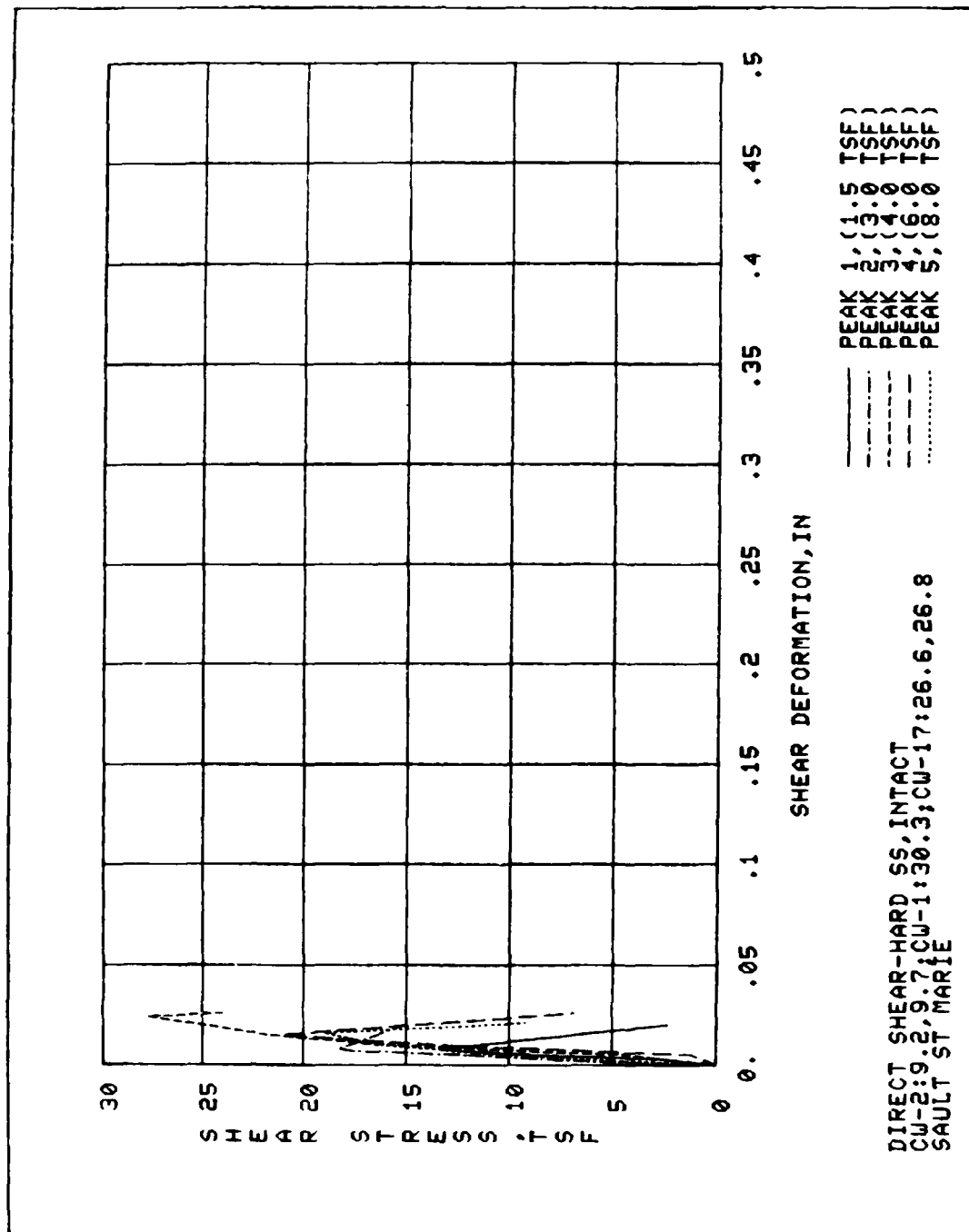
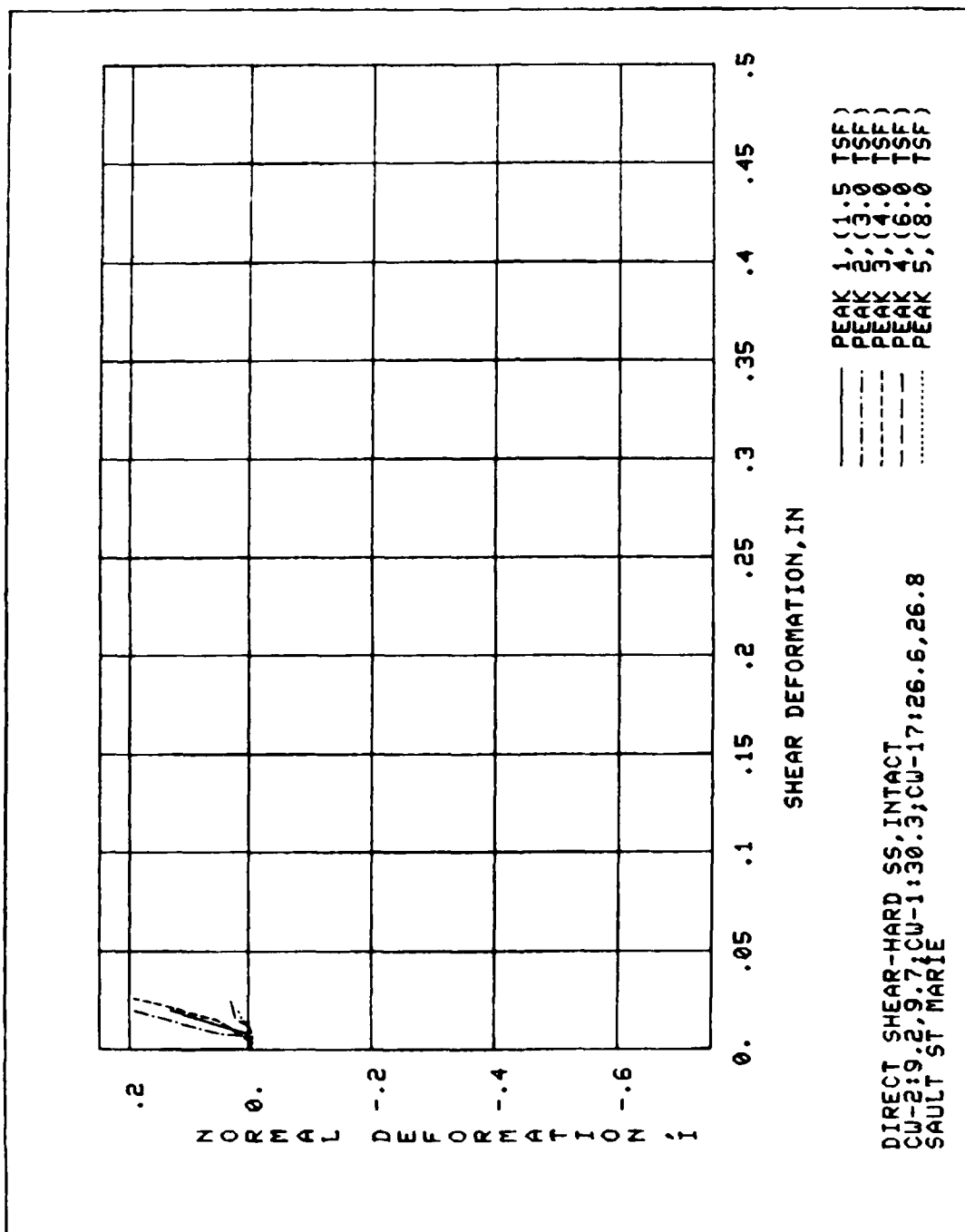


PLATE E62





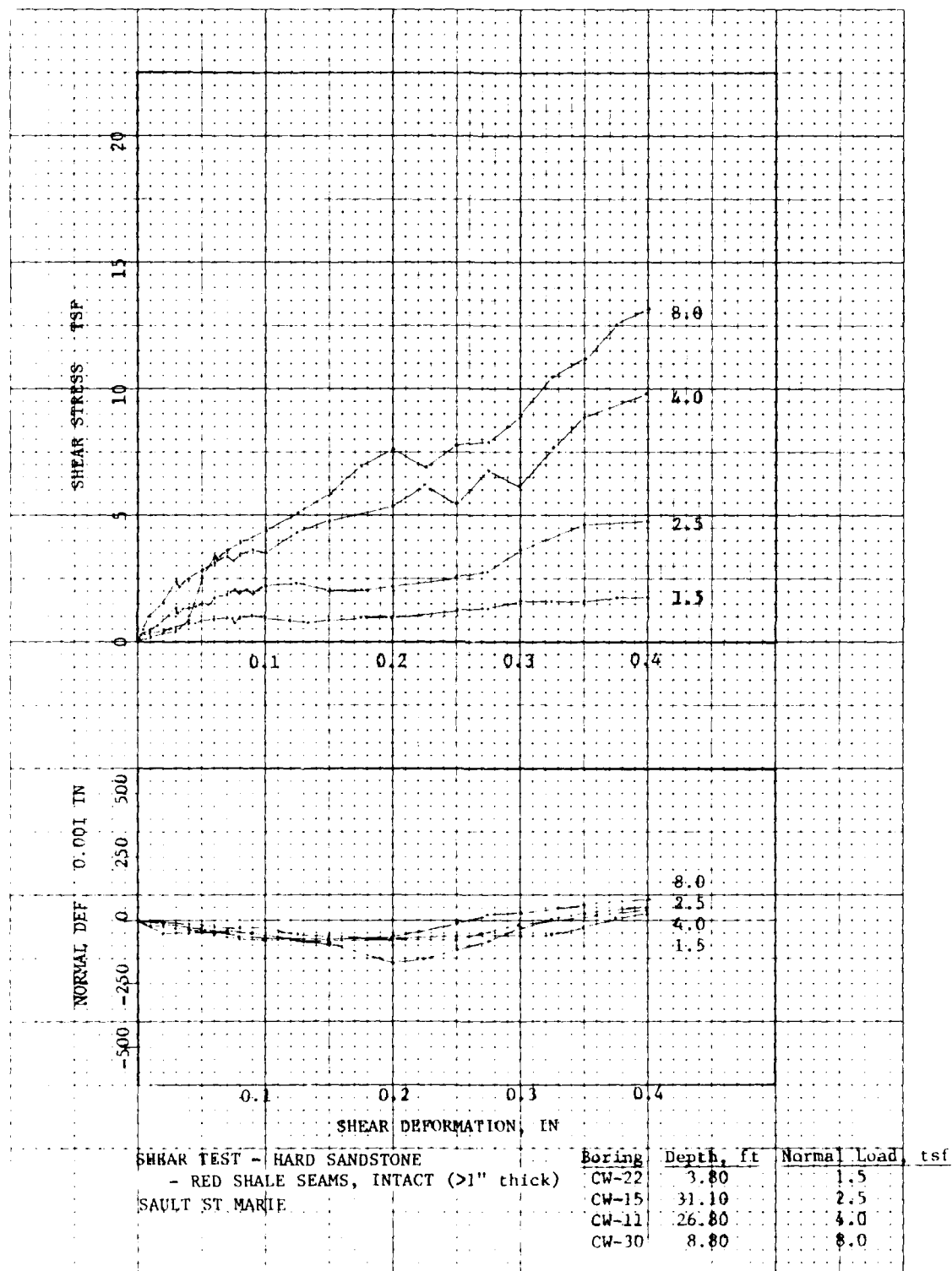
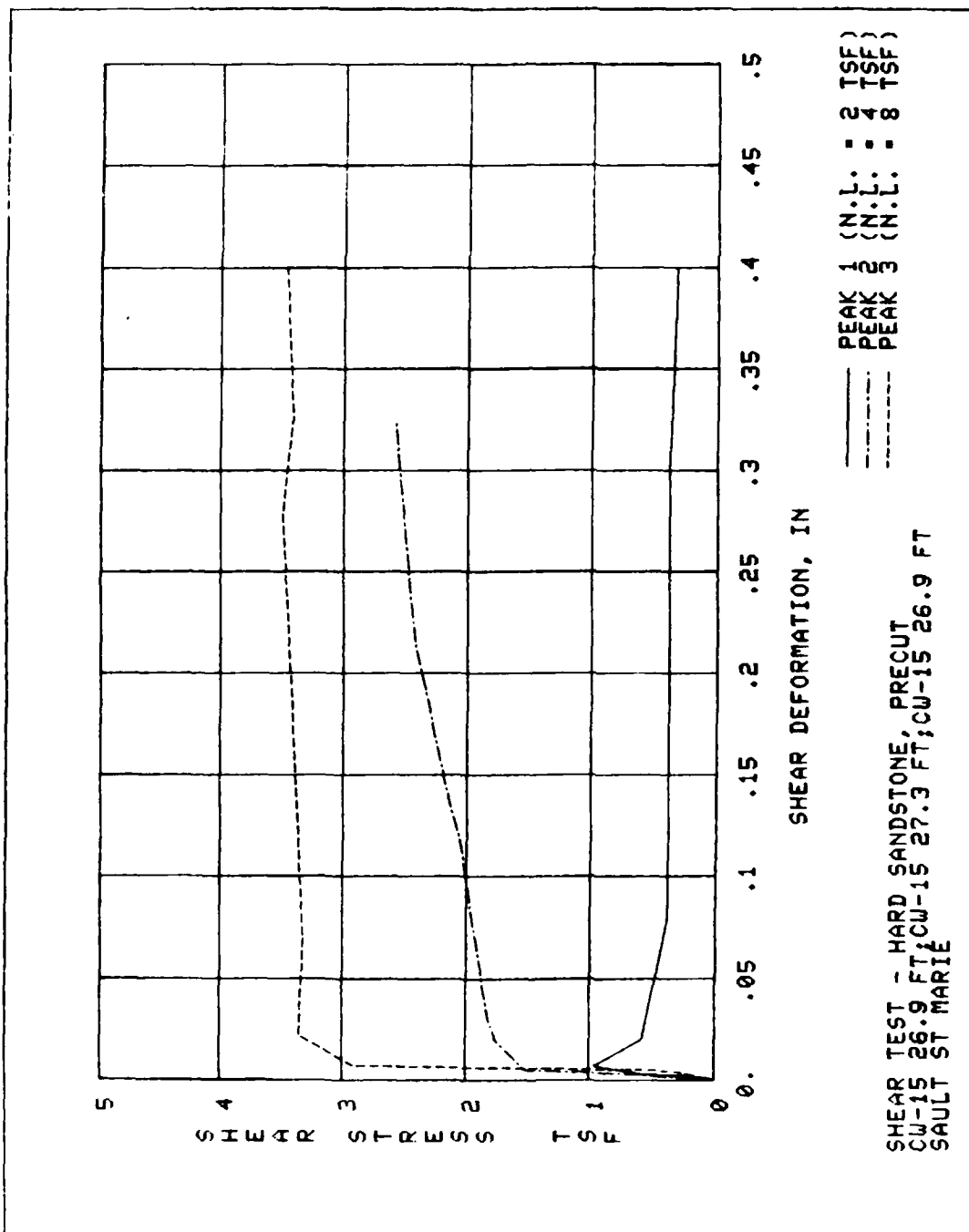
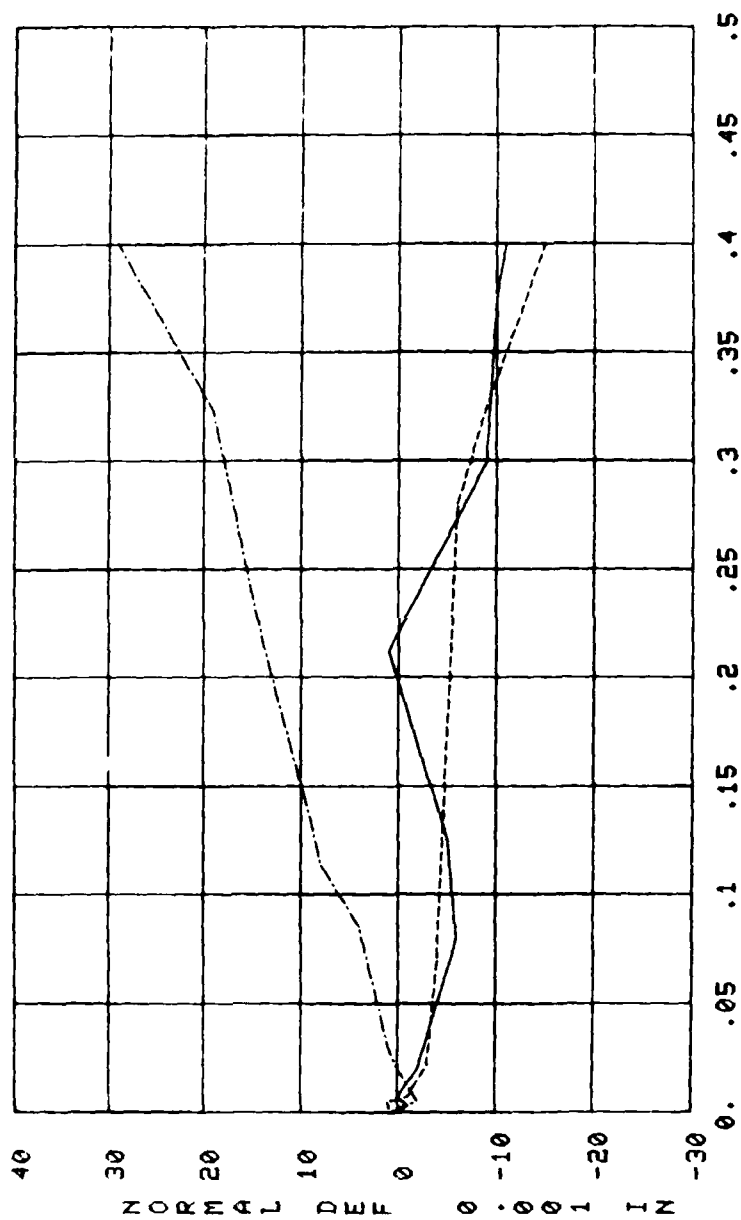


PLATE E64

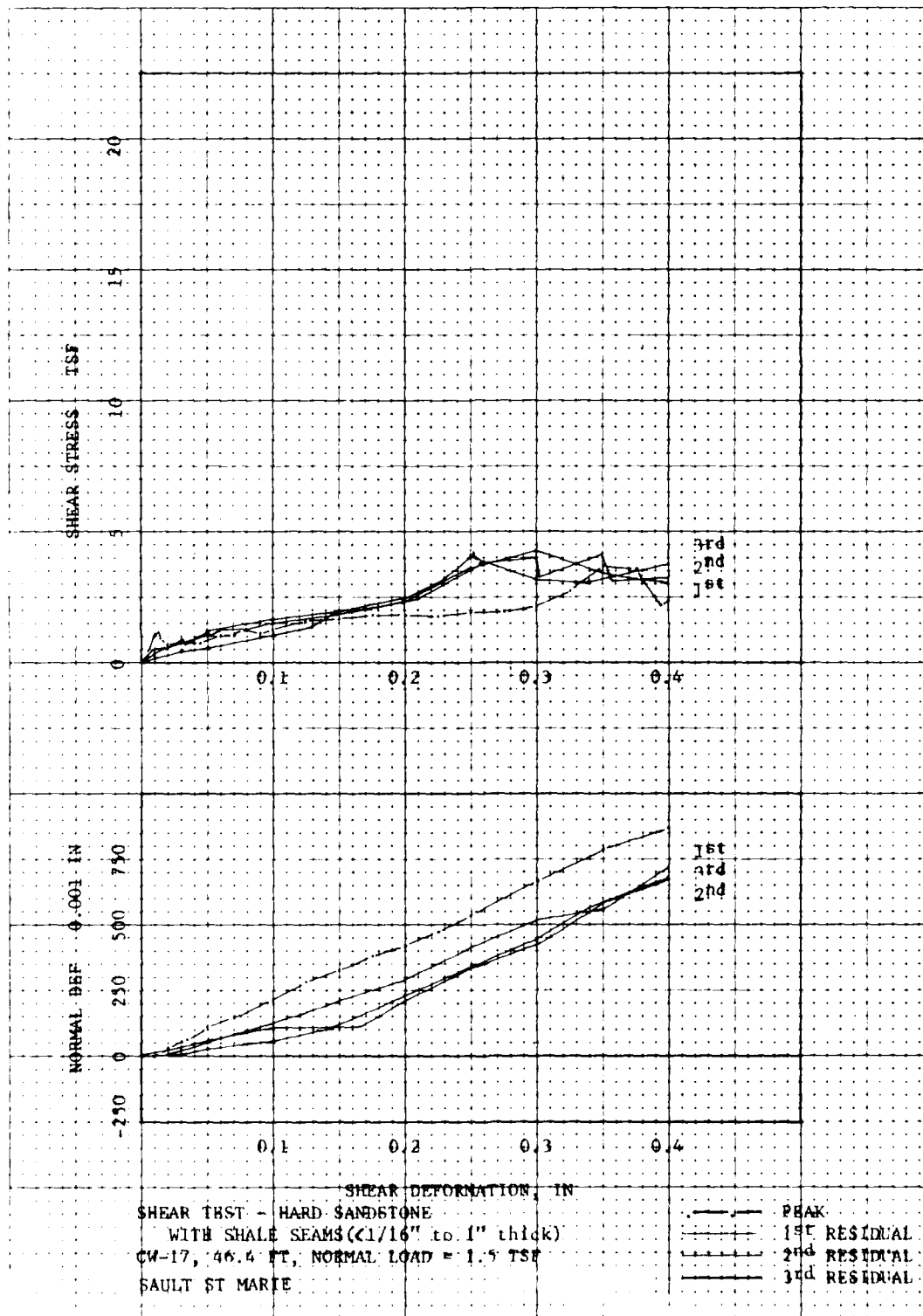




SHEAR DEFORMATION, IN

PEAK 1 (N.L. - 2 TSF)  
 PEAK 2 (N.L. - 4 TSF)  
 PEAK 3 (N.L. - 8 TSF)

SHEAR TEST - HARD SANDSTONE, PRECUT  
 CU-15 26.9 FT; CU-15 27.3 FT; CU-15 26.9 FT  
 SAULT ST MARIE



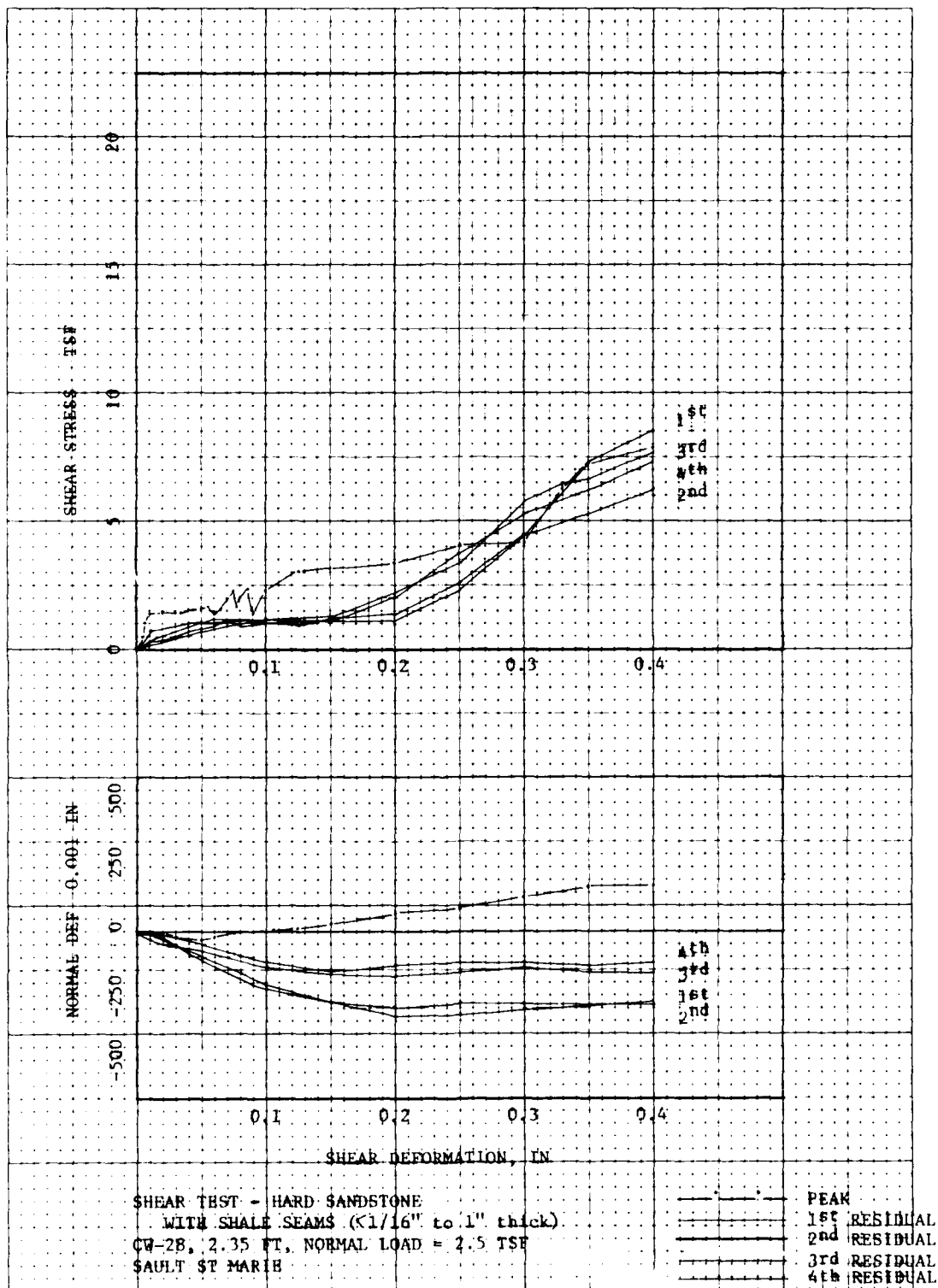
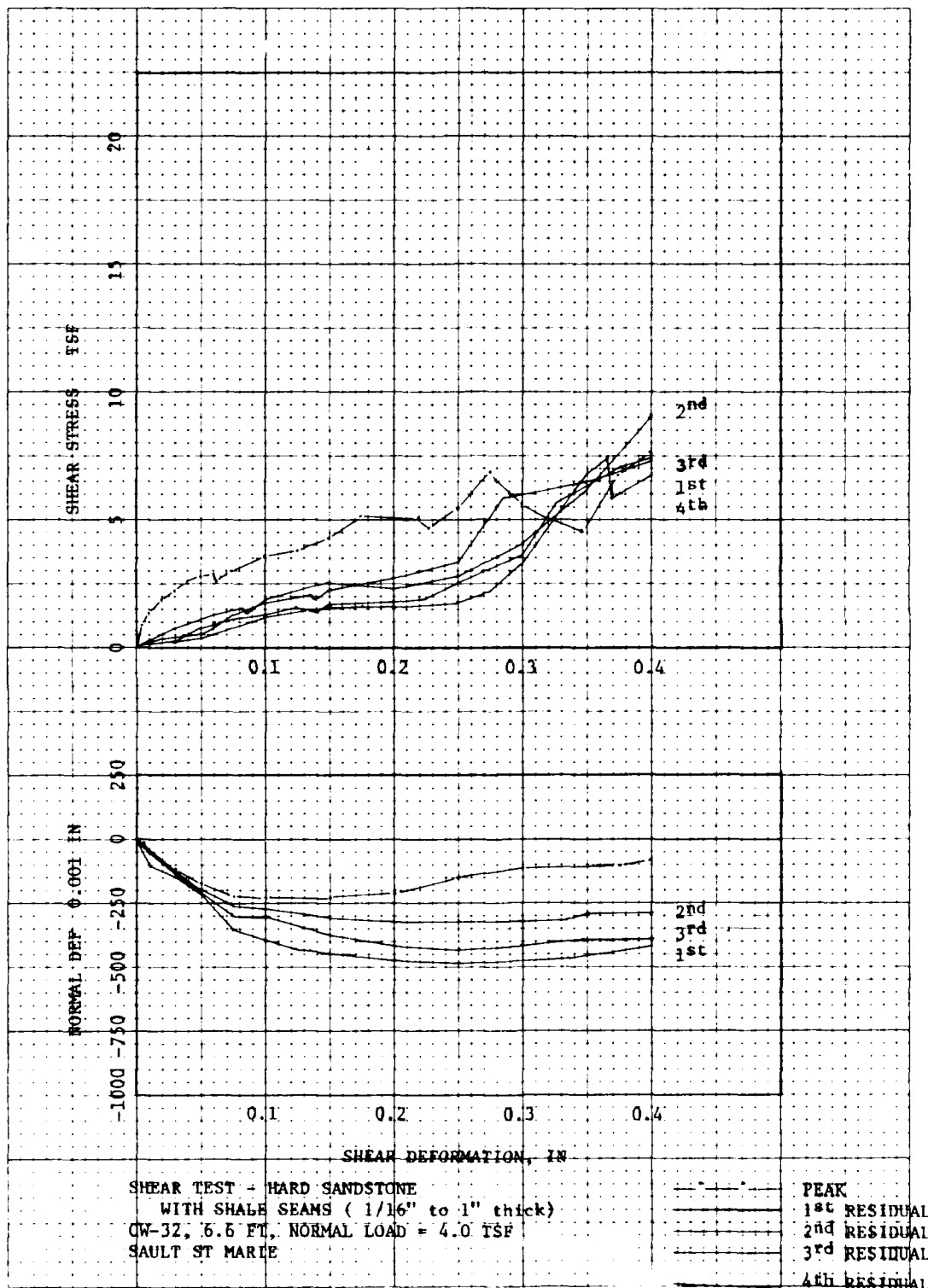


PLATE E68



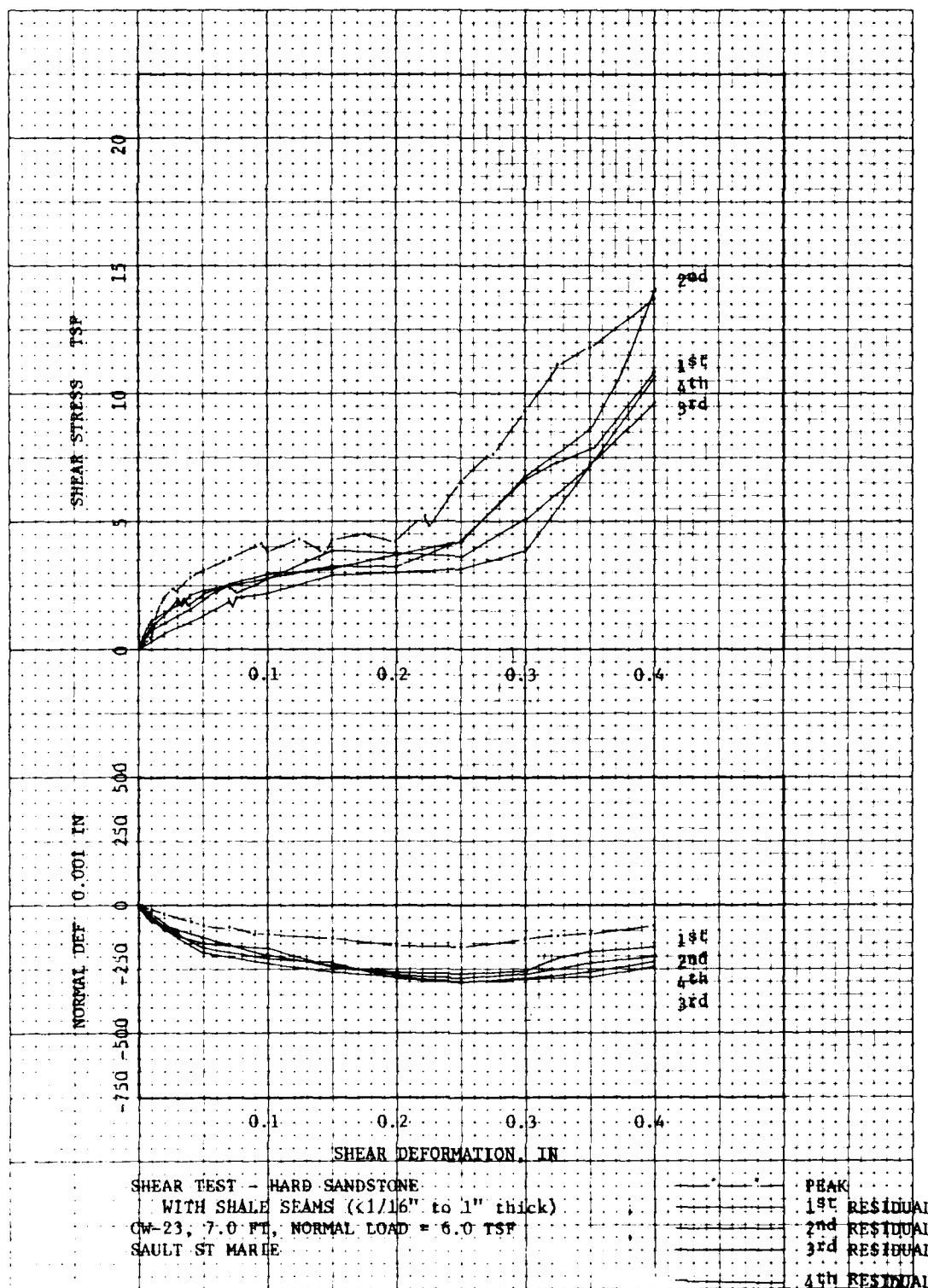
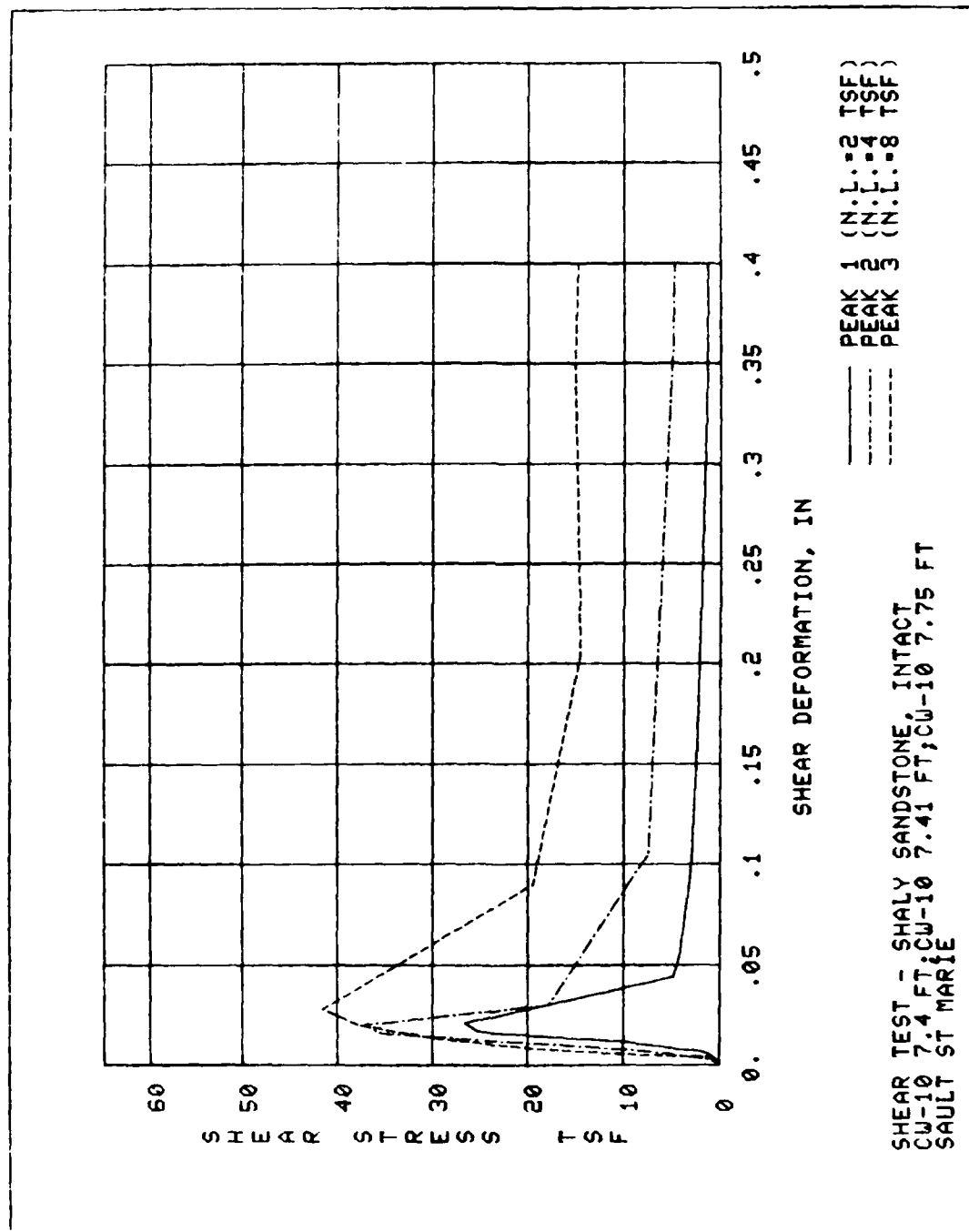


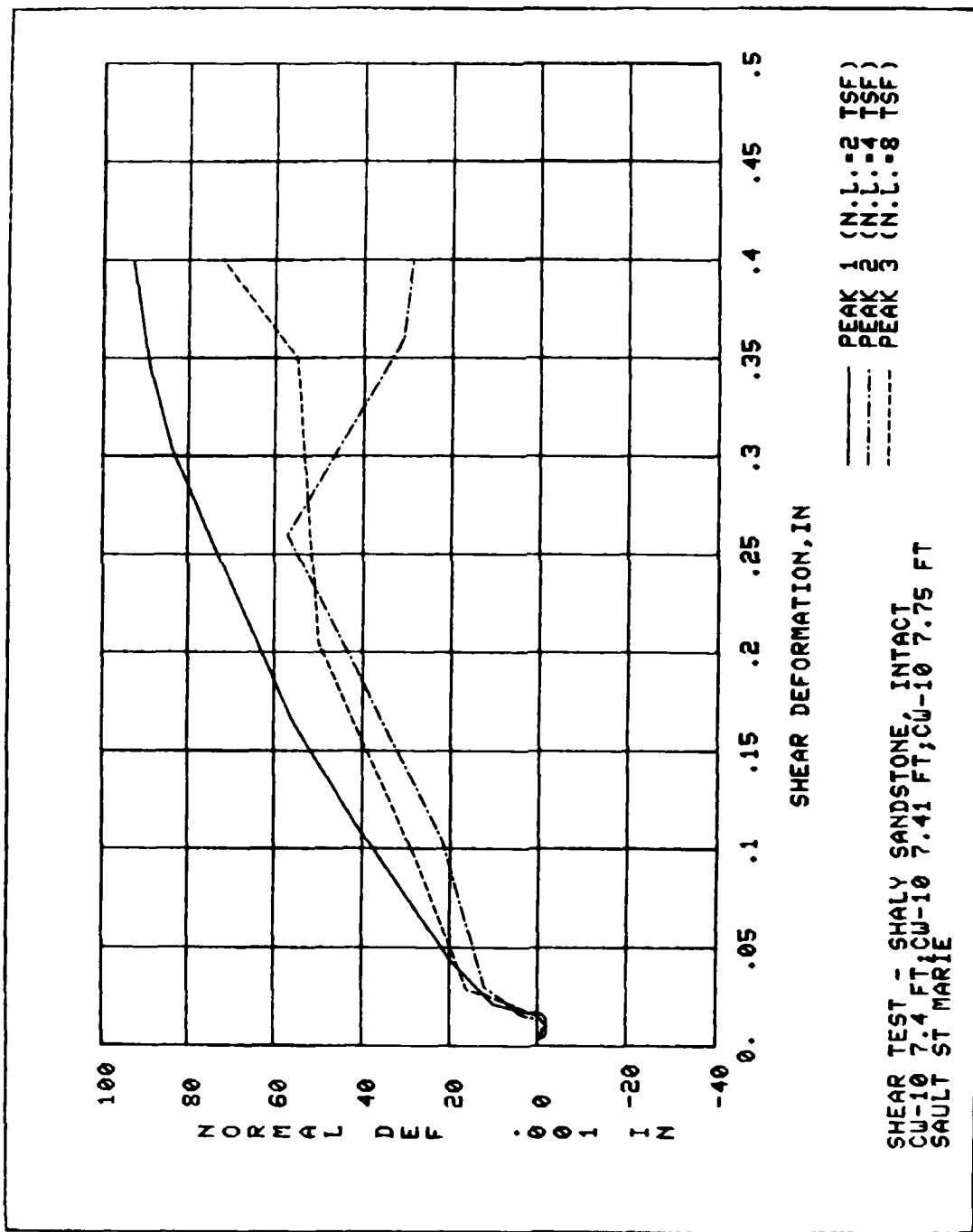
PLATE E70



PLATE E71







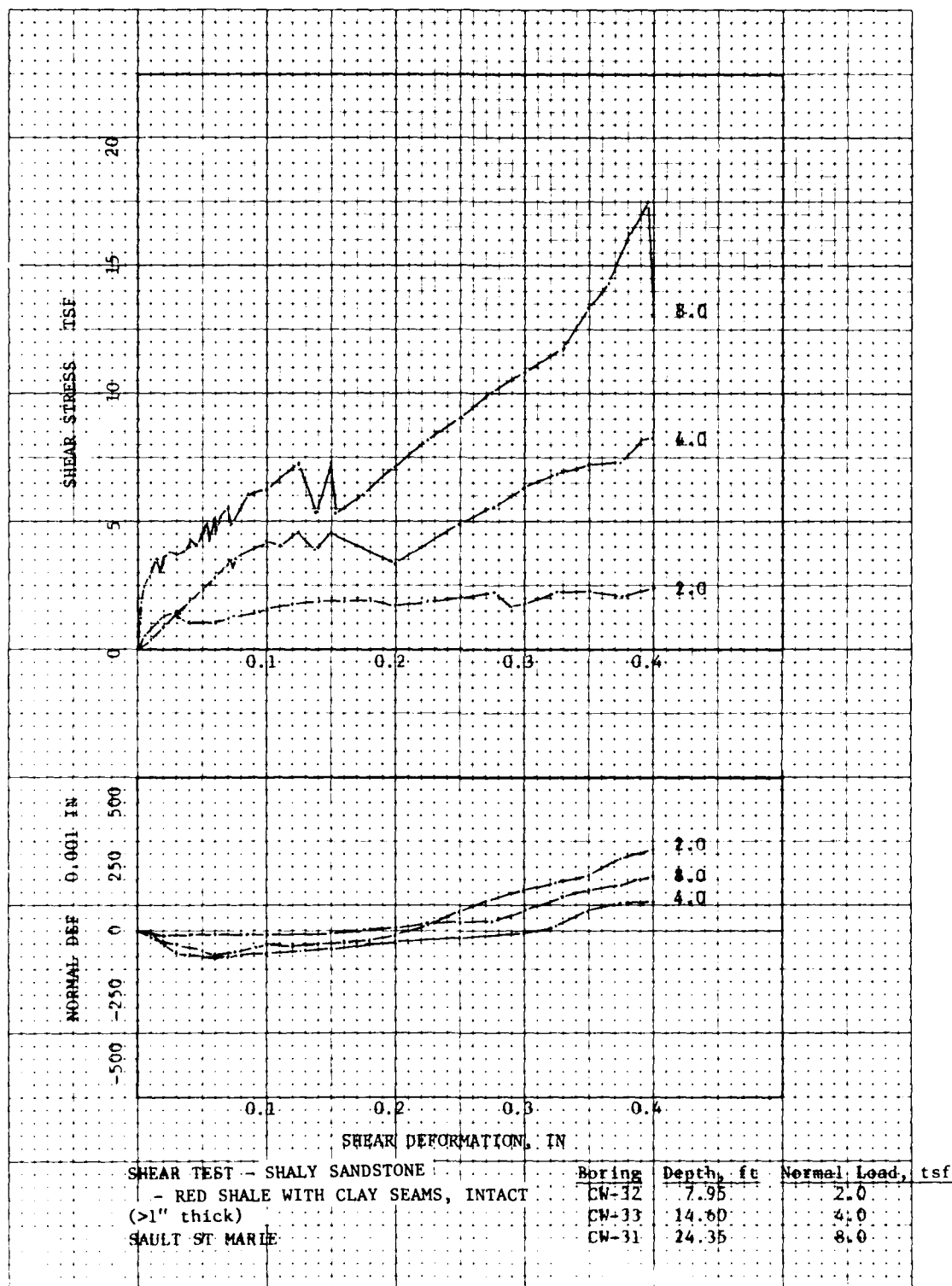
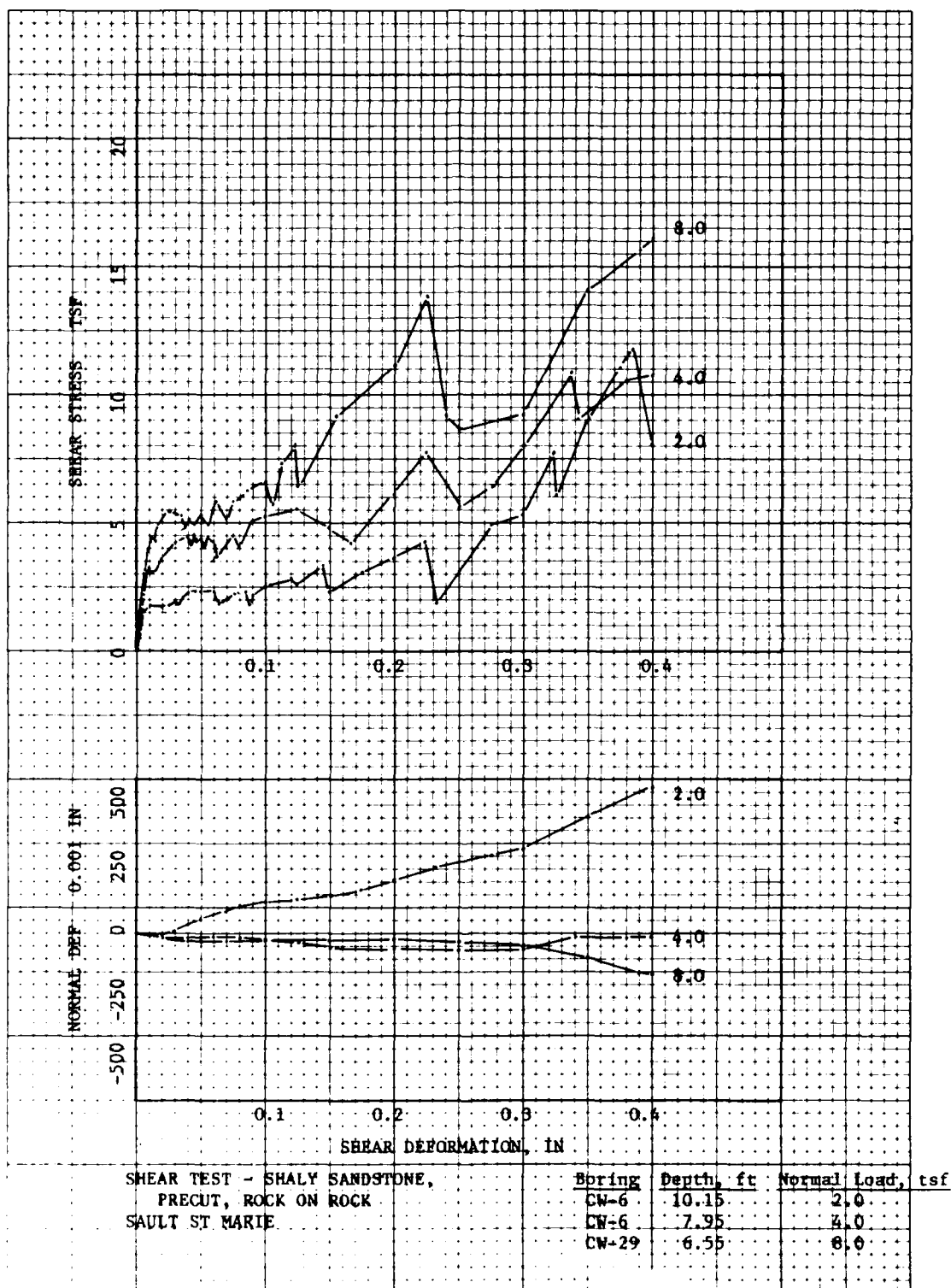


PLATE E74



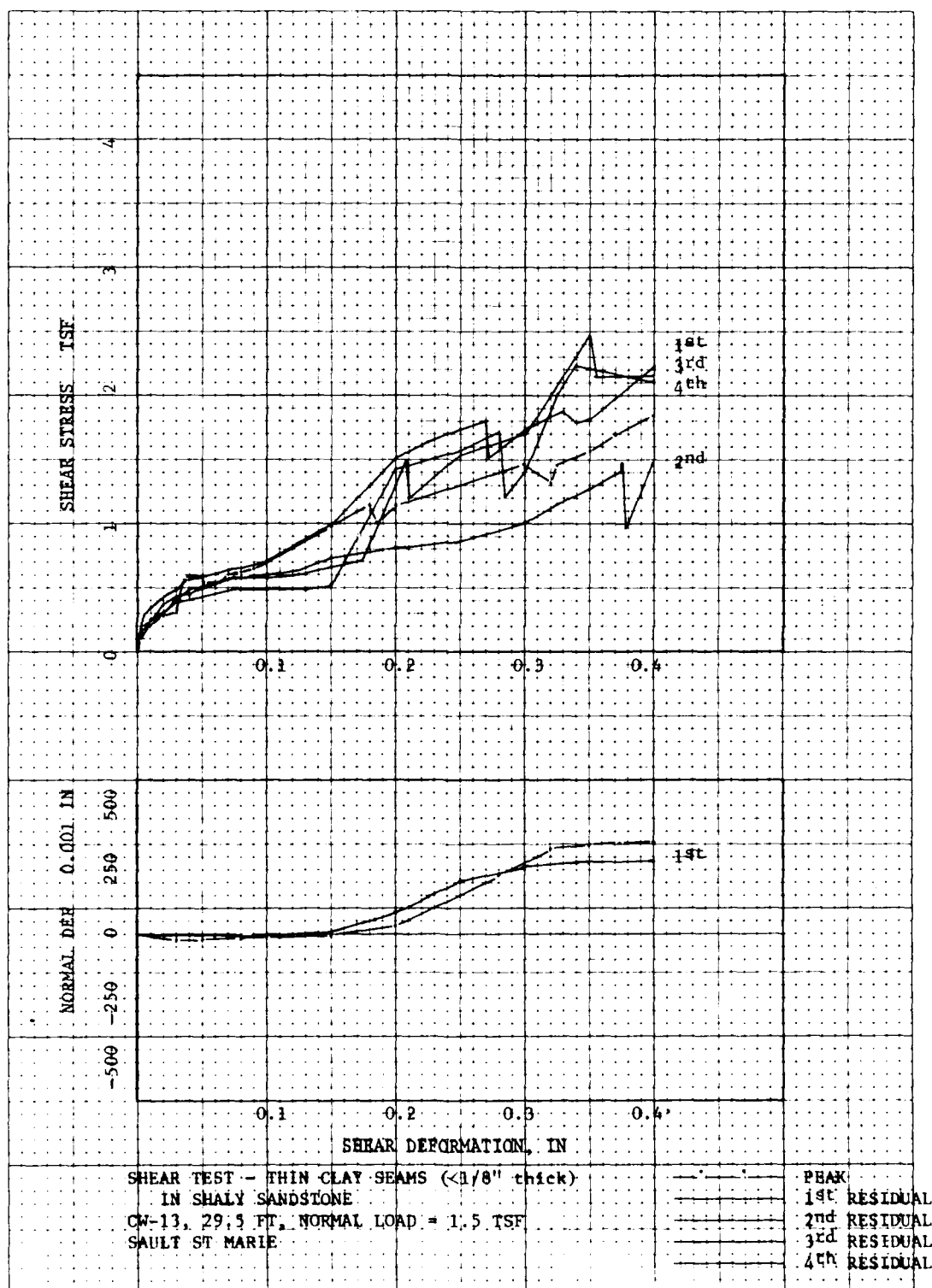
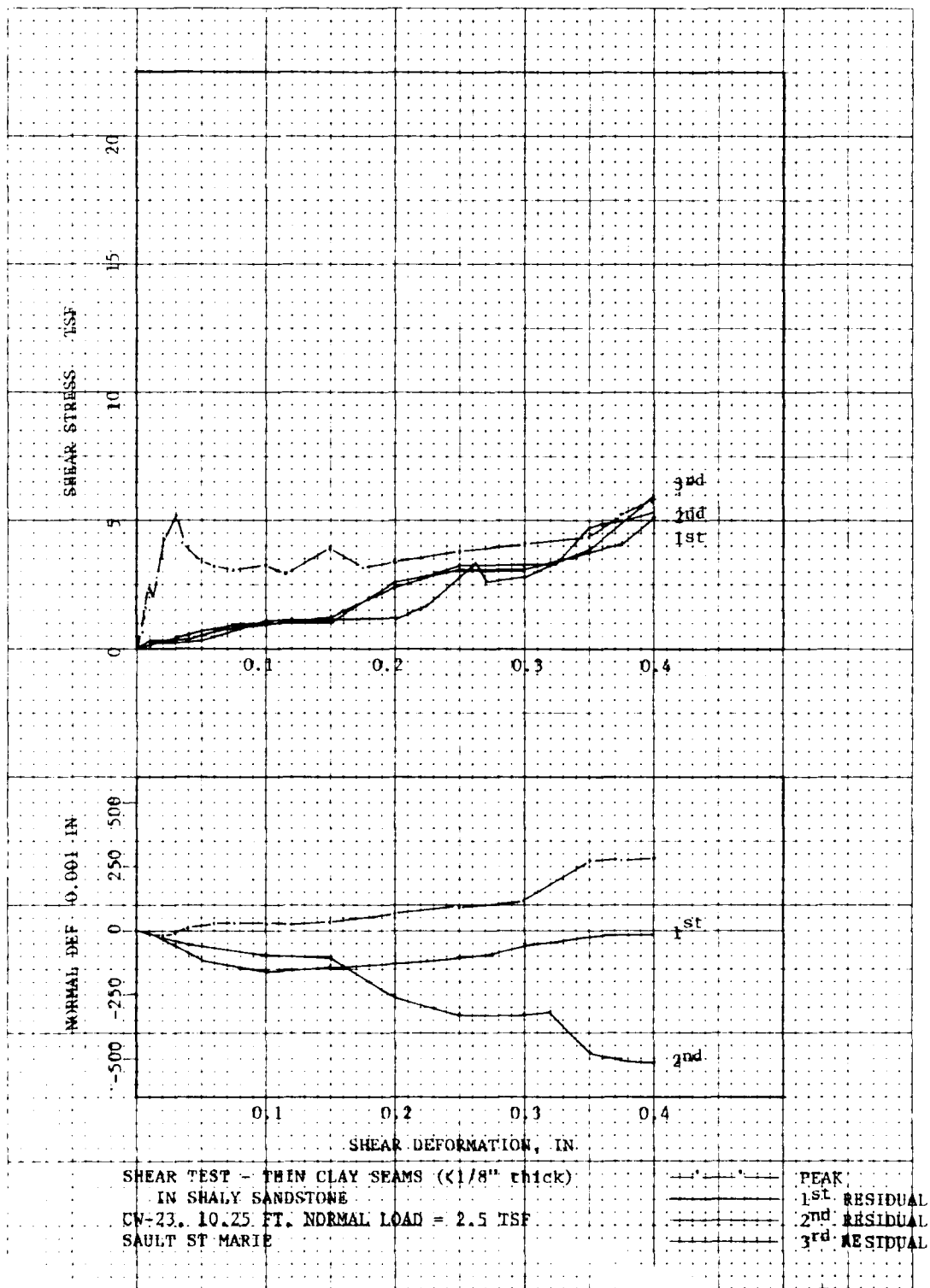


PLATE E76



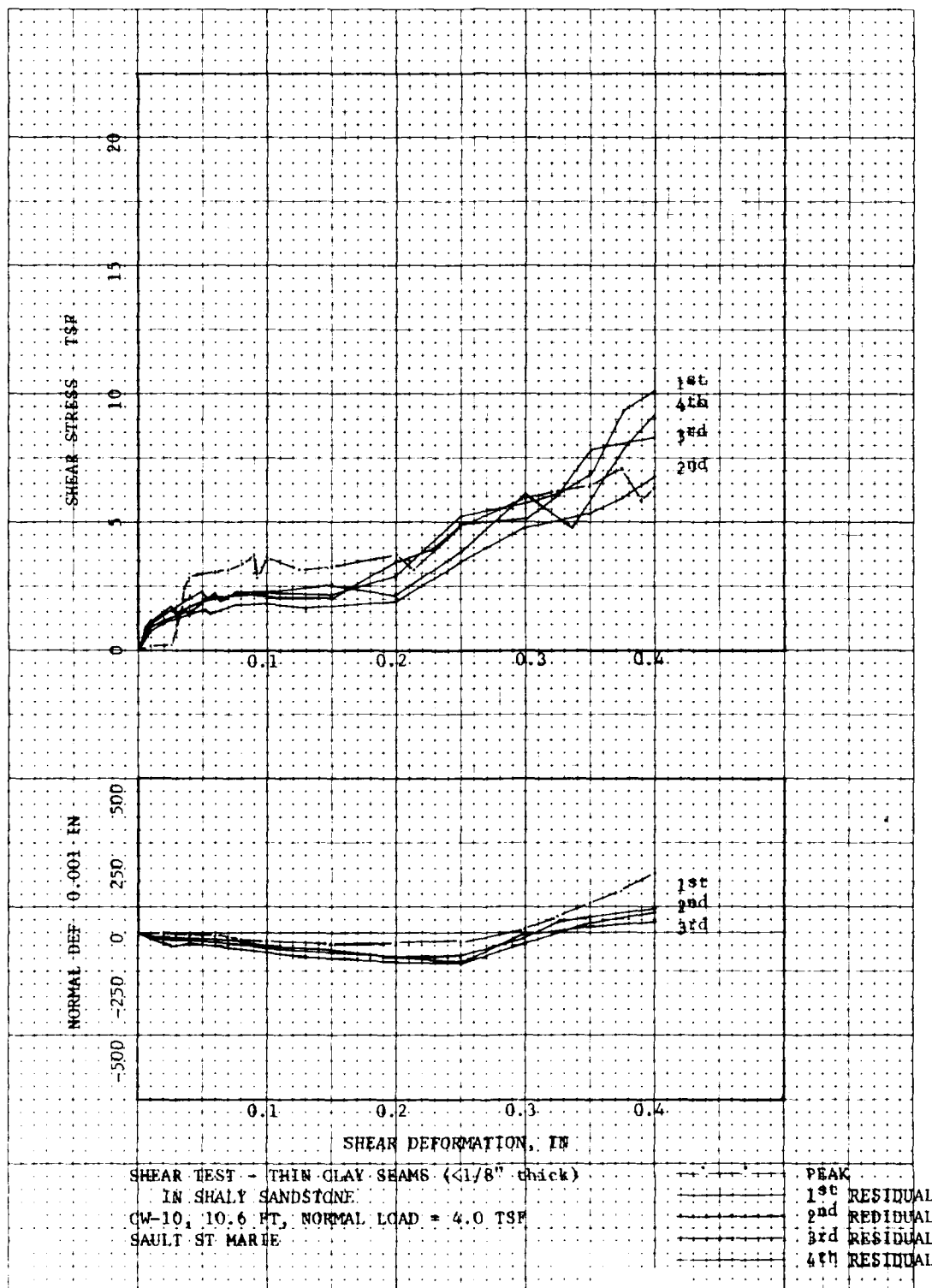
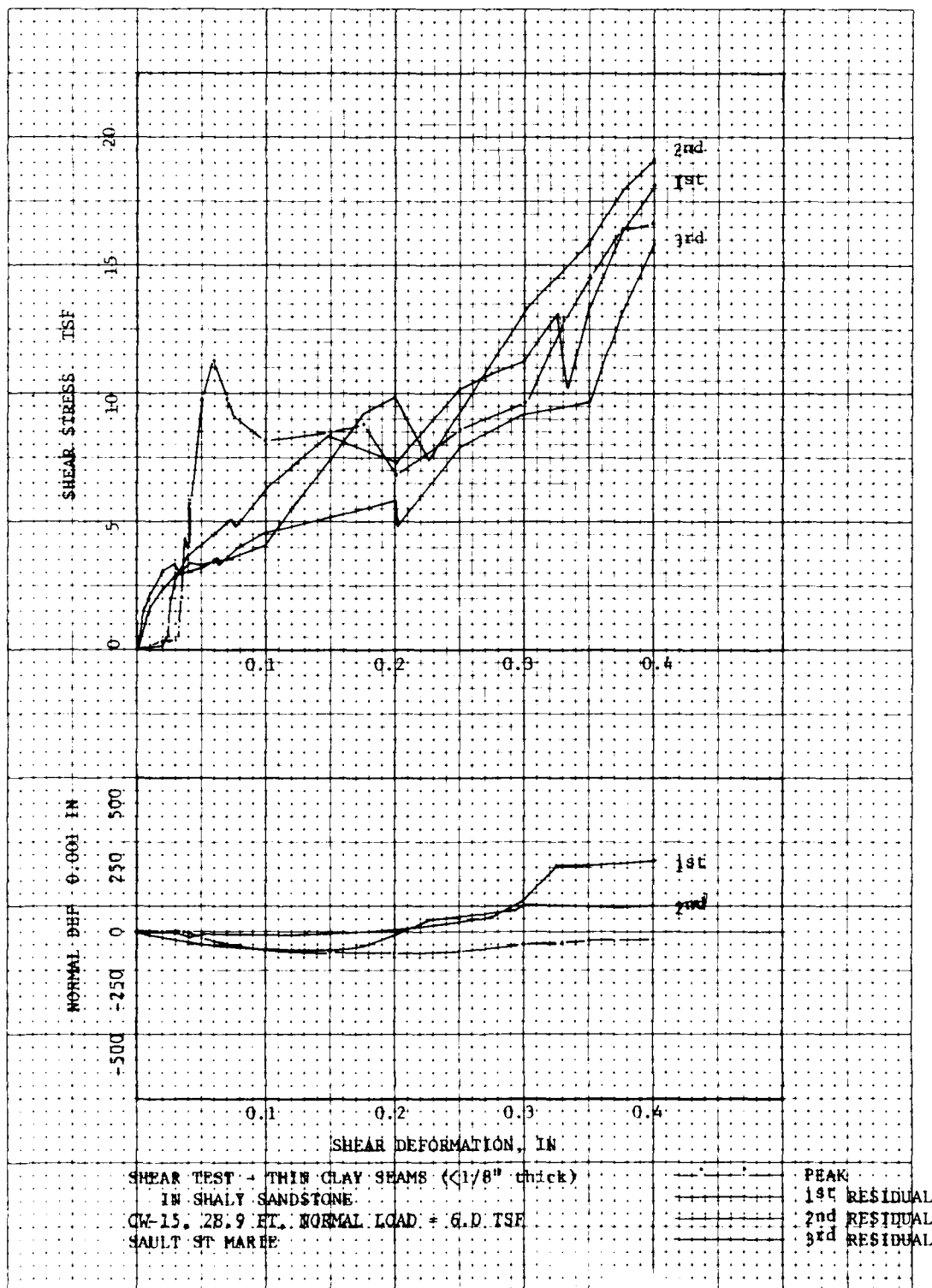
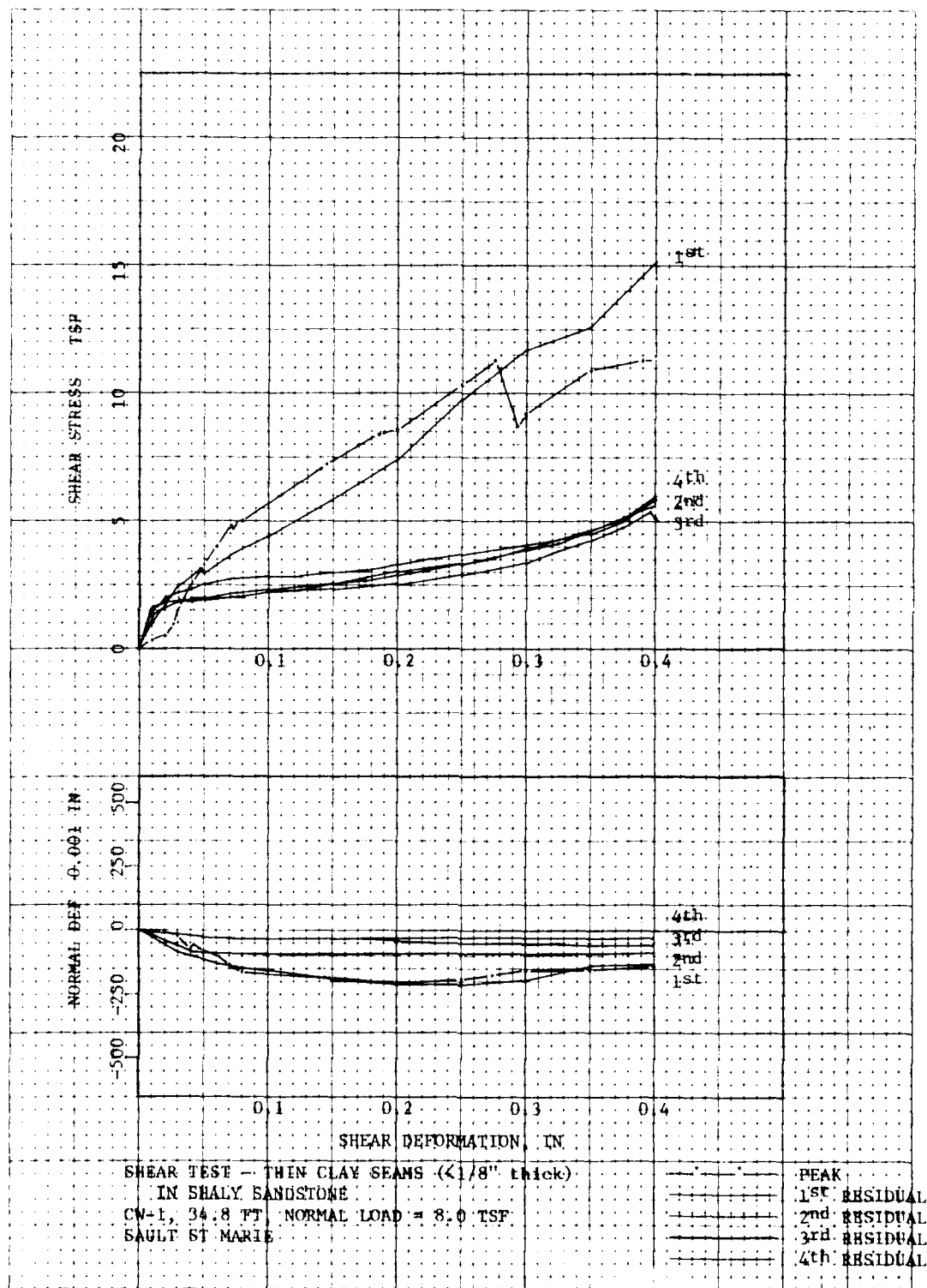
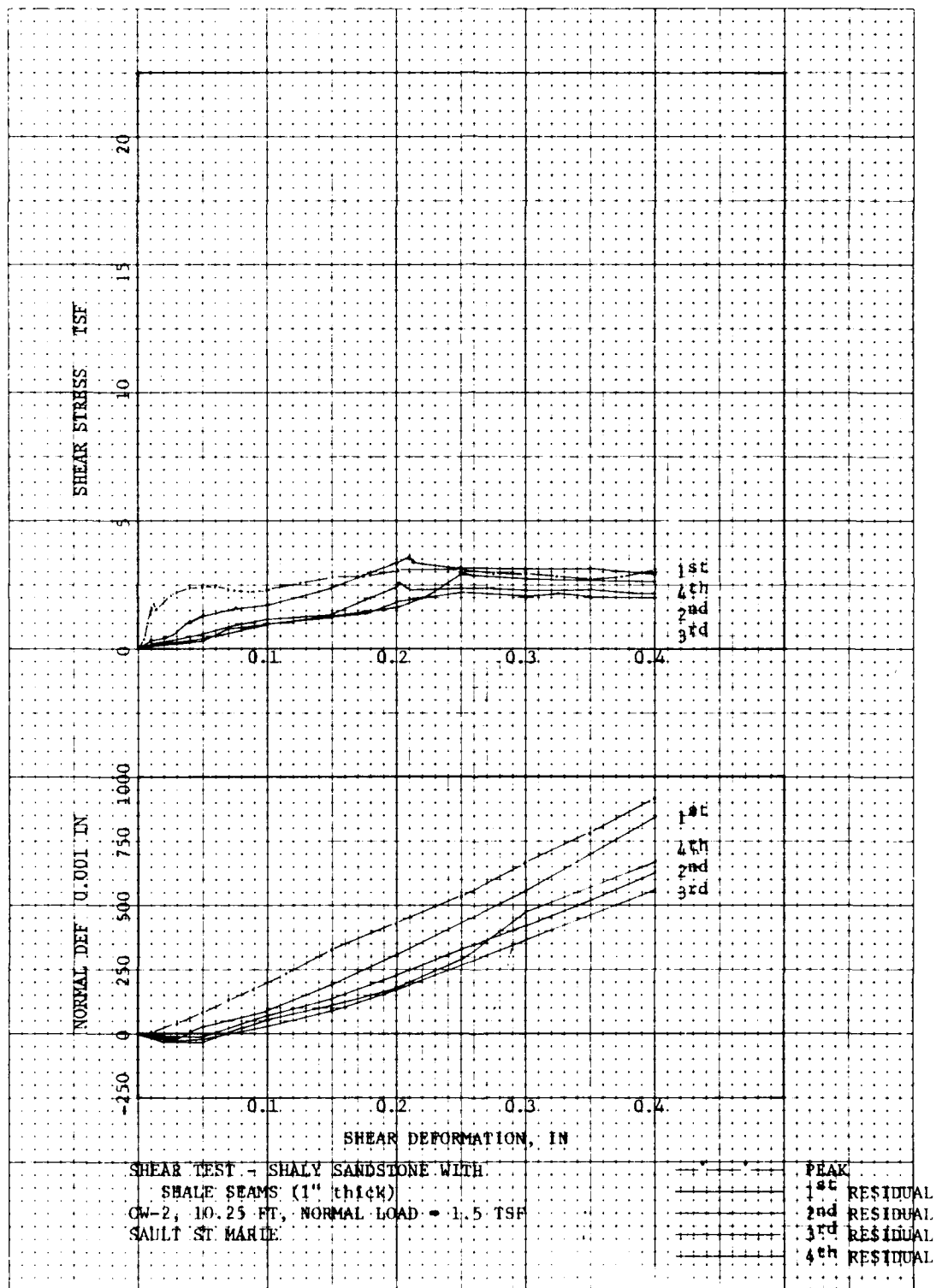


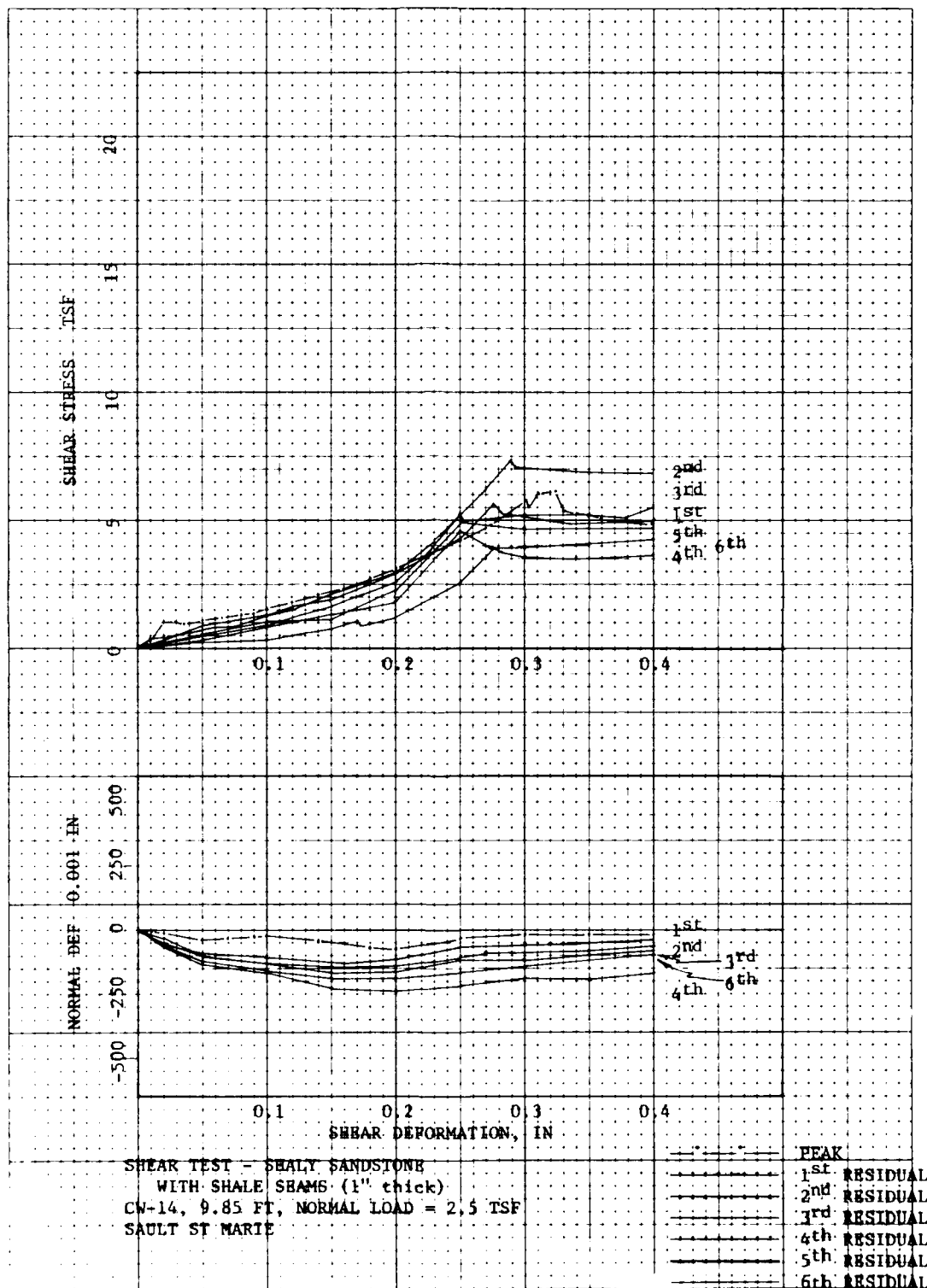
PLATE E78

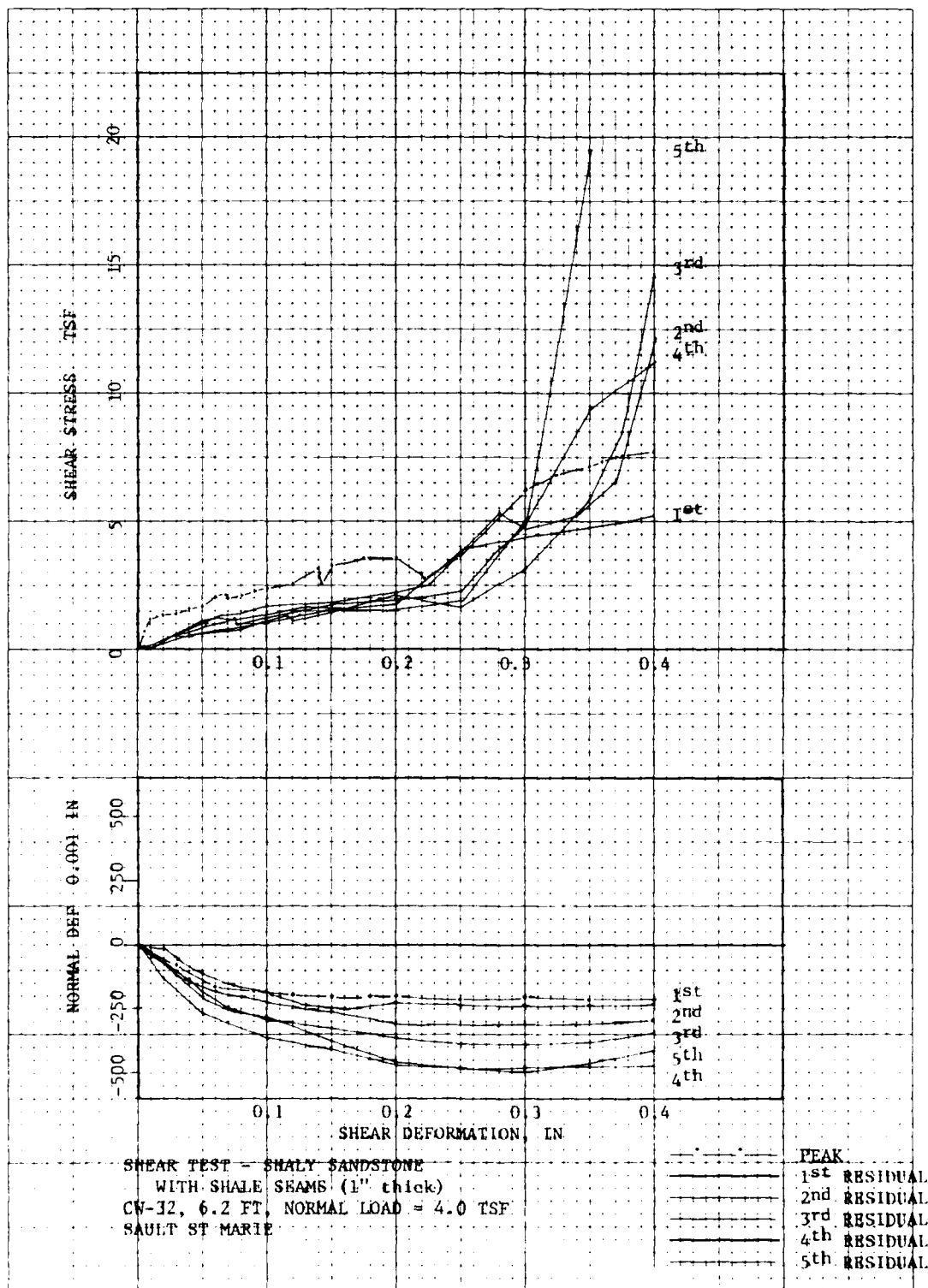












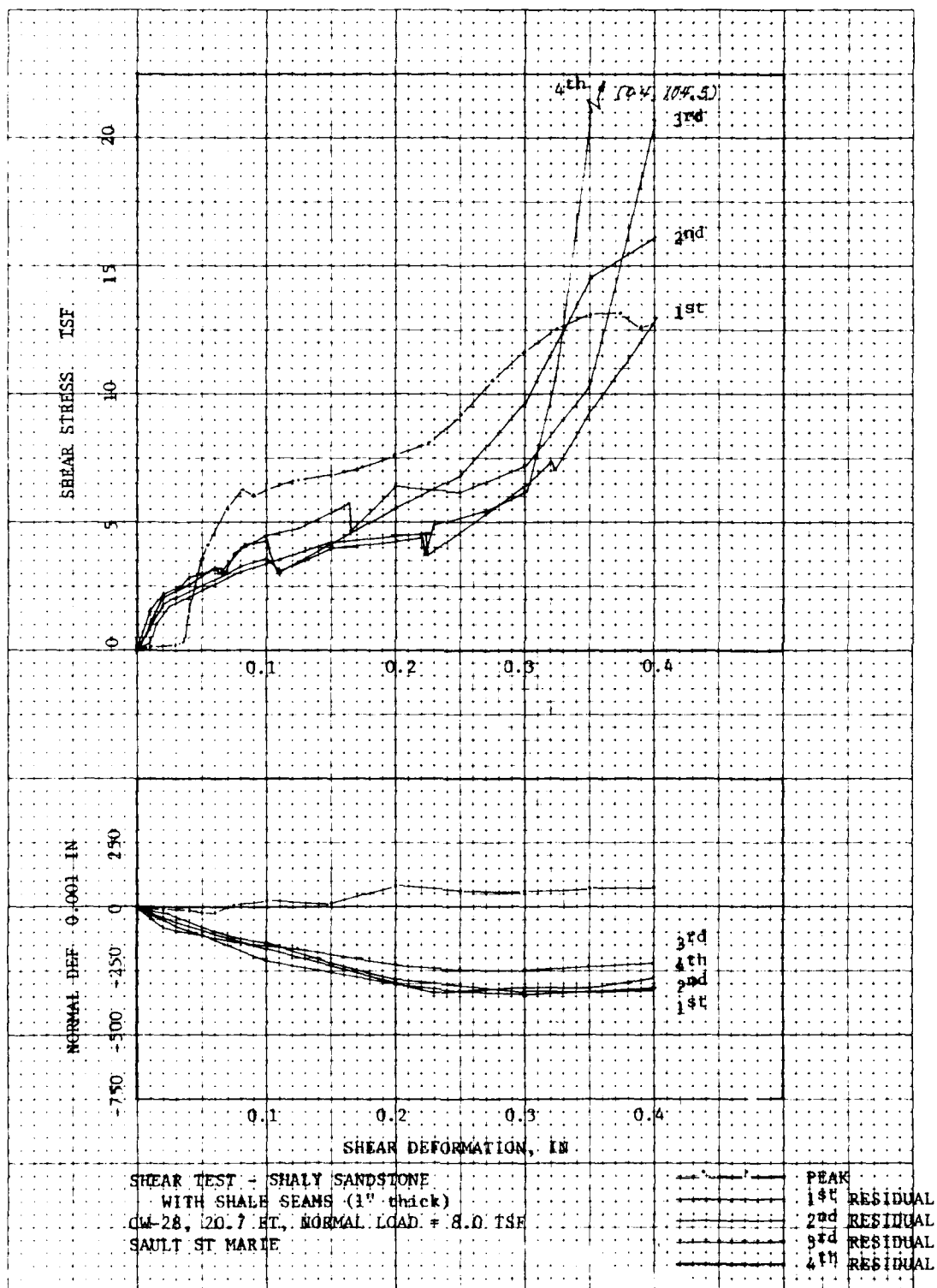
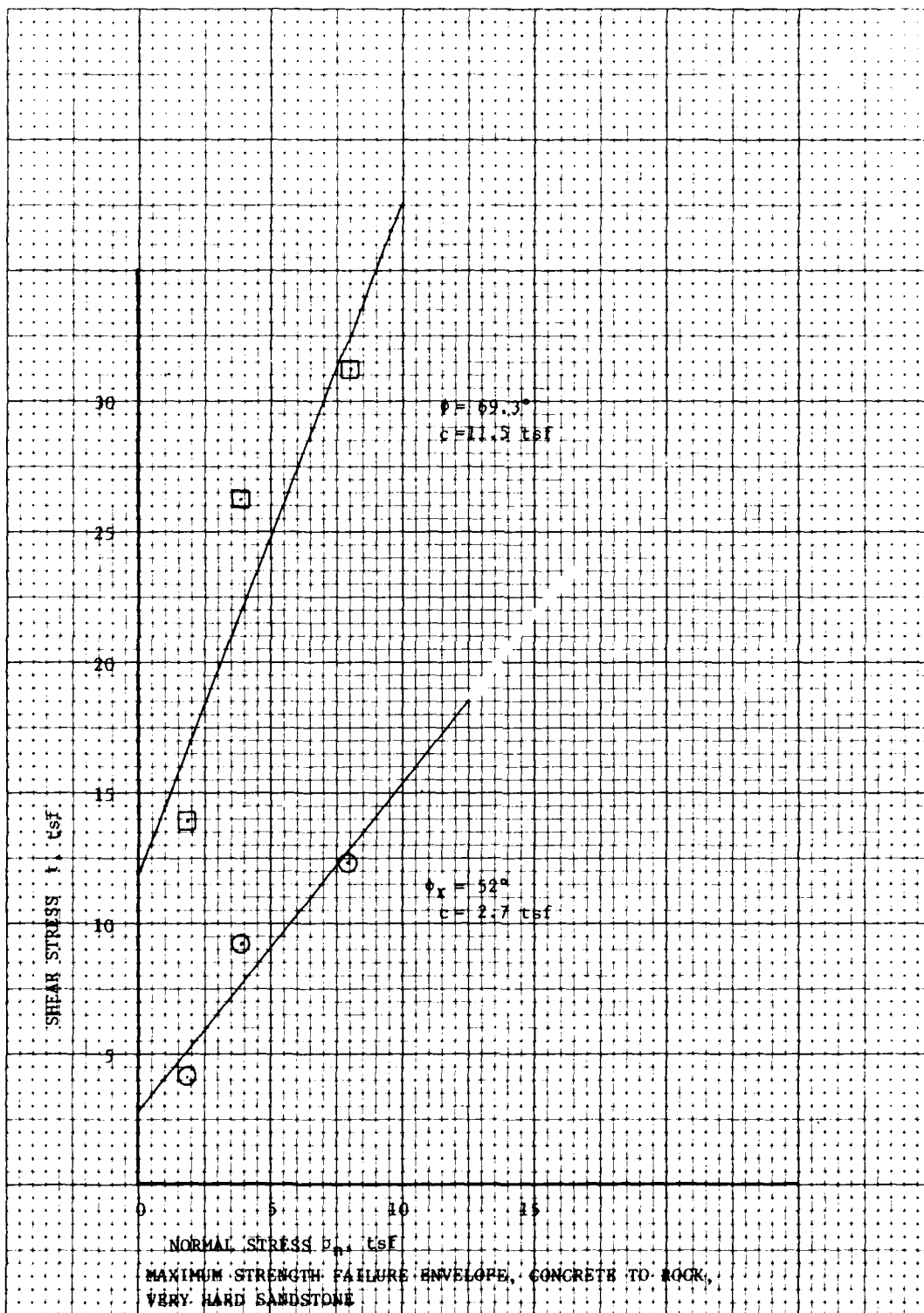
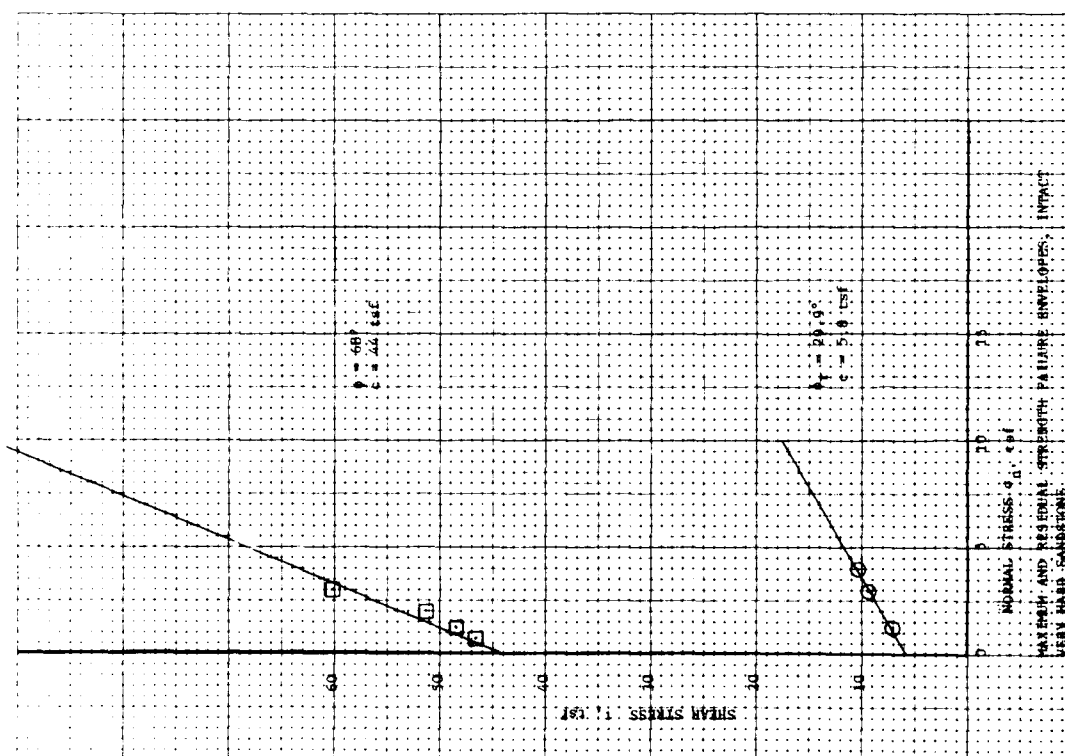
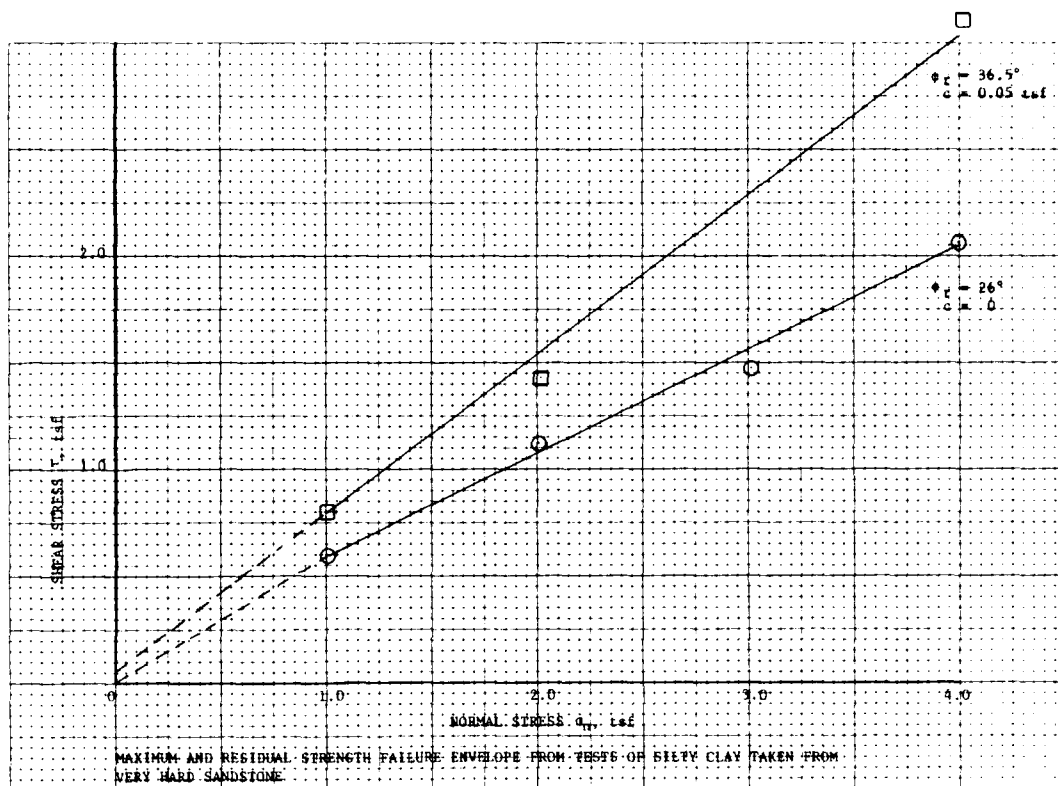
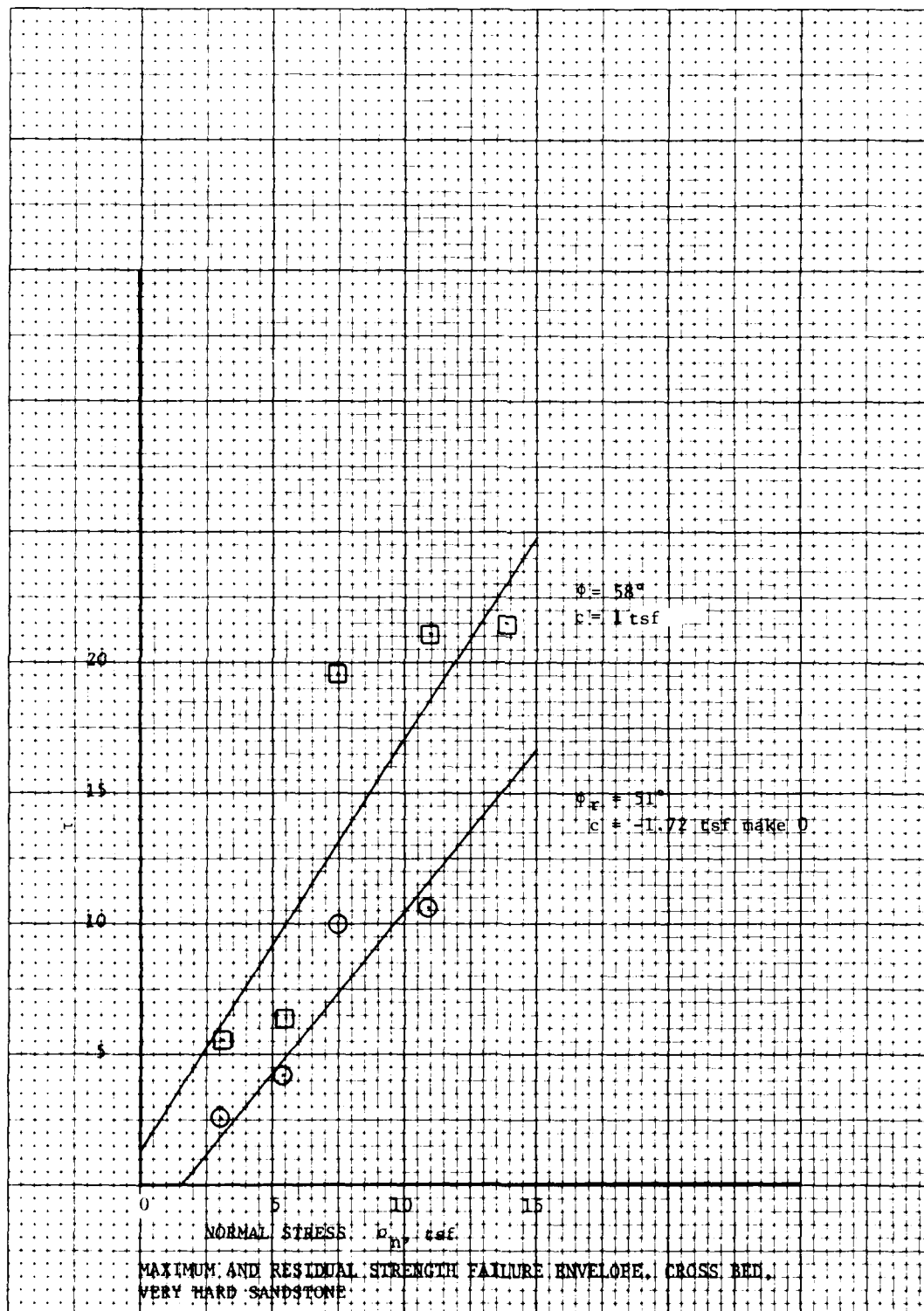


PLATE E84









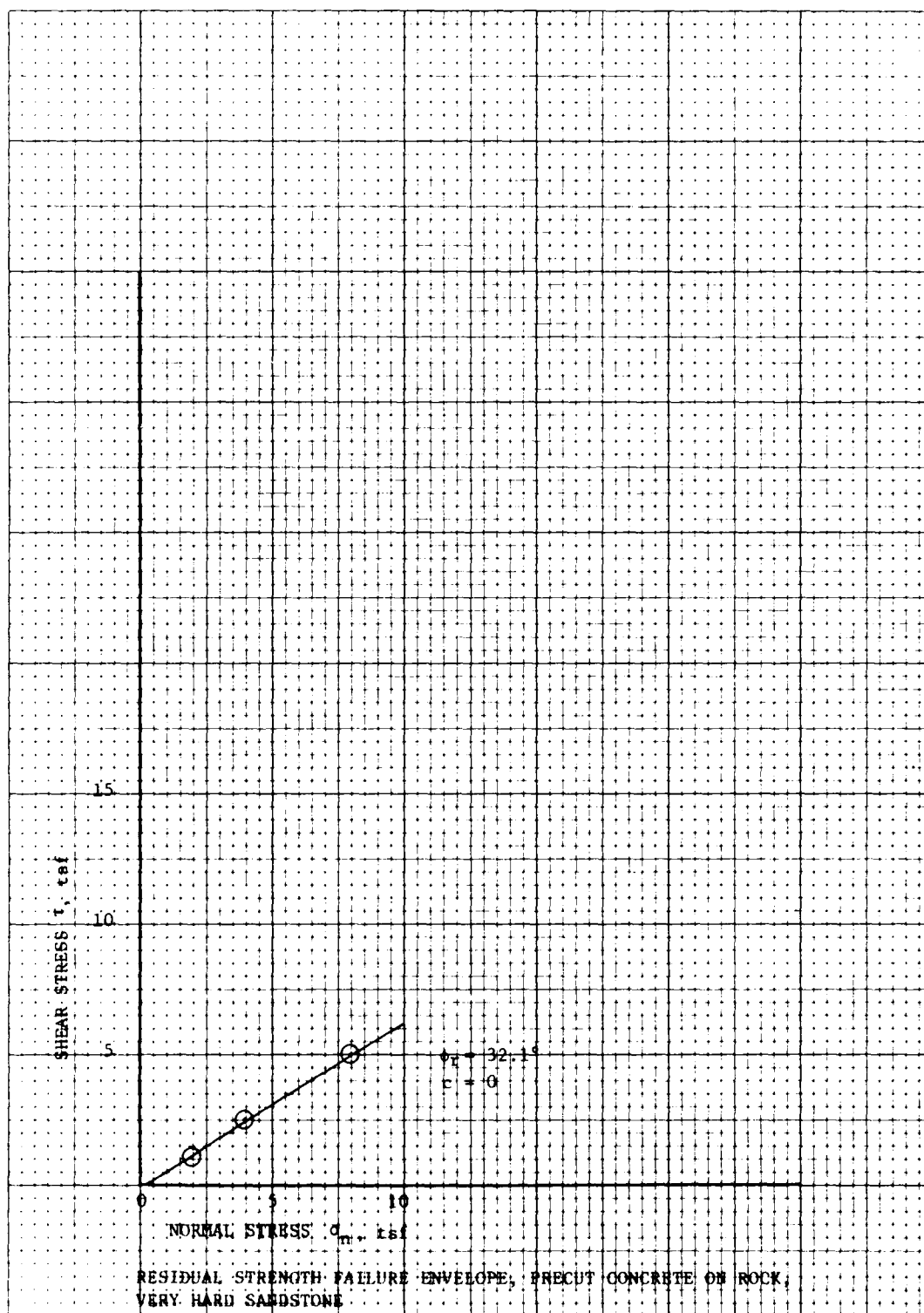
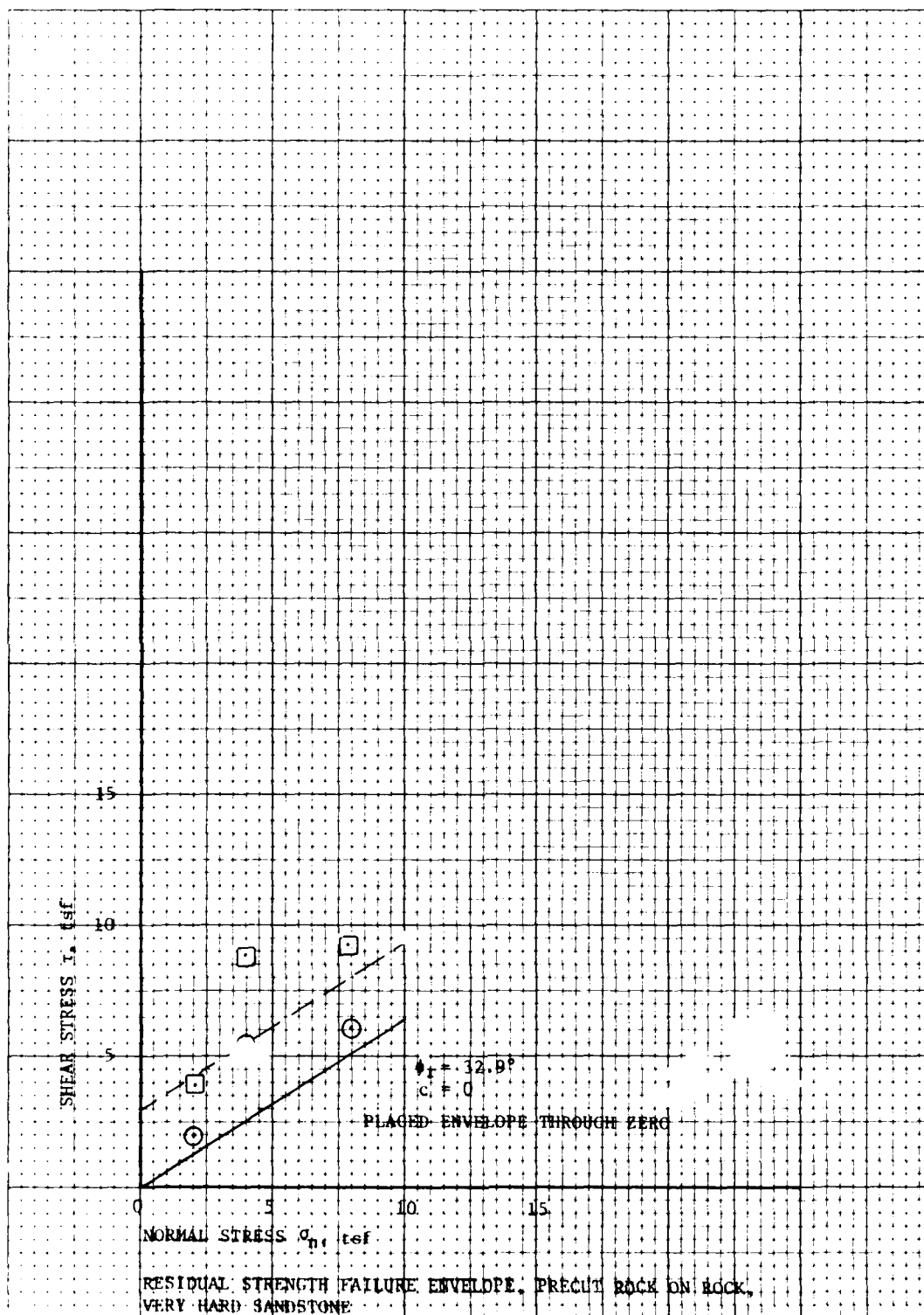
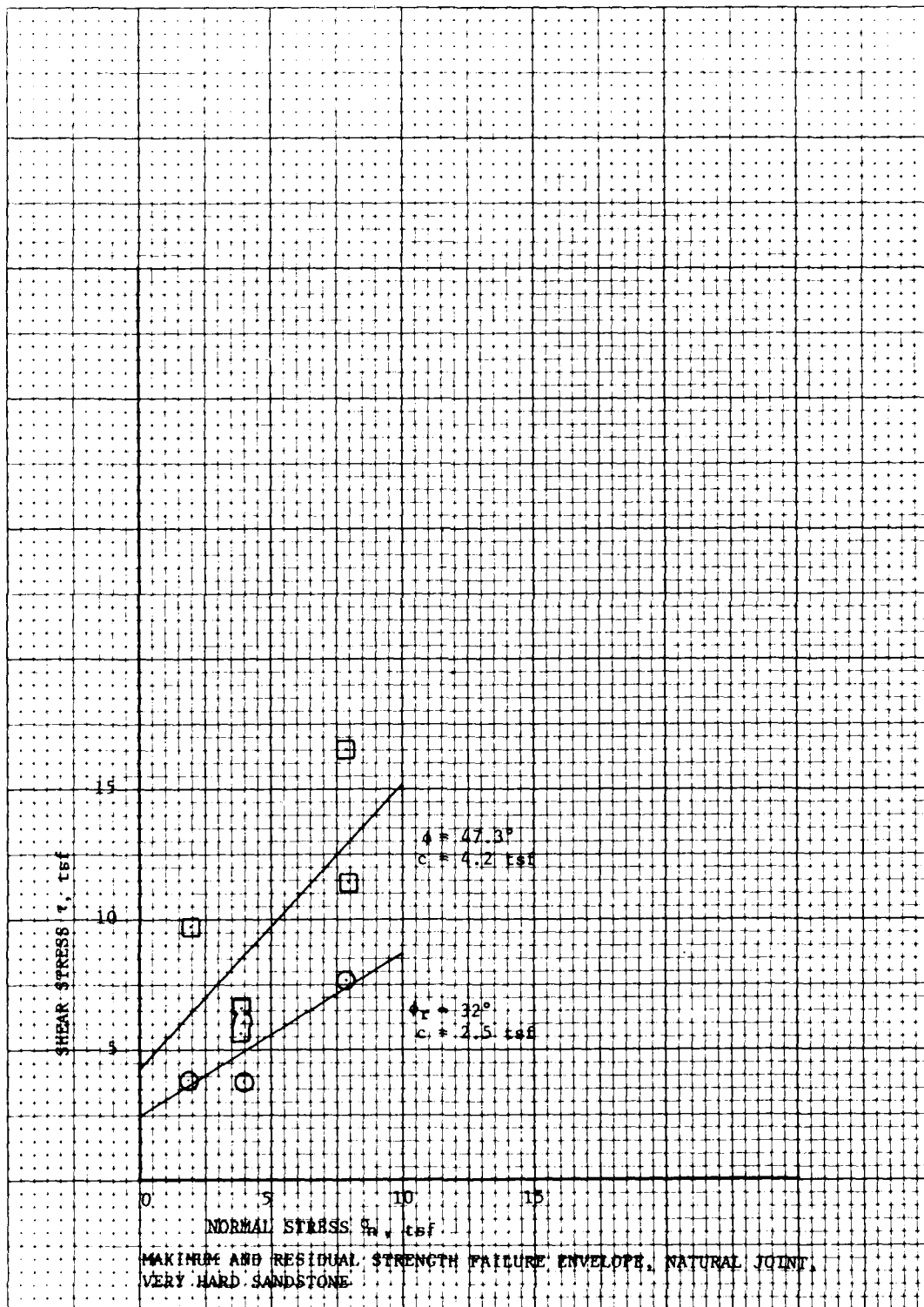
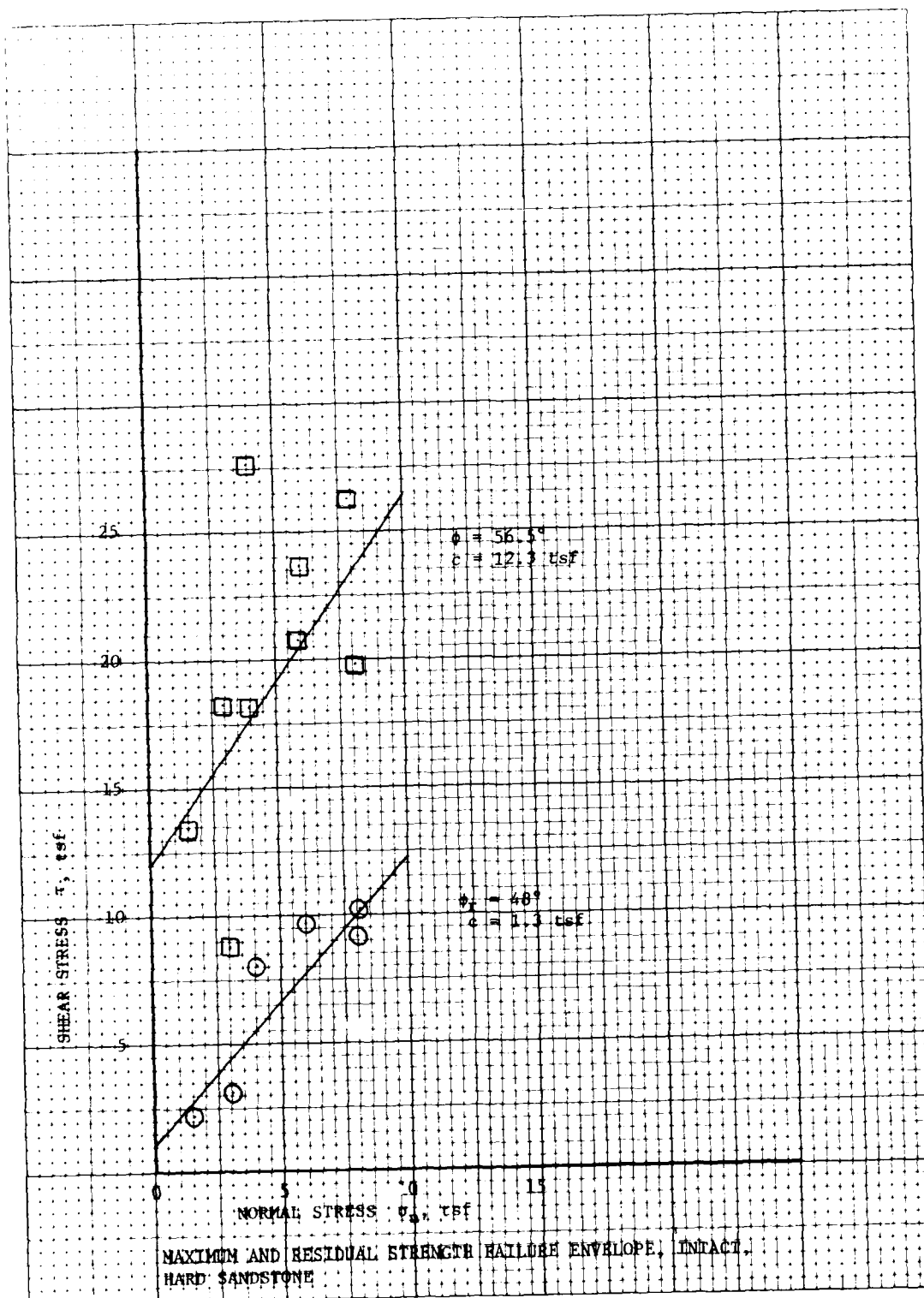


PLATE E88







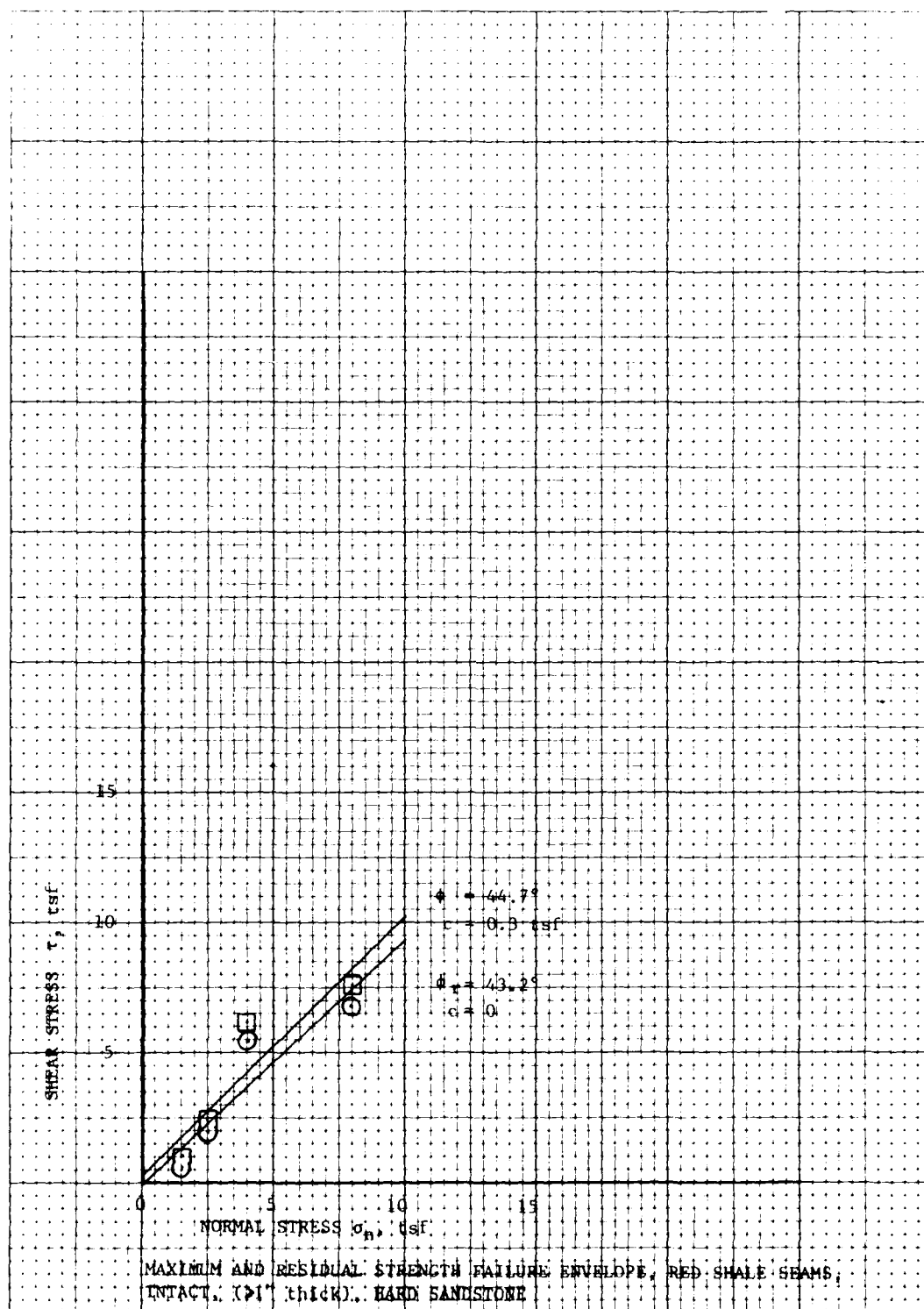
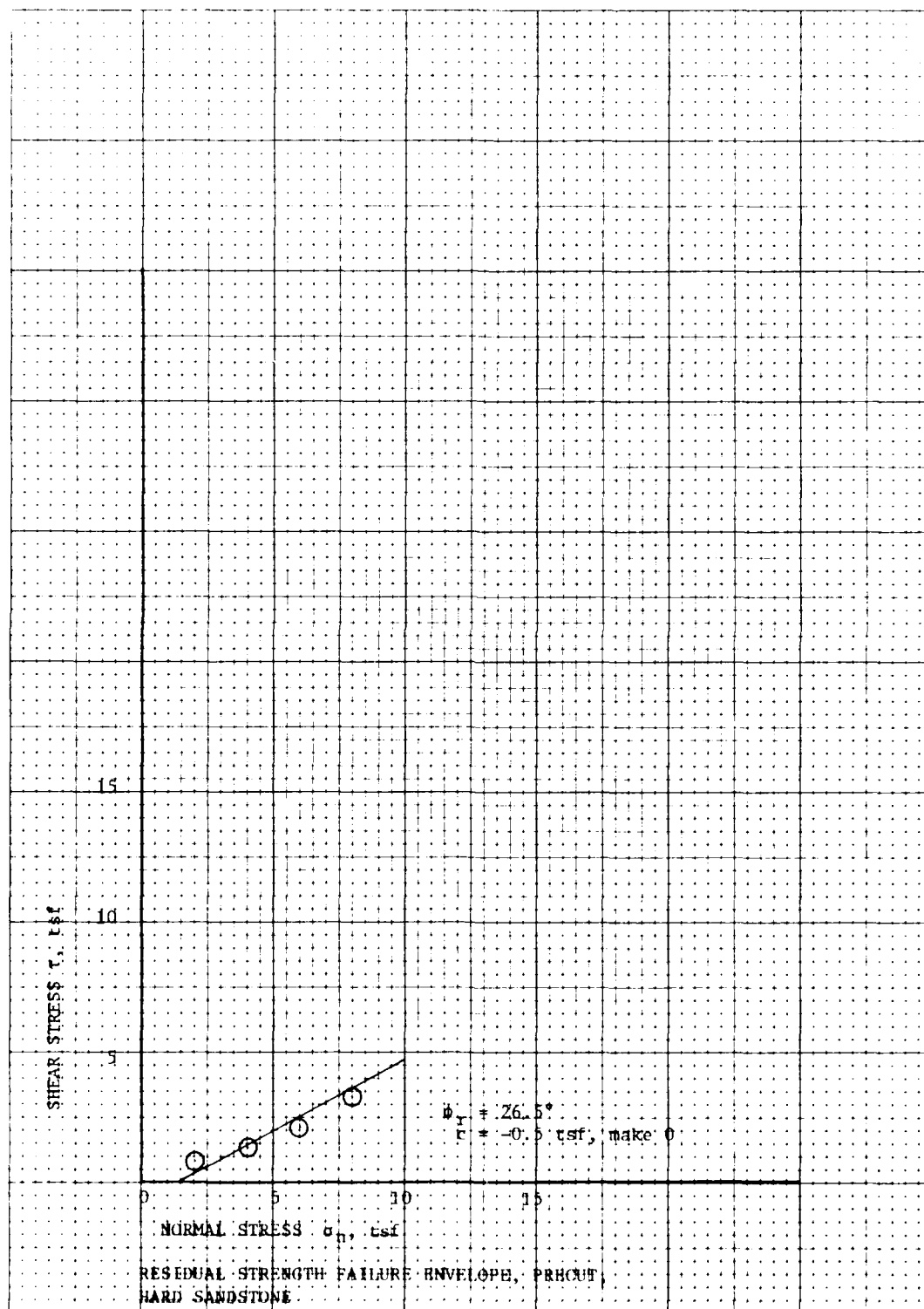
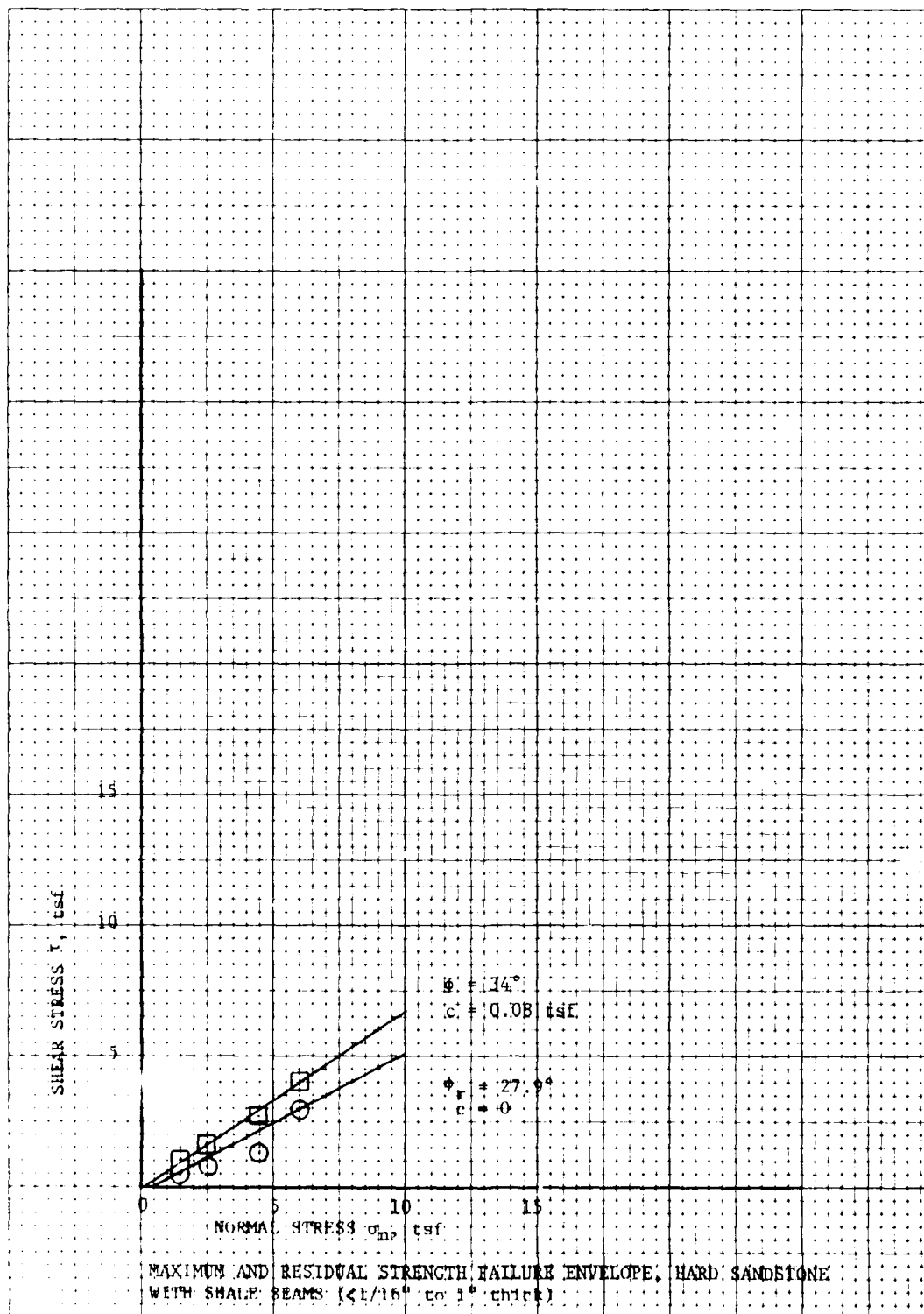
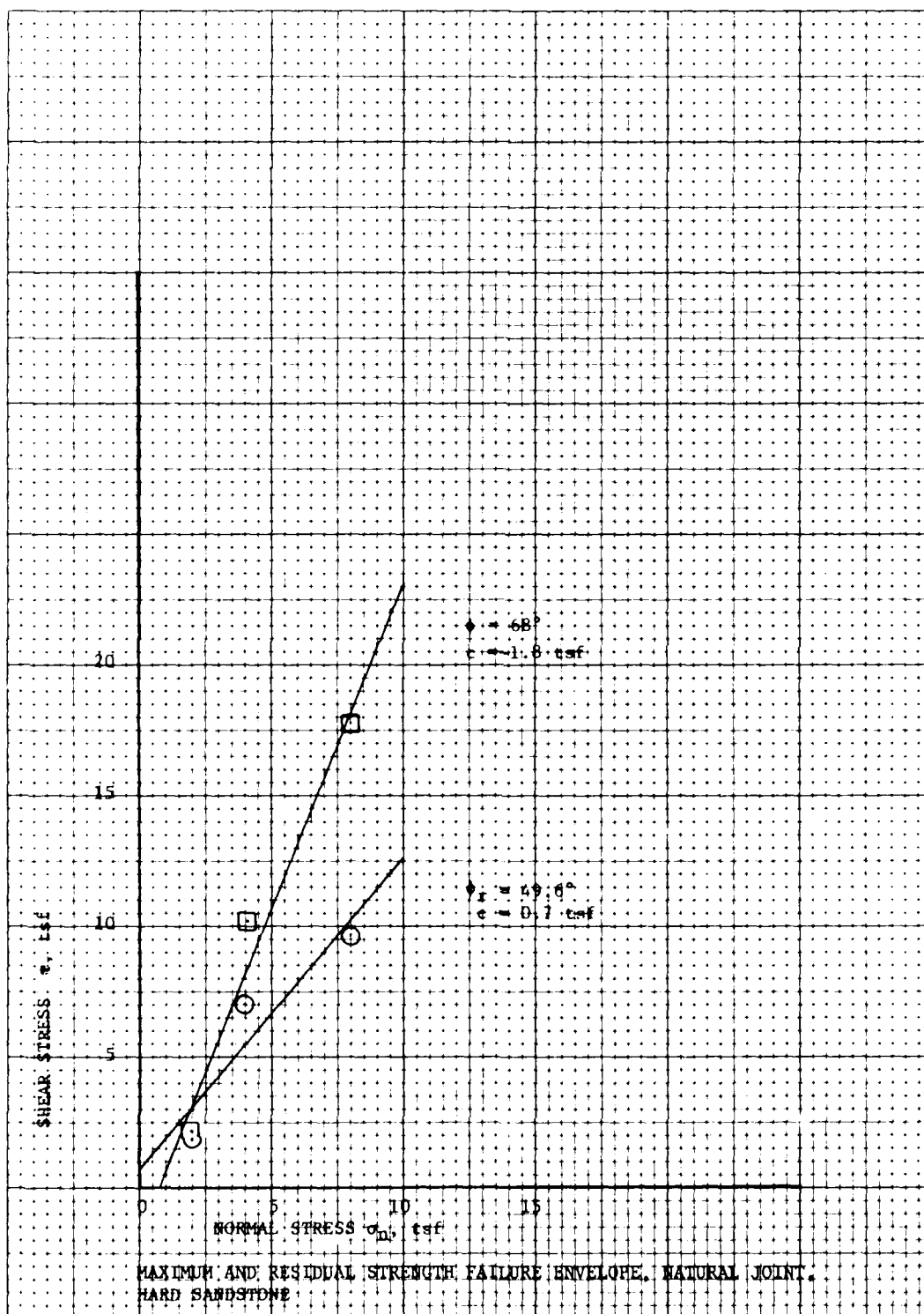


PLATE E92









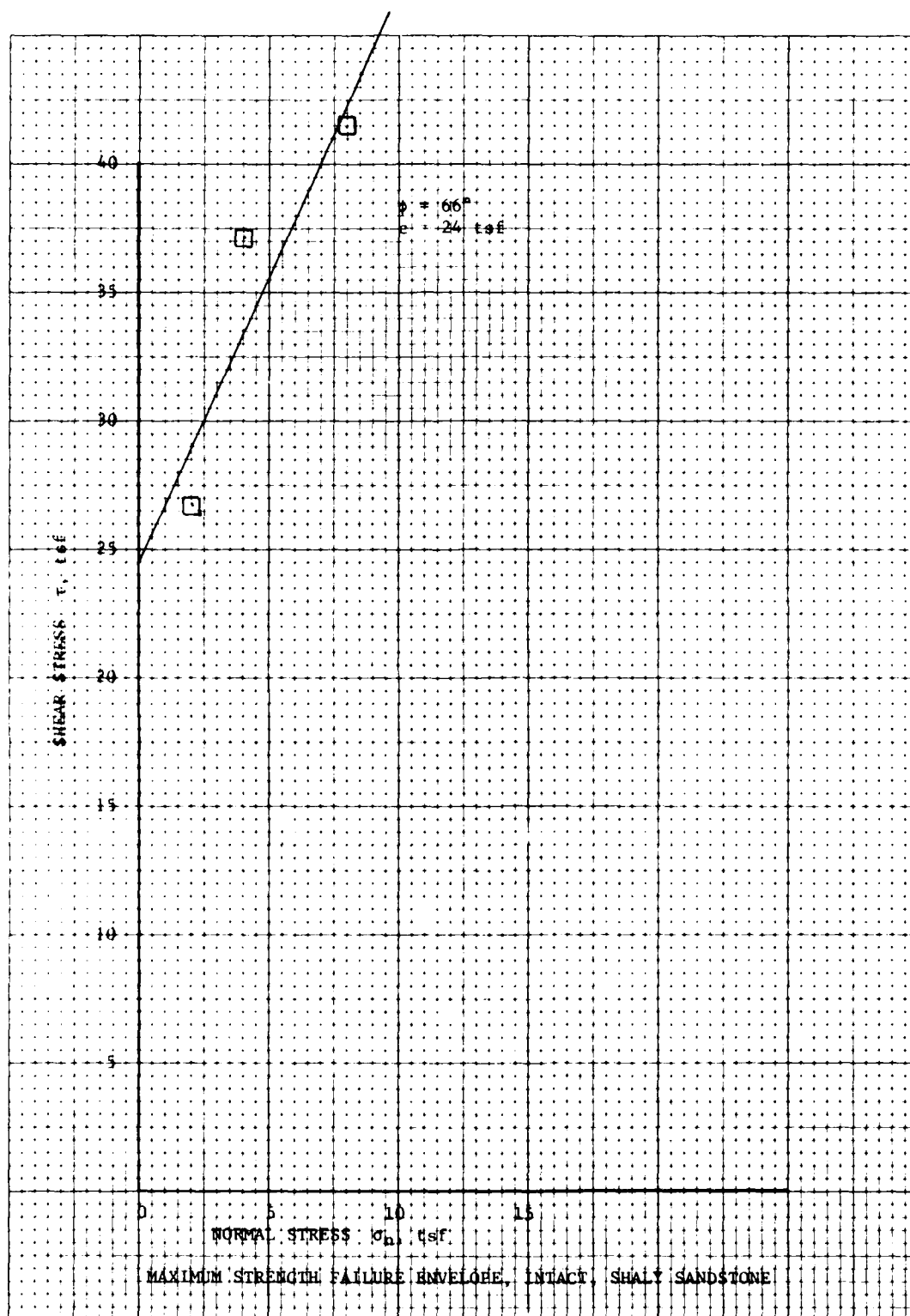
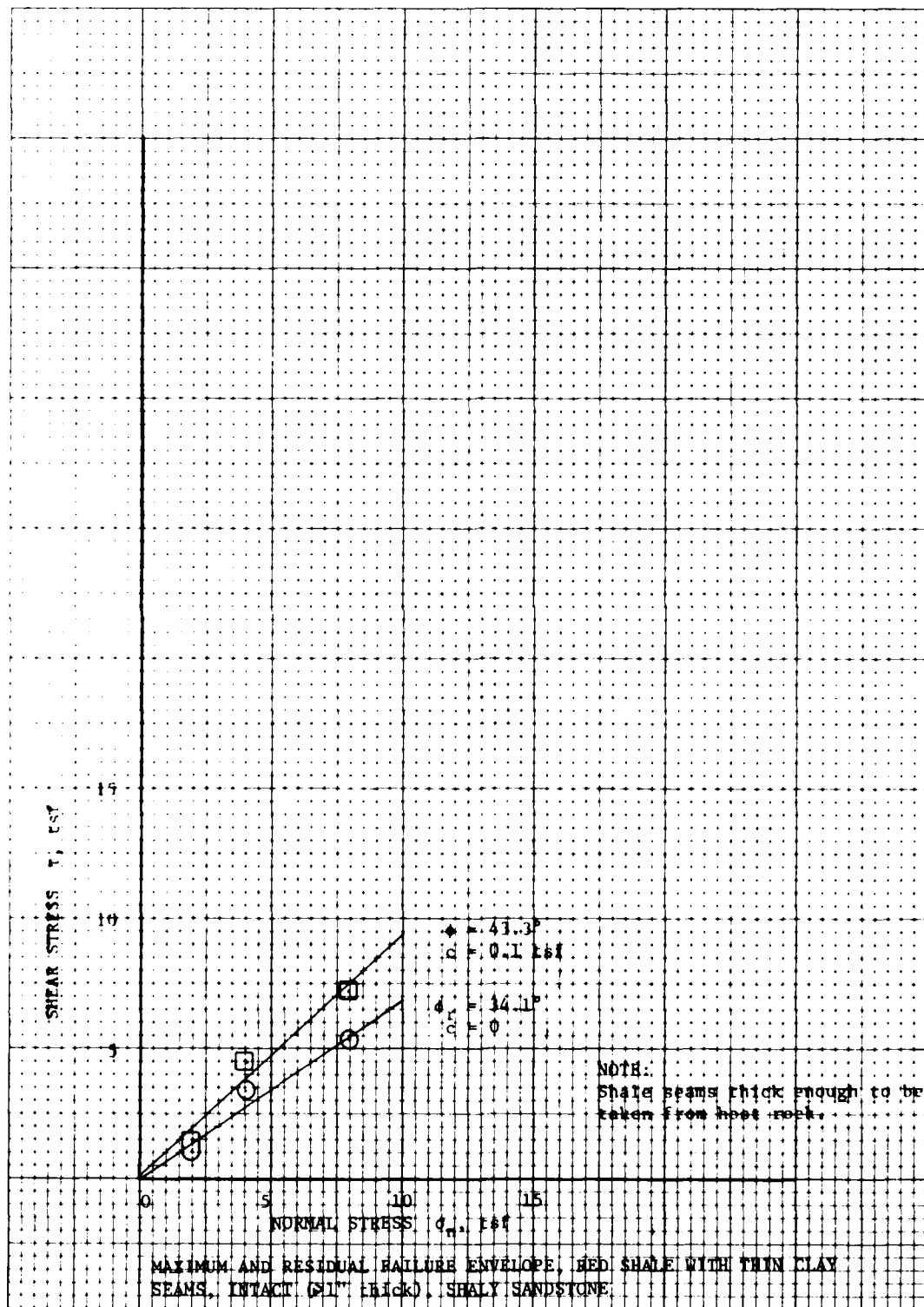


PLATE E96



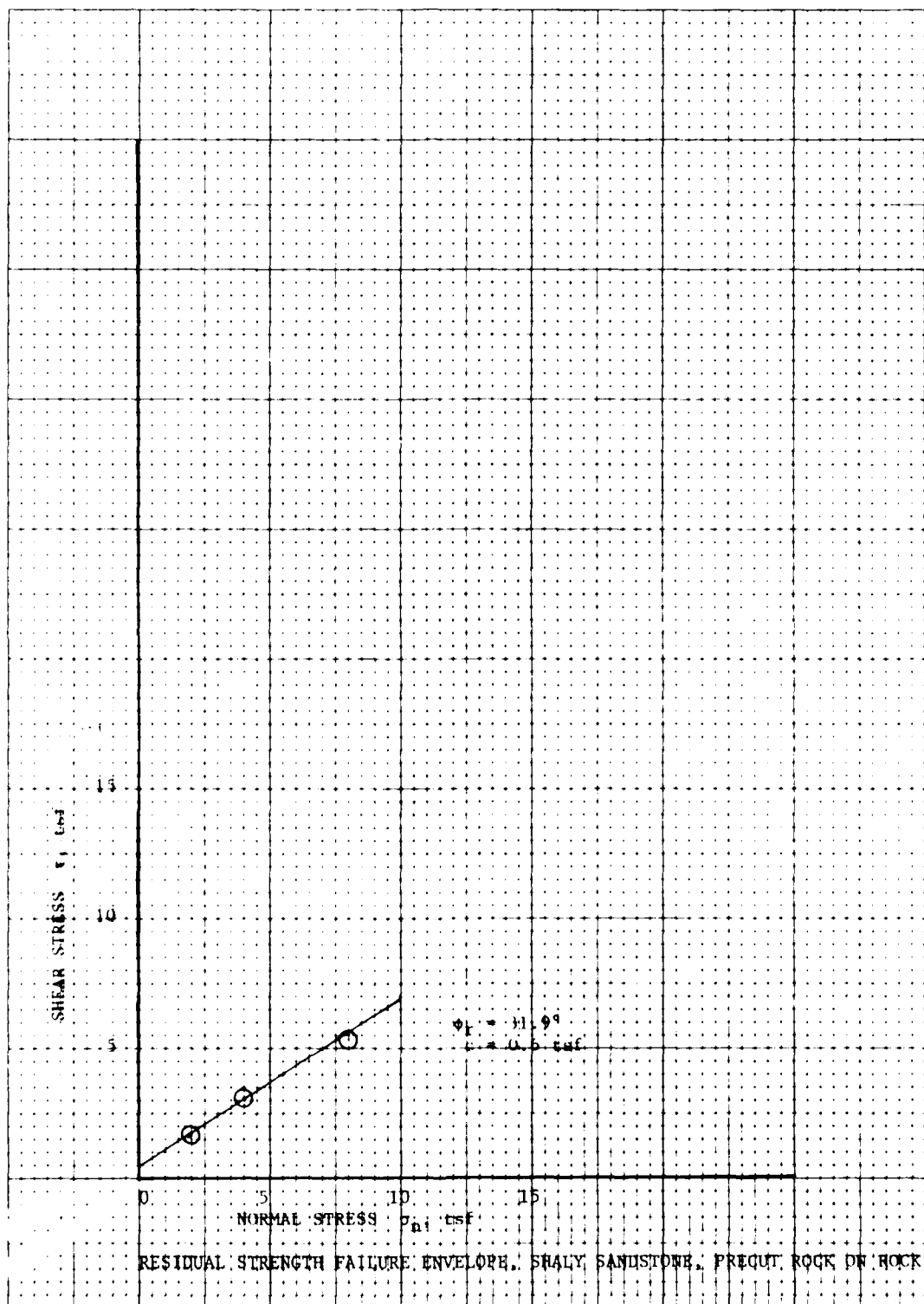
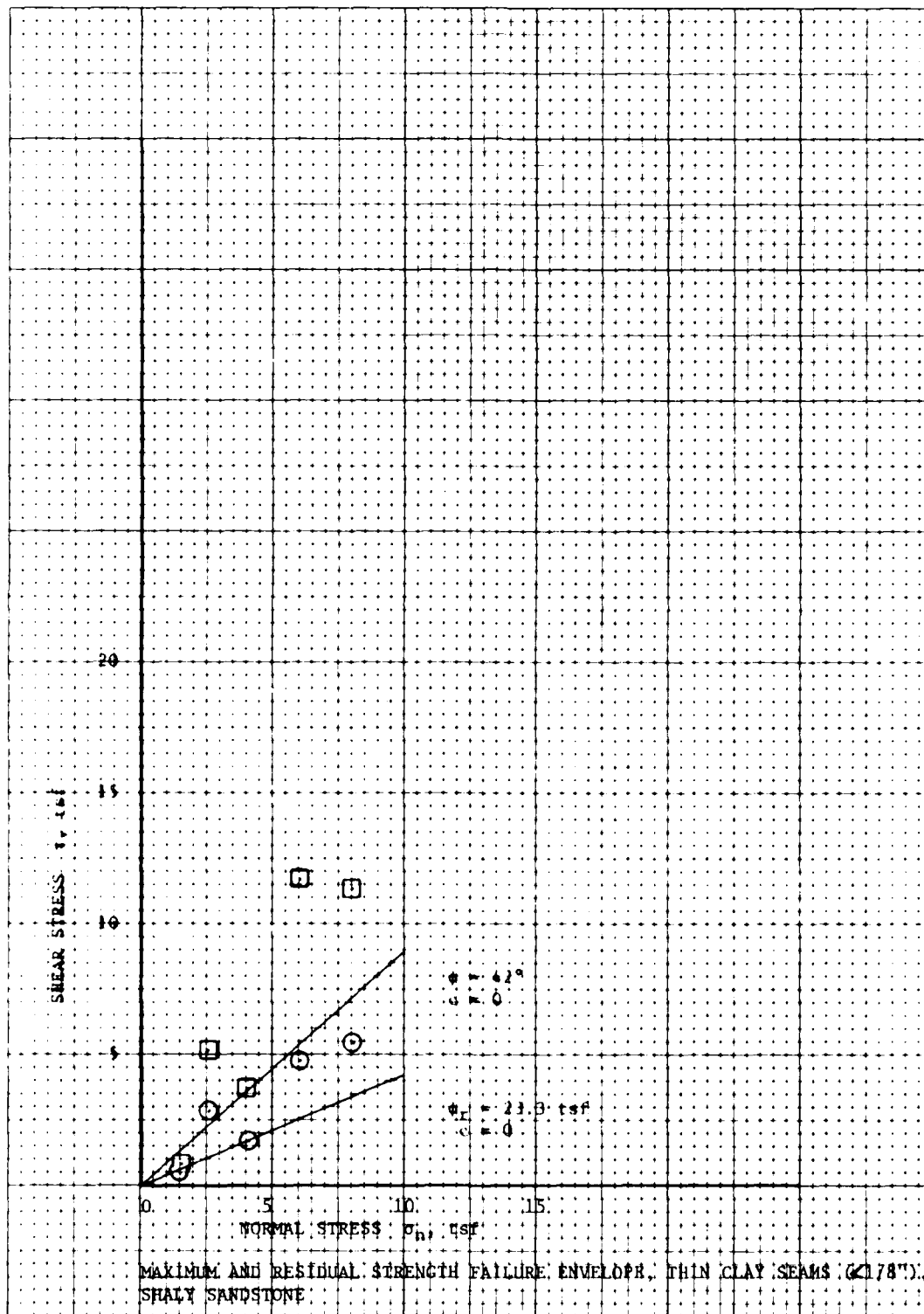


PLATE E98



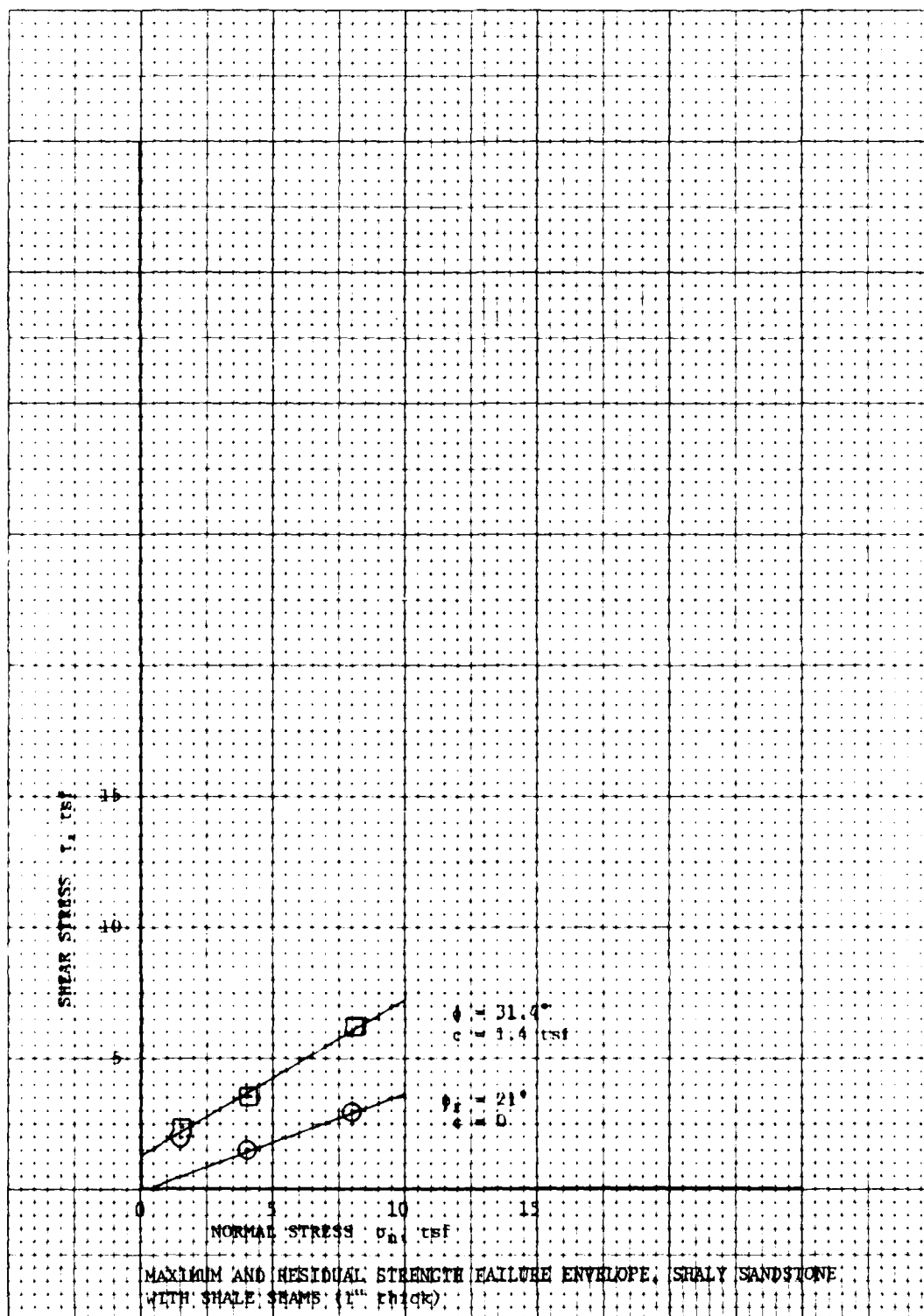


PLATE E100

**DIRECT SHEAR**

**CW-7      CW-15**

**EL. 25.3   EL. 24.7**

**GROUT TO ROCK VH**



**DIRECT SHEAR**

**CW-10      CW-10**

**EL. 7.75   EL. 7.4**

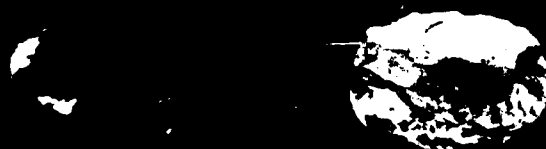
**INTACT SS**



Typical photographs of concrete to rock and intact

PLATE E101

**DIRECT SHEAR**  
**CW-15      CW-10**  
**EL. 28.9   EL. 10.25**  
**CLAY SEAM   SS**



**DIRECT SHEAR**  
**CW-34      CW-34**  
**EL. 13.8   EL. 27.6**  
**PRECUT**



Typical photographs of precut and clay seam

**DIRECT SHEAR**

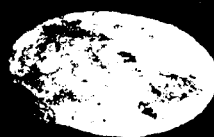
**CW-32**

**CW-17**

**EL. 6.6**

**EL. 46.4**

**SHALE SEAM HS**



**DIRECT SHEAR**

**CW-1**

**CW-1**

**EL. 27.9**

**EL. 27.6**

**NATURAL JOINT HS**



Typical photographs of shale seam and natural joint



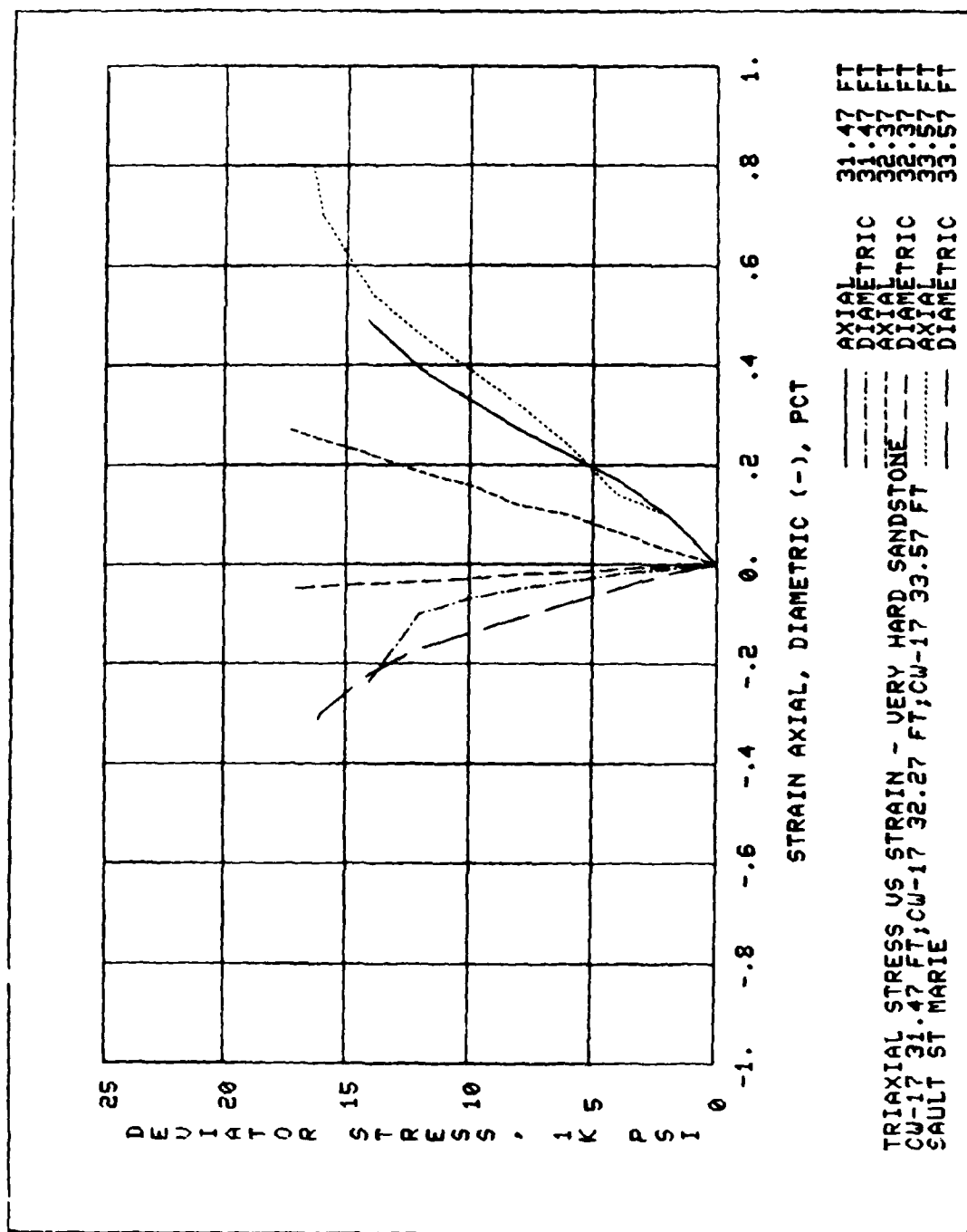
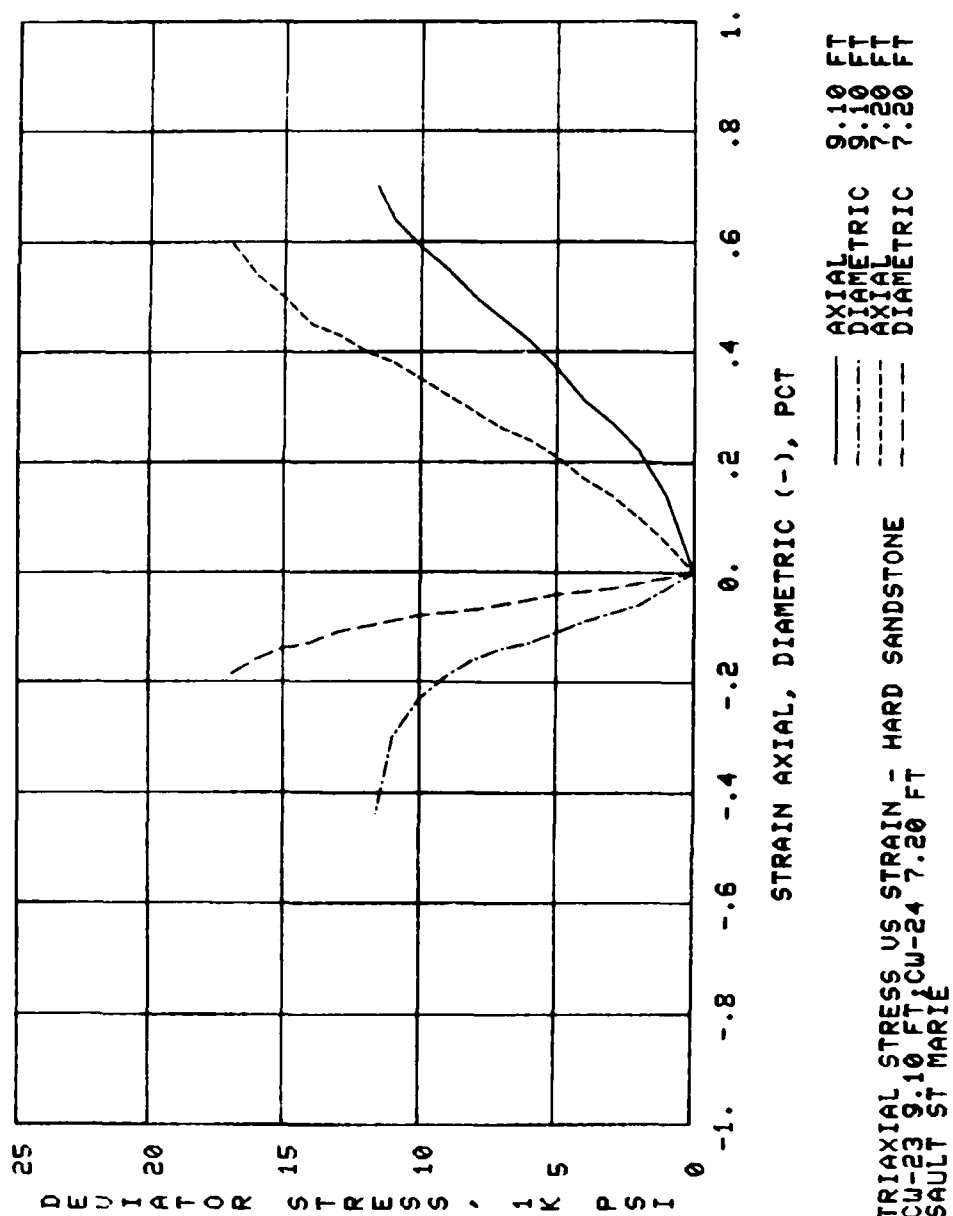


PLATE E104



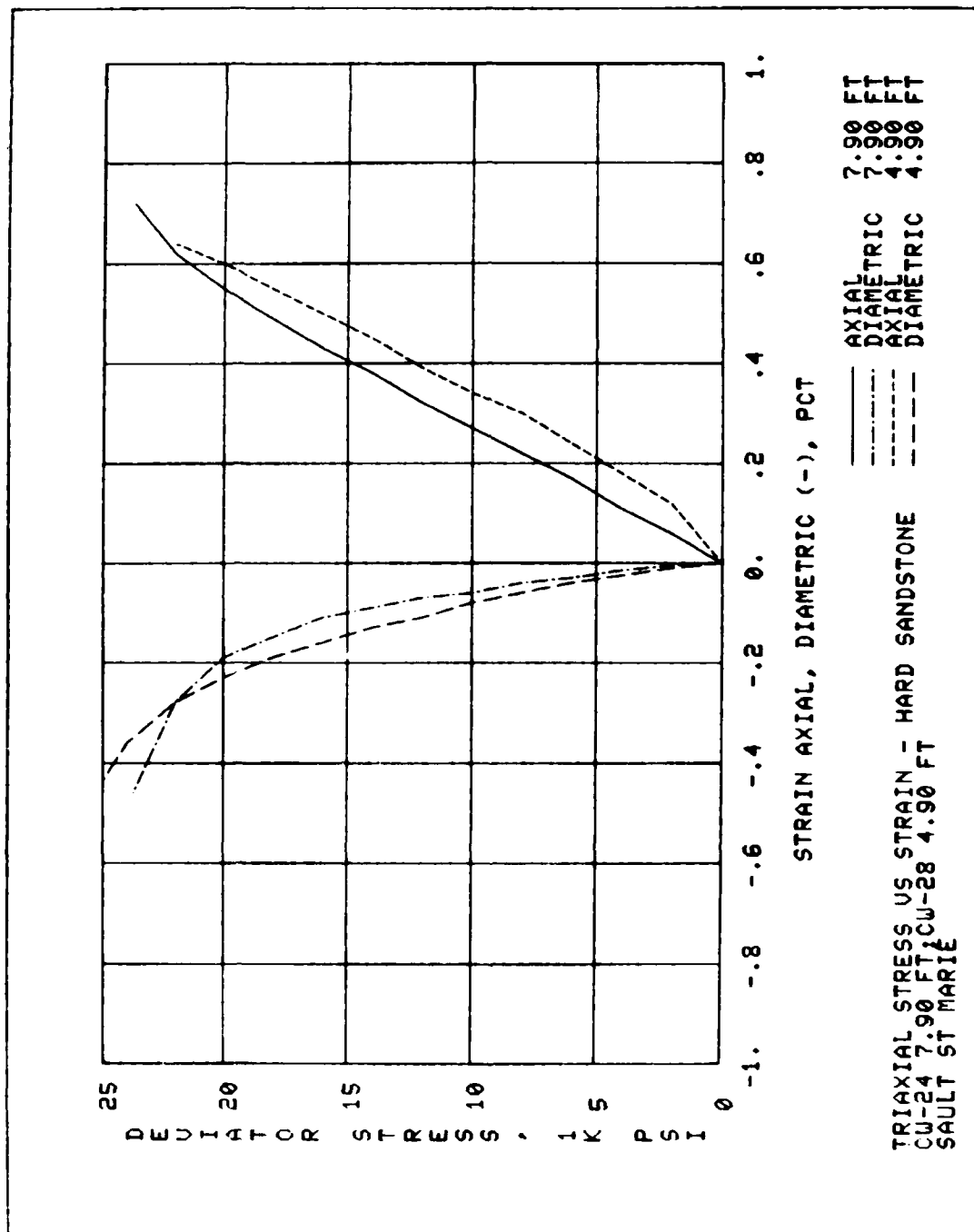
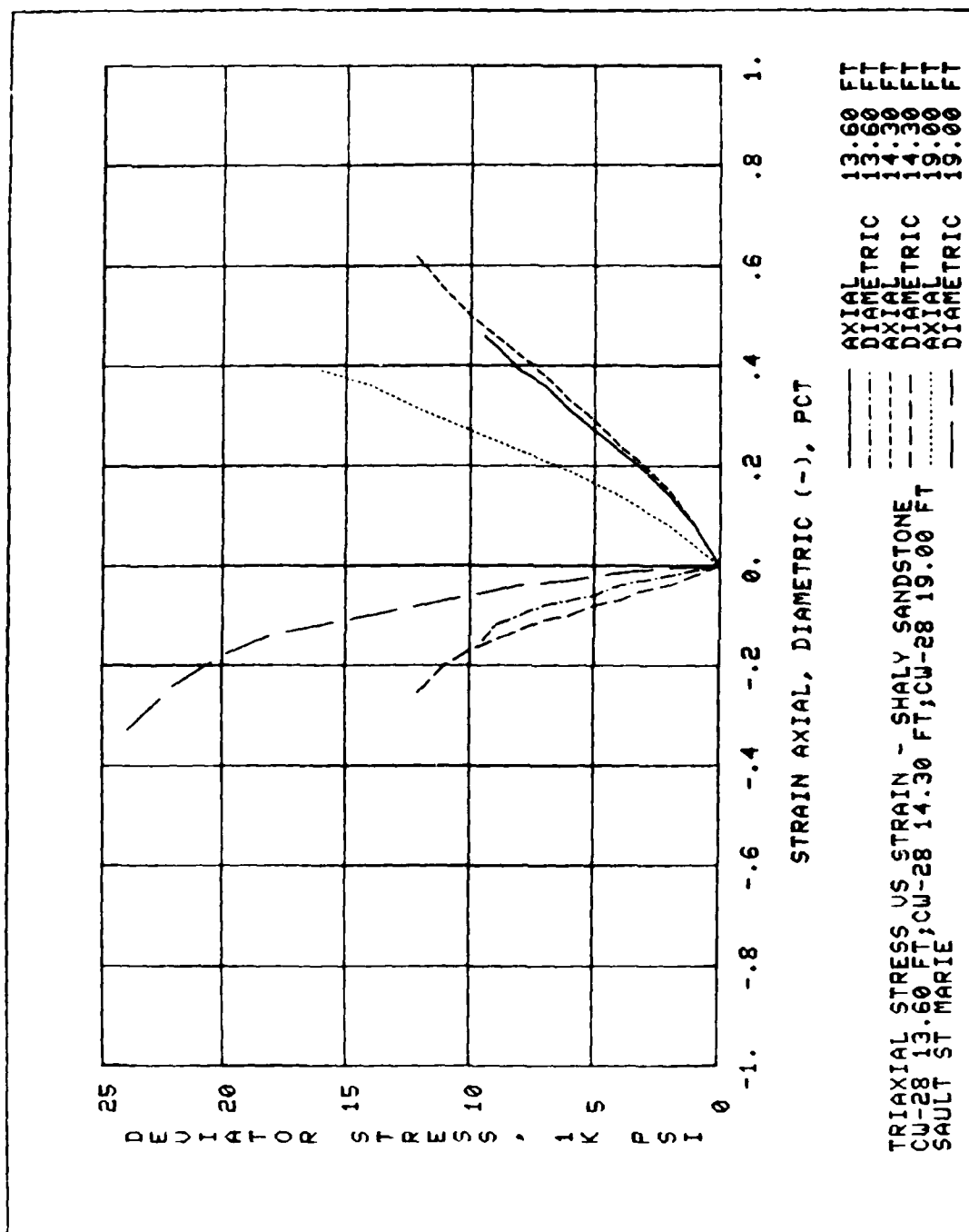


PLATE E106



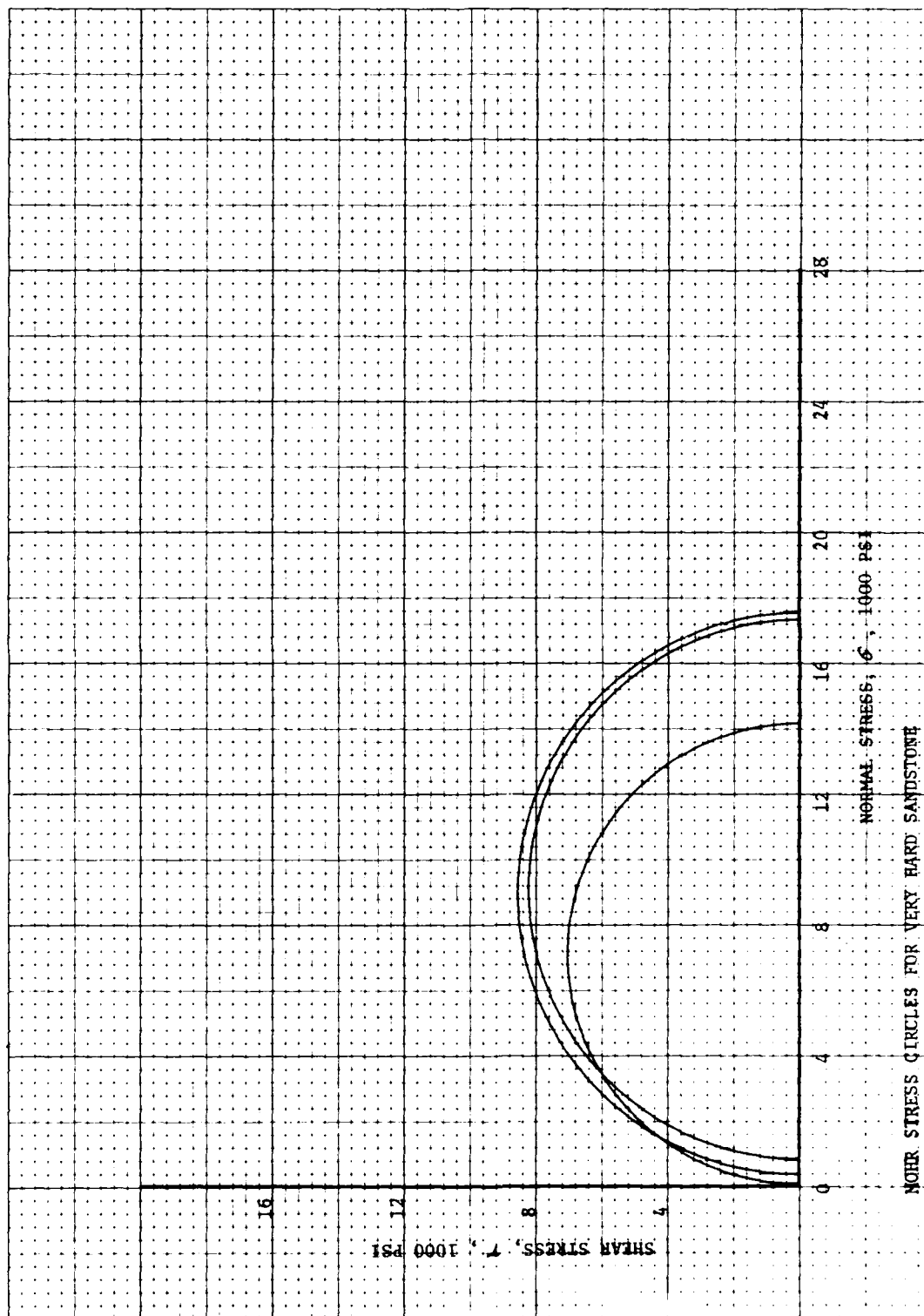
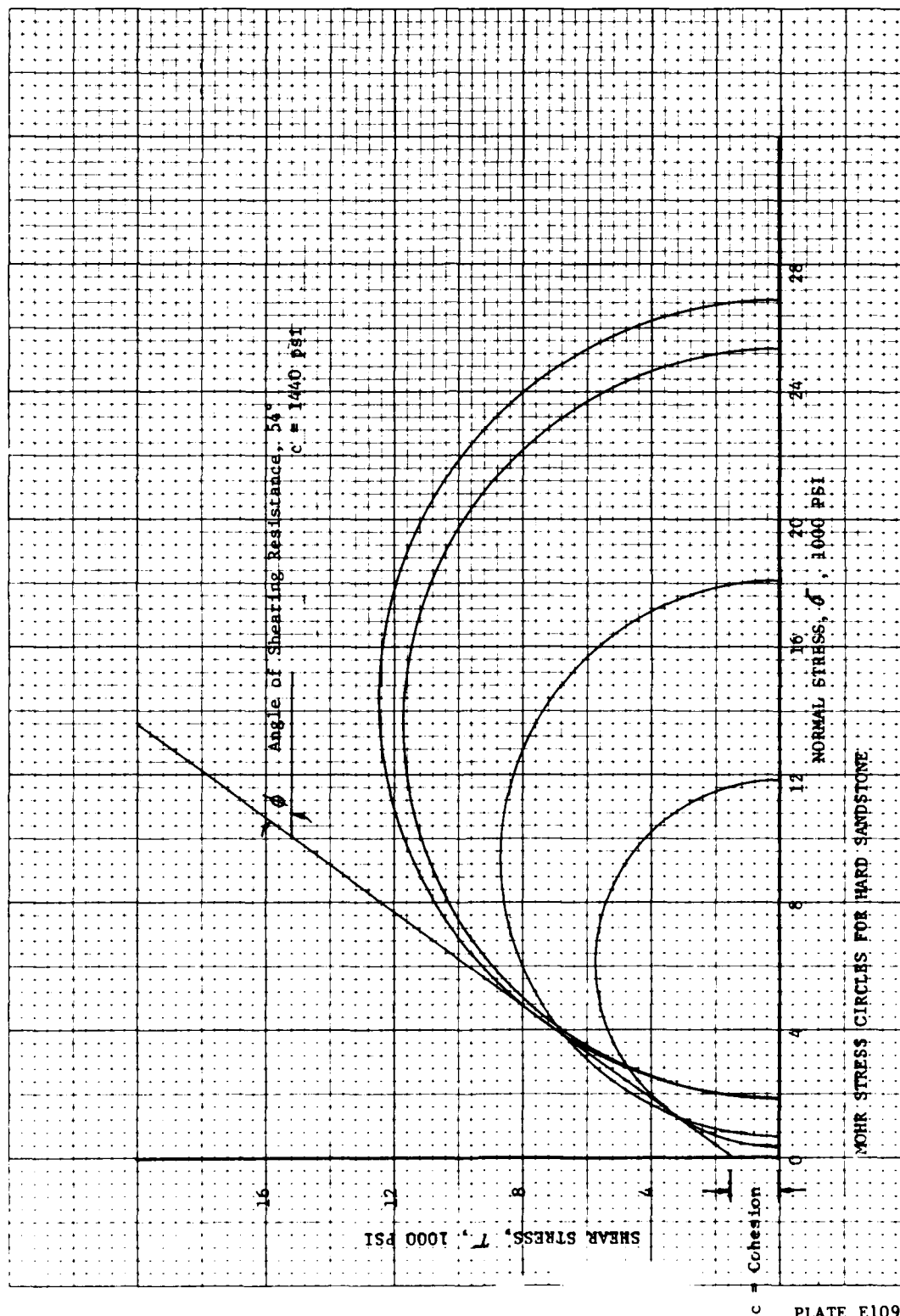


PLATE E108



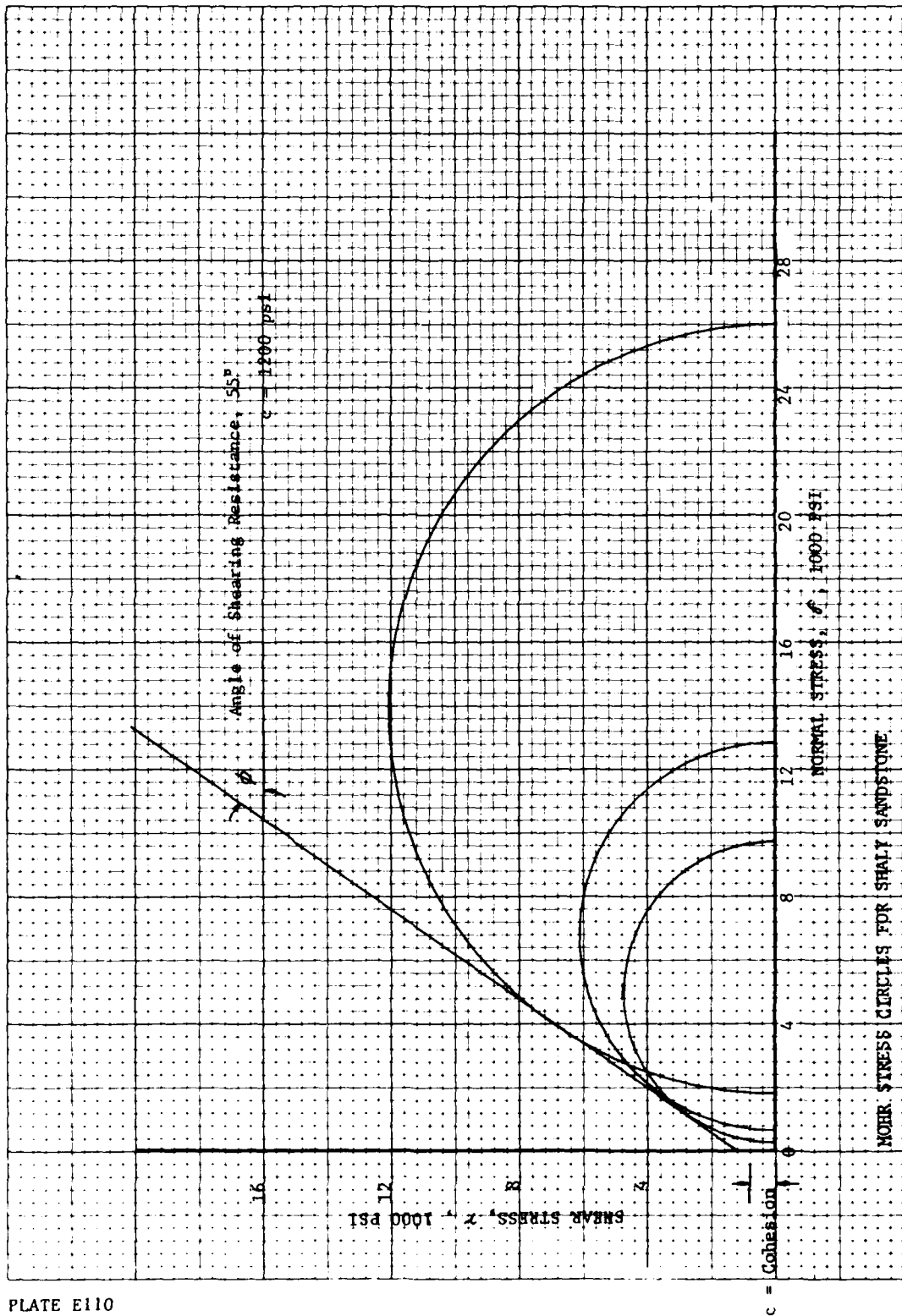


PLATE E110

APPENDIX F  
STRUCTURAL STABILITY ANALYSIS,  
FIGURES AND COMPUTATIONS



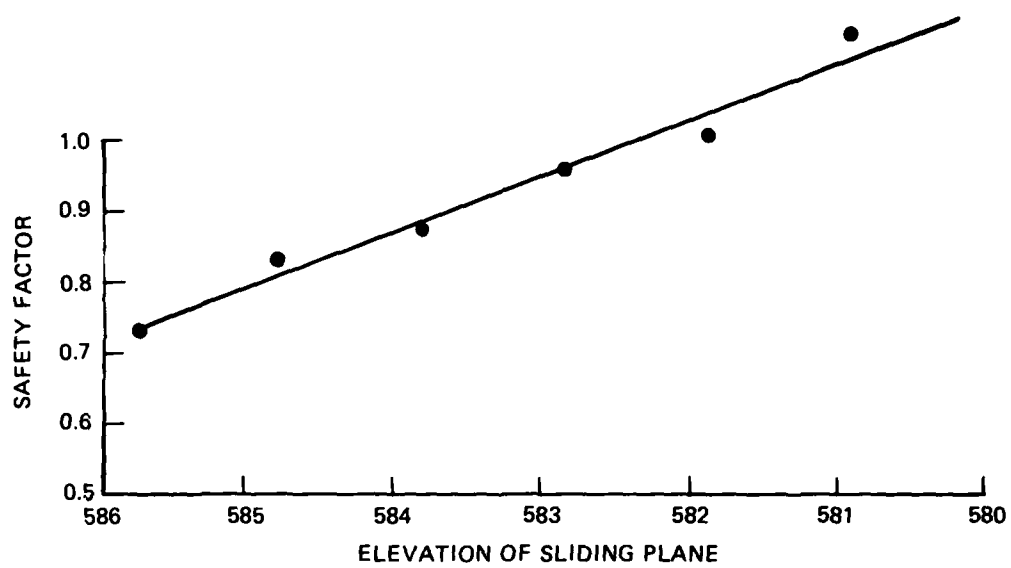


Figure F1. Safety factor versus elevation of sliding plane in foundation

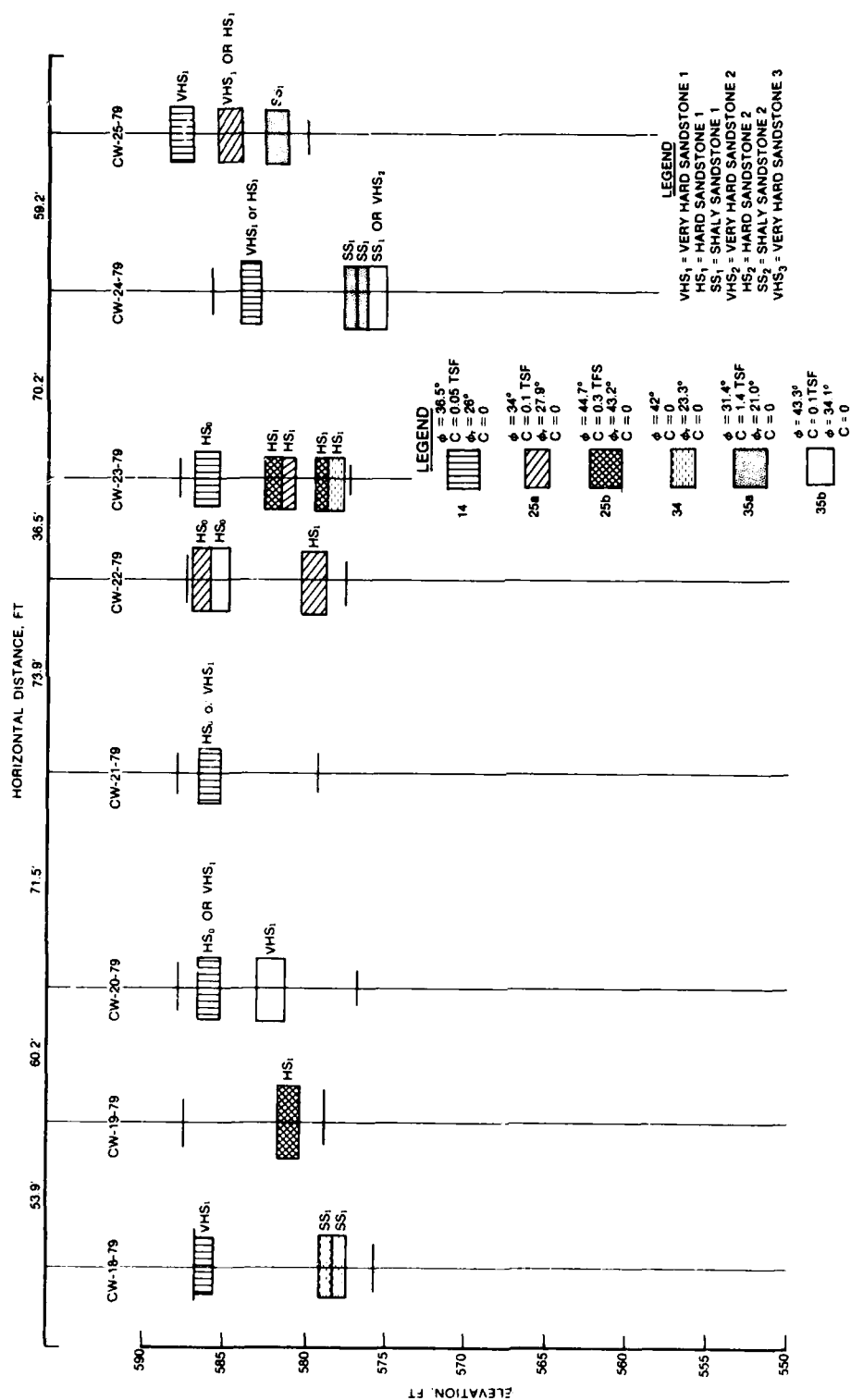


Figure F2. Location of clay and shale seams in upstream section (Section A-A', Plate D1) of core holes

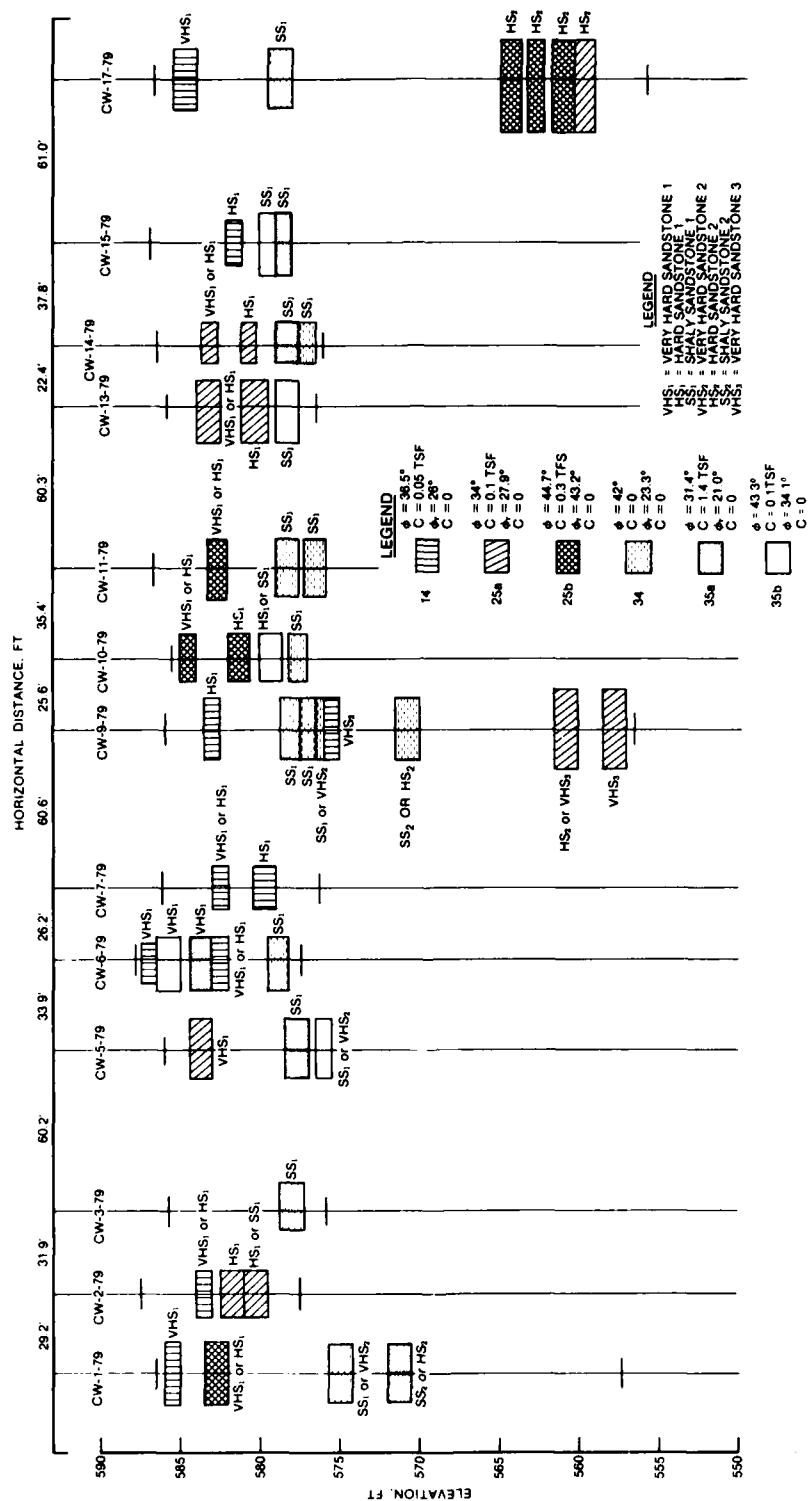


Figure F3. Location of clay and shale seams in downstream section (Section D-D', Plate D1) of core holes

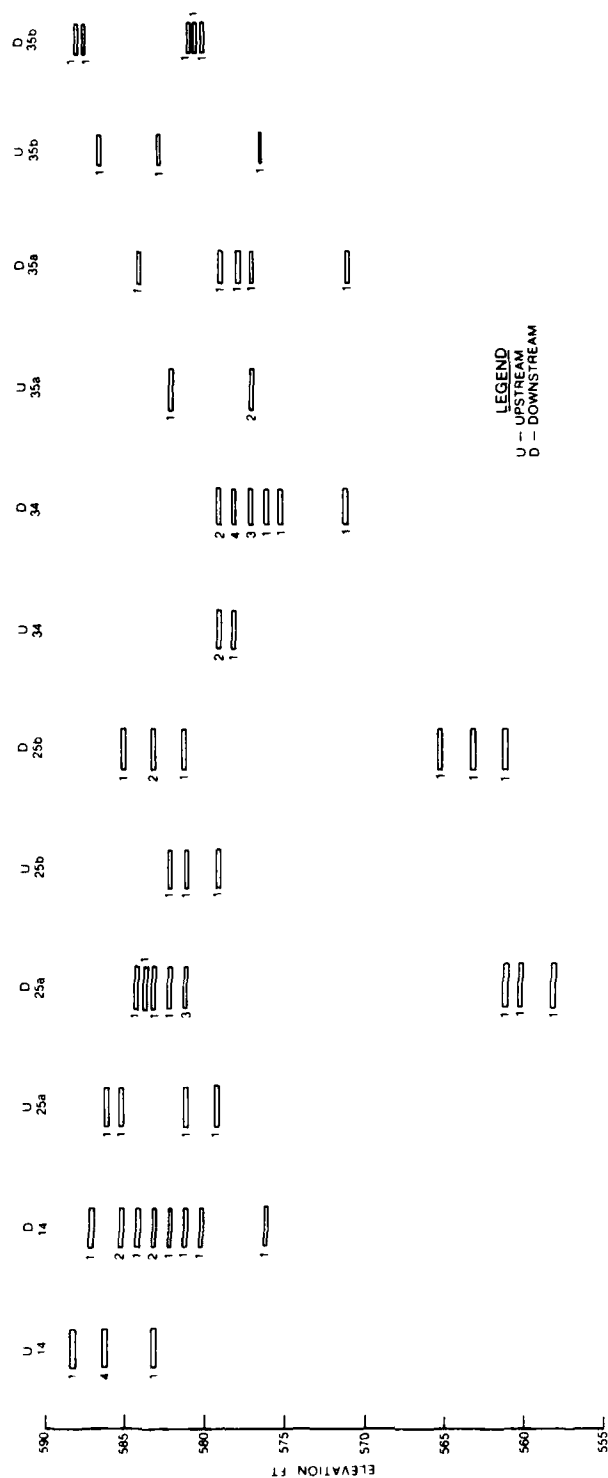


Figure F4. Composite location of clay and shale seams in core holes of Section A-A' and Section D-D' (Plate D1)

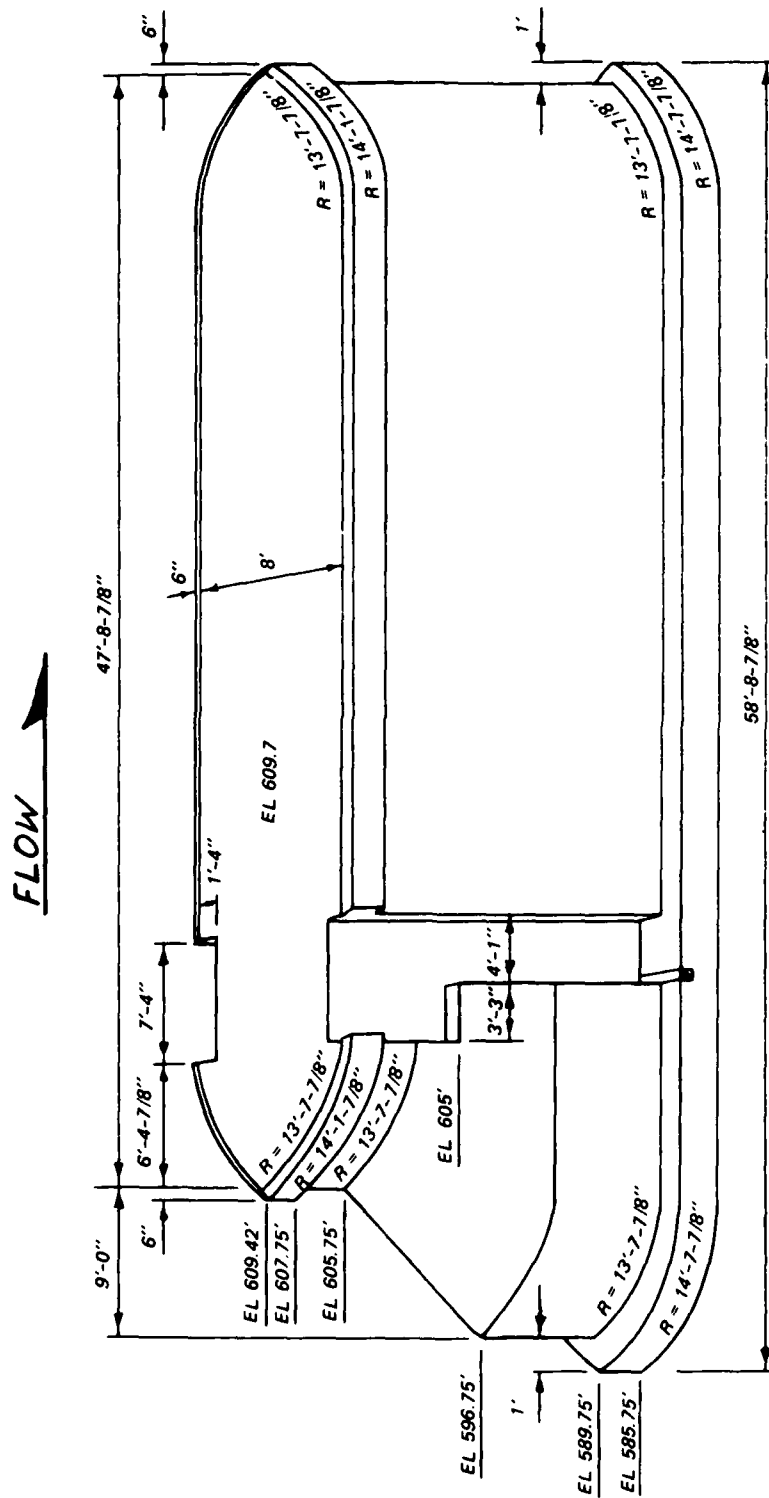


Figure F5. Typical geometry for dam piers 10, 11, 12, 14, 15, and 16, Soo Dam

SUBJECT DAM PIERS 10, 11, 12, 14, 15, AND 16 - PERCENT EFFECTIVE BASE, CONCRETE-FOUNDATION INTERFACE		COMPUTED BY:	DATE
		CHECKED BY:	DATE

LOAD CASE	TOTAL AREA OF PIER BASE	AREA OF PIER BASE IN COMPRESSION	PERCENT EFFECTIVE BASE
	$A_o$	$A_c$	$\frac{A_c}{A_o} \times 100$
	FT <sup>2</sup>	FT <sup>2</sup>	%
NORMAL OPERATION	519.76	519.76	100.0
NORMAL OPERATION WITH ICE	519.76	486.53 *	93.6
HIGH-WATER CONDITION	519.76	519.76	100.0
NORMAL OPERATION WITH EARTHQUAKE	519.76	519.76	100.0

\* Iterative solution used to determine area of base in compression

Figure F6. Percent of pier base in compression, concrete-foundation interface, dam piers 10, 11, 12, 14, 15, and 16, Soo Dam

SUBJECT DAM PIERS 10, 11, 12, 14, 15, AND 16 - FACTOR OF SAFETY AGAINST SLIDING ALONG										DATE	DATE
CONCRETE - FOUNDATION INTERFACE										COMPUTED BY	DATE
CHECKED BY										DATE	DATE
LOAD CASE	SUM OF VERTICAL FORCES	SUM OF HORIZONTAL FORCES	FRICTION ANGLE	COHESIVE STRENGTH	BASE AREA	STRUT RESISTANCE	SHEAR RESISTANCE	COHESIVE RESISTANCE	TOTAL SLIDING RESISTANCE	FACTOR OF SAFETY AGAINST SLIDING	
	$F_v$ (KIPS)	$F_H$ (KIPS)	$\phi$ (DEGREES)	$C$ (KSF)	$A$ ( $FT^2$ )	$R_s$ (KIPS)	$R_s = F_v \tan \phi$ (KIPS)	$R_c = CA$ (KIPS)	$R = R_s + R_c$ (KIPS)	$FS = \frac{R}{F_H}$	
NORMAL OPERATION	1,285.4	264.9	32.1	0	519.76	717.0	806.3	0.0	1,523.3	5.75	
NORMAL OPERATION WITH ICE	1,285.4	867.0	32.1	0	486.53	717.0	806.3	0.0	1,523.3	1.76	
HIGH-WATER CONDITION	1,266.4	313.8	32.1	0	519.76	717.0	794.4	0.0	1,511.4	4.82	
NORMAL OPERATION WITH EARTHQUAKE	1,285.4	366.9	32.1	0	519.76	717.0	806.3	0.0	1,523.3	4.15	

253A  
253A

PAGE 1 OF 1

Figure F7. Factor of safety against pier sliding, concrete-foundation interface, dam piers 10, 11, 12, 14, 15, and 16, Soo Dam

SUBJECT DAM PIERS 10, 11, 12, 14, 15, AND 16 - MAXIMUM BASE PRESSURES, CONCRETE-FOUNDATION INTERFACE														
		COMPUTED BY		CHECKED BY		DATE		DATE						
LOAD CASE	SUM OF VERTICAL FORCES	SUM OF MOMENTS	RESULTANT ARM	DISTANCE TO CENTROID OF AREA IN COMPRESSION	AREA OF PIER BASE IN COMPRESSION	INERTIA OF BASE AREA IN COMPRESSION	LOCATION	DISTANCE TO OUTER-MOST FIBER OF BASE	AXIAL PRESSURE	PRESSURE DUE TO BENDING MOMENT	INTERMEDIATE PRESSURE	UPLIFT HEAD	UPLIFT PRESSURE	TOTAL BASE PRESSURE
	$F_v$	$M$	$e = \frac{M}{F_v}$	$D$	$A$	$I$	—	$C$	$f_a = \frac{F_v}{A}$	$f_b = \frac{E b d C}{I}$	$f = f_a + f_b$	$h$	$f_u = 0.05 h$	$f = f_u + f$
—	—	—	—	—	—	—	—	—	KSF	KSF	KSF	FT	KSF	KSF
NORMAL OPERATION	1,285.4	33,870	26.35	29.37	519.76	120,322	HEEL	29.37	2.47	-0.95	1.52	16.0	1.00	2.52
							TOE	29.37	2.47	0.95	3.42	7.5	0.47	3.89
NORMAL * OPERATION WITH ICE	1,285.4	24,838	19.32	27.67	487.30	100,419	HEEL	24.67	2.64	-2.64	0.00	16.0	1.00	1.00
							TOE	27.67	2.64	2.96	5.60	7.5	0.47	6.07
HIGH-WATER CONDITION	1,266.4	32,726	25.84	29.37	519.76	120,322	HEEL	29.37	2.44	-1.04	1.35	17.0	1.06	2.41
							TOE	29.37	2.44	1.04	3.53	7.5	0.47	4.00
NORMAL OPERATION WITH EARTHQUAKE	1,285.4	32,581	25.35	29.37	519.76	120,322	HEEL	29.37	2.47	-1.26	1.21	16.0	1.00	2.21
							TOE	29.37	2.47	1.26	3.73	7.5	0.47	4.20

PAGE 1 OF 1

\* Iterative solution used to determine base properties when less than 100% of base in compression

Figure F8. Maximum base pressure (pier section only), concrete-foundation interface, dam piers 10, 11, 12, 14, 15, and 16, Soo Dam



SUBJECT: DAM PIERS 10, 11, 12, 14, 15, AND 16 - FACTOR OF SAFETY AGAINST SLIDING ALONG FOUNDATION SEAM										COMPUTED BY:		DATE:	
										CHECKED BY:		DATE:	
LOAD CASE	SUM OF VERTICAL FORCES	SUM OF HORIZONTAL FORCES	FRICTION ANGLE	COHESIVE STRENGTH	BASE AREA	STRUT RESISTANCE	SHEAR RESISTANCE	CONCRETE RESISTANCE	TOTAL SLIDING RESISTANCE	FACTOR OF SAFETY AGAINST SLIDING			
	$F_v$ (KIPS)	$F_H$ (KIPS)	$\phi$ (DEGREES)	C (KSF)	A ( $ft^2$ )	$R_s$ (KIPS)	$R_s = F_v \tan \phi$ (KIPS)	$R_c = CA$ (KIPS)	$R = R_s + R_c$ (KIPS)	$FS = \frac{R}{F_H}$			
NORMAL OPERATION	1,285.4	264.9	21.0	0.0	519.76	717.0	493.4	0.0	1,210.4	4.57			
			36.5	0.1	519.76	717.0	951.2	52.0	1,720.2	6.49			
NORMAL OPERATION WITH ICE	1,285.4	867.0	21.0	0.0	486.53	717.0	493.4	0.0	1,210.4	1.80			
			36.5	0.1	486.53	717.0	951.2	48.7	1,716.9	1.98			
HIGH - WATER CONDITION	1,266.4	313.8	21.0	0.0	519.76	717.0	486.1	0.0	1,203.1	3.83			
			36.5	0.1	519.76	717.0	931.1	52.0	1,706.1	5.44			
NORMAL OPERATION WITH EARTHQUAKE	1,285.4	366.9	21.0	0.0	519.76	717.0	493.4	0.0	1,210.4	3.30			
			36.5	0.1	519.76	717.0	951.2	52.0	1,720.2	4.69			

SEE COVER SHEET 1253A  
RECEIVED 1964

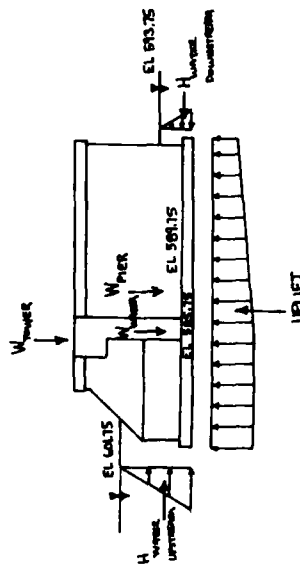
PAGE 1 OF 1

Figure F9. Factor of safety against pier sliding, foundation seam, dam piers 10, 11, 12, 14, 15, and 16, Soo Dam

SUBJECT DAM PIERS 10, 11, 12, 14, 15, AND 16, STABILITY ANALYSIS - NORMAL OPERATION			COMPUTED BY		DATE	
			CHECKED BY		DATE	
ITEM	FORCE COMPUTATIONS	$F_v$ (KIPS)	$F_h$ (KIPS)	ARM (FT)	MOMENT (FT-K)	
$W_{PIER}$	SEE FIGURE F14	1488.0		27.65	41,143	
$W_{TOWER}$	SEE FIGURE F15	179.0		38.83	6,951	
$W_{WATER}$	SEE FIGURE F16	47.8		37.43	1,789	
UPLIFT	SEE FIGURE F17	-429.4		32.44	-13,930	
$H_{TURNER PIER}$	$-(.0455)(\frac{1}{2})[601.75-585.75]^2(8)$ $(.0455)(\frac{1}{2})[593.25-585.75]^2(8)$		-64.0 14.1 -49.9	5.33 2.50	-341 35 -306	
$H_{TURNER GATE}$	$-(.0455)(\frac{1}{2})[601.75-585.75]^2(52.21)$ $(.0455)(\frac{1}{2})[593.25-585.75]^2(52.21)$		-235.0 20.0 -215.0	8.00 6.17	-1,880 103 -1,777	
TOTAL		1,285.4	-264.9		33,870	

PAGE 1 OF 1

Figure F10. Stability analysis summary for normal operation load case, dam piers 10, 11, 12, 14, 15, and 16, Soo Dam



W15 Cont No. 1253A  
Revised 10/80



SUBJECT DAM PIERS 10, 11, 12, 14, 15, AND 16, STABILITY ANALYSIS - HIGH - WATER CONDITION				COMPUTED BY CHECKED BY:		DATE	DATE
ITEM	FORCE COMPUTATIONS	$F_v$ (kips)	$F_h$ (kips)	ARM (ft)	MOMENT (ft-k)		
$W_{PIER}$	SEE FIGURE F14	1,488.0		27.65	41,143		
$W_{TOWER}$	SEE FIGURE F15	179.0		38.83	6,951		
$W_{WATER}$	SEE FIGURE F16	50.2		37.95	1,905		
UPLIFT	SEE FIGURE F17	-450.8		32.62	-14,705		
$H_{WATER PIER}$	$-(0.025)(1/4)[602.75 - 585.75]^2 (8)$ $(0.025)(1/4)[593.35 - 585.75]^2 (8)$		-72.2 14.1 -58.1	5.67 2.50	-409 35 -374		
$H_{WATER GATE}$	$-(0.025)(1/4)[602.75 - 585.75]^2 (52.21)$ $(0.025)(1/4)[593.35 - 585.75]^2 (52.21)$		-275.7 20.0 -255.7	8.33 5.17	-2,297 103 -2,194		
TOTAL		1,266.4	-313.8		32,726		

PAGE 1 OF 1

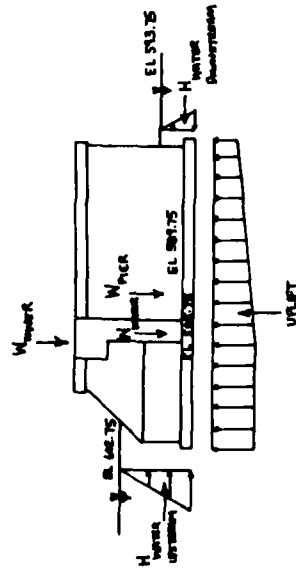


Figure F12. Stability analysis summary for high-water condition, dam piers 10, 11, 12, 14, 15, and 16, Soo Dam

SUBJECT: DAM PIERS 10, 11, 12, 14, 15, AND 16, STABILITY ANALYSIS - NORMAL OPERATION WITH EARTHQUAKE					
COMPUTED BY:		DATE:		CHECKED BY:	
ITEM	FORCE COMPUTATIONS	$F_v$ (KIPS)	$F_h$ (KIPS)	ARM (FT)	MOMENT (FT-K)
NORMAL OPERATION LOADS	SEE FIGURE F10	1,285.4	-264.9		33,870
EARTHQUAKE					
$P_{e1}$	$(0.05)(1488 + 179 + 478)$		-85.7	13.46	-1154
$P_{e2}$	$(\frac{1}{2})(51)(0.05)(16)^2(8)(\frac{1}{1000})$		-3.5	6.40	-22
	$(\frac{1}{2})(51)(0.05)(12)^2(52.21)(\frac{1}{1000})$		-12.8	8.80	-113
			-102.0		-1289
TOTAL		1,285.4	-366.9		32,581

PAGE 1 OF 1

441 Form No. 253A  
FEBRUARY 1964

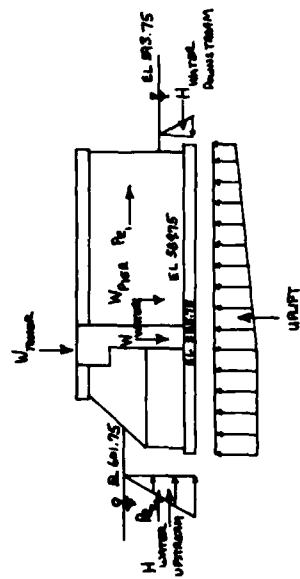


Figure F13. Stability analysis summary for normal operation with earthquake load case, dam piers 10, 11, 12, 14, 15, and 16, Soo Dam

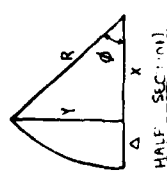
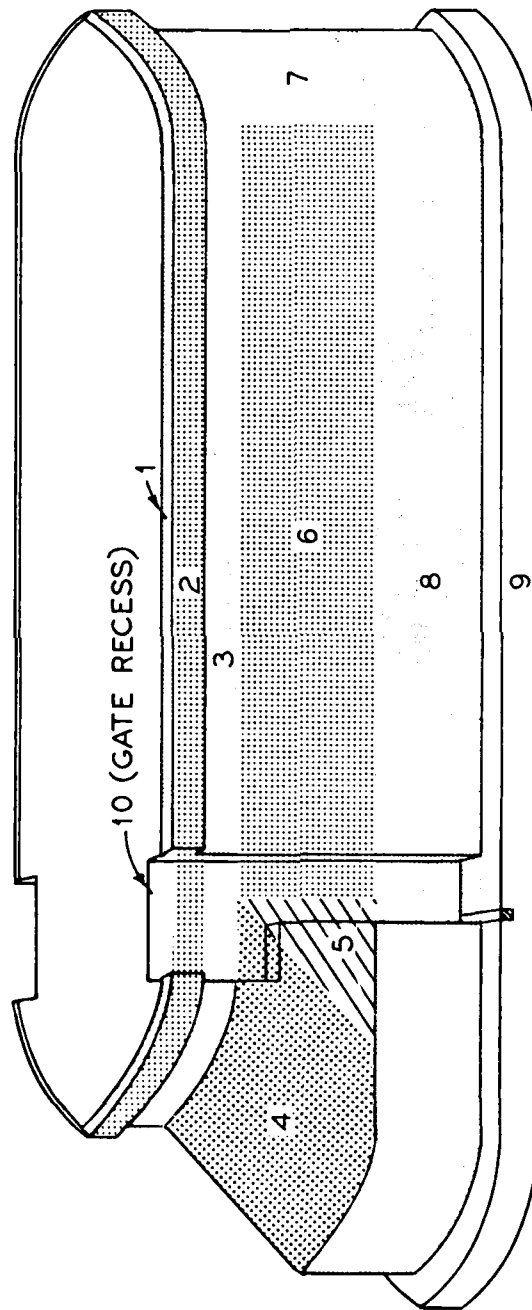
PROJECT	DAM PIERS 10, 11, 12, 14, 15, AND 16 - WEIGHT OF PIER	COMPUTED BY	DATE
		CHECKED BY	DATE
<p><u>GEOMETRY OF PIER NOSE</u></p> <div style="display: flex; justify-content: space-around; align-items: center;">  <div style="text-align: center;"> <p>EL 509.75 - EL 509.75</p> <p>HAIR SECTION</p> <p>GIVEN: R = 14.66 ft    Δ = 5.00 ft</p> <p>X = 14.66 - 5 = 9.66 ft</p> <p>Y = <math>\sqrt{(14.66)^2 - (9.66)^2}</math> = 11.03 ft</p> <p>φ = ArcTan <math>\frac{11.03}{9.66}</math> = 48.79°</p> </div> </div>			
<p>EL 609.63</p> <p>GIVEN: R = 13.91 ft    Δ = 4.25 ft</p> <p>X = 13.91 - 4.25 = 9.66 ft</p> <p>Y = <math>\sqrt{(13.91)^2 - (9.66)^2}</math> = 10.01 ft</p> <p>φ = ArcTan <math>\frac{10.01}{9.66}</math> = 46.02°</p>			
<p>EL 607.75 - 609.42</p> <p>GIVEN: R = 14.16 ft    Δ = 4.50 ft</p> <p>X = 14.16 - 4.50 = 9.66 ft</p> <p>Y = <math>\sqrt{(14.16)^2 - (9.66)^2}</math> = 10.35 ft</p> <p>φ = ArcTan <math>\frac{10.35}{9.66}</math> = 46.97°</p>			
<p>EL 509.75 - 596.75 AND EL 605.75 - 607.75</p> <p>GIVEN: R = 13.60 ft    Δ = 4.00 ft</p> <p>X = 13.60 - 4.00 = 9.66 ft</p> <p>Y = <math>\sqrt{(13.60)^2 - (9.66)^2}</math> = 9.66 ft</p> <p>φ = ArcTan <math>\frac{9.66}{9.66}</math> = 45.00°</p>			

Figure F14. Weight of pier, dam piers 10, 11, 12, 14, 15, and 16, Soo Dam (Sheet 1 of 6)



MONOLITH AREAS

Figure F14. (Sheet 2 of 6)

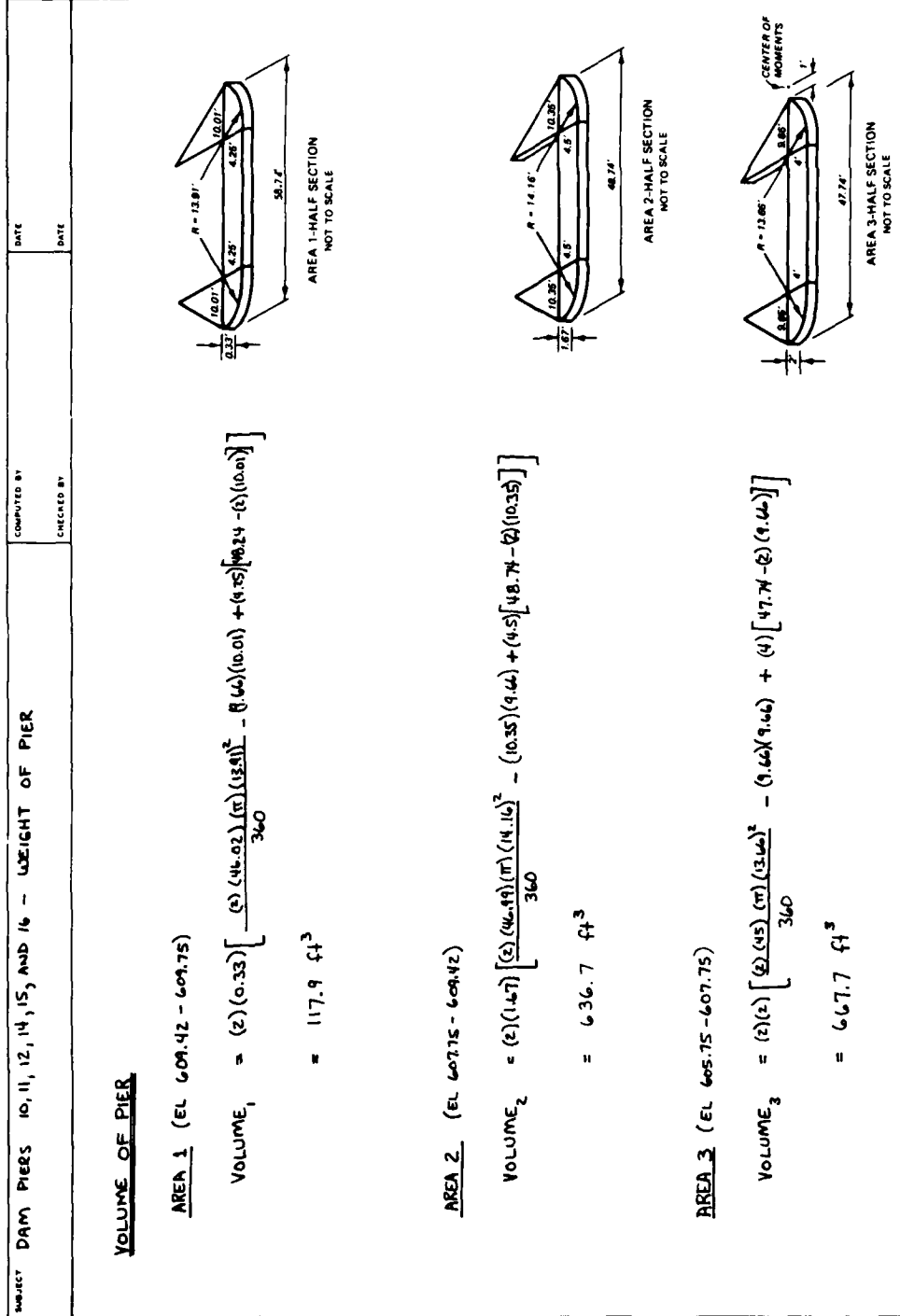


Figure F14. (Sheet 3 of 6)



SUBJECT: DAM PIERS 10, 11, 12, 14, 15, AND 16 - WEIGHT OF PIER	COMPUTED BY:	DATE:
	CHECKED BY:	DATE:

VOLUME OF PIER (CONTINUED)

AREA 4 (EL 596.75 - 605.75)

$$\text{VOLUME}_4 = (9)(9) \left[ \frac{(45)(\pi)(13.66)^2}{360} - \left(\frac{1}{2}\right)(9.66)(9.66) \right]$$

$$= 479.1 \text{ ft}^3$$

AREA 5 (EL 596.75 - 605.75)

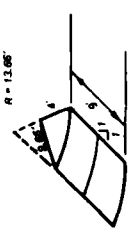
$$\text{VOLUME}_5 = \left(\frac{1}{2}\right)(9)^2(8)$$

$$= 324.0 \text{ ft}^3$$

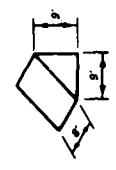
AREA 6 (EL 596.75 - 605.75)

$$\text{VOLUME}_6 = (9)(8)(28.43)$$

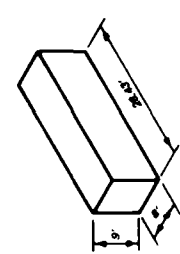
$$= 2047.0 \text{ ft}^3$$



AREA 4 - HALF SECTION  
NOT TO SCALE



AREA 5  
NOT TO SCALE



AREA 6  
NOT TO SCALE

Figure F14. (Sheet 4 of 6)

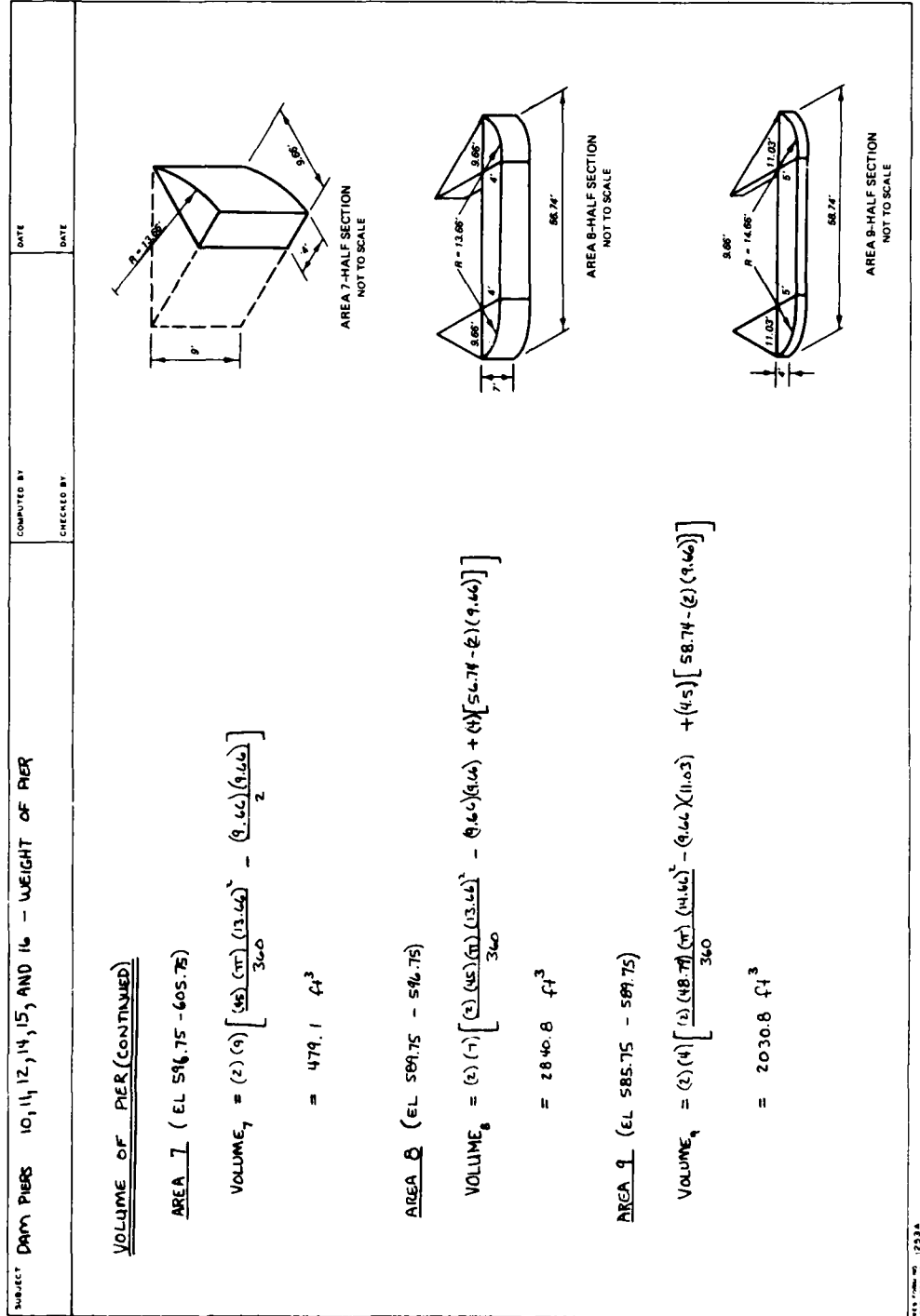
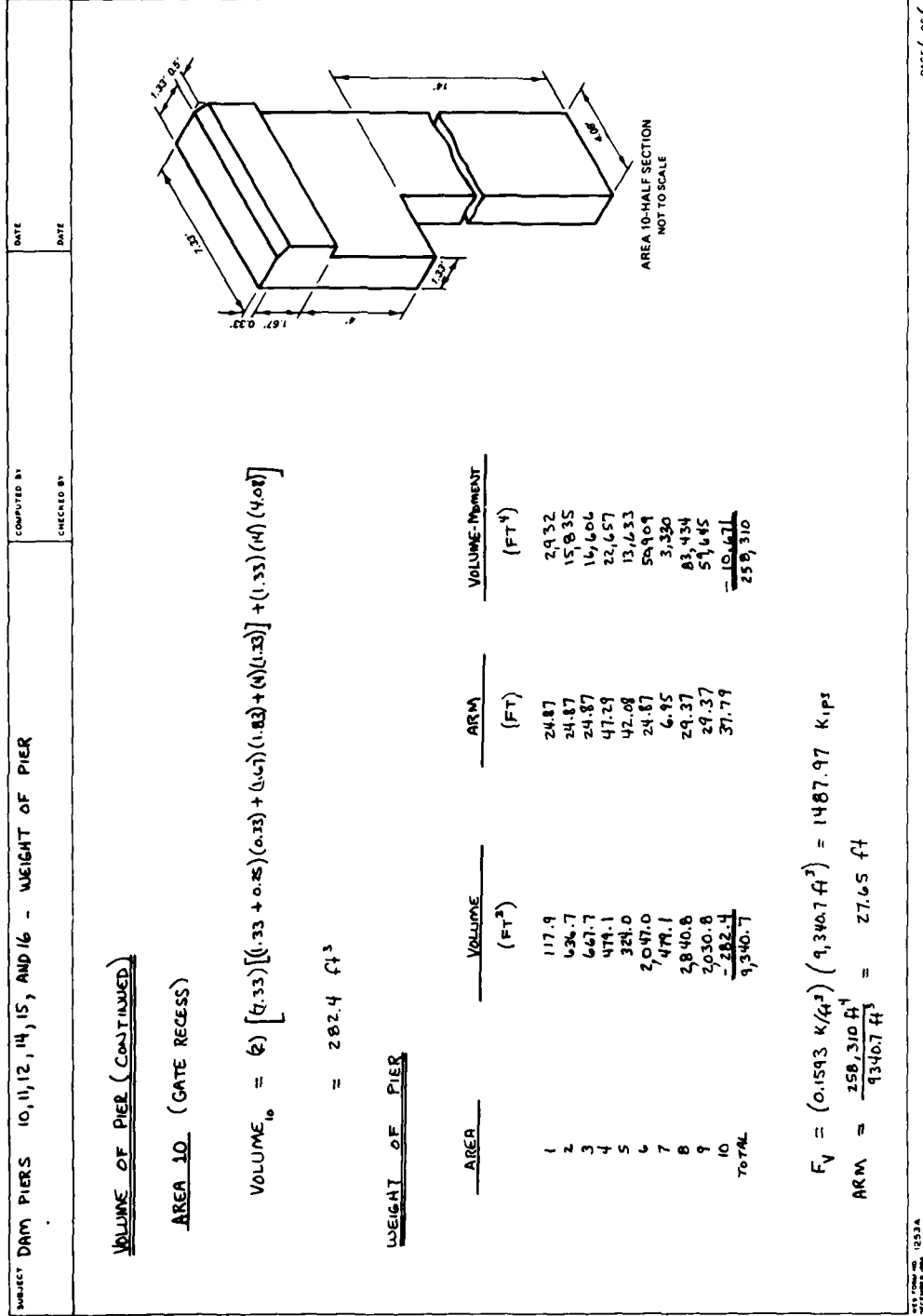


Figure F14. (Sheet 5 of 6)



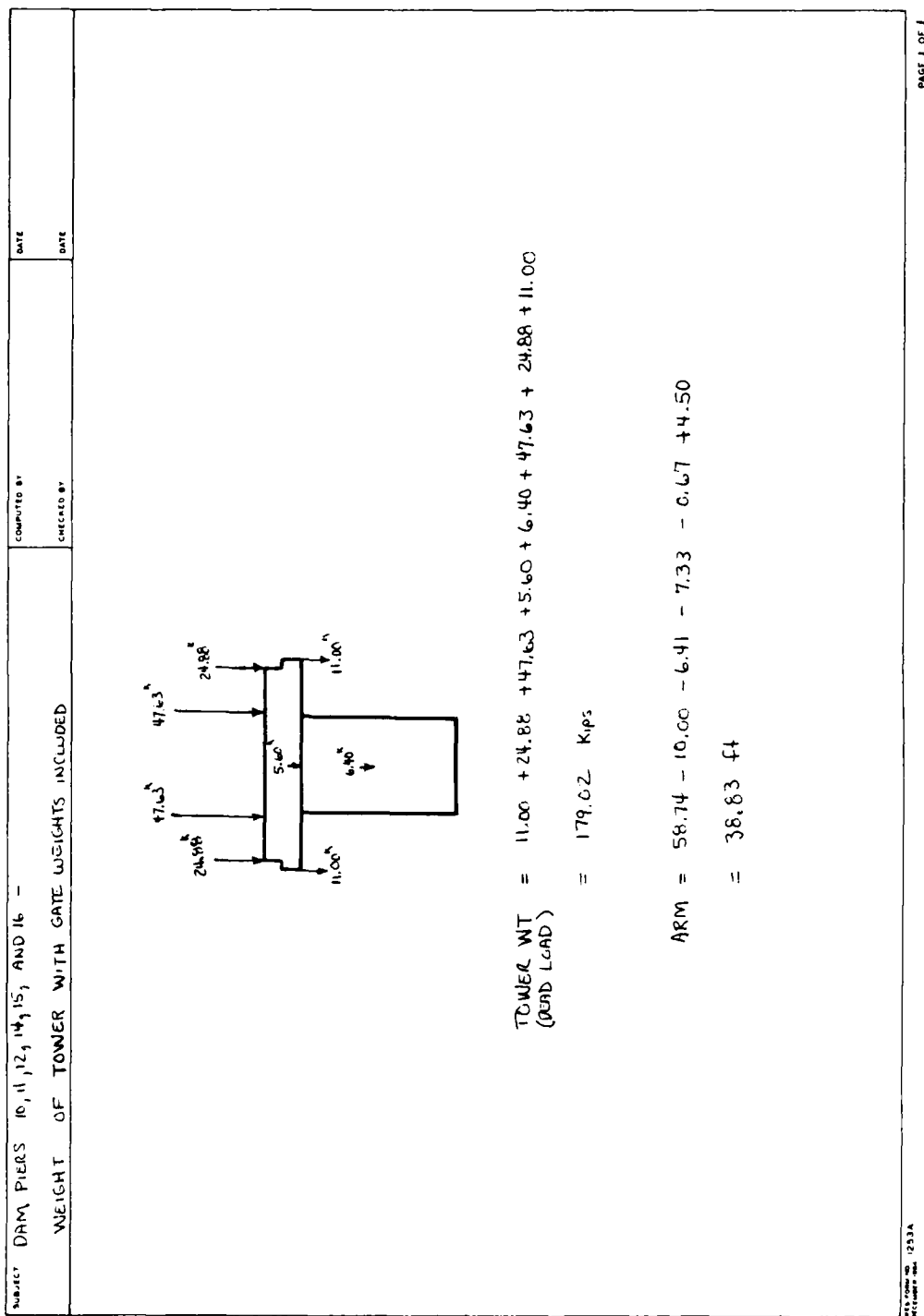


Figure F15. Weight of tower on pier, dam piers 10, 11, 12, 14, 15, and 16, Soo Dam

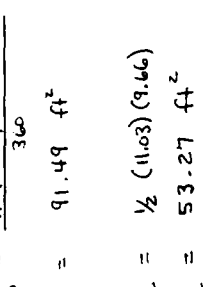
SUBJECT	DAM PIERS 10, 11, 12, 14, 15, AND 16 - WEIGHT OF WATER ON PIERS	COMPUTED BY	DATE
		CHECKED BY	DATE
<p align="center"><u>WEIGHT OF WATER UPSTREAM</u></p> <p align="center"><u>TOTAL AREA AT ELEVATION 509.75</u></p>			
			
<p align="center">HALF SECTION OF UPSTREAM NOSE (TOTAL AREA)</p>			
<p align="center"><math>\tan 2\alpha = \frac{11.03}{9.66}</math></p> <p align="center"><math>\alpha = 24.39^\circ</math></p>			
<p align="center"><math>\bar{X}_{ABO} = \frac{2(14.66) \left[ \sin(24.39^\circ) \right]^2}{3(24.39) (\pi/180)}</math></p> <p align="center"><math>\bar{X}_{ABC} = 3.91 \text{ ft}</math></p>			
<p align="center"><math>\bar{X}_{OBC} = \frac{1}{3} (11.03)</math></p> <p align="center"><math>\bar{X}_{OBC} = 3.68 \text{ ft}</math></p>			
<p align="center"><math>A_{ABO} = \frac{\pi (14.66)^2 (24.39)}{360}</math></p> <p align="center"><math>A_{ABO} = 91.49 \text{ ft}^2</math></p>			
<p align="center"><math>A_{OBC} = \frac{1}{2} (11.03) (9.66)</math></p> <p align="center"><math>A_{OBC} = 53.27 \text{ ft}^2</math></p>			
<p align="center"><math>A_{ABC} = 91.49 - 53.27</math></p> <p align="center"><math>A_{ABC} = 38.22 \text{ ft}^2</math></p>			
<p align="center"><math>\bar{X}_{ABC} = \frac{(91.49)(3.91) - (53.27)(3.68)}{38.22}</math></p> <p align="center"><math>\bar{X}_{ABC} = 4.23 \text{ ft}</math></p>			
<p align="center"><math>ARM_{ABC} = 4.23 + 36.69 + 11.03</math></p> <p align="center"><math>ARM_{ABC} = 51.95 \text{ ft}</math></p> <p align="center"><math>AM_{ABC} = (38.22)(51.95)</math></p> <p align="center"><math>AM_{ABC} = 1985.53 \text{ ft}^3</math></p>			

Figure F16. Weight of water on pier, dam piers 10, 11, 12, 14, 15, and 16, Soo Dam (Sheet 1 of 8)

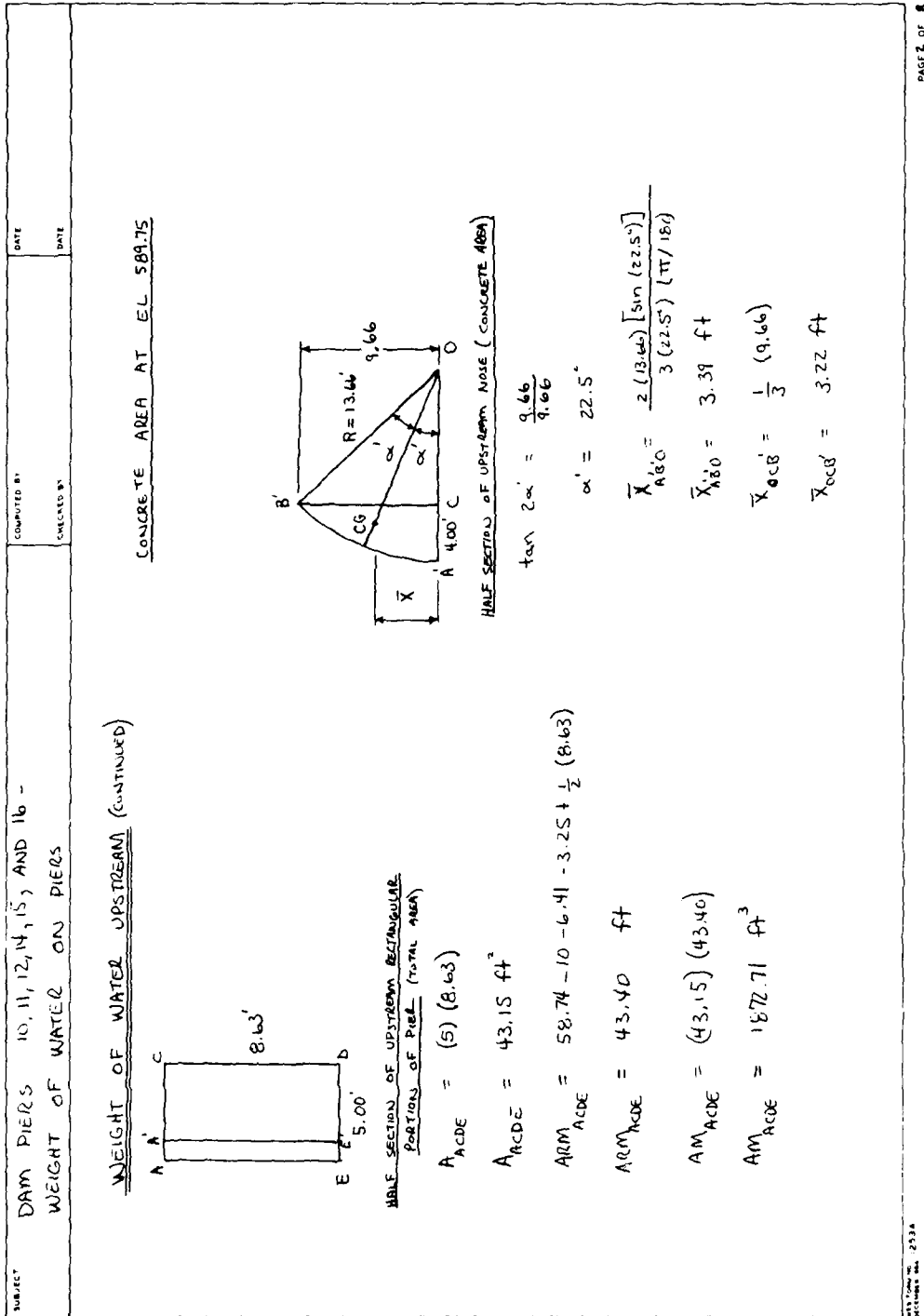


Figure F16. (Sheet 2 of 8)

SUBJECT	DAM PIERS 10, 11, 12, 14, 15, AND 16 - WEIGHT OF WATER ON PIERS	COMPUTED BY	DATE
		CHECKED BY:	DATE

WEIGHT OF WATER UPSTREAM (CONTINUED)

$$A_{AB'O} = \frac{\pi (13.66)^2 (2) (22.5)}{360}$$

$$A_{AB'O} = 73.28 \text{ ft}^2$$

$$A_{OCB'} = \frac{1}{2} (9.66) (9.66)$$

$$A_{OCB'} = 46.66 \text{ ft}^2$$

$$A_{AB'C} = 73.28 - 46.66$$

$$A_{AB'C} = 26.62 \text{ ft}^2$$

$$\bar{X}_{AB'C} = \frac{(73.28) (3.39) - (46.66) (3.22)}{26.62}$$

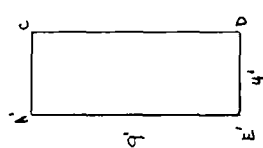
$$\bar{X}_{AB'C} = 3.69 \text{ ft}$$

$$ARM_{AB'C} = 3.69 + 58.74 - 1.00 - 9.66$$

$$ARM_{AB'C} = 51.77 \text{ ft}$$

$$AM_{AB'C} = (26.62) (51.77)$$

$$AM_{AB'C} = 1378.12 \text{ ft}^3$$



HALF SECTION OF UPSTREAM RECTANGULAR  
PORTION OF PIER (CONCRETE AREA)

$$A_{ACDE'} = 4.00 (9.00)$$

$$A_{ACDE'} = 36.00 \text{ ft}^2$$

$$ARM_{ACDE'} = 58.74 - 10.00 - 6.41 - 3.25 + \frac{1}{2} (9.00)$$

$$ARM_{ACDE'} = 43.58 \text{ ft}$$

$$AM_{ACDE'} = (36.00) (43.58)$$

$$AM_{ACDE'} = 1568.88 \text{ ft}^3$$

Figure F16. (Sheet 3 of 8)

SUBJECT	DAM PIERS 10, 11, 12, 14, 15, AND 16 - WEIGHT OF WATER ON PIERS	COMPUTED BY:	DATE:
		CHECKED BY:	DATE:

WEIGHT OF WATER UPSTREAM (CONTINUED)

WEIGHT OF WATER ON UPSTREAM PORTION OF PIER

$$A_u = 2 [38.22 + 43.15 - 26.62 - 36.00]$$

$$A_u = 37.50 \text{ ft}^2$$

$$AM_u = 2 [1985.53 + 1872.71 - 1378.12 - 1568.88]$$

$$AM_u = 1822.48 \text{ ft}^3$$
  

$$ARM_{WATER_u} = \frac{1822.48}{37.50}$$

$$ARM_{WATER_u} = 48.60 \text{ ft}$$
  

$$W_{WATER_u} = (0.0625) (37.50) (601.75 - 581.75)$$

$$W_{WATER_u} = 28.13 \text{ Kips (FOR NORMAL OPERATION)}$$

$$W_{WATER_u} = (0.0625) (37.50) (602.75 - 589.75)$$

$$W_{WATER_u} = 30.47 \text{ Kips (FOR HIGH WATER CONDITION)}$$

Figure F16. (Sheet 4 of 8)



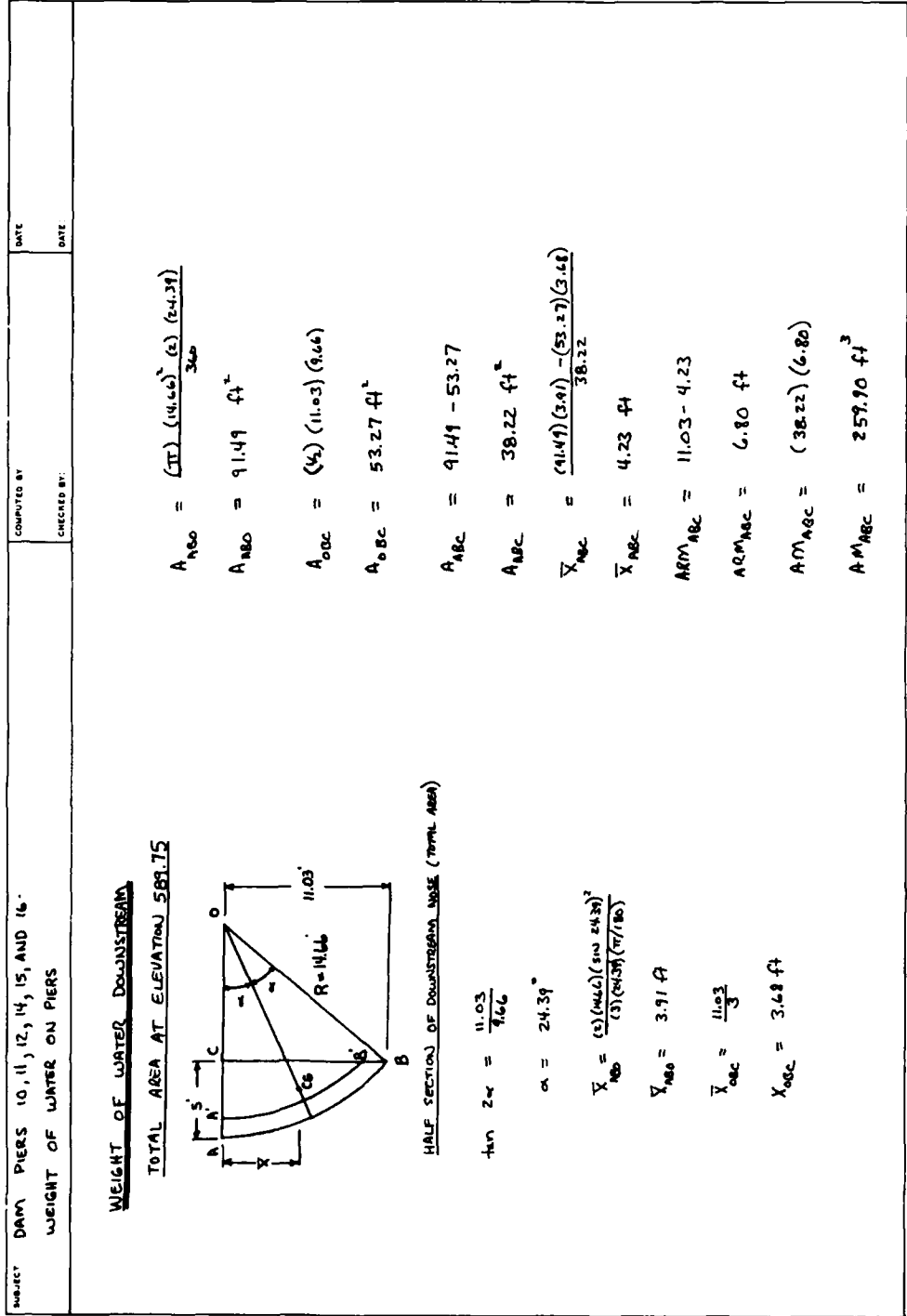


Figure F16. (Sheet 5 of 8)

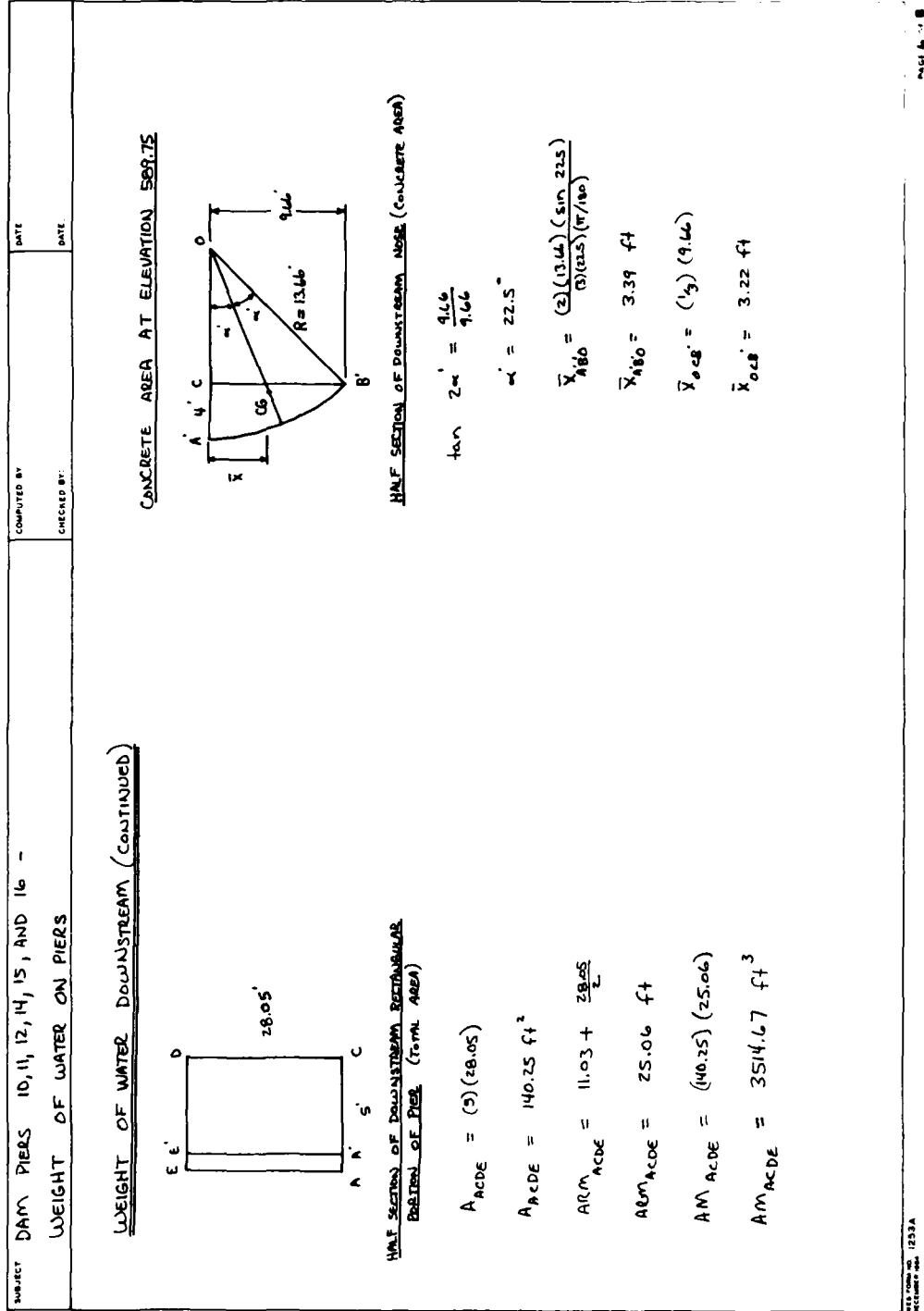


Figure F16. (Sheet 6 of 8)

SUBJECT. DAM PIERS 10, 11, 12, 14, 15, AND 16 -  
WEIGHT OF WATER ON PIERS

DATE:	COMPUTED BY:
DATE:	CHECKED BY:

WEIGHT OF WATER DOWNSTREAM (CONTINUED)

$$A_{AB'D} = \frac{(11)(13.66)^2(2)(22.5)}{360}$$

$$= 73.28 \text{ ft}^2$$

$$A_{occ} = (1/2) (9.66) (9.66)$$

$$A_{OCB'} = 46.66 \text{ ft}^2$$

$\Delta_{\text{air}} = 73.28 - 46.66$

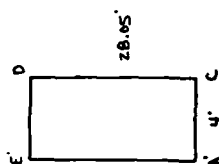
$$= 26.62 \text{ ft}^2$$

$$PRM_{AIC} = 11.03 - \frac{(73.28)(3.39) - (46.66)(5.22)}{2662}$$

$$ARM_{ABC} = 7.34 \text{ ft}$$

$$AM_{Agg} = (26.42)(7.34)$$

$$AM_{\text{air}} = 195.39 \text{ ft}^3$$



HALF SECTION OF DOWNSTREAM RECTANGULAR  
PORTION OF PIER (CONCRETE AREA)

$$A'_{ACDE} = (4)(28.03)$$

$$A'_{\text{cde}} = 112.70 \text{ ft}^2$$

$$ARM' = 11.03 + \frac{28.05}{2}$$

$$ARM_{ACDE} = 25.06 \text{ Ft}$$

$$AM_{ACDE} = (112.2) (25.06)$$

$$AM_{\text{c DE}} = 2811.73 \text{ ft}^3$$

AREA OF WATER IN GATE RECESS

$$A_{\text{recess}} = (4.08)(1.33) = 5.43$$

$$A_{\text{gross}} = 5.43 \text{ ft}^2$$

$$AD_{\text{process}} = (5.43)(37.04) = 201.13 \text{ ft}^3$$

Figure F16. (Sheet 7 of 8)

SUBJECT DAM PIERS 10, 11, 12, 14, 15, AND 16 - WEIGHT OF WATER ON PIERS	COMPUTED BY: _____ CHECKED BY: _____	DATE: _____ DATE: _____
<u>WEIGHT OF WATER DOWNSTREAM (CONTINUED)</u>		
<u>WEIGHT OF WATER ON DOWNSTREAM PORTION OF PIER</u>		
$A_p = 2 [38.22 + 140.25 - 26.62 - 112.20 + 5.43]$	$AM_p = 2 [259.90 + 3514.67 - 195.39 - 2811.73 + 201.13]$	
$A_p = 90.16 \text{ ft}^2$	$AM_p = 1937.16 \text{ ft}^3$	
$ARM_{water, p} = (1937.16 / 90.16)$	$W_{water, p} = (.0625) (90.16) (593.25 - 589.75)$	
$ARM_{water, p} = 21.49 \text{ ft}$	$W_{water, p} = 19.72 \text{ KIPS (FOR NORMAL OPERATION AND HIGH WATER CONDITIONS)}$	
<u>TOTAL WEIGHT OF WATER ON PIER</u>		
<u>NORMAL OPERATION</u>		
$W_{water} = 28.13 + 19.72$	<u>HIGH-WATER CONDITION</u>	
$W_{water} = 47.85 \text{ KIPS}$	$W_{water} = 30.47 + 19.72$	
$ARM_{water} = \frac{(28.13) (49.60) + (19.72) (21.49)}{47.85}$	$ARM_{water} = \frac{(30.47) (49.60) + (19.72) (21.49)}{50.19}$	
$ARM_{water} = 37.43 \text{ ft}$	$ARM_{water} = 37.95 \text{ ft}$	

Figure F16. (Sheet 8 of 8)

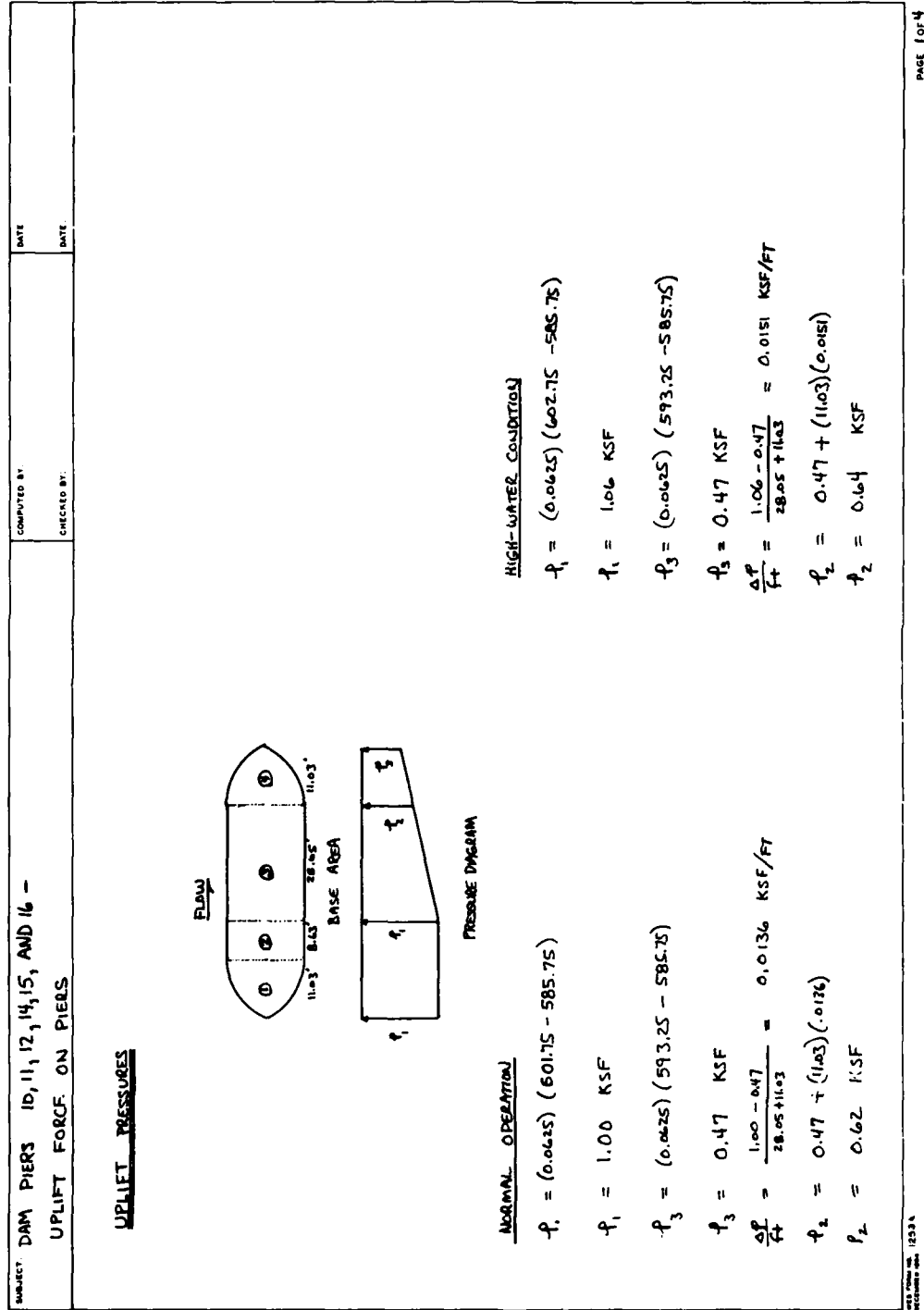


Figure F17. Uplift force on pier, dam piers 10, 11, 12, 14, 15, and 16, Soo Dam (Sheet 1 of 4)

SUBJECT DAM PIERS 10, 11, 12, 14, 15, AND 16 - UPLIFT FORCE ON PIERS	COMPUTED BY: _____ CHECKED BY: _____	DATE: _____ DATE: _____
---	---	----------------------------

UPLIFT FORCE

NORMAL OPERATION

SECTION 1

$$F_v = (2)(38.22)(1.00) = 76.44 \text{ KIPS}$$

$$ARM_v = 58.74 - 11.03 + 4.23 = 51.94 \text{ FT}$$

$$MOMENT_v = (76.44)(51.94) = 3970.29 \text{ FT-K}$$

SECTION 2

$$F_v = (2)(5)(8.63)(1.00) = 86.30 \text{ KIPS}$$

$$ARM_v = 58.74 - 11.03 - (8.63/2) = 43.40 \text{ FT}$$

$$MOMENT_v = (86.30)(43.40) = 3745.42 \text{ FT-K}$$

SECTION 3

UNIFORM LOAD

$$F_v = (2)(5)(28.05)(0.62) = 173.91 \text{ KIPS}$$

$$ARM_v = \frac{28.05}{2} + 11.03 = 25.06 \text{ FT}$$

$$MOMENT_v = (173.91)(25.06) = 4358.18 \text{ FT-K}$$

HIGH - WINTER CONDITION

SECTION 1

$$F_v = (2)(38.22)(1.06) = 81.03 \text{ KIPS}$$

$$ARM_v = 58.74 - 11.03 + 4.23 = 51.94 \text{ FT}$$

$$MOMENT_v = (81.03)(51.94) = 4208.7 \text{ FT-K}$$

SECTION 2

$$F_v = (2)(5)(8.63)(1.06) = 91.48 \text{ KIPS}$$

$$ARM_v = 58.74 - 11.03 - (8.63/2) = 43.40 \text{ FT}$$

$$MOMENT_v = (91.48)(43.40) = 3970.23 \text{ FT-K}$$

SECTION 3

UNIFORM LOAD

$$F_v = (2)(5)(28.05)(0.64) = 179.52 \text{ KIPS}$$

$$ARM_v = \frac{28.05}{2} + 11.03 = 25.06 \text{ FT}$$

$$MOMENT_v = (179.52)(25.06) = 4498.77 \text{ FT-K}$$

Figure F17. (Sheet 2 of 4)

SUBJECT DAM PIERS 10, 11, 12, 14, 15, AND 16 - UPLIFT FORCE ON PIERS	COMPUTED BY:  CHECKED BY:	DATE:  DATE:
--	---------------------------------	--------------------

UPLIFT FORCE (CONTINUED)  
NORMAL OPERATION

SECTION 3

UNIFORMLY VARYING LOAD

$$F_{uV} = \left(\frac{1}{2}\right) (2) (5) (28.05) (1.00 - 0.42) = 53.30 \text{ KIPS}$$

$$ARM_{uV} = \left(\frac{2}{3}\right) (28.05) + 11.03 = 29.73 \text{ FT}$$

$$MOMENT_{uV} = (53.30) (29.73) = 1584.61 \text{ FT-K}$$

SECTION 4

UNIFORM LOAD

$$F_{uV} = (2) (38.22) (0.47) = 35.93 \text{ KIPS}$$

$$ARM_{uV} = 11.03 - 4.23 = 6.80 \text{ FT}$$

$$MOMENT_{uV} = (35.93) (6.80) = 244.32 \text{ FT-K}$$

UNIFORMLY VARYING LOAD

$$F_{uV} = 3.52 \text{ KIPS}^*$$

$$ARM_{uV} = 7.88 \text{ FT}$$

$$MOMENT_{uV} = (3.52) (7.88) = 27.74 \text{ FT-K}$$

HIGH - WATER CONDITION

SECTION 3

UNIFORMLY VARYING LOADS

$$F_{uV} = \left(\frac{1}{2}\right) (2) (5) (28.05) (1.06 - 0.64) = 58.90 \text{ KIPS}$$

$$ARM_{uV} = \left(\frac{2}{3}\right) (28.05) + 11.03 = 29.73 \text{ FT}$$

$$MOMENT_{uV} = (58.90) (29.73) = 1751.10 \text{ FT-K}$$

SECTION 4

UNIFORM LOAD

$$F_{uV} = (2) (38.22) (0.47) = 35.93 \text{ KIPS}$$

$$ARM_{uV} = 11.03 - 4.23 = 6.80 \text{ FT}$$

$$MOMENT_{uV} = (35.93) (6.80) = 244.32 \text{ FT-K}$$

UNIFORMLY VARYING LOAD

$$F_{uV} = 3.94 \text{ KIPS}^*$$

$$ARM_{uV} = 7.88 \text{ FT}$$

$$MOMENT_{uV} = (3.94) (7.88) = 31.05 \text{ FT-K}$$

\* Iterative solution used to solve force for uniformly varying load acting on nose portion of pier base

Figure F17. (Sheet 3 of 4)





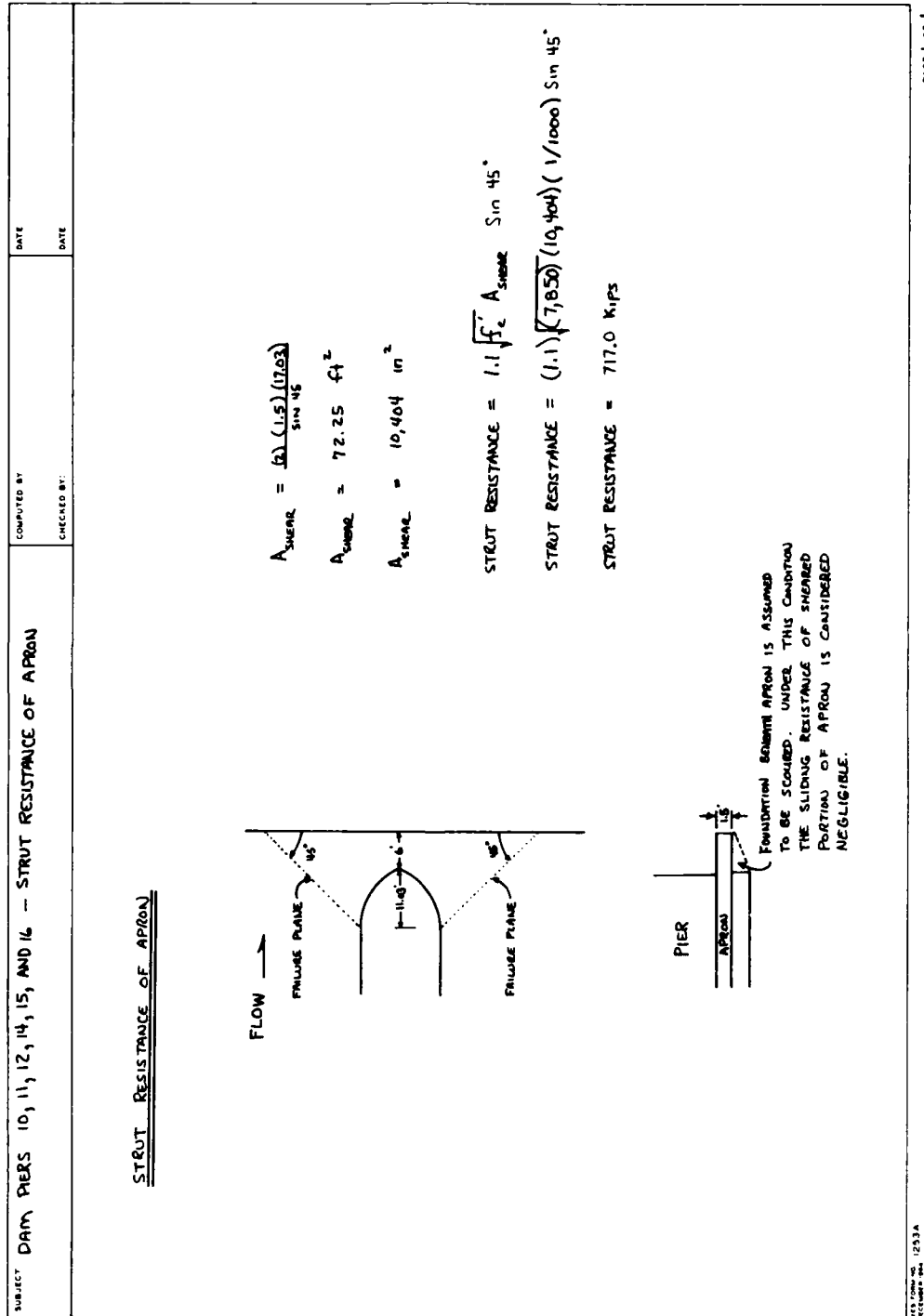


Figure F18. Strut resistance of apron, dam piers 10, 11, 12, 14, 15, and 16, Soo Dam

SUBJECT DAM PIERS 10, 11, 12, 14, 15 AND 16 - SLIDING STABILITY ALONG SEAM AT ELEVATION 585.75

COMPUTED BY: DATE: CHECKED BY: DATE:

SLIDING STABILITY - NORMAL OPERATION

UPLIFT

ITEM	FORCE COMPUTATIONS	$F_v$ (KIPS)	$F_h$ (KIPS)
$W_{PIER}$	SEE FIGURE F14	1,488.0	
$W_{TOWER}$	SEE FIGURE F15	174.0	
$W_{WATER}$	$(.1593)(1.5)(53.71)(60.21)$ $-(.1893)(1.5)(43.15+40.22)(2)$	772.7	
$W_{UPLIFT}$	$(.1943)(588.25 - 585.75)(53.71)(60.21)$ $-(.1563)(2.5)(43.15+40.22)(2)$	-105.9	
$W_{TOTAL}$		666.8	
$W_{TOTAL}$		1,243.6	
$W_{TOTAL}$		-173.2	
$W_{TOTAL}$		1,090.4	
$W_{TOTAL}$	WEIGHT OF WATER (SEE FIGURE F12)	47.8	
$W_{TOTAL}$	$(.0425)(593.75-582.75)(53.71)(60.21)$ $-(.0425)(593.75-582.75)(43.15+40.22)(2)$ $(.0425)(601.75-593.25)(9)(60.21)$ $-(.0425)(601.75-593.25)(4)(10)$	707.4	
$W_{TOTAL}$		-97.0	
$W_{TOTAL}$		287.9	
$W_{TOTAL}$		-47.8	
$W_{TOTAL}$		898.3	
UPLIFT	$-(.0425)(1/2)(601.75+593.25-445.5)(53.71)(60.21)$ $-(.0425)(601.75-585.75)(38.22)(2)$	-2,374.9	
$H_{WATER}$	$-(.0425)(1/2)(601.75-585.75)^2(60.21)$ $(.0425)(1/2)(593.25-585.75)^2(60.21)$	-76.4	
$H_{WATER}$		-2,451.3	
$H_{WATER}$		-481.7	
$H_{WATER}$		105.8	
$H_{WATER}$		-375.9	
TOTAL		1,871.2	-375.9

PAGE 1 OF 8

Figure F19. Sliding stability summary for pier and apron section along foundation seams, dam piers 10, 11, 12, 14, 15, and 16, Soo Dam (Sheet 1 of 8)

SUBJECT	COMPUTED BY	DATE
DAM PIERS 10, 11, 12, 14, 15 AND 16 - SLIDING ALONG SEAM AT ELEVATION 585.75		
<p><u>SUM OF FORCES</u></p> <p><u>NORMAL OPERATION</u></p> <p><math>F_v = 1,871.2 \text{ KIPS}</math></p> <p><math>F_H = 375.9 \text{ KIPS}</math></p> <p><u>NORMAL OPERATION WITH ICE</u></p> <p><math>F_v = 1,871.2 \text{ KIPS}</math></p> <p><math>F_H = 375.9 + (2)(5)(60.21) = 978.0 \text{ KIPS}</math></p> <p><u>HIGH WATER CONDITION</u></p> <p><math>W_{\text{WATER}} = 898.3 + 50.2 - 47.8 + (0.0625)(9)(60.21 - 10) = 928.9 \text{ KIPS}</math></p> <p><math>\text{UPLIFT} = (0.0625) \left[ \left( \frac{1}{2} \right) (602.75 + 513.25 - 42)(585.75) \right] + (602.75 - 585.75)(2)(38.22) = 2,557.1 \text{ KIPS}</math></p> <p><math>F_v = W_{\text{PIER}} + W_{\text{TOWER}} + W_{\text{APRON}} + W_{\text{FOUNDATION}} + W_{\text{WATER}} - \text{UPLIFT}</math></p> <p><math>F_v = 1,488 + 179 + 666.8 + 1,090.4 + 928.9 - 2,557.1 = 1,796.0 \text{ KIPS}</math></p> <p><math>F_H = (0.0625) \left( \frac{1}{2} \right) (60.21) \left[ (602.75 - 585.75)^2 - (593.45 - 585.75)^2 \right] = 437.9 \text{ KIPS}</math></p> <p><u>NORMAL OPERATION WITH EARTHQUAKE</u></p> <p><math>F_v = 1,871.2 \text{ KIPS}</math></p> <p><math>F_H = 375.9 + (1.05) \left[ 1485 + 174 + 666.8 + 1,090.4 \right] + \left( \frac{1}{2} \right) (51)(.05) \left( \frac{1}{1000} \right) (16)^2 (8) = 550.6 \text{ KIPS}</math></p>		

Figure F19. (Sheet 2 of 8)

SUBJECT DAM PIERS 10,11,12,14,15 AND 16 - SLIDING STABILITY ALONG SEAM AT ELEVATION 585.75										COMPUTED BY		DATE	
										CHECKED BY		DATE	
LOAD CASE	SUM OF VERTICAL FORCES	SUM OF HORIZONTAL FORCES	FRICTION ANGLE (DEGREES)	CONCRETE STRENGTH	AREA OF SLIDING PLANE	STILT RESISTANCE	SHEAR RESISTANCE	COHESIVE RESISTANCE	TOTAL SLIDING RESISTANCE	FACTOR OF SAFETY AGAINST SLIDING			
	$F_v$ (KIPS)	$F_H$ (KIPS)	$\phi$ (DEGREES)	C (KSE)	$A$ ( $FT^2$ )	$R_s$ (KIPS)	$R_s = F_v \tan \phi$ (KIPS)	$R_c = CA$ (KIPS)	$R = R_s + R_c$ (KIPS)	$F.S. = \frac{R}{F_H}$			
NORMAL OPERATION	1,871.2	375.9	36.5	0.1	2234	0	1,384.6	323.4	1,708.0	4.54			
			26.0	0.0			912.6	0.0	912.6	2.43			
			34.0	0.2			1,262.1	646.8	1,908.9	5.08			
			27.9	0.0			990.8	0.0	990.8	2.64			
			31.4	2.8			1,142.2	9,055.2	10,197.4	27.13			
NORMAL OPERATION WITH ICE			21.0	0.0			718.3	0.0	718.3	1.91			
	1,871.2	978.0	36.5	0.1	3234	0	1,384.6	323.4	1,708.0	1.75			
			26.0	0.0			912.6	0.0	912.6	0.93			
			34.0	0.2			1,262.1	646.8	1,908.9	1.95			
			27.9	0.0			990.8	0.0	990.8	1.01			
HIGH WATER CONDITION			31.4	2.8			1,142.2	9,055.2	10,197.4	10.43			
			21.0	0.0			718.3	0.0	718.3	0.73			
	1,796.0	437.9	36.5	0.1	3234	0	1,329.0	323.4	1,652.4	3.77			
			26.0	0.0			876.0	0.0	876.0	2.00			
			34.0	0.2			1,211.4	646.8	1858.2	4.24			
			27.9	0.0			450.9	0.0	450.9	2.17			

11-10-60 1253A  
RECEIVED

PAGE 3 OF 8

Figure F19. (Sheet 3 of 8)

SUBJECT: DAM PIERS 10,11,12,14,15 AND 16 - SLIDING STABILITY ALONG SEAM AT ELEVATION 585.75										
COMPUTED BY					DATE					
CHECKED BY:					DATE					
LOAD CASE	SUM OF VERTICAL FORCES	SUM OF HORIZONTAL FORCES	FRICTION ANGLE (DEGREES)	COHESIVE STRENGTH (KSF)	AREA OF SLIDING PLANE	STRUT RESISTANCE (KIPS)	SHEAR RESISTANCE (KIPS)	COHESIVE RESISTANCE (KIPS)	TOTAL SLIDING RESISTANCE (KIPS)	FACTOR OF SAFETY AGAINST SLIDING
	$F_v$ (KIPS)	$F_H$ (KIPS)	$\phi$ (DEGREES)	C (KSF)	A (FT <sup>2</sup> )	$R_s$ (KIPS)	$R_s = F_v \tan \phi$ (KIPS)	$R_c = CA$ (KIPS)	$R = R_s + R_c$ (KIPS)	$F.S. = \frac{R}{F_H}$
HIGH WATER CONDITION	1,746.0	437.9	31.4	2.8	3234	0	1,096.3	9,055.2	10,151.5	23.18
			21.0	0.0			689.4	0.0	689.4	1.57
NORMAL OPERATION WITH EARTHQUAKE	1,871.2	550.6	34.5	0.1	3234	0	1,384.6	323.4	1,708.0	3.10
			26.0	0.0			912.6	0.0	912.6	1.66
			34.0	0.2			1,262.1	646.8	1,908.9	3.47
			27.9	0.0			990.8	0.0	990.8	1.80
			31.4	2.8			1,142.2	9,055.2	10,197.4	18.52
			21.0	0.0			718.3	0.0	718.3	1.30

WES FORM NO. 1253A  
DECEMBER 1966

PAGE 4 OF 5

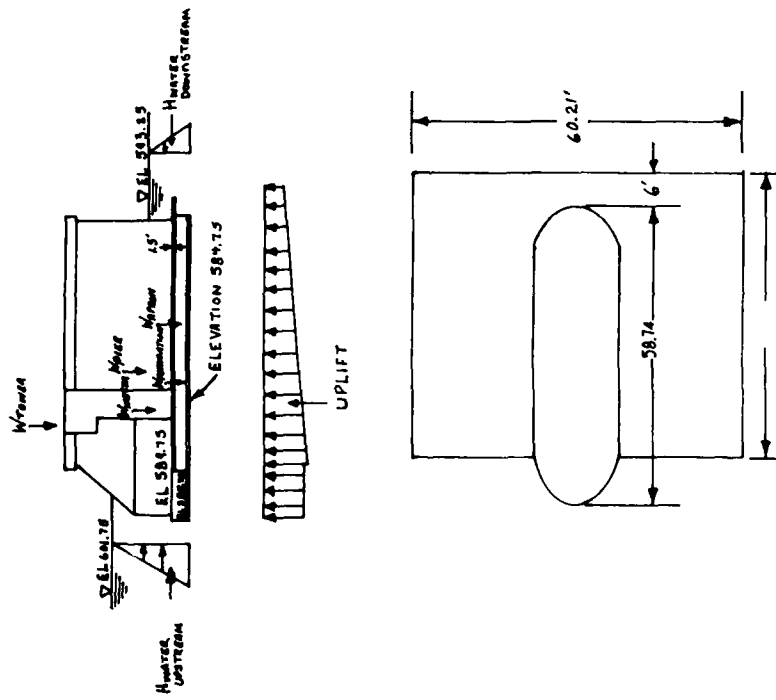
Figure F19. (Sheet 4 of 8)

SUBJECT DAM PIERS 10, 11, 12, 14, 15 AND 16 - SLIDING STABILITY ALONG SEAM AT ELEVATION 584.75		COMPUTED BY:	DATE:		
		CHECKED BY:	DATE:		
ITEM	FORCE COMPUTATIONS	$F_v$ (KIPS)	$F_h$ (KIPS)		
$N_{PIER}$	SEE FIGURE F14	1,488.0			
$W_{TOWER}$	SEE FIGURE F15	174.0			
$W_{WATER}$	$(.1593)(1.5)(63.71)(60.21)$ $- (.1593)(1.5)(43.51)(40.25 + 38.22)(2)$	772.7 -105.9			
$W_{FOUNDATION}$	$(.1593)(588.25 - 584.75)(53.71)(60.21)$ $- (.1593)(62.5)(43.15 + 40.25 + 38.22)(2)$	1,709.1 -173.2			
$W_{WATER}$	WEIGHT OF WATER ON PIER (SEE FIGURE F16) $(.0425)(593.25 - 584.75)(53.71)(60.21)$ $- (.0425)(593.25 - 584.75)(43.15 + 40.25 + 38.22)(2)$ $(.0425)(601.75 - 593.25)(41)(60.21)$ $- (.0425)(601.75 - 593.25)(41)(10)$	47.8 707.4 -47.0 287.9 -47.8			
$UPLIFT$	$(.0425)(43)(601.75 - 584.75)(53.71)(60.21)$ $- (.0425)(601.75 - 584.75)(38.22)(2)$	898.3 -2,517.0 -16.4 -2,653.4			
$H_{WATER}$	$-(.0425)(1/2)(601.75 - 584.75)(60.21)$ $(.0425)(1/2)(593.25 - 584.75)(60.21)$		- 543.8 135.9 - 407.9		
TOTAL		2,174.6	- 407.9		

PAGE 5 OF 8

Figure F19. (Sheet 5 of 8)

SLIDING STABILITY-NORMAL OPERATION



SEE DAM NO. 1233A  
DECEMBER 1964

SUBJECT	DAM PIERS 10, 11, 12, 14, 15 AND 16 - SLIDING STABILITY ALONG SEAM AT ELEVATION 584.75	COMPUTED BY	DATE
		CHECKED BY:	DATE

SUM OF FORCES

NORMAL OPERATION

$F_V = 2,174.6 \text{ KIPS}$

$F_H = 407.9 \text{ KIPS}$

NORMAL OPERATION WITH ICE

$F_V = 2,174.6 \text{ KIPS}$

$F_H = 407.9 + (2)(5)(60.21) = 1010.0 \text{ KIPS}$

HIGH WATER CONDITION

$W_{\text{WATER}} = 898.3 + 50.2 - 47.8 + (.0625)(4)(60.21 - 10) = 928.9 \text{ KIPS}$

$UPLIFT = (.0625)[(1/2)(602.75 + 593.25 - 0)(584.75)](53.7)(60.21) + (602.75 - 584.75)(2)(38.22) = 2,764.0 \text{ KIPS}$

$F_V = W_{\text{PIER}} + W_{\text{TOWER}} + W_{\text{APRON}} + W_{\text{FOUNDATION}} + W_{\text{WATER}} - UPLIFT$

$F_V = 1,488 + 179 + 646.8 + 1,595.9 + 928.9 - 2,764.0 = 2,094.6 \text{ KIPS}$

$F_H = (.0625)(1/2)(60.21)[(602.75 - 584.75)^2 - (593.25 - 584.75)^2] = 473.7 \text{ KIPS}$

NORMAL OPERATION WITH EARTHQUAKE

$F_V = 2,174.6 \text{ KIPS}$

$F_H = 407.9 + (.05)(1488 + 179 + 646.8 + 1595.9) + (1/2)(51)(.05)(1/1,000)(60)^2(8) = 607.9 \text{ KIPS}$

111 1253A

PAGE 6 OF 8

Figure F19. (Sheet 6 of 8)

SUBJECT DAM PIERS 10, 11, 12, 14, 15 AND 16 - SLIDING STABILITY ALONG SCAM AT ELEVATION 584.75										COMPUTED BY		DATE	
										CHECKED BY		DATE	
LOAD CASE	SUM OF VERTICAL FORCES	SUM OF HORIZONTAL FORCES	FRICTION ANGLE	CONSSIVE STRENGTH	AREA OF SLIDING PLANE	STRUT RESISTANCE	SHEAR RESISTANCE	CONSSIVE RESISTANCE	TOTAL SLIDING RESISTANCE	FACTOR OF SAFETY AGAINST SLIDING			
	$F_v$ (KIPS)	$F_h$ (KIPS)	$\phi$ (DEGREES)	C (NSF)	A (FT <sup>2</sup> )	$R_s$ (KIPS)	$R_s = F_v \tan \phi$ (KIPS)	$R_c = CA$	$R = R_s + R_c$ (KIPS)	$F.S. = \frac{R}{F_h}$			
NORMAL OPERATION	2,174.6	407.9	36.5	0.1	3234	0	1,609.1	323.4	1,932.5	4.74			
			26.0	0.0			1,060.6	0.0	1,060.6	2.60			
			34.0	0.2			1,466.8	646.8	2,113.6	5.18			
			27.9	0.0			1,151.4	0.0	1,151.4	2.82			
			31.4	2.8			1,327.4	9,055.2	10,382.6	25.45			
NORMAL OPERATION WITH ICE	2,174.6	1010.0	36.5	0.1	3234	0	1,609.1	323.4	1,932.5	1.91			
			26.0	0.0			1,060.6	0.0	1,060.6	1.05			
			34.0	0.2			1,466.8	646.8	2,113.6	2.09			
			27.9	0.0			1,151.4	0.0	1,151.4	1.14			
			31.4	2.8			1,327.4	9,056.2	10,382.6	10.28			
HIGH WATER CONDITION	2,094.6	473.7	36.5	0.1	3234	0	1,549.9	323.4	1,873.3	3.95			
			26.0	0.0			1,021.6	0.0	1,021.6	2.16			
			34.0	0.2			1,412.8	646.8	2,059.6	4.35			
			27.9	0.0			1,109.0	0.0	1,109.0	2.34			

115 FORM NO. 1253-A  
MAY 1964 EDITION

PAGE 7 OF 8

Figure F19. (Sheet 7 of 8)





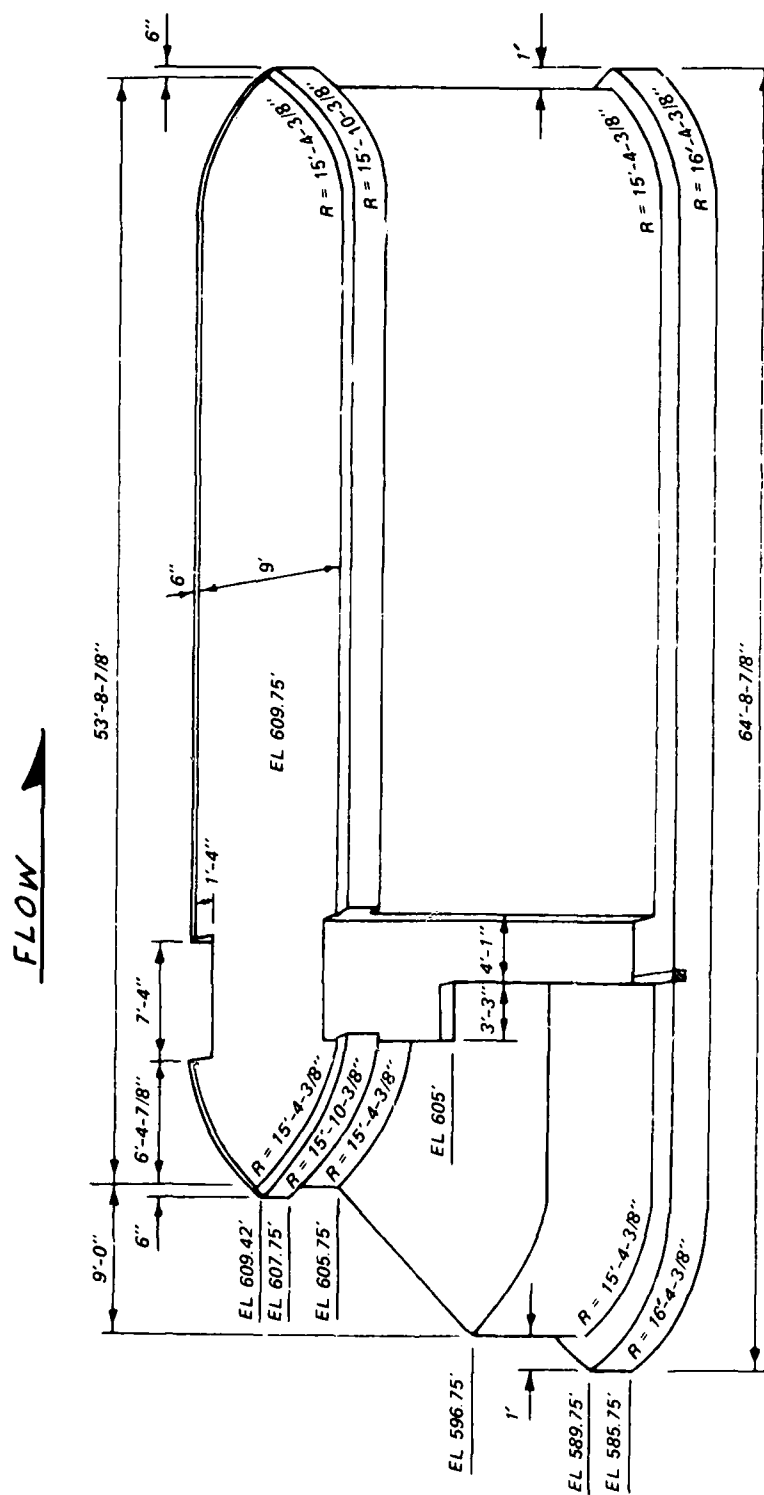


Figure F20. Typical geometry for dam piers 9 and 13, Soo Dam

SUBJECT DAM PIERS 9 AND 13 - FACTOR OF SAFETY AGAINST SLIDING ALONG CONCRETE - FOUNDATION INTERFACE		COMPUTED BY		DATE					
LOAD CASE		CHECKED BY		DATE					
SUM OF VERTICAL FORCES	SUM OF HORIZONTAL FORCES	FRICTION ANGLE	CONESIVE STRENGTH	BASE AREA	STRUT RESISTANCE	SHEAR RESISTANCE	CONESIVE RESISTANCE	TOTAL SLIDING RESISTANCE	FACTOR OF SAFETY AGAINST SLIDING
$F_v$ (KIPS)	$F_H$ (KIPS)	$\phi$ (DEGREES)	C (KSF)	A (FT <sup>2</sup> )	$R_s$ (KIPS)	$R_s = F_v \tan \phi$ (KIPS)	$R_c = CA$ (KIPS)	$R = R_s + R_c$ (KIPS)	$FS = \frac{R}{F_H}$
1,573.3	269.1	32.1	0	629.18	515.3	986.9	0	1,502.2	6.38
1,573.3	876.2	32.1	0	629.18	515.3	986.9	0	1,502.2	1.96
1,549.8	331.7	32.1	0	629.18	515.3	972.2	0	1,487.5	5.13
1,573.3	310.2	32.1	0	629.18	515.3	986.9	0	1,502.2	4.40
NORMAL OPERATION WITH EARTHQUAKE									

WES CONCRETE 253A  
RECEIVED 1964

PAGE 1 OF 1

Figure F21. Factor of safety against pier sliding, concrete-foundation interface, dam piers 9 and 13, Soo Dam

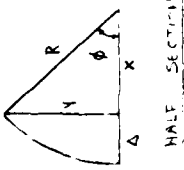
SUBJECT DAM PIERS 9 AND 13 - FACTOR OF SAFETY AGAINST SLIDING ALONG FOUNDATION SEAM									
COMPUTED BY					DATE		CHECKED BY		
LOAD CASE	SUM OF VERTICAL FORCES $F_v$ (KIPS)	SUM OF HORIZONTAL FORCES $F_H$ (KIPS)	FRICTION ANGLE $\phi$ (DEGREES)	COHESIVE STRENGTH $C$ (KSF)	BASE AREA $A$ (FT <sup>2</sup> )	STRIUT RESISTANCE $R_s$ (KIPS)	SHEAR RESISTANCE $R_f = F_v \tan \phi$ (KIPS)	COHESIVE RESISTANCE $R_c = CA$ (KIPS)	FACT OF SAFETY AGAINST SLIDING $FS = \frac{R}{F_H}$
NORMAL OPERATION	1,573.3	269.1	21.0	0.0	629.18	515.3	653.9	0.0	4.16
			36.5	0.1	629.18	515.3	1,164.2	62.9	6.47
NORMAL OPERATION WITH ICE	1,573.3	876.2	21.0	0.0	629.18	515.3	653.9	0.0	1.28
			36.5	0.1	629.18	515.3	1,164.2	62.9	1.99
HIGH - WATER CONDITION	1,549.8	331.7	21.0	0.0	629.18	515.3	594.9	0.0	3.35
			36.5	0.1	629.18	515.3	1,146.8	62.9	5.20
NORMAL OPERATION WITH EARTHQUAKE	1,573.3	390.2	21.0	0.0	629.18	515.3	653.9	0.0	2.87
			36.5	0.1	629.18	515.3	1,164.2	62.9	4.47

Figure F22. Factor of safety against pier sliding, foundation seam, dam piers 9 and 13, Soo Dam

SUBJECT	DAM PIERS : AUL 13 - WEIGHT OF PIER	COMPUTED BY	DATE
		CHECKED BY	DATE

EL 585.75 - EL 589.75



HALF SECTION

GIVEN:  $R = 16.36 \text{ ft}$      $\Delta = 5.50 \text{ ft}$

$X = 16.36 - 5.50 = 10.86$

$Y = \sqrt{(16.36)^2 - (10.86)^2} = 12.24 \text{ ft}$

$\phi = \text{ARCTAN } \frac{12.24}{10.86} = 48.42^\circ$

EL 589.75 - 596.75 AND EL 605.75 - 607.75

GIVEN:  $R = 15.36 \text{ ft}$      $\Delta = 4.50 \text{ ft}$

$X = 15.36 - 4.50 = 10.86 \text{ ft}$

$Y = \sqrt{(15.36)^2 - (10.86)^2} = 10.86 \text{ ft}$

$\phi = \text{ARCTAN } \frac{10.86}{10.86} = 45.00^\circ$

EL 609.63

GIVEN:  $R = 15.61 \text{ ft}$      $\Delta = 4.75 \text{ ft}$

$X = 15.61 - 4.75 = 10.86 \text{ ft}$

$Y = \sqrt{(15.61)^2 - (10.86)^2} = 11.21 \text{ ft}$

$\phi = \text{ARCTAN } \frac{11.21}{10.86} = 45.91^\circ$

EL 607.75 - 609.42

GIVEN:  $R = 15.86 \text{ ft}$      $\Delta = 5.00 \text{ ft}$

$X = 15.86 - 5.00 = 10.86 \text{ ft}$

$Y = \sqrt{(15.86)^2 - (10.86)^2} = 11.56 \text{ ft}$

$\phi = \text{ARCTAN } \frac{11.56}{10.86} = 46.79^\circ$

Figure F23. Weight of pier, dam piers 9 and 13, Soo Dam (Sheet 1 of 6)

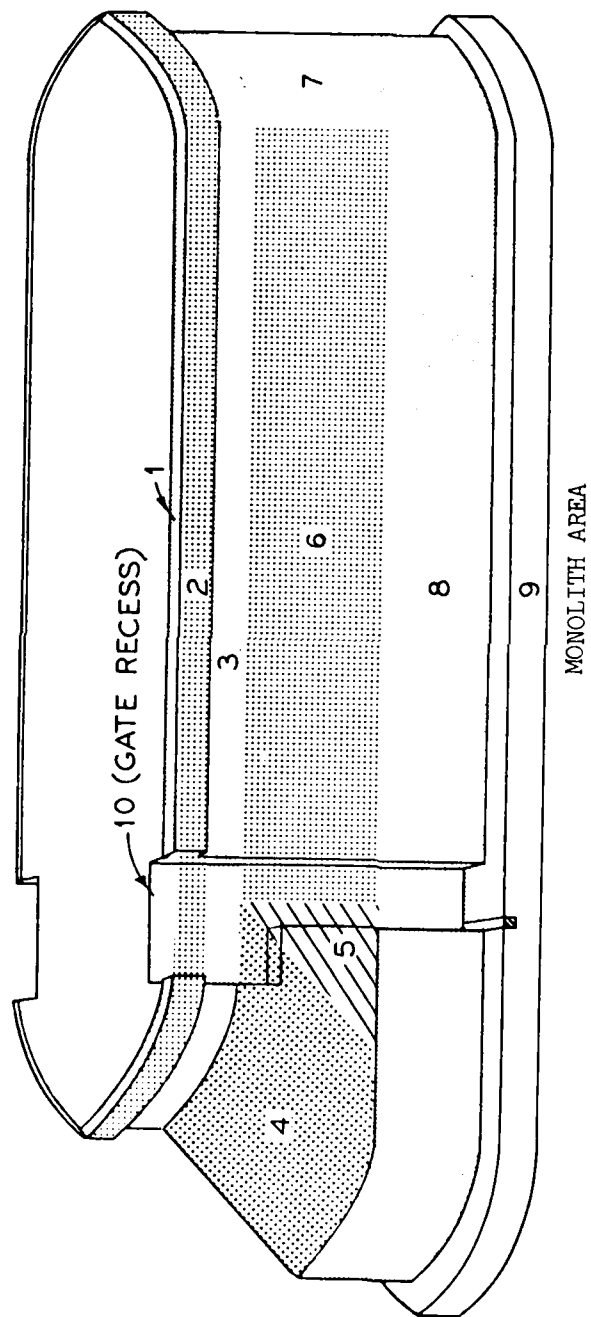


Figure F23. (Sheet 2 of 6)

SUBJECT	DAM PIERS 9 AND 13 - WEIGHT OF PIER	COMPUTED BY	DATE
		CHECKED BY	DATE

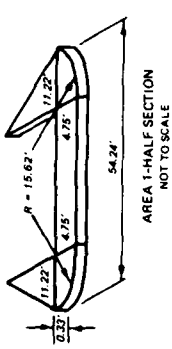
  

**VOLUME OF PIER**

**AREA 1** (EL 609.42 - 609.75)

$$\text{VOLUME}_1 = (2) (.33) \left[ \frac{(2)(45.81)(\pi)(15.63^2)}{360} - (10.86)(11.22) + (4.75) [54.24 - (2)(11.22)] \right]$$

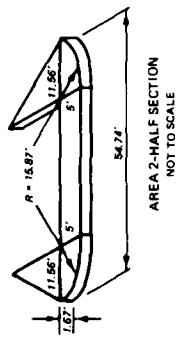
$$= 148.14 \text{ ft}^3$$



**AREA 2** (EL 607.75 - 609.42)

$$\text{VOLUME}_2 = (2) (1.67) \left[ \frac{(2)(46.78)(\pi)(15.84^2)}{360} - (10.86)(11.56) + (5) [54.74 - (2)(11.56)] \right]$$

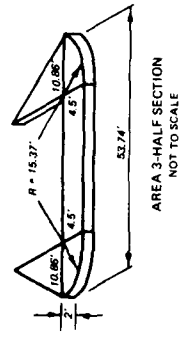
$$= 744.69 \text{ ft}^3$$



**AREA 3** (EL 605.75 - 607.75)

$$\text{VOLUME}_3 = (2) (2) \left[ \frac{(2)(45)(\pi)(15.36^2)}{360} - (10.86)(10.86) + (4.5) [53.74 - (2)(10.86)] \right]$$

$$= 845.8 \text{ ft}^3$$



SEE FORM NO. 1233-A  
RECEIVED MAY

Figure F23. (Sheet 3 of 6)

SUBJECT	DAM PIERS 9 AND 13 - WEIGHT OF PIER		DATE	
	COMPUTED BY		DATE	
	CHECKED BY			

VOLUME OF PIER (CONTINUED)

AREA 4 (EL 596.75 - 605.75)

$$\text{VOLUME}_4 = (2)(9) \left[ \frac{(45)(\pi)(15.36)^2}{360} - \frac{(10.06)(10.06)}{2} \right]$$

$$= 606.23 \text{ ft}^3$$

AREA 5 (EL 596.75 - 605.75)

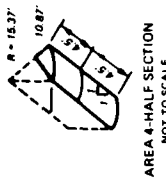
$$\text{VOLUME}_5 = (1/2)(9)^2(9)$$

$$= 364.50 \text{ ft}^3$$

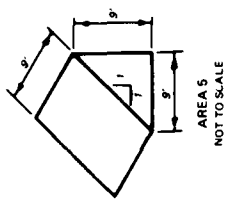
AREA 6 (EL 596.75 - 605.75)

$$\text{VOLUME}_6 = (9)(9)(32.01)$$

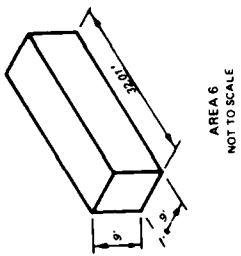
$$= 2592.81 \text{ ft}^3$$



AREA 4 - HALF SECTION  
NOT TO SCALE



AREA 5  
NOT TO SCALE



AREA 6  
NOT TO SCALE

WESCAM INC. 1253A

PAGE 4 OF 6

Figure F23. (Sheet 4 of 6)



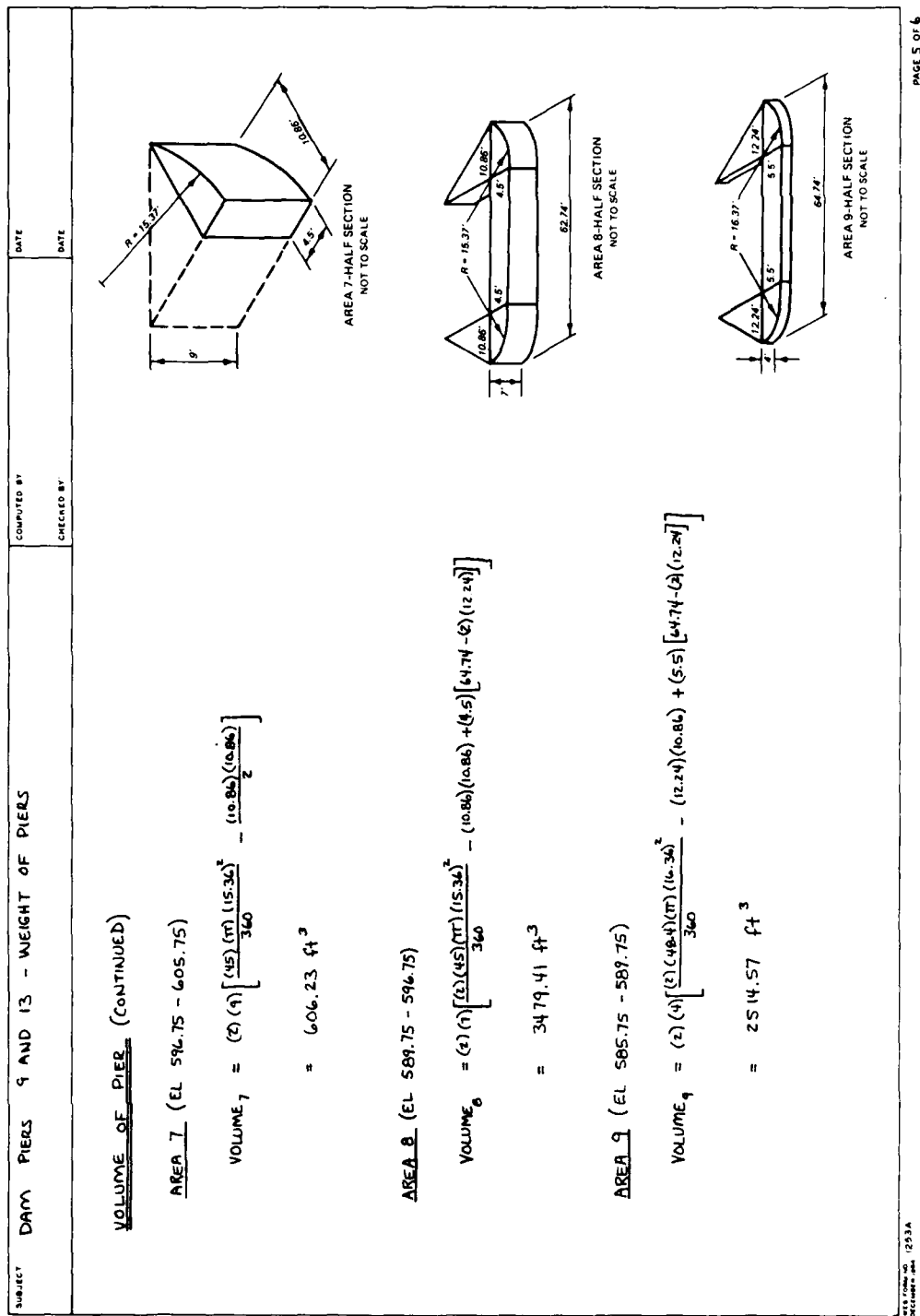


Figure F23. (Sheet 5 of 6)



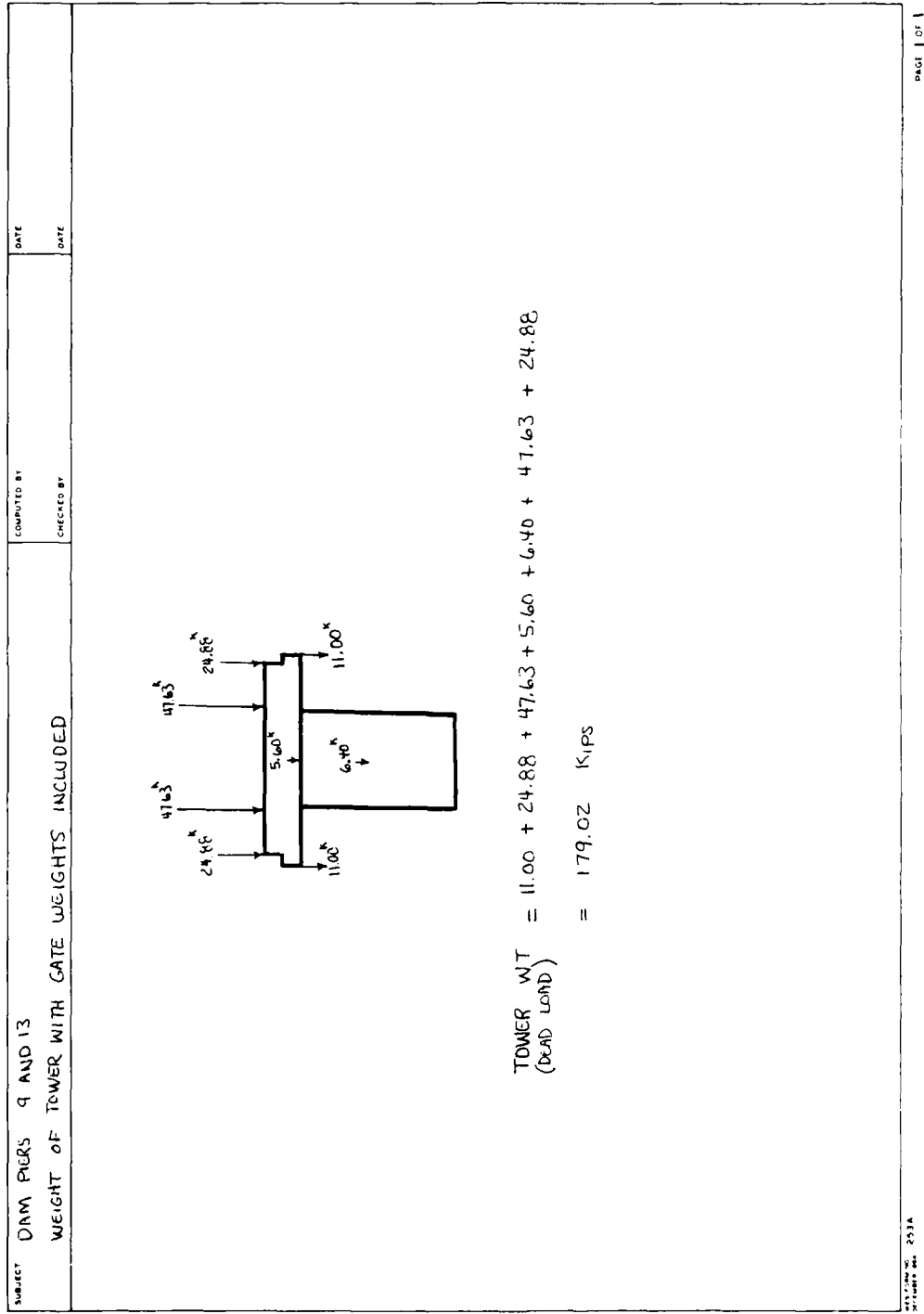


Figure F24. Weight of tower on pier, dam piers 9 and 13, Soo Dam

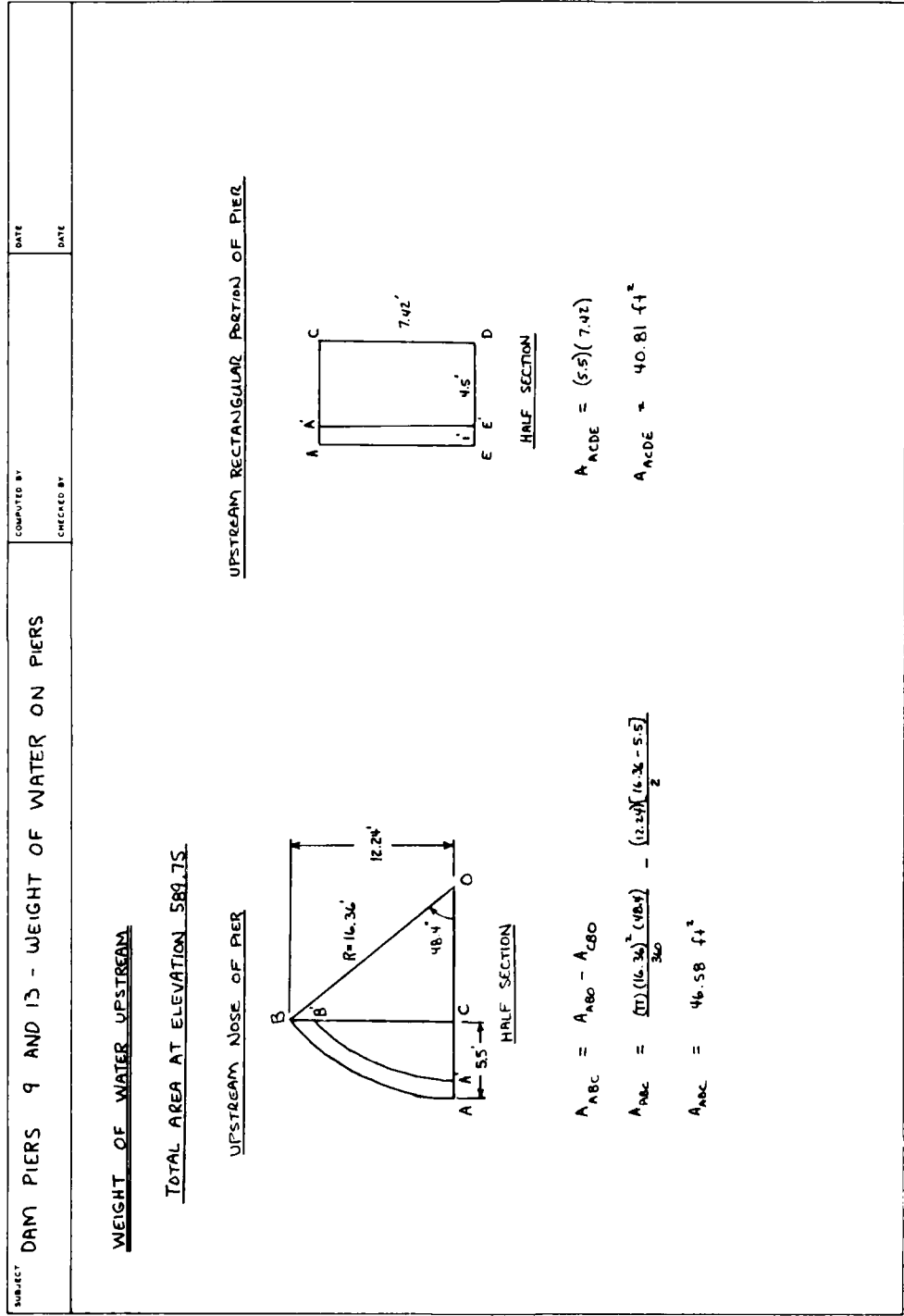


Figure F25. Weight of water on piers, dam piers 9 and 13, Soo Dam (Sheet 1 of 5)

SUBJECT	DAM PIERS 9 AND 13 - WEIGHT OF WATER ON PIERS		COMPUTED BY	DATE
			CHECKED BY	DATE
<p align="center"><u>WEIGHT OF WATER UPSTREAM (CONTINUED)</u></p> <p align="center"><u>CONCRETE AREA AT ELEVATION 589.75</u></p>				
<p align="center"><u>UPSTREAM NOSE OF PIER</u></p> <div style="display: flex; justify-content: space-around; align-items: flex-start;"> <div style="text-align: center;"> <p>Diagram of the upstream nose of the pier showing a quarter-circle sector B'AC with radius R = 15.36' and a 45-degree angle at vertex B'. A vertical line segment CO is drawn from the center of the arc to the pier axis, with a length of 10.86'. The horizontal distance from the pier axis to the arc is 4.5'.</p> </div> <div style="text-align: center;"> <p><u>HALF SECTION</u></p> <math display="block">A_{B'C} = A_{B'O} - A_{CBO}</math> <math display="block">A_{B'C} = \frac{(\pi)(15.36)^2(45)}{360} - \frac{(10.86)(15.36-4.5)}{2}</math> <math display="block">A_{B'C} = 33.68 \text{ ft}^2</math> </div> </div>				
<p align="center"><u>UPSTREAM RECTANGULAR PORTION OF PIER</u></p> <div style="display: flex; justify-content: space-around; align-items: flex-start;"> <div style="text-align: center;"> <p>Diagram of the rectangular portion of the pier showing a rectangle A'CDE with a width of 4.5' and a height of 7.42'.</p> </div> <div style="text-align: center;"> <p><u>HALF SECTION</u></p> <math display="block">A_{A'CDE} = (4.5)(7.42)</math> <math display="block">A_{A'CDE} = 33.39 \text{ ft}^2</math> </div> </div>				
<p align="center"><u>WEIGHT OF WATER - NORMAL OPERATION</u></p> $W_{water_u} = (62.5)[46.58 + 46.81 - 33.68 - 33.39][61.75 - 589.75][2]$ $W_{water_u} = 30.48 \text{ KIPS}$				
<p align="center"><u>WEIGHT OF WATER - HIGH WATER CONDITION</u></p> $W_{water_h} = (62.5)[46.58 + 46.81 - 33.68 - 33.39][602.75 - 589.75][2]$ $W_{water_h} = 33.02 \text{ KIPS}$				

Figure F25. (Sheet 2 of 5)

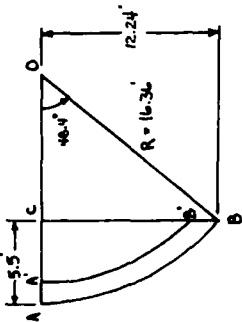
SUBJECT DAM PIERS 9 AND 13 - WEIGHT OF WATER ON PIERS	COMPUTED BY  CHECKED BY  	DATE  DATE  
--	---------------------------------------	--------------------------

WEIGHT OF WATER DOWNSTREAM

TOTAL AREA AT ELEVATION 589.75

DOWNSTREAM NOSE OF PIER



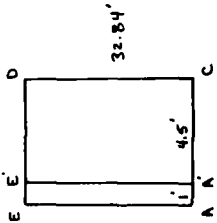
HALF SECTION

$$A_{ABC} = A_{BOC} - A_{BCO}$$

$$A_{ABC} = \frac{(\pi) (16.36')^2 (40.4)}{360} - \frac{(12.24) [(16.36 - 5.5)]}{2}$$

$$A_{ABC} = 46.58 \text{ ft}^2$$

DOWNSTREAM RECTANGULAR PORTION OF PIER



HALF SECTION

$$A_{ACDE} = (5.5) (32.84)$$

$$A_{ACDE} = 180.62 \text{ ft}^2$$

1253A  
 1253A  
 1253A

Figure F25. (Sheet 3 of 5)

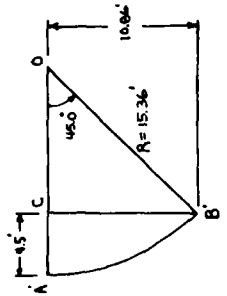
SUBJECT: DAM PIERS 9 AND 13 - WEIGHT OF WATER ON PIERS	COMPUTED BY: _____ CHECKED BY: _____	DATE: _____ DATE: _____
--	---	----------------------------

WEIGHT OF WATER DOWNSTREAM (CONTINUED)

CONCRETE AREA AT ELEVATION 589.75

DOWNSTREAM NOSE OF PIER



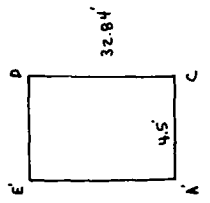
HALF SECTION

$$A_{A'B'C} = A_{A'B'O} - A_{C'B'O}$$

$$A_{A'B'C} = \frac{(\pi)(15.36)^2(45)}{360} - \frac{(10.86)[15.36-4.5]}{2}$$

$$A_{A'B'C} = 33.68 \text{ ft}^2$$

DOWNSTREAM RECTANGULAR PORTION OF PIER



HALF SECTION

$$A_{A'CDE} = (45)(32.84)$$

$$A_{A'CDE} = 147.78 \text{ ft}^2$$

WES FORM NO. 253-A  
REVISED 1966

PAGE 4 OF 5

Figure F25. (Sheet 4 of 5)

SUBJECT	DAM PIERS 9 AND 13 - WEIGHT OF WATER ON PIERS	COMPUTED BY	DATE
		CHECKED BY	DATE

WEIGHT OF WATER DOWNSTREAM (CONTINUED)

GATE ACCESS AREA

$A_{\text{ACCESS}} = (4.08)(4.33)$

$A_{\text{ACCESS}} = 5.43 \text{ ft}^2$

WEIGHT OF WATER - NORMAL OPERATION AND HIGH WATER CONDITION

$W_{\text{WATER}} = (6.25)(2)[4.58 + 180.62 - 33.69 - 147.78 + 5.43] [593.25 - 589.75]$

$W_{\text{WATER}} = 22.39 \text{ KIPS}$

TOTAL WEIGHT OF WATER ON PIER

NORMAL OPERATION

$W_{\text{WATER}} = W_{\text{WATER}_L} + W_{\text{WATER}_D}$

$W_{\text{WATER}} = 30.48 + 22.39$

$W_{\text{WATER}} = 52.87 \text{ KIPS}$

HIGH-WATER CONDITION

$W_{\text{WATER}} = W_{\text{WATER}_L} + W_{\text{WATER}_D}$

$W_{\text{WATER}} = 33.02 + 22.39$

$W_{\text{WATER}} = 55.41 \text{ KIPS}$

11-10-60 1253A  
 11-10-60 1253A  
 11-10-60 1253A

PAGE 5 OF 5

Figure F25. (Sheet 5 of 5)



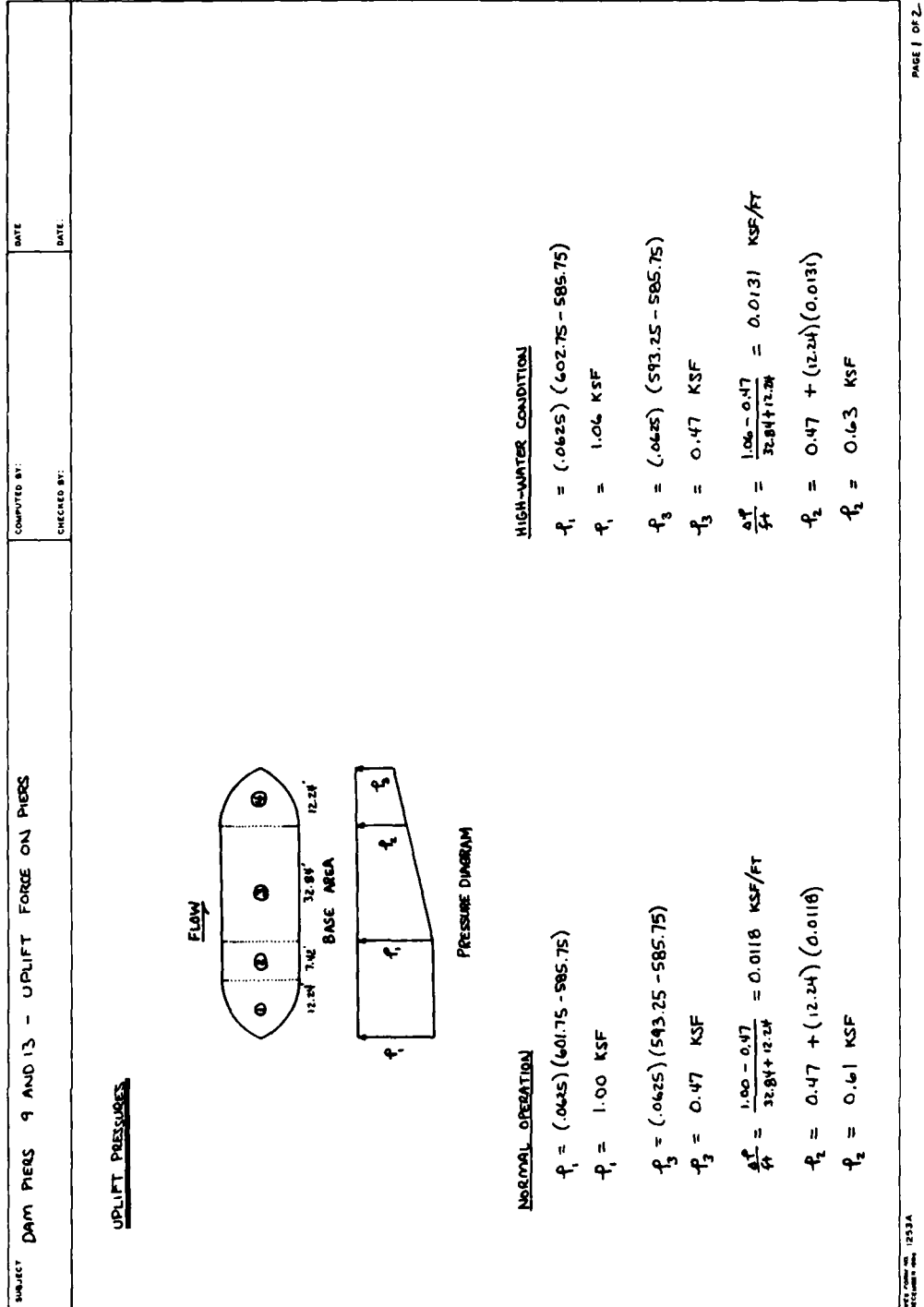


Figure F26. Uplift force on piers, dam piers 9 and 13, Soo Dam (Continued)

SUBJECT	PIERS 9 AND 13 - UPLIFT FORCE ON PIERS	COMPUTED BY:	DATE:
		CHECKED BY:	DATE:

UPLIFT FORCE

NORMAL OPERATION

SECTION 1

$$F_{V_1} = (2)(46.58)(1.00) = 93.16 \text{ KIPS}$$

SECTION 2

$$F_{V_2} = (2)(40.81)(1.00) = 81.62 \text{ KIPS}$$

SECTION 3

$$F_{V_3} = (2)(180.62)(1.00 + 0.01)(\frac{1}{2}) = 240.80 \text{ KIPS}$$

SECTION 4

$$F_{V_4} = (2)[(46.58)(0.47)^2 + 4.13] = 52.04 \text{ KIPS}$$

TOTAL UPLIFT FORCE

$$F_V = 93.16 + 81.62 + 240.80 + 52.04$$

$$F_V = 517.62 \text{ KIPS}$$

HIGH-WATER CONDITION

SECTION 1

$$F_{V_1} = (2)(46.58)(1.06) = 98.75 \text{ KIPS}$$

SECTION 2

$$F_{V_2} = (2)(40.81)(1.06) = 86.52 \text{ KIPS}$$

SECTION 3

$$F_{V_3} = (2)(180.62)(1.06 + 0.03)(\frac{1}{2}) = 305.25 \text{ KIPS}$$

SECTION 4

$$F_{V_4} = (2)[(46.58)(0.47)^2 + 4.62] = 53.03 \text{ KIPS}$$

TOTAL UPLIFT FORCE

$$F_V = 98.75 + 86.52 + 305.25 + 53.03$$

$$F_V = 543.55 \text{ KIPS}$$

\* Iterative solution used to solve force for uniformly varying load acting on nose portion of pier base

Figure F26. (Concluded)

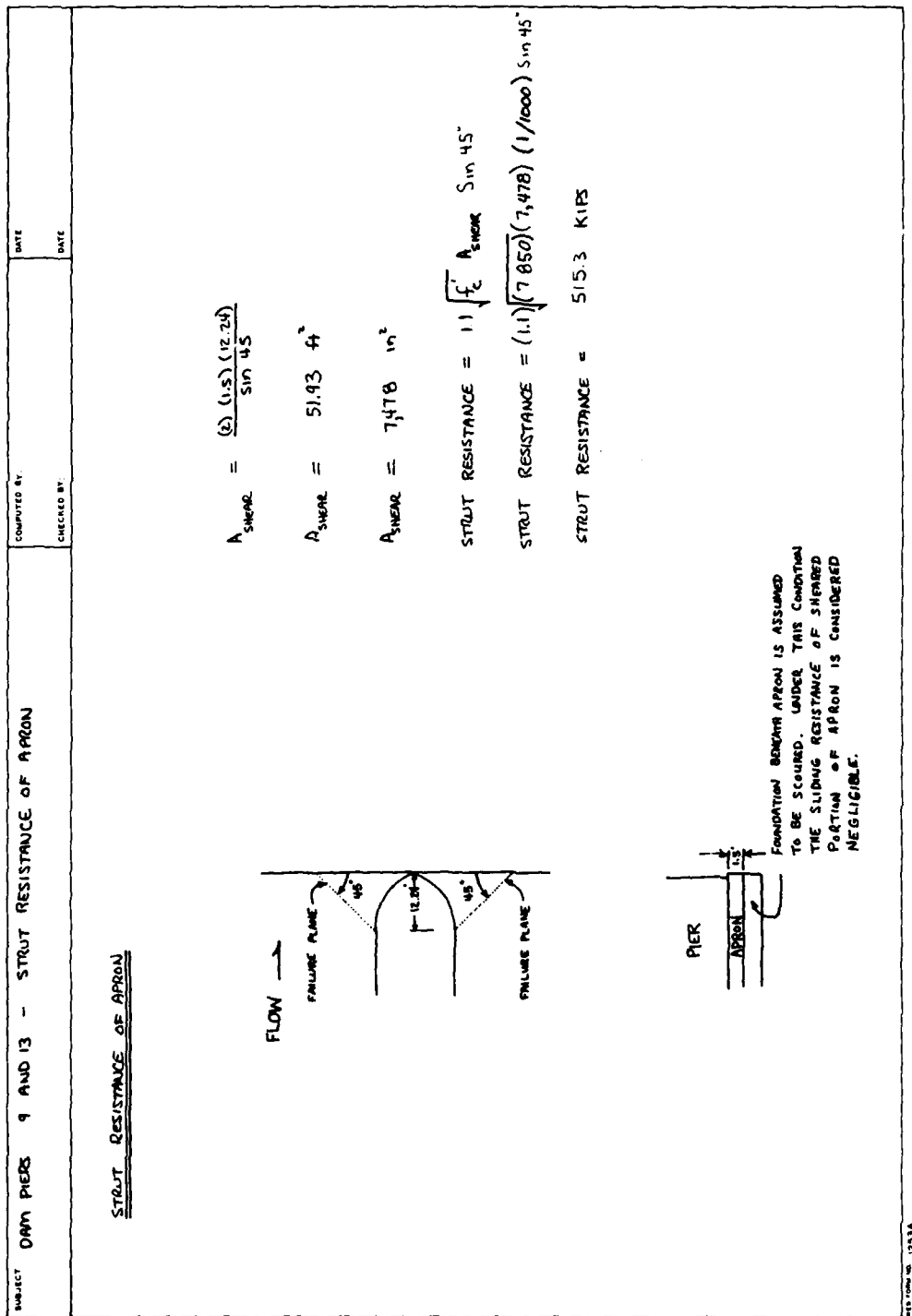


Figure F27. Strut resistance of apron, dam piers 9 and 13, Soo Dam

DATE

COMPUTED BY

PROJECT DAM PIERS 4 AND 13 - SLICING STABILITY AT CONCRETE - FOUNDATION

INTERFACE

DATE

CHECKED BY

FACTOR OF SAFETY AGAINST SLIDING

NORMAL OPERATION

ITEM	DESCRIPTION	$F_v$ (KIPS)
Water	SEE FIGURE F23	1,859.0
Wingwall	SEE FIGURE F24	171.0
Wingwall	SEE FIGURE F25	52.9
UPLIFT	SEE FIGURE F26	-517.6
		<u>1,573.3</u>

$$\begin{aligned}\text{RESISTING FORCE} &= F_v \tan \phi + \text{STRUT RESISTANCE OF APRON} \\ &= 1,573.3 \tan 32.1 + 728.8 \\ &= 1,715.7\end{aligned}$$

$$\begin{aligned}\text{DRIVING FORCE} &= (0.0435) \left( \frac{1}{4} \right) [(601.75 - 585.75)^2 - (513.25 - 585.75)^2] (4) + [(601.75 - 585.75)^2 - (513.25 - 585.75)^2] (51.71) \\ &= 269.1 \text{ KIPS}\end{aligned}$$

$$\begin{aligned}\text{F.S.} &= \frac{\text{RESISTING FORCE}}{\text{DRIVING FORCE}} = \frac{1,715.7}{269.1} = 6.38\end{aligned}$$

NORMAL OPERATION WITH ICE

$$\text{DRIVING FORCE} = 269.1 + (2)(5) (60.71) = 876.2 \text{ KIPS}$$

$$\text{F.S.} = \frac{1,715.7}{876.2} = 1.96$$

HIGH-WATER CONDITION

$$\begin{aligned}\text{ITEM} \quad \text{DESCRIPTION} \quad F_v \text{ (KIPS)} \\ \text{Water} \quad \text{SEE FIGURE F23} \quad 1,859.0 \\ \text{Wingwall} \quad \text{SEE FIGURE F24} \quad 171.0 \\ \text{Wingwall} \quad \text{SEE FIGURE F25} \quad 55.4 \\ \text{UPLIFT} \quad \text{SEE FIGURE F26} \quad -513.6 \\ \hline 1,571.8\end{aligned}$$

$$\begin{aligned}\text{DRIVING FORCE} &= 269.1 + (0.0435) [(0.5 + 601.75 - 585.75) (60.71)] \\ &= 331.7 \text{ KIPS}\end{aligned}$$

$$\begin{aligned}\text{RESISTING FORCE} &= (1,571.8) \tan 32.1 + 728.8 \\ &= 1,701.0\end{aligned}$$

$$\text{F.S.} = \frac{1,701.0}{331.7} = 5.13$$

NORMAL OPERATION WITH EARTHQUAKE

$$\text{DRIVING FORCE} = 269.1 + (0.05) [1,859 + 179 + 52.9] + \left( \frac{2}{3} \right) (51) (\cos(1/2 \text{ wave})) [(1/4)^2 (4) + (1/8)^2 (51.71)]$$

$$= 390.2 \text{ KIPS}$$

$$\text{F.S.} = \frac{1,715.7}{390.2} = 4.40$$

Figure F28. Sliding stability summary for pier section, concrete-foundation interface, dam piers 9 and 13, Soo Dam



SUBJECT	COMPUTED BY	DATE
DAM PIER 9 AND 13 - SLIDING STABILITY ALONG SEAM AT ELEVATION 585.75	CHECKED BY:	DATE
<u>SUM OF FORCES</u>		
<u>NORMAL OPERATION</u>		
$F_v = 2,138.6$ KIPS		
$F_H = 379.0$ KIPS		
<u>NORMAL OPERATION WITH ICE</u>		
$F_v = 2,138.6$ KIPS		
$F_H = 379.0 + (2)(5)(60.7) = 986.1$ KIPS		
<u>HIGH WATER CONDITION</u>		
$W_{WATER} = 872.6 + 55.4 - 52.4 + (.005)(9)(60.71 - 11)$		$= 903.1$ KIPS
$UPLIFT = (.005) \left[ \left( \frac{1}{2} \right) (602.75 + 593.25 - (2)(585.75)) (53.71)(60.71) + (602.75 - 585.75)(2)(46.58) \right]$		$= 2,595.5$ KIPS
$F_v = W_{PIER} + W_{TOWER} + W_{APRON} + W_{FOUNDATION} + W_{WATER} - UPLIFT$		
$F_v = 1,859.0 + 179.0 + 651.1 + 1,064.7 + 903.1 - 2,595.5$		$= 2,061.4$ KIPS
$F_H = \left( \frac{1}{2} \right) (.005)(60.71) \left[ (602.75 - 585.75)^2 - (593.25 - 585.75)^2 \right]$		$= 441.6$ KIPS
<u>NORMAL OPERATION WITH EARTHQUAKE</u>		
$F_v = 2,138.6$ KIPS		
$F_H = 379.0 + (0.05) [1,859 + 179 + 651.1 + 1,064.7] + \left( \frac{1}{3} \right) (51)(.05) \left( \frac{1}{1000} \right) (16)^2 (8)$		$= 570.2$ KIPS

Figure F29. (Sheet 2 of 8)

SUBJECT DAM PIERS 9 AND 13 -SLIDING ALONG SEAM AT ELEVATION 585.75										COMPUTED BY		DATE	
										CHECKED BY:		DATE	
LOAD CASE	SUM OF VERTICAL FORCES	SUM OF HORIZONTAL FORCES	FRICTION ANGLE (DEGREES)	COHESIVE STRENGTH (KSF)	AREA OF SLIDING PLANE	STRET RESISTANCE	SHEAR RESISTANCE	CONESIVE RESISTANCE	TOTAL SLIDING RESISTANCE	FACTOR OF SAFETY AGAINST SLIDING			
	F <sub>V</sub> (KIPS)	F <sub>H</sub> (KIPS)	φ (DEGREES)	C (KSF)	A (FT <sup>2</sup> )	R <sub>s</sub> (KIPS)	R <sub>f</sub> = F <sub>H</sub> tan φ (KIPS)	R <sub>c</sub> = CA (KIPS)	R = R <sub>s</sub> + R <sub>f</sub> + R <sub>c</sub> (KIPS)	F.S. = $\frac{R}{F_H}$			
NORMAL OPERATION	2,138.6	379.0	36.5	0.1	3261	0	1,582.5	326.1	1,908.6	5.04			
			26.0	0.0			1,043.1	0.0	1,043.1	2.75			
			34.0	0.2			1,442.5	652.2	2,094.7	5.53			
			27.9	0.0			1,132.3	0.0	1,132.3	2.99			
			31.4	2.8			1,305.4	9,130.8	10,436.2	27.54			
NORMAL OPERATION WITH ICE	2,138.6	986.1	36.5	0.1	3261	0	1,582.5	326.1	1,908.6	1.94			
			26.0	0.0			1,043.1	0.0	1,043.1	1.06			
			34.0	0.2			1,442.5	652.2	2,094.7	2.12			
			27.9	0.0			1,132.3	0.0	1,132.3	1.15			
			31.4	2.8			1,305.4	9,130.8	10,436.2	10.58			
HIGH WATER CONDITION			21.0	0.0			820.9	0.0	820.9	0.83			
	2,061.4	441.6	36.5	0.1	3261	0	1,525.4	326.1	1,851.5	4.19			
			26.0	0.0			1,005.4	0.0	1,005.4	2.28			
			34.0	0.2			1,390.4	652.2	2,042.6	4.63			
			27.9	0.0			1,091.5	0.0	1,091.5	2.47			

Figure F29. (Sheet 3 of 8)

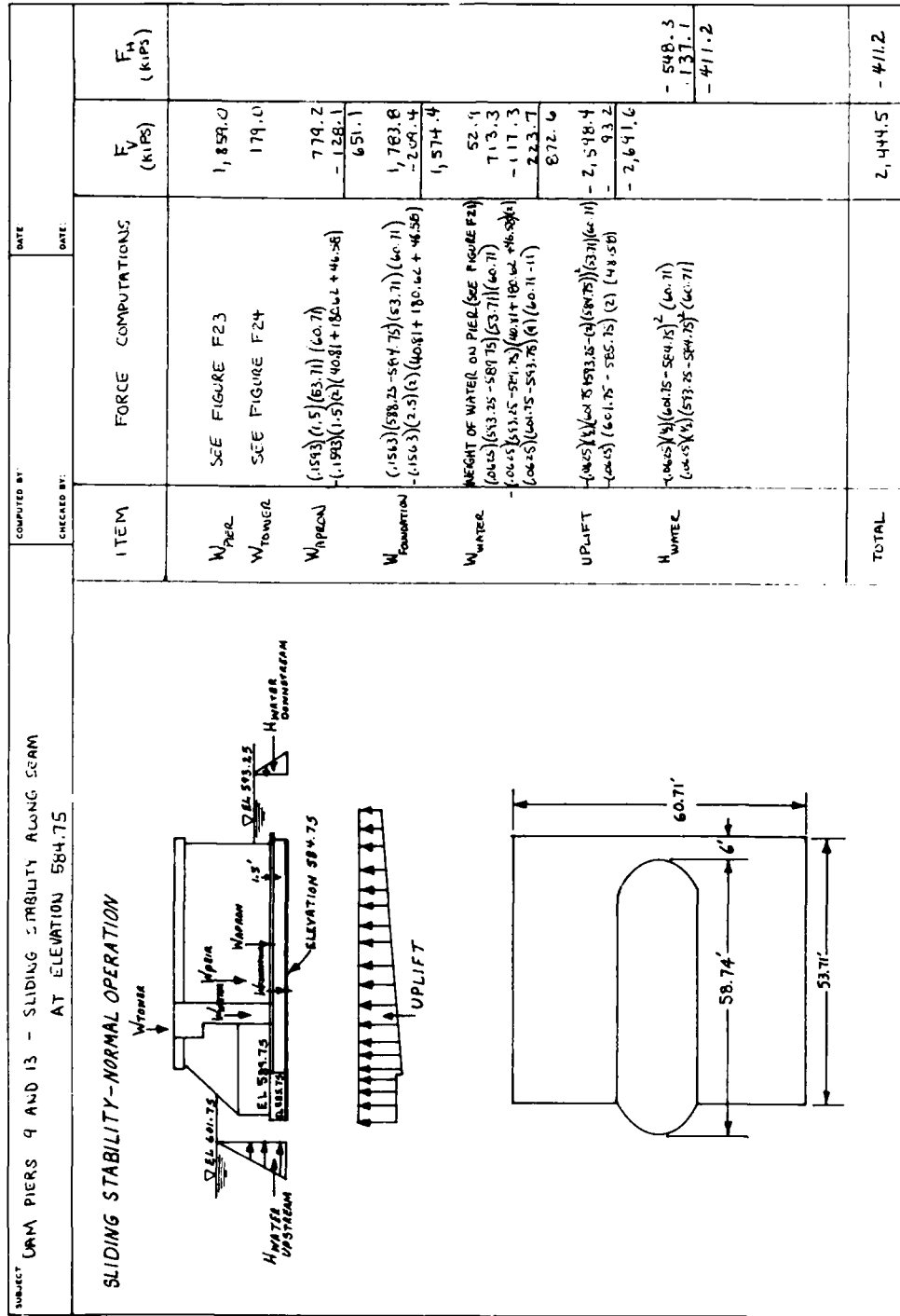
DAM PIERS 9 AND 13 - SLIDING STABILITY ALONG SEAM AT ELEVATION 585.75							COMPUTED BY		DATE	
LOAD CASE							CHECKED BY		DATE	
	SUM OF VERTICAL FORCES	SUM OF HORIZONTAL FORCES	FRICTION ANGLE (DEGREES)	CONESUE STRENGTH (KSF)	AREA OF SLIDING PLANE (FT <sup>2</sup> )	STRAUT RESISTANCE (KIPS)	SHEAR RESISTANCE (KIPS)	CONESUE RESISTANCE (KIPS)	TOTAL SLIDING RESISTANCE (KIPS)	FACTOR OF SAFETY AGAINST SLIDING
	$F_v$ (KIPS)	$F_h$ (KIPS)	$\phi$ (DEGREES)	$C$ (KSF)	$A$ (FT <sup>2</sup> )	$R_s$ (KIPS)	$R_g = F_v \tan \phi$ (KIPS)	$R_c = CA$ (KIPS)	$R = R_g + R_c$ (KIPS)	$F.S. = \frac{R}{F_h}$
HIGH WATER CONDITION	2,061.4	441.6	31.4	2.8	3261	0	1,258.3	9,130.8	10,389.1	23.53
			21.0	0.0			791.3	0.0	791.3	1.79
NORMAL OPERATION WITH EARTHQUAKE	2,136.6	570.2	36.5	0.1	3261	0	1,582.5	326.1	1,908.6	3.35
			26.0	0.0			1,043.1	0.0	1,043.1	1.83
			34.0	0.2			1,442.5	652.2	2,094.7	3.67
			27.9	0.0			1,132.3	0.0	1,132.3	1.99
			31.4	2.8			1,305.4	9,130.8	10,436.2	18.30
			21.0	0.0			820.9	0.0	820.9	1.44

W&S, Inc. No. 1253A  
December 1961

PAGE 4 OF 8

Figure F29. (Sheet 4 of 8)





SUBJECT DAM PIERS 9 AND 13 - SLIDING STABILITY ALONG SEAM AT ELEVATION 564.75	COMPUTED BY: CHECKED BY:	DATE: DATE:
--	-----------------------------	----------------

SUM OF FORCES

NORMAL OPERATION

$F_V = 2,444.5 \text{ KIPS}$

$F_H = 411.2 \text{ KIPS}$

NORMAL OPERATION WITH ICE

$F_V = 2,444.5 \text{ KIPS}$

$F_H = 411.2 + (2)(5)(60.71) = 1,018.3 \text{ KIPS}$

HIGH WATER CONDITION

$W_{\text{WATER}} = 872.6 + 55.4 - 52.9 + (.0625)(q)(60.71 - 11) = 903.1 \text{ KIPS}$   
 $\text{UPLIFT} = (.0625) \left[ \left( \frac{1}{2} \right) (602.75 + 593.25 - (2)(584.75)) (53.71)(60.71) + (602.75 - 584.75)(2)(46.58) \right] = 2,865.1 \text{ KIPS}$

$F_V = W_{\text{PIER}} + W_{\text{TOWER}} + W_{\text{APPROX}} + W_{\text{FOUNDATION}} + W_{\text{WATER}} - \text{UPLIFT}$   
 $F_V = 1,859 + 179 + 651.1 + 1,574.4 + 903.1 - 2,865.1 = 2,361.5 \text{ KIPS}$   
 $F_H = \left( \frac{1}{2} \right) (.0625)(60.71) \left[ (602.75 - 584.75)^2 - (593.25 - 584.75)^2 \right] = 477.6 \text{ KIPS}$

NORMAL OPERATION WITH EARTHQUAKE

$F_V = 2,444.5 \text{ KIPS}$

$F_H = 411.2 + (.05)(1,859 + 179 + 651.1 + 1,574.4) + \left( \frac{2}{3} \right) (51)(.05) \left( \frac{1}{602.5} \right) (164)(8) = 6,279 \text{ KIPS}$

Figure F29. (Sheet 6 of 8)

PROJECT		COMPUTED BY				DATE			
DAM PIERS 9 AND 13 - SLIDING STABILITY ALONG SEAM		CHECKED BY				DATE			
AT ELEVATION 584.75									
LOAD CASE	SUM OF VERTICAL FORCES	SUM OF HORIZONTAL FORCES	FRICTION ANGLE	COHESIVE STRENGTH	AREA OF SLIDING PLANE	SHEAR RESISTANCE	COMBINED RESISTANCE	TOTAL SLIDING RESISTANCE	FACTOR OF SAFETY AGAINST SLIDING
	$F_v$ (KIPS)	$F_h$ (KIPS)	$\phi$ (DEGREES)	$c$ (KSF)	$A$ ( $FT^2$ )	$R_f = F \tan \phi$ (KIPS)	$R_c = CA$ (KIPS)	$R = R_f + R_c$ (KIPS)	$FS = \frac{R}{F_h}$
NORMAL OPERATION	2,444.5	411.2	36.5	0.1	326.1	0	326.1	2,134.9	5.19
			26.0	0.0			0.0	1,192.3	2.90
			34.0	0.2			652.2	2,301.6	5.60
			27.9	0.0			0.0	1,294.3	3.15
			31.4	2.8			9,130.8	10,622.9	25.83
NORMAL OPERATION WITH ICE	2,444.5	1,018.3	36.5	0.1	326.1	0	326.1	2,134.9	2.28
			26.0	0.0			0.0	1,192.3	1.17
			34.0	0.2			652.2	2,301.6	2.26
			27.9	0.0			0.0	1,294.3	1.27
			31.4	2.8			9,130.8	10,622.9	10.43
HIGH WIND CONDITION	2,361.5	477.6	36.5	0.1	326.1	0	326.1	2,073.5	4.34
			26.0	0.0			0.0	1,151.8	2.41
			34.0	0.2			652.2	2,245.1	4.70
			27.9	0.0			0.0	1,250.4	2.62

411 Form No. 1233A  
REVISION 02

PAGE 7 OF 8

Figure F29. (Sheet 7 of 8)

SUBJECT DAM PIERS 9 AND 13 - SLIDING STABILITY ALONG SCAM AT ELEVATION 584.75										COMPUTED BY DATE		CHECKED BY DATE	
LOAD CASE	SUM OF VERTICAL FORCES	SUM OF HORIZONTAL FORCES	FRICTION ANGLE (DEGREES)	COHESIVE STRENGTH (K.S.F)	AREA OF SLIDING PLANE (FT <sup>2</sup> )	STRAUT RESISTANCE (KIPS)	SHEAR RESISTANCE (KIPS)	COHESIVE RESISTANCE (KIPS)	TOTAL SLIDING RESISTANCE (KIPS)	FACTOR OF SAFETY AGAINST SLIDING			
	$F_v$ (KIPS)	$F_H$ (KIPS)	$\phi$ (DEGREES)	$C$ (K.S.F)	$A$ (FT <sup>2</sup> )	$R_s$ (KIPS)	$R_f = F_v \tan \phi$ (KIPS)	$R_c = CA$ (KIPS)	$R = R_s + R_f + R_c$ (KIPS)	$F.S. = \frac{R}{F_H}$			
HIGH WATER CONDITION	2,364.5	477.6	31.4	2.8	3261	0	1,441.5	9,130.8	10,572.3	22.14			
			21.0	0.0			906.5	0.0	906.5	1.90			
NORMAL OPERATION WITH EARTHQUAKE	2,444.5	627.9	36.5	0.1	3261	0	1,808.8	326.1	2,134.9	3.40			
			26.0	0.0			1,192.3	0.0	1,192.3	1.90			
			34.0	0.2			1,648.8	652.2	2,301.0	3.66			
			27.9	0.0			1,244.3	0.0	1,244.3	2.06			
			31.4	2.8			1,492.1	9,130.8	10,622.9	16.92			
			21.0	0.0			438.4	0.0	438.4	1.49			

1253A

Figure F29. (Sheet 8 of 8)

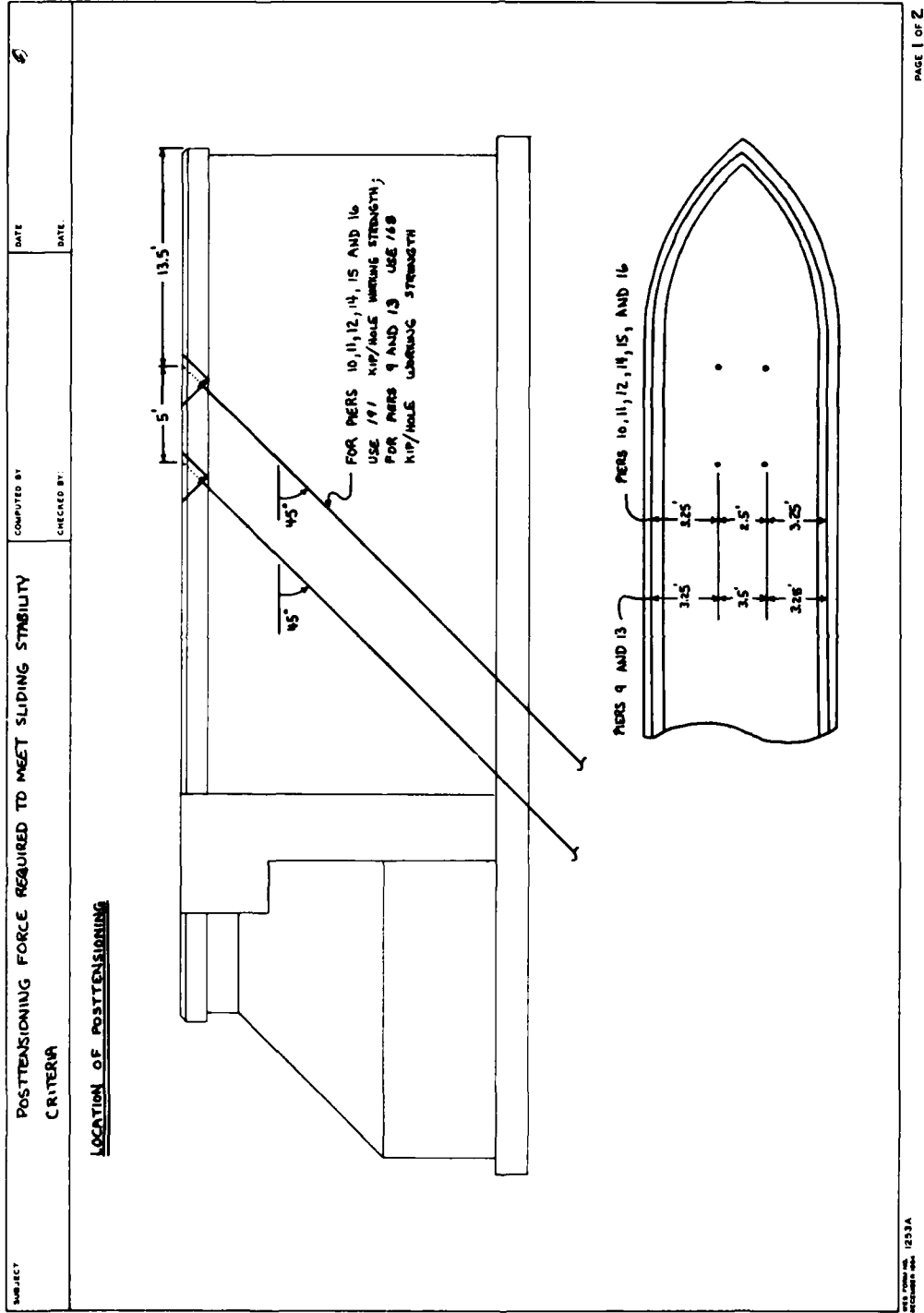


Figure F30. Layout of posttensioning required to meet sliding stability, Soo Dam (Continued)

SUBJECT  POSTTENSIONING FORCE REQUIRED TO MEET SLIDING STABILITY CRITERIA	COMPUTED BY:  CHECKED BY:	DATE:  DATE:
<p><u>REQUIRED POSTTENSIONING</u></p> <p>FSR = FACTOR OF SAFETY AGAINST SLIDING REQUIRED TO MEET STABILITY CRITERIA  <math>F_v</math> = SUM OF VERTICAL FORCES (KIPS)  <math>\phi</math> = ANGLE OF SLIDING FRICTION (DEGREES)  <math>C</math> = COHESIVE STRENGTH ALONG SLIDING PLANE (KSF)  <math>A</math> = AREA OF SLIDING  <math>\theta</math> = ANGLE POSTTENSIONING MAKES WITH HORIZONTAL (DEGREES)  <math>P</math> = POSTTENSIONING FORCE REQUIRED TO MEET SLIDING STABILITY (KIPS)</p> $FSR = \frac{\text{RESISTING FORCE}}{\text{DRIVING FORCE}} = \frac{(F_v + P \cos \theta) \tan \phi + P \sin \theta + CA}{F_H}$ $P = \frac{FSR \cdot F_H - F_v \tan \phi - CA}{\cos \theta \tan \phi + \sin \theta}$ <p>PIERS 10, 11, 12, 14, 15, AND 16 - NORMAL OPERATION WITH ICE</p> <p>FOR FSR = 1.5, <math>\phi = 21.0</math>, AND <math>C = 0.0</math></p> $P = \frac{(1.5)(978) - (871.2) \tan 21 - (0)(3234)}{\cos 45 \cdot \tan 21 + \sin 45} = 765 \text{ KIPS}; \quad P = \frac{765}{4} = 191 \text{ KIPS/HOLE}$ <p>FOR FSR = 2.0, <math>\phi = 36.5</math>, AND <math>C = 0.1</math></p> $P = \frac{(2.0)(978) - (1,871.2) \tan 36.5 - (0.1)(3234)}{\cos 45 \cdot \tan 36.5 + \sin 45} = 202 \text{ KIPS}$ <p>PIERS 9 AND 13 - NORMAL OPERATION WITH ICE</p> <p>FOR FSR = 1.5, <math>\phi = 21.0</math>, AND <math>C = 0.0</math></p> $P = \frac{(1.5)(986.1) - (438.6) \tan 21 - (0)(3241)}{\cos 45 \cdot \tan 21 + \sin 45} = 673 \text{ KIPS}; \quad P = \frac{673}{4} = 168 \text{ KIPS/HOLE}$ <p>FOR FSR = 2.0, <math>\phi = 36.5</math>, AND <math>C = 0.1</math></p> $P = \frac{(2.0)(986.1) - (2,138.6) \tan 36.5 - (0.1)(3241)}{\cos 45 \cdot \tan 36.5 + \sin 45} = 52 \text{ KIPS}$		

Figure F30. (Concluded)

SUBJECT DAM PIERS 10, 11, 12, 14, 15, AND 16 - FORCES AND MOMENTS AFTER POSTTENSIONING										COMPUTED BY:	DATE:
										CHECKED BY:	DATE:
LOAD CASE	SUM OF VERTICAL FORCES $F_v$	VERTICAL COMPONENT OF POSTTENSIONING FORCE $P_v = P \sin 45^\circ$	SUM OF VERTICAL FORCES AFTER POSTTENSIONING $F_v = F_v + P_v$	SUM OF HORIZONTAL FORCES $F_h$	SUM OF HORIZONTAL FORCES AFTER POSTTENSIONING $F_h = F_h + P_h$	SUM OF MOMENTS $M$	MOMENT DUE TO POSTTENSIONING $M_p = 46.5 P'$	SUM OF MOMENTS AFTER POSTTENSIONING $M = M + M_p$	FT-KIPS		
<u>PIER ONLY</u>											
NORMAL OPERATION	1,285.4	540.9	1,826.3	264.9	33,870	21,906	55,776				
NORMAL OPERATION WITH ICE	1,285.4	540.9	1,826.3	867.0	24,838	21,906	46,744				
HIGH - WATER CONDITION	1,266.4	540.9	1,807.3	313.8	32,726	21,906	54,632				
NORMAL OPERATION WITH EARTHQUAKE	1,285.4	540.9	1,826.3	366.9	32,581	21,906	54,487				
<u>PIER AND FOUNDATION</u>											
NORMAL OPERATION	1,285.4	540.9	1,826.3	264.9	33,870	21,906	55,776				
NORMAL OPERATION WITH ICE	1,285.4	540.9	1,826.3	867.0	24,838	21,906	46,744				
HIGH - WATER CONDITION	1,266.4	540.9	1,807.3	313.8	32,726	21,906	54,632				
NORMAL OPERATION WITH EARTHQUAKE	1,285.4	540.9	1,826.3	366.9	32,581	21,906	54,487				
<u>PIER AND MASON SECTION AT ELEV. 565.75</u>											
NORMAL OPERATION	1,871.2	540.9	2,412.1	375.9	*	—	—				
NORMAL OPERATION WITH ICE	1,871.2	540.9	2,412.1	978.0	*	—	—				
HIGH - WATER CONDITION	1,796.0	540.9	2,336.9	437.9	*	—	—				
NORMAL OPERATION WITH EARTHQUAKE	1,871.2	540.9	2,412.1	550.6	*	—	—				

\* NOT COMPUTED BECAUSE SLIDING STABILITY WAS MORE CRITICAL AND THEREFORE COVERED IN THE ANALYSIS

\* NOT COMPUTED BECAUSE SLIDING STABILITY WAS MORE CRITICAL AND THEREFORE COVERED IN THE ANALYSIS

Figure F31. Forces and moments after posttensioning, dam piers 10, 11, 12, 14, 15, and 16, Soo Dam (Continued)

SUBJECT

DOWN PIERS 10, 11, 12, 14, 15, AND 16 - FORCES AND MOMENTS AFTER

POSTTENSIONING

COMPUTED BY:

DATE:

CHECKED BY:

DATE:

LOAD CASE	SUM OF VERTICAL FORCES $F_v$	VERTICAL COMPONENT OF POSTTENSIONING FORCE $P' = P \sin 45^\circ$	SUM OF VERTICAL FORCES AFTER POSTTENSIONING $F_v' = F_v + P'$	SUM OF HORIZONTAL FORCES $F_H$	SUM OF MOMENTS $M$	MOMENT DUE TO POSTTENSIONING $M_p = 48.5 P'$	SUM OF MOMENTS AFTER POSTTENSIONING $M' = M + M_p$
<u>PIER AND PIER SECTION AT ELEV. 534.75</u>							
NORMAL OPERATION	2,174.6	540.9	2,715.5	407.9	*	—	—
NORMAL OPERATION WITH ICE	2,174.6	540.9	2,715.5	1,010.0	*	—	—
HIGH-WATER CONDITION	2,094.6	540.9	2,635.5	473.7	*	—	—
NORMAL OPERATION WITH EARTHQUAKE	2,174.6	540.9	2,715.5	607.9	*	—	—

Drawing No. 1253A

WES Form No. 1252-A  
OCTOBER 1960

PAGE 2 OF 2

Figure F31. (Concluded)



SUBJECT DAM PERS 10, 11, 12, 14, 15, AND 16 - PERCENT EFFECTIVE BASE AFTER POSTTENSIONING, CONCRETE-FOUNDATION INTERFACE		COMPUTED BY:	DATE:
		CHECKED BY:	DATE:
LOAD CASE	TOTAL AREA OF PIER BASE $A_t$ FT <sup>2</sup>	AREA OF PER BASE IN COMPRESSION $A_c$ FT <sup>2</sup>	PERCENT EFFECTIVE BASE $\frac{A_c}{A_t} \times 100$ %
NORMAL OPERATION	519.76	519.76	100.0
NORMAL OPERATION WITH ICE	519.76	519.76	100.0
HIGH- WATER CONDITION	519.76	519.76	100.0
NORMAL OPERATION WITH EARTHQUAKE	519.76	519.76	100.0

432 Form No. 1231A  
RECEIVED 10/1/54

PAGE 1 OF 1

Figure F32. Percent of pier base in compression after posttensioning, concrete foundation interface, dam piers 10, 11, 12, 14, 15, and 16, Soo Dam

SUBJECT DAM PIERS 10, 11, 12, 14, 15, AND 16 - FACTOR OF SAFETY AGAINST SLIDING AFTER POSTTENSIONING										COMPUTED BY: DATE:	CHECKED BY: DATE:
LOAD CASE	SUM OF VERTICAL FORCES	SUM OF HORIZONTAL FORCES	FRICTION ANGLE (DEGREES)	COHESIVE STRENGTH (KSF)	BASE AREA (FT <sup>2</sup> )	STAY RESISTANCE (KIPS)	STEM RESISTANCE (KIPS)	HORIZONTAL COMPONENT OF POSTTENSIONING FORCE (KIPS)	TOTAL SLIDING RESISTANCE (KIPS)	FACTOR OF SAFETY AGAINST SLIDING	
<u>PIER ONLY</u>	$F_v$ (KIPS)	$F_H$ (KIPS)	$\phi$ (DEGREES)	C (KSF)	A (FT <sup>2</sup> )	$R_s$ (KIPS)	$R_s = \frac{1}{3} \sum w_i + C_A$ (KIPS)	$R_p$ (KIPS)	$R = R_s + R_p$ (KIPS)	$FS = \frac{R}{F_H}$	
NORMAL OPERATION	1,826.3	264.9	32.1	0.0	520	717.0	1,145.6	540.9	2,403.5	9.07	
NORMAL OPERATION WITH ICE	1,826.3	867.0	32.1	0.0	520	717.0	1,145.6	540.9	2,403.5	2.77	
HIGH-WATER CONDITION	1,807.3	313.8	32.1	0.0	520	717.0	1,133.7	540.9	2,391.6	7.62	
NORMAL OPERATION WITH EARTHQUAKE	1,826.3	366.9	32.1	0.0	520	717.0	1,145.6	540.9	2,403.5	6.55	
<u>PIER AND FOUNDATION</u>											
NORMAL OPERATION	1,826.3	264.9	21.0	0.0	520	717.0	701.0	540.9	1,958.9	7.39	
NORMAL OPERATION WITH ICE	1,826.3	867.0	21.0	0.0	520	717.0	701.0	540.9	1,958.9	2.26	
HIGH-WATER CONDITION	1,807.3	313.8	21.0	0.0	520	717.0	693.8	540.9	1,951.7	6.22	
NORMAL OPERATION WITH EARTHQUAKE	1,826.3	366.9	21.0	0.0	520	717.0	701.0	540.9	1,958.9	5.34	
<u>PIER AND AROUND SECTION A ELEV. 585.75</u>											
NORMAL OPERATION	2,412.1	375.9	21.0	0.0	3234	0.0	925.9	540.9	1,466.8	3.90	
NORMAL OPERATION WITH ICE	2,412.1	978.0	21.0	0.0	3234	0.0	925.9	540.9	1,466.8	1.50	
HIGH-WATER COND	2,336.9	437.9	21.0	0.0	3234	0.0	897.0	540.9	1,437.9	3.28	
NORMAL OPERATION WITH EARTHQUAKE	2,412.1	550.6	21.0	0.0	3234	0.0	925.9	540.9	1,466.8	2.66	

WES CONSTRUCTION DIST. 1253A

PAGE 1 OF 2

Figure F33. Factor of safety against sliding after posttensioning, dam piers 10, 11, 12, 14, 15, and 16, Soo Dam (Continued)

SUBJECT DAM PIERS 10,11,12,14,15, AND 16 - FACTOR OF SAFETY AGAINST SLIDING AFTER POSTTENSIONING										COMPUTED BY:	DATE:
										CHECKED BY:	DATE:
LOAD CASE	SUM OF VERTICAL FORCES	SUM OF HORIZONTAL FORCES	FRICTION ANGLE (DEGREES)	CONCRETE STRENGTH (KSF)	BASE AREA (FT <sup>2</sup> )	STROT RESISTANCE (KIPS)	SHEAR RESISTANCE (KIPS)	HORIZONTAL COMPONENT OF POSTTENSIONING FORCE (KIPS)	TOTAL SLIDING RESISTANCE (KIPS)	FACTOR OF SAFETY AGAINST SLIDING $FS = \frac{R}{F_h}$	
	$F_v'$ (KIPS)	$F_h$ (KIPS)	$\phi$ (DEGREES)	$C$ (KSF)	$A$ (FT <sup>2</sup> )	$R_s$ (KIPS)	$R_s + F_v' \tan \phi + C$ (KIPS)	$P_p$ (KIPS)	$R = R_s + P_p$ (KIPS)		
<u>PIER AND APPROX. SECTION AT ELEV 524.75</u>											
NORMAL OPERATION	2,715.5	407.9	21.0	0.0	3234	0.0	1,042.4	540.9	1,583.3	3.88	
NORMAL OPERATION WITH ICE	2,715.5	1,010.0	21.0	0.0	3234	0.0	1,042.4	540.9	1,583.3	1.57	
HIGH - WATER CONDITION	2,635.5	473.7	21.0	0.0	3234	0.0	1,011.7	540.9	1,552.6	3.28	
NORMAL OPERATION WITH EARTHQUAKE	2,715.5	607.9	21.0	0.0	3234	0.0	1,042.4	540.9	1,583.3	2.60	

SEE COVER OF 1253A  
CONTINUED ON 1253A

PAGE 2 OF 2

Figure F33. (Concluded)

SUBJECT DAM PIERS 10,11,12,14,15,AND 16- MINIMUM BASE PRESSURES AFTER POST-TENSIONING, CONCRETE-FOUNDATION INTERFACE										COMPUTED BY		DATE		
										CHECKED BY		DATE		
LOAD CASE	SUM OF VERTICAL FORCES	SUM OF MOMENTS	RESULTANT MOMENT ARM	DISTANCE TO CENTROID OF AREA IN COMPRESSION	AREA OF PIER BASE IN COMPRESSION	INERTIA OF BASE AREA IN COMPRESSION	LOCATION	DISTANCE TO OUTER FIBER OF BASE	AXIAL PRESSURE	PRESSURE DUE TO BENDING MOMENT	INTERGRAVITY PRESSURES	UP-LIFT HEAD	UP-LIFT PRESSURE	TOTAL BASE PRESSURE
—	$F_v$	$M$	$e = \frac{M}{F_v}$	D	A	I	—	C	$f_a = \frac{F_v}{A}$	$f_b = \frac{M}{S}$	$f_c = f_a + f_b$	h	$f_u = \gamma_w h$	$f = f_c + f_u$
—	KIPS	FT-K	FT	FT	FT <sup>2</sup>	FT <sup>4</sup>	—	FT	KSF	KSF	KSF	FT	KSF	KSF
NORMAL OPERATION	1,826.3	55,776	30.54	29.37	519.76	120,322	HEEL	29.37	3.51	0.52	4.03	16.0	1.00	5.03
							TOE	29.37	3.51	-0.52	2.99	7.5	0.47	3.46
NORMAL OPERATION WITH ICE	1,826.3	46,744	25.59	29.37	519.76	120,322	HEEL	29.37	3.51	-1.69	1.82	16.0	1.00	2.82
							TOE	29.37	3.51	1.69	5.20	7.5	0.47	5.67
HIGH-WATER CONDITION	1,807.3	54,632	30.23	29.37	519.76	120,322	HEEL	29.37	3.48	0.38	3.86	17.0	1.06	4.92
							TOE	29.37	3.48	-0.38	3.10	7.5	0.47	3.57
NORMAL OPERATION WITH EARTHQUAKE	1,826.3	54,487	29.83	29.37	519.76	120,322	HEEL	29.37	3.51	0.21	3.72	16.0	1.00	4.72
							TOE	29.37	3.51	-0.21	3.30	7.5	0.47	3.77

WES FORM NO. 1233A  
FEBRUARY 1961

PAGE 1 OF 1

Figure F34. Maximum base pressures after posttensioning (pier section only), concrete-foundation interface, dam piers 10, 11, 12, 14, 15, and 16, Soo Dam

SUBJECT

DAM PIERS 4 AND 13 - FORCES AFTER POSTTENSIONING

COMPUTED BY

DATE

CHECKED BY:

DATE

LOAD CASE	SUM OF VERTICAL FORCES $F_v$	VERTICAL COMPONENT OF POSTTENSIONING FORCE $P_v = P \sin 45^\circ$	SUM OF VERTICAL FORCES AFTER POSTTENSIONING $F_v = F_v + P_v$	SUM OF HORIZONTAL FORCES $F_h$
<u>PIER ONLY</u>	KIPS	KIPS	KIPS	KIPS
NORMAL OPERATION	1,573.3	475.9	2,049.2	269.1
NORMAL OPERATION WITH ICE	1,573.3	475.9	2,049.2	876.2
HIGH - WATER CONDITION	1,549.8	475.9	2,025.7	331.7
NORMAL OPERATION WITH EARTHQUAKE	1,573.3	475.9	2,049.2	370.2
<u>PIER AND FOUNDATION</u>				
NORMAL OPERATION	1,573.3	475.9	2,049.2	269.1
NORMAL OPERATION WITH ICE	1,573.3	475.9	2,049.2	876.2
HIGH - WATER CONDITION	1,549.8	475.9	2,025.7	331.7
NORMAL OPERATION WITH EARTHQUAKE	1,573.3	475.9	2,049.2	370.2
<u>PIER AND APRON SECTION AT ELEVATION 545.95</u>				
NORMAL OPERATION	2,138.6	475.9	2,614.5	379.0
NORMAL OPERATION WITH ICE	2,138.6	475.9	2,614.5	986.1
HIGH - WATER CONDITION	2,061.4	475.9	2,537.3	441.6
NORMAL OPERATION WITH EARTHQUAKE	2,138.6	475.9	2,614.5	570.2

1253A

PAGE 1 OF 2

Figure F35. Forces after posttensioning, dam piers 9 and 13, Soo Dam (Continued)

SUBJECT DAM PIERS 9 AND 13 -- FORCES AFTER POSTTENSIONING		COMPUTED BY:	DATE:	
		CHECKED BY:	DATE:	
LOAD CASE	SUM OF VERTICAL FORCES $F_v$	VERTICAL COMPONENT OF POSTTENSIONING FORCE $P' = P \sin 45^\circ$	SUM OF VERTICAL FORCES AFTER POSTTENSIONING $F_v' = F_v + P'$	SUM OF HORIZONTAL FORCES $F_H$
	KIPS	KIPS	KIPS	KIPS
<u>PIER AND APRON SECTION AT ELEVATION 564.75</u>				
NORMAL OPERATION	2,444.5	475.9	2,920.4	411.2
NORMAL OPERATION WITH ICE	2,444.5	475.9	2,920.4	1,018.3
HIGH - WATER CONDITION	2,361.5	475.9	2,837.4	471.6
NORMAL OPERATION WITH EARTHQUAKE	2,444.5	475.9	2,920.4	627.9

WES. FORM NO. 125.3A  
OCTOBER 1966

PAGE 2 OF 2

Figure F35. (Concluded)

SUBJECT: DAM PIERS 9 AND 13 - FACTOR OF SAFETY AGAINST SLIDING AFTER POSTTENSIONING										COMPUTED BY:	DATE
										CHECKED BY:	DATE
LAND CASE	SUM OF VERTICAL FORCES	SUM OF HORIZONTAL FORCES	PRICITION ANGLE (DEGREES)	COHESIVE STRENGTH (KSF)	BASE AREA (FT <sup>2</sup> )	SHAFT RESISTANCE (KIPS)	SHEAR RESISTANCE (KIPS)	HORIZONTAL COMPONENT OF POSTTENSIONING FORCE (KIPS)	TOTAL SLIDING RESISTANCE (KIPS)	FACTOR OF SAFETY AGAINST SLIDING $FS = \frac{R}{F_H}$	
<u>PIER ONLY</u>	$F_v'$ (KIPS)	$F_H$ (KIPS)	$\phi$ (DEGREES)	$c$ (KSF)	$A$ (FT <sup>2</sup> )	$R_s$ (KIPS)	$R = \frac{1}{4} \sum c \cdot b_i$ (KIPS)	$R_p$ (KIPS)	$R = R_s + R_p$ (KIPS)		
NORMAL OPERATION	2,049.2	249.1	32.1	0.0	629	515.3	1,285.5	475.9	2,276.7	8.46	
NORMAL OPERATION WITH ICE	2,049.2	876.2	32.1	0.0	629	515.3	1,185.5	475.9	2,276.7	2.60	
HIGH WATER CONDITION	2,025.7	331.7	32.1	0.0	629	515.3	1,270.7	475.9	2,261.9	6.82	
NORMAL OPERATION WITH EARTHQUAKE	2,049.2	390.2	32.1	0.0	629	515.3	1,285.5	475.9	2,276.7	5.83	
<u>PIER AND FOUNDATION</u>											
NORMAL OPERATION	2,049.2	249.1	21.0	0.0	629	515.3	786.6	475.9	1,777.8	6.61	
NORMAL OPERATION WITH ICE	2,049.2	876.2	21.0	0.0	629	515.3	786.6	475.9	1,777.8	2.03	
HIGH-WATER CONDITION	2,025.7	331.7	21.0	0.0	629	515.3	777.6	475.9	1,768.8	5.33	
NORMAL OPERATION WITH EARTHQUAKE	2,049.2	390.2	21.0	0.0	629	515.3	786.6	475.9	1,777.8	4.56	
<u>PIER AND APRON SECTION AT ELEV. 595.5</u>											
NORMAL OPERATION	2,114.5	379.0	21.0	0.0	3,261	0.0	1,003.6	475.9	1,476.5	3.90	
NORMAL OPERATION WITH ICE	2,164.5	986.1	21.0	0.0	3,261	0.0	1,003.6	475.9	1,476.5	1.50	
HIGH-WATER CONDITION	2,153.3	441.6	21.0	0.0	3,261	0.0	974.0	475.9	1,449.9	3.28	
NORMAL OPERATION WITH EARTHQUAKE	2,164.5	570.2	21.0	0.0	3,261	0.0	1,003.6	475.9	1,476.5	2.59	

1233A

PAGE 1 OF 2

Figure F36. Factor of safety against sliding after posttensioning, dam piers 9 and 13, Soo Dam (Continued)

SUBJECT DAM PIERS 9 AND 13 - FACTOR OF SAFETY AGAINST SLIDING AFTER POSTTENSIONING										COMPUTED BY	DATE
										CHECKED BY:	DATE
LOAD CASE	SUM OF VERTICAL FORCES	SUM OF HORIZONTAL FORCES	FRICTION ANGLE	COHESIVE STRENGTH	BASE AREA	STILT RESISTANCE	SHEAR RESISTANCE	HORIZONTAL COMPONENT OF ACTING FORCE	TOTAL SLIDING RESISTANCE	FACTOR OF SAFETY AGAINST SLIDING	
	$F_v$ (KIPS)	$F_H$ (KIPS)	$\phi$ (DEGREES)	C (KSF)	A ( $FT^2$ )	$R_s$ (KIPS)	$R_f = F_v \tan \phi + CA$ (KIPS)	$R_p$ (KIPS)	$R = R_s + R_f + R_p$ (KIPS)	$FS = \frac{R}{F_H}$	
<u>PIER AND ABUT SECTION AT ELEV 547.75</u>											
NORMAL OPERATION	2,920.4	411.2	21.0	0.0	3,261	0.0	1,121.0	475.9	1,596.9	3.88	
NORMAL OPERATION WITH ICE	2,920.4	1,018.3	21.0	0.0	3,261	0.0	1,121.0	475.9	1,596.9	1.57	
HIGH-WATER CONDITION	2,837.4	477.6	21.0	0.0	3,261	0.0	1,049.2	475.9	1,565.1	3.28	
NORMAL OPERATION WITH EARTHQUAKE	2,920.4	627.9	21.0	0.0	3,261	0.0	1,121.0	475.9	1,596.9	2.54	

SEE FORM NO. 1233A  
REVISION ONE

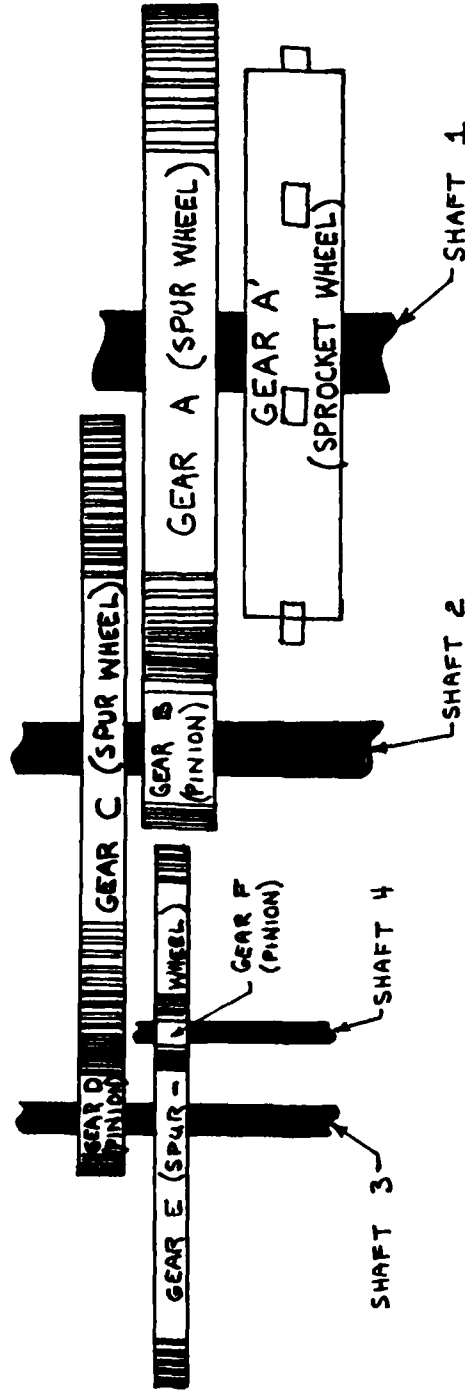
Figure F36. (Concluded)



APPENDIX G  
STRESS ANALYSIS OF GATES AND OPERATING MACHINERY,  
FIGURES AND COMPUTATIONS

# GEAR AND SHAFT LOCATIONS

— FLOW



PLAN VIEW

SUBJECT	GATE MACHINERY	COMPUTED BY	DATE
		CHECKED BY	DATE

GEAR DETAILS

GEAR	TYPE MATERIAL	NUMBER TEETH	PITCH (IN)	INVOLUTE (DEGREES)	PITCH DIAMETER (IN)	SHAFT DIAMETER (IN)
A	CAST STEEL	9	16.84	—	48.00	6.75
A	CAST STEEL	68	2.75	15	59.52	6.75
B	CAST STEEL	15	2.75	15	13.13	4.50
C	CAST IRON	92	2.00	15	58.57	4.50
D	CAST IRON	15	2.00	15	9.55	2.50
E	CAST IRON	121	1.25	15	48.14	2.50
F	CAST IRON	15	1.25	15	5.97	1.50

Figure G1. (Sheet 2 of 6)

SUBJECT GATE MACHINERY

COMPUTED BY

DATE

CHECKED BY

DATE

# FORCES AND TORQUES ON GEARS

## GEAR A' (SPROCKET WHEEL)

$$F_A' = \frac{\text{WEIGHT OF GATE} - \text{COUNTERWEIGHT}}{2} = \frac{36,400 - 28,800}{2} = 7,600 \text{ lbs}$$

$$T_A' = (7,600) (48) (1/2) = 182,400 \text{ lb-in.}$$

## GEAR A (SPUR WHEEL)

$$F_A = \frac{(7,600) (48)}{59.52} = 6,129 \text{ lbs}$$

$$T_A = T_A' = 182,400 \text{ lb-in.}$$

## GEAR B (PINION)

$$F_B = F_A = 6,129 \text{ lbs}$$

$$T_B = (6,129) (13.13) (1/2) = 40,237 \text{ lb-in.}$$

## GEAR C (SPUR WHEEL)

$$F_C = \frac{(6,129) (13.13)}{58.57} = 1,374 \text{ lbs}$$

$$T_C = T_B = 40,237 \text{ lb-in.}$$

## GEAR D (PINION)

$$F_D = F_C = 1,374 \text{ lbs}$$

$$T_D = (1,374) (9.55) (1/2) = 6,561 \text{ lb-in.}$$

## GEAR E (SPUR WHEEL)

$$F_E = \frac{(1,374) (9.55)}{48.14} = 273 \text{ lbs}$$

$$T_E = T_D = 6,561 \text{ lb-in.}$$

## GEAR F (PINION)

$$F_F = F_E = 273 \text{ lbs}$$

$$T_F = (273) (5.97) (1/2) = 815 \text{ lb-in.}$$

Figure G1. (Sheet 3 of 6)

SUBJECT GATE MACHINERY		COMPUTED BY	DATE
		CHECKED BY	DATE

STRESS IN GEARS

GEAR	PRESSURE ANGLE	TRANSMITTED LOAD	TANGENTIAL COMPONENT OF LOAD	RADIAL COMPONENT OF LOAD	LENGTH OF GEAR TOOTH	WIDTH OF GEAR TOOTH AT ROOT FILLET	INERTIA OF AREA AT BASE OF TOOTH	DISTANCE FROM OUTRA-MOUTH FACE OF GEAR TO BASE AREA	MOMENT ARM FOR LOAD $W_e$	MOMENT ARM FOR LOAD $W_t$	MOMENT	AXIAL STRESS	BENDING STRESS	MAXIMUM TENSILE STRESS	MAXIMUM COMPRESSIVE STRESS
—	$\phi$	$W$	$W_t = W \cos \phi$	$W_r = W \sin \phi$	$L$	$W$	$I = \frac{W^3}{12}$	$C = \frac{W}{2}$	$Q_e$	$Q_t = W_e \cdot W_t$	$in \cdot lb$	$\sigma = \frac{W_t}{L \cdot W}$	$\sigma = \frac{M}{I}$	$\sigma = \sigma_b - \sigma_a$	$\sigma = \sigma_b + \sigma_a$
—	DEGREES	LBS	LBS	LBS	in	in	in <sup>4</sup>	in	in	in	in	PSI	PSI	PSI	PSI
A	0°	7,600	7,600	0	2	3.00	4.50	1.50	2.50	1.45	19,000	0	6,333	6,333	6,333
A	15	6,129	5,920	1,586	6	1.59	2.01	0.80	1.56	0.85	7,887	166	3,139	2,973	3,305
B	15	6,129	5,920	1,586	6	1.26	1.00	0.63	1.44	0.72	7,383	210	4,651	4,441	4,861
C	15	1,374	1,327	356	4	1.19	0.56	0.60	1.14	0.34	1,392	75	1,491	1,416	1,566
D	15	1,374	1,327	356	4	0.90	0.24	0.45	1.05	0.30	1,287	99	2,413	2,314	2,512
E	15	273	264	71	2.5	0.76	0.04	0.38	0.71	0.21	173	37	730	693	767
F	15	273	264	71	2.5	0.53	0.03	0.26	0.65	0.18	159	54	1,378	1,324	1,432

\* ASSUMED MOST CRITICAL PRESSURE ANGLE

Figure G1. (Sheet 4 of 6)

SUBJECT

GATE MACHINERY

COMPUTED BY

DATE

CHECKED BY

DATE

STRESS IN SHAFTS

SHAFT	TORQUE	DIAMETER OF SHAFT	POLAR MOMENT OF INERTIA	DISTANCE FROM CENTROID TO OUTER-MOST FIBER	SHEARING STRESS
—	T	d	$J = \frac{\pi d^4}{32}$	$C = \frac{d}{2}$	$\tau = \frac{T C}{J}$
—	LBS	IN	IN <sup>4</sup>	IN	PSI
1	182,400	6.75	203.8	3.38	3,025
2	40,237	4.50	40.3	2.25	2,247
3	6,561	2.50	3.8	1.25	2,158
4	815	1.50	0.5	0.75	1,222

REVISED BY

1253A

DATE

PAGE

5 OF 6

Figure G1. (Sheet 5 of 6)

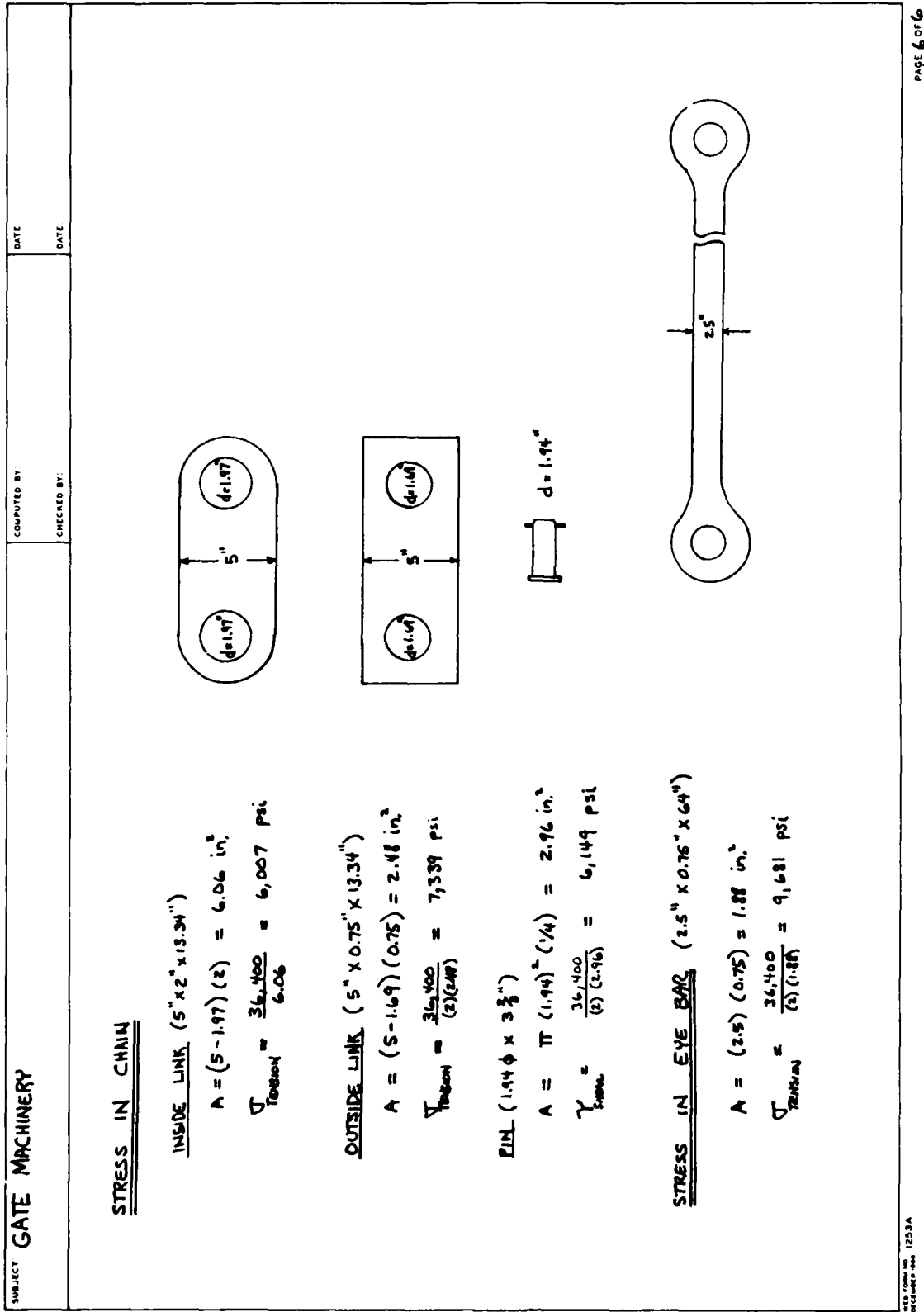


Figure G1. (Sheet 6 of 6)

SUBJECT	SLUICE GATE	COMPUTED BY:	DATE:
		CHECKED BY:	DATE:

STRESS ANALYSIS WITH GIRDER AS RIB - NORMAL OPERATION WITH ICE

LOADS ON GIRDERS

DISTRIBUTION FACTORS

$$DF_{AB} = \frac{5.42}{5.42 + 6.67} = 0.4483$$

$$DF_{BC} = \frac{6.67}{5.42 + 6.67} = 0.5517$$

FIXED END MOMENTS DUE TO ICE LOADING

$$M_B = \frac{10,000 (5.07) (1.00)^2}{(4.67)^2} = 2,917 \text{ lb-ft}$$

$$M_C = -\frac{10,000 (5.07) (1.60)}{(4.67)^2} = -9,245 \text{ lb-ft}$$

FIXED END MOMENTS DUE TO WATER LOADINGS

$$M_A = \frac{(8)(6.25)(5.42)^2}{12} = 1,224 \text{ lb-ft}$$

$$M_B = -M_A = -1,224 \text{ lb-ft}$$

Figure G2. Stress analysis of sluice gates, Soo Dam (Sheet 1 of 18)



SUBJECT SLUICE GATE

COMPUTED BY:

DATE:

CHECKED BY:

DATE:

FIXED END MOMENT DUE TO WATER LOADS (CONTINUED)

$$EI\theta_1 = 0$$

$$\frac{V_L l^2}{2} - M_L l = \frac{w l^3}{6} \frac{a}{4}$$

$$\frac{V_L (6.07)}{2} - M_L = \frac{(6.25)(6.07)^3}{24}$$

$$3.34 V_L - M_L = 530.03 \quad (1)$$

$$EI\Delta_1 = 0$$

$$\frac{V_L l^3}{6} - \frac{M_L l^2}{2} = \frac{w l^4}{24} \frac{a}{5}$$

$$\frac{V_L (6.07)}{3} - M_L = \frac{(6.25)(6.07)^5}{(120)(4.47)^2}$$

$$2.22 V_L - M_L = 192.94 \quad (2)$$

$$EQ (1) - EQ (2)$$

$$1.12 V_L = 337.09$$

$$V_L = 301.0 \text{ lbs}$$

$$M_L = 192.94 - (2.22)(301.0)$$

$$M_L = -475.28 \text{ lb-ft}$$

$$M_B = \frac{(6.25)(6.07)^3}{6} + 475.28 - (301)(6.07)$$

$$M_B = 797.28 \text{ lb-ft}$$

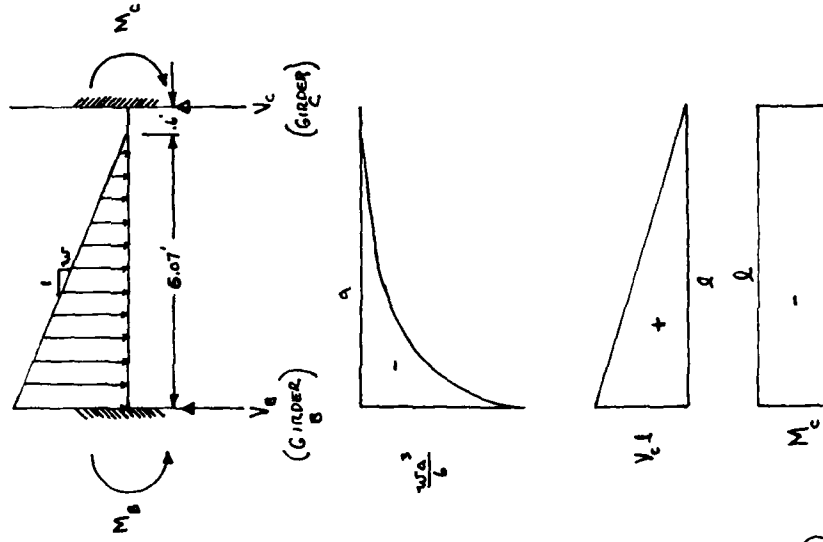


Figure G2. (Sheet 2 of 18)

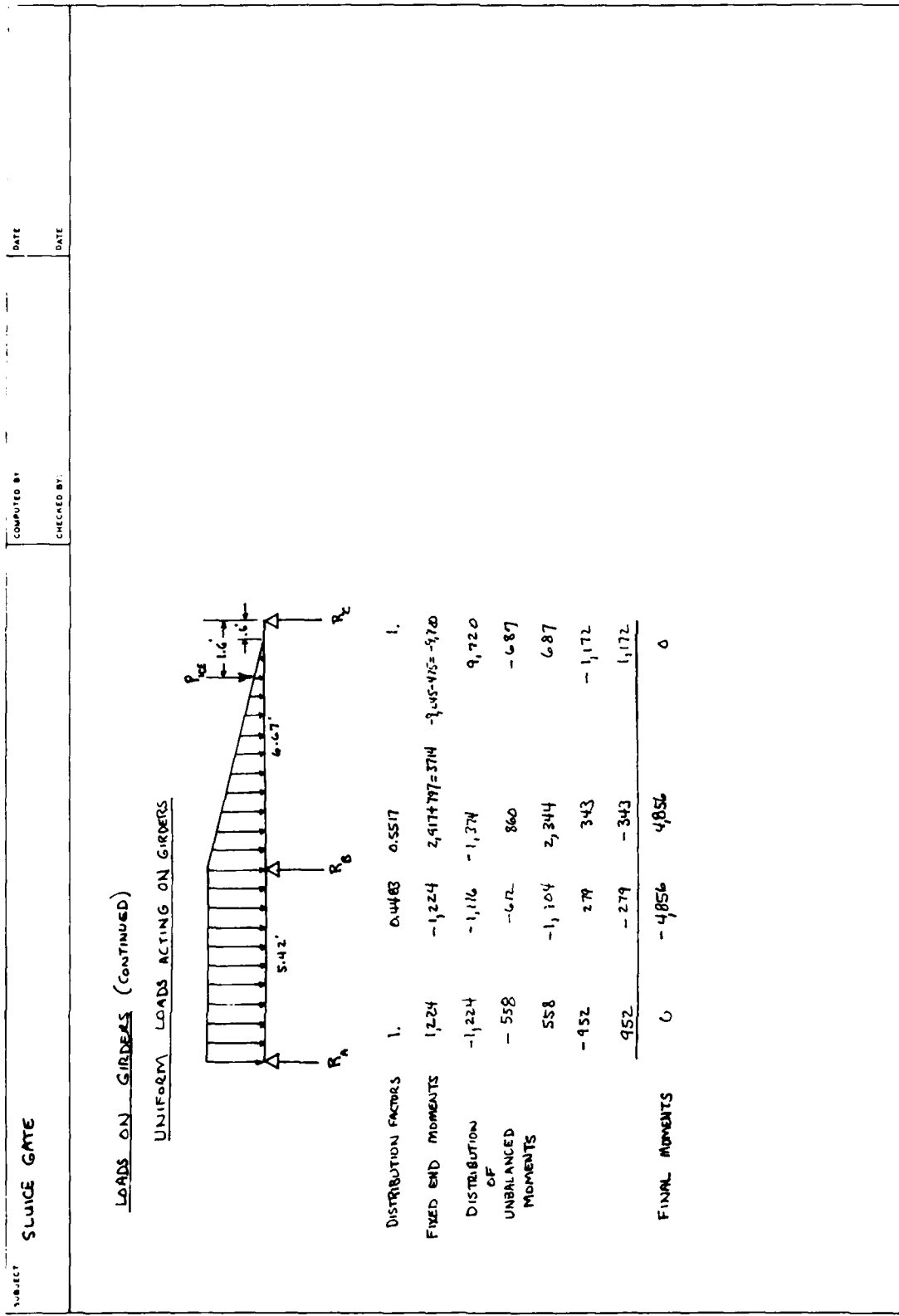


Figure G2. (Sheet 3 of 18)

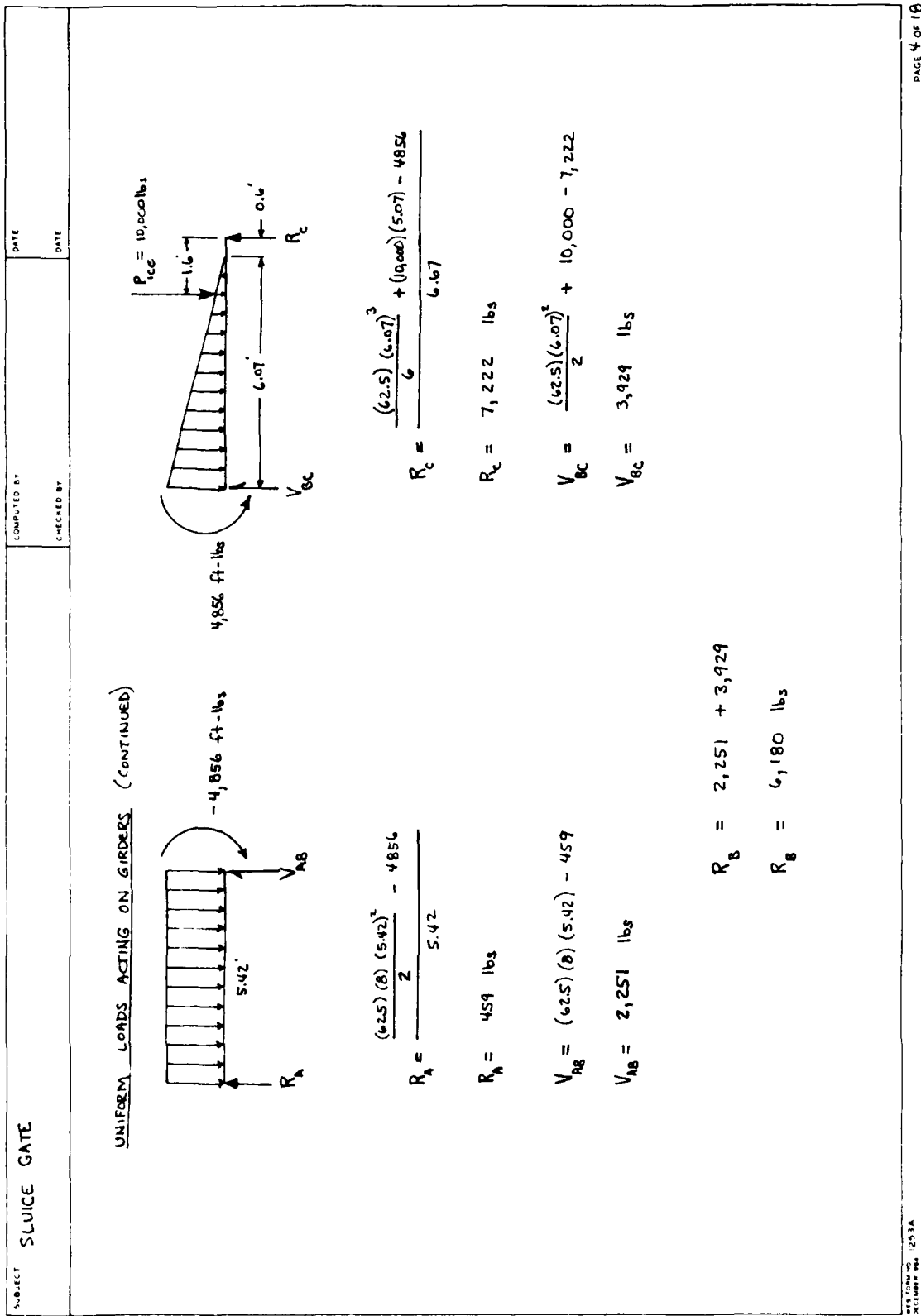


Figure G2. (Sheet 4 of 18)

SUBJECT	SLUICE GATE	COMPUTED BY	DATE
		CHECKED BY	DATE

### STRESS IN GIRDER B

ITEM	AREA, A	INERTIA, I	DISTANCE FROM CENTROID TO DOWNSTREAM EDGE OF GIRDER, y	A <sub>y</sub>	A <sub>y</sub> <sup>2</sup>
—	IN <sup>2</sup>	IN <sup>4</sup>	IN	IN <sup>3</sup>	IN <sup>4</sup>
SKIN PLATE	6.3	0	32.06	202.0	6,475
2-L's 6"x4"x $\frac{5}{8}$ "	11.7	42	24.95	349.2	10,425
WEB PLATE (31"x $\frac{3}{8}$ " x $\frac{5}{8}$ )	11.7	954	14.25	190.1	3,090
2-L's 6"x6"x $\frac{5}{8}$ "	14.2	48	2.36	33.5	79
BACK PLATE (6"x $\frac{3}{8}$ " x 5')	4.2	0	0.31	1.3	0
SUM	48.1	1,044	—	776.1	20,069

$$\bar{y} = \frac{776.1}{48.1} = 16.14 \text{ in.}$$

$$I_{CG} = 1044 + 20,069 - (48.1)(16.14)^2 = 8,583 \text{ in.}^4$$

$$S_{CG_{RHS}} = \frac{8,583}{16.14} = 531.8 \text{ in.}^3$$

$$S_{CG_{LATE}} = \frac{8,583}{32.28-16.14} = 532.8 \text{ in.}^3$$

$$M = \frac{(6,180)(53.49)^2(12)}{(12)} = 17,682,000 \text{ in.-lb}$$

$$f_{RHS} = \frac{17,682,000}{531.8} = 33,249 \text{ psi}$$

$$f_{LATE} = \frac{17,682,000}{532.8} = 33,187 \text{ psi}$$

$$\text{EFFECTIVE WIDTH OF SKIN PLATE} = \frac{253(.375)}{\sqrt{32}}$$

$$= 16.77 \text{ in.}$$

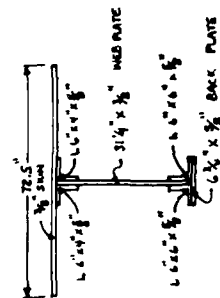


Figure G2. (Sheet 5 of 18)

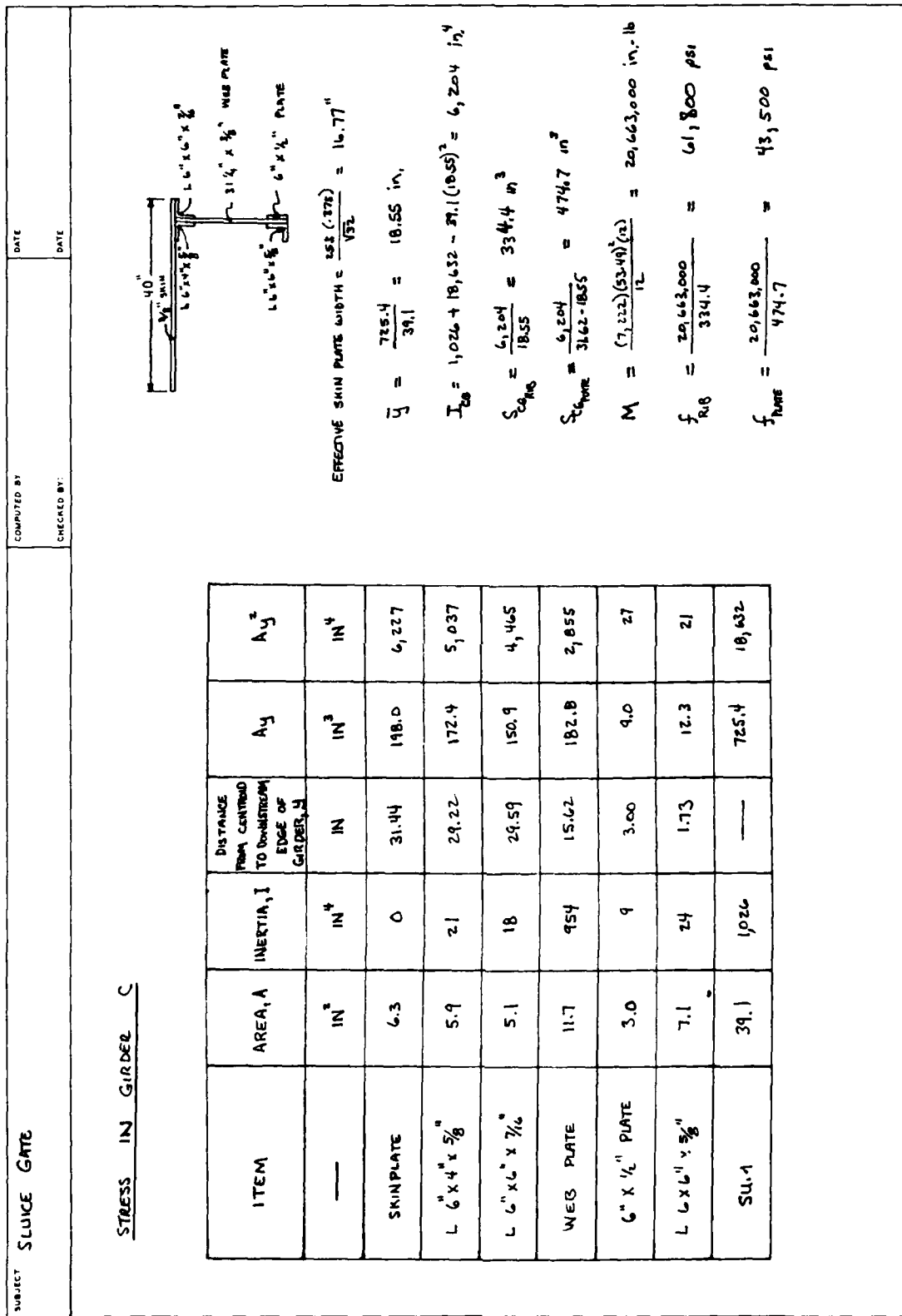


Figure G2. (Sheet 6 of 18)

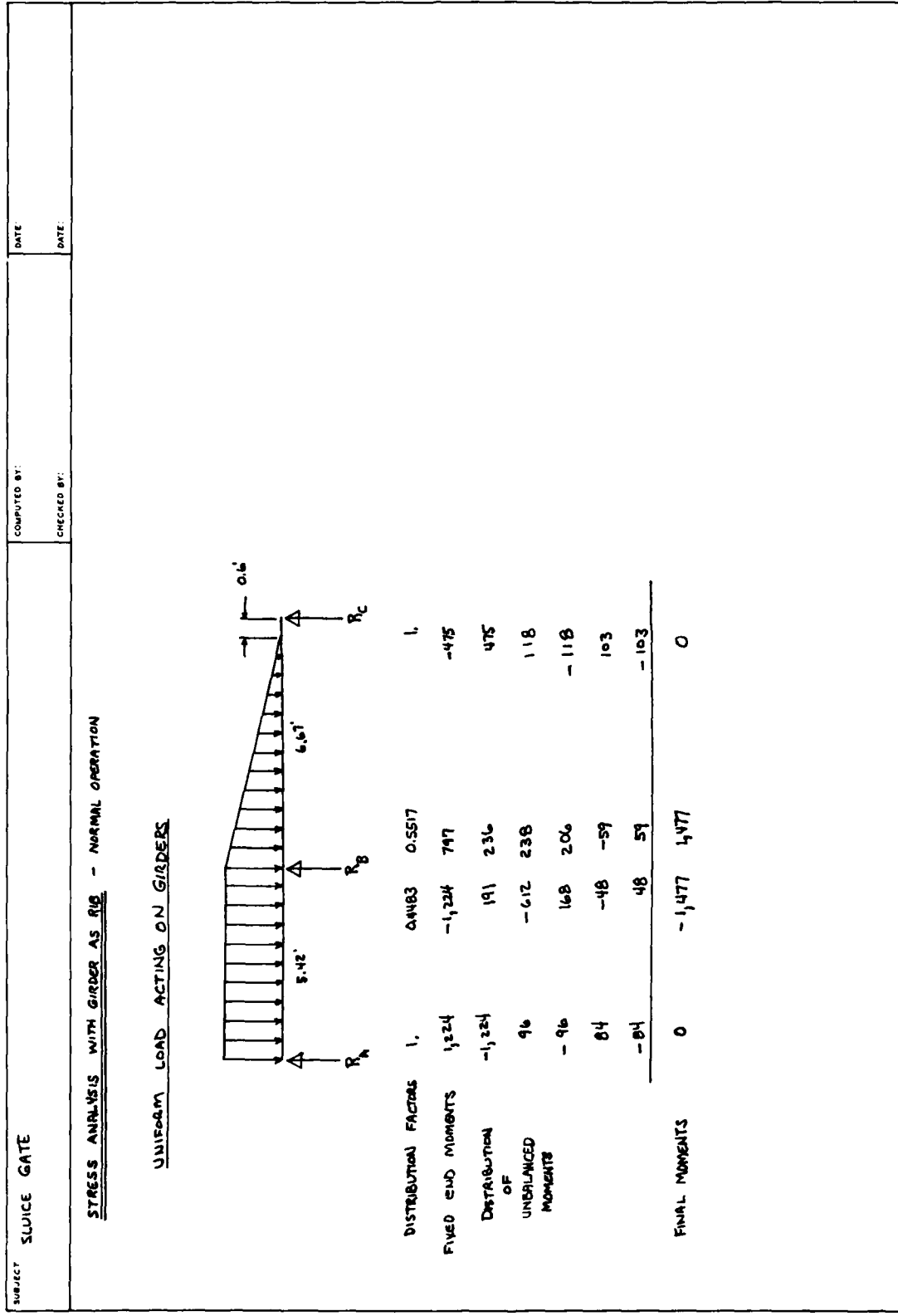


Figure G2. (Sheet 7 of 18)

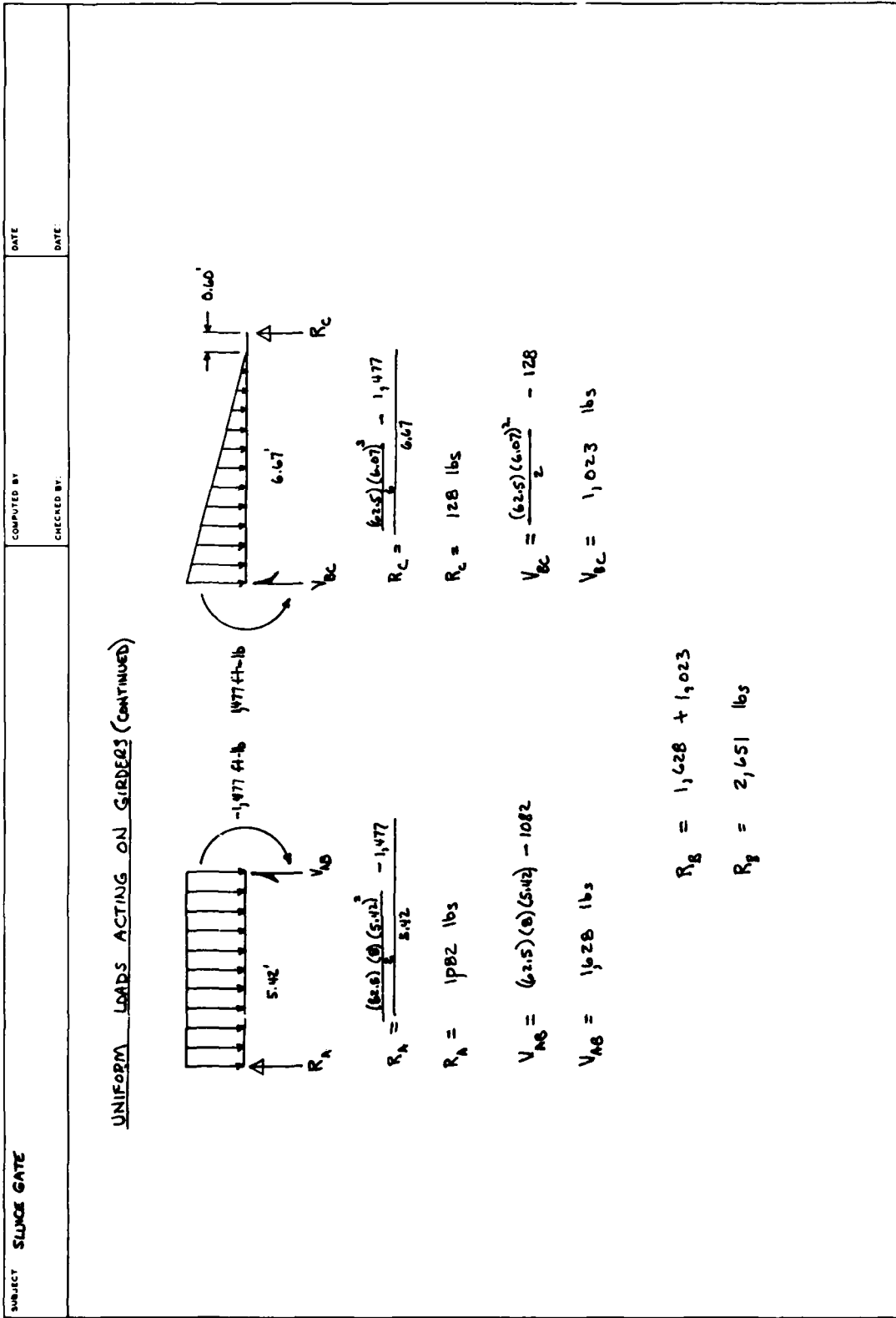


Figure G2. (Sheet 8 of 18)

SUBJECT	SLUICE GATE		COMPUTED BY:	DATE
			CHECKED BY:	DATE

STRESS IN GIRDER B

$$S_{CG_{RIB}} = 531.8 \text{ in}^3$$

$$S_{CG_{PLATE}} = 532.8 \text{ in}^3$$

$$M = \frac{(2,651)(53.49)^2(12)}{(12)} = 7,585,000 \text{ in.-lb}$$

$$f_{RIB} = \frac{7,585,000}{531.8} = 14,260 \text{ psi}$$

$$f_{PLATE} = \frac{7,585,000}{532.8} = 14,236 \text{ psi}$$

STRESS IN GIRDER C

$$S_{CG_{RIB}} = 334.4 \text{ in}^3$$

$$S_{CG_{PLATE}} = 474.7 \text{ in}^3$$

$$M = \frac{(128)(53.49)^2(12)}{(12)} = 366,200 \text{ in.-lb}$$

$$f_{RIB} = \frac{366,200}{334.4} = 1,095 \text{ psi}$$

$$f_{PLATE} = \frac{366,200}{474.7} = 771 \text{ psi}$$

Figure G2. (Sheet 9 of 18)



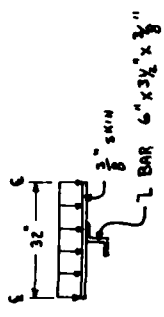
SUBJECT SLUICE GATE	COMPUTED BY	DATE	CHECKED BY	DATE
<p><u>STRESS ANALYSIS WITH SKINPLATE AS A BEAM - NORMAL OPERATION WITH ICE</u></p> <p><u>BETWEEN L BAR SUPPORTS IN AREA BETWEEN GIRDERS A AND B</u></p> <div style="display: flex; justify-content: space-between; align-items: flex-start;"> <div style="width: 45%;"> <p>CLEAR SPAN = 32 - 3.5 = 28.5 in.</p> <math display="block">w = \frac{(625) (401.75 - 593.75) (28.5)}{(12)^3} = 98.96 \text{ lb/in.}</math> <math display="block">M = \frac{(98.96) (28.5)^2}{10} = 8,038 \text{ in.-lb}</math> <math display="block">S = \frac{28.5 (.375)^2}{6} = 0.668 \text{ in.}^3</math> <math display="block">f = \frac{8038}{0.668} = 12,033 \text{ psi}</math> </div> <div style="width: 45%; text-align: right;">  </div> </div>				
<p><u>BETWEEN L BAR SUPPORTS IN AREA BETWEEN GIRDERS B AND C</u></p> <div style="display: flex; justify-content: space-between; align-items: flex-start;"> <div style="width: 45%;"> <math display="block">f_{ave} = \frac{(625) (607)^2}{6.67} + \frac{(5,000) (2)}{6.67} = 1,672 \text{ lb/in.}^2</math> <math display="block">w = \frac{(1,672) (28.5)}{(12)^2} = 330.92 \text{ lb/in.}</math> <math display="block">M = \frac{(330.92) (28.5)^2}{10} = 24,879 \text{ in.-lb}</math> <math display="block">f = \frac{24,879}{0.668} = 40,238 \text{ psi}</math> </div> </div>				

Figure G2. (Sheet 10 of 18)

SUBJECT	SLUICE GATE	COMPUTED BY	DATE
		CHECKED BY:	DATE:

STRESS ANALYSIS WITH SHEAR PLATE AS A BEAM - NORMAL OPERATION

BETWEEN 2 BAR SUPPORTS IN AREA BETWEEN GIRDERS A AND B

$$w = \frac{(62.5)(601.75 - 573.75)(28.5)}{(12)^3} = 98.96$$

$$M = \frac{(98.96)(28.5)^2}{10} = 8,038 \text{ in.-lb}$$

$$S = \frac{(28.5)(0.375)^2}{6} = 0.648 \text{ in.}^3$$

$$f = \frac{8,038}{0.648} = 12,033 \text{ psi}$$

BETWEEN 2 BAR SUPPORTS IN AREA BETWEEN GIRDERS B AND C

$$f_{ave} = \frac{(62.5)(6.07)^2}{(5)(6.67)} = 172.6$$

$$w = \frac{(172.6)(28.5)}{(12)^3} = 34.16 \text{ lb/in.}$$

$$M = \frac{(34.16)(28.5)^2}{10} = 2,775 \text{ in.-lb}$$

$$f = \frac{2,775}{0.668} = 4,154 \text{ psi}$$

Figure G2. (Sheet 11 of 18)

SUBJECT	SLUICE GATE	COMPUTED BY	DATE
		CHECKED BY	DATE

STRESS ANALYSIS WITH L BAR AS RIB - NORMAL OPERATION WITH ICE

AREA BETWEEN GIRDERS A AND B

ITEM	AREA, A IN. <sup>2</sup>	INERTIA, I IN. <sup>4</sup>	DISTANCE FROM CENTROID TO DOWNSTREAM EDGE OF GIRDER, Y IN.	A <sub>y</sub> IN. <sup>3</sup>	A <sub>y</sub> <sup>2</sup> IN. <sup>4</sup>
SKIN PLATE	6.29	0.07	6.19	38.9	241.01
L BAR	4.59	4.55	3.00	13.8	41.31
SUM	10.88	4.62	—	52.7	282.32

$$\text{EFFECTIVE SKINPLATE WIDTH} = \left[ \frac{253 (375)}{\sqrt{32}} \right]^* = 16.77 \text{ in.}$$

$$\bar{y} = \frac{52.7}{10.88} = 4.84 \text{ in.}$$

$$I_{CG} = 4.62 + 282.32 - (10.88)(4.84)^2 = 32.07 \text{ in.}^4$$

$$S_{PLATE} = \frac{32.07}{6.38-4.84} = 20.82 \text{ in.}^3$$

$$S_{L-BAR} = \frac{32.07}{4.84} = 6.63 \text{ in.}^3$$

\* FROM SECTION 1.9.2.2, 1969 AISI CODE

Figure G2. (Sheet 12 of 18)

SUBJECT	SWIPE GATE	COMPUTED BY	DATE
		CHECKED BY:	DATE

STRESS ANALYSIS WITH L BAR AS RIB - NORMAL OPERATION WITH ICE

AREA BETWEEN GIRDERS A AND B (CONTINUED)

$$M = 4,856 \quad \text{ft-lb}$$

$$M = 58,272 \quad \text{in-lb}$$

$$f_{\text{tune}} = \frac{58,272}{20.82} = 2,799 \text{ psi}$$

$$f_{\text{rib}} = \frac{58,272}{6.63} = 8,789 \text{ psi}$$

$$\left. \begin{array}{l} \text{COMBINED BIAxIAL} \\ \text{STRESS FACTOR} \\ \text{(SKIN PLATE)} \end{array} \right\} = \frac{(15,033)^2 - (12,033)(2,799) + (2,799)^2}{0.75 (82,000)^2} = 0.15$$

AREA BETWEEN GIRDERS B AND C

$$M = (7,222)(1.6) = 11,555 \text{ ft-lb}$$

$$M = 138,660 \text{ in-lb}$$

$$f_{\text{tune}} = \frac{138,660}{20.82} = 6,660 \text{ psi}$$

$$f_{\text{rib}} = \frac{138,660}{6.63} = 20,914 \text{ psi}$$

$$\left. \begin{array}{l} \text{COMBINED BIAxIAL} \\ \text{STRESS FACTOR} \\ \text{(SKIN PLATE)} \end{array} \right\} = \frac{(40,238)^2 - (40,238)(20,914) + (20,914)^2}{0.75 (32,000)^2} = 1.58$$

Figure G2. (Sheet 13 of 18)

SUBJECT <b>SLUICE GATE</b>	COMPUTED BY:  CHECKED BY:	DATE	DATE
-------------------------------	---------------------------------	------	------

**STRESS ANALYSIS WITH 1 BAR A3 RB - NORMAL OPERATION**

AREA BETWEEN GIRDERS A AND B

$M = 1477 \text{ ft-lb}$

$M = 17,724 \text{ in.-lb}$

$f_{\text{FUTE}} = \frac{17,724}{20.82} = 851 \text{ psi}$

$f_{\text{RUB}} = \frac{17,724}{6.63} = 2,673 \text{ psi}$

COMBINED BIASIAL STRESS FACTOR (SKIN PLATE)  $= \frac{(14,033)^2 - (14,033)(851) + (851)^2}{(0.75)(32,000)^2} = 0.18$

AREA BETWEEN GIRDERS B AND C

$M = 1,477 \text{ ft-lb}$

$M = 17,724 \text{ in.-lb}$

$f_{\text{FUTE}} = \frac{17,724}{20.82} = 851 \text{ psi}$

$f_{\text{RUB}} = \frac{17,724}{6.63} = 2,673 \text{ psi}$

COMBINED BIASIAL STRESS FACTOR (SKIN PLATE)  $= \frac{(4,154)^2 - (4,154)(851) + (851)^2}{(0.75)(32,000)^2} = 0.02$

Figure G2. (Sheet 14 of 18)

SUBJECT: SLUDGE GATE	COMPUTED BY	DATE
	CHECKED BY	DATE

SHEAR STRESS IN RIVETS CONNECTING SKINPLATE AND L BAR - NORMAL OPERATION WITH ICE

AREA BETWEEN GIRDERS A AND B

$$V = 2,251 (32) \left(\frac{1}{2}\right) = 6,003 \text{ lbs}$$

$$Q = (16.77)(0.375) [6.38 - 4.84 - (0.375)(0.5)] = 8.51 \text{ in.}^2$$

$$q = \frac{(6,003)(851)}{32.07} = 1,593 \text{ lb/in.}$$

$$A_{\text{rivet}} = \pi \left(\frac{1}{8}\right)^2 = 0.40 \text{ in.}^2$$

$$\tau_{\text{rivet}} = \frac{(1,593)(9)}{(0.40)} = 23,895 \text{ psi}$$

AREA BETWEEN GIRDERS B AND C

$$V = (7,222)(32) \left(\frac{1}{2}\right) = 19,259 \text{ lbs}$$

$$q = \frac{(19,259)(851)}{32.07} = 5,111 \text{ lb/in.}$$

$$\tau_{\text{rivet}} = \frac{(5,111)(9)}{(0.40)} = 76,665 \text{ psi}$$

Figure G2. (Sheet 15 of 18)

SUBJECT	SLUICE GATE	COMPUTED BY	DATE
		CHECKED BY	DATE

SHEAR STRESS IN RIVETS CONNECTING SKINPLATE AND L BAR - NORMAL OPERATION

AREA BETWEEN GIRDERS A AND B

$$V = (1,028) (32) \left(\frac{1}{2}\right) = 4,341 \text{ lbs}$$

$$q = \frac{(4,341) (851)}{32.07} = 1,152 \text{ lb/in.}$$

$$\tau_{\text{RIVET}} = \frac{(1,152) (9)}{0.60} = 17,280 \text{ psi}$$
  

AREA BETWEEN GIRDERS B AND C

$$V = (1,023) (32) \left(\frac{1}{2}\right) = 2,728 \text{ lbs}$$

$$q = \frac{(2,728) (851)}{32.07} = 724 \text{ lb/in.}$$

$$\tau_{\text{RIVET}} = \frac{(724) (9)}{0.60} = 10,860 \text{ psi}$$

Figure G2. (Sheet 16 of 18)

SUBJECT	SLUICE GATE	COMPUTED BY:	DATE:
		CHECKED BY:	DATE:

SHEAR STRESS IN RIVETS CONNECTING SKINPLATE AND GIRDERS — NORMAL OPERATION WITH ICE

GIRDER B

$$V = \frac{(6,180)(53.47)}{2} = 165,284 \text{ lb}$$

$$Q = (16.77)(0.375) [32.25 - 16.14 - (0.5)(0.375)] = 100.13 \text{ in.}^3$$

$$q = \frac{(165,284)(0.0013)}{8503} = 1,928 \text{ lb/in.}$$

$$A = \frac{\pi (\frac{7}{8})^2}{4} = 0.40 \text{ in.}^2$$

$$\tau = \frac{(1,928)(2)}{(0.40)} = 6,427 \text{ psi}$$
  

GIRDER C

$$V = \frac{(7,222)(53.47)}{2} = 193,152 \text{ lb}$$

$$Q = (16.77)(0.375) [31.25 + (0.5)(0.375) - 18.55] = 81.05 \text{ in.}^3$$

$$q = \frac{(193,152)(0.0013)}{6,204} = 2,523 \text{ lb/in.}$$

$$\tau = \frac{(2,523)(2)}{0.16} = 8,410 \text{ psi}$$

Figure G2. (Sheet 17 of 18)



SUBJECT  SLUICE GATE	COMPUTED BY  CHECKED BY	DATE  DATE
<p><u>SHEAR STRESS IN RIVETS CONNECTING SKINPLATE AND GIRDERS - NORMAL OPERATION</u></p> <p><u>GIRDER A</u></p> <p>(GEOMETRY OF GIRDER A SAME AS THAT OF GIRDER C)</p> $V = \frac{(1982)(53.49)}{2} = 28,938 \text{ lbs}$ $q = \frac{(28,938)(81.05)}{6,204} = 378 \text{ lb/in.}$ $\tau = \frac{(378)(2)}{0.60} = 1,260 \text{ PSI}$ <p><u>GIRDER B</u></p> $V = \frac{(2,651)(53.49)}{2} = 70,901 \text{ lbs}$ $q = \frac{(70,901)(81.05)}{6,204} = 827$ $\tau = \frac{(827)(2)}{0.60} = 2,757 \text{ PSI}$		

WES FORM NO. 1253A  
RECEIVED 1961

Figure G2. (Sheet 18 of 18)

In accordance with letter from DAEN-RDC, DAEN-ASI dated 22 July 1977, Subject: Facsimile Catalog Cards for Laboratory Technical Publications, a facsimile catalog card in Library of Congress MARC format is reproduced below.

Evaluation of condition of Lake Superior regulatory structure, Sault Ste. Marie, Michigan : final report / by Henry T. Thornton ... [et al]. (Structures Laboratory, U.S. Army Engineer Waterways Experiment Station). -- Vicksburg, Miss. : The Station, [1981]. 228 p. in various pagings, 82 leaves of plates (some folded) in various pagings : ill. ; 27 cm. -- (Miscellaneous paper / U.S. Army Engineer Waterways Experiment Station ; SL-81-14)

Cover title.

"June 1981."

"Prepared for U.S. Army Engineer District, Detroit."

Bibliography: p. 93-94.

1. Concrete construction. 2. Concrete-testing.  
3. Foundations. 4. Hydraulic structures. 5. Lake Superior. I. Thornton, Henry T. II. United States Army. Corps of Engineers. Detroit District. III. U.S.

Evaluation of condition of Lake Superior regulatory : ... 1981.  
(Card 2)

Army Engineer Waterways Experiment Station. Structures Laboratory. IV. Title V. Series: Miscellaneous paper (U.S. Army Engineer Waterways Experiment Station) ; SL-81-14. TA7.W34m no.SL-81-14